Improving the Hydrogen Yield of Microbial Electrolysis Cell with Facilitated Electron Transfer Using Mediators, Choice of Environmental Conditions and Anode Treatment with Conductive Materials

A thesis submitted in partial fulfillment for the degree of Doctor of Philosophy

Submitted by:

A.L.Popov

June
2015

Table of Contents

List of Units and Abbreviations

A ..... adenine

A ..... absorbanc (no units)

A ..... Tafel slope

AD ..... anaerobic digestion

ADP ..... adenosine diphosphate

AEM ..... anion exchange membrane

AFC ..... ammonium perusulfate

APS ..... alkaline fuel cell

AQDS ..... 9,10-anthraquinone-2,7-disulphonic acid

ATP ..... adenosine triphosphate

BA ..... bicarbonate alkalinity

C and / or conc ..... concentration ($mmolL^{-1}$)

C ..... cytosine

$C_{initial}$ ..... initial concentration ($mmolL^{-1}$)

C_{final} ..... final concentration ($mmolL^{-1}$)

CE ..... coulombic efficiency

CEM ..... cation exchange membrane

CE_t ..... theoretical coulombic efficiency

CE_p ..... coulombic efficiency calculated from data obtained practically

CNT ..... carbon nano tube

COD ..... chemical oxygen demand

CoTMPP ..... cobalt (II) tetramethoxyphenylporphyrin

DGGE ..... denaturing gradient gel electrophoresis

DMFC ..... direct-methanol fuel cell

DNA ..... deoxyribonucleic acid

Da ..... dalton (a non-SI unit of atomic and molecular mass)

E .....energy recoverey (J)

E_t ..... theoretical energy recoverey (J)

$\Delta E^{\ominus}$ .....standard electrode potentioal (V)

E_{anode} .....anode electrode potentioal (V)

$E_{cathode}$ ..... cathode electrode potentioal (V)

E_{cell} ..... cell electrode potentioal (V)

$E_{half\ cell}$ .....half cell electrode potentioal (V)

E_i ..... ionic losses (V)

E_{pH} ..... pH gradient losses (V)

E_t ..... transport losses (V)

EAB .....electrochemically active biofilm

EDTA .....ethylenediaminetetraacetic acid

EFC ..... enzymatic fuel cell

Eq ..... equation

F .....Faraday's constant (96500 c mol $^{-1}$)

FAD^{+} .....flavine adenine dinucleotide

FADH..... flavine adenine dinucleotide (reduced form)

FePc..... iron–phthalocyanine

FID .....flame ionization detector

G ..... guanine

ΔG .....Gibbs free energy constant

GC .....gas chromatograph

GC primer..... primer with high guanine and cytosine content

$GtCO_2$..... giga tonnes CO_2

HPLC.....high performance liquid chromatography

HRT .....hydrolic retention time

i ..... current density (A m^{-2})

i_0 ..... current density dependent on the electrolytic process (A m^{-2})

IPCC ..... Intergovernmental Panel on Climate Change

l ..... path length (distance between walls of the cuvette)

MB ..... methylene blue

MCFC ..... molten catbonate fuel cell

MEC ..... microbial electrolysis cell

MFC ..... microbial fuel cell

MV ..... methyl viologen

n ..... number of samples or repeat (see in text definition)

n ..... number of electrons in chamical reaction

NAD^+ ..... nicotinamide adenine dinucleotide

NADH ..... reduced NAD (reduced form)

$NADP^+$ ..... nicotinamide adenine dinucleotide phosphate

NADPH ..... nicotinamide adenine dinucleotide phosphate (reduced form)

NQ .....naphthoquinone

NR ..... neutral red

OCP .....open circuit potential

OECD countries ..... 34 countries that originally signed the Convention on the Organization for Economic Co-operation and Dvelopment

OME .....Other Major Economies and baseline emissions that would occur without 50 % CO_2 reduction policy intervention

P ..... power density

P_{max} .....maximum power density

PAFC..... phosphoric acid fuel cell

PCR .....polymerase chain reaction

PEM .....proton exchange membrane

PMFC .....polymer electrolyte membrane fuel cell

P-MFC .....photo-microbial fuel cell

PMEC .....pilot scale microbial electrolysis cell

PTFE ..... polytetrafluoroethylene

R ..... molar gas constant (8.314 J $K^{-1}mol^{-1}$)

r .....hydrogen recovery

r_{cat} .....cathodic hydrogen recovery

RFC ..... regenerative fuel cell

RNA .....ribonucleic acid

RVC .....reticulated vitreous carbon

SBR ..... sequencing batch reactor

SOFC .....solid oxide fuel cells

SOP .....standard operating procedure

STM ..... scanning tunneling electron microscopy

SS .....suspended solids

T ..... temperature (K or ^{o}C)

T .....thymine

Taq ..... polymerase enzyme which enables running the PCR at high temperatures ≥60 ^{o}C

TAE .....Tris, acetic acid and EDTA solution used to prepare actylamide gel

TCD ..... thermal conductivity detector

TEME .....N',N,N,N'-tetra-methylethylenediamine

TPB ..... tripple phase boundary

Tris .....tris(hydroxymethyl)aminomethane)

TS ..... total solids

UF .....ultra filtration membrane

VFA ..... volatile fatty acids

W .....weight (mg)

$W_{adsorbed}$.....adsorbed weight (mg)

$W_{initial}$.....initial weight (mg)

W_{final} ..... final weight (mg)

W_{H_2} ..... heat of combustion for hydrogen (286 KJ mol^{-1})

W_S .....heat of combustion for a partiular substrate (KJ mol^{-1})

W_{in} .....the electric input need to make hydrogen from a particular substrate (V)

Y ..... hydrogen yield

$Y_{H2\ per\ mol\ substrate\ destroyed}$ .....hydrogen yield per mol substrate destroyed

Greek letters

α .....class of proteobacteria

β .....class of proteobacteria

δ .....class of proteobacteria

η ..... efficiency of the process (W h^{-1})

η_{W+S} .....cathodic energy recovery

η .....overpotential

$\eta_{(anode)}$..... anode overpotential

$\eta_{(cathode)}$..... cathode overpotential

μ .....specific growth rate (h^{-1})

ε ..... extinction coefficient

List of Units

A .....Amper

Å .....Angstrom

c .....Coulomb

^{o}C ..... degree (Celcius)

d .....Dalton

F ..... Faraday

J .....Joule

K ..... Kelvin

L ..... Liter

m .....Meter

mol ..... Mol

V .....Volt

W .....Watt

List of Figures

List of Tables

List of Equations

List of Equivalence Statements

1. Abstract

The fermentative conversion of organic substrate to biohydrogen produces volatile fatty acid (VFA) rich effluents, typically a 40 % acetate and 60 % butyrate mixture. These VFA products can be used as feedstock for microbial fuel cells (MFC), to recover more energy as electricity, or microbial electrolysis cells (MEC), to recover more hydrogen. The effect of pH and temperature on hydrogen production rate in MECs from acetate using continuous flow MEC was evaluated from daily hydrogen production rates and yield per mol substrate (acetate). The highest hydrogen production rate was achieved at 850 mV, pH $5_{cathode}$ amounting to 200 cm^3 $L_{(anode)}^{-1}$ day^{-1} and H_2 yield 1.1 mol / mol substrate converted to hydrogen. The temperature of 30 ± 1 ^oC, was found to be best for hydrogen production in the system tested, with the performance of the reactor being reduced at a higher temperature, 42 ± 4 ^oC and at a lower temperature of 23 ± 2 ^oC.

Experiments on the effect of immobilized electron mediators methylene blue (MB) and neutral red (NR) on the maximum power densities (P_{max}) and voltage generation from acetate were conducted. The results showed that the improvement the power generation of a MFC (with MB anode) by the factor of 2 at temperatures of 8 ± 1 ^oC, 23 ± 2 ^oC and 33 ± 2.5 ^oC. The highest peak power density of P_{max} (MB) = 11.78 W m^{-3} (7.5 mA) was achieved for the MFC (MB treated anode), compared to P_{max} (control, plain carbon veil) =5.3 W m^{-3} (5.2 mA) at 35.5 ^oC. Neutral red however inhibited MFC performance at temperatures of 8 ± 1 ^oC, 23 ± 2 ^oC and 33 ± 2.5 ^oC with MFCs (NR) producing highest power density P_{max} (NR) = =3.06 W m^{-3} (3.19 mA) at 35.5 ^oC.

The effect of different acetate and butyrate concentrations, along with a full substrate switch on MEC performance was assessed. Two MEC cells were operated, one containing a bioanode acclimated to acetate (AC) and another with bioanode acclimated to butyrate (BU), for 20 mmol L^{-1} substrate. When the substrate concentration was changed from 20 mmol L^{-1} to 10 mmol L^{-1} and to 5 mmol L^{-1}, to acetate and butyrate mixtures (10 mmol L^{-1} and 10 mmol L^{-1}) and then finally changed over from acetate to butyrate and vice versa were evaluated. The highest hydrogen production rate was observed with 20 mmol L^{-1} acetate amounting to 250 cm^3 $L_{(anode)}^{-1}$ day^{-1} for the reactor (BU), when the substrate was switched from butyrate to acetate. The optimal concentration for butyrate was 10 mmol L^{-1} with a hydrogen production rate of 203 cm^3 $L_{(anode)}^{-1}$ day^{-1} and H_2 yield 0.5 mol / mol of substrate destroyed. These results indicate that the hydrogen yield from the acetate and butyrate present in hydrogen fermentation effluent could be used to produce hydrogen in a MEC.

The effect of four different electrode configurations on MEC performance was evaluated. Untreated carbon cloth roll (UCC) anodes; stainless steel mesh and carbon cloth roll anodes (RR); J cloth (artificial cloth made from non conductive fibers of the same as stainless steel cloth) carbon cloth roll (JC) and methylene blue treated cloth roll (MB) anodes were built. The MEC with RR anode performed best 175±5 $cm^3 L_{(anode)}^{-1} day^{-1}$ and H_2 yield 0.67 mol / mol for 20 mmol L^{-1} acetate. The hydrogen production decreased after several days of operation, biofilm coming off the electrode surface. MEC (UCC) had most stable hydrogen production 165±5 $cm^3 L_{(anode)}^{-1} day^{-1}$ and H_2 yield 0.46 mol / mol) whilst (MEC JC and MEC (MB) produced small amounts of hydrogen 20.5±1.5 $cm^3 L_{(anode)}^{-1} day^{-1}$ and 7.75±0.25 $cm^3 L_{(anode)}^{-1} day^{-1}$ respectively. A design for a scaled up 19 L MEC reactor was produced from this experimental data.

2. Introduction

Hydrogen is proposed as an alternative energy vector to reduce the reliance on conventional hydrocarbon fuels for powering vehicles (De Boer et al., 1976, White et al., 2006). Hydrogen possesses a high energy content of 141.9 J kg^{-1} compared to other energy vectors such as methane (55.7 J kg^{-1}) and biodiesel (mostly mono-alkyl esters, 37 J kg^{-1}) (Midilli et al., 2005). Hydrogen is an alternative energy vector that produces relatively negligible amounts of carbon dioxide emissions to adversely impact either on human health or the environment compared to, for example, bioethanol and biodiesel fuel eg:- mono-alkyl esters (Patterson et al., 2011, Patterson et al., 2008). On utilization in fuel cells, hydrogen produces solely water compared to fossil fuels in internal combustion engines, which produce carbon dioxide, carbon monoxide (if combustion is incomplete), nitrogen oxides and sulfur oxides.

Anthropogenic (man made) carbon dioxide emissions also contribute to so called green house effect, a process by which thermal radiation from a planetary surface is absorbed by atmospheric greenhouse gases, and is re-radiated in all directions elevating the average surface temperature above what it would be in the absence of the gases (Kuramochi et al., 2012, Kesicki, 2012). Various environmental experts argue that a reduction of 90 % is required in order to reduce the impacts of climate change (Watson et al., 1996). In 1988 the Intergovernmental Panel on Climate Change (IPCC), a scientific intergovernmental body under the auspices of the United Nations (UN) was set up at the request of member governments to target reductions in CO_2 emissions (IPCC, 2014). The UK Government target for CO_2 emissions is 20 % below 1990 levels by 2020 (Chitnis and Hunt, 2012, Kesicki, 2012). The larger term goal of 50 % reduction by 2050 (Fig. 1) is in progress (Akimoto et al., 2013).

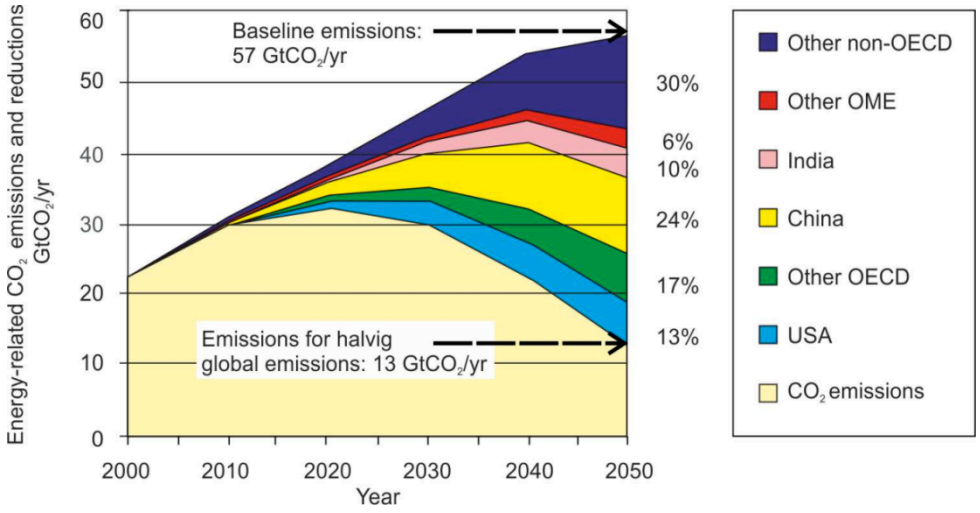

Figure 1 – Predicted increase in CO_2 emissions by region compared to predicted 50 % reduction by 2050 (Modified from Akimoto, 2013).

The Kyoto Protocol (1997), which targets reductions in CO_2 emissions in developed countries to 450 parts per million was a landmark agreement to try and limit the emissions of anthropogenic carbon dioxide. To reach these targets an alternative energy vector has to be found which is carbon free and could be sustainably produced. Fossil fuel reserves are also finite and crude oil reserves, for example, are being reduced at the rate of 4 billion tonnes a year. So if fossil fuel consumption carries on at this rate without any increase in exploitable reserves for our growing population or aspirations, known oil deposits will be gone by 2052 (Hogue, 2012). Hydrogen is a possible substitute for fossil fuels, however 96 % of this gas is currently produced from finite fossil fuels, such as coal or gas reforming process (Flohn, 1980, Cherryman et al., 2008). Steam reforming, a process most commonly used in industry, utilizes fossil fuels and produces carbon dioxide emissions (Angenent et al., 2004). Hydrogen can also be produced using electrolysis (Wang et al., 2014) with electricity produced by low carbon resources such as wind turbines (Pino et al., 2011, Khalilnejad and Riahy, 2014), solar power (Dou and Andrews, 2012, Giaconia and Caputo, 2014). Hydrogen production via fermentation which combines hydrogen production with removal of organic waste from wastewater streams is an potential alternative to water electrolysis method for sustainable hydrogen production (Intanoo et al., 2014). Therefore an interesting development of wastewater treatment technologies in the future may be aimed more towards fuel and energy production.

The first steps towards replacing conventional fuels with hydrogen are already being made. A hydrogen industry is already well established with a growth rate estimated at 5-10 % a year (Logan, 2004a, Clark and Rifkin, 2006, Keskin and Hallenbeck, 2012). According to California Senate Transportation Committee in 2013, $9 billion was invested by US government and various private companies into 300 hydrogen and fuel cell projects in United States per year (Thompson et al., 2013). The United States has formed an International Partnership in Hydrogen Economy with Australia, Brazil, Canada, China, France, Germany, Iceland, India, Italy, Japan, Korea, Norway, Russia and United Kingdom. Oil industries already recognise the importance of hydrogen as well and it's potential to replace gasoline in cars, in particular. Royal Dutch Shell group, for example, formed Shell Hydrogen Group and one of it's members stated that "fuel cell technology will eventually replace the internal combustion engine" (Hanisch, 1999). In 2014 Honda has developed and selling hydrogen powered fuel cell vehicles (Ito, 2014). Similar technologies were developed by Hyundai (Lim, 2010) and Shell (French, 2014). A key need is to identify sustainably produced hydrogen routes and the biological route for hydrogen production via fermentation of wastewater and microbial electrolysis (MEC) is a potential hydrogen production technology that can contribute to an overall low carbon hydrogen economy.

2.1 Biological Hydrogen Production

Fermentative hydrogen production is a potential renewable hydrogen production route, which can also treat organic wastes in a sustainable way (Dewan et al., 2008, Kundu and Sharma, 2010, Logan, 2010). This is particularly interesting for any industry producing large volumes of organic waste (i.e., food waste treatment industries) because the compounds present in biomass-based feedstocks can be used for biohydrogen production (Hawkes et al., 2002)). Hydrogen production via fermentation has been studied for many years (Massanet-Nicolau et al., 2008, Massanet-Nicolau et al., 2010, Das and Veziroglu, 2001, Wong et al., 2014).

Both pure and mixed cultures have been evaluated with mixed cultures obtained from "seed" sludges, sediments and soils extracts shown to produce more hydrogen because the diverse micro flora present in these extracts provides synergistic interactions that improve substrate degradation (Shi et al., 2010). Mixed microbial cultures found in sludge and soil were shown to adapt more easily to environmental stresses including changes in temperature, pH and to a range of substrates more easily than pure cultures (Ginkel et al., 2001, Argun et al., 2008). Examples of microorganisms responsible for hydrogen production are *Clostridium* sp. such as *Clostridium acetobutyricum* and *Clostridium butyricum* (Kamalaskar et al., 2010)*, Bacillus* sp. (Liu and Wang, 2012), *Enterobacter* sp. (Ren et al., 2008) and *Thermoanaerobacterium* sp. (O-Thong et al., 2009).

In these proteobacteria, glucose undergoes glycolysis to produce pyruvate with electron carrier NADH as the electron donor. The electrons generated from the oxidative decarboxylation of pyruvate are transferred to protons and then hydrogenase reduces the protons to molecular hydrogen. This process can be divided into two main routes: acidogenesis (acid production) where the main products are hydrogen, acetate and butyrate; or solventogenesis (solvent production) where the main products are hydrogen, ethanol and butanol (Shi et al., 2010, Akutsu et al., 2009).

Unfortunately, microflora in inoculum (sludge, soil and sediment samples) usually consists of both hydrogen producing bacteria and hydrogen consuming bacteria and archaea. Fermentative hydrogen production systems have been widely researched as various innovations allowed reduced the amount of hydrogen converted into methane by archaea. These innovations were various physical inoculum pre treatments eg:- heat treatment (Argun and Kargi, 2009) and untrasonication (Kotay and Das, 2007), chemical inoculum pre treatments eg:- reduction of pH to 3 for 24 h (Wu and Chang, 2007) and combination inoculum pre treatments (Venkata Mohan et al., 2008) which selectively reduce the number of archaea in the mixed microbial consortium.

If hexose undergoes complete oxidation, 12 moles of hydrogen can be recovered per mol of hexose utilized, however yields are typically much lower at 2-3 moles per mole of hexose. A maximum yield of 4 mol of hydrogen could only be obtained from 1 mol of hexose if the main product of hydrogen fermentation is acetate (Eq 26, p. 22). In practice, however a mixture of acetate and butyrate and so smaller hydrogen yields are obtained (Fang and Liu, 2002, Hussy et al., 2005). Depending of the environmental conditions other fermentation products, such as formate, propionate, lactate and ethanol could also be produced (Logan, 2004a). These by-products consume hydrogen during their production and should be avoided. Fermentative hydrogen production, which converts carbohydrate rich waste into hydrogen and acetate, has 33 % hydrogen conversion efficiency, whilst microbial electrolysis (MEC) converts acetate and/or butyrate into hydrogen, with hydrogen production efficiency close to 70 % (Heidrich et al., 2013, Zhang et al., 2013) (see "Integration of Microbial Fermentation Microbial Electrolysis (MECs) to Increase Energy Recovery" section 2.6 for further details).

Two stage biogas production is an elegant approach to the integration of bio hydrogen producing technologies to increase the energy yield, as each phase of the process can be optimised separately, resulting in more efficient removal of organic contaminants from the wastewater overall. The two stage process has been applied in the treatment and conversion of a wide range of wastes including food waste (Han and Shin, 2004) and agro-industrial waste (Rincón et al., 2009). Either a methane fermenter, microbial electrolysis cell (MEC) or microbial fuel cell (MFC) can be used as second stage process to convert byproducts of the hydrogen fermentation (first stage), which are mostly acetate and butyrate mixtures into methane, hydrogen or electricity (Guwy et al., 2011).

An example of the development of integrated hydrogen production process from biomass is the non-thermal production of pure hydrogen from biomass project (HYVOLUTION project, (see Fig. 2)). This project involves members of 10 EU countries as well as Turkey and Russia, represented with prominent specialists in academia and industries. The aim of HYVOLUTION was to deliver prototypes of process modules that are needed to produce hydrogen of high quality in a bioprocess that is fed by multiple biomass feedstocks (Panagiotopoulos et al., 2012). HYVOLUTION is the combination of a thermophilic fermentation with photo heterotrophic fermentation. During the first stage (thermophilic fermentation, at temperatures ≥70 ^{o}C) thermophilic bacteria are used to start the bioprocess that offers advantages, compared to more common mesophilic (at temperatures 22-35 ^{o}C).

In thermophilic fermentation glucose is converted to, on the average, 3 moles of hydrogen and 2 moles of acetate as the main by-product. In contrast, for mesophilic fermentation, the average yield is only 1 to 2 moles of hydrogen per mole of glucose and butyrate, propionate, ethanol and/or butanol are the main by-products. The production of acetate as the main by-product in the first fermentation is also very important because acetate is a prime substrate for photo heterotrophic bacteria (second stage). Through the combination of thermophilic fermentation with a photo heterotrophic fermentation (Liu et al., 2013), complete conversion of the substrate to hydrogen and CO_2 can be established. This two step process allows hydrogen to be produced from molasses, thick juice, potato steam peels and barley straw in a two step fermentation process using thermophilic bacteria and photo fermentative bacteria, consecutively. The overall efficiency in the combined fermentative steps was 53 % and increased to 64 % if a genetically modified mutant was used for the photo fermentation (Claassen and de Vrije, 2006, Claassen et al., 2010, Claassen et al., 2009, Liu et al., 2013a).

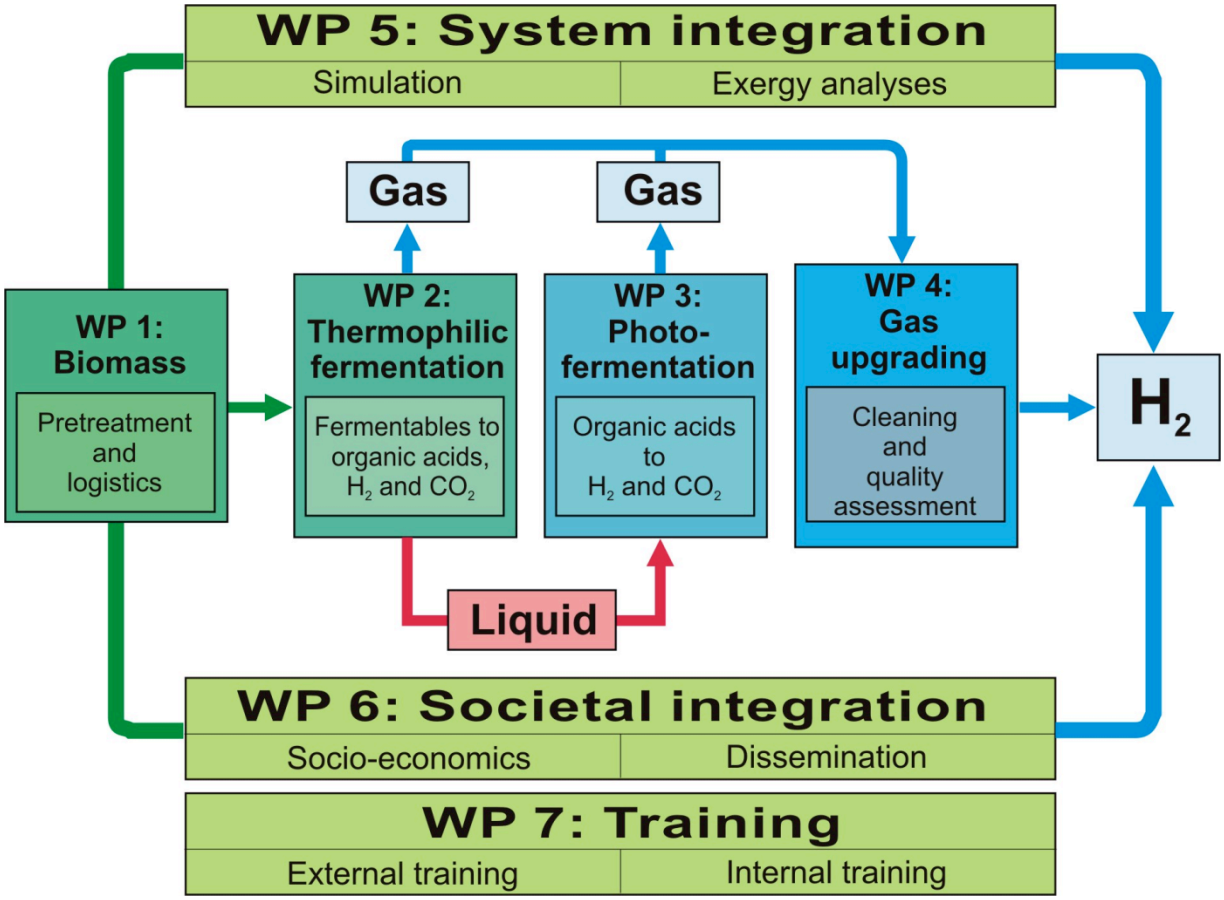

Figure 2 – A diagram for HYVOLUTION project based on material by Claassen et al (2008).

2.2 Bioelectrical Systems

Bioelectrical systems (BESs) convert chemical energy in organic compounds, to electrical energy and other products, by the metabolic reaction of electrochemically active microorganisms. The reductive energy in BESs cathodes can be used to produce energy rich fuels i.e. H_2 (Escapa et al., 2012), CH_4 (Cusick et al., 2011, Logan et al., 2010) and other applications which include H_2O_2 production (Jian-Xiao et al., 2009), desalination (Luo et al., 2012), treating dyes in wastewater (Kalathil et al., 2011), recovering radioactive waste (Lovley et al., 1991) and heavy metal ion removal from wastewater (Strandberg et al., 1981, Dollhopf et al., 2000, Liu et al., 2002). Two types of BESs were used in this thesis: - the microbial fuel cell (MFC), which converts the chemical energy into electricity and the microbial electrolysis cell (MEC) (Logan, 2008), which produces hydrogen by the electrolysis and is based on the architecture of MFC (Liu et al., 2005c, Logan and Cheng, 2007, Wang et al., 2010a).

2.3 Fuel Cells

A fuel cell is a device that converts energy generated by a chemical reaction directly into electricity. Fuel cells can be split into 3 main categories, microbial fuel cells (MFCs), enzymatic fuel cells and chemical fuel cells. These 3 categories can be split into sub categories determined by the kind of chemical reactions that take place in the cell, the kind of catalysts required, the temperature range in which the cell operates, the fuel required, and designs such as electrode materials.

2.3.1 Chemical Fuel Cells and Enzymatic Fuel Cells (EFCs)

Chemical fuel cells convert chemical energy of fuels, such as hydrogen and methanol into electrical energy (Andersson et al., 2010). Fuel cells can be split into 7 sub categories according to chemical reactions that take place in the fuel cells and the catalysts used:-

i) Polymer electrolyte membrane fuel cells (PEMs) deliver high-power density and offer the advantages of a smaller volume and lower weight, compared with other chemical fuel cells (Kramm et al., 2012, Tian et al., 2013). PEM fuel cells use a solid polymer as an electrolyte and porous carbon electrodes containing a platinum or palladium catalyst. They consume hydrogen and oxygen from the air, and operate at low temperatures ≈ 80 °C compared to other chemical fuel cells and do not use corrosive fluids. They are typically operated on pure hydrogen supplied from storage tanks. Low temperature operation allows them to start quickly (less warm - up time) and also results in less wear on system components resulting in better durability.

However PEM fuel cells require a precious metal catalyst (typically platinum) to be used to separate the hydrogen's electrons and protons, which add significantly to system cost (Genorio et al., 2011). The platinum catalyst is also extremely sensitive to carbon monoxide (CO) poisoning, making it necessary to install an additional filter to reduce CO in the fuel gas, if the hydrogen, is derived from an alcohol or hydrocarbon fuel. Today most research on PEMs is focused on exploring use of alloys such as platinum/ruthenium catalysts that are more resistant to CO poisoning (Roth et al., 2005).

ii) Direct-methanol fuel cells (DMFCs) are powered by methanol, which is mixed with steam and fed directly into the fuel cell anode chamber (Chen et al., 2013, Sharma et al., 2013). Methanol has a higher energy volumetric density than hydrogen, so the size of a fuel tank for DMFC can be significantly smaller than those used for hydrogen powered fuel cells (Sharma et al., 2013).Methanol is also easier to transport and supply to the public using our current infrastructure because it is present in a liquid form (Rahimpour and Elekaei, 2009).

iii) Regenerative fuel cells (RFCs) produce electricity from hydrogen and oxygen and generate heat and water as by-products (Wan et al., 2010). However, regenerative fuel cell systems can also use electricity from solar power or another electrical energy source to split water into oxygen and hydrogen fuel.

iv) Solid oxide fuel cells (SOFCs) use a hard, non - porous ceramic compound as the electrolyte (Oh et al., 2012). These cells do not have to be constructed in the plate-like configuration typical of other fuel cell types, because the electrolyte is a solid. The biggest advantage of SOFCs is that they can convert around 50 % - - 60 % the embedded energy in the fuel into electricity. If the system's waste heat is also converted into electricity (co-generation), overall fuel use efficiencies could reach 80 % - 85 %. Solid oxide fuel cells operate at high temperatures - around 1,000 °C, and therefore have longer warm-up times than PEM fuel cells. Most research on SOFCs today is focused on the development of SOFCs capable of operating at or below 800 °C, and therefore will have fewer durability problems and cost less. However, lower temperature SOFCs produce less electrical power, PEM fuel cells and stack materials that will function efficiently in this lower temperature range have not yet been identified (Raza et al., 2012). SOFCs are not poisoned by carbon monoxide (CO), which can even be used as fuel. This allows SOFCs to use gases made from coal (Oh et al., 2012).The development of low-cost materials with high durability at cell operating temperatures is the most important technical challenge facing this technology. High temperature operation, however, removes the need for a precious-metal catalyst, thereby reducing cost. It also allows SOFCs to reform fuels internally, which enables the use of a variety of fuels.

v) Phosphoric acid fuel cells use liquid phosphoric acid as an electrolyte with the acid typically contained in a Teflon - bonded silicon carbide matrix along with the porous carbon electrodes containing a platinum catalyst (Zeng et al., 2013). Phosphoric acid fuel cells (PAFCs) are usually used for stationary power generation, but some PAFCs have been used to power large vehicles such as city buses. PAFCs are more tolerant of impurities in fossil fuels that have been reformed into hydrogen than PEM cells, which are easily "poisoned" by carbon monoxide (CO) (Hwang et al., 2006). PAFC converts fuel to current with 85 % efficiency when used for the co-generation of electricity and heat but only 37 % - 42 % efficient at generating electricity alone. PAFCs produce less power (measured as Wm^{-3}) than other fuel cells, for the same weight and volume. In order to deliver, the required power for a small house or a vehicle for example, these fuel cells are typically large and heavy compared to PEM fuel cells. PAFCs are also expensive, like PEM fuel cells, PAFCs require an expensive platinum catalyst, which increases the cost of the fuel cell (Zeng et al., 2013).

vi) Molten carbonate fuel cells (MCFCs) are high-temperature fuel cells that use an electrolyte composed of a molten carbonate salt mixture suspended in a porous, chemically inert ceramic lithium aluminum oxide ($LiAlO_2$) matrix (Jung et al., 2012). They operate at temperatures of 650 °C, which makes it possible to use non-precious metals as catalysts at the anode and cathode, reducing costs of building electrodes. When the waste heat is captured and used, overall fuel efficiencies can be as high as 85 %. Unlike alkaline, phosphoric acid, and polymer electrolyte membrane fuel cells, MCFCs do not require an external reformer to convert more energy-dense fuels to hydrogen (Jung et al., 2012, Locher et al., 2012).

vii) Alkaline fuel cells (AFCs) use a solution of potassium hydroxide (KOH) in water as the electrolyte and can use a variety of non-precious metals as a catalyst at the anode and cathode (Li et al., 2013a). High-temperature AFCs operate at temperatures between 100 °C - 250 °C. Newer low temperature AFCs operate at 20 °C - 70 °C with fuel to electricity conversion efficiencies reaching near 60 %.

The disadvantage of this fuel cell type is that it is efficiency is easily reduced by carbon dioxide (CO_2). Even the small amount of CO_2 in the air can affect this cell's operation, making it necessary to purify both the hydrogen and oxygen used in the cell to remove any carbon dioxide. This purification process can be costly. Susceptibility to poisoning by CO_2 also affects the cell's lifetime (the amount of time before it must be replaced), further adding to the cost of operation (Li et al., 2013b).

viii) Enzymatic fuel cells (EFCs) use enzymes as catalysts to oxidize its fuel, rather than precious metals. EFCs consist of relatively inexpensive components (the anode and cathode contain enzymes instead of precious metals) and convert low cost substrates.

Most often reported in literature are glucose and sacharides, but are also capable of utilizing lipids, carbohydrates and fatty acids) into electricity (Jenkins et al., 2012, MacAodha et al., 2013). The size of EFCs can be reduced to fit into small implants powered by glucose in the blood stream (Yamamoto et al., 2013) and micro EFCs offer potential power source for small implants, such as pacemakers in the future. Unfortunately comparison between devices (anodes, cathodes, assemblies), in terms of operating conditions, performance benchmarks and stability benchmarks, is difficult with no adopted standardized procedures for testing or reporting of data (Uk Lee et al., 2013).

2.3.2 Microbial Fuel Cells (MFCs) and Photo Microbial Fuel Cells (P- MFCs)

Microbial fuel cells (MFCs) convert the chemical energy in liquid organic waste into electricity via electrochemically active microorganisms growing on the anode surface (Logan et al., 2006). MFCs have been studied for wastewater treatment because they convert organic waste into electricity at ambient temperatures and may not require any additional energy input (Logan, 2008) for heating. In MFCs, the fuel substrate is organic compounds found in wastewater, which are then converted into acetate and then into water and carbon dioxide. Biochemical electricity generation was reported as early as 1910 (Logan et al., 2006) and has been extensively investigated since 1960's. Research has used two main types of MFCs:- microbial fuel cells (MFCs) and photo microbial fuel cells (P-MFCs). P-MFCs contain microalgae instead of bacteria used in MFCs. PMFCs require less external organic carbon than MFCs as they convert CO_2 in the atmosphere into organic matter (Pandit et al., 2012). The work on approaches to integrate photosynthesis is still in the early stages of development and primarily concerns bioremediation and metal oxidation applications. The biggest problem however is building a chamber for photosynthetic culture, so that as much of biomass as possible would be exposed to the light source for a scaled up system (Pandit et al., 2012). MFCs and P-MFCs can be split into 3 sub types:-

i) Product microbial fuel cells are used for the production of a electrochemical product from organic substrate such as carbohydrates (Malki et al., 2008), wastewater containing lipids (Daniel et al., 2009), volatile fatty acids (VFAs) (Xing et al., 2008), antibiotics (Wen et al., 2011) and dyes (Li et al., 2010b). Product MFC cells are mediatorless i.e. do not require dissolved electron carrier in the solution or immobilized electron carrier on the anode surface.

ii) Redox cells (used for conversion of electrochemical product into electrochemical reactants, which can be again converted into electrochemical product) (Young et al., 1966). The term redox MFC cells refer to mediated MFC (these require dissolved electron carrier in the solution or immobilized electron carrier on the anode surface). Electron mediators could be electron carriers, such as neutral red (Park and Zeikus, 1999), resazurin (Sund et al., 2007), methyl viologen (Park and Zeikus, 2000), metal ions, such as Fe^{2+} (Park and Zeikus, 2003) and mediators, such as phenazine produced by cells themselves. Product or redox MFCs and P-MFCs can be either one chamber with air cathodes or two chamber MFCs with second chamber containing an electron acceptor. The cathodes could consist of a catalyst immobilized on a carbon cloth surface (Cheng et al., 2006b) or a biofilm on carbon cloth (biocathode) in a solution containing a fuel substrate (He and Angenent, 2006).

iii) The term sedimentary MFC refers to either a product MFC (ii) or redox MFC (iii) implemented as a one chamber MFCs where the anode is placed at the bottom of the chamber containing sediment and water and cathode is placed above it (Logan et al., 2007d). The devices are typically used for electricity production from marine sediments.

One promising application of MFC technology is to extract useful energy from organic wastes, thus reducing the negative environmental impacts associated with conventional waste treatments, such as activated sludge processes, landfill and incineration (Wang et al., 2012). MFCs have been used to treat a range of liquid organic waste: - biodiesel waste (Sukkasem et al., 2011) and liquid food wastes (Cusick et al., 2011) with the concurrent production of energy. In order to become commercialized microbial fuel cells need to have similar performance factors, such as power density and voltage to chemical fuel cells and be able to treat waste at a similar rate to conventional biological waste treatment systems. The power densities of MFCs are approximately 10 times smaller than that of chemical fuel cells (Aelterman et al., 2006b, Logan et al., 2006). This is one reason why a significant amount of research today focuses on improving voltage production and power density of MFCs (Lanas and Logan, 2013, Logan et al., 2006, Logan, 2008).

2.4 Principles of Microbial Fuel Cell (MFCs) Operation

A microbial fuel cell (MFC) consists of an anode and cathode separated by an ion exchange membrane (see Fig. 3). In the anode compartment, substrate is oxidized by microorganisms, generating electrons and protons. The electrons are transferred to the cathode compartment through the external circuit, and the protons are transferred from the anode to the liquid cathode compartment or open-air cathode through the ion exchange or microfiltration membrane (Li et al., 2010a). Electrons and protons are consumed at the cathode, combining with a terminal electron acceptor (TEA) which accepts electrons and becomes reduced (Rabaey and Verstraete, 2005). The TEAs could be oxygen (Kim et al., 2010), ferricyanide (Chaudhuri and Lovley, 2003) and anaerobic bacteria, if a biocathode is used (Clauwaert et al., 2007b). Electron acceptors such as ferricyanide are not practical to use compared to atmospheric oxygen because they are not easily regenerated and expensive (Logan et al., 2006, Willner et al., 1998). If the oxygen in atmospheric air is used as electron acceptor in single chamber MFCs, it eliminates the need for building a second chamber which is an advantage for scale up (Cheng et al., 2006b).

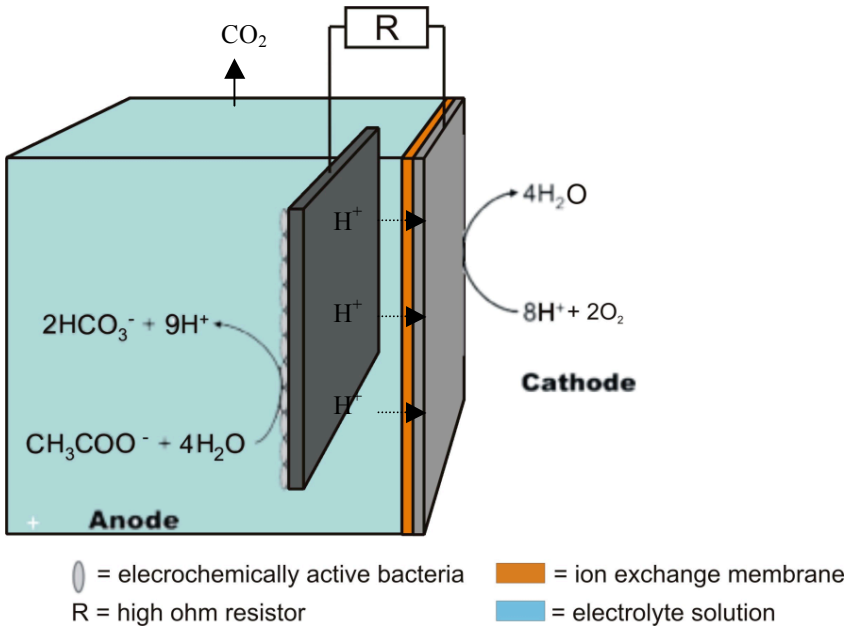

Figure 3 – Single chamber cubic microbial fuel cell (MFC) schematic.

Bacteria in microbial fuel cells (MFCs) do not constantly produce electricity at the same rate. If an external resistor not placed between the anode and cathode, the voltage production would increase and then rapidly decrease with time (Menicucci et al., 2006). Placing a resistor (100 Ω - 1000 Ω) between the anode and cathode, in MFCs, allows voltage production at a steady rate to be produced.

The power generated by the MFC is also limited by the charge-transfer resistance to the electrode, including kinetic and / or mass transfer limitations (Sleutels et al., 2009b, Sleutels et al., 2009a) and the external resistance (Aelterman et al., 2008, Christy et al., 2011, Coronado et al., 2013, Hong et al., 2011, Katuri et al., 2011). The impact of charge-transfer could be demonstrated by increasing the convection of electro active species in a solution, which in turn increases the ionic transport, electricity production and power density in MFCs. The effect of the internal mass transfer resistance is described in "Performance Inhibitors in Microbial Fuel Cells (MFCs) and Microbial Electrolysis Cells (MECs)" section 2.16 in greater detail. The voltage between the cathode and the anode is measured and can be compared to theoretical overall electrode potential $E_{(cell)}$, (see equations 12 and 18). This is calculated from the half cell potentials $E_{(half\ cell)}$. Half cell potentials are calculated via the Nernst Equation. The Nernst Equation relates the equilibrium reduction potential of a half cell in an electrochemical cell to the standard electrode potential and temperature, as shown:

$$E_{(half\ cell)} = E^{\ominus} - \frac{RT}{nF} \ln (K) \qquad \text{Eq 1}$$

Where the half cell is a structure that contains conductive electrode and a surrounding conductive electrolyte separated by ion exchange membrane. For experiments conducted in this thesis, $E_{(half\ cell)}$ is half cell potential, $E^{\ominus}$ is standard half cell potential, R=8.314 J $K^{-1}mol^{-1}$, T = temperature, F= Faraday's constant (96500 c mol^{-1}), n = number of electrons (8 for acetate (Eq 5) and 4 for butyrate (Eq 14), 20 (if it is considered that butyrate oxidized to acetate and acetate is converted into carbonate (Logan et al., 2006)) and K is equilibrium constant (the function of concentration when the reaction has reached equilibrium). In order to simplify the equation:

$$(R\ (J\ K^{-1}\ mol^{-1}) \times T\ (K)) / F\ (c\ mol^{-1}) = 25.693 \times 10^{-2}\ J\ c^{-1} = 25.693mV \qquad \text{Eq 2}$$

Acetate oxidation, for example can be represented by 2 half equations. Equilibrium constant (K) for substance concentration X, which could be any substance, is always represented as:-

$$K = [X_{(reduced)}] / [X_{(oxidized)}] \qquad \text{Eq 3}$$

(Aelterman et al., 2006a, Logan et al., 2006, Logan, 2008)

so that all half equations are written in reduction direction $X_{(oxidized)} \rightleftharpoons X_{(reduced)}$. Eq 4

Both half equations for acetate oxidation (Eq 5 and Eq 14), used as an example, are written in reduction direction despite that this is an oxidation reaction. The overall equations 11 and 17 however can be written in the oxidation direction.

Acetate is used as an example because it is most common substrate of choice in MFCs and because it produces highest voltages and power densities reported in the literature (Logan et al., 2006).

Half cell equation for anode for MFC with acetate:

$2HCO_3^-{}_{(aq)} + 9H^+_{(aq)} + 8e^- \rightleftharpoons CH_3COO^-{}_{(aq)} + 4H_2O_{(l)}$ Eq 5

$$\ln(K) = \ln\left(\frac{[CH_3COO^-_{(aq)}]}{[HCO^-_{3(aq)}]^2 \times [H^+_{(aq)}]^9}\right) = \ln\left(\frac{[0.02]}{[0.02]^2 \times [10^{-7}]^9}\right) \approx 149 \text{ (no units)} \quad \text{Eq 6}$$

$$E_{(half\ cell)} = E^{\ominus}_{(half\ cell)} - \frac{RT}{nF}\ln(K) = 0.187 - \left(\frac{1}{8} \times 25.693 \times 10^3 \times 149\right) = -0.292V \quad \text{Eq 7}$$

Half cell equation for cathode for MFC with acetate:

$4H^+_{(aq)} + O_{2(g)} \rightleftharpoons 2H_2O$ Eq 8

This is a special case where the percentage of oxygen in air (21%) has to be taken into the account:

$$\ln(K) = \ln\left(\frac{1}{[H^+_{(aq)}]^4 \times 0.21}\right) = \ln\left(\frac{1}{[10^{-7}]^4 \times 0.21}\right) = \ln\left(\frac{1}{[10]^{-28} \times 0.21}\right) \approx 66 \text{ (no units)} \quad \text{Eq 9}$$

$$E_{(half\ cell)} = E^{\ominus}_{(half\ cell)} - \frac{RT}{nF}\ln(K) = 1.23 - \left(\frac{1}{4} \times 25.693 \times 10^{-3} \times 66\right) = 1.23 - 0.424 = 0.806V \quad \text{Eq 10}$$

Overall: $CH_3COO^-_{(aq)} + 2O_{2(g)} \rightleftharpoons 2HCO_3^-{}_{(aq)} + H^+_{(aq)}E$ Eq 11

$E_{(cell)} = E_{(half\ cell\ cathode)} - E_{(half\ cell\ anode)} = 0.806 - (-0.292) = 1.01\ V$ Eq 12

Eq 11 and Eq 12 show that 1.01V is potentially produced by a microbial fuel cell (MFC) from 20 mmol L^{-1} acetate solution. In reality however approximately 0.6V are produced in close circuit conditions due to overpotential and ionic transport losses described as “Performance Inhibitors in Microbial Fuel Cells (MFCs) and Microbial Electrolysis Cells (MECs)” (see section 2.16). The electrode potential $E_{(cell)}$ does not only show how much voltage can be produced by the MFC in theory it can also be used to calculate the Gibbs free energy constant ΔG (a thermodynamic potential which indicates the spontaneousness of a chemical reaction solution (Bard and Faulkner, 1976)). The relationship between ΔG and $E_{(cell)}$ is determined by the equation:

$\Delta G = -nFE_{(cell)}$ Eq 13

where n=number of electrons involved in a chemical reaction and F is Faraday’s constant (96500).

If ΔG is negative a chemical reaction is spontaneous and if ΔG is positive energy has to be applied to drive the chemical reaction. If $E_{(cell)}$ is positive for example, it results in negative Gibbs free energy, so the reaction does proceed and voltage is produced, in MFC.

The oxidation of butyrate is described by equations 14 - 16. Butyrate is 1st oxidized to acetate and then acetate is converted by bacteria into carbonate (Liu et al., 2005b). Butyrate oxidation to acetate produces 4 electrons (Eq 14 and Eq 17) and 2 mol of acetate (8+8 electrons) that are then converted into carbonate (Eq 5 and Eq 12).

Half cell equation for anode for MFC with butyrate:

$$2CH_3COO^-_{(aq)}+5H^+_{(aq)}+4e^- \rightleftharpoons C_3H_7COO^-_{(aq)}+2H_2O_{(l)} \quad \text{Eq 14}$$

$$\ln(K) = \ln\left(\frac{[CH_3CH_2COO^-_{(aq)}]}{[H_3CCOO^-_{(aq)}]^2 \times [H^+_{(aq)}]^5}\right) = \ln\left(\frac{[0.02]}{[0.02]^2 \times [10^{-7}]^5}\right) \approx 85 \text{ (no units)} \quad \text{Eq 15}$$

$$E_{(half\ cell)} = E^{\ominus}_{(half\ cell)} - \frac{RT}{nF}\ln(K) = 0.184 - \left(\frac{1}{4} \times 25.693 \times 10^{-3} \times 85\right) = -0.362V \quad \text{Eq 16}$$

Half cell equation for cathode for MFC with butyrate:

$$4H^+_{(aq)}+O_{2(g)} \rightleftharpoons 2H_2O \quad \text{Eq 8}$$

This is a special case where the percentage of oxygen in air (21%) has to be taken into the account

$$\ln(K) = \ln\left(\frac{1}{[H^+_{(aq)}]^4 \times 0.21}\right) = \ln\left(\frac{1}{[10^{-7}]^4 \times 0.21}\right) = \ln\left(\frac{1}{[10]^{-28} \times 0.21}\right) \approx 66 \text{ (no units)} \quad \text{Eq 9}$$

$$E_{(half\ cell)} = E^{\ominus}_{(half\ cell)} - \frac{RT}{nF}\ln(K) = 1.23 - \left(\frac{1}{4} \times 25.693 \times 10^{-3} \times 66\right) = 1.23\text{-}0.424 = 0.806V \quad \text{Eq 10}$$

Overall: $C_3H_7COO^-_{(aq)}+O_{2(g)} \rightleftharpoons 2CH_3COO^-_{(aq)} + H^+_{(aq)}$ Eq 17

$$E_{(cell)} = E_{(half\ cell\ cathode)} - E_{(half\ cell\ anode)} = 0.806 - (-0.362) = 1.17\ V \quad \text{Eq 18}$$

Electrode and half cell potentials ($E_{(cell)}$ and $E_{(half\ cell)}$) for 5, 10 and 20 mmol L^{-1} acetate or butyrate concentrations are shown in Table 1.

Table 1 – Electrode and half cell potential values ($E_{(cell\ MFC)}$ and $E_{(half\ cell\ MFC)}$) for butyrate and acetate oxidation reactions calculated using Nernst Equation.

	Conc. (mmol L^{-1})	$E_{(half\ cell\ anode\ MFC)}$ (V)	$E_{(half\ cell\ cathode\ MFC)}$ (V)	$E_{(cell\ MFC)}$ (V)
acetate	5	- 0.295	0.806	1.101
$E^{e}_{(half\ cell)}$ = 0.187 (V)	10	- 0.295	0.806	1.101
(Logan et al., 2006)	20	- 0.292	0.806	1.098
butyrate	5	- 0.368	0.806	1.174
$E^{e}_{(half\ cell)}$ = 0.184 (V)	10	- 0.362	0.806	1.170
(Thauer et al., 1977)	20	- 0.362	0.806	1.170

2.5 Principles of Microbial Electrolysis Cell (MEC) Operation

Microbial electrolysis cell (MEC) can convert organic pollutants in wastewater into hydrogen (Guo et al., 2010). The hydrogen yield of an MEC using 1g Chemical Oxygen Demand (COD, an indirect method used to determine how much substrate is consumed described in "Offline Analysis Methods" section 4.8), could liberate 1.4 L of hydrogen at 25 ^{o}C and 1 atm (Oh and Logan, 2005, Liu et al., 2005c).

Microbial electrolysis cell (MEC) is a technology related to microbial fuel cells (MFCs) and has many similar characteristics, such as anode chamber designs. There are however five important differences:-

i) MFC's produce electric current from the microbial decomposition of organic compounds; MEC's however require electric current to generate hydrogen.

ii) The cathode chamber in MEC has to be sealed to prevent loss of hydrogen (Fig. 4).

iii) In a microbial electrolysis (MEC) there is a loss of hydrogen, through the diffusion membrane from cathode into the anode chamber and hydrogen consumption by methanogenic bacteria, but there is no comparable process in microbial fuel cells (MFC). Hydrogen therefore has to be generated in a manner that reduces the diffusion back into the anode chamber (Hamelers et al., 2006, Logan et al., 2007c).

iv) Methane production in the cathode chamber from hydrogen or substrate is called cathodic methanogenesis (Hamelers et al., 2007), explained further in ”Cathodic Methanogenesis” in “Performance Inhibitors in Microbial Fuel Cells (MFCs) and Microbial Electrolysis Cells (MECs)” section 2.16. This problem arises from archaea (methane producing microorganisms) reaching into the cathode chamber, of a two chamber microbial electrolysis cells (MECs). The reasons for this could be small holes (imperfections) on the membrane surface big enough to let substrate to pass through and contamination by bacteria from the anode chamber, when MECs are taken apart for cleaning. This problem could be greatly reduced, if the electrolyte solution, ion exchange membrane and the cathode surface are sterilized before next experiment begins. In microbial fuel cells (MFCs), which do not produce hydrogen this problem is avoided.

v) This difference only applies to MFC with air cathodes. Oxygen diffusion through the membrane into the anode chamber kills anaerobic bacteria. Therefore coulombic efficiency (CE for MFC and R_{CE} for MEC), the efficiency with which the substrate is converted into current is lower for MFCs with air cathodes compared to coulombic efficiencies for MECs. In MECs this problem is avoided because cathode chamber is anaerobic resulting in much higher coulombic efficiencies (R_{CE}^{S}), as high as 97 % compared to 10 % and 78 % in MFCs with open air cathodes, depending on designs and their internal resistances (Liu et al., 2005a, Oh et al., 2004).

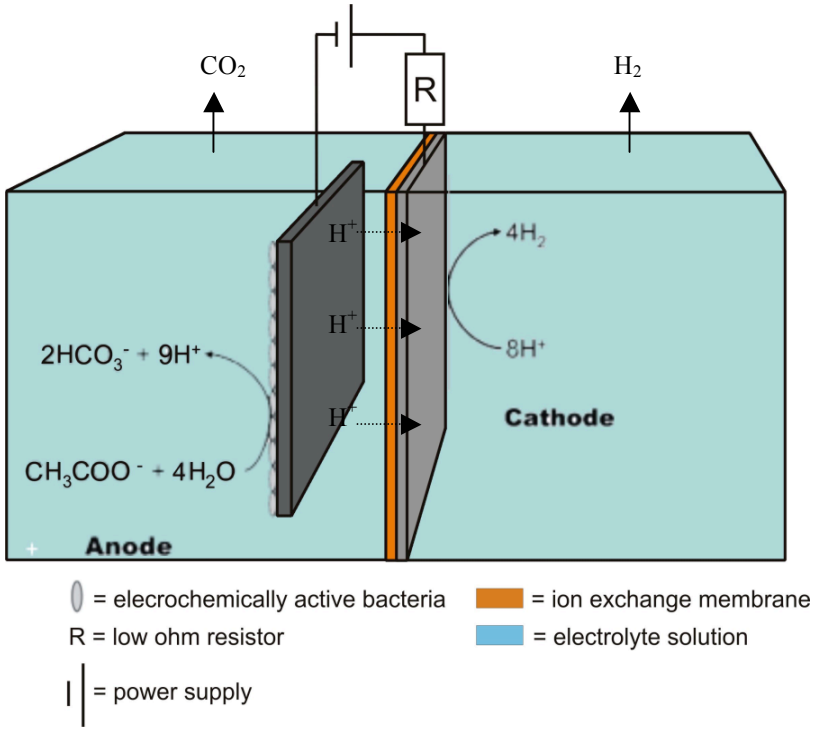

Figure 4 – Two chamber cubic microbial electrolysis cell (MEC) schematic.

Figure 4 shows a typical microbial electrolysis cell (MEC) consisting of an anode and a cathode chamber, where the anode chamber contains electrolyte solution and substrate for the bacteria grown on the porous bioanode surface (usually carbon cloth). Anion (AEM) or cation (CEM) exchange membrane separates both chambers. The cathode is usually platinum (Pt) treated carbon cloth or Pt coated titanium mesh (Rozendal et al., 2007). The cathode chamber (usually abiotic) contains a terminal electron acceptor (TEA) dissolved in electrolyte (Mohan et al., 2009). If a gaseous cathode is used, the cathode is placed directly over the membrane (Tartakovsky et al., 2008). A biocathode can then be used as alternative to precious metal catalyst based cathode and contains bacteria on the carbon cloth surface, as in the MFC anode (Rozendal et al., 2007). The hydrogen in a MEC is usually produced by *Proteobacteria* (Logan et al., 2008). The side product methane is produced by archaea, if a mixed microbial culture, grown from anaerobically digested sludge is used.

The hydrogen produced by MECs can be stored and used to produce electricity by means of an additional PEM fuel cell or internal combustion engine for domestic use and/or in gas powered and hydrogen fuel cell vehicles (Hirose, 2010). Microbial electrolysis (MEC) process, requires 0.5-0.8 V in practice, utilizes less voltage than water electrolysis, which requires a minimum voltage of 1.23 V to produce hydrogen (Hamelers et al., 2007). MEC offers potential for even greater efficiency. Theoretical voltage required to drive the process is much lower 0.119 V, if electron transport and overpotenial losses (described in detail in “Performance Inhibitors in Microbial Fuel Cells (MFCs) and Microbial Electrolysis Cells (MECs)” section 2.16) are not taken into the account.

The theoretical voltage needed to drive the process is calculated, using the same method as described in "Principles of Microbial Fuel Cells (MFC) Operation" section 2.4 with all half cell equation written in the reduction direction and overall equation written in the direction it occurs in practice:-

Half cell equation for anode for MEC with acetate:

$2HCO_3^-{}_{(aq)} + 9H^+_{(aq)} + 8e^- \rightleftharpoons CH_3COO^-{}_{(aq)} + 4H_2O_{(l)}$ Eq 5

$$\ln(K) = \ln\left(\frac{[CH_3COO^-_{(aq)}]}{[HCO^-_{3(aq)}]^2 \times [H^+_{(aq)}]^9}\right) = \ln\left(\frac{[0.02]}{[0.02]^2 \times [10^{-7}]^9}\right) \approx 149 \text{ (no units)} \quad \text{Eq 6}$$

$$E_{(\text{half cell})} = E^{\ominus}_{(\text{half cell})} - \frac{RT}{nF}\ln(K) = 0.187 - \left(\frac{1}{8} \times 25.693 \times 10^3 \times 149\right) = 0.187 - 0.479 = -0.292\text{V} \quad \text{Eq 7}$$

Half cell equation for cathode for MEC with acetate:

$2H^+_{(aq)} + 2e^- \rightleftharpoons H_2$ Eq 19

$$\ln(K) = \ln\left(\frac{1}{[H^+_{(aq)}]^2}\right) = \ln\left(\frac{1}{[10^{-7}]^2}\right) = \ln\left(\frac{1}{[10]^{-14}}\right) \approx 32 \text{ (no units)} \quad \text{Eq 20}$$

$$E_{(\text{half cell})} = E^{\ominus}_{(\text{half cell})} - \frac{RT}{nF}\ln(K) = 0 - \left(\frac{1}{2} \times 25.693 \times 10^{-3} \times 32\right) = 0 - 0.414 = -0.414\text{V} \quad \text{Eq 21}$$

Overall: $CH_3COO^-_{(aq)} + 4H_2O_{(g)} \rightleftharpoons 2HCO_3^-{}_{(aq)} + H^+_{(aq)} + 4H_{2\,(g)}$ Eq 22

$E_{(\text{cell})} = E_{(\text{half cell cathode})} - E_{(\text{half cell anode})} = -0.414 - (-0.292) = -0.122\text{V}$ Eq 23

Eq 21 and 22 show that 0.122V is required to drive acetate oxidation to hydrogen in (MEC) from 20 mmol L^{-1} acetate solution. In reality, however approximately 0.5-1V are required. Electrode potential $E_{(cell)}$ does not just show how much voltage can be produced by MFC in theory it can also be used to calculate Gibbs free energy constant ΔG could be calculated, as described in "Principles of Microbial Fuel Cell (MFC) Operation" section 2.4. Gibbs free energy is positive for acetate oxidation to hydrogen that means that energy has to be applied to drive this reaction. The butyrate oxidation is described by equations 14 and 25. Butyrate is first oxidized to acetate and then acetate is converted by bacteria into carbonate (Liu et al., 2005b). Butyrate oxidation to acetate produces 4 electrons (Eq 5), and 2 mols of acetate (8+8 electrons, Eq 13), which are than converted into, carbonate.

Half cell equation for anode for MEC with butyrate:

$2CH_3COO^-_{(aq)}+5H^+_{(aq)}+4e^- \rightleftharpoons C_3H_7COO^-_{(aq)}+2H_2O_{(l)}$ Eq 14

$\ln(K) = \ln\left(\frac{[CH_3CH_2COO^-_{(aq)}]}{[H_3CCOO^-_{(aq)}]^2 \times [H^+_{(aq)}]^5}\right) = \ln\left(\frac{[0.02]}{[0.02]^2 \times [10^{-7}]^5}\right) \approx 85$ (no units) Eq 15

$E_{(\text{half cell})} = E^{\ominus}_{(\text{half cell})} - \frac{RT}{nF}\ln(K) = 0.184 - \left(\frac{1}{4} \times 25.693\times10^{-3}\times85\right) = -0.362$ V Eq 16

Half cell equation for cathode for MEC with butyrate:

$2H^+_{(aq)}+2e^- \rightleftharpoons H_2$ Eq 19

$\ln(K) = \ln\left(\frac{1}{[H^+_{(aq)}]^2}\right) = \ln\left(\frac{1}{[10^{-7}]^2}\right) = \ln\left(\frac{1}{[10]^{-14}}\right) \approx 32$ (no units) Eq 20

$E_{(\text{half cell})} = E^{\ominus}_{(\text{half cell})} - \frac{RT}{nF}\ln(K) = 0 - \left(\frac{1}{2} \times 25.693\times10^{-3}\times32\right) = 0 - 0.414 = -0.414$ V Eq 21

Overall: $C_3H_7COO^-_{(aq)} + 2H_2O_{(l)} \rightleftharpoons 2CH_3COO^-_{(aq)} + H^+_{(aq)} + 2H_{2\,(aq)}$ Eq 24

$E_{(\text{cell})} = E_{(\text{half cell cathode})} - E_{(\text{half cell anode})} = -0.414 - (-0.362) = -0.052$ V Eq 25

Electrode and half cell potentials ($E_{(\text{cell})}$ and $E_{(\text{half cell})}$) for 5, 10 and 20 mmol L^{-1} acetate or butyrate concentrations are shown in Table 2.

Table 2 – Electrode and half cell potential values ($E_{(\text{cell MFC})}$ and $E_{(\text{half cell MFC})}$) for acetate and butyrate oxidation reactions calculated using the Nernst Equation.

	Conc. (mmol L^{-1})	$E_{(\text{half cell anode MFC})}$ (V)	$E_{(\text{half cell cathode MFC})}$ (V)	$E_{(\text{cell MFC})}$ (V)
acetate	5	- 0.295	- 0.414	- 0.119
$E^{\ominus}_{(\text{half cell})}$ =0.187 (V)	10	- 0.295	- 0.414	- 0.119
(Logan et al., 2006)	20	- 0.292	- 0.414	-0.122
butyrate	5	- 0.368	- 0.414	-4.6×10^{-2}
$E^{\ominus}_{(\text{half cell})}$ =0.184 (V)	10	- 0.362	- 0.414	-5.2×10^{-2}
(Thauer et al., 1977)	20	- 0.362	- 0.414	-5.2×10^{-2}

2.6 Integration of Biohydrogen Fermentation with BES to Increase Energy Recovery

Hydrogen can be produced from wastewater containing food waste and/or dyes (Catanho et al., 2006, Li et al., 2010b) using hydrogen fermentation integrated with microbial electrolysis (MEC) cell. This is the most efficient way to remove organic waste from wastewater in terms of energy recovery and treatment of organic waste (Guwy et al., 2011). Hydrogen fermentation is the process that converts organic wastewater, mostly containing carbohydrates, lipids and proteins by hybrid process into hydrogen and volatile fatty acids (Vass). Anaerobic fermentation converts organics in wastewater to hydrogen with 17-33 % efficiency with 4 mol (Eq 26) or 2 mol (Eq 27) of hydrogen obtained per mol of carbohydrate compared to theoretical amount of 12 mol of hydrogen per mol carbohydrate, use:- eg. Eq 28), with acetate or butyrate mixtures as main aqueous products (Logan, 2004a).

$$C_6H_{12}O_6 + 2H_2O \rightleftharpoons 2C_2H_4O_2 + CO_2 + 4H_2 \qquad \text{Eq 26}$$

$$C_6H_{12}O_6 \rightleftharpoons C_4H_8O_2 + 2CO_2 + 2H_2 \qquad \text{Eq 27}$$

$$C_6H_{12}O_6 + 6H_2O \rightleftharpoons 6CO_2 + 12H_2 \qquad \text{Eq 28}$$

Therefore another step is needed to consume the remaining volatile fatty acids such as acetate and butyrate in order to completely remove organic pollutants and to increase the energy yield (Collet et al., 2004, Massanet-Nicolau et al., 2008, Guwy et al., 2011). If a hydrogen fermenter is connected to microbial electrolysis cell (MEC), as shown in figure 5, the hydrogen yield could be increased by up to 60-80% (Hallenbeck and Benemann, 2002).

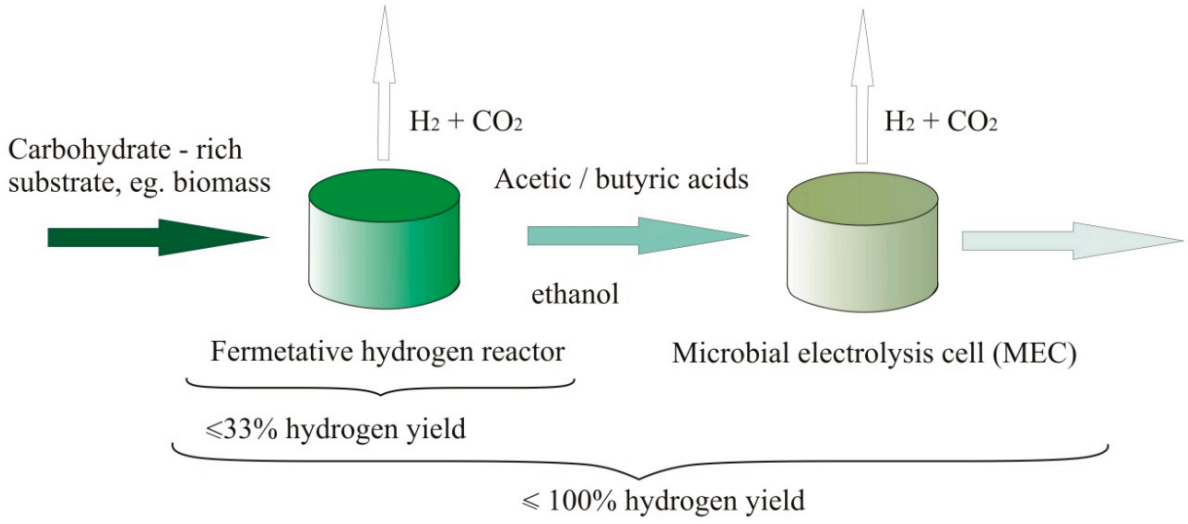

Figure 5 – Fermentative hydrogen reactor coupled to MEC cell.

For photo fermentation, increased yields ranging from 53 to 64% have been reported (Claassen and de Vrije, 2006, Claassen et al., 2010, Claassen et al., 2009, Liu et al., 2013a). The overall yield of the hydrogen fermentation process combined with microbial electrolysis (MEC) could be increased even closer to 100 % in the near future (Chaudhuri and Lovley, 2003, Logan and Cheng, 2007, Liu and Fang, 2003). It could be suggested that hydrogen fermentation combined with MEC will replace conventional methods used to produce hydrogen such as steam reforming (see "Introduction" (section 2) for more details). If the hydrogen fermenter is connected to microbial fuel cell (MFC) the percentage organic removal can be increased to 70-90 % (Lu et al., 2009) with 17-33 % of organics converted into hydrogen and remaining 37-73 converted into electricity (Wang et al., 2011). Hydrogen production by (MEC) however is considered to be more profitable then production of electricity from wastewater (Foley et al., 2010), so research in near future is more likely to focus on the development of hydrogen fermenters integrated with microbial electrolysis cells (MECs) and microbial fuel cell (MFC) technology. Hydrogen fermentation combined with MEC is considered to better than conventional wastewater treatment technologies, such as activated sludge treatment (Anastasi et al., 2012), which has already been taken to industrial level and dominates the wastewater treatment industry. Activated sludge treatment process involves pumping air or oxygen into sewage or industrial wastewater in order to promote growth of organisms to develop a biofilm, which reduces the organic content in treated wastewater (Dey and Magbanua, 2012). MFC integrated with hydrogen fermentation however produces gas and electricity and does not require as much energy as activated sludge treatment, which only removes organic waste (Liu et al., 2011c).

Three key research areas, for improving the performance of hydrogen fermenters, microbial electrolysis cells (MECs) and microbial fuel cells (MFCs) have to be addressed:

i) New materials for better configurations of fermenters, MECs and MFCs.

ii) Low material costs as well as low operational costs, dry cathodes that have high affinity to oxygen and use O_2 directly from air, for MFCs.

iii) A reliable output for "non commodity" electricity produced by MFCs (Pham et al., 2006). Studies on the integrated anaerobic hydrogen fermentation treatment / MEC systems (Foley et al., 2010, Guwy et al., 2011) suggest that there is sufficient cause, from an environmental perspective, to pursue the development and commercialization of this technology.

2.7 Electrochemically Active Microorganisms

Electrochemically active bacteria are bacteria required for electricity production in microbial fuel cell (MFC) or hydrogen production in microbial electrolysis cell (MEC) at applied voltage (Mu et al., 2010). It was shown that presence of *Aeromonas, Geobacter* and / or *Shewanella* bacteria was required for the current generation of 0.80 - 0.89 V at open circuit potential (Sharma et al., 2008). In their experiment a microbial fuel cell having only substrate (acetate) in abiotic environment did not produce any current. However, when bacteria were added to the system, there was a rapid increase in the open circuit potential (OCP) to 0.2 V and a gradual increase in the potential to 0.89 V, there after. Bacteria, such as *Geobacter* and *Shewanella*, capable of transferring electrons to outer membrane without aid of artifical electron carriers are sometimes referred to as exoelectrogenic bacteria Logan (2008). The term electrochemically active or electrogenic bacteria refers to both exoelectrogens and becteria, such as *Escherichia coli*, which require artificial electron mediators to facilitate electricity production. Electrochemically active bacteria have the ability to transfer electrons to an electrode by anaerobic respiration from various organic compounds such as carbohydrates proteins and lipids found in sewerage and food waste wastewaters (Allen and Benetto, 1993, Moon et al., 2006, Oh et al., 2005), from dyes (Mu et al., 2009), metals (Strandberg et al., 1981) and even radioactive metals (Lovley et al., 1991).

Electrochemically active bacteria evolved over millions of years using various compounds to support their metabolism, without gaseous oxygen to drive their respiration. In anaerobic environments where the availability of electron acceptors is limited, bacteria have ability to generate energy by fermentative metabolism (Thauer et al., 1977). Fermentative metabolism is a process that occurs in the absence of electron transport chain which oxidizes a carbon source, such as glucose (substrates used in MFCs and MECs are reviewed in greater detail in “Substrates Used for Microbial Fuel Cells (MFCs) and Microbial Electrolysis Cells (MECs)” section 2.13), converting it into products like lactic acid or acetate which requires more energy than respiration (a process where the chemical energy of organic molecules is released in a series of metabolic steps involving the consumption of oxygen and the liberation of carbon dioxide and water (Logan, 2008)). Anaerobic glycolysis is responsible for hydrogen production in hydrogen fermentation (Cheng and Liu, 2011) and is the first step for electricity production in microbial fuel cells (MFC) operated on glucose (Catal et al., 2008).

There is no name for the pathways for fatty acid oxidation process in anaerobic bacteria, which produces electrons when acetate is converted into carbonate. In electrochemically active bacteria, in anaerobic environment, these electrons are not used directly for energy generation but to create the proton gradients across the cell membranes to re-generate electron carrier molecules, such as adenosine triphosphate (ATP).

In order to transfer electrons to exogenous (outside the cell) electron acceptor *Geobacter* species have conductive pilli (nanowires) (Reguera et al., 2005), *Pseudomonas aeruginosa* species produce exógenos electron carrier phenazine (Venkataraman et al., 2010) and *Escherichia coli* can use a artificial electron acceptor such as neutral red (Park et al., 1999, Park and Zeikus, 1999). Electrochemically active bacteria may also use methanogenic bacteria as electron acceptors (Reguera et al., 2005, Gorby et al., 2008). It has been observed that *Pelotomaculum* species produced conductive pilli like appendages connecting them to methanogens, more specifically *M. thermoautotrophicus* (Gorby et al., 2006).

Shewanella species, which have electron conductive pilli (Inman, 2006) and *E. Coli*, capable of utilizing exogenous electron carriers are often used in microbial fuel cells (MFCs) to produce electricity. *Geobacter* species are used in microbial electrolysis cells (MECs) to create the proton gradients across the cell membranes to generate hydrogen (Call et al., 2009b). A lot of information has been obtained on *Shewanella* and *Geobacter* species and mechanisms used to generate electricity from organic substrate (Dollhopf et al., 2000, Logan, 2008), and their genetic sequence (Heidelberg et al., 2002, Methe et al., 2003). The full diversity of bacteria capable of generating electricity however is just beginning to be discovered.

While most of the electrochemically active bacteria has been reported to be Gram-negative, such as *Geobacter* and *Shewanella* species, some Gram-positive bacteria such as *Micrococcus luteus*, *Bacillus subtilis*, and *Staphylococcus carnosus were* also shown to perform direct electron transfer (Berge et al., 2010, Delia et al., 2010) in micro scale microbial fuel cell (MFC) which were focused on proving that the bacteria were capable of electron transport. Gram-positive bacteria however have not yet been used in large scale bio electrochemical systems (BES) with aim to produce electricity or hydrogen.

Electrochemically active bacteria have great importance in natural environment, principally in metal oxidation, reduction and associated effects of mineral dissolution, the carbon cycle and sorption of phosphorus and heavy metals. These microorganisms could have great potential for organic waste treatment combined with energy production (Margesin and Schinner, 2001, Logan, 2008) and also in the removal of inorganic waste such as heavy metals (Lee and Kim, 2010) and radioactive materials (Pedersen, 2002). Electrochemically active bacteria are relatively easy to obtain because rich sources of these microorganisms are wastewaters, anaerobically digested sludge and sediments. Often mixed cultures are used in microbial electrolysis fuel cells (MFCs) and microbial electrolysis cells (MECs). This means that there are a large number of bacteria that are not electrochemically active in the community. Robust rapid selection methods have been recently developed for exoelectrogens (Wang et al., 2010b).

2.8 Electron Transport Mechanisms in Electrogenic Bacteria

Electrogenic bacteria are known to use two electron transfer mechanisms: shuttling via self produced mediators, as produced by *Pseudomonas aeruginosa* produces phenazine-1-carboxamide (Sell et al., 1989, Rabaey et al., 2005a) or electrically conductive pilli "nanowires" as produced by *Geobacter* and *Shewanella* species (Reguera et al., 2005, Gorby, 2006, Gorby, 2007). Although both species are capable of producing "nanowires", gene deletion studies have shown that *Shewanella* species are also capable or shuttling via self produced mediators *Geobacter* species however, could only transfer electricity through pilli, as shown by Gorby et al (2006).

2.8.1 Use of Endogenous and Exogenous Electron Carriers for Indirect (Mediated) Electron Transport in Electrogenic Bacteria

Shuttling or mediated electron transport usually involves a molecule accepting electrons from the bacteria and releasing these electrons to the anode. The electrode potential (E), for the mediator molecule, has to be higher than that of substrate oxidation but lower than E of the reaction occurring on the cathode surface. These chemicals could be exogenous (not produced by the cell) such as rezazurin (Sund et al., 2007), or endogenous compounds produced by the bacteria. *Pseudomonas aeruginosa*, for example, can produce endogenous mediators, such as phenazine. Studies on endogenous electron mediators were done to identify genes responsible for electron transport mechanisms and electron mediator production (Venkataraman et al., 2010). This study investigated the effect of deletion of various genes from bacterial DNA on the electron mediator (phenazine) until the genes responsible for phenazine production were identified. Studies on the effect of endogenous electron mediators have only been performed on laboratory scale (Cusick et al., 2011, Escapa et al., 2012, Heidrich et al., 2013).

Artificial electron mediators facilitate electricity production by yeast and bacteria such as *E. coli* (Wang et al., 2010c) which are unable to use the electrode directly and therefore produce low voltages and power densities (Bond and Lovley, 2003). The desirable characteristics for an artificial electron mediator are (i) capability to penetrate or attach itself to the receptors on cytoplasm membrane in prokaryotic bacteria; (ii) capability of accepting electrons from the cell and discharging these electron on the anode, (iii) high solubility and stability and finally (iv) low toxicity to microorganisms and environment (Bon et al., 2007) (Das et al., 2008, Wang et al., 2010c).

Large variety of chemicals has been determined to facilitate electron transport from the bacteria to anode; exogenous mediators such as neutral red (NR) (Park et al., 1999, Park and Zeikus, 1999), thiamin (Choi et al., 2003, Lithgow et al., 1986), potassium ferricyanide (Mohan et al., 2009, Logan, 2008), ubiquinone (Rajalakshmi et al., 2010), methyl viologen (MV) (Logan et al., 2006, Das et al., 2008), methylene blue (MB) (Das and Mohan, 2009, Daniel et al., 2009, Wang et al., 2010c), and naturally produced chemicals by bacteria (endogenous mediator) such as phenazine (Rabaey et al., 2005a) have been documented. Methylene blue (MB) has been used in MFC research as well as a mediator in bioelectrochemical systems because it is cheap, low toxicity and soluble in bacterial media than other chemicals (Guilherme et al., 2003).

2.8.2 Direct (Mediatorless) Electron Transport in Electrogenic Bacteria

Direct electron transport involves electron transfer to electron acceptor through conductive pilli. Gorby and coworkers were the first to report conductive pilli in *Geobacter*, which were termed as nanowires (Gorby et al., 2006). The conductivity of these nanowires was examined via conductive scanning tunneling electron microscopy (STM). In nature electrically conductive pilli enable *Geobacter* species to transport electrons to archaea, which use these electrons to produce methane and act as electrons acceptors for electrochemically active bacteria. The electron transport for *Geobacter* species has been studied as a model to understand enzymatically catalyzed reactions (Reguera et al., 2005) and electron transport chains that enable *Geobacter* species to transport electrons to outside of their cell walls (Mehta et al., 2005). *G. Sulfurreducens* is the organism of choice for research since its complete genetic sequence is now available (Heidelberg et al., 2002, Methe et al., 2003). Similar “nanowires” were observed in *Shewanella* species (Inman, 2006). *Shewanella putrefaciens* IR-1, for example, was shown to achieve high Fe(III)-reduction activity without addition of exogenous mediators (Hyun et al., 1999). Several other strains of *Shewanella* species were shown to be electrochemically active (Park et al., 2001, Pham et al., 2003, Chaudhuri and Lovley, 2003).

Electron transport chains in processes linked to anaerobic glycolysis (a process that allows bacteria to produce energy by substrate oxidation in anaerobic environment) have been extensively studied (Brooijmans et al., 2009, Fuller et al., 2014). An electron transport chain (ETC) couples electron transfer between an electron donor (such as NADH or Cytochrome *b*) and an electron acceptor with the transfer of H^+ ions (protons) across a membrane. The resulting electrochemical proton gradient is used to generate chemical energy in the form of adenosine triphosphate (ATP). Other processes linked to electricity production by electrochemically active bacteria such as dissimulatory metal reduction have also been studied (Lovley, 1993).

Dissimulatory metal reduction is a process that is utilized by microbes to conserve energy through oxidizing organic or inorganic electron donors (metal ions) and reducing a metal or metalloid (Lovley et al., 1991). Fe (III) ions in the outer membrane is linked to production of energy carrier, adenosine triphosphate (ATP) and endogenous electron carrier Cytochrome *b*. Generation of ATP using cytochrome-linked to anaerobic electron transport in *Propionibacterium freudenreichii* was investigated as early as 1972 (Devries et al., 1973) and compared to electron acceptors other than Fe (III) (Kieft et al., 1999). The study determined that enzyme Cytochrome *b*, was therefore involved in the anaerobic electron transport from glycerol-1-phosphate to fumarate (reaction observed in anaerobic glycolysis).

It has been shown that c-type cytochrome acts as endogenous electron carrier from acetate oxidation to Fe (III) inside the outer membrane of *Geobacter sulfurreducens* (Seeliger et al., 1998, Lloyd et al., 1999). Understanding these processes and genes responsible makes it possible to improve selection procedures for selection of electrochemically active bacteria (Liu et al., 2008) and the genetic engineering of bacteria incapable of producing electricity, such as *E. coli* (Yong et al., 2013).

Chemical reactions responsible for electricity production in bacteria capable of direct electron transport such as *Geobacter* species may also be linked to production of exogenous electron mediators. It was also proposed that *G. sulfurreducens* releases *c*-type cytochrome, as the extracellular shuttle, into the extracellular environment in order to promote the reduction of insoluble Fe (III) oxide (Lloyd et al., 2003). More recently an in vivo method to detect the orientation of c type cytochromes of outer membrane cytochromes via analysis of electron transfer reactions between these enzymes in *S. odeniensis* (Gescher et al., 2010) and role of periplasmic triheme *c*-type cytochromes of PpcA family in electron transfer (Dantas et al., 2013).

2.9 Applications of Electrically Active Bacteria in Microbial Fuel Cell (MFC) and Microbial Electrolysis Cell (MEC) Technology

The use of bacteria capable of direct electron transfer is particularly effective in microbial fuel cells (MFCs), since it saves the cost of replacing electron mediators in the electrolyte solution. A simple fuel cell device capable of harnessing low-level power for long periods of time could be built from cheap materials, excluding the cathode. Examples of such devices are sediment MFCs, which consist of an anode electrode embedded in anaerobic sediment and a cathode electrode suspended in aerobic water column above the anode electrode and can be built from cheap materials (Reimers et al., 2001).

An ion exchange membrane is not necessary in sediment MFCs, because the decreasing oxygen gradient over the depth of water and sediment columns creates the necessary potential difference naturally (Angenent et al., 2007). This however does not mean that mediators are completely redundant. A carbon cloth anode with permanently immobilized mediator can be used in continuous flow microbial fuel cells (MFCs) to improve carbon cloth anode conductivity. Studies involving small scale MFC designs with immobilized neutral red (NR) showed 1000 fold increase in power density for *Shewanella putrefaciens*, although also capable of direct electron transport (Park and Zeikus, 2002). It has also been reported that bacterial nanowire could facilitate the electron transfer to the solid Fe (III) in the electron acceptor deficient conditions (Loveley et al., 2004, Lovley, 1997, Childers et al., 2002, Lovley et al., 2002), which may allow to use wastewater without electrolyte added to it to increase its conductivity (Xu et al., 2013). This is important for removal of contaminant heavy metals in soils and wastewaters (Aralp et al., 2001, Lee and Kim, 2010, Sekomo et al., 2012). Fe (III) reducing bacteria were shown to be the most useful in the removal organic contaminants from wastewaters, due to their ability to degrade a wide variety of organic materials (Loveley et al., 2004, Lovley, 1997, Childers et al., 2002, Lovley et al., 2002).

2.10 Electrochemically Active Anodic Biofilm Overview

2.10.1 Microbial Groups within Mixed Electrogenic Biofilm

The term biofilm refers to bacteria growing in the anode chamber of microbial fuel cell (MFC) or microbial electrolysis cell (MEC) capable of converting fermentable substrates carbohydrates, lipids or non fermentable substrates (volatile fatty acids) into electricity (Lee et al., 2008, de Carcer et al., 2011). Microorganisms can be viewed as existing in planktonic for (i.e. they are floating free in solution) or sessile (attached to the surface) states (Davey and O'Toole G, 2000). The development of enriched electrochemically active biofilms has successfully demonstrated a capacity to remove organic compounds whilst also being able to generate electricity. More complex and fermentable substrates were shown to produce different and more complex microbial profiles (Lee et al., 2003). It has been further observed that loosely associated bacterial clumps within the anode biofilm can form when MFCs are fed with fermentable substrate. DNA analysis via denaturing gel electrophoresis (DGGE), (where chemicals are used to denature DNA as it moves across an acrylamide gel) has shown that these clumps consist of community profiles distinct from the main body of the anode biofilm (described in “Offline Analysis Methods” section 4.8 in greater detail). It has been suggested that the clumps functionally act to ferment complex electron donors to produce volatile fatty acids that can be utilized by the electrochemically active bacteria (EAB) in the anode biofilm, and so facilitate the donation of electrons to the electrode (Kim et al., 2004).

The view that fermentative processes are not competing with anodophiles but facilitating an energetically favorable syntrophic association was examined by looking at electron fluxes associated with glucose conversion pathways. It was found that the majority of glucose is first converted to hydrogen and acetate but electron flow to the anode could be lost to other electron sinks such as:- bacteria in mixed microbial culture which are not chemically active (Logan et al., 2008), residual organic acids (Lee et al., 2008) and methanogenesis (methane production by archaea) (Freguia et al., 2008).

2.10.2 Biofilm Development on the Anode Surface

The process of bacterial biofilm attachment to the carbon anode surface can bring physiological and genetic changes in the biofilm (Shen et al., 2013) and is the most preferential form of growth (Zobell, 1943). A key feature of all biofilms is the production exopolymeric substances (EPS), which facilitates bacteria to form muticellular structures which provide protection from many environmental stresses, such as:- temperature; pH changes (Yuan et al., 2011); antibiotics (Wen et al., 2011) and other nitrogenous heterocyclic compounds (Hu et al., 2011) found in wastewater in the form of sulfa drugs, disinfectants; high shear rates (Shen et al., 2013); low nutrient stress (Modin and Wilen, 2012) and drying (Ahn et al., 2014). The development of biofilm depends on constituent microbial species and different environmental conditions and can be broken down into 3 stages (Matos and Lopes da Silva, 2013).

i) Prior to the attachment of microorganisms, the anode surface is conditioned due to the adsorption of macromolecules such as proteins, polysaccharides, glycoproteins and humic acids. This was demonstrated by an investigation into the kinetics of conditioning biofilm layer formation on stainless steel sheets immersed in seawater (Compère et al., 2001). The initial adhesion of bacteria to the surface is driven by short range Van der Waal forces and facilitated through expression of specific adhesion receptors, such as hair like appendages found on the surface of many bacteria referred to as pilli and fimbriae (Busscher et al., 1992). The expression and presence of these adhesion receptors in different bacterial groups dictates the bacterial colonization process. Bacteria that can undergo direct electron transfer (members of *Geobacteriaceae* family) produce these pilli appendages and are known to produce high power densities.

ii) Once a biofilm is established, it may then continue to colonize a surface through a number of mechanisms such as bacterial motility, binary division of microbial cells and the possible adsorption of cells into the biofilm from the planktonic phase. The way these mechanisms develop and how they are controlled determines the biofilm structure during this stage of development.

iii) The final step is irreversible bacterial attachment, where bacterial cells develop into a mature electro-facilitating biofilm is the production of extracellular polymeric substances (EPS). This matrix is made up of proteins, DNA from dead bacteria and polysaccharides, which can all act to maintain the structural and organizational components of the biofilm (Hall-Stoodley et al., 2004).

The matrix composition and rates of EPS production will thus determine how much current is produced by the mature biofilm; this again depends on the types of microbial species present and environmental factors such as pH and temperature. Other mechanisms apart from exocellular matrices can conduct electricity produced by electrochemically active bacteria. Conductive reticular / extra-cellular activity is also possible through syntropic direct electron transfer between members of the biofilm consortium (Summers et al., 2010). The connection between the overall conductivity of the biofilm matrix and the ability of the anode respiring bacteria to produce high current densities was established as being of critical importance in MFC systems (Torres et al., 2010) and follows work that has established links between anode biofilm development and MFC performance (Ramasamy et al., 2008). To achieve maximum current density, for MFC or MEC with electrochemically active biofilms, non conductive EPS matrix bacteria should be in direct electrical contact with the solid electrode to enable efficient electron transfer, preferably as a cellular monolayer. Most anodic biofilms are complex 3-dimensional structures of >50 μm thickness and can take up to 6 months to form (Reguera et al., 2006). This has been demonstrated by real-time imaging of anode biofilms which show that the most active cellular respiration is associated with microorganisms in close proximity to the anode interface (Franks et al., 2009). However, the generation of high current densities requires deeper electrogenic biofilm development that would require respiratory activity to be undertaken via more remote electron transfer mechanisms to the anode. It could be suggested that in the near future the research will focus on engineering biofilms containing bacteria capable of both direct (to the anode surface via conductive pilli) and indirect (from outer layers to inner biofilm layers via self produced mediators) electron transfer.

In order for microorganisms to act as effective biocatalysts in microbial fuel cells (MFCs) and microbial electrolysis cells (MECs) it is necessary to use a conductive anode electrode as the terminal electron acceptor to drive cellular catabolism. A material of choice is either carbon cloth or carbon mesh as poor attachment of bacteria to metals is reported (Dumas et al., 2007). Various methods have been used to improve carbon anode conductivities ranging from immobilizing mediators (Park et al., 2000) to treatment with metal particles (Lowy et al., 2006, Lowy and Tender, 2008), described in “Comparison of Different Microbial Fuel Cell (MFC) and Microbial Electrolysis Cell (MEC) Designs” section 2.14 in greater detail.

2.11 Advantages of a Diverse Mixed Culture Biofilm

Many different species of bacteria have been shown to be electrochemically active, reports generally concur that pure culture microbial fuel cells (MFCs) produce less power than mixed culture systems (Logan, 2009). For comparison purposes for a MFC with mixed culture grown from wastewater produces the peak power density P_{max}=766 mW m^{-2} (Cheng et al., 2006b) compared to P_{max}=77 mW m^{-2}, for pure *Pseudomonas aerginosa* (Rabaey et al., 2005a) and P_{max}=13 mW m^{-2}, for pure *Geobacter sulfureducens* (Bond and Lovley, 2003). There are however exceptions because higher power densities have been reported using pure cultures, experiments have been carried out under specific conditions i.e. using *G. sulfurreductans* an MFC that used a ferricyanide catholyte and a cathode surface area eight times larger than that of the anode produced more power using a pure culture (1.9 W m^{-2}) compared with a mixed culture (1.6 W m^{-2}) (Nevin et al., 2008). If however these conditions, such as pH and temperature are not kept exactly the same mixed microbial cultures perform better and changes in pH and temperature are likely to fluctuate if the process is to be scaled up. This would seem to indicate that electrogenic biofilms are able to utilize and structure the networks of biofilm electron transfer mechanisms (previously described in "Electron Transport Mechanisms" section 2.8) to produce these higher power densities, this has been shown to be achieved through the reduction in the internal resistance in mixed culture biofilms (Watson and Logan, 2010).

However even more important to the successful operation of MFCs and MECs is the capacity to breakdown complex substrates (i.e. food waste materials in water) containing lipids, carbohydrates and proteins converted into volatile fatty acids (VFAs) by one species of bacteria and VFAs converted into CO_2 and water by another. This was demonstrated, in MFCs, by LaPara et al (2002) who subjected a wastewater community to decreasing nutrient concentrations. This resulted in maintenance of functionality but it was found that redundant populations were eliminated. Decreasing microbial diversity is also linked to a decreased community stability and functional resilience to perturbation events (Girvan et al., 2005). Comparison studies between pure and mixed cultures were performed for MECs (Call et al., 2009b) and no new publications to the knowledge of the author have been published since then. That study compared hydrogen production rates for pure hydrogen utilizing exoelectrogenic bacterium (*Geobacter sulfurreducens*) to both a nonhydrogen oxidizer (*Geobacter metallireducens*) and a mixed microbial consortium. At an applied voltage of 0.7 V, both *G. sulfurreducens* and the mixed culture generated similar current densities (ca. 160 A m^{-3}), resulting in hydrogen production rates of ca. 1.9 m^{-3} H_2 m^{-3} day^{-1}, whereas *G. metallireducens* exhibited lower current densities and hydrogen production rates of 110±7 A m^{-3} and 1.3±0.1 m^{-3} H_2 m^{-3} day^{-1}, respectively.

The MEC with the mixed consortium achieved the highest overall energy recovery (energy produced from the biomass relative to both electricity and substrate energy inputs) of 82±8 % compared to *G. sulfurreducens* (77±2 %) and *G. metallireducens* (78±5 %). When the voltage applied was decreased to 0.4V, methane production from the mixed culture increased from 1.87 cm^3 to 6 cm^3 (calculated from methane percentages and total gas volumes produced). However the actual amount of energy recovery from produced methane decreased to 38±16 % compared to 80±5 % for *G. sulfurreducens* and 76±0 % for *G. metallireducens*. Previous studies also support these findings and also suggests that mixed bacterial consortium produces more hydrogen and allows higher energy recovery than pure culture but methanogenesis (methane production from hydrogen by archaea in mixed consortium) can also develop causing hydrogen production to decrease (Zhang et al., 2012b). Voltages above 0.7 V are possibly inhibitory to archaea, which explains low methane production at voltages of 0.7-0.9 V (Van Eerten-Jansen et al., 2013).

2.12 Effect of Environmental Conditions on Electrogenic Activity in Biofilms

Operational environmental conditions such as substrate type (eg: acetate, butyrate or glucose), substrate concentration, temperature, pH, anode architecture, buffering capacity/conductivity and flow rate will all effect anodic / MFC or MEC performance (Feng et al., 2008) and the potential power densities achievable from the MFCs. This is directly related to the anode (Eq 5 and Eq 14) and cathode electrode potentials (Eq 8 and Eq 19) and subject to parameters set by the Nernst Equation (Eq 1) (Thauer et al., 1977) and overpotentials (discussed in "Performance Inhibitors in Microbial Fuel Cells (MFCs) and Microbial Electrolysis Cells (MECs)", section 2.16), which also have a direct effect on the internal resistance. Even though each of these factors will have a direct influence on the electrochemically active biofilm activity and all parameters may also exhibit a degree of operational interdependency.

2.12.1 Operation of Microbial Fuel Cell (MFCs) and Microbial Electrolysis Cells (MECs) at Thermophilic, Mesophilic and Psychrophilic Conditions

The effects of temperature on MFC operation have been previously reported to have a direct effect on electrochemical processes (Moon et al., 2006) and hydrogen production in MEC (Omidi and Sathasivan, 2013). This can be directly observed when MFC reactors are run at ambient temperatures where cell voltages have been reported to cycle up and down with the temperature fluctuations (Ahn and Logan, 2010, Kim et al., 2010). The system constraints usually considered are cathode and / or anode size and distance between the anode and the cathode that will directly affect MFC operation.

Other, not so obvious factors that also have to be considered are how electrode configurations in MFCs influence voltage production and power generation through the conversion of electrons in biomass to electricity. The percentage recovery of electrons, termed as the coulombic efficiency (CE), can often achieve levels of 70 %, for MFC systems, when non fermentable substrates such as acetate, butyrate or propionate are used (Kim et al., 2009a, Liu et al., 2005b). Low CEs reflect the activity of alternative electron sinks such as those used in archaea (converting metabolic energy obtained from acetate oxidation and/or hydrogen into methane) and bacteria that do not produce electricity, competing for substrate with electrochemically active bacteria and non-electrogenic metabolic pathways being utilized by electrochemically active bacteria on the anode biofilm and in planktonic microbial populations (Lee et al., 2008). Since conventional anaerobic digestion (AD) does not optimally operate at psychrophilic temperatures (15 ± 5 ^{o}C), if MFC or MEC is used as a part of hydrogen fermentation – either as part of MFC or MEC 2 stage system psychrophilic conditions are likely to be used to decrease losses via archaeal methanogenesis which is limited at psychrophilic temperatures.

When AD systems are subjected to sub-mesophilic conditions methanogenic AD efficiency/activity typically decreases with the resultant elevated production of volatile fatty acids (VFAs); however it has been demonstrated that AD systems may also be adapted to operate at both high temperatures and low temperatures through long-term reactor acclimatization (McHugh et al., 2006). MFCs and MECs have also been shown to operate and produce electricity over a range of thermophilic (55 ± 10 ^{o}C), mesophilic (30 ± 15 ^{o}C) and psychrophilic (≤15 ^{o}C) operating conditions (Cusick et al., 2010, Logan et al., 2011, Jadhav and Ghangrekar, 2009). A similar experiment to the experiment designed by Jadhav and Ghangrekar (2009) investigated performance of single chamber MFCs in greater detail at operational temperatures 10 °C, 20 °C and 35 °C was performed by Michie et al (2011).

i) Operation in MFCs and MECs at Thermophilic Conditions

As in AD systems MFC operation at thermophilic temperatures can provide advantages in terms of increased rates of enzymatic activity and pathogen removal when compared with lower temperature systems (Suryawanshi et al., 2010). A few studies have looked at high temperature MFC operation and demonstrated that MFCs can be operated effectively at temperatures of 45 - 60 ^{o}C with power densities of 375 mW m^{-2} (Jong et al., 2006, Carver et al., 2011) but MFC design was seen to be a potential issue due the increased rates of evaporation at higher operational temperatures. It was determined that 50% predominance of *Firmicutes thermicola* strains occurred in thermophilic current producing MFCs (Wrighton et al., 2008), which were reported to be responsible for electricity production at thermophilic conditions.

The advantages of increased enzymatic activity at thermophilic temperatures also apply to MECs. A study on hydrogen production in thermophilic environments showed that hydrogen production rates of 0.63 m^3 H_2 m^{-3} was observed at currents of 1.1 A m^{-2} when a biocathode in electrolyte containing acetate as substrate (Croese et al., 2011). The bacterial population consisted of 46 % *Proteobacteria*, 25 % *Firmicutes*, 17 % *Bacteroidetes*, and 12 % various mesophilic phyla unlikely to survive in thermophilic conditions for prolonged time periods. The high effiencies of substrate converted into electricity (coulombic efficiencies, CEs), calculated from current in the reactors, for both MFCs and MECs (from 85 % to 97 %) (Marshall and May, 2009, Croese et al., 2011) would seem to suggest that there was little alternative metabolic competition for electrons in these communities at thermophilic conditions. The only problem with this approach would be the amount of energy needed to be used to heat the reactors (Lubken et al., 2007).

ii) Operation of in MFCs and MECs at Mesophilic and Psychrophilic Conditions

A number of studies have looked at low strength wastewater treatment at ambient and mesophilic temperatures (21 - 35 ^oC), but since most waste treatment systems in temperate climates work and discharge effluents at temperatures lower than this (10 - 20 ^oC) these processes would still require a significant input of energy as heat, but not as much as thermophilic systems (Lettinga et al., 2001). More recently the performances of two double-chamber microbial fuel cells (MFCs) were examined at 25 °C and 15 °C (Liu et al., 2013b) and performance of single chamber MFCs at operational temperatures 10 °C, 20 °C and 35 °C was compared (Michie et al., 2011). Sediment MFCs, for example, were been for in situ operation in marine sediments at room temperature (22 ± 1 °C). They are able to generate electricity from anaerobic anode respiring bacteria, which grow within the sediment. Microorganisms of the family *Geobacteraceae* have been isolated from electrodes in marine sediment fuel cells (Bond et al., 2002). This family of bacteria are also commonly found in mesophilic MFC and MEC anodic biofilms (Logan and Regan, 2006), where *Geobacter* species have often been identified as the dominant electrochemically active bacteria. Two psychrotolerant *Geobacteraceae* strains (A1 (T) and A2) grow over a range of 4 °C to 30 °C have also been isolated from these types of sediment MFCs (Holmes et al., 2004), however adaptation and change of the ARB communities derived from mixed culture biofilms at different temperatures has not been studied in detail. A similar approach could be used to build scaled up MECs with sediment anode submerged in large container with cathode chamber and cathode placed above it (Guo et al., 2010).

The capacity to run MFC and MEC reactors at temperatures of 10-20 ^{o}C reduces the operating costs by eliminating the power input needed for heating. At psychrophilic conditions there is a real potential for MFCs and MECs to be an economically viable alternative to conventional aerobic processes in temperate sewage treatment operations. Psychrophiles, that only grow at temperatures below 10 ^{o}C, and psychrotolerant bacteria, that can grow at less than 20 ^{o}C but have optimal growth temperatures of greater than 20 ^{o}C, have both been found in a wide variety of natural and processed environments e.g. wastewater, soil and sediment (Morita, 1975). In these habitats cold adapted biofilm communities can consist of a diverse range of archival and bacterial populations and this observed variability might also include transitions between different thermal types. Indeed it has been found that bacteria isolated from cold boreal ground waters (4 ^{o}C) may be predominantly psychrotolerant (Mannisto and Puhakka, 2002). This suggests there is an inherent adaptability of cold tolerant microorganisms to mesophilic environments and a capacity for growth over a wide temperature range.

2.12.2 pH Effects on MFC and MEC Operation

pH is another important parameter in the operation of MFC and MEC reactors, as the chemical formation and movement of protons from the anode to the cathode is integral to system operation. The Nernst Equation (Eq 1) shows that each pH unit change across a cell membrane represent a potential loss (overpotential) of 60mV through the development of high anodic equilibrium potentials (Rozendal et al., 2006a). In dual chamber MFC and MEC systems He et al (2008) found that reducing the anode chamber to pH 5 also reduced the current density 10-fold. The pH gradient losses are discussed in “Performance Inhibitors in Microbial Fuel Cell (MFCs) and Microbial Electrolysis Cells (MECs)“, section 2.16 in greater detail. Anodic pH particularly important because it can rapidly drop due to the formation of acidic products by fermentative metabolism, but it has also been reported that even if low pH values cause a reduction in power production, this power can again recover if the pH is again re-adjusted to 7 (Ren et al., 2007). The optimal operational pH level in an air cathode MFC system was found to be pH 6.5 by (Jadhav and Ghangrekar, 2009), and when MFC anodes were run for a period of time at pHs 4, 5, 6 and 7 in dual chamber MFCs (Zhang et al., 2011a) reported that operation at pH 6 only reduced by maximum power density (P_{max}) by 0 %, and voltage production 8 % and pH 5 reduced (P_{max}) by 32 % and voltage by 16 %. pH can also have a direct effect on the respiratory activity of electrochemically active biofilm and it has been demonstrated that this can be a particular concern in anodic biofilms where the build-up of protons due to mass transfer limitations can lead to significant localized drops in pH close to the electrode (Torres et al., 2008). It was shown that bacteria such as *Shewanella* species can be acclimated to operation at pH levels as low as 5 (Biffinger et al., 2008).

2.13 Substrates used in Microbial Fuel Cells (MFCs) and Microbial Electrolysis Cells (MECs)

The most commonly used substrates are acetate (Kim et al., 2009b, Liu et al., 2005b), glucose (Logan et al., 2009b, Kim et al., 2010), lactate (Ringeisen et al., 2006) and cellulose from non woody plants (Logan et al., 2009b). Acetate, in particular, has produced the highest reported voltages in MFCs (Logan et al., 2006). Electricity could also be produced from other components found in wastewater such as antibiotics eg:- penicillin – glucose mixtures where used as substrate (Wen et al., 2011). Wen's study reported a maximum power density P_{max}, (see "Electrochemical Analysis Methods", section 4.7 for details and calculations for P_{max}) for 1 g L^{-1} glucose + 50 mg L^{-1} penicillin (101.2 Wm^{-3}) was 6-fold higher than the sum of that for 1 g L^{-1} glucose (14.7 W m^{-3}) and 50 mg L^{-1} penicillin (2.1 W m^{-3}) as the sole substrate.

The maximum current density with 50 mg L^{-1} penicillin (10.73 A m^{-2}) was 3.5-fold greater if compared to that without penicillin (3.03 A m^{-2}). MFCs are capable of converting a wide variety of organic wastes other than fatty acids (Pant et al., 2010) ranging from benzene (Wu et al., 2013a), xylose (Catal et al., 2008) and other humic acids (Huang and Angelidaki, 2008), starch (Niessen et al., 2004b) to industrial azo dyes (Li et al., 2010b) (see Table A-1.1 in "Appendix A1" section 9.1).

Carbon dioxide is the carbon source for photosynthetic algae, such as *Chlorella vulgaris* (Feng et al., 2010a). A photosynthetic MFC produced a voltage output of 610±50 mV, at 1000 Ω resistance and maximum power densities increased from 4.1 W m^{-3} to 5.6 W m^{-3}, see Table A-1.1 in "Appendix A-1" section 9.1.

Acetate is most common substrate for MECs (Table A-1.2 in "Appendix A-1" section 9.1) Acetate and butyrate mixtures are the most common waste products of hydrogen production via dark carbohydrate fermentation (Hawkes et al., 2007, Jung et al., 2011) and therefore MECs can be used to treat hydrogen fermentation effluent. Acetate also has the highest power densities reported in MFCs (Logan, 2008) and the highest reported amounts of hydrogen produced in MECs compared to other substrates (Cheng and Logan, 2007a). Other VFAs, such as butyrate and propionate and carbohydrates, cellulose, sucrose and glucose have been used as substrates in MECs as well, with hydrogen yields of up to 8 mol of hydrogen per mol of butyrate being reported (Cheng and Logan, 2007a).

2.14 Comparison of Different Microbial Fuel Cell (MFC) and Microbial Electrolysis Cell (MEC) Designs

An ideal microbial fuel cell (MFC) must produce current while sustaining a steady voltage and an ideal microbial electrolysis cell (MEC) must have stable hydrogen production as long as the substrate and voltage is supplied. Some limitations with MFC or MEC performance arise from the design (cathode and anode surface areas) or charge transport through the electrolyte solution in the anode chamber (see "Performance Inhibitors in Microbial Fuel Cells (MFCs) and Microbial Electrolysis Cells (MECs)" section 2.16 for details) and/or the choice of electron acceptor at the cathode. In order to understand the design limitations it is important to understand how the anode and cathode work, and what improvements have to be made in order to engineer practical systems for bioenergy production at larger scales. Ideally these improvements should decrease the cost of production whilst increasing the performance of the reactor. Tables A-2.1-A-2.7 in "Appendix A-2" section 9.2 show that more research has been put into improving the anodes and cathodes used in MFCs rather than specifically in MECs.

2.14.1 Comparison of Different Anode and Cathode Designs for Microbial Fuel Cells (MFCs)

i) Introduction Comparison of Different Anode Designs for MFCs

In an MFC, the anode acts as an artificial, external electron acceptor for the microorganisms thus most improvements are focused on making the anode surface more conductive (Park and Zeikus, 2002) and increasing the anode surface area (Rabaey et al., 2005b). The most important performance indicators for MFCs are voltage, the relationship between the current produced by MFC and percentage of substrate removed by the bacteria (i.e. coulombic efficiency or CE) and the maximum power produced by the reactor. The power is typically calculated per unit area or unit volume of the anode or cathode (in W m^{-2} and in W m^{-3}, see "Electrochemical Analysis Methods" section 4.7 for details and calculations) and the highest value is referred to as the maximum power density (P_{max}). However other factors that may have an influence of MFC performance, such as the methodology used to prepare growth media for the bacteria, microbial culture and substrates, all of which may vary between different research groups. Ideally the designs have to be explicitly described and a benchmark design and microbial culture for MFC or MEC has to be used to be able to compare all modifications to anodes and/or cathodes.

Most MFC studies have been limited to the laboratory scale mainly because of their low power densities when applied in larger scale deployment. Higher power densities, such as 68.4 W m^{-3} (compared to cathodic wet volume) were reported for smaller MFCs with 40 cm^3 or smaller anode chambers (You et al., 2009), but as the size of the device is increased there will be loss in the performance due to charge transport losses in larger electrolyte volumes. Described in "Performance Inhibitors in Microbial Fuel Cells (MFCs) and Microbial Electrolysis Cells (MECs)" section 2.16 in greater detail. The highest maximum power density (P_{max}) 1010 W m^{-3} was reported in the literature for an MFC with air cathode compared to the anode chamber size at a current density of 0.9 mA cm^{-2} was obtained (Fan et al., 2007) for MFC with ≈ 12 cm^3 anode chamber. An two chamber MFC containing ferricyanide as an electron acceptor instead of oxygen can produce a maximum power density up to 500 W m^{-3} (anode chamber vol. 1.18 cm^3) on micro scale with *Shewanella oneidensis* DSP10 in a growth medium with lactate (Ringeisen et al., 2006). One of the highest voltages reported for MFC was an open circuit potential (OCP) 1.05±0.05 V, for MFC with anode modified with Fe/ferric oxide, compared to OCP values usually observed in literature, within the range of 0.70±0.05 V (Fu et al., 2014). This design achieved maximum power density (P_{max}) 7.4 × 10^{-2} mW cm^{-2} compared to anode (4 cm × 4 cm × 2 cm) in tubular MFC with 3L anode chamber (17.4-fold higher than that of the plain graphite, for tubular MFC with granular graphite anode.

A larger version of this MFC design was built in 2008 (Rabaey et al., 2005b, Logan, 2010). It has a volume of approximately 1 m^3 and consists of 12 modules. Carbon fiber anodes and cathodes are used, based on a brush design. In a second phase, 12 additional modules with varying designs will be constructed. A more recent study reported maximum power density of 23.8 W m^{-3} was observed between 25±2 ^oC (Zhu et al., 2013) for single chamber MFC with 1 L anode chamber volume. This reactor has an advantage because it does not have a cathode soaked in potassium ferricyanide which has to be replaced (Logan, 2008, Rabaey et al., 2005b) and was aimed towards removal of organics from wastewater than electricity generation. A higher power density of 90 W m^{-3}, was reported for a smaller "semi pilot scale" sized MFC with a single 560 cm^3 anode chamber (Table A-2.2 in "Appendix A-2" section 9.2) was where maximum power density was calculated per anode chamber unit volume (Rabaey et al., 2005b).

ii) Comparison of Different Anode Designs for MFCs

Porous carbon materials have the largest surface areas and, theoretically, can accommodate the most exoelectrogenic bacteria, but an MFC with graphite plate anode containing pure *Shewanella oneidensis* (MR – 1) has a reported power density of 1410 mW m^{-2} anode surface area (Dewan et al., 2008), compared to 893 mW m^{-2}, anode surface area, 45 W m^{-3} anode chamber volume, for MFC with carbon mesh anode containing a unidentified pre acclimated mixed bacteria culture from an active MFC, (Wang et al., 2009b). A lower power density of 27 W m^{-3} calculated on the volume of the anode chamber, or 661 W m^{-3} calculated, on the volume of anode material, was also reported for *Shewanella oneidensis* (MR – 1) for flexible nickel - graphene foam anodes (Wang et al., 2013).

Another option is to immobilize metal particles on the anode surface. An effective but costly, example of this is a MFC design containing Pd or Au nanoparticle treated graphite disk anode that produced 50-150 % or 20 fold increase in the current density, for MFC containing *Shewanella oneidensis* MR-1. Again the apparatus and most importantly microbial culture variation between different research groups making it difficult to compare MFC with either Pd or Au nanoparticle treated anodes. Relatively few researchers report on controlled comparisons (Lowy et al., 2006), for MFC (Table A-2.2 in "Appendix A-2" section 9.2), and (Cheng and Logan, 2007a), for MEC (Table A-2.5 in "Appendix A-2" section 9.2) thus making effective material comparative evaluations very difficult.

Compounds such as anthraquinone-2,6-disulfonate (AQDS) and 1,4-naphthoquinone (NQ) have been added to the liquid media solutions containing nutrients and carbon substrate and have resulted in an 0.7 and 0.5 fold increase in kinetic activity (Lowy et al., 2006). These electron mediators however were not immobilized and therefore could represent an environmental risk if used in a continuous flow scaled up reactor and discarded with wastewater. However if these mediators were bonded into the anode material higher power densities might be seen. The highest, 1000-fold increase in power density (P_{max}) mW, per anode surface area m^2 was observed for an MFC that incorporated electron mediators into graphite electrodes (Park and Zeikus, 2003). Three new electrodes containing bound electron mediators including a neutral red (NR), covalently linked to woven graphite cloth anode, Mn^{4+} graphite anode, both with Fe^{3+} solid graphite cathodes were developed. The maximum power densities (P_{max}) were 5.32 mW m^{-2} (NR treated graphite anode), 788 mW m^{-2} (Mn^{4+} treated graphite anode), 0.65 mW m^{-2} (woven graphite anode, control), with current densities following similar trend.

These results also imply that sewage sludge contain mixed culture with unique electrophilic microbes that transfer electrons the performance of which can be enhanced via immobilized mediators and that microbial fuel cells using the new NR or Mn^{4+} graphite anodes and Fe^{3+}- graphite cathodes may have commercial utility for producing low amounts electrical power whilst removing organic waste from wastewater. These experiments were performed on single chamber fuel cells composed of a rubber bunged bottle, a window-mounted cathode containing an internal, proton-permeable porcelain layer and an anode inserted at the centre by Park et al (1999). Another 10 fold increase in (P_{max}), from 1 to 9.1 mW m^{-2} (NR treated anode) and 10.2 mW m^{-2} (Mn^{4+} treated anode) was reported by the same authors for MFCs containing *Shewanella putrefaciens* culture (Park and Zeikus, 2002) with the same design as in later 2003 publication, see Table A-2.2 in "Appendix A-2" section 9.2.

From results in Tables A-2.1 and A-2.2 it's possible to make following conclusions:- dye treated anodes for MFCs produce the same improvement in MFC performance as metal particle treated anodes. However the use of dyes such as neutral red (organic electron carriers such as NR are dyes) is cheaper and therefore could be used for scaled up systems for industrial applications. However if dyes are ejected into wastewaters in large amounts, this represents a serious potential problem (Franke and Franke, 1999). Dyes in wastewater prevent sunlight from reaching deep into the water killing algae and depriving fish of oxygen (Wang et al., 2005), so an efficient method has to be found for dye immobilization on the anode. Chemiadsorption could be used to immobilize the mediator on the activated carbon cloth anode surface for BES such as MFC or MEC for enhanced performance. For textile wastewater treatment an integrated system consisting of a dye treatment tank, for MFC and/or MEC, and hydrogen fermenter connected to MFC and/or MEC, with dye treated anodes, and could also be a future of wastewater treatment technology that could be researched.

iii) Introduction into Comparison of Cathode Designs for MFCs

As previously mentioned in "Principles of Microbial Fuel Cell (MFC) Operation" section 2.4, the anode acts as an artificial, external electron acceptor for the microorganisms, in a MFC. The electrons travel through a resistor or a device that is to be powered, generating electricity until reaching the cathode. While the electrons travel through the circuit, the corresponding protons migrate to the cathodic compartment through a proton-exchange membrane to maintain charge neutrality (Logan, 2008). At the cathode an electron acceptor (e.g., oxygen) is reduced by the electrons via the circuit and the protons via the membrane (Rismani-Yazdi et al., 2008).

The cathode is the most challenging aspect of the MFC design due to the need to have a three-phase interface: air (oxygen) or another electron acceptor, such as ferricyanide, electrolyte solution (protons), and solid (electricity), so that protons and electrons in these three phases can meet at the same point (Logan et al., 2006). This boundary is called 3-phase boundary (TPB), a zone where oxidation (loss of electrons) reaction occurs. It was previously shown that the cathode is more likely to limit power generation than the anode due to being limited to the amount of active sites on the catalyst surface (Rismani-Yazdi et al., 2008). The electrochemical reactions in all MFCs are comparable but the kinetics and coulombic efficiencies may vary depending on the physical, chemical and biological operating conditions, see tables A-2.3 and A-2.4. When comparing power produced by these systems, it makes the most sense to compare them on the basis of equally sized anodes, cathodes, and membranes (Cheng et al., 2006a, Cheng et al., 2006b, Zhang et al., 2010).

iv) Comparison of Cathode Designs for MFCs

Platinum is considered to be the benchmark catalyst for oxygen reduction in MFCs, because of its electrochemical properties and as it is also the benchmark catalyst in chemical fuel cells (Rozendal et al., 2009b, Rozendal et al., 2009a). Despite its good oxygen reduction properties, many disadvantages are also associated with the use of platinum in BESs. These include cost and environmental impact. Platinum extraction from ore and the production of platinum containing cathodes is not considered environmentally friendly (Chassary et al., 2005) and conflicts with the sustainable nature of BESs. There is also a high economic cost associated with the use of platinum as a catalyst, (Clauwaert et al., 2007b). Within this scope, replacing expensive cathode catalysts, like platinum, with cheaper materials and finding the suitable ion exchange membranes in order to maintain electro neutrality in the system form an important challenge of BES research.

It is likely that platinum will be replaced by cheaper stainless steel (Table A-2.3) for use in industrially deployed units, which can produce power densities (P_{max}) of up to 1610±56 mW m^{-2}, for a cathode area of 7 cm^2 (Zhang et al., 2010). The use of plain granular graphite with nanoscale pores (Table A-2.4), which can produce a power density (P_{max}) up to 50 W m^{-3}, per anode chamber (Freguia et al., 2007a) is another option to replace platinum. Another promising alternative is the use of biocathodes. (i.e. cathodes containing biocatalysts such as microbes or enzymes (Duma and Minteer, 2006) instead of inorganic catalyst particles made from graphite fibre brush can produce 68.4 W m^{-3}, but the cathode size and chamber volume were not reported (You et al., 2009).

Some of the most significant problems associated with use of biocathodes are reproducibility of results, time consuming determination of the optimal growth conditions for the bacteria, (particularly important if mixed cultures are used) and the requirement for a two chamber system, which may have higher capital and operational cost then a single chamber system (Logan, 2008). The use of algae for example is a potentially effective approach to make a biocathode (Wu et al., 2013b) because these organisms can act as efficient in situ oxygenators, there by facilitating the cathodic reaction. In this example the maximum power density of 24.4 mW m^{-2} was obtained. There are however factors like the requirement for continuous illumination, which can shorten the algal lifetime and require additional equipment and energy requirement for continuous operation. These results demonstrate that intermittent illumination and cathode material-coated catalyst are beneficial to a more efficient and prolonged operation of MFC with *Chlorella vulgaris* biocathode. Although this is an important finding it is however hard to compare the performance of this MFC to other literature values as the size of MFC, anode and cathode were not specified in Wu et al (2013b).

The use of immobilized enzymes on carbon cloth would require complex laboratory procedures and use of expensive reagents for the immobilization. This cost of could be avoided by the use of stainless steel or plain granular graphite instead (Selembo et al., 2009a). The main challenge is to bring these technologies out of the laboratory and engineer practical systems for bioenergy production at larger scales (Logan, 2010). Single chamber air-cathode microbial fuel cells (MFCs) hold great promise for many practical applications due to their simple configuration and their low operational cost and no recycling or chemical regeneration of the catholyte is required. Thus the overall operation is simplified and smaller cell volume is achieved, thus a higher volumetric power density, can be achieved more easily (Fan et al., 2007).

Another important and often overlooked part of MFC design, is the ion exchange membrane. It is important for the membrane to be permeable to hydrogen protons and to keep the liquid within the anode chamber (Rismani-Yazdi et al., 2008). In MFC systems a loss in the buffering capacity of the electrolyte is often observed, if an anion exchange membrane (AEM) is used instead of a cation exchange membrane (CEM), for example. This results in a smaller voltage output and P_{max} values observed for these systems (Kim et al., 2007a). Nafion is the most frequently used ion exchange membrane, however it transports other cation species (Na^+, K^+, NH_4^+, Ca^{2+}, and Mg^{2+}) that are typically 10^5 times higher than the proton concentration. Nafion, however, is not the perfect choice for the membrane. If other cationic species than protons, which are consumed in the cathode reaction, are transported across the membrane this will then result in an increased pH in the cathode chamber and a decrease in the MFC`s performance (Rozendal et al., 2006a).

No solution to this problem has yet to be reported in literature apart from various ways to reduce this problem such as the use of cation exchange membranes (CEMs), as previously reported by Kim et al (2007a) and seems to be the best choice of membrane at the moment.

2.14.2 Comparison of Anode and Cathode Designs for Microbial Electrolysis Cells (MECs)

i) Introduction into Comparison Anode Designs for MECs

In a MEC system, the anode acts as an electron acceptor for the bacteria and the electrons travel, through a low ohm resistor, to generate hydrogen when reaching the cathode from the corresponding protons which migrate to the cathodic compartment through a proton-exchange membrane to maintain the charge neutrality of the system (Logan, 2008). MEC technology has potentially the same limitations as MFCs. The fact that energy has to be applied to drive the process does not change the system limitations, such as the flow of hydrogen protons in the solution and the number of active sites on the cathode catalyst. The main difference, between two chamber MFC and MECs is the choice of membrane for the two chamber MEC. Different membranes were tested in two chamber MEC systems and the results indicate that AEMs performed better than CEMs in MEC systems (Table A-2.6). This is probably because the loss in the buffering capacity is not an issue for a continuous flow system where the electrolyte in the anode chamber is constantly replaced and system performance is measured according to the volume of hydrogen produced i.e. more hydrogen indicates better performance. The most important performance factors for MECs are coulombic efficiency (C_E), the efficiency with which charge (electrons) are transferred in the system facilitating an electrochemical reaction, hydrogen recovery (Y), the moles of hydrogen produced from the measured current, and hydrogen yield per mol of acetate utilized can be compared to different anode treatments and configurations (Table A-2.5, also see “Electrochemical Analysis Methods” section 4.7 and “Offline Analysis Methods” section 4.8 for more details). One and two chamber MECs have similar anode configurations and any modifications to the anodes affect them in the same way. These differences, however, have to be addressed when cathodic performance is discussed. In a two-chamber system, the cathode, electron acceptors (e.g., hydrogen protons) are reduced to hydrogen by the electrons via the circuit via the membrane (Rismani-Yazdi et al., 2008).

In MEC’s microorganisms are grown in the anode and the cathode is usually abiotic, if a precious metal catalyst is used. In a one chamber a MEC system the membrane is not used. This reduces the cost of buying a membrane and building a second chamber is avoided. The biggest problem with one chamber devices, however, is the build up of methanogens in the cathode compartment (Rader and Logan, 2010).

The solution to this problem may be to place the cathode above the anode, between the headspace and the aqueous phase, in a continuous flow system, where the substrate is quickly replaced (Guo et al., 2010). Such system could be referred to as a single chamber with head space or a two - chamber, membrane less system with gas cathode.

ii) Comparison Anode Designs for MECs

Carbon is usually used as the anode material for MECs. Little research however has been done in perfecting the anode designs in MEC systems and since for example mediator treatments worked in MFCs, there is no reason to why the same improvements would not work in MEC systems. Most research performed on MECs to date approaches MECs from the engineering perspective and very little research was done on investigating the actual processes that allow exoelectrogenic bacteria to produce hydrogen from acetate in detail. For all MECs with platinated carbon cloth cathodes and that used acetate as substrate, unless stated otherwise, the hydrogen yields could be described as follows:-

i) Carbon felt (cloth) 6.32 $m^3\ m^{-3}_{(anode)}\ day^{-1}$ for two chamber MEC with gaseous cathode, with each chamber 50 cm^3 in volume (Tartakovsky et al., 2009)

ii) Ammonia treated graphite brushes 3.12 $m^3\ m^{-3}_{(anode)}\ day^{-1}$; for single chamber MEC anode 28 cm^3 in volume (Call and Logan, 2008)

iii) Graphite granules, 1.58 $m^3\ m^{-3}_{(anode)}\ day^{-1}$, C_E =95 % for 300 cm^3 single chamber MEC (Guo et al., 2010); 1.1 $m^3\ m^{-3}_{(anode)}\ day^{-1}$, C_E=77 %, for two chamber (14 cm^3 each) MEC operated on butyrate, (Cheng and Logan, 2007a); carbon cloth 0.69 $m^3\ m^{-3}_{(anode)}\ day^{-1}$, C_E=73 % for MEC with anode with surface area 9 cm^2 (volume not specified) (Hu et al., 2008)

iv) Carbon foam and a hydrogen production rate of 5.60 $m^3\ m^{-3}_{(anode)}\ day^{-1}$, current density 16.40 A m^{-2} C_E=60 % for two chamber MEC with each chamber 280 cm^3 in volume (Sleutels et al., 2009b).

These results show that increasing the surface area for exoelectrogenic bacteria on conductive matrix, increases the MEC performance and other volatile fatty acids (VFAs) such as butyrate could be used as substrates.

A number of other design changes have been shown to improve hydrogen yields. Immobilized metal ions on the anode surface or in the substrate solution could be used as electron carriers. The anode acts as artificial electron acceptor for anaerobic respiration, so any improvement in electron transport in solution and / or anode conductivity will result an increase in anaerobically respiring bacteria. Addition of iron hydroxide ($Fe(OH)_3$) to the substrate was found to give improved hydrogen gas production at the cathode, using mixed cultures and *Geobacter sulfurreducens* performance of MECs built from 100 cm^3 single chamber MECs made from pyrex bottles, presumably by improving electron transfer from the bacteria to the anode (Ren et al., 2012). $Fe(OH)_3$ addition to the feedstock in the anode chamber increased the maximum current density of both the mixed cultures (from 6.1 ± 0.9 A m^{-2} to 8.8 ± 0.3 A m^{-2}) and pure cultures (from 4.8 ± 0.5 A m^{-2} to 7.4 ± 1.1 A m^{-2}). The hydrogen production rate increased from 23.2 ± 0.1 cm^3 $L^{-1}_{(anode)}$ day^{-1} to 26.5 ± 0.1 $L^{-1}_{(anode)}$ day^{-1}, for both reactors with anode and cathode made from same materials with electrode dimensions of 4.5 cm × 2 cm. Improved current and hydrogen production was sustained even after iron was no longer added to the medium. It could be argued that anode with immobilized ($Fe(OH)_3$) will have exactly the same effect on current density in MECs and hydrogen production as iron hydroxide in solution.

iii) Comparison of Cathode Designs for Microbial Electrolysis Cells (MECs)

The most commonly used cathode is platinum immobilized on carbon. For example, in a small 2 chamber MECs, with each chamber of 12 cm^3 in volume yield of 3.12 cm^3 $L_{(anode)}^{-1}$ day^{-1}, C_E = 98% (Call and Logan, 2008) was achieved with Pt treated carbon cloth. A number of reports on improving cathode performance have been reported (see Table A-2.6), where carbon cloth with immobilized platinum particles was replaced with for example titanium meshes and stainless steel brushes. Stainless steel looks likely to replace platinum in the near future due to the cost of platinum. Some stainless steel alloys, such as alloy A 286, were more effective for hydrogen production than platinum giving 1.5 ± 0.04 cm^3 $L_{(anode)}^{-1}$ day^{-1} (Selembo et al., 2009a) or NiW coated carbon cloth 1.5 cm^3 $L_{(anode)}^{-1}$ day^{-1}, C_E =73 % (Hu et al., 2009). MECs with stainless steel mesh cathodes are more scalable then MECs with platinum coated carbon cathodes (Table A-2.7). Other promising alternatives to platinum catalysts are nickel foam, stainless steel, and molybdenum disulfide (MoS_2) and these were tested as substitute for platinum on a MFC with anode chamber 28 cm^3 and cathode chamber 34 cm^3 (Ribot-Llobet et al., 2013) with cathode electrode 12 cm^2 in size. Pt produced the highest volume of recoverable hydrogen gas (37.9 ± 0.5 cm^3), followed by nickel foam (34.5 ± 0.8 cm^3), with about the same amount of gas produced using either the MoS_2 (29.9 ± 0.1 cm^3).

The improvement of MEC performance goes beyond modifying cathodes and anodes. Such factors as cathode and anode arrangement in the MEC reactor have to be taken into consideration. A good example of this is a study by Gil Carrera (2011) that investigated the influence of anode and cathode size and arrangement on hydrogen production in a membraneless flat-plate microbial electrolysis cell (MEC). Two continuous flow MECs, MEC-1 and MEC-2, were constructed with a series of nylon plates. MEC 1 had a 50 cm^3 anodic compartment and MEC 2 had a 100 cm^3 anodic compartment. The measurements of proteins produced by bacteria were used to evaluate microbial density in the carbon cloth anode. The protein concentration was observed to decrease with the increase in distance from the anode–cathode interface. Cathode placement on both sides of the carbon cloth anode was found to increase the current, but also led to increased losses of hydrogen to hydrogenotrophic activity leading to methane production (see "Performance Inhibitors Microbial Fuel Cells (MFCs) and Microbial Electrolysis Cells (MECs)" section 2.16 for details). Overall, the best performance was obtained in the flat-plate MEC with a two-layer 10 mm thick carbon cloth anode and a single gas-diffusion cathode sandwiched between the anode and the hydrogen collection compartments.

2.15 Scaled up Microbial Electrolysis Cells (s - MECs)

Only a few scaled up examples for microbial electrolysis cells (MECs) have been reported to date. The reason for this is that this is a relatively new technology that still needs significant improvement to compete with existing commercial hydrogen or wastewater treatment systems. Studies conducted on large scale for a single chamber MEC (1 m^3 in volume), revealed that even though it is a promising technology for urban and winery wastewater treatment (Cusick et al., 2011, Heidrich et al., 2013), the maximum gas production for this scaled up MEC was 0.19 ± 0.04 cm^3 $L_{(anode)}^{-1}$ day^{-1}. Although most of the product gas was converted to methane (86 ± 6 %) with only 14 ± 6 % remaining as hydrogen. Several difficulties still need to be overcome in order to increase hydrogen recovery in MECs (see "Performance Inhibitors Microbial Fuel Cells (MFCs) and Microbial Electrolysis Cells (MECs)" (section 2.16) for details). For example, better methods will be needed to isolate hydrogen gas produced at the cathode. The results of the study by Cusick et al (2011) show that inoculation and enrichment procedures (choice of culture and growth conditions for mixed microbial culture promoting growth of electrochemically active bacteria) are critical to the initial success of larger-scale systems. Acetate amendments, warmer temperatures, and pH control during startup were found to be critical for proper enrichment of exoelectrogenic biofilms and improved reactor performance.

The ability of an MEC to treat real wastewater was assessed by Gil-Carriera et al (2013). A MEC consisting of two 2 L one chamber MEC modules was used to treat wastewater in a two stage process, combining hydrogen fermentation with microbial electrolysis cell. A H_2 production rate of 45 cm^3 $L^{-1}_{(anode)}$ day^{-1} was reported (Gil-Carrera et al., 2013). Another report involved operating a 120 L microbial electrolysis cell was operated on site in Northern England for a period of over 3 months, converting domestic wastewater to produce hydrogen gas at a rate of 15 cm^3 $L^{-1}_{(anode)}$ day^{-1} (100 ± 6.4 %) (Heidrich et al., 2013). The reactor had a coulombic efficiency (CE), (the percentage of substrate converted into hydrogen) of 55 %. It was noted that improved hydrogen capture and reactor design could increase the performance levels substantially. Most importantly, these scaled up designs show that a 'proof of concept' was made and microbial electrolysis technology is capable of energy capture as hydrogen gas from both vinery and low strength domestic wastewaters at ambient temperatures.

2.16 Performance Inhibitors in Microbial Fuel Cells (MFCs) and Microbial Electrolysis Cells (MECs)

There are a number of phenomena which can reduce the efficiency of MFC`s and MEC`s, these include for example cathode methanogenesis, pH and gradient losses

2.16.1 Cathodic Methanogenesis in MECs

Cathodic methanogenesis refers to production of methane by archaea. Methanogenesis is a significant problem, because methanogenic archaea compete for the acetate substrate with exoelectrogenic bacteria species under anaerobic conditions (Wang et al., 2009a). Methanogens also consume hydrogen, in hydrogenotrophic methanogenesis:

$$4H_{2\,(g)} + CO_{2\,(g)} \rightarrow CH_{4(g)} + 2H_2O_{(l)} \qquad \text{Eq 29}$$

The other form of methanogenesis converts acetate into methane (acetoclastic methanogenesis),

$$H_3CCOO^- + H^+ \rightarrow CH_{4(g)} + CO_{2\,(g)} \qquad \text{Eq 30}$$

A number of studies show that the increase in methane concentration in MEC cells was accompanied by the consumption of hydrogen and carbon dioxide, which indicated that hydrogenotrophic methanogenesis was involved in the microbial electrolysis cell (Tartakovsky et al., 2008, Rozendal et al., 2008b). No evidence of acetoclastic methanogenesis was reported in the same cell.

In mixed biofilms, acetate oxidizing electrochemically active bacteria (EAB) in microbial fuel cell (MFC) or microbial electrolysis cell (MEC) will out-compete the acetoclastic methanogens present but not hydrogenotrophic methanogens in MECs, (Parameswaran et al., 2011).

As most methanogens are strict anaerobes (Koizumi et al., 2003), a way to reduce this problem is to periodically bubble oxygen in small volumes, through the anode chamber, which selects towards facultative anaerobes, such as *Sewanella* species, which are capable of producing electricity in their anaerobic respiration (Kim et al., 2009b).

2.16.2 Transport and pH Gradient Losses

Performance of BES's is assessed via the comparison of actual performance to the ideal theoretical performance. Where the ideal performance refers to the way BES performs without pH gradient, ionic and mass transport limitation or cathodic and anodic overpotential losses. The ideal total hydrogen production volume in a MEC, for example, takes place where the number of moles of hydrogen recovered is the same as the maximum number of moles of hydrogen produced from the reduction in acetate concentration.

Actual performance is typically lower than the ideal performance because of the potential losses. A simplified version of what happens is described by the following equations, based on the approach by Sleutels et al (2009b). The wide range of chemical losses occurs because of the different current densities used in each study, different biofilm anode composition, different biofilm thickness, donor concentration, pH, electrode material, electrode distance and the membrane type used (Torres et al., 2008).

The most important losses are:

i) pH gradient losses refer to flow of H^+ protons from low to high pH areas.

The pH gradient losses are described by equation:

$$E_{\Delta pH} = \frac{RT}{F} \ln (10^{(pHcathode - pHanode)}) = \frac{RT}{F} \ln(10^{(7-7)}) = 0 \qquad \text{Eq 31}$$

Where RT/F is a constant equivalent to 25.693mV and $E_{\Delta pH}$ = 0, is a pH gradient loss when the pH in the cathode chamber is the same as that in the anode chamber. The problem with cathodic methanogenesis that could also be also reduced by keeping the pH in the cathode chamber at pH 5 and results in a small pH gradient loss.

ii) Ionic losses refer to electrolyte resistance that is related to concentration of ions in the electrolyte solution. Ionic losses are described by equation:

$$E_{ionic}=I_{ions}\times\left(\frac{1}{2R_{anode}}+\frac{1}{2R_{cathode}}\right) \quad \text{Eq 32}$$

Where I_{ions} is the flow of ions (Am^{-2}) and R_{anode} and $R_{cathode}$ are anode and cathode resistances (ohms).

iii) Transport losses refer to movement of ions in the electrolyte solution. Transport losses are described by equation:

$$E_T\,(mV) = E_{emf} - E_{\Delta pH} - \eta_{an} - \eta_{cat} - E_{ionic} - E_{cell} \quad \text{Eq 33}$$

Where η_{an} and η_{cat} are anodic and cathodic overpotentials.

iv) Coulombic losses explain why the value for coulombic efficiency (CE), obtained experimentally for a particular BES, is lower than the theoretical value due to some of the energy from the substrate conversion by bacteria is used for parasitic processes other than electricity production.

The coulombic efficiency indicates the ratio between the coulombs recovered as current over the total amount of coulombs from the electron donor added (eg:- 8 mol electrons per mol acetate). On one hand, there is incomplete substrate removal in the effluent and on the other hand there is occurrence of alternative reactions that do not result in current production. For a biocatalyzed anode, this means that at first, fermentation or anaerobic respiration of organic compounds in the anode can occur in a way that some products (eg:- gaseous compounds like methane) are not converted into electrical current production. If these anaerobic products, like acetate or dihydrogen sulfide, could be completely recovered as current, the coulombic efficiency is not affected (however the energy liberated in these processes is lost), as reported by Rabaey et al (2006). Secondly, the build-up of biomass in the anode gives rise to a lower coulombic efficiency due to the presence of non conductive exopolimeric substances excreted by the bacteria and dead cells. Thirdly, crossover of substrate or mixing of the anodic and cathodic reagents, also gives rise to a low coulombic efficiency. In membraneless MFCs, a high influx of oxygen in the anode gives rise to the aerobic conversion of the organic substrate resulting in a low coulombic efficiency as a result (Liu and Logan, 2004a).

2.16.3 Overpotential Losses

Overpotential is an electrochemical term which refers to the potential difference between the half-reaction's at which the redox event is experimentally observed (Bard and Faulkner, 2001). The term is directly related to a cell's voltage efficiency and can be described by the equation:

$$E_{cell} = S_{eem} - E_{spy} - a_n - c_{at} - I_{onic} - E_T \quad \text{Eq 34}$$

In Eq 34 the potential used to produce hydrogen, where E_{emf} (mV) is the potential measured across the resistor, where $E_{\Delta pH}$ (mV) is the pH gradient over the membrane, where η_{an} is anode overpotential, where η_{cat} is cathode overpotential, where E_{ionic} are ionic losses and where E_T are transport losses.

Due to the overpotential the following occurs:

i) An electrolytic cell's anode is more positive because it uses more energy than thermodynamics require (anode overpotential), described by equation:

$$\text{Anode overpotential, } \eta_{an} = E_{anode,\ measured} - E_{anode} \quad \text{Eq 35}$$

Where $E_{anode,\ measured}$ is the anode electrode potential measured with respect to the reference electrode and E_{anode} is the theoretical anode potential, at 289K and 1 atmosphere pressure.

ii) An electrolytic cell's cathode is more negative because it uses more energy than thermodynamics require (cathode overpotential), described by equation:

$$\text{Cathode overpotential } (\eta_{cat}) = E_{cathode} - E_{cathode,\ measured} \quad \text{Eq 36}$$

$E_{cathode,\ measured}$ is the cathode electrode potential measured with respect to the reference electrode and $E_{cathode}$ is -414 mV, the theoretical cathode potential, at 289K and 1 atmosphere pressure.

The overpotentials could be split into three categories: activation, concentration and resistance, as shown in figure 6, where V_e= voltage and V_{cell}= measured voltage, as described by Rabaey et al (2010).

$$V_{cell} = V_e - \sum \eta_a - |\sum \eta_c| - IR$$ Eq 37

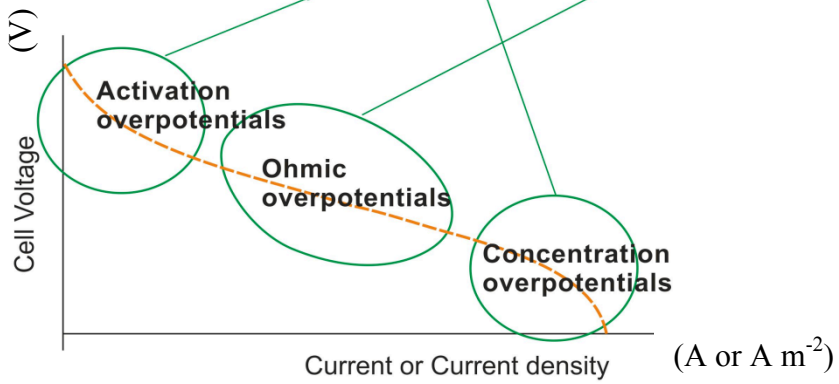

Figure 6 – Indication of overpotential losses and their region of dominance as current.

Activation overpotentials are considered to be amongst the main limitations in MFC performances (Rabaey and Verstraete, 2005). Activation overpotentials are the potential differences required to produce a current that depends on the activation energy of the redox reaction. Activation overpotentials accompany the kinetic slowness of the redox-reactions.

Tafel equations could be used to calculate the exchange current (i_0) if the concentration polarization is not taken into account, however this never happens in reality (Rabaey and Verstraete, 2005, Logan et al., 2006). The Tafel equation relates to the rate of an electrochemical reaction to the overpotential:

$$\eta = A \times ln \left(\frac{i}{i_0} \right)$$ Eq 38

Where η is the overpotential, where A is the so-called "Tafel slope", where i = current density (A m^{-2}) and where i_0 = current density dependent on the electrolytic process (A m^{-2}).

Equation 38 shows that there is a linear correlation between the activation overpotential and the logarithmic value of the current. Therefore if the activation overpotentials are low, the exchange current density is high (Freguia et al., 2007b). Thus, activation overpotentials are the most dominant overpotentials in the low current density range and the activation overpotentials increase slowly with increasing current densities (see Fig. 6). The current density is typically expressed per total electrode surface. However, the electrochemical reactions only occur at specific reactive catalyst sites. In the case of a chemical catalyst, the catalyst loading will determine the number of reactive sites, therefore increasing the number of reactive sites, by using more catalyst, lowers the associate activation losses (Cheng et al., 2006b).

Catalyst poisoning inactivates reactive sites and further increases electrode overpotentials (Niessen et al., 2004a). For biologically catalyzed reactions in BESs, the amount of biocatalyzing microorganisms in relation to the available surface area and the biological activity of the microbial consortium will determine the magnitude of the overpotentials. This bio-catalytic activity is dependent on the environmental conditions (e.g. vitamin and mineral composition, temperature, toxic compounds, electrode properties and electrode potential) and the biological competition within the microbial consortium (Cheng and Logan, 2007b, Clauwaert et al., 2007b, Rabaey and Verstraete, 2005).

Concentration overpotentials are associated with the concentration gradient of reagents and products in the proximity of the electrode. They are determined through migration, diffusion and convection of substrate and removal of products. The use of a more concentrated electrolyte, or the use of stirring may increase the electron transfer rate (Bard and Faulkner, 2001). The best way to address concentration overpotentials is to use highly conductive electrolytes or to reduce the distance between the anode and the cathode when the composition of wastewater can not be altered (Bard and Faulkner, 2001). This was therefore the reason identified to avoid the use of H type MFC's and MEC's in the experimental work in this thesis. This is particularly important if wastewater is to be used as substrate due to its low natural conductivity.

The resistivity of wastewater at room temperature is typically between 20 Ωm (0.5 mS cm^{-1} for potable water based wastewaters) and up to 0.2 Ωm (50 mS cm^{-1}, for seawater based wastewaters). This is the main reason why a small BES, with higher conductivity due to reduced distance between the anode and cathode will perform better than larger ones with a greater distance between the anode and the cathode. To minimize the resistivity in BESs used for wastewater treatment, where typically it would be difficult and costly to alter the electrolyte composition, it is particularly important to minimize the distance between the electrodes.

Ohmic or resistance overpotentials are the overpotentials due to a particular cell design. This includes "junction overpotentials" which describe overpotentials occurring at electrode surfaces and the interfaces with the electrolyte membranes. This can include aspects of electrolyte diffusion, surface polarization (capacitance), and other sources of counter electromotive forces. In order to overcome the problems associated with resistance overpotentials, highly conductive precious metals are used as the electrode materials (Bard and Faulkner, 2001).

Further research is needed to determine the contribution of different overpotentials in combination with the energy consuming nature of the biocatalysts, as it is difficult to make a clear distinction at this moment between these factors.

2.16.4 Power Overshoots (MFC only)

Power overshoots were identified as a problem in numerous BES studies (Liu et al., 2011b, Winfield et al., 2010, Winfield et al., 2011, Hong et al., 2011, Nien et al., 2011). Power overshoots occur when electrical resistance of the MFC increases leading to both decrease in cell voltage and current, as the external load decreases (Hong et al., 2011). It was shown that power overshoots occur during the early stages of enrichment, when exoelectrogenic biofilm density is small, as shown in figure 7, where the circled area highlights overshoot peaks. (Winfield et al., 2010, Winfield et al., 2011) One way to resolve this problem, which is associated with mass transport in the electrolyte is either to adopt low resistances (Hong et al., 2011), increase the stirring rate or to reduce the electrode spacing (Nien et al., 2011).

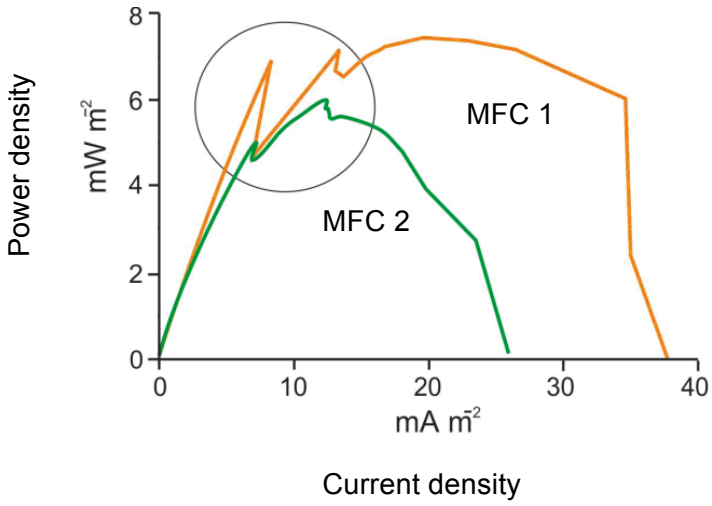

Figure 7 – Power density curves with overshoots for microbial fuel cells (MFCs) 1 and 2.

2.16.5 Voltage Reversal (MFC only)

Voltage reversal can occur if a chemical fuel cell receives an inadequate supply of substrate. In order to pass current, reactions other than fuel oxidation may take place at the fuel cell anode, including water electrolysis and oxidation of anode components. The latter may result in significant degradation of the anode (Knights et al., 2001). In a MFC, however a cell charge reversal, where the voltage in one cell is abruptly reversed. Polarity reversal can also be observed when using a continuously fed MFC system is connected in series (Aelterman et al., 2006b). Serial linking is one way, commonly used to increase the voltage output in a MFC system (Wilkinson, 2000).

2.16.6 Improvements in Anode and Cathode Designs to Reduce Performance Inhibitors in Microbial Fuel Cells (MFCs) and Microbial Electrolysis Cells (MECs)

i) Improvements in Anodic Performance

Exoelectrogenic bacteria can use a carbon cloth anode as a final electron acceptor in their anaerobic respiration (Torres et al., 2010). A chemical mediator facilitates the electron transport between the bacteria and the electrode surface in most exoelectrogenic bacteria systems (Logan, 2009). The maximum cell potential that can be developed by the oxidized and reduced form of mediator is determined by the Nernst Equation (Torres et al., 2010):

$$E = E^{\theta} \times \frac{RT}{nF} \ln\left[\frac{\text{Mediator}_{(\text{reduced})}}{\text{Mediator}_{(\text{oxidised})}}\right] \quad \text{Eq 39}$$

However a small portion of the immobilized mediator on the anode surface may be metabolized by the bacteria and dissolved from the carbon cloth electrode into the acetate solution. This can be described by Ficks law (Picioreanu et al., 2007). Fick's first law relates to the diffusive flux to the concentration under the assumption of steady state. It postulates that the mediator adsorbed goes from regions of high concentration to regions of low concentration, with a magnitude that is proportional to the concentration gradient. Since it is unlikely that the mediator is re-adsorbed back on the electrode in a continuous flow system, as it will be discarded in the environment with the effluent, this is not taken into the account. Electron transport involving electron carrier molecules is called mediated electron transfer (MET) (Sund et al., 2007, Blankenship and Parson, 1979, Logan et al., 2009a).

ii) Improvements in Cathodic Performance

Platinum is used widely in MFC and MEC as a cathode catalyst (Call and Logan, 2008). Platinum is the most efficient heterogeneous catalyst that converts protons into hydrogen in the cathode chamber of MEC. However platinum is expensive, $ 38.0 per gram (Zhao et al., 2006). Recently, alternative cathode catalysts were investigated, such as stainless steel alloy A286 (Selembo et al., 2009a), NiMo (Damian and Omanovic, 2005, Hu et al., 2009), cobalt tetromethoxyphenylporphyrin CoTMPP, and FePc (Zhao et al., 2005) and these could be used to significantly reduce the cost of building a microbial electrolysis cell.

3. Aims of this Thesis

3.1 Determine the Influence of Temperature and Catholyte pH on the Hydrogen Production in Microbial Electrolysis Cells (MECs)

Hypothesis

Before the work on investigating the anodes used in microbial fuel cells (MFCs) and microbial electrolysis cells (MECs) was started, it was important to assess how the novel tubular reactor was operated in regard to the selected temperature and pH. Microbial electrolysis cells (MEC) could be integrated with dark fermentative production to increase the overall hydrogen production that could operate at a range of temperatures and pH. Tubular reactors were shown to perform better than most other designs (Gil-Carrera et al., 2013, Kim et al., 2009b, Rabaey et al., 2005b) and could be scaled up. It is important to know how the change in temperature or pH, which will happen if the process is taken to industrial scale, will affect the hydrogen production rate and coulombic efficiency (CE). According to authors knowledge the performance of an up flow MEC was not assessed in detail under different temperature and pH levels, in the literature, when the experimental work was done.

Objectives

i) To construct a microbial fuel cell built around an untreated carbon cloth anode (UCC) and to operate it for several weeks, under a 150 Ω resistance, in sequencing batch mode, in order to develop exoelectrogenic biofilm. This method (Liu et al., 2011a, Cusick et al., 2011) should allow faster biofilm development on the electrode surface.

ii) To remove the anode and to place the conditioned anode into microbial electrolysis cell and evaluate the effect of temperature and pH on the hydrogen production rate and efficiency in MECs.

iii) To investigate the performance factors in detail that include the hydrogen production rate, current density at the cathode, conductivity, pH and the amount of acetate consumed by the bacteria and to assess the how these performance factors are affected by the changes in the pH.

iv) If the performance of MFC comparable to results reported in literature to use this MEC as control in future work.

3.2 Investigate the Effect of Immobilized Methylene Blue and Neutral Red on the Current Production in Microbial Fuel Cells (MFCs)

Hypothesis

In order to become, commercialized microbial fuel cells need to have similar performance factors, such as power density to chemical fuel cells. The performance of microbial fuel cells (MFCs) is lower than that of chemical fuel cells by the factor of 10. The potential inefficiency of large scale microbial fuel cell (MFC) reactors was investigated by Logan and Cheng (2011) and electron transport losses were highlighted as one of the major problems. The effect of various electron mediators on the performance of MFCs was investigated (Sund et al., 2007). Much of the work on the immobilization of mediators on the electrode surface was performed by Park et al (1999). Passive adsorption on carbon had not previously investigated as a means to attach mediator to the carbon cloth anode. This approach has the advantages because it avoids the use of a non conductive matrix that holds the electron mediator molecules to the carbon surface.

Objectives

i) To immobilize a mediator on the carbon cloth anode via passive adsorption and to determine the most efficient way to immobilize the mediator on the carbon anode surface (experiment 2). To build and operate the microbial fuel cells (MFCs) with different mediator treated anodes, at 150 Ω resistance, for several weeks, in sequencing batch mode (experiment 2.1), such that it would be possible to compare these results to work published by Kim et al (2009b).

ii) To investigate the performance factors in detail including voltage production, current, power density and the amount of acetate consumed by the bacteria on both the control MFCs and MFCs with mediator treated anodes.

3.3 Investigate the Influence of Changes in Acetate and Butyrate Concentrations and Full Substrate Switch on Gas Production from Two Microbial Electrolysis Cells (MECs) Acclimated to either Acetate or Butyrate

Hypothesis

If a microbial electrolysis cell (MEC) is to be integrated with dark fermentative hydrogen production reactor, which typically produces an acetate and butyrate mixture in approximate ratio of 4 to 6. Then it is important to investigate how fluctuations in acetate and butyrate concentrations would effect the hydrogen production on such an integrated process. If a mixed microbial culture is acclimated to butyrate, there may be a natural selection towards more exoelectrogenic bacteria and / or a reduction in methanogens (Regan and Jung, 2011). Previous work by Cheng and Logan (2007a) showed that it is possible to operate MECs on butyrate, propionate and valerate. This process was not however investigated in detail and minimal information on the experimental procedures was published. According to the author`s knowledge information on how small shifts in the substrate concentration and full substrate switch effects the hydrogen production was not previously published in literature.

Objectives

i) To build and operate microbial fuel cells (MFCs) with untreated carbon cloth (UCC) anodes and to operate one on acetate and another on butyrate for several weeks at 1000 Ω resistance, to compare these results to previously published work such as Michie et al (2011) and Liu and Logan (2004b). The results will compare all performance factors previously addressed in the literature which should include voltage production, current, power density and the amount of acetate consumed by the bacteria to see if there are any significant differences between the acclimated electrodes.

ii) To build continuous flow microbial electrolysis cells (MECs) and to investigate the effect of changes in substrate concentration and full substrate switch on hydrogen production rate. Other performance factors such as current density at the cathode, conductivity, pH and the amount of substrate consumed by the bacteria, previously reported in literature, should also be investigated. The percentage of exoelectrogenic bacteria and archaea on anodes acclimated to acetate (AC) or butyrate (BU) should be determined if there is a significant difference in the MEC performance. This type of work on MEC anodes has not been reported in the literature before.

3.4 Compare four Anode Types on the Voltage Production in Microbial Fuel Cells (MFCs) and Hydrogen Production in Microbial Electrolysis Cells (MECs)

Hypothesis

Mediators are not the only substances that can enhance MFC and MEC performance. Iron and manganese particles immobilized on carbon electrodes can also act as mediators (Seo et al., 2009). The anode in a microbial electrolysis cell (MFC) or MEC could be made more conductive, if a stainless steel anode is used instead of pure carbon with carbon cloth. Previous work by Dumas et al (2007) showed that most bacteria in mixed culture could not attach itself to the stainless steel plate anode surface. Stainless steel has a higher conductivity than carbon (Wang et al., 2003) and carbon materials with metal particles immobilized on their surface were shown to perform better than MFCs with carbon anodes (Lv et al., 2012, Kim et al., 2005, Park and Zeikus, 2003, Fan et al., 2011).

Objectives

i) To build and operate the microbial fuel cells (MFCs) with untreated carbon cloth roll (UCC) anodes; stainless steel cloth and carbon cloth roll anodes (RR); J cloth (artificial cloth made from non conductive fibers) of the same thickness as stainless steel cloth) carbon cloth roll (JC) and methylene blue treated cloth roll (MB) and to operate these MFCs on acetate for several weeks at 1000 Ω resistance, so that it would be possible to compare these results to (Michie et al., 2011, Liu and Logan, 2004b). The results should compare all performance factors previously addressed in literature which should include voltage production, current, power density and the amount of acetate consumed by the bacteria to see if there are any significant differences.

ii) To build and operate microbial electrolysis cells (MECs) with 4 different anodes for a comparison study and to investigate the effect of changes in substrate concentration and full substrate switch from acetate to butyrate on hydrogen production rate. Other performance factors such as current density at the cathode, conductivity, pH and the amount of substrate consumed by the bacteria, previously reported in literature, were also investigated in detail.

3.5 Design scaled Up Multi Anode Chamber Microbial Electrolysis Cell (Revolver Reactor)

Hypothesis

The industrial large scale microbial electrolysis (MEC) system has to be run continuously at high volumes (>m^3) and should be designed in such a way that it could be possible to move large amounts of liquid through these devices. At the time when the work on the designs started several types of such scalable reactors were investigated including systems based on up-flow systems based on graphite granules Rabaey et al (2005b) and one MEC with 1m^3 chamber was described in the article published by Cusick et al (2011). A microbial electrolysis (MEC) cell used in Part 1 is not large enough to take the process to the next step of MEC development. A larger MEC system has to be built in order to be able to operate on industrial scale.

Objectives

i) To design a scaled up MEC cell consisting of separate modules placed inside 18L cathode chamber, made from old hydrogen fermenter case, capable of processing the effluent produced by hydrogen fermenter, as part of two step hydrogen production process.

ii) To design anode chamber modules and novel anodes for a scaled up MEC based on conclusions from previous experimental work from this thesis.

4. Materials and Methods

4.1 Anode Materials and Anode Designs Used

The anodes used in experiments 6.1 - 6.4 unless stated otherwise in “Results” section 6. Untreated carbon cloth (UCC), methylene blue treated carbon cloth (MB) and neutral red treated carbon cloth (NR) designs were assembled around the carbon cloth anodes, (o.d. 17.2 mm. 200 mm long) and each anode (Fig. 11 c) with either untreated or dye treated (see “Methods to Determine how Much Mediator was Adsorbed on the Electrode Surface” section 4.84, for carbon cloth dye treatment procedures) carbon cloth veil 475/200/0.3mm (plain carbon cloth, PRF composite materials, Dorset, UK), see figure 13 b, wrapped around the graphite rod of diameter 6.5 mm and length 200 mm (graphite rod, Alfa Aesar, A Johnson Matthey Company, Lancashire, UK).

Stainless steel mesh carbon cloth roll (RR) was assembled around a carbon cloth anode, o.d. 17.2mm. 200mm tall and each anode (Fig. 8 a) was assembled with carbon cloth veil 475/200/0.3 mm (plain carbon cloth, PRF composite materials, Dorset, UK) shown in figure 8b, stainless steel cloth 475/200/0.1 mm (200 mesh, 0.07 mm aperture, wire diameter 0.066 Mesh Direct, Burslem, UK) wrapped around the carbon rod of diameter 6.5 mm and length 200 mm (graphite rod, Alfa Aesar, A Johnson Matthey Company, Lancashire, UK). J cloth carbon cloth roll anode (JC, control 2, Fig. 8 c) consisted of artificial wool fibers 475/200/0.1 mm / aperture 0.07, fiber diameter 0.07 (blue non conductive artificial synthetic fiber cloth, product code: 7444300**,** Vegware, Edinburgh, UK) instead. Fig. 8 shows untreated carbon cloth roll (UCC, also control 1 for the experiment with RR electrode) anode (8 a), stainless steel mesh carbon cloth roll (RR) anode (8 b) and J cloth carbon cloth roll (JC, control 2 for the experiment with RR electrode) anode (8 c), before assembly.

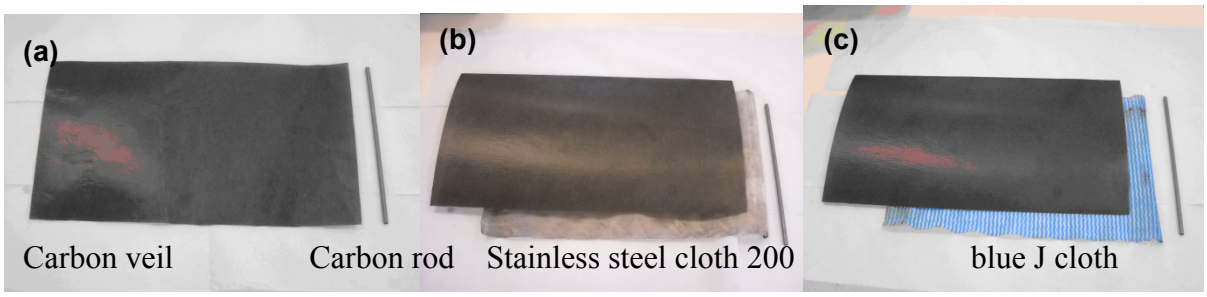

Figure 8 – Materials used for anode assembly.

4.2 Method for Immobilization of Dye on Anodes

For the preparation of methylene blue (MB) treated carbon cloth anodes a carbon veil electrode (950 cm^3) (plain carbon cloth, PRF composite materials, Dorset, UK) was placed into 1.56 mmol L^{-1} methylene blue ([7-(dimethylamino) phenothiazin-3-ylidene]-dimethylazanium chloride C.I. 52015, Fisher Scientific, Loughborough, UK) solution at pH12 (adjusted from pH 5.5 to pH 12, using NaOH as described in the previous studies on adsorption of MB on saw dust (Hameed et al., 2007a, Hameed et al., 2007b), for 28 h and dried for another 28 h (MB-carbon anode treatment). This method works because MB is more likely to be adsorbed on the surface at high pH (i.e. 10 to 12) at which most MB molecules exist in an oxidized form as shown in the previous study (Senthilkumaar et al., 2005). The anode was then placed into microbial fuel cell (MFC) module that operated at pH 7. The prepared electrodes were assembled into a membrane electrode assembly MFC as previously described (Kim et al., 2009b).

The same procedure was repeated for neutral red (NR8-N, 8-N, 3-trimethylphenazine-2,8-diamine hydrochloride, C.I.50040, Fisher Scientific, Loughborough, UK) treated anodes carbon cloth anodes.

4.3 Methods and Materials Used to Construct Microbial Fuel Fells (MFCs)

Each MFC cell consisted of one tubular cell to contain the anode. The tubular cell was made from polyethene tubes (Marley Extrusions, part number WPP40WX, RS components, Pontypridd, Wales, UK) with an internal diameter of 40 mm, wall thickness 2 mm and 216 mm length (Fig. 10 a). The volume of the anode tube was 200 cm^3 with 53 holes 1.0 cm in diameter, drilled into its side. These holes were covered with the cation exchange membrane (CMI 7000, Membranes International, NJ, USA), the area of which was 240 cm^2. The cation exchange membrane was then covered with the carbon veil cathode (75 cm^2, 0.5 mg cm^{-2} Pt, BASF fuel cell, NJ USA). Copper wire (Tined copper wire TCW 25, Rowan House, Hertfordshire, UK) was wrapped around the assembled anode chamber and any gaps were sealed before the cathode sleeve was placed to hold the membrane in place. A 150 Ω resistor was connected between the anode and cathode (Fig. 11) for enrichment, at the beginning of MFC operation. Sludge containing bacteria is added to the substrate in the MFC anode chamber and the microbial culture was allowed to establish for 2 weeks (Kim et al., 2005).

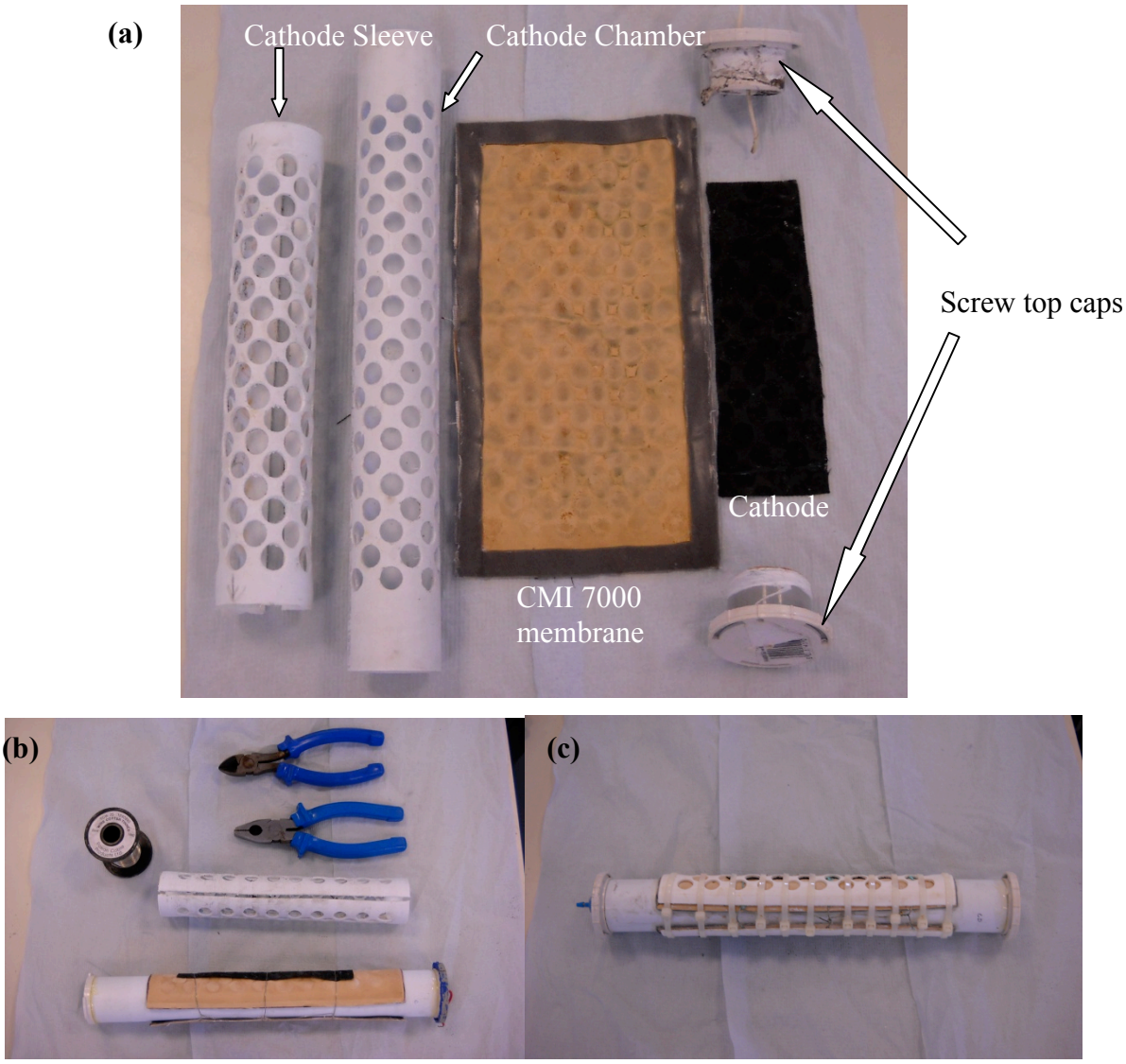

With CMI 7000 membrane attached to anode chamber

Complete assembly

Figure 9 – Single chamber (MFC) at various stages of the construction process.

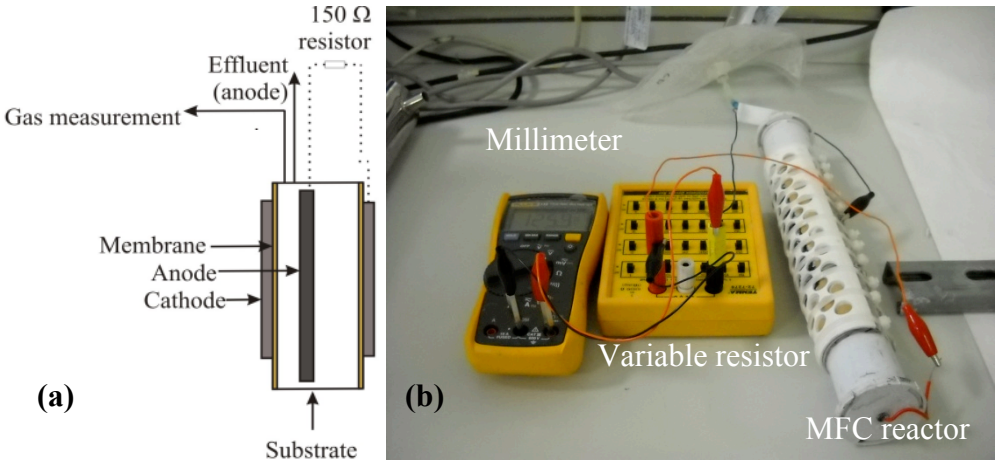

Figure 10 – Complete MFC assembly diagram (a) and photograph (b).

4.3.1 Temperature Control for MFC Reactors

Specific MFC temperatures were controlled by placing reactors in incubators (Oxitop, WCW, Germany). Incubator temperatures were checked once a day using a glass alcohol thermometer.

4.4 Method and Materials used for Microbial Electrolysis Cells (MECs) Construction

A schematic of the MEC setup is shown in Fig. 11 – Fig. 13 and more detailed design in Appendix A-6. The MEC consisted of two concentric tubular clear acrylic cells (i.d. 40 mm and 74 mm). The plastic sheets for the lids and acrylic tubes, (see "Appendix A-6" for detailed diagrams), were made with materials from Dipec Plastics, (Cardiff, UK). The smaller, inner tube (326 cm^3 volume) shown in figure 11 (a) was radially perforated (39 holes each 8 mm in diameter) on one side of the tube (subtending 150^0 of the 360^0 circumference) and inserted in the larger diameter tube (1290 cm^3 inner volume).

The inner tube was assembled with the anode electrode removed from a MFC, after several weeks of operation and placed into microbial electrolysis cell (MEC). The reference electrode (RE 5b Ag/AgCl, Basinc, Warwickshire, UK) was located on the top lid of the anode chamber. The anion exchange membrane (AMI 7001, Membranes International, NJ, USA) was attached to the outer surface of the inner tube so as to cover the perforations, thus separating the internal volumes of the two tubes. The cathode electrode (carbon cloth, area 75 cm^2 coated with 0.5 mg cm^2 Pt, BASF fuel cell, NJ, USA) was used to form a membrane electrode assembly identical to the MFC design.

Copper wire (plastic jacketed copper wire RG 178, Farnell Ltd, Cheshire, UK) was wrapped around the assembled anode chamber and any gaps were sealed with liquid gasket (Locktite Quick Gasket 5180, Halfords, Cardiff, UK) before the cathode sleeve was placed to hold the membrane in place. Fig. 11 a shows anodes RR, JC and UCC before transfer from microbial fuel cell (MFC) into microbial electrolysis cell (MEC) modules, MB and NR only used for comparison (figure 11c).

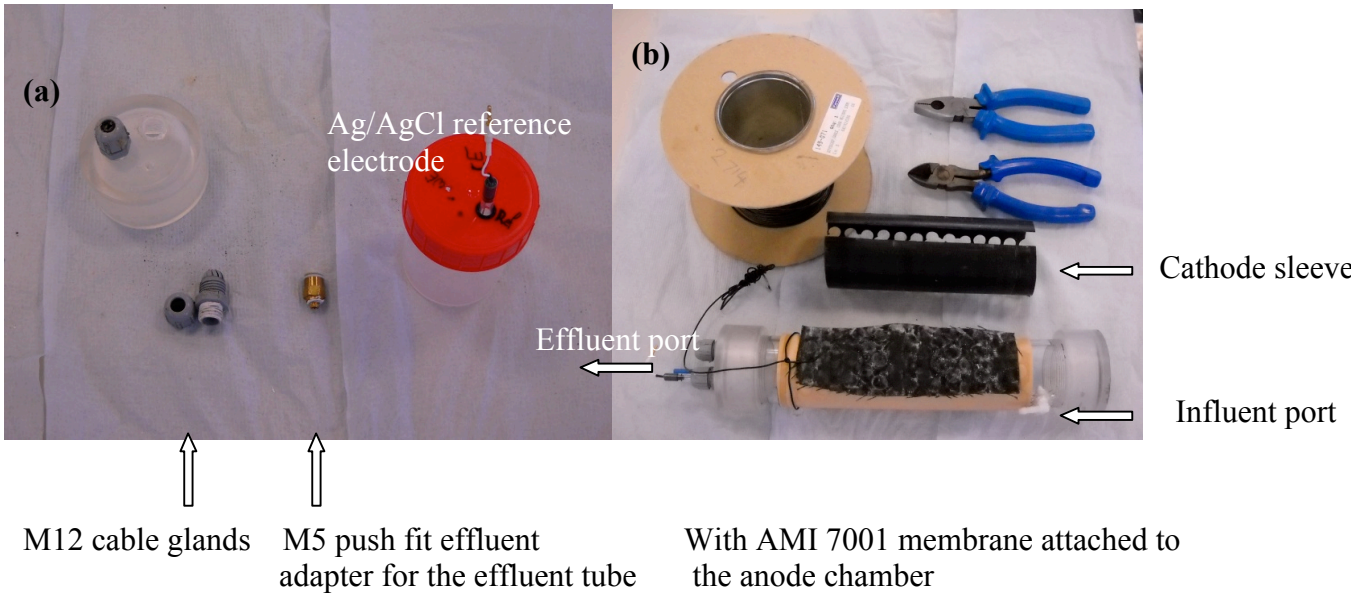

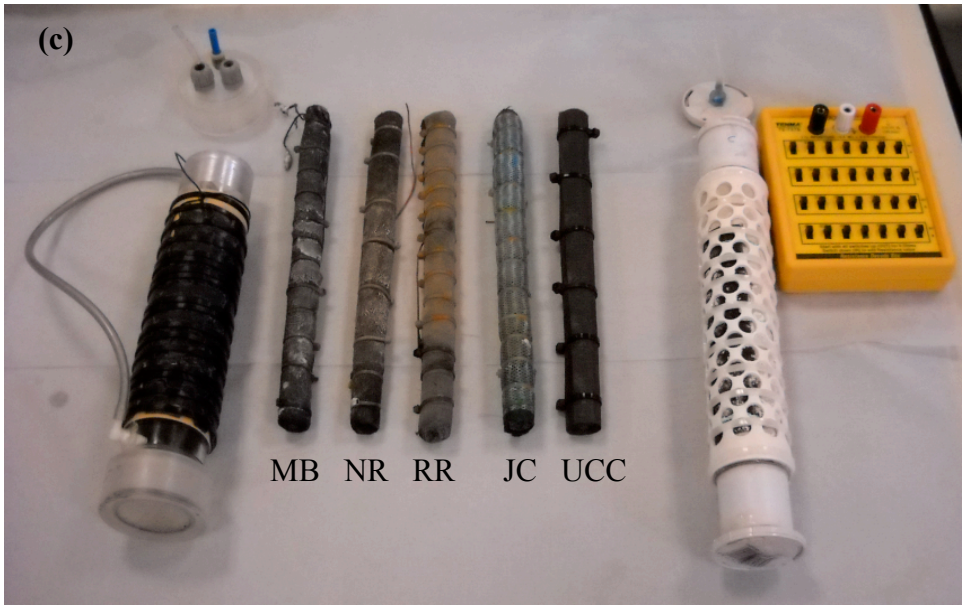

Figure 11 – A top cap microbial electrolysis cell (11 a), anode chamber (11 b) and complete MEC anode module (11 c).

The inner tube was equipped with shoulder connector (RS Stock No: 419-7221 adapter, RS Components, Pontypridd, Wales, UK) for supplying the substrate (Fig. 11 a) at the bottom of the tube. The substrate was supplied via Watson Marlow, 323Du with MC8 head cassette pump (, Watson and Marlow, Cornwall, UK), from a 5 L feed tank in a fridge, where the temperature was maintained at 8 ^{o}C. AM5 adapter (KQ2H01-M5, Bestneumatics, Lancashire, UK) was inserted in to the top lid for removing the substrate. Two M12 cable glands (RS Stock No: 361-9994, RS Components, Pontypridd, Wales, UK) were installed in the anode and cathode top chamber lids for connecting the anode and cathode to the power supply (Array 0-18 V, 5A, 90 W DC Programmable Power Supply, Carrog, UK) whilst keeping the environment inside the reactor anaerobic. A second reference electrode (RE 5b Ag/AgCl, Basinc, Warwickshire, UK) was attached to the top lid in the cathode chamber for simultaneous on line data logging from anode and cathode (explained in section 4.5 "Flow Rates, pH, Temperature and Current Monitoring in Microbial Electrolysis Cells (MECs)") in greater detail). The top and bottom lids on the outer tube (the cathode chamber) were fitted with M10 push fit connectors (KQ2H01-M10, Bestneumatics, Lancashire, UK) for recirculation of catholyte in the cathode chamber using a Watson-Marlow 323Du peristaltic pump with 313D and 313X pump heads (Watson-Marlow Pumps Group, Cornwall, UK) (see Fig. 12, Fig. 13 a and Fig. 13 b). The catholyte was water with 30 g L^{-1} NaCl, added to prevent any methanogens growing in the cathode chamber (de Baere et al., 1984). A pressure valve was installed on the top lid of the cathode chamber and another, another on the small plexiglas bottle attached to the effluent tube from the anode chamber. The headspace was also maintained at 100 cm^3, with the evolved gas collected into separate gas bags with FEP on / off valves (Tedlar BagStock No: 24633, Sigma Aldrich, Dorset, UK) attached both to the cathode and anode headspace.

4.5 Flow Rates, pH, Temperature and Current Monitoring in Microbial Electrolysis Cells (MECs)

In order to allow effective comparison in continuous flow reactors the substrate flow rate in MECs has to be controlled. The flow rate in all continuous flow reactors was 36 cm^3 h^{-1} giving 9h hydraulic retention time (HRT) for 326 cm^3 reactor and 5.5h HRT for 200 cm^3 reactor. In order to avoid problems in varying flow rate, the flow rate was checked twice a day and the peristaltic tubing was replaced as necessary. Antibacterial tubes with an antibacterial lining were used to connect the pump peristaltic tubing to the substrate container (Tygon LTD, Hanwell, London, UK). The substrate was supplied to the anode chamber by a Watson Marlow 323Du pump fitted with a MC8 head attached (Watson-Marlow, Cornwall, UK), from a 5 L feed tank in a fridge at 8 ^{o}C).

The substrate pH in the anode chamber remains at 7, as feedstock solution had very high buffering capacity, as described in “Method for Preparing Feed Stock Solution (FS) used for Reactor Operation” section 4.6. The cathode pH however tends to increase as the reaction proceeds. In order to achieve a stable performance for the continuous flow MEC cell, the pH, in the cathode chambers, was maintained at pH 5.3, 7 or 9 via addition of 1.2M hydrochloric acid (HCl), a required for the different experiments.

The temperature was maintained at 23 ± 2 ^{o}C, depending on conditions required for each experiment. Temperature was controlled by recirculation of warm water through the coils of silicone tubing (T10X1ST60, Polymax, Burdon, Hampshire, UK), wound a round the vertical surface area of outer cathode chamber MEC reactors. The water was heated using Grant flow heaters (Grant Instruments, Cambridge, UK) as shown in figures 12 a and 13 b. For logging voltages between cathode and cathode reference and anode and anode reference, electrodes (MF-2052, model RE-5B Ag/AgCl reference electrode, with flexible connector) were used (Fig. 11a, Fig. 12 a and Fig. 13a).

The voltage between and reference electrode and cathode and reference was logged for reference purposes to compare to the values previously reported in literature on hydrogen production. During the course of the experiment, the pH in the cathode chamber, temperature, voltage in cathode and anode chambers and current applied were measured via Labview TM (National Instruments Co., Newbury, UK) system. All outputs were analogue signals logged via a Labview card (NI USB - 6212) on a Viglen Pentium III computer used for data logging at 1 second intervals (see “Appendix A-4” pages 230 - 233 for VI diagrams). Two pH meters / temperature controllers (M300 Model, Mettler-Toledo, Leicester, U.K.) were connected to Model InPro4010/120/PT1000 pH probes (Mettler - Toledo, Leicester, U.K) and the acid dosing pump model 323Du/MC8 (Watson-Marlow Pumps Group,) to maintain pH in the cathode chamber at either 5, 7 and 9, in experiment 1.1, or at pH 5.3 only, in experimental sections 6.1, 6.3 and 6.4 (Fig.13 a).

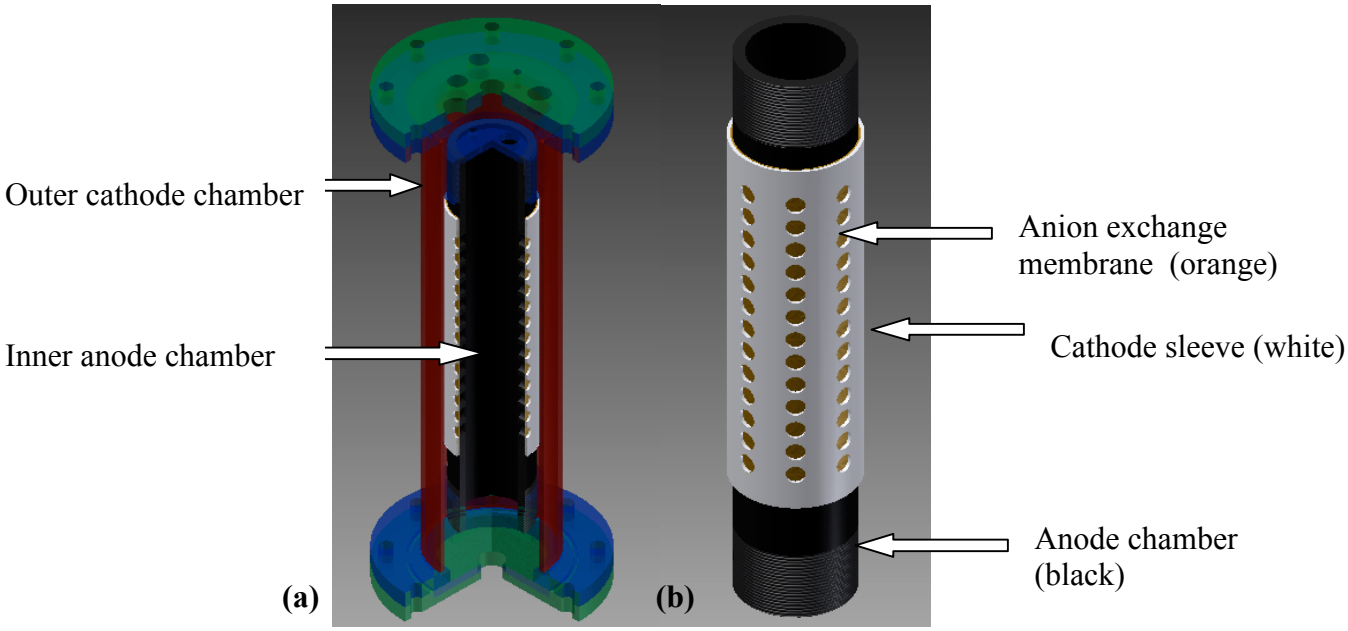

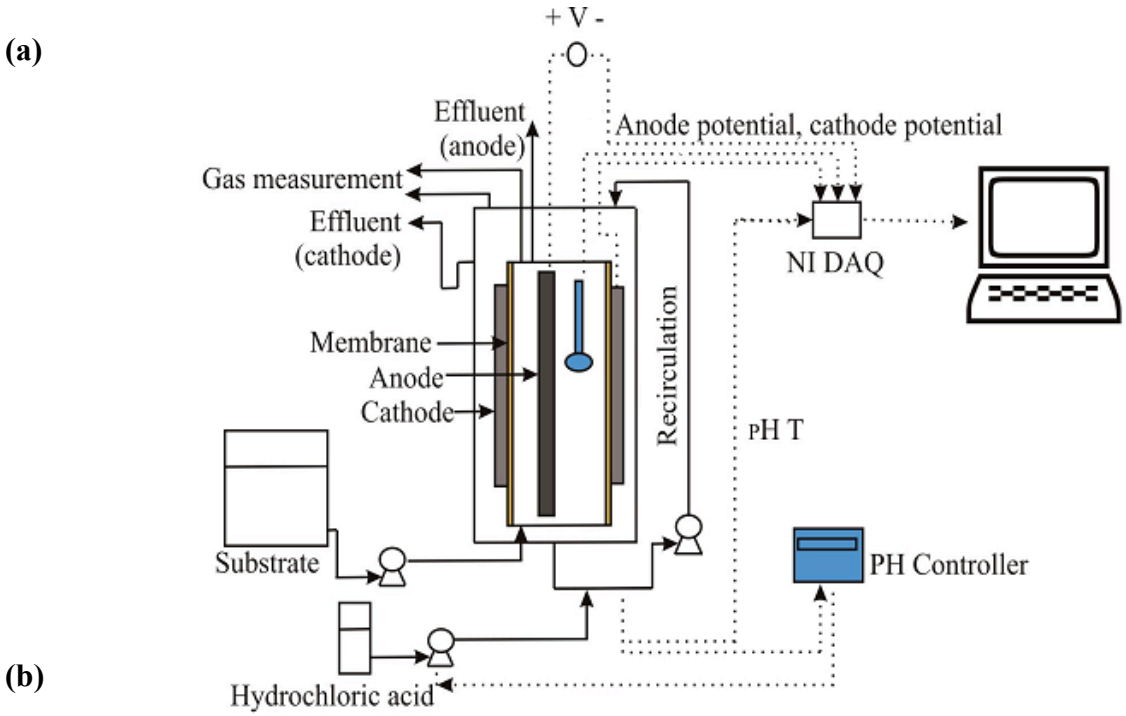

Figure 12 – 3d drawing of cathode and anode chamber assembly (12 a) and anode (12 b).

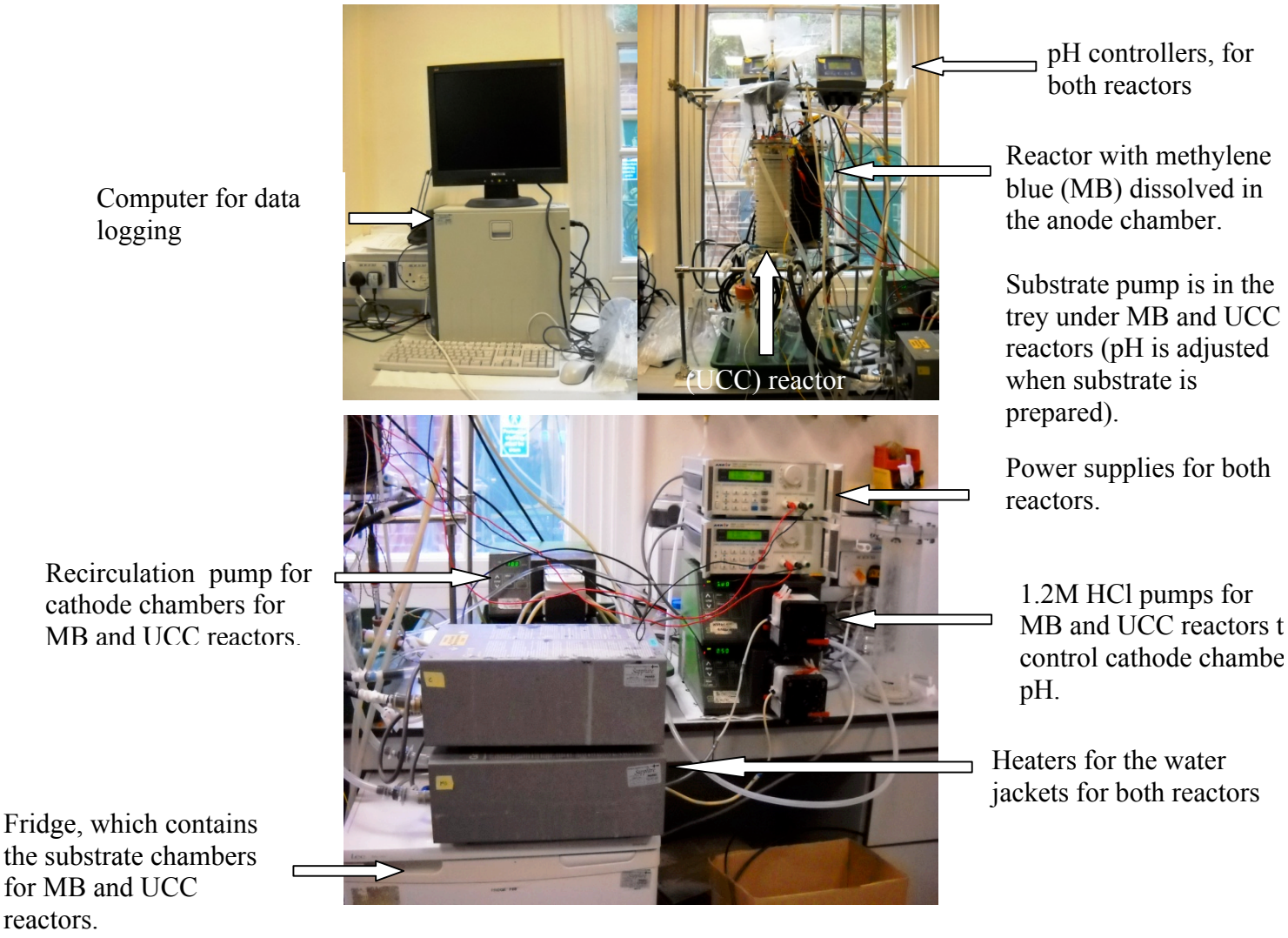

Figure 13 b – Two chamber tubular upflow MEC reactor (13 a) schematic and photograph (13 b).

4.6 Method for Preparing Feedstock Solution (FS) used for Reactor Operation

The feedstock solution (FS) was prepared in 5 L containers filled with media containing acetate or butyrate with concentrations ranging from 5 to 20 mmol L^{-1}, depending on the experimental protocol, as the carbon substrate. The substrate preparation could be split in 2 stages: preparation of buffer solution S1 and preparation of mineral and vitamin solutions S2 and S3. In order to minimize the volume of buffer solution stored, concentrated solution (twice the required concentration) was kept in 20 L container. In buffer solution, the pH changes very little when a small amount of strong acid or bases added to it and thus it is used to prevent changes in the pH of a solution. In the anode chamber it is necessary to keep the correct pH for many electricity or hydrogen producing microorganisms to work.

The substrate solution for MFC and MEC anodes was prepared using concentrated electrolyte solution (S1, 2.5 L), mineral solution (S2, 62.5 cm^3 (see table 3) and vitamin solution (S3, 62.5 cm^3) were added containing nutrients in excess, to promote bacterial growth (Kim et al., 2010, Kim et al., 2009b) diluted with deionized water to 5 L. For cathodes in MECs and two compartment MFCs pure solution S1 (without minerals or vitamins added), diluted by the factor of 2, was used with NaCl (30 g L^{-1}) added to prevent growth of methanogenic archaea.

Concentrated buffer solution S1 prepared as shown on table 3 was kept in 20L container. All buffer, mineral and vitamin solutions were diluted with deionized water, which contained dissolved antifoam (polydimethylsiloxane, Dow Corning), Coventry, UK). Antifoam was used to prevent the build up of foam which represented problems associated with slow drainage in continues flow MEC reactors.

Vitamin and mineral solutions (S2 and S3) were prepared as shown in Table 3. In order to minimize the volumes of vitamin and minerals solutions, twice the required concentration, was made up and stored in 1L containers in the fridge. Prior to use in the experiments the concentrated solution from each 1L container was diluted with deionized water.

Table 3 – Ingredients used to prepare vitamin and mineral solutions S1, S2 and S3.

Buffer solution (S1):		Mineral solution (S2):		Vitamin solution (S3):	
Name:	Weight (g L^{-1}):	Name:	Weight (g L^{-1}):	Name:	Weight (g L^{-1}):
$NaH_2PO_4 \cdot H_2O$	107.6	NTA	1.5	biotin	2
Na_2HPO_4	173.2	$MgSO_4$	3	folic acid	2
KCl	5.2	$MnSO_4 \cdot H_2O$	0.5	pyridoxine (HCl)	10
NH_4Cl	12.4	NaCl	1	riboflavin	5
		$FeSO_4 \cdot 7H_2O$	0.1	thiamin	5
		$CaCl_2 \cdot 6H_2O$	0.1	nicotinic acid	5
		$CoCl_2 \cdot 6H_2O$	0.1	pantothenic acid	5
		$ZnCl_2$	0.13	b-12	0.1
		$CuSO_4 \cdot 5H_2O$	0.01	p-aminobenzoic acid	5
		$AlK(SO_4)_2 \cdot 12H_2O$	0.01	thioctic acid	5
		H_3BO_3	0.01		
		Na_2MO_4	0.025		
		$NiCl_2 \cdot 6H_2O$	0.024		
		$Na_2WO_4 \cdot 2H_2O$	0.025		

4.7 Electrochemical Analysis Methods

4.7.1 Microbial Fuel Cell (MFC) Operation

i) Voltage Monitoring:

For the results in experiment 1.2 (see section 6.1 for details), which was performed simultaneously with experiment 2.1 (see section 6.2 for details), the voltage between the anode and cathode was monitored manually once a day (average of three readings at 11:00, 15:00 and 18:00), across a 150 Ω resistor.

For "The Influence of Changes in Acetate and Butyrate Concentrations and full Substrate Switch on Gas Production from two Microbial Electrolysis Cells (MECs) Acclimated to Acetate and Butyrate" (see section 6.3 for details) and "The Comparison of four Anode Types on the Voltage Production in Microbial Fuel Cells (MFCs) and Hydrogen Production in Microbial Electrolysis Cells (MECs)" (see section 6.4 for details) potential difference across a 1000 Ω resistor signals were measured via labview TM (National Instruments Co., Newbury, UK) based system at 60 second intervals (averages of 60 readings, 1 reading per second), as shown on "Appendix A-4" for VI diagrams and figures 31 and 34.

ii) Power Density Monitoring and Polarization Curves:

The power curve (Fig. 14 a) is one of the ways to assess the performance of a fuel cell and to determine its maximum power. The power performance curve relates to the power delivered across the external load to its impedance. The power delivered is 0 for both an open circuit and a short circuit (infinite and zero external impedance) and is a maximum when the external load impedance matches the internal resistance of the fuel cell (Benziger et al., 2006).

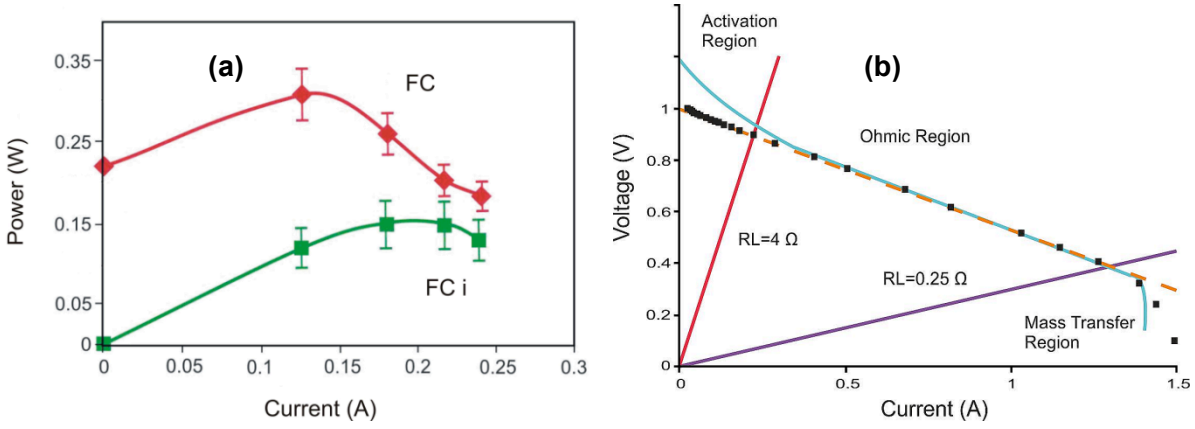

Figure 14 – Sketches of typical power for fuel cells (FC) and (imaginary data, used as an example, 14 a) and polarization (14 b) curves based material published by Bezinger at al (2006).

Polarization curves (Fig. 14 b) allow to determine the differences and/or improvements in mass transport and ohmic regions, as shown in figure 6. The slope ohmic (linear) portion of polarization curves is used to determine internal resistance.

Power density plots were produced once per week (once per batch cycle including start up) when the voltage in MFCs stabilized, 3 days after the substrate was added. Start up refers to one or two week period when MFC reactors were filled with fresh solution containing substrate, vitamins and minerals (80 %), prepared as described in ("Method for Preparing Feed Stock Solution (FS) used for the Reactors", section 4.6), and 20 % sludge (Fan et al., 2007, Liu and Logan, 2004b). At the end of the start up period the sediments were removed, at the end of 1st week, fresh substrate solution was added once per weak, prepared as described in "Materials and Methods" (section 4). One week periods during which the substrate solution (without sludge) was replaced were referred to as batch cycles. MFCs were usually operated for 7-10 batch cycles, same as the number of power density plots produced. For each power density plot the resistance was increased to open circuit resistance (∞), for 2hours, and decreased to lower resistances for ten 1hour periods to allow voltage stabilization until lowest resistance on the variable resistor 10 Ω was reached, as shown on Table 5, for 200 cm^3 MFC (see "Electrochemical Analysis Methods" (section 4.7), for detailed calculations and examples). In literature the power produced is either compared to the volume of anode chamber or anode or cathode surface areas, depending on what performance factors are investigated in the experiment.

iii) Coulombic Efficiency (CE) and Energy Efficiency:

The coulombic efficiency describes the efficiency with which charge (electrons) are transferred in a system facilitating an electrochemical reaction. It correlates charge (coulombs) with the amount of substance (moles) (Liu and Logan, 2004b, Logan et al., 2006). For fuel cells coulombic efficiency is the fraction of coulombs recovered as current per batch cycle (7 day period, between times when the substrate was replaced) divided by the theoretical number of coulombs recovered from the starting organic matter, acetate or butyrate for example. The coulombic efficiency (CE) and energy efficiency for a MFC and MEC in sequencing batch (SBR) operation were calculated via equation 40 (Logan et al., 2006).

$$CE = \sum_{n=1}^{n} \int_{0}^{t} Idt / (CE_t) \times 100 \quad \text{(Logan, 2008)} \qquad \text{Eq 40}$$

Where CE is coulombic efficiency (%), $I\,dt$ (C) is the average of total number of coulombs recovered per batch cycle, from the substrate and (CE_t) theoretical number of coulombs that could be recovered, from the same amount of substrate.

iv) Calculation of Coulombs Recovered as Current (CE):

Total energy recovered from the substrate is the area under the current vs time curve divided by the number of batch cycles (the voltage measured across the resistor (each data point on the curve) as shown in figure 15 converted into current via Eq 41 (Logan, 2008):

Current (*I*) *I* = Voltage (*V)* / resistance (*R)* Eq 41

Each MFC reactor was re filled with fresh substrate once a week (reason for dividing curve total area by the number of batch cycles) and the total number of coulombs recovered from current increases as the number of microbes in the biofilm on the anode surface increases, with each batch cycle represented as arrow (Fig. 15). During 1st batch cycle almost no current was produced and only small amount of substrate was consumed. During 2nd batch cycle the amount of current produced and substrate consumed goes up. During 3rd batch cycle the amount of current produced and substrate consumed stabilizes. After 3rd batch cycle the biofilm continues to grow slowly hence current and energy recovered from substrate slowly goes up from batch cycle 3 to batch cycle 7.

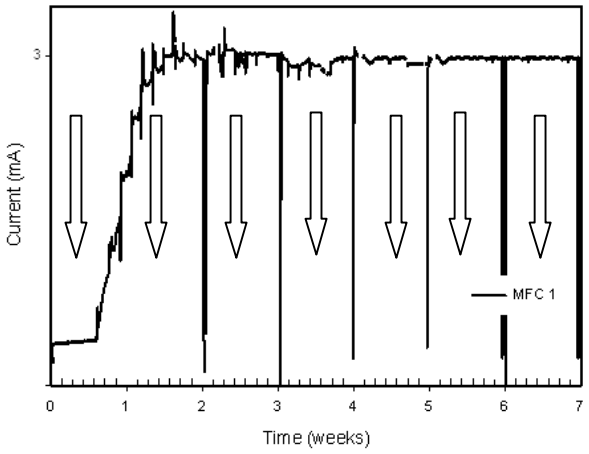

Figure 15 – A sketch of a typical power current vs time (hours) curve.

v) Calculation of Theoretical Number of Coulombs (CE_t) Recovered from Starting Organic Matter:

Theoretical number of coulombs (CE_t) refers to coulombs recovered from the starting organic matter, assuming 100 % of starting organic substrate is converted into current. It does not take looses associated with ionic transport into the account.

Theoretical number of coulombs (CE_t) = z (electrons per mol of substrate) × F (Faradays constant) × n (number of moles of substrate, in 200 cm^3 MFC reactor) (Logan, 2008). Eq 42

n (number of moles of substrate, in 200 cm^3 MFC reactor) is 0.02 mmol L^{-1} × 0.2L=0.004mol of acetate or butyrate Eq 43

Theoretical CE values for the coulombs that could be recovered from 20mmol L^{-1} acetate and butyrate is calculated as follows: one acetate molecule requires 8 electrons and one butyrate molecule requires 20 (4 electrons from butyrate oxidation and 16 electrons for 2 acetate molecules produced from butyrate, if a two step process is considered (Liu et al., 2005b).

Theoretical Coulombic Efficiency (CE_t) for 20 mmol L^{-1} Acetate:

8 mole e^- /mole (electrons per mol of substrate) × 96485 c/mole e^- (Faradays constant) ×
× 0.004 mol (in 200 cm^3 MFC reactor) = 3088 c (Logan, 2008) Eq 44

Theoretical Coulombic Efficiency (CE_t) for 20 mmol L^{-1} Butyrate:

20 mole e- /mole (electrons per mol of substrate) × 96485 c/mole e^- (Faradays constant) ×
× 0.004mol (in 200 cm^3 MFC reactor) = 7719 c (Liu et al., 2005b) Eq 45

vi) Energy Efficiency (E):

Energy recovery compares the energy recovered from the system to energy stored in the starting material. It correlates the energy recovered with the amount of substance (moles) and heat of combustion of organic substrate (Logan, 2008).

$$E = \sum_{n=1}^{n} \int_{0}^{t} Pdt / (E_t) \times 100 \quad \text{Eq 46}$$

Where E is energy recovered (%), *P dt* (Joules) is the average of total number of Joules recovered per batch cycle, from the substrate and (E_t) theoretical number of Joules that could be recovered, from the same amount of substrate.

Calculation of Energy Recovered as Current (P):

Total energy recovered from the substrate is the area under the power vs time curve, is divided by the number of batch cycles, where the voltage across the resistor (each data point on the curve, see figure 15 is converted into power using:

$P = V^2/R$ (Logan, 2008), where V= voltage (V) *R* is external resistance (Ω) Eq 47

Calculation of Theoretical Energy (E_t) Recovered from Starting Organic Matter:

Theoretical energy recovered (E_t) refers to the Joules recovered from starting organic matter, if 100% of starting material is converted into current. It does not take looses associated with ionic transport into the account.

Theoretical number of coulombs (CE_t) = E (energy recovered per mol of substrate) × n (number of moles of substrate, in 200 cm^3 MFC reactor). Eq 48

Where n (number of moles of substrate, in 200 cm^3 MFC reactor) is 0.004 mol for 20mmol L^{-1} acetate or butyrate solution (see equation 41 - 45).

Theoretical Energy Recovery (E_t) for 20 mmol L^{-1} Acetate:

Enthalpy change of combustion for acetate ($\Delta H_{combustion}$)= -875200J/mol (Logan, 2008, Logan et al., 2008)

*E*t = (-875200J/mol ($\Delta H_{combustion}$)) x 0.004mol (in 200 cm^3 MFC reactor)= 3501J Eq 49

Theoretical Energy Recovery (E_t) for 20 mmol L^{-1} Butyrate:

Enthalpy change of combustion for acetate ($\Delta H_{combustion}$)= -2183500J/mol (Lebedeva, 1964, Linstrom and Mallard, 2010)

*E*t = -(-2183500J/mol ($\Delta H_{combustion}$)) x 0.004mol (in 200 cm^3 MFC reactor) = 8734J Eq 50

The theoretical energy (E_t) recovered from butyrate is always higher than energy recovered from acetate because enthalpy change of combustion for butyrate is higher (Liu et al., 2005b).

4.7.2 Cyclic Voltammetry Tests on the Liquid Samples

Cyclic voltammetry (CV) is generally used to study the electrochemical properties of an analyte in solution and/or determine its reduction and oxidation potential peaks. For this work however cyclic voltammetry examination was performed in order to determine whether methylene blue was adsorbed on the electrode surface without bacteria and to investigate if cytochorome redox peaks (enzyme present in exoelectrogenic bacteria) were taller on the plot for effluent samples from MFC that produced higher voltage.

Cyclic voltammetry is a type of potentiodynamic electrochemical measurement. In a cyclic voltammetry experiment the working electrode potential is ramped linearly versus time like linear sweep voltammetry (Cheng et al., 2009).

Unlike sweep voltammetry, which ends when it reaches a set potential, the working electrode's potential ramp is inverted in cyclic voltammetry and this inversion can happen multiple times during a single experiment (Bard and Faulkner, 2001). The current at the working electrode is plotted versus the applied voltage to give the cyclic voltammogram trace.

i) Preparation of Mediator Treated Anode Material for CV Scans

In order to investigate physico-chemisorption of MB on the carbon electrode, cyclic voltammetry tests were conducted in the electrolyte S1 solution diluted by the factor of 2 (prepared as described in "Method for Preparing Feed Stock Solution (FS) used for the Reactors") at pH 7, respectively (Fig. 23). Four electrodes were prepared:- untreated carbon cloth (control), methylene blue in buffer solution with untreated carbon cloth anode (MB in solution), methylene blue treated carbon cloth (MB) prepared using 1.56 mmol L^{-1} solutions as described in experiment 2 ii, after 4 buffer washes.

ii) Preparation of Liquid Samples for CV Scans

For effluent samples obtained at the end of each batch operation cycle each sample was split into two. The first one was taken to analysis, and the second one was centrifuged in a Sorvall Legend P 76^{TM} T centrifuge (Kendro Laboratory Products Plc, Bishop's Stortford, UK) for 10 minutes at 13400xg, same as samples used for COD analysis. Cyclic voltammetry (CV) was performed on 3 samples:- (a) the MFC culture in its medium (see figure 24, for experimental result), (b) the supernatant of centrifuged MFC culture and (c) the MFC culture after centrifugation and re-suspension (Logan et al., 2006). Experiments a, b and c produced exactly the same results.

iii) Procedure for CV Scans

In these experiments, the working electrode potential was linearly ramped versus time; then, when the potential changed it was repeated in the reverse direction. The measurement cycle was conducted in multiplicate during the experiment, 3 times (-0.7 OC, 0.7 OC, 10mV/S, x3), where OC is open circuit. The current on the working electrode (y axis) was plotted against the applied voltage to produce the cyclic voltammogram (x axis).

4.7.3 Microbial Electrolysis Cell (MEC) Operation

Unlike MFCs that were operated in sequencing batch mode microbial electrolysis cells (MECs) were operated in continuous flow mode, which had to be taken into account when coulombic efficiency (CE) was calculated. The voltages between the anode and the reference electrode in the anode chamber and cathode and the reference electrode in the cathode chamber and the voltage across 1Ω resistor connecting the power supply via labview TM (National Instruments Co., Newbury, UK) system was used for data logging at 1 second intervals for experiment 1 and at 60 second intervals (averages of 60 readings, 1 reading per second, for experiments 2 and 3) and all outputs were analogue signals installed on a Viglen Pentium III computer (see "Appendix A-4" for VI diagrams). Averages of 60 readings were used in experiments 3 and 4 to reduce the number of data points on the plot.

The data was extracted on daily basis and the averages for anode vs anode reference and cathode vs reference electrodes were calculated by adding all values in anode and cathode columns, separately. The sums of voltages in each column were divided by 1440 (minutes in 24hours). For data recorded voltages across 1 Ω resistor each data point was converted into current using equation 30, divided by 75 cm^2 (cathode surface area) and multiplied by 1000 to get values in A m^{-2} and added to graph time (weeks (x axis) vs current density (A m^{-2})). The standard performance factors for MEC performance are coulombic efficiency (CE), cathodic hydrogen recovery (actual hydrogen production divided by the amount of hydrogen produced) and hydrogen yield per mol of substrate destroyed calculated as previously described by Logan et al (2006). The amount of hydrogen produced on daily basis had to be determined via gas chromatography see "Offline Analysis Methods" section 4.8 for more details) of the contents of the gas bags and the amount of acetate or butyrate consumed had to be determined offline. In literature the amount of gas produced is either compared to the volume of anode chamber or anode surface area. For all experiments performed the gas production was compared to the volume of anode chamber in order to allow comparison with other work performed by the research group at the Univeristy of South Wales. The substrate concentration was determined via chemical oxygen demand (COD) analysis (see "Offline Analysis Methods" section 4.8 for more details).

i) Coulombic Efficiency (CE) and Energy Efficiency:

For continuous flow microbial electrolysis cells coulombic efficiency (CE) is the fraction of coulombs recovered as current per 8 or 9 hour cycle (hydraulic retention time, time needed for electrolyte to pass through the reactor) divided by the theoretical number of coulombs recovered from the starting organic matter, acetate or butyrate for example (see equations 13 - 23, and 14 - 25). All other calculations were performed in exactly the same way, as previously described in "Electrochemical Analysis Methods" section 4.7.

ii) Cathodic Hydrogen Recovery ($rH_{2(cat)}$) and Analysis of Hydrogen Obtained in Gas Bags:

Cathodic hydrogen recovery compares the amount of hydrogen produced by microbial to electrolysis cell per 24 h to theoretical amount of hydrogen recovered from the current in the system (for determining actual amount of hydrogen measured on daily basis, see "Electrochemical Analysis Methods" section 4.7 and "Results" (section 6) for examples).

iii) Theoretical Amount of Hydrogen Produced for the Current Measured Across 1Ω Resistor ($rH_{2(cat)}$):

From Faradays second law 2F (2x96500 c mol^{-1}≈2 $x10^5$ c mol^{-1})

is required to liberate 1mol of hydrogen at the cathode (Logan, 2008, Logan et al., 2008) and the expected production rate (cm^3) is 10×I (current calculated from the voltage logged across 1 Ω resistor (mA)), so that 1 mA gives theoretical 1 cm^3 of hydrogen. Eq 51

iv) Calculating Cathodic Hydrogen Recovery ($rH_{2(cat)}$):

The cathodic hydrogen recovery (r_{Cat}, %) is actual hydrogen production rate (n_{H2}, cm^3, manually measured once a day via gas chromatography) divided by the expected hydrogen production rate (calculated from current measured across 1Ω resistor between power supply

and cathode (n_{CE})): $$\frac{n_{H2}}{n_{CE}} = r_{Cat}$$ Eq 52

(Logan et al., 2008)

Values for r_{Cat} previously reported in literature range from 31% (Nam et al., 2011) to 100% (Logan et al., 2008).

v) Overall Hydrogen Yield and Hydrogen Yield per mol of Substrate Destroyed:

Overall hydrogen yield compares the volume of hydrogen produced by the microbial electrolysis cell per 24h to the theoretical volume of hydrogen that could recovered if it undergoes 100% oxidation (for determining actual amount of hydrogen measured on daily basis, see "Offline Analysis Methods" section 4.8). It is also possible to determine number of mols of hydrogen produced per mol of substrate utilized (Logan et al., 2008).

Theoretical Volume of Hydrogen Produced from the Substrate Consumed:

The substrate concentration for influent and effluent was determined via chemical oxygen demand (COD) analysis from which the amount of substrate (acetate or butyrate, mg L^{-1}) utilized by the bacteria in 24 hours in the microbial electrolysis cell (MEC) was calculated. The theoretical amount and the volume of hydrogen produced from the substrate oxidation (n_s) was calculated from the change in the amount of substrate concentration of substrate in the influent.

Overall Hydrogen Recovery and Hydrogen Yield per mol of Substrate Consumed:

Overall hydrogen yield (%, Y_{H2}) is the volume of hydrogen produced by microbial electrolysis cell (MEC) every 24h, (n_{H2}, cm^3, manually measured once a day via gas chromatography) divided by theoretical volume of hydrogen (n_s) that could recovered if it undergoes 100% oxidation (Logan et al., 2008), for determining actual amount of hydrogen measured on daily basis, see "Offline Analysis Methods" section 4.8, described by equation 52:

$$\frac{n_{H2}}{n_S} = Y_{H2} \qquad \text{Eq 53}$$

(Logan et al., 2008)

vi) Hydrogen Yield per mol of Substrate Destroyed:

Using the equivalence statement 1g COD (organic material utilized) ≡ 1400 cm^3 of hydrogen produced at the cathode calculated from the equations and procedures used in Gavala et al (2006), Logan (2008), Logan et al (2008), at standard conditions (298K and 1ATP pressure. The amount of substrate (acetate or butyrate, mg L^{-1}) utilized by the bacteria in 24 hours in microbial electrolysis cell (MEC)) was determined first and then converted into hydrogen that could be produced from substrate utilization.

The actual hydrogen production rate (n_{H2}, cm^3, manually measured once a day) divided by the theoretical volume of hydrogen (n_{COD}) that could recovered from the amount of utilized substrate, (see section 4.7.5, for examples to determine hydrogen recovery based on the COD reduction (Y_{COD}), (Logan et al., 2008).

$$\frac{n_{H2}}{n_{COD}} = Y_{COD} \qquad \text{Eq 54}$$

(Logan et al., 2008)

From the stoichiometry (1 mol of acetate produces 4 mol of hydrogen (equations 19 - 23) and 1 mol of butyrate produces 10 (2+4+4) mol of hydrogen (equations 14 and 25). It is possible to calculate yield of hydrogen per mol of substrate destroyed ($Y_{H2\ per\ mol\ substrate\ destroyed}$) (Cheng and Logan, 2007a).

4.7.4 Experimental Methodology and Example Online Calculations for Microbial Fuel Cells (MFCs)

i) Coulombic Efficiency (CE) and Energy Efficiency:

The coulombic efficiency (CE) and energy efficiency for sequencing batch (SBR) operation were calculated, as previously described in "Electrochemical Analysis Methods" section 4.7. The voltage readings for voltage production vs time curve similar to that in figure 36 are converted into current area under AC curve (Fig. 15). CE is the fraction of coulombs recovered as average of 60 current readings recorded in a minute (CE_p, currents recorded) divided by the theoretical number of coulombs (CE_t) recovered from the starting organic matter, acetate or butyrate (see "Electrochemical Analysis Methods" section 4.7 for details).

ii) Calculation of Coulombs Recovered as Current (CE):

Total number of coulombs (amperes per second) recovered from current is the area under the current vs time curve (Fig. 15), divided by the number of batch cycles, for example experiment it's area under control MFC (AC) curve divided by 7 (number of weeks, because each batch cycle was 1 week long). If the voltage was recorded manually 3 times a day it was assumed that same voltage was produced per minute between times the voltage was recorded. If voltage was logged on line and it was assumed that same voltage was produced per second for each average of 60 readings per minute, so (CE_p, currents recorded (4.2336×10^6 data points divided by 7 weeks) divided by the theoretical number of coulombs (CE_t) recovered from the starting organic matter, acetate or butyrate (see "Electrochemical Analysis Methods" section 4.7 for details).

The reason MFC data was recorded manually experiments in "The Effect of Immobilized Methylene Blue and Neutral Red on the Current Production in Microbial Fuel Cells (MFCs)" section 6.2 was due to problems with data acquisition system. The reason the current was not recorded one reading per second for experiments involving use of acetate and/or butyrate as substrate (see "Results" sections 6.3 and 6.4 for details) was background noise caused by connection problems (sloppy soldering on the wires connected to each other and moist in the air), so that the averages provide more accurate results. The values were then converted into current separately, for each value, and added together. Replacing substrate in MFCs on weekly basis is a standard operating procedure for all MFCs used in publications to allow comparison between work done on all projects by the research team).

The example practical values, in coulombs, are 1820 c for MFC (operated on acetate AC) and 1850 c for MFC (operated on butyrate BU). Theoretical number of coulombs (CE_t) refers to coulombs recovered from starting organic matter, if 100 % of starting material is converted into current calculated as shown in the "Electrochemical Analysis Methods" section 4.7. For acetate in 200 cm^3 MFC CE_t= 3088 c and for butyrate CE_t= 7719 c. Table 4 represents practical values divided by theoretical CE values multiplied by 100.

iii) Calculation of Energy Recovery (E):

The energy recovery (E) is the fraction of coulombs recovered as current per batch cycle (E_p, 7 day period, between times when the substrate was replaced) divided by theoretical energy recovery (E_t).

Practical energy recovery (E_p) is calculated in exactly the same way as (CE_p) where the only difference is power used instead of current, from the voltage per second, as described in "Electrochemical Analysis Methods" section 4.7. The practical values used as example, in Joules, are 630 J for MFC (AC), 655 J for MFC (BU).

Theoretical energy recovery (E_t) is calculated, as described in the "Electrochemical Analysis Methods" section 4.7, which is 3501 J, for MFC (AC) and 8734 J, for MFC (BU).

Table 4 – Comparison of coulombic efficiency (CE) and energy recovery (E) values for example MFCs (BU and AC).

Substrate	MFC	CE_p (c)	CE_t (c)	CE (%)	E (%)	E_p (J)	E_t (J)
butyrate	BU	1850	7719	26	7.5	655	8734
acetate	AC	1820	3088	59	18	630	3501

i) Power Density Monitoring:

Knowing the coulombic efficiency (CE) and energy recovery (E) does not sufficiently describe how the power is generated by specific microbial fuel cell (MFC) architecture. Power is normalized across the volume of the anode chamber or anode surface area is another performance factor, which has to be assessed, compulsory for publications in journals such as "Biotechnology and Bioprocess Engineering". Power density plots (Table 5) were created as described in "Electrochemical Analysis Methods" section 4.7.

Table 5 – Example power density plot data for microbial fuel cell (MFC) with acclimated to butyrate (BU) and acetate (AC) .

	Resistance (Ω)	Voltage (mV)	Current (mA) I=V/R	Power (mW) $P=V^2/R$	Power (W m^{-3})
MFC (BU) (wk 7)	10	21	2.10	0.04	0.22
	40	90	2.25	0.20	1.01
	60	135	2.25	0.30	1.52
	100	200	2.00	0.40	2.00
	150	250	1.67	0.42	2.08 (P_{max})
	300	310	1.03	0.32	1.60
	500	347	0.69	0.24	1.20
	700	356	0.51	0.18	0.91
	1000	500	0.0	0.00	0.00
	400000	530	0.00	0.00	0.00
	∞	550	0.00	0.00	0.00
MFC (AC) (wk 7)	10	36	3.60	0.13	0.65
	40	130	3.25	0.42	2.11
	60	175	2.92	0.51	2.55
	100	240	2.40	0.58	2.88 (P_{max})
	150	278	1.85	0.52	2.58
	300	330	1.10	0.36	1.82
	500	360	0.72	0.26	1.30
	700	375	0.54	0.20	1.00
	1000	390	0.39	0.15	0.76
	400000	550	0.00	0.00	0.00
	∞	550	0.00	0.00	0.00

Power (W) is for 200 cm^3 MFC chamber. 1 m^3= Power (W) / 200 cm^3 ×10^6

All plots were produced for microbial fuel cells (MFCs) acclimated to 23±2 ^oC, as an example

For each power density plot the resistance was increased to the open circuit resistance (∞), for 2 hours, and decreased to lowest resistance 10 Ω, for 1 hour periods, for 200 cm^3 MFCs used in all experiments. The data was used to plot figure 16. Power density plots were created once a week 4 days after substrate was added to sludge and then 4 days after the substrate was replaced in MFCs, if operated in sequencing batch (SBR) mode. Data in Table 5, with maximum power densities marked as (P_{max}) can then be converted into figure 16 with (P_{max}) as tallest peaks on power density plots. P_{max} values slowly increase every week and shift from high to low resistance region. The current at 10 Ω resistance also increased (measured as shown on Table 5) as biofilm was established on the anode surface for all experiments. Currents and power densities at 10 Ω resistance from power density plots were used to create figure 17.

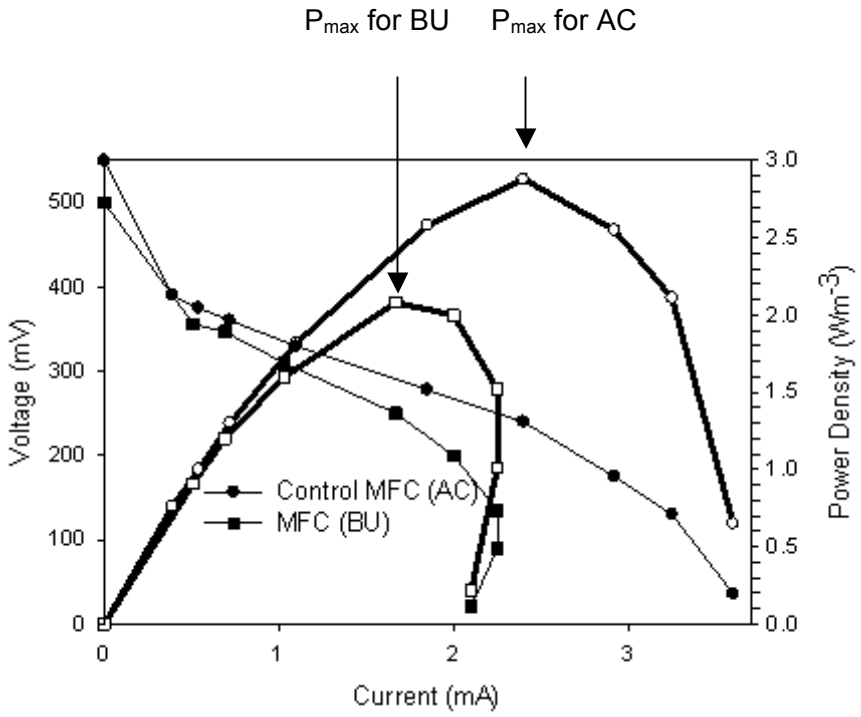

Figure 16 – Power density plot (open symbols) and polarization plot (closed symbols). For space reasons only closed symbol key shown but symbol shape is same for the reactors for the power densities when the symbol is open.

Currents at low resistances are good indicators of anaerobic respiration, where the anode acts as artificial final electron acceptor for electrogenic bacteria. Microbial electrolysis cells (MECs) which are operated at low (1 - 10 Ω) resistances utilize electrogenic bacteria, so one of the aims of this work was to check if anode from MFC producing high currents at 10 Ω region does produce more hydrogen when transferred into MEC.

Similar plots to figure 17 (p. 84) can be produced for powers at low resistances and P_{max} values depending on what data is needed to support results for a particular publication or patent.

The error bars for these histograms in “Results” section 6 are based on variations from the average for experimental repeats (standard deviations) for experimental repeats (usually 3, see “Analysis” 4.7 and 4.8 and “Experimental Regime” section 5).

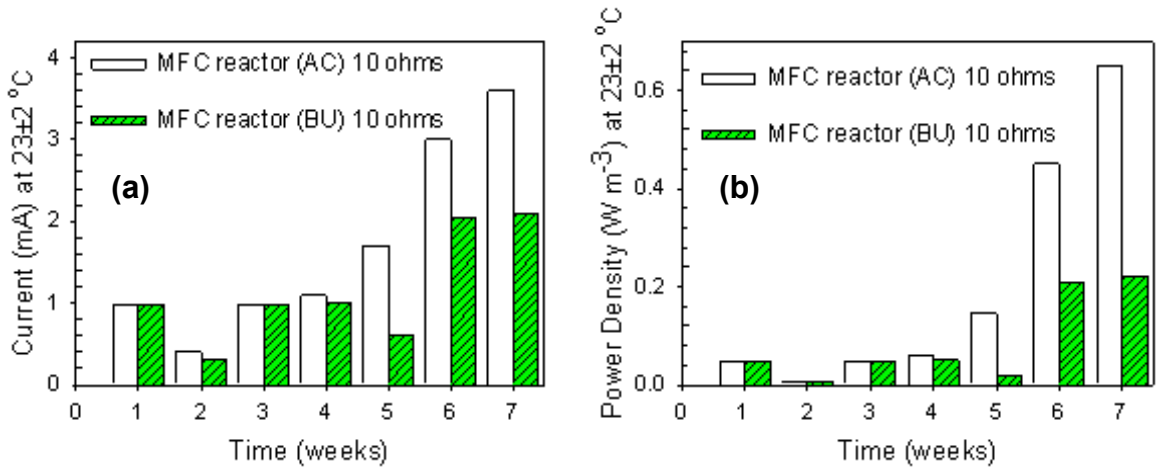

Figure 17 – Histograms that shows a gradual increase in current (a) and power density (b) for MFCs (AC and BU) during 7 week period.

4.7.5 Experimental Methodology and Example Online Calculations for Microbial Electrolysis Cells (MECs)

Calculations for the Performance Factors

All performance factors, described in "Electrochemical Analysis Methods" section 4.7, such as coulombic efficiency (CE), cathodic hydrogen recovery (r_{cat}), see equation 51, overall hydrogen recovery (Y_{H2}), see equation 52, hydrogen yield with respect to the substrate consumed ($Y_{H2\ per\ mol\ substrate\ destroyed}$), see equation 53, were calculated, from data obtained, as shown below, based on Logan (2008). The calculations were exactly the same as in "The Influence of pH and Temperature on Hydrogen Production in Continuous Flow Microbial Electrolysis Cell (MEC) Reactor " with the only difference being the HRT, was changing from 8.1 to 9.6 h instead of 9 h, because tubing was replaced. Calculations of CE and hydrogen yield were different for butyrate one molecule which requires 20 instead of 8 electrons (as required for one acetate molecule) to completely converted into hydrogen and carbon dioxide (Liu et al., 2005b, Cheng and Logan, 2007a).

For daily performance factors calculations liquid and gas samples were collected every 24 hours for microbial electrolysis cell operated on acetate (MEC AC) and for MEC operated on butyrate (MEC BU). Lets consider following experimental results: COD reduction of 240 mg COD L^{-1} obtained experimentally but initial COD reduction for 10 mmol L^{-1} acetate solution 640 mg COD L^{-1}. COD reduction (478 mg COD L^{-1}) is obtained for butyrate experimentally, but initial 10 mmol L^{-1} butyrate solution gives 1625 mg COD L^{-1}. Please see "Offline Analysis Methods" (section 4.8) for detailed description of COD analysis, where the concentration of organic material is determined via indirect dichromate oxidation method where change in color. The gas production is 42 cm^3 day^{-1} (MEC AC) and 65 cm^3 day^{-1} (MEC BU) and currents measured across 1 Ω resistor are 9.2 A (MEC AC) and 11.7 A (MEC BU). These specific examples are not results but based on them to show how all MEC performance factors were calculated.

i) Calculation of Coulombic Efficiency (CE) Using Experimentally Obtained Results:

$$1\text{gCOD} \equiv \frac{1}{16}\text{mol } H_2 \equiv \frac{1}{8} \times F \equiv \frac{1}{8} \times 96500 \text{ c mol}^{-1} \qquad \text{Eq 55}$$

(Logan, 2008, Logan et al., 2008)

COD reduction (240 mg COD L^{-1}) is obtained experimentally but initial 10 mmol L^{-1} acetate solution (640mg COD L^{-1}), so 640 - 240 = 400 mg COD L^{-1} is consumed by the bacteria, a COD reduction of 400 / 640×100 = 62.5 % in 8.15 hours, time taken for the substrate solution to pass through the anode chamber in MEC reactor. COD reduction (478 mg COD L^{-1}) is obtained experimentally but initial 10 mmol L^{-1} butyrate solution (1625 mg COD L^{-1}), so 1625- - 478 = 1147 mg COD L^{-1} is consumed by the bacteria, a COD reduction of 1147 / 1628 × ×100 = 70.5 % in 9.58 hours, time taken for the substrate solution to pass through the anode chamber in MEC reactor.

Calculating COD Reduction in an Hour:

[(COD degraded in 1h, mg COD)×(F, c mol^{-1}) / (number of electrons needed for substrate oxidation)], represented by the equation below (Logan, 2008, Logan et al., 2008):

For acetate:
COD degraded in 1h = (COD in from 10 mmol L^{-1} acetate)×(anode chamber volume (L)/ hydraulic retention time (HRT)) × (COD reduction %)=(640mg L^{-1}) × (0.326L/8.15h) × 0.625= = 16.0 mg COD (Logan, 2008, Logan et al., 2008). Eq 56

For butyrate:
COD degraded in 1h = (COD in from 20 mmol L^{-1} butyrate)×(anode chamber volume (L)/ hydraulic retention time (HRT))×(COD reduction %)=(1625mgL^{-1})×(0.326L/9.58 h)×0.705= =39.0 mg COD (Cheng and Logan, 2007a, Liu et al., 2005b). Eq 57

Calculating CE from COD Reduction in an Hour:

For acetate:

$$\left[\frac{16\times 96500}{8}\right] = [I(mA)\times 3600], \text{ so } [16\times 96500]\div[3600\times 8] = I\ (mA), \text{ for 1g COD} \quad \text{Eq 58}$$

Current needed to convert acetate into water and CO_2 = *I (mA)* = 53.6 mA acetate.
Current observed across 1 Ω resistor is 9.2 mA, hence CE= (9.2/53.6)×100=17.2 % for acetate (Logan, 2008, Logan et al., 2008).

For butyrate:

$$\left[\frac{39\times 96500}{20}\right] = [I(mA)\times 3600], \text{ so } [39\times 96500]\div[3600\times 20] = I\ (mA), \text{ for 1g COD} \quad \text{Eq 59}$$

Current needed to convert butyrate into water and CO_2 = *I (mA)* = 52.3 mA

Current observed across 1 Ω resistor is 11.7 mA, hence CE= (11.7 /52.3)×100 = 22.4 % (Cheng and Logan, 2007a, Liu et al., 2005b).

ii) Calculation of Cathodic Hydrogen Recovery (r_{cat}):

From Faradays second law 2 F (Faradays) is required to liberate 1mol of hydrogen at the cathode (Logan, 2008, Logan et al., 2008), so current 9.2 mA produces 92 cm^3 of hydrogen for MEC (AC), in theory, and current 11.7 mA produces 117 cm^3 of hydrogen for MEC (BU), in theory.

For acetate:
The cathodic hydrogen recovery is actual hydrogen production rate (42 cm^3 day^{-1}, measured experimentally) divided by the expected hydrogen production rate (92 cm^3 day^{-1}) = 45.6 %, for acetate (Logan, 2008, Logan et al., 2008).

For butyrate:
Actual hydrogen production rate (65 cm^3 day^{-1}) at pH 5.3 and the temperature 25 ^oC divided by the expected hydrogen production rate (117 cm^3 day^{-1}) = 55.5% for butyrate (Cheng and Logan, 2007a, Liu et al., 2005b).

iii) Calculation of the Hydrogen Yield with Respect to the Substrate Consumed ($Y_{H2\ per\ mol\ substrate\ destroyed}$):

1g COD ≡ 1400 cm^3 of hydrogen produced at the cathode taken from standard operating procedure (SOP) manual calculated from equations in Gavala et al (2006), Logan (2008) and Logan et al (2008). Eqs 1

Calculating COD Reduction in 24 Hours:

For acetate:
In a day, COD converted is COD converted in an hour×24 h= 16.0 mg×24h=
=384 mg COD (Logan, 2008, Logan et al., 2008) Eq 60

For butyrate:
In a day, COD converted is 39 mg × 24h = 936.0 mg COD (Cheng and Logan, 2007a, Liu et al., 2005b) Eq 61

From this value the number of moles of hydrogen produced per mol of substrate can be calculated:

Calculating Hydrogen Yield from COD Reduction in 24 Hours:

For acetate:

Actual amount of hydrogen produced in a day is: (experimentally measured amount of hydrogen produced in a day)/((COD converted in a day)×(amount of hydrogen produced per gram of COD)= (42 cm^3)/(0.384 g×1400)×100=7.8 %

(Logan, 2008, Logan et al., 2008). Eq 62

In theory 1mol of acetate gives 4mol of hydrogen. 7.8×4/100=0.31mol mol^{-1} Eq 63

For butyrate:

Actual amount of hydrogen produced in a day is: (experimentally measured amount of hydrogen produced in a day)/((COD converted in a day)×(amount of hydrogen produced per gram of COD) = (65 cm^3) / (0.936 g × 1400) × 100 = 5.0 %, for butyrate (Cheng and Logan, 2007a, Liu et al., 2005b).

In theory 1mol of butyrate gives 10 mol of hydrogen. Butyrate consumed and
5 × 10/100 = 0.5 mol mol^{-1} of butyrate are consumed.

4.8 Offline Analysis Methods

4.8.1 Gas Composition Analysis

The gas syringe was flushed 3 times with nitrogen prior to taking samples from the gas bags attached to the head space in the anode chamber on microbial fuel cells (MFCs) and anode and cathode chambers for the microbial electrolysis cells (MECs). A sample of 5-10 cm^3, depending on how much gas was produced was taken and injected into micro gas chromatographer (Varian Ltd, Walton-upon-Thames, UK). The syringe was flushed four times with the gas bag contents before the final sample was taken. A Varian CP-4900 Micro-GC Varian Ltd, Walton-upon-Thames, UK) was used for the gas composition analysis. The GC was equipped with a thermal conductivity detector and two columns: a MolSieve 5Å Plot column which separates H_2, CO, CH_4, N_2 and O_2 ; and a HayeSep A, column which separates O_2, CH_4, C_2H_2, C_2H_4, C_2H_6 and CO_2. The injected gas sample was split on both columns. The GC was operated at an oven temperature of 150^oC and column pressure of 30 psi for the MolSieve 5Å Plot column and at an oven temperature of 60^oC P, column pressure 20 psi for the HayeSep A column. The carrier gas was argon. By activating the start option within the data handling package, a vacuum pump drew the gas sample through a loop (10 µl) and then the injector injected the gas sample from the sample loop into the carrier gas stream. The run time was 1 minute. The GC was calibrated for H_2, CO_2, CH_4 and N_2 using calibration gases of the following compositions:

Gas 1: 5%H_2 and 95%N_2 (BOC, Guildford, UK)
Gas 2: 100%H_2 (BOC, Guildford, UK)
Gas 3: 40%CO_2 and 60% CH_4 (BOC, Guildford, UK)
Gas 4: 100% CO_2 (BOC, Guildford, UK)
Gas 5: 10.047% H_2, 30.256% N_2, 27.764% CH_4 and 31.933% CO_2 (Scientific and Technical Gases Ltd., Newcastle-under-Lyme, UK)
Gas 6: 19.901% H_2, 30.150% N_2 and 49.949% CH_4 (Scientific and Technical Gases Ltd., Newcastle-under-Lyme, UK)

The calibration was checked daily when machines were started up.

4.8.2 Liquid Sample Analysis

i) Inoculum Characterization

Anaerobic digester sludge from a mesophilic sewage digester (Cog Moors Sewage Treatment Works, Cardiff, UK), was used as an inoculum. Typical total solids (TS) = 24.8 ± 0.1g/L, ash content (TA) = 11.5 ± 0.1g/L, total volatile suspended solids (TVS) and pH 7.52, see "Offline Analysis Methods" (section 4.8) for details). The inoculum was stored for up to 7 weeks, at room temperature, in a sealed vessel before use.

ii) Total solids (TS)

Total solids were determined for inoculums used for 10 cm^3 homogeneous samples for the bioelectrochemical cells (BESs) by standard method APHA (1989). Total solids were determined by drying in an oven (Gallenkamp, Leicester, UK) to constant weight at 103 ^oC – 105 ^oC. The increase in weight over that of the empty container represented the total solids. Because of the particulate nature of the samples, wide bore pipettes were used. Samples were analysed in duplicates. Duplicate samples were within ±5 % of their average and calculated via equation 64:

$$mg\ total\ solids/L = \frac{(A-B)\times 1000}{V} \qquad \text{Eq 64}$$

where A = Weight of dried residue + dish, mg; B = Weight of empty dish, mg; V = sample volume, cm^3.

iii) Ash Content

The ash content in dry inoculum samples was determined by the combustion of an oven dried sample. Three crucibles were pre-heated in a furnace at 550^oC, cooled in a desiccator and weighed. Approximately 1 g of sample was transferred to each of the crucibles and dried at 105^oC to constant weight. The dried samples were then put in a furnace at 550 ^oC. After 3 hours, the samples were removed, allowed to cool and placed in a desiccator. The residue was weighed when cooled to room temperature.

Ash was determined from the equation:

$$Ash(\%) = \frac{A(g)}{B(g)} \times 100 \qquad \text{Eq 65}$$

Where A is the ash weight and B is the oven dry weight.

iv) Total Volatile Solids (TVS)

Total volatile solids (TVS) are calculated by subtracting total ash (TA) from total solids (TS).

Total volatile solids was determined from the equation:

$$TVS(\%) = TS(\%) - TA(\%) \quad \text{Eq 66}$$

For typical total solids (TS) = 24.8 ± 0.1g/L, ash content (TA) = 11.5 ± 0.1g/L total volatile solids (TVS) = TS – TA = (24.8 ± 0.1) – (11.5 ± 0.1) = 13.3 ± 0.1g/L

v) Determination of Residual Sugars and Carbohydrates

Soluble carbohydrates were determined spectrophotometrically. This method is based on the reaction where 5 carbon (pentoses) and 6 carbon (hexoses) sugars are converted into furfural and hydroxymethyl furfural (Gerhardt, 1994). Anthrone then reacts with the furfurals to give coloured product with the colour intensity proportional to concentration. Samples were centrifuged in a Sorvall Legend^{TM} T centrifuge (Kendro Laboratory Products Plc, Bishop's Stortford, UK) for 5 minutes at 13400 x g and the supernatant diluted 100 times with deionised water. To 0.4 cm^3 of the diluted solution of 5 % phenol in water solution and 2.5 cm^3 of concentrated sulphuric acid (98 % analytical grade from Fisher Scientific, Loughborough, UK) was added. The test tubes were allowed to stand for 10 minutes, then vortex mixed and allowed to stand for a further 20 minutes. The absorbance of the characteristic orange colour was measured at 490 nm using a Unicam UV 1 spectrophotometer (Unicam, Cambridge, UK) against a reagent blank. The colour was stable for several hours and readings could be taken later if necessary.

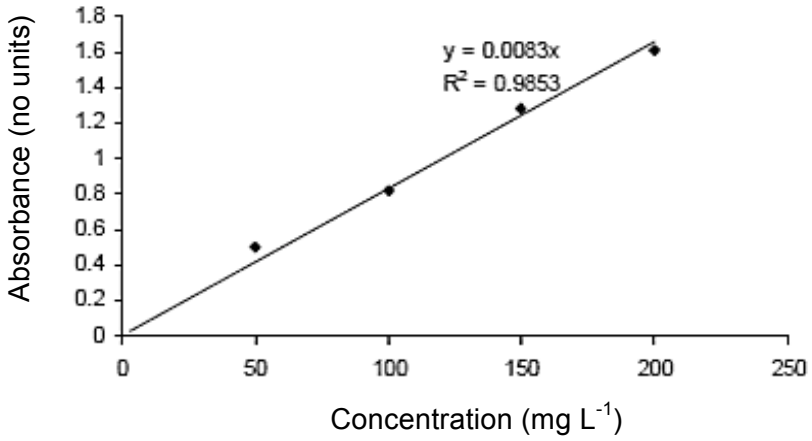

Figure 18 – Example of a calibration plot for determining the concentration of residual sugar (as sucrose).

Concentrations were read off a calibration graph as shown in figure 18 made from standard solutions of sucrose. Determinations were made in triplicate. The accuracy of the method was within ±2%.

vi) Tests on the Influent and Effluent Samples from Bioelectrochemical Systems Reactors

Two samples per reactor (one 20 cm^3 liquid influent and one 20 cm^3 liquid effluent sample) were collected using 50 cm^3 medical syringes from the liquid sampling ports on the reactors once per 7 days for microbial fuel cells (MFCs) and on daily basis for microbial electrolysis cells (MECs) and stored at -20 ^oC inside a commercial Bosch no frost fridge freezer, (Currys, Pontypridd, Wales, UK). Three 2 cm^3 samples were removed from 20 cm^3 bulk, prior to being placed in the freezer, as all tests were performed in triplicate, for chemical oxygen demand (COD), pH, conductivity as well as 1 cm^3 sample was removed for DGGE computational analysis (DNA analysis to evaluate diversity of microbial communities). If tests had to be repeated the frozen samples were removed from the freezer and allowed to defrost for 3 hours in the laboratory up to the point of use.

vii) Soluble Chemical Oxygen Demand (sCOD)

The chemical oxygen demand (COD) test is commonly used to indirectly measure the degree of organic compounds in water (APHA, 1989). The analysis is expressed in milligrams O_2 per liter (mg L^{-1}), which indicates the mass of oxygen consumed to oxidize the organic matter in a liter of solution. The COD indirect method relies on dichromate reduction where dichromate changes colour from orange (Cr^{6+}) to green (Cr^{3+}). The color change is proportional to the concentration of organics in wastewater. This oxidation process for organics in waste can be described by simplified equation:

$$C_nH_aO_bN_c+(n+\frac{a}{4}-\frac{b}{2}-\frac{3c}{4})O_2 \rightarrow n\ CO_2+(\frac{a}{2}-\frac{3c}{2})H_2+cNH_3 \quad \text{Eq 67}$$

This equation for oxidation can be simplified to Eq 68 for acetate and Eq 69 butyrate:

$$CH_3COO^-_{(aq)}+H^+_{(aq)}+2O_{2(g)} \rightleftharpoons CO_{2(g)}+H_2O_{(l)} \quad \text{Eq 68}$$

1 mol L^{-1} (16×4) = 64 g

20 m mol L^{-1} 64×2/100=1.28 g L^{-1} = 128 0 mg L^{-1}, experimental 1290-1300 mg L^{-1}

10 m mol L^{-1} 64/100=0.64 g L^{-1} = 640 mg L^{-1}, experimental 640-645 mg L^{-1}

5 m mol L^{-1} (64/2)/100=0.32g L^{-1} = 320 mg L^{-1}, experimental 319-330 mg L^{-1}

$CH_3\ CH_2CH_2COO^-_{(aq)} + H^+_{(aq)} + 5O_{2(g)} \rightleftharpoons 4CO_{2(g)} + 4H_2O_{(l)}$ Eq 69

1 mol L^{-1} (16×10) = 160 g

20 mmol L^{-1} 160×2/100=3.20 g L^{-1} = 3200 mg L^{-1}, experimental 3200-3300 mg L^{-1}

10 mmol L^{-1} 160/100=1.60 g L^{-1} = 1600 mg L^{-1}, experimental 1600-1650 mg L^{-1}

5 mmol L^{-1} (160/2)/100=0.800 g L^{-1} = 800 mg L^{-1}, experimental 800-830 mg L^{-1}

The effluent required 30-60 % less oxygen COD (influent) – COD (effluent) is the amount of oxygen need to oxidise the organics consumed by the bacteria from which the amount of acetate or butyrate consumed by the bacteria can be calculated.

2 cm^3 of liquid from the 20 cm^3 bulk sample for COD analysis was taken. Each sample was centrifuged in a Sorvall LegendP 76™ T centrifuge (Kendro Laboratory Products Plc, Bishop's Stortford, UK) for 10 minutes at 13400xg in order to remove traces of particulate solids. Each sample was diluted 0-2 times for acetate and 4-16 times for butyrate, with de-ionized water, prior to the COD analysis to 200 - 640 mg L^{-1} for greater accuracy.

Soluble COD (sCOD) was measured using a commercial method kit (Method 5220, HACH COD system, HACH Co., Loveland, CO, USA) derived from the standard method as described in APHA (1989). 2 cm^3 of diluted sample was added to 1 disposable HACH vial containing COD solution. The samples were heated on heating block at 110 ^oC for 2 hours and allowed to cool for 1 hour before the dichromate change in colour was analysed via spectrophotometer (DR 2700™ Portable Spectrophotometer, HACH, Loveland, CO, USA).

viii) Volatile Fatty Acids (VFAs)

Volatile fatty acid analysis (VFA), for acetic, propionic, *i*-butyrate, *n*-butyrate, *i*valerate and *n*-valerate was performed to confirm and support the COD results. The VFAs were determined by the method of Cruwys *et al* (2002) using a Perkin Elmer HS 40 XL automatic headspace sampler connected to a Perkin Elmer Autosystem XL GC system (Perkin Elmer, Beaconsfield, UK). The determination was linear in the range 0 to 1000 mg L^{-1} (R^2 > 0.99 for each acid) and the limit of detection was 4 mg L^{-1}. To prepare the samples 1 cm^3 of reactor sample, 1 cm^3 of de-ionized water, 1 cm^3 of $NaHSO_4$ (62 % w/v) and 0.1 cm^3 of 2 – ethylbutyric acid (1800 mg L^{-1}, stored at 4 ^oC as internal standard) were pipetted into a standard 22.3 cm^3 vial, fitted with PTBE septum. For higher concentrations of fatty acids (>2 g L^{-1}) the reactor sample was diluted twice or four times as required.

In the headspace unit, vials were heated for 30 min until the fatty acids evaporated and the equilibrium between the gas and liquid phases was established at the boiling above the boiling temperature for *n*-valerate (187 ^{o}C). The needle connecting the column to the headspace in the vial was inserted through the septum and the headspace was filled with the carrier gas (nitrogen at 14 psi) for 3 min allowing pressure to build up and transfer the sample to the GC injection port. The sample injection period was 0.1 min. Each sample was followed with 2 washes, from sample vials containing de-ionized water instead of samples, to minimize sample carry over. The injection port was maintained at 200 and split flow of 5.0 cm^3 / min. The column used was a free fatty acid phase fused-silica capillary column, initially at 60 ^{o}C, which was increased at 10 ^{o}C /min to 200 ^{o}C where it was held for 1 min. The detector was a flame ionization detector held at 250 ^{o}C.

ix) pH and Conductivity Measurements

pH and conductivity measurements were performed on sludge samples used as inoculum, influent and effluent samples from the reactors and used in the experiments and pH controllers were used to maintain pH in the cathode chambers of microbial electrolysis cells (MECs). The pH of the reactors was maintained at 5.0 - 5.5 by preparing the buffer solutions by adding 1.2 mol L^{-1} HCl (Sigma-Aldrich, Dorset, UK) to buffer solution S1 diluted by the factor of 2 (see "Materials and Methods" (section 4) for details) and replacing the media. For MFCs, the pH was measured using a pre-calibrated Mettler-Toledo, Gmbh 860 or Thermo Orion, Hydrus 300 pH (Thermo Fischer Scientific Inc., MA) pH meters and the conductivity was measured using pre-calibrated Inlab 737 or Metller-Toledo, SG7, FK2 conductivity meters (Kyazze et al., 2007). The pH and conductivity of the reaction mixtures was also measured at the end of each weekly batch cycle, when the MFCs were operated in sequencing batch (SBR) modes.

4.8.3 Statistical Analysis

All experiments were repeated 3 times, unless stated otherwise in the "Experimental Regime" section 5. For both offline and online analysis standard deviations were calculated, where averages of experimental repeats for experiment *n*, n_2 (repeat 1) and n_2 (repeat 2) were added together and divided by 3 to create error bars on the graphs.

4.8.4 Methods to Determine Mediator Adsorption on the Electrode Surface

Two quantitative techniques were used to determine exactly how much mediator was adsorbed on the carbon anode surface. Adsorption of methylene blue (MB) and neutral red (NR) on carbon veil (plain carbon cloth, PRF composite materials, Dorset, UK) was determined by weight difference and the amount of dye remaining in the solution.

All dye adsorption experiments were performed in triplicate. Experiments 2 i - iii investigated MB or NR adsorption by change in sample weight and experiment 2 iv investigated how much MB or NR was remaining or coming off into the solution. The dye solutions were continuously stirred for 48 h before pieces of the carbon veil were placed in the dye solutions for 28 h. The carbon veils were then removed from the dye solutions and dried at 90 ^{o}C for 2 hours. The weight measurements were performed on dry carbon veils on 5 point balance (see "Determination of Electron Mediator Adsorption by Weight Difference" section on page 96). For UV absorption tests 10 cm^3 solution sample was removed from each 1 L container, after carbon veil was removed, portions and tested for how much dye was still present in the solution. Solutions containing MB were scanned at 608 - 669 nm (base of the adsorption peak) and solutions containing NR were scanned at 529 - 571 nm (base of the adsorption peak) using a UV / Vis spectrophotometer (Lambda 25, model L6020060). The adsorptions for the tops of the peaks can shift, so points at the base were selected (see "Methods to Determine Mediator was Adsorption on the Electrode Surface", section 4.8.4).

Experiments 2i - 2iv

(MB) and (NR) solutions of concentrations of 0.94 mmol L^{-1}, 1.25 mmol L^{-1} and 1.56 mmol L^{-1} (i.e. 3 × 3 = 9 solutions of each concentration at 1 L per carbon veil sample) were prepared and a piece of carbon veil (material from which the carbon anode was made) were cut from the roll, weight ≈ 0.1 - 0.15 g, 13 cm^2 in size, placed into either the methylene blue (MB) or neutral red (NR) solution, 1 L, pH 5.5, for 28 hours.

For experiment 2ii (MB) and (NR) solutions of concentrations 0.94 mmol L^{-1}, 1.25 mmol L^{-1} and 1.56 mmol L^{-1} (3 × 3 = 9 solutions of each concentration) were prepared the same as in experiment 2 i with each carbon veil piece being conditioned at pH 12 used instead of pH 5.5.

For experiment 2iii (MB) and (NR) solutions of concentrations 0.94 mmol L^{-1}, 1.25 mmol L^{-1} and 1.56 mmol L^{-1} (3×3=9 solutions of each concentration) were prepared the same as in experiment 2ii with each carbon veil piece being previously conditioned in NaOH, pH 5.5, for 28 hours prior to being placed into dye solution.

For experiment (2iv), each piece of carbon veil, form experiments 2i, 2ii and 2iii, was placed into dye free, phosphate buffer solution (S1, see "Materials and Methods" section 4 for preparation details), 13 cm^2, pH 5.5, for 28 hours, and dried at 90 ^{o}C, for 2 hours. UV spectroscopy and weight difference were used to determine how much, methylene blue (MB) or neutral red (NR) came off on the buffer solution. This was repeated 3 times, until MB or NR stopped coming off into the buffer solution.

Determination of Electron Mediator Adsorption by Weight Difference

For weight difference experiments each carbon veil was removed from the solution and dried at 90 ^{o}C (Gallenkamp, Hotbox Oven with Fan), for 2 hours at the end of 28 hour experiments 2i, 2ii and 2iii and after each 24 hour wash for experiment 2iv. The weight measurements were performed on a 5 point balance (Mettler Toledo AE 163, analytical digital scale balance). For experiments 2i, 2ii and 2iii initial weight of each sample was determined and the difference $W_{final} - W_{initial} = W_{adsobed}$. For experiment 2iv the weight of methylene blue (MB) or neutral red (NR) permanently adsorbed was determined as follows:

$$W_{adsobed} - W_{wash\ 1} - W_{wash\ 2} - W_{wash\ 3} - W_{wash\ 4} = W_{permanently\ adsorbed} \quad \text{Eq 70}$$

Determination of Electron Mediator Adsorption by UV Spectrospcopy

Before experiments were started linear calibration plots were produced for ten solutions of known concentrations as shown on Table 6. The calibration plots have R^2 values ≥ 98, which indicates that points fit into a straight line with good accuracy.

All calibration plots were expected to obey Beer Lamberts law: $A = \varepsilon Cl$ Eq 71

where A = absorbance (no units), C = concentration (mmol L^{-1}), l = path length (distance between cuvette walls=1cm) and ε = extinction coefficient.

The solutions were later diluted × 50 for methylene blue (MB) and × 10 for neutral red (NR) to meet the detection limits for the UV spectrometer. Only 7 from 11 points were needed for the calibration plots as written in the instruction manual, so seven points that best fitted the trend lines where used for the calibration plots (Table 6, Fig. 21 a and Fig. 21 b).

Table 6 – The concentrations (mmol L^{-1}) and amounts of dye used to prepare methylene blue (MB) and neutral red (NR) solutions.

$mmolL^{-1}$	0	0.47	0.63	0.78	0.94	1.09	1.25	1.40	1.41	1.56	1.72
gL^{-1}(MB)	0	0.15	0.20	0.25	0.3	0.35	0.4	0.45	0.5	0.55	0.6
gL^{-1}(NR)	0	0.14	0.18	0.22	0.27	0.31	0.36	0.41	0.45	0.50	0.54

UV absorption for known dye concentrations (Table 6, Fig. 21 and Fig. 21b) from the calibration plot ($C_{initial}$) values were compared to MB and NR concentrations after carbon veil pieces were placed in those solutions for 28 hours C_{final} values.

Concentration of MB or NR adsorbed ($C_{adsobed}$) was determined via equation:

$$C_{final} - C_{initial} = C_{adsobed} \quad \text{Eq 72}$$

C_{final} values were determined for Experoments 2i – iii to confirm tests by weight difference.

For the leaching experiment 2iv, the concentration of dye in the buffer $C_{wash\ 1}$, $C_{wash\ 2}$, $C_{wash\ 3}$ and C_{wash4} were determined. The buffer solutions, containing unknown concentrations of methylene blue, which leached from the carbon veils were diluted: - 1st wash × 10, 2nd wash × 1, 3rd wash × 1, 4th wash × 1 and scanned. The concentration of dye methylene blue (MB) or neutral red (NR) permanently adsorbed on the carbon surface was calculated as:

$$C_{adsobed} - C_{wash\ 1} - C_{wash\ 2} - C_{wash\ 3} - C_{wash\ 4} = C_{permanently\ adsorbed} \quad \text{Eq 73}$$

5. Experimental Regime

5.1 The Influence of Catholyte pH and Temperature on the Hydrogen Production in Microbial Electrolysis Cell (MEC)

Batch Start up and Continuous Flow MFC Operation

Batch start up (when the sludge containing bacteria was added at time = 0 to the nutrient electrolyte mixture, when the MFC was assembled. During batch start up (1^{st} two weeks approx. (16 days) of batch operation) the anodes for the two microbial fuel cells (MFCs 1 and 2 (control)) with untreated carbon cloth (UCC) anodes were inoculated with anaerobically digested sludge (20 % v/v) obtained from a local wastewater treatment plant (Cog Moors, Cardiff, UK). The media supplied to the anode chamber consisted of 30 mmol L^{-1} CH_3COONa and feedstock solution (FS), as described in "Method for Preparing Feed Stock Solution (FS) used for Reactor Operation" section 4.6. Another 2 MFCs (MFCs 3 and 4) were prepared without sludge.

The start-up stage ended when the sediments in the anode chamber were removed and replaced with fresh anode media, without further sludge addition, once a week, for 4 weeks (30 days), if the start up period is included, with 150 Ω applied resistance. The influent had a pH of 7.0 and a conductivity of 7.24 mS cm^{-1}.

Continuous Operation in Microbial Electrolysis Cell (MEC) Mode

Anodes acclimated to acetate for 4 weeks (30 days) in MFC mode were then removed and placed into two tubular microbial electrolysis cells (MECs) operated at a 9 h hydraulic retention time (HRT) (time it takes for the substrate to move through the anode chamber). All MECs were assembled as described in "Materials and Methods" section 4. They were connected to a 3 Ω resistors, so that the potential differences, and hence the current through the circuits, between the anodes and cathodes could be logged on line (see "Electrochemical Analysis Methods" section 4.7). The reactor was operated at room temperature at 23±1.4 ^{o}C (temperature controller switched off) and the pH was maintained at 7, in the anode chamber. The MEC cells for were operated on 10 mmol L^{-1} acetate for 48 days (weeks 4-11, days 30-78), until hydrogen production became stable at the applied voltage of 600 mV.

Experiment 1.1 lasted from week 11 till week 21 (from day 78 to day 149). The voltages of 600 and 850 mV were applied between anode and cathode. In the first experiment (weeks 11-15, days 78-108), pH in the cathode chamber was decreased to 5, increased to 7 and then to 9 (5 day periods per pH), at the applied voltage of 600 mV.

Experiment 1.1 lasted from week 11 till week 13, days 78-93. Experiment 1.1i was a repeat of experiment 1.1 at an applied voltage 850 mV (weeks 13-15, days 93-108).

For experiment 1.2 (weeks 17-21, days 117-149) experiments 1.1 and 1.1i were repeated to confirm the results. There was a break of approx. 1.2 weeks, 9 days between experiments 1.1 and 1.2 (weeks 15-17, days 108-117) and a delay of 6 days before experiment 1.3 (weeks 21-22, days 149-155). During these periods the abiotic cathode compartment was drained and fresh electrolyte solution S1, (adjusted to pH 7) was added, (prepared as described in "Materials and Methods", section 4).

In experiment 1.3 (weeks 22-30, days 155-211) the effect of temperature on the hydrogen production was investigated. Temperature 30±1.4 ^{o}C was applied (weeks 22-23, days 155--167), 43±0.4 ^{o}C (weeks 23-25, days 167-177), 50±3.0 ^{o}C (weeks 25-26, days 177-187) and room temperature 23±1.4 ^{o}C (weeks 26-28, days 187-201, temperature controller switched off). Cold water from refrigerator was circulated through the silicone tubes wound around cathode chamber on MEC and connected to the flow temperature controller, for weeks 28-30, days 201-211 to maintain the temperature at 19±1.2 ^{o}C. (see Materials and Methods for further details).

In experiment 1.4 (weeks 31-39, days 218-274) experiment 1.3 was repeated to confirm the results. There was a 7 day break between experiments 1.3 and 1.4 (weeks 30-31, days 211-218). During these periods the abiotic cathode compartment was drained and fresh electrolyte solution S1, pH 7 was added, prepared, as described in "Method for Preparing Feed Stock Solution (FS) used for Reactor Operation" (section 4.6).

5.2 The Effect of Immobilized Methylene Blue and Neutral Red on the Current Production in Microbial Fuel Cell (MFC)

Batch Start up and Sequencing Batch MFC Operation

In experiment 2 (see "Results" section 6, for details) various methods for methylene blue and neutral red passive adsorption methods were tested. When the best method for mediator adsorption was determined three methylene blue and three neutral red treated anodes were prepared.

For experiment 2.1 the anodes for nine MFCs (three with untreated carbon cloth anodes (UCC), three with methylene blue treated carbon cloth anodes (MB) and three with neutral red treated carbon cloth anodes (NR)) were inoculated with anaerobically digested sludge (20% v/v) obtained from a local wastewater treatment plant (Cog Moors, Cardiff, UK). During the start-up (time t=0 weeks, when sludge containing bacteria was added to nutrient electrolyte mixture, when MFCs were assembled), the media supplied to the anode chamber consisted of 20 mmol L^{-1} CH_3COONa and feedstock solution (FS), as described in "Method for Preparing Feed Stock Solution (FS) used for Reactor Operation" section 4.6.

After start-up, the sediments in the anode chamber were removed and replaced with fresh anode media, without sludge, once a week, for 15 weeks (105 days), 17 weeks if start up is included, at 150 Ω resistance and temperature 23±2 ^{o}C. The influent had a pH of 7.0 and a conductivity of 7.23 mS cm^{-1}. At the beginning of week 22 the temperature was increased from 23±2 ^{o}C to 35.5 ^{o}C and the power densities were recorded. On week 23 the temperature was decreased from 35.5 ^{o}C to 8 ^{o}C and the power densities were recorded. Experiment 2.2 was a repetition of experiment 2.1 designed to confirm the results obtained.

5.3 The Influence of Changes in Acetate and Butyrate Concentrations and Full Substrate Switch on Gas Production from Two Microbial Electrolysis Cells (MECs) Acclimated to either Acetate or Butyrate

Batch Start up and Continuous Flow MFC Operation

For experiment 3.1 the anodes for six MFCs (three MFCs (AC) and three MFCs (BU)) were inoculated with anaerobically digested sludge (20 % v/v) obtained from a local wastewater treatment plant (Cog Moors, Cardiff, UK). During the start-up (when sludge containing bacteria was added at time zero, t = 0 weeks). The media supplied to the anode chamber to each MFC consisted of 20 mmol L^{-1} (CH_3COONa, for the MFC reactor AC or CH_3 CH_2 CH_2COONa, for the MFC reactor BU) and feedstock solution (FS), as described in "Materials and Methods", section 4.

After start-up, the sediments in the anode chamber were removed and replaced with fresh anode media, without sludge, once a week, for 8 weeks (56 days) or 9 weeks if start up is included, at 1000 Ω resistance. The influent had a pH of 7.0 and a conductivity of 7.24 mS cm^{-1}.

Continuous Operation of Microbial Electrolysis Cell (MEC) Operation

For experiment 3.2 and 3.3 best performing anode acclimated to acetate (AC) and another butyrate (BU), for 9 weeks, were the removed and placed into two tubular MECs and operated at 8 h HRT (time it takes for the substrate to move through the anode chamber). Only 2 pilot MEC reactors were available and could be operated at the same time. All MECs were assembled as described in "Materials and Methods" section 4, however the difference was that the cathode electrode, attached to anion exchange membrane was placed between two stainless steel mesh sheets (200 mesh, 0.07 mm aperture, Mesh Direct, Burslem, UK) to improve cathodic conductivity. Both MECs AC and BU were connected to 1Ω resistors, so that the potential differences, and hence the current through the circuits, between the anodes and cathodes could be logged on line. The temperature was maintained at 29±3 ^{o}C to allow highest possible gas production and pH was kept at 7, in the anode chamber, as described in "Results" section 6. In the cathode chamber pH was kept at 5.3 and 26 g L^{-1} of NaCl was added to the electrolyte, in the cathode chambers only, in both reactors to prevent cathodic methanogenesis in both AC and BU reactors. The MEC cells for were operated on 20 mmol L^{-1} acetate (MEC AC) or butyrate (MEC BU) for 15 days (weeks 9 -11, days 65-80), until hydrogen production became stable.

Two reactors, MEC (AC) and MEC (BU), were later used for experiments 3.2 and 3.3, which lasted weeks 11-18 (from day 80 to day 130), where the voltage of 850mV was applied between anode and cathode. In the experiment 3.2 (weeks 11-13, days 80-95) substrate concentration was decreased. During weeks 11-13 (days 80-95), the acetate (MEC AC) or butyrate (MEC BU) concentration, in the feedstock, was 20 mmol L^{-1}, and decreased to 10 and 5 mmol L^{-1}. These concentrations were maintained for 5 day periods to allow microbial culture to acclimate to each concentration. For experiment 3.3 (weeks 13-15, days 95-105) acetate for MEC (AC) and butyrate for MEC (BU) were replaced with 10 mmol L^{-1} acetate and 10 mmol L^{-1} butyrate mixture, for 5 days (weeks 13-14, days 95-100) and fully switched to 20 mmol L^{-1} pure butyrate or acetate solution (5 day full substrate switch, weeks 14-15, days 100-105).

In the Experiment 3.2i and 3.3i (weeks 15-18, days 105-130) Experiments 3.2 and 3.3 were repeated. The gas produced was collected by the displacement of water saturated with sodium chloride. The gas composition in the anode and cathode chambers using two separate gas samples on a daily basis, starting from week 11.

5.4 The Comparison of Four Anode Types and their Effect on the Voltage Production in Microbial Fuel Cells (MFCs) and Hydrogen Production in Microbial Electrolysis Cells (MECs)

Batch Start up and Continuous Flow MFC Operation

Batch start up (1st 2 week, 16 day batch operation after sludge containing bacteria was added at time t = 0 weeks). The anodes for eight MFCs (3 with untreated carbon cloth anode (UCC), control 1), 3 with carbon cloth stainless steel cloth anode roll (RR), 3 with carbon cloth J cloth anode roll (JC, control 2) and methylene blue treated carbon cloth roll anode (MB, MBi if contains microbial culture acclimated to 1000 Ω resistance) prepared as described in "Materials and Methods", section 4) were inoculated with anaerobically digested sludge (20% v/v) obtained from a local wastewater treatment plant (Cog Moors, Cardiff, UK). During the start-up period weeks 1-2), the media supplied to the anode chamber consisted of 40 mmol L^{-1} CH_3COONa and feedstock solution (FS), as described in "Method for Preparing Feed Stock Solution (FS) used for Reactor Operation" section 4.6.

After start-up, the sediments in the anode chamber were removed and replaced with fresh anode media, without sludge, once a week, for experiment 4.1 which lasted for 5 weeks (35 days), 7 weeks if start up is included, at 1000 Ω resistance. The influent had a pH of 7.0 and a conductivity of 7.24 mS cm^{-1}.

Continuous Operation in Microbial Electrolysis Cell (MEC) Operation

Anodes acclimated to acetate for 7 weeks (one best performing from 3 of each, 1 UCC, 1 RR, 1 JC and 1 MBi) were the removed and placed into two tubular microbial electrolysis (MECs) and operated at 8 h HRT (time it takes for the substrate to move through the anode chamber). Only 4 MECs could be operated at the same time. All MECs were assembled as described in "Materials and Methods" section 4, however the difference was that the cathode electrode, attached to anion exchange membrane was placed between two stainless steel mesh sheets (200 mesh, 0.07 mm aperture, Mesh Direct, Burslem, UK) to improve cathodic conductivity. All MECs were connected to 1 Ω resistors, so that the potential differences, and hence the current through the circuits, between the anodes and cathodes could be logged on line. The temperature was maintained at 29±3 ^oC for optimal gas production and pH was kept at 5.3, in the anode chamber, as described in "Results" section 6. The MEC cells for were operated on 20 mmol L^{-1} acetate for 15 days (weeks 7-9, days 49-63), until hydrogen production became stable.

Four reactors, UCC, RR, JC and MBi, were later used for experiments 4.2 and 4.2 i, which lasted weeks 9-12 (from day 63 to day 88), where the voltage of 850 mV was applied between anode and cathode. In experiment 4.2 (week 9-12, days 63-88), weeks 9-11 (days 63-78), the acetate concentration, in the feed stock, was 20 mmol L^{-1}, and decreased to 10 and 5 mmol L^{-1} (5 day periods to allow microbial culture to acclimate to each concentration), replaced with 10 mmol L^{-1} acetate and 10 mmol L^{-1} butyrate mixture, for 5 days, (week 11, days 78-83) and operated on 20 mmol L^{-1} butyrate (weeks 11-12, days 83-88).

In experiment 4.2 i (weeks 13 - 17, days 95 - 120) experiment 4.2 was repeated. The gas produced was collected by the displacement of water saturated with sodium chloride. The gas composition in the anode and cathode chambers using two separate gas samples on a daily basis, starting from week 9. There was 1 week break between experiments 4.2 and 4.2 i

6. Results

6.1 The Influence of Temperature and Catholyte pH on the Hydrogen Production in Microbial Electrolysis Cells (MECs)

The objective for this experiment was to build and operate a continuously fed 1 L microbial electrolysis cell and evaluate the effect of pH in the abiotic cathode chamber on pH gradient losses, hydrogen production rate and the effect of temperature on gas production rate in MECs. In order to prepare the anodes two, 200 cm^3 microbial fuel cells (MFCs 1 and 2) were built and operated for 4 weeks (30 days) at 150 Ω resistance and a room temperature (23±1.4 ^oC). The anodes were removed from MFCs on day 30 and placed into 326 cm^3 anode chambers in two tubular MECs and operated at a 9 h hydraulic retention time (HRT). Currents, pH and temperature were logged on line, as described in "Electrochemical Analysis Methods" (section 4.7) at 1 second intervals. All MECs were assembled as described in "Materials and Methods" section 4.6 with the 150 Ω resistor replaced with a 3 Ω resistor to minimize the energy input into the system. This also enabled the potential differences, and hence the current through the circuits, between the anodes and cathodes to be logged on line. The MECs were operated for 7 weeks, 48 days (weeks 4-11, days 30-78), until the hydrogen production rate became stable. MFCs 3 and 4 (prepared without sludge inoculum) did not produce any current. When the anodes from control MFCs 3 and 4 were placed into the microbial electrolysis cells (MECs) no gas was produced and no COD reduction was observed.

6.1.1 The Influence of pH on the MEC Performance

The effect of pH 5, pH 7 and pH 9 at an applied voltage of 600 mV (experiments 1.1) was evaluated and repeated at an applied voltage of 850 mV (experiment 1.1 i). In experiment 1.1, the pH in the cathode chamber, which was maintained at pH 7, was decreased to pH 5, increased to pH 7 and than increased again to pH 9, for 5 day periods per pH. The pH in the anode chamber remained the same, at a pH of 7. In experiments 1.2 and 1.2 i, which were repetitions of 1.1 and 1.1 i designed to confirm the findings. The aim of this experiment was to reduce the pH gradient losses and to find the optimal pH for gas production in the cathode chamber. Daily hydrogen production and cathode current densities were logged on line from experiments 1.1, 1.1 i, 1.2 and 1.2i. These were used to plot figure 19 a and 19 b.

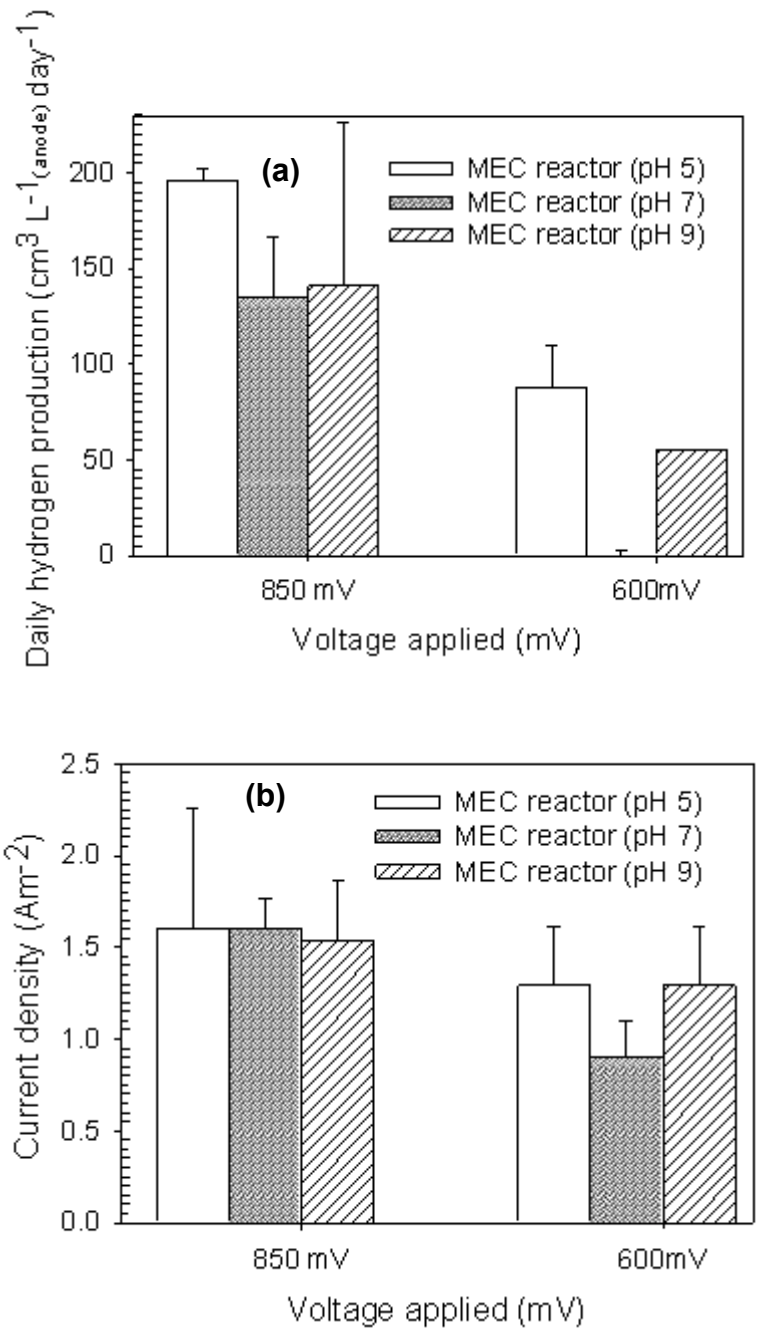

Error bars represent variations from the average for *n* experimental repeats (*n*=2).

Figure 19 – Influence of pH (19 a) and the current density (19 b) on the hydrogen production rate.

The pH in the cathode chamber influenced hydrogen production rate as did the voltage applied. When a voltage of 850 mV was applied, it accompanied the highest hydrogen production rate and highest current density at pH 5 (Fig. 19 a and Fig. 19 b). Figures 19 a and b show that at 850 mV, the hydrogen production rate (cm^3 $L_{(anode)}^{-1}$ day^{-1}) and corresponding current densities were: 199±3 cm^3, 1.93±0.33 A m^{-2} (pH 5, *n*=2); 150±15.5 cm^3, 1.68±0.08 A m^{-2} (pH7, *n*=2); 183±42.5 cm^3, 1.70±0.16 A m^{-2}, (pH9, *n*=2) respectively, where *n* refers to experimental repeats as described in "Statistical Analysis" section 4.8.3.

An applied voltage of 600 mV accompanied lower hydrogen production rates but the effect of catalyte pH was more significant at the applied voltage of 600 mV than at 850 mV (Fig. 19 a and Fig. 19 b). At the applied voltage 600 mV, the hydrogen production rates and corresponding current densities in the cathode ($cm^3 L_{(anode)}^{-1} day^{-1}$) were 99 ± 16.5 cm^3, 1.45 ± 0.16 A m^{-2} (pH 5, *n* = 2); 0 cm^3, 0 A m^{-2} (pH7, *n* = 2) and 38.5 ± 11 cm^3, 0.6 9 ± 0.0 A m^{-2} (pH 9, *n* = 2) respectively (Fig. 19 a and Fig. 19 b).

Performance factors such as coulombic efficiency (CE), cathodic hydrogen recovery (r_{cat}), which relates current to hydrogen production, hydrogen recovery ($Y_{H2\ per\ mol\ substrate\ destroyed}$) and COD reduction (see Table 7 and "Electrochemical Analysis Methods" section 4.7, for more detailed information). The changes in pH in the cathode chamber had an effect on the hydrogen production rate (Table 7; Fig 19 a and Fig. 19 b) and associated parameters but COD reduction (Table 8) only changed when pH was changed to from pH 7 to pH 9 at 600 mV.

Table 7 – The variation of CE, r_{cat} and the overall hydrogen yield with pH and the voltage applied.

	600 mV			850 mV		
	pH 5	pH 7	pH 9	pH 5	pH 7	pH 9
CE (%)	40	28	54	60	52	57
cathodic hydrogen recovery r_{cat} (%)	32	2.5	25	45	39	47
overall hydrogen yield per mol of acetate (mol/mol)	0.52	0.13	0.5	1.1	0.81	1.0
highest volumetric production ($cm^3 L_{(anode)}^{-1} day^{-1}$)	92	0	61	200	153	190
All performance factors for highest gas productions and currents See figure 19 for details						

The highest volumetric hydrogen production 200 $cm^3 L_{(anode)}^{-1} day^{-1}$ and highest yield of 1.1 mol / mol were observed at pH 5 at 850 mV (Table 7). Other important performance factors such as hydrogen yield per mol substrate destroyed and coulombic efficiencies (CEs), which show how much substrate is converted into current in the system follow same trend as hydrogen production rate. Hydrogen yield values, which depend on the volumetric hydrogen production, were affected more strongly than CEs (Table 7) but COD reductions (the amount of substrate consumed by bacteria) remained roughly the same (between 25% and 37%) as pH was increased from pH 5 to pH 9 at 850 mV (Table 8).

COD reductions between 27% and 37% were observed when the reactor with pH 5 at the applied voltage 600mV was increased to pH 7. A further increase in pH was followed by 18% drop in COD reduction at pH 9 (Table 8). The hydrogen production rate and hydrogen yields decreased with increase in pH with highest values observed at pH 5, lowest values observed at pH 7 and slight increase at pH 9 (Table 7). A slight increase in anode and cathode potentials, which did not follow the same trend as hydrogen production rate and hydrogen yields at 600 mV and 850 mV was seen as the pH was increased from 5 to 9 (Table 8).

Table 8 – The COD reduction values for MECs at cathodic and anodic potentials vs Ag/AgCl reference electrode of 600 mV and 850 mV.

	600 mV				850 mV			
pH	COD reduction (%)	Anode potential vs Ag/AgCl (V)	Cathode potential vs Ag/AgCl (V)	1.2M HCl dosed per day (cm^3)	COD reduction (%)	Anode potential vs Ag/AgCl (V)	Cathode potential vs Ag/AgCl (V)	1.2M HCl dosed per day (cm^3)
5	32±5 (2)	-52±20	-652±20	9±1.4 (2)	30.5±5 (2)	-100±18	-750±20	6.5±1(2)
7	30±2 (2)	-150±86	-750±86	5.4±1.7 (2)	31±6 (2)	-170±2	-1020±15	5.0±0(2)
9	12±5 (2)	-256± 44	-856±44	7.1±2.5 (2)	29.7±7 (2)	-213±55	-1056±44	7.2±0.7(2)

± refers to the variation from the average for (2) experimental repeats

(see "Offline Analysis Methods, section 4.8")

A comparison of hydrogen yields from the continuous flow MECs (Table 7) to literature values (Table A-2.5 – Table A-2.7 in "Appendix A-2" section 9.2) indicates that there is still a need to further improve the efficiency of MECs in order to produce overall yields ≥ 2 mol of hydrogen per mol of acetate (mol/mol), as described by Logan (2004 a). The volumetric hydrogen production and hydrogen yield per mol of acetate converted into hydrogen is comparable to the hydrogen production rates (measured as volumetric hydrogen production per day) reaching 300 $cm^3\ L^{-1}_{(anode)}\ day^{-1}$ reported by Rozendal et al (2007) for MEC with 3.3 L anode chamber and a yield of for a MEC with $1m^3$ anode chamber by Cusick et al (2011). More recently MECs with anode chamber volumes 120 L and 2 L were reported to average hydrogen production rate of 15 $cm^3\ L^{-1}_{(anode)}\ day^{-1}$ (Heidrich et al., 2013) and 45 $cm^3\ L^{-1}_{(anode)}\ day^{-1}$ (Gil-Carrera et al., 2013) respectively, which are considerably lower than the values reported here. Apart from the problem of methanogenesis in the anode and a low cathodic hydrogen recovery, low COD reduction in MECs (Table 8) needs improvement to produce results similar to 1418 ± 0.08 $cm^3\ L^{-1}_{(anode)}\ day^{-1}$ that reported by Lu et al (2009).

6.1.2 The Influence of Temperature on the MEC Performance

The influence of catholyte temperature on the hydrogen production rate in microbial electrolysis cell (MEC) was investigated. Temperatures 19 ^{o}C, 23, ^{o}C 30 ^{o}C, 43 ^{o}C and 53 ^{o}C were tested (experiment 1.3) by decreasing the temperature from 23 ± 1.4 ^{o}C to 19 ± 1.2 ^{o}C and then increasing it from 19 ± 1.2 ^{o}C to 50 ± 3.0 ^{o}C for five day periods, for each temperature, and then decreasing it back to 23 ± 1.4 ^{o}C (Fig. 20 a and Fig. 20 b).

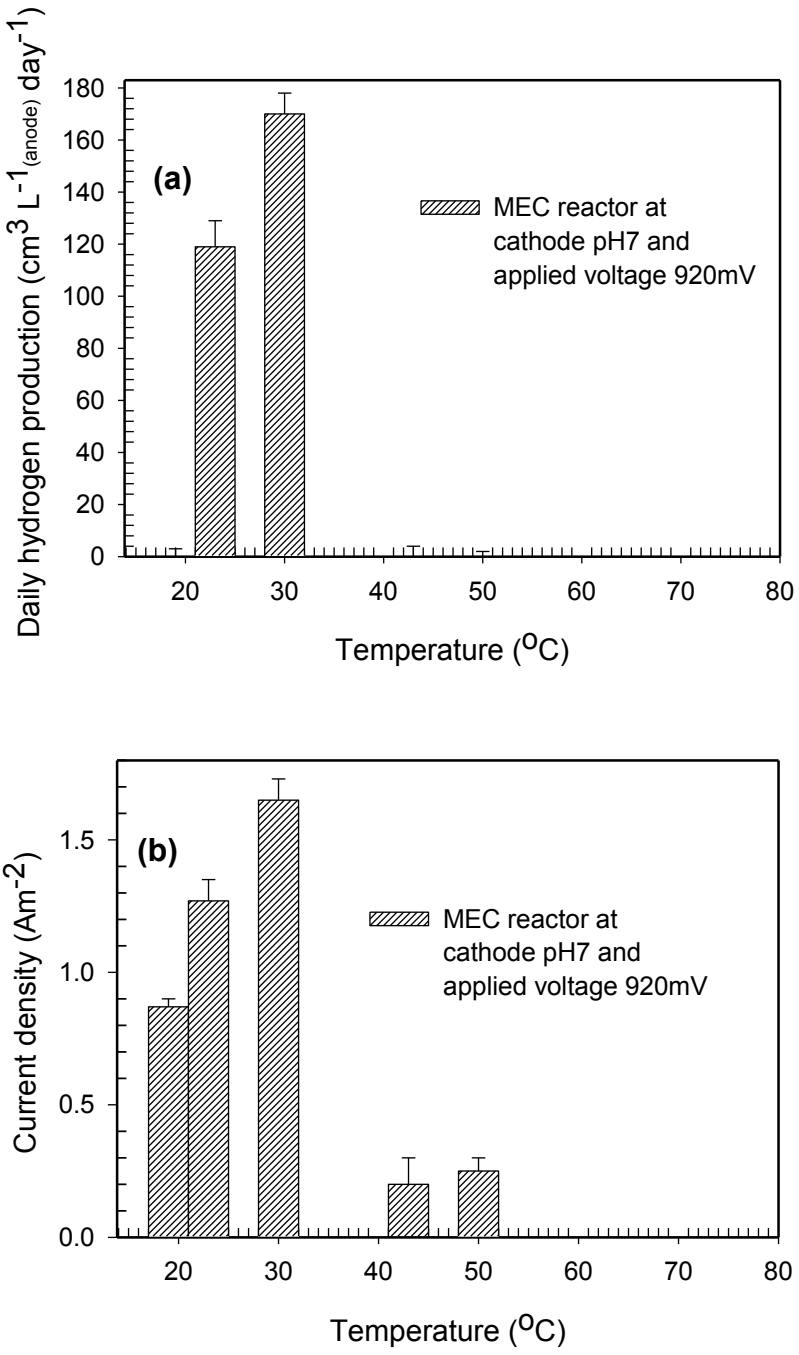

Error bars represent variations from the average for *n* experimental repeats (*n*=2).

Figure 20 – Influence of temperature on the hydrogen production rate (20 a) and current density (20 b).

The results in Fig. 20 a and Fig. 20 b show that the increase in temperature from 19 ^{o}C to 31 ^{o}C (mesophilic conditions) increased the hydrogen production rate and current density (A m^{-2}), with the highest hydrogen production rate obtained at 31 ^{o}C (as shown in the three temperature points i-iii), where *n* refers to the number of experimental repeats:-

i) At 19 ± 1.2 ^{o}C the hydrogen production rate was 1.60 ± 1.4 0 cm^3 $L_{(anode)}^{-1}$ day^{-1} (*n* =2) shown in figure 20 a, with a current density of 0.88 ± 0.02 A m^{-2} (Fig. 20 b).

ii) At 23 ± 1.4 ^{o}C the hydrogen production rate increased to 124 ± 5.00 cm^3 $L_{(anode)}^{-1}$ day^{-1} (*n*=2) shown in figure 20 a, with a current density of 1.31 ± 0.04 A m^{-2} (Fig. 20 b).

iii) At 30 ± 1.4 ^{o}C the maximum hydrogen production rate was achieved amounting to 174 ± 5.00 cm^3 $L_{(anode)}^{-1}$ day^{-1} (*n*=2) shown in figure 20 a, with a current density of 1.69 ± 0.04 A m^{-2} (Fig. 20 b).

A further increase in temperature from 42 ^{o}C to 53 ^{o}C (thermophilic conditions) decreased the hydrogen production rate and current density (A m^{-2}) further with the lowest rate of hydrogen produced at 53 ^{o}C (see the two temperature points below iv-v):-

iv) At 43 ± 0.4 ^{o}C the hydrogen production rate was 2.10 ± 1.90 cm^3 $L_{(anode)}^{-1}$ day^{-1} (*n*=2) shown in figure 20 a, current density 0.25 ± 0.05 A m^{-2} (Fig. 20 b).

v) At 50 ± 3.0 ^{o}C the hydrogen production rate was 1.10 ± 0.90 cm^3 $L_{(anode)}^{-1}$ day^{-1} (*n*=2) shown in figure 20 a, current density 0.28 ± 0.03 A m^{-2} (Fig. 20 b).

6.1.3 Discussion

This work can be split into two parts:- (i) where the effect of pH on the hydrogen production rate was investigated and (ii) where the effect of temperature on the hydrogen production rate was investigated:-

i) The aim of this work was to assess how changes in the pH of the abiotic cathode chamber effect hydrogen production rate and how other performance factors such as current density, COD reduction (the amount of substrate consumed) and pH of the anode chamber (separated from cathode via cation exchange membrane). The effect of applied voltage on the hydrogen production rate was previously investigated by Rozendal et al (2008b), see Table A-2.6 in Appendix A-2 section 9.2. According to author's knowledge, the relationship between pH changes, the current and hydrogen production rate has not been assessed in detail before.

Experimental findings, such as the effect of catholyte pH on the current density being more significant at the lower applied voltage of 600 mV than at 850 mV have not been reported previously in literature.

ii) The highest volumetric hydrogen production was obtained at an applied voltage of 850 mV, pH $5_{cathode}$ amounting to 200 $cm^3\ L_{(anode)}^{-1}\ day^{-1}$ (n=2, for MEC1) (a coulombic efficiency of 60 %, a $H_{2\ (anode)}$ yield of 1.1 mol / mol $_{(acetate)}$ and a COD reduction of 30.5 %). Since volumetric hydrogen production is directly proportional to the current density in the MEC cell it is expected that at higher applied voltages will produce more hydrogen (Logan, 2008). It could also be suggested that hydrogen production rate becomes more dependant on the pH gradient losses as the voltage applied is decreased. Lower pH results in an increase in hydrogen protons (Bard and Faulkner, 1976), which are converted into hydrogen, so the gradual decrease in hydrogen production rate would be expected, when the pH is increased (Logan, 2008). The drop in hydrogen production rate (measured as 5 consecutive daily volumetric hydrogen productions per pH) at pH 7, which was lower than hydrogen production rate at pH 9, still can not yet be explained since the same a linear decrease in hydrogen production rate is expected but the same as the abrupt drop in hydrogen production rate was observed for MECs 1 and 2 (control) when the experiment was repeated. These results also showed that a lower pH in the cathode chamber improves the hydrogen production rate and that pH control at lower pH levels may be needed if the potentials applied to MECs are to be minimised. These result were as described in the published work by Kyazze et al., (2010) from data in this thesis.

iii) The effect of temperature on the hydrogen production rate from the microbial electrolysis process was investigated by increasing the temperature from 19 ^oC to 30 ^oC and then to 43 ^oC and 50 ^oC. Temperature changes were investigated over a 5 day (0.7 week) periods. The relationship between the increase in the current density and the increase in the hydrogen production rate, $cm^3\ L_{(anode)}^{-1}\ day^{-1}$, for 5 day period during which a particular temperature was used (Fig.19 a – Fig. 19 b and Fig. 20 a – Fig. 20 b) is not an original finding, previously reported by Logan et al (2008). At the temperature of 30 ^oC, the highest hydrogen production rate was observed in the systems tested. The performance of the however the MEC reactor being significantly lower at 50 ^oC. The reactor was enriched from a mesophilic culture and exhibits a typical response of mesophilic cultures in that activity increases until a maxima is reached around 40 ^oC with then a subsequent decline as the temperature increases beyond 40 ^oC, as shown by Lettinga et al (2001) in anaerobic digestion.

The cell was not operated between 30 - 35 ^{o}C as this would lead to a significant degree of competition from methanogens in the cell. Experiments were operated outside this range to determine an optimum temperature for hydrogen production rate and would not favour mesophilic methangens significantly.

6.1.4 Conclusion

A novel continuous flow microbial electrolysis cell (MEC) was designed, assembled and the operating conditions that gave the highest hydrogen production rate were determined. All performance factors were assessed in detail with highest hydrogen production rate observed at the temperature of 30 ^{o}C at a cathode chamber pH of 5. It was important to assess the response of a mixed microbial culture grown from sludge inoculum to different temperature changes so that a suitable temperature for the further development and implementation of industrial scale MECs. The hydrogen producing bacterial consortium was determined to predominantly mesophilic in character, with temperatures above 35 ^{o}C and below 19 ^{o}C inhibiting the hydrogen production rate, as shown in figure 20. Lower anode also overpotentials developed at lower temperatures due to better mass transfer capabilities. With coulombic efficiencies ranging from 57 % to 62 % at an applied voltage of 850 mV and cathode pH 5, the highest hydrogen yield 1.1 $mol_{(hydrogen)}$ $mol_{(acetate)}^{-1}$, corresponding to volumetric production of 200 cm^3 $L_{(anode)}^{-1}$ day^{-1} were comparable to results reported in literature Table A-2.7 in Appendix A-2 section 9.2. There is however room for improvement with lower daily hydrogen production rate observed for larger, 6.6 L systems with hydrogen production of 20 cm^3 $L_{(anode)}^{-1}$ day^{-1}, (molar yield not specified) by Rozendal et al (2006b), see Table A-2.7 in Appendix A-2 section 9.2. The performance of MFCs, for example, can be enhanced by addition of artificial electron carriers (electron mediators), see Table A-2 in Appendix A-2.2 section 9.2, but have not been extensively used for MECs.

Hydrogen production rate at 600 mV and at temperatures as low as 19 - 23 ^{o}C as well as at 43 and 50 ± 3.0 ^{o}C was also shown to be possible, as mentioned in “Results” (sections 6.1.2 - 6.1.3). For a larger scale continuous flow system to be used with typical industrial waste waters, this could make the process more efficient in terms of the energy consumption, as the industrial wastewaters are produced at ambient temperatures.

It was also shown that the current density, which is proportional to the hydrogen production, could be logged continuously on line and was successfully used to monitor MEC performance. This would allow industrially deployed units to be monitored and controlled by computer based systems.

6.2 The Effect of Immobilized Methylene Blue and Neutral Red on the Current Production in Microbial Fuel Cells (MFCs)

The purpose of this experiment was to investigate the effect of immobilized mediators on the performance of bioelectrical systems (BESs). Microbial fuel cells (MFCs), BESs that convert the chemical energy into electricity were chosen for this experiment as a relatively quick way of determining the effect of immobilized mediators on electrogenic activity and can be compared to a relatively large body of information where soluble mediators have been used. The voltage produced by a MFC can be used to calculate the efficiency with which organics in the feedstock were converted into electricity by the exoelectrogenic bacteria on the anode surface. Voltage generation, power density and the percentage of substrate consumed by bacteria in MFCs (standard MFC performance factors) were also assessed. Cyclic voltammetry and UV spectroscopy were used to determine how much electron mediator was adsorbed on the electrode surface (described in "Methods to Determine how Much Mediator was Adsorbed on the Electrode Surface" (section 4.8.4) in greater detail).

All MFC reactors were run under the same conditions. Temperature was maintained at 23±2 ^{o}C (room temperature) and pH of the solution containing substrate (20 mmol L^{-1} acetate) was maintained at pH 7. All sequencing batch mode reactors (SBR) (Mohan et al., 2008a, Logan et al., 2009b) were operated in MFC mode for 50 weeks, seven months, and refilled once a week after two week start up (MFC operation with sludge in them). The reason MFCs were operated for such a long period of time was to allow the development of a biofilm on the anode surface and colonization being a slow process that can be split into bacterial to the anode surface attachment during two week start up (MFC operation with sludge) and the development of mature biofilm, after the sludge was removed, can take several month to complete (Hall-Stoodley et al., 2004, Xie et al., 2010). Performance factors, such as voltage production, power density; coulombic efficiency (CE) and energy recovery were calculated as shown in "Electrochemical Analysis Methods" section 4.7.

6.2.1 Dye Adsorption Tests Preformed Prior to the Experimental Run

Two quantitative techniques were used to determine exactly how much dye was adsorbed on the carbon anode surface. Adsorption of methylene blue (MB) and neutral red (NR) on carbon veil was determined by weight difference and the amount of dye adsorbed on the carbon surface (experiments 2 I - iii). Experiment 2 iv investigated how much dye was coming of into the solution. Before Experiments 2 i – iv calibrations plots were produced as described in "Offline Analysis Methods" section 4.8.4.

The calibration plots (Fig. 21 a and Fig. 21 b) had R^2 values ≈ 99, which indicates that points fit into a straight line with high degree of accuracy (see Table 6 for concentration and absorbance peaks scanned to plot the calibration graphs).

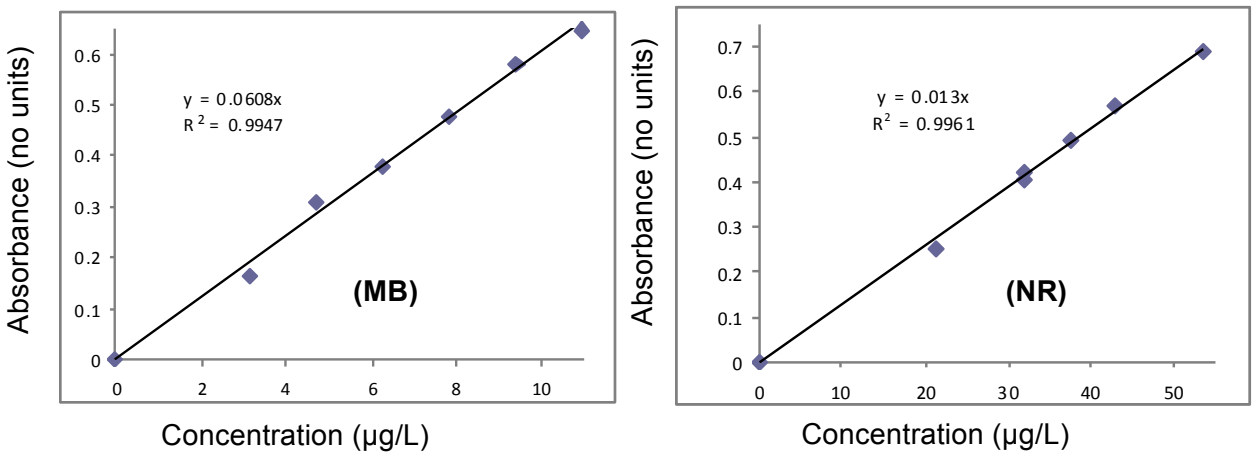

Figure 21 – Examples of calibration curves for determining the concentrations of methylene blue (MB) and neutral red (NR).

The aim of these experiments was to determine how much dye remained in solution and then to determine how much dye was coming off in 4 sequential washes, which were applied until no dye was coming off at pH 5.5 (experiment 2i). Experiments 2 ii – iii were designed to access the effect of increase in pH from 5.5 to 12 on methylene blue (MB) and neutral red (NR) adsorptions on the material from which the carbon anodes for microbial fuel cells (MFCs) were made. All methodology is described at the end of "Offline Analysis Methods" section 4.8. UV adsorption tests showed that at pH 12, similar amounts of MB ≈ 1.23 ± 0.23 mg cm^{-2} were initially adsorbed, after 4 washes however ≈ 0.54 mg cm^{-2} remained for material treated with MB at pH 12 and ≈ 0.23 ± 0.1 mg cm^{-2} remained for material treated with MB at pH 5.5. Determination of amounts of MB adsorbed by weigh difference produced similar results to UV spectroscopy analysis with more variability and confirmed this observation.

The results for UV spectrophotometry analysis and determination of MB adsorbed by weight difference were included into (Fig. 22 a – Fig. 22 d) with error bars being variations from the average (standard deviations) for results obtained via UV spectroscopy and changes in weights. Figure 22 shows the amounts of dye adsorbed on the carbon veil surfaces from 1.56 mmol L^{-1} solutions at different pHs (22 a and 22 b) and from 0.94 mmol L^{-1}, 1.25 mmol L^{-1}, 1.56 mmol L^{-1} dye solutions (22 c and 22 d) at pH 5.5. 6 samples were for each concentration (3 determined via UV adsorption changes in dye solution into which the samples were placed and 3 determined by weight differences for MB and neutral red (NR) solutions). The experimental results (Fig. 22 a – Fig. 22 d) showed that the increase in pH increases the dye adsorption from dye and buffer solution.

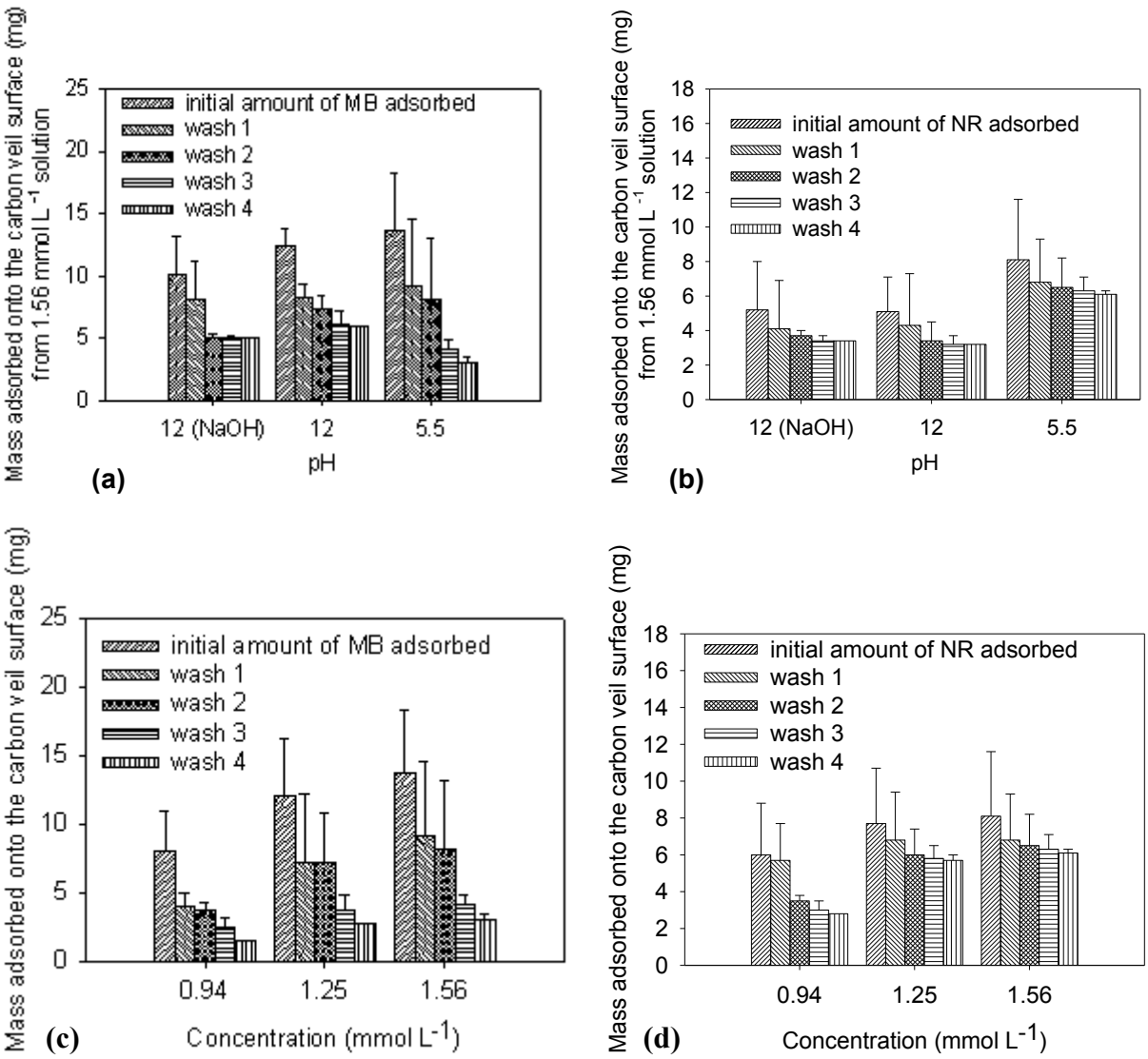

Error bars represent variations from the average for *n* experimental repeats (*n*=3)

Figure 22 – The effect of increase in concentration (a and b) and pH (c and d) on the amounts of dye adsorbed on the carbon veil surfaces.

Similar results were previously obtained by Foo and Hameed (2012), Hameed et al (2008), who used activated charcoal to remove methylene blue from the wastewater. According to our knowledge however no similar work was attempted with carbon veils used as anode material for microbial fuel cells (MFC) nor has it been attempted to investigate if immobilized electron mediator could enhance the performance of MFC for prolonged time periods in sequencing batch (SBR) mode.

6.2.2 Cyclic Voltammetry Tests for Determination of Dye Concentration on the Anodes and Presence of Cytochromes in the Effluent Samples

Cyclic voltammery (CV) can be used to confirm if methylene blue (MB) or neutral red (NR) was adsorbed on the carbon anode surface, if the adsorption was strong or weak and even to confirm the presence of presence of exoelectrogenic bacteria in the effluent samples. Most exoelectrogeic proteobacteria species contain cytochrome enzymes, which produce oxidation and reduction peaks which could be detected by CV.

CV allows to confirm passive adsorption of electron mediators, such as methylene blue (MB) or neutral red (NR) on the carbon veil anode surface solution (Bard and Faulkner, 1976). It is however impossible to determine exactly how much mediator was adsorbed on the carbon anode surface, therefore it's referred to as a qualitative technique. The presence of so-called pre or post peaks confirms strong adsorption. Pre peaks indicate that adsorbed mediator has slightly lower redox potential than mediator in the solution and post peaks indicate slightly higher redox potential for the adsorbed mediator compared to mediator in the solution (Bard and Faulkner, 1976). When weak adsorption occurs a larger and wider peak is observed for CV spectrum for the carbon anode in the mediator solution compared to that for the anode in the mediator solution where no adsorption occurs.

In order to investigate physico-chemisorption of MB on the carbon electrode, cyclic voltammetry tests were conducted, as described in "Electrochemical Analysis Methods" section 4.7. Figure 23 shows reduction and oxidation peaks were obtained from MB treated carbon electrode at pH12 (0.69 mA at -0.13 V and -0.85 mA at -0.29 V, respectively), compared to those for the same material treated at pH5.5 (0.10 mA at -0.20 V and -0.38 mA at -0.27 V, respectively) and 1.34 mmol L^{-1} MB in solution (0.10 mA at 0.20 V and -0. 23 mA at 0.14 V, respectively). The peaks at (-0.13 V at 0.69 mA and -0.29 V at -0.85 mA) shown in figure 23 for the MB treated carbon veil anode at pH 12 and (-0.20 V at 0.10 mA and -0.27 V at -0.38 mA) for the MB treated carbon veil anode at pH 5.5 (Fig. 23) are pre-peaks observed for strongly adsorbed substance on the carbon veil anode surface (Bard and Faulkner, 1976). Small peaks for MB electrode treated at pH 12 (0.20 mA at 0.3 V and -0.16 mA at 0.2 V) shown in figure 23 could be contributed to the mediator dissolving back into the solution from the electrode surface. The reason that peaks for MB in solution were not present, was because the MB treated electrode was washed in 4 sequential buffer aliquots, as described in "Offline Analysis Methods" section 4.8.

It is highly unlikely that any mediator that could dissolve back into the solution would remain on the carbon veil anode surface after four 28 hour washes with buffer solution as previously described in experiment 2 ii in "Experimental Regime" section 5.

The control untreated carbon veil anode, in buffer solution S1 produced no redox peaks. CV analysis was only performed on methylene blue (MB) treated anode samples since it was shown to improve microbial fuel cell (MFC) performance, as described in "Electrochemical Analysis Methods" section 4.7.

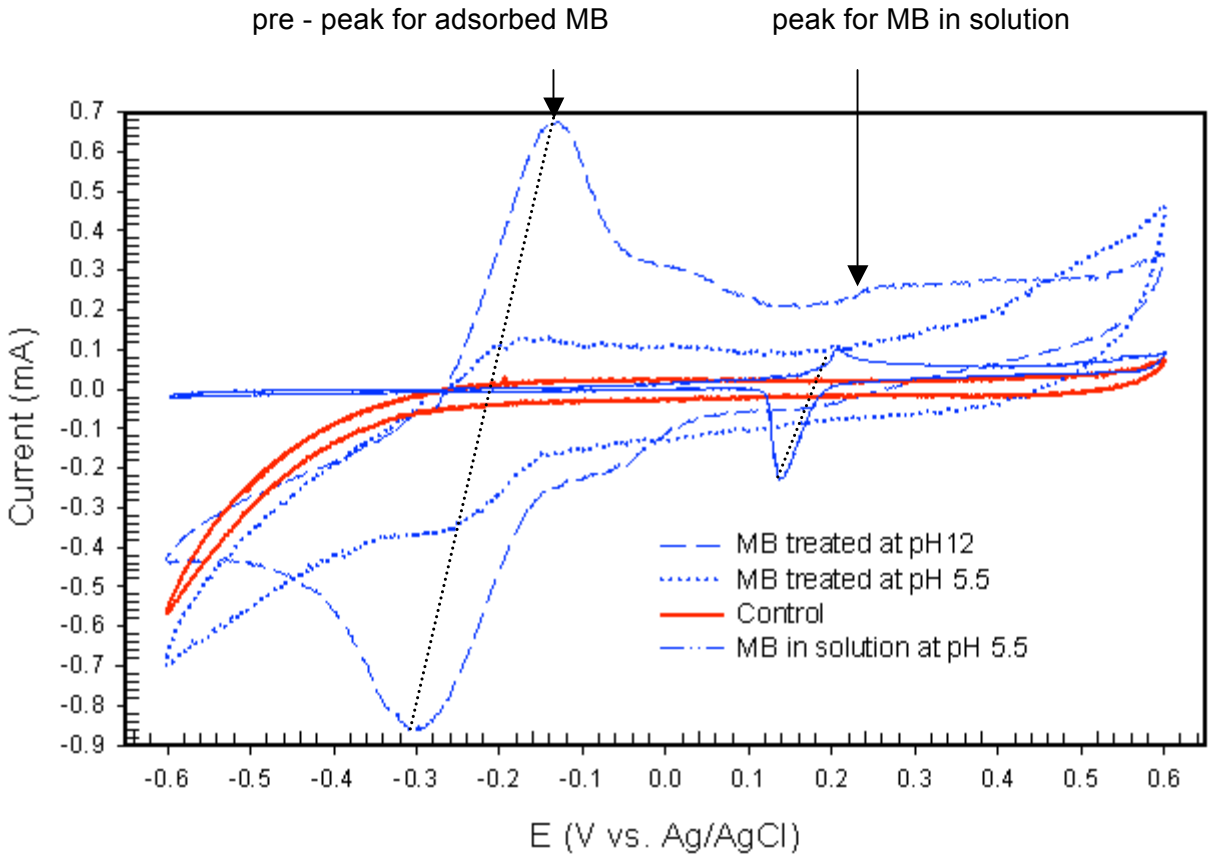

The dashed lines connect the oxidation and reduction peaks of MB.

Figure 23 – Cyclic voltammogram showing methylene blue (MB) pre-treated carbon electrodes as compared to control and MB in solution.

Cyclic voltammetry is also a useful tool in detecting redox peaks for cytochromes in effluent samples or to discern whether or not bacteria use redox shuttles in order to transfer their electrons. It could also be argued that mediators such as methylene blue (MB) and neutral red (NR) promote the growth of exoelectrogenic bacteria, such as *Geobacter*, for example. If this is true then the effluent from the microbial fuel cells (MFCs) with mediator treated anodes will contain more cytochrome enzymes, which are present in membranes of many exoelectrogenic bacteria (Logan, 2009) compared to MFCs with untreated carbon veil anodes.

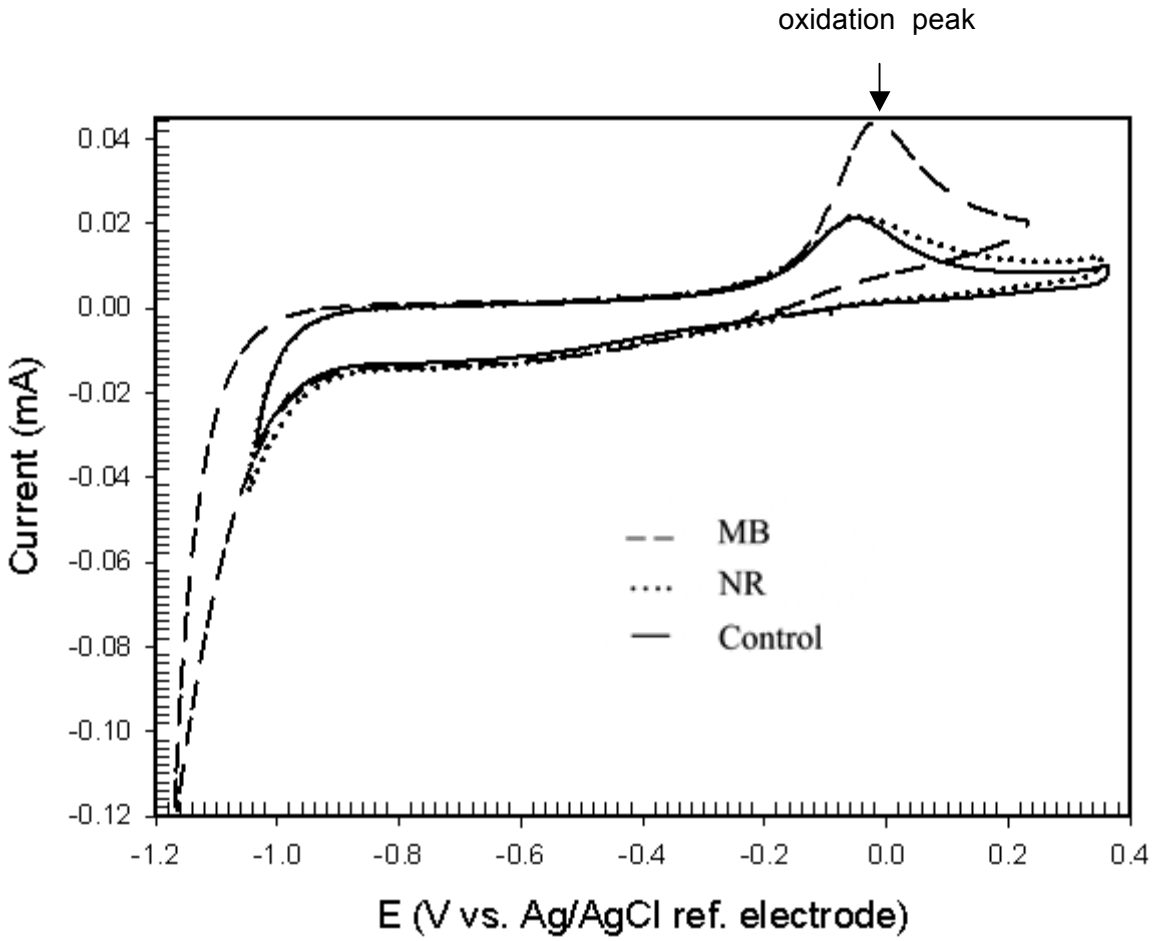

Figure 24 – Cyclic voltammogram of MFC effluent of MFC effluent containing bacteria, with MB and NR and carbon only (control).

The aim of analyzing effluent samples from the MFCs in weeks 15-20 after the beginning of batch operation was to see if the effluent samples from MFCs with mediator treated anodes produced taller cytochome oxidation peaks (Fig. 24), since it was very unlikely that any mediator was coming off after 15-20 sequencing batch (SBR) operational cycles. All samples were prepared and all CV tests were carried out as described in the "Electrochemical Analysis Methods" section 4.7.

The results showed taller peaks in the cytochrome voltammogram region at -0.02 V and 0.042 mA for the MFC with MB treated anodes, which supports the hypothesis that effluent from the MB MFC contained more exoelectrogenic bacteria.

6.2.3 Microbial Fuel Cell (MFC) Operation

i) Time Dependant Voltage Plots:

For experiment 2.1, the voltage was monitored manually once a day across a 150 Ω resistor at room temperature (23±2 ^{o}C) using a multimeter (Fluke 115 low input impedance multimeter) and logged manually once daily for each of the 3 replicate MFCs. The average of the readings from the three experimental replicates is represented by a single data point on the plot shown in figure 25. Before describing the data it is important to mention that when the voltage readings are described at a particular resistance the power obtained from that resistance was added in the text description next to the voltage values for the sake of clarity and facilitate interstudy comparison. In the text *n* refers to the number of experimental repeats for all the data points for voltages are averages of 1 reading from 3 replicate reactors and ± values refer to voltage fluctuations on the plot. Figure 25 shows the development of voltage generation in the MFC with adsorbed MB and NR treated carbon electrode, compared to a control with an untreated carbon anode. For the MFCs with the MB modified anodes the voltage generation began to noticeably increase from 6 days after the sludge was placed into the acetate / buffer solution (Fig. 25), reaching 153 ± 10 mV (0.78 ± 0.01 W m^{-3}), on week 2, day 8; and slowly increased/stabilized at 286 ± 20 mV (2.73 ± 0.01 W m^{-3}), on day 20, in week 3.

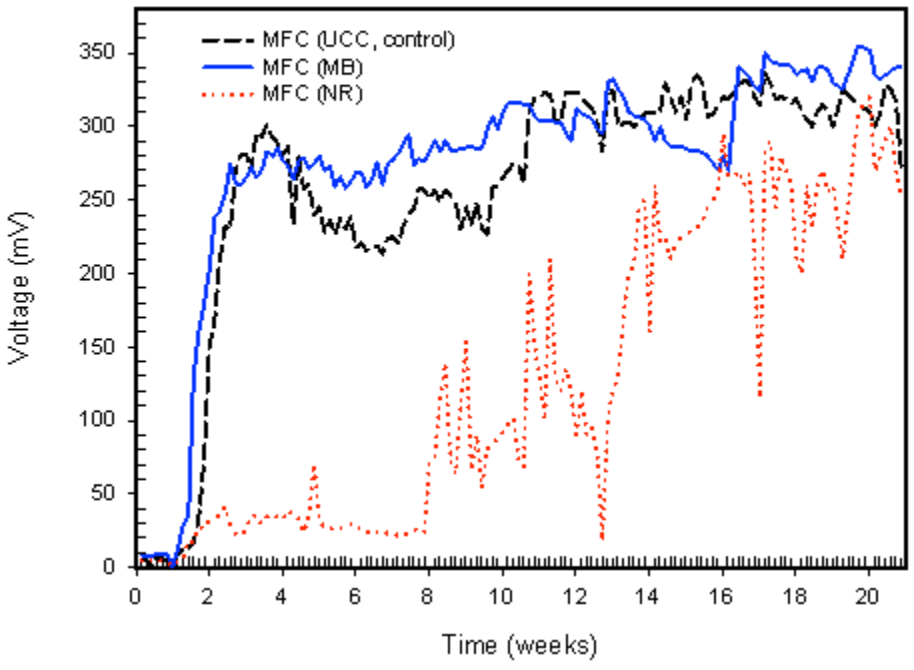

All values on this figure are averages of *n* experimental repeats (*n*=3).

Figure 25 – The development of voltages in MFCs with immobilized MB and NR compared to a control without mediator over 21 week operation.

In the later period of the experiment from days 23 – 71 in weeks 3-10; the voltage continuously increased and reached 366 ± 30 mV (4.47 ± 0.03 W m^{-3}) on day 118, week 16; and then stabilized at 353 ± 20 mV (4.15 ± 0.01 W m^{-3}) on day 154; (week 22), with a 150 Ω resistance.

The NR treated carbon electrode, however, showed a relatively low voltage for 154 days (22 week) period (Fig. 25). The voltage slowly increased from 0.45 ± 0.2 mV (0±0 W m^{-3}) on week 1, (days 1-5), to 43.4 ±20 mV (0.6±0.01 W m^{-3}) on day 23, week 3, and stabilized at 40±10 mV (0.6±0 W m^{-3}) on days 28-63, week 4-8, slowly stabilising at 280 ± 30 mV (2.61 ± ±0.03 W m^{-3}) on days 140 – 154, weeks 20 - 22.

The control (UCC, without mediator) showed a lag phase of 1 week (8 days), then rapidly increased and stabilized to approximately 301.7 ± 30 mV (3.03 ± 0.03 W m^{-3}) on week 2, day 19, (see figure 25 for details). In the later period of the experiment (weeks 3 - 10, days 23 - 71), the voltage slowly increased and subsequently peaked at 338 mV ± 30 mV (3.81 ± ± 0.03 W m^{-3}) on day 141, week 21.

ii) Coulombic Efficiency (CE) and Energy Efficiency:

One of the aims of microbial fuel cell (MFC) research is to extract as many electrons as possible and to recover as much energy as possible from the available biomass substrate. The coulombic efficiency (CE) and energy efficiency for sequencing sequencing batch (SBR) operation were calculated, as previously described in "Electrochemical Analysis Methods" section 4.7. Table 9 represents coulombic efficiency (CE) and energy recovery (E) values observed for the MFC with a MB treated anode and control at 150 Ω resistance. Coulombs recovered (CE_p) and energy recovered (E_p) were added for comparison purposes. The MFCs with MB treated anodes had the highest CE and E values (Table 9) that were 4% higher than the control, at 150 Ω resistance.

Table 9 – Comparison of coulombic efficiency (CE) and energy recovery (E) values for MFCs fed with acetate (20 mmol L^{-1}).

Resistance		CE_p (c)	CE (%)	E_p (J)	E (%)
150Ω	control (UCC)	2408	78	728	21
	MB	2532	82	770	22
	NR	1637	53	385	11
CE_t (AC) = 3088 c, E_t (AC) = 3501 J					
Where all CE_p, E_p, values are calculated from curves in figure 25					

It could be argued, however that if a lower resistance was used, such as 60 Ω resistor CE values would be much higher for the MFC with MB treated anodes (as described in a "Electrochemical Analysis Methods" section 4.7). The reason, a 60 Ω resistor was not used for this experiment was because it was designed to compare to work previously published by Kim et al (2009b) and Kim et al (2010).

iii) Power Density Monitoring:

Knowing the coulombic efficiency (CE) and energy recovery (E) does not sufficiently describe how the power is generated by specific microbial fuel cell (MFC) architecture. Power is normalized across the volume of the anode chamber or anode surface area and is another performance factor, which has to be assessed to perform comparative evaluation. Power density plots (Fig. 26) were created as described in "Electrochemical Analysis Methods" section 4.7 and examples with detailed calculations. For each power density plot the resistance was increased to the open circuit resistance (∞), for 2 hours, and decreased to the lowest resistance 10 Ω, for 1 hour periods. All values for figures 25 and 26 were calculated from as the average for *n* experimental repeats (*n*=3) voltages used to calculate powers and cell potentials.

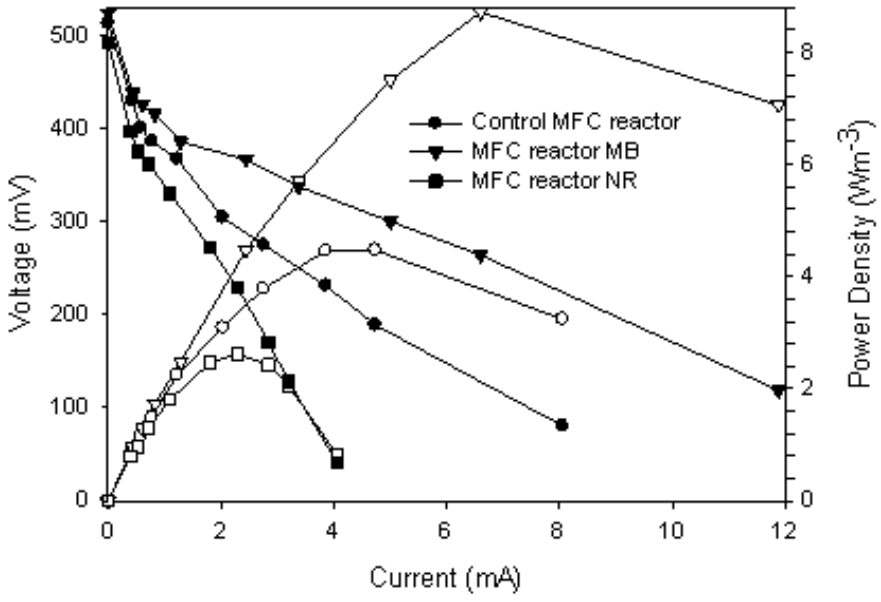

All values are calculated average voltage values for *n* experimental repeats (*n*=3) voltages.

Figure 26 – Comparison of voltages (closed symbols) corresponding to highest power densities (open symbols) for MFCs with MB and NR immobilized carbon electrode on day 118. For space reasons only closed symbol key shown but symbol shape is same for the reactors for the power densities when the symbol is open.

This experiment was operated over 21 weeks, after the voltage output for MFC (MB) stabilized at 323±20 mV, (*n*=3) with 150 Ω resistance (Fig. 27). The power densities at low resistances were measured once a week, (as described in "Electrochemical Analysis Methods" section 4.7). Power densities and currents at a 40 Ω resistance (resistance was dropped from 150 to 10 Ω once a week were used to produce figure 26 as explained in section 4.7.4 in greater detail) were used to produce figures 27 a and 27 b. A 40 Ω resistance was chosen for figure 27 because it was the resistance at which the highest power densities and currents were recorded on week 20 (Fig. 26).

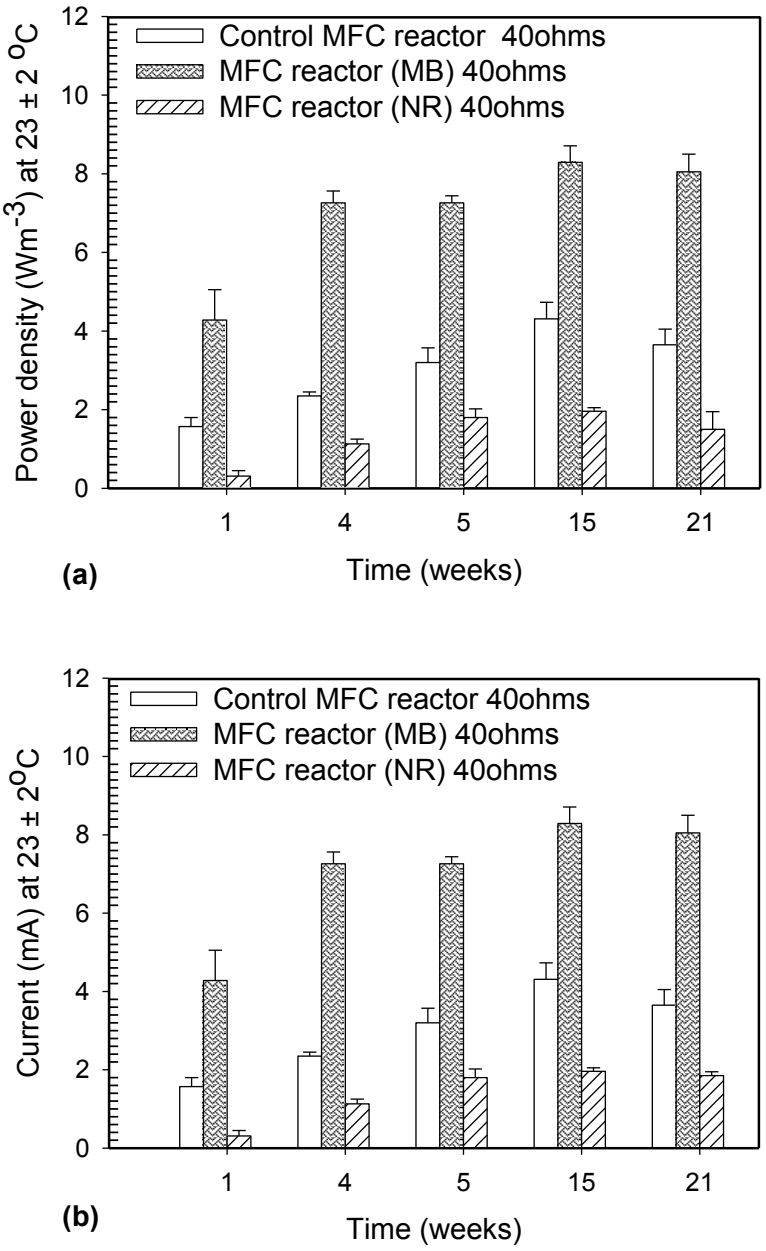

Error bars represent variations from the average for *n* experimental repeats (*n*=3)

Figure 27 – Comparison of power densities (27 a) and currents (27 b) for control MFC and MFCs with MB and NR treated anode.

Figures 27 a and 27 b show the increase in current production and power density observed for the MFC with MB treated anode. The MFC with MB treated anode was shown to produce 3 times more maximum power during initial 4 weeks compared to control and two times as much as control on weeks 15 – 21. The methylene blue treated anode had long lasting positive effect on power current production and allowed power to develop faster reaching steady state after 4 weeks compared to control (15 weeks). MFCs with neutral red (NR) treated anodes also reached steady state after 4 weeks with inhibitory effect on electricity production (approximately 3-4 times less than control).

The purpose of the temperature variation experiments was to determine if the biofilm grown at room temperature was mesophilic and to determine if the MFCs with MB treated anodes still performed better at different temperatures. The temperature experiments were carried out on week 21 (Fig. 28), when the highest power density was recorded at room temperature (23±2 ^{o}C) for MFC (MB) P_{max} = 8.7 Wm^{-3} (6.6 mA) and MFC (NR) P_{max} = 2.63 W m^{-3} (2.29 mA) as shown in figure 27, as compared to MFC (control) P_{max} = 4.5 W m^{-3} (4.7 mA). A series of pilot experiments were carried out to determine the initial temperature range tested in this experiment (data not shown). Temperatures above 40 ^{o}C and below 7 ^{o}C were shown to irreversibly reduce the voltage production, the power densities and the substrate consumption for MFCs. For the temperature control, experiments the temperature was initially increased to 35.5 ^{o}C (highest temperature found to be tolerated by bacteria in this study) for a week (power density was recorded on the last day of that week) and then decreased to 8 ^{o}C for a week and power density was recorded again on the last day (see “Experimental Regime” section 5 for details). The peak power was higher by a factor of two for the MFC with MB treated anode compared to the control, as well as the power densities at low load resistance and high current regions. The highest power density for MFC (MB) P_{max} = 11.78 W m^{-3} (7.5 mA) was obtained as compared to MFC (control) P_{max} = 5.3 W m^{-3} (5.2 mA) and MFC (NR) P_{max} = 3.06 W m^{-3} (3.19 mA) at 35 ^{o}C (Fig. 28). The lowest power density P_{max} for MFC (MB) = 7.3 W m^{-3} (6.05 mA) was obtained as compared to MFC (control) P_{max} = 4.05 W m^{-3} (4.5 mA) and MFC (NR) P_{max} = 2.46 W m^{-3} (2.21 mA) at 8 ^{o}C. The increase in the maximum power densities with MB treated carbon electrode was more pronounced compared to those of the control and NR electrode, when the temperature was increased from 8 to 35.5 ^{o}C (Fig. 28) simultaneously. Also, no methane production occurred indicating lower methanogenic activity with MB electrode (Table 10). The results shown in figure 28 are comparable to other reports that investigated the influence of temperature on microbial fuel cell performance (Catal et al., 2011, Michie et al., 2011).

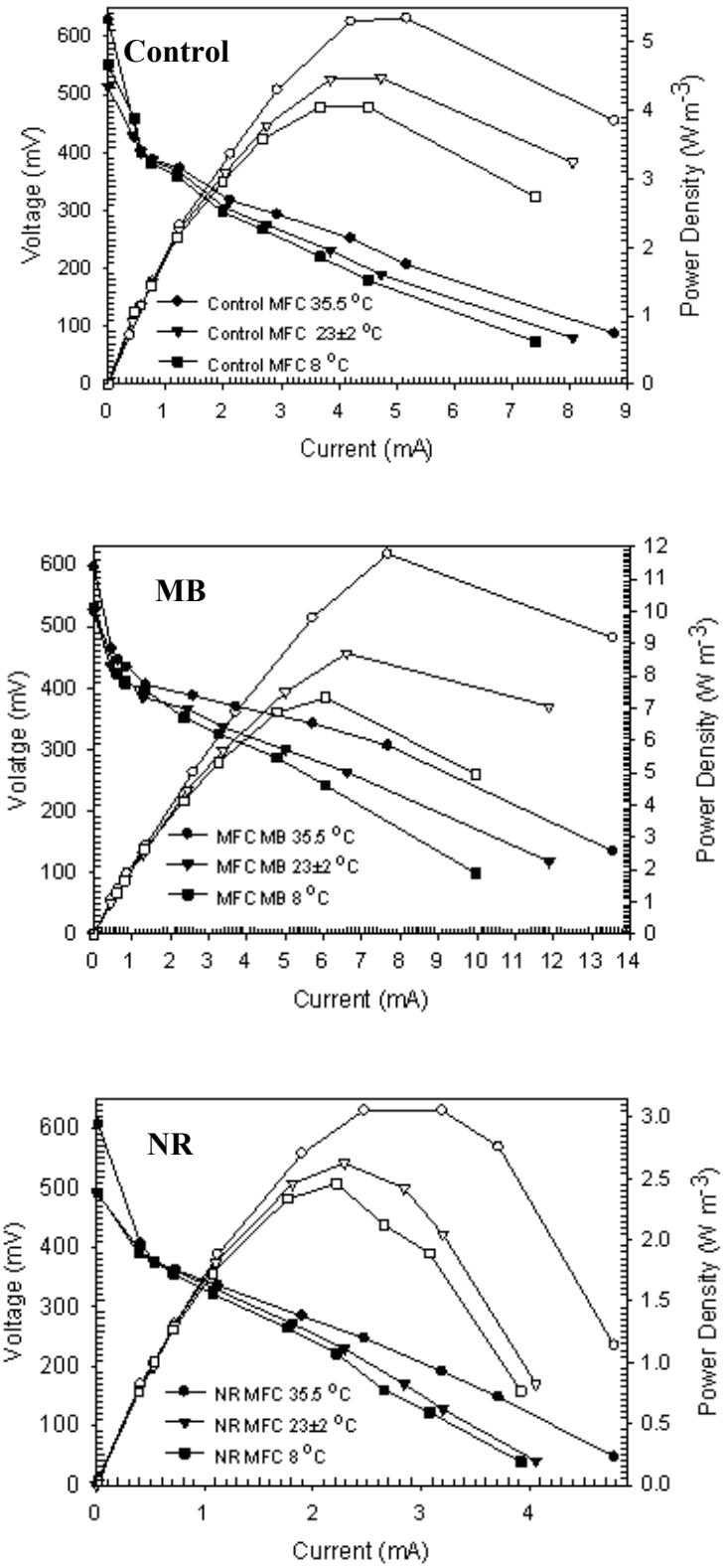

All values are calculated for average voltages for *n* experimental repeats (*n*=3).

Figure 28 – Comparison of currents to voltages (closed symbols) and power densities (open symbols) for MFCs at different temperatures on day 118. For space reasons only closed symbol key shown but symbol shape is same for the reactors for the power densities when the symbol is open.

iv) VFA Removal Rates:

The percentage VFA (predominately acetate) removal for the microbial fuel cells (MFCs) with either control, methylene blue (MB) or neutral red (NR) treated carbon electrodes are shown in figure 29. It shows that similar amounts of substrate were consumed by the bacteria but the voltage (Fig. 25) and the power produced by MFCs was different (Fig. 26 – Fig. 27b). As shown on in figure 29 initial average VFA removal (%) values in the MFCs were 7.4 mg / L / day (9.7 %, *n* = 3 where error bars which refer to the number experimental repeats) for the control; 30 mg / L / day (39.7 %, *n* = 3) for NR, and 23 mg / L / day (30.5 %, *n* = 3) with MB treated carbon anodes, respectively. Higher percentage VFA removal in the MFC with MB treated carbon anode was accompanied by a higher voltage generation during the initial increase in voltage over days 5 - 16 in the start-up Period. The percentage VFA removal increased for all reactors, for example from 9.7% to 87 % (67mg / L / day, *n* = 3) for the control MFC, from 30.5 to 83 % (63 mg / L / day, *n* = 3) for the MB MFC and 39.7 to 82 % (63mg / L / day, *n* = 3) for NR MFC.

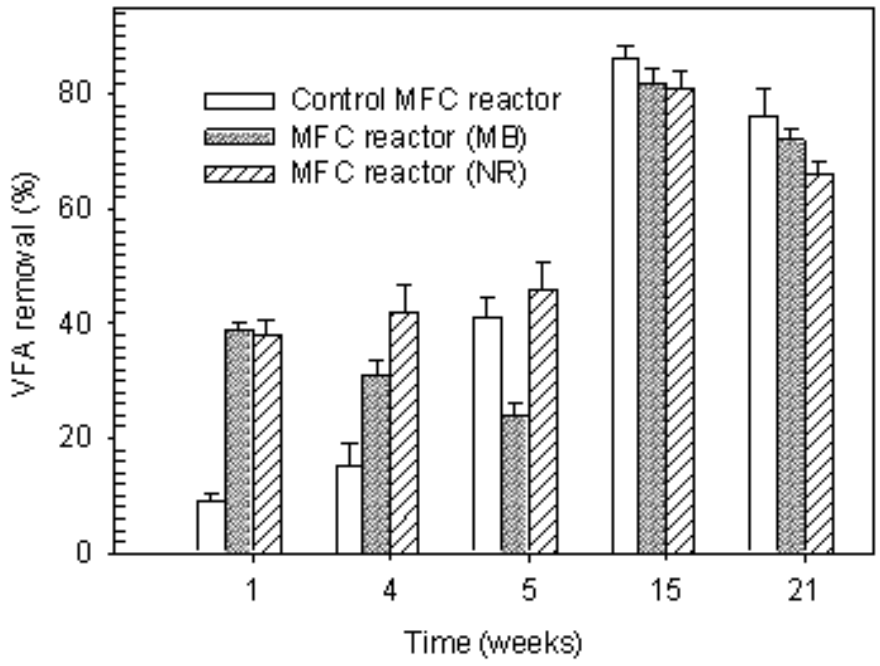

Error bars represent variations from the average for *n* experimental repeats (*n*=3)

Figure 29 – VFA removal (%) in MFCs with MB, NR modified anodes and a control, with carbon electrode.

v) Comparison of Gas Production:

The purpose of monitoring gas composition of the headspace in microbial fuel cells (MFCs) was to determine the amount of methane given off by the MFC. This may explain the small voltage production combined with high percentage VFA removal (substrate consumption) in particular cells or experiments. Methane producing archaea act as electron sinks for electricity producing bacteria, so a high methane percentage in the headspace combined with low voltage production indicates presence of archaea in MFCs (Wang et al., 2009a, Parameswaran et al., 2011).

The amount of gas produced was very small in these experiments. The headspace size, inside the reactor, was 12.56 cm^3 in volume. It was periodically exposed to air, when the substrate was replaced. Then it would be expected to have 2.64 cm^3 of oxygen present in the head space, since air contains 21% oxygen (Dominguez et al., 2004). The gas analysis showed that the oxygen in the samples was largely consumed, as shown in Table 10. The nitrogen percentage in the gas in all reactors was almost the same as that in air, without oxygen. This suggests that the oxygen was consumed by aerobic bacteria. It is reasonable to suggest:- that the biofilm had complex structure and contained both aerobic and anaerobic bacteria. The voltage output in microbial fuel cell is a good indicator that the electrogenic bacteria are utilizing the substrate (Dietel et al., 1983). Since there are no aerobic electrogenic bacteria identified to date and the voltage went up and stabilized after one, sometimes two days, it is reasonable to suggest that the process was occurring in two stages.

The first stage occurred when the oxygen was consumed by aerobic bacteria and then, when the voltage went up, the anaerobic environment was created favorable for the metabolism of exoelectrogenic bacteria. An increase in methane production was seen on day 7 and it then decreased after the sludge was removed and replaced with fresh media on day 14 (Table 10) and was also accompanied by a low carbon dioxide concentration which could be attributable to hydrogenotrophic methanogenesis (Tartakovsky et al., 2008, Rozendal et al., 2008b). Methanogenic activity decreased significantly from days 14 to 147 (data not shown), in the MFC containing an MB treated carbon anodes, while 0.07 - 0.14 % of methane was detected in the control and the NR treated carbon anode MFC. An increase in carbon dioxide production on day 7 was also accompanied by an increase in VFA removal (Fig. 29), voltage (Fig. 25), power density and a gradual increase in power density and current in all reactors (Fig. 27).

Table 10 – The average values for gas compositions over time.

Time (weeks)	Material / treatment	H_2 (%)	O_2 (%)	N_2 (%)	CH_4 (%)	CO_2 (%)	Total gas volume (cm^3 day^{-1})
1	NR / carbon anode	0	0	80.5±5	2.5±0.5	0.44 ±0.2	0.5±0.1
	MB / carbon anode	0	0	83.1±7	4 ±1	0.39±0.2	0.4±0.1
	control (carbon electrode)	0	0	77.3±3	0.3±0.1	1.01±1	0.5±0.1
2	NR / carbon anode	0	0	76.5±5	0	2.05±0.9	5±2
	MB / carbon anode	0	0	77±5	0	1.83±0.5	1.75±5
	control (carbon electrode)	0	0	77±5	0	0.76±0.1	2.4±0.7
22	NR / carbon anode	0.02±0.01	0	75±5	0.14±0.02	1.05±0.3	1.05±0.6
	MB / carbon anode	0	0	77±2	0	4.56±0.5	8±2
	control (carbon electrode)	0	0	74±5	0.1±0.02	0.89±0.1	0.5±0.1

± represents variations from the average for *n* experimental repeats (*n*=3)

6.2.4 Discussion

Up to 0.54 mg cm^{-2} of MB was successfully and permanently adsorbed from a 1.56 mmol L^{-1} MB solution on the carbon veil electrode surface when pH of the buffer solution was changed to pH 12 for 28 h compared to 0.23 mg cm^{-2} mg adsorbed at pH 5.5 during 28 h period. This was confirmed by determining how much dye was adsorbed from the buffer / dye solution on the carbon surface (Fig. 22) and cyclic voltammetry (CV) data (Fig. 23). Although MB has been used as a mediator in many studies (Daniel et al., 2009, Wang et al., 2010c, Mohan et al., 2008b), immobilization of MB on the electrode by a physico-chemical adsorption of pH shifting has not been done before in microbial fuel cells (MFCs). This could be a feasible activation method for carbon electrodes for electrogenic bacteria, which could simultaneously treat contaminated wastewater (e.g. dye), and generate electrical power (Fernando et al., 2014). The increase in MB concentration in buffer solution and the increase in pH from 7 to 12 for 28 hours facilitated dye adsorption onto thecarbon veil electrode. The reason for higher MB adsorption at higher pH could be that H^+ ions are significantly smaller than other cation groups and more likely to cluster around sligtly negatively charged carbon fibres due to presence of delocolized electrons, as shown in figure 9 (Senthilkumaar et al., 2005). It is likely that MB, in its ionic form, interacts with delocolized electrons on carbon at higher pH, when the concentration is H^+ protons is small. These results are confirmed by the studies on MB adsorption on saw dust (Hameed et al., 2007a, Hameed et al., 2007b) to form an activated MB-carbon anode.

NR was poorly adsorbed on the carbon suface (Fig. 22) at pH 12. This can be explained by Henderson–Hasselbalch equation describes the derivation of pH as a measure of acidity (using pK_a, the negative log):

$$pK_a+\log_{10}((NR)/(NR^+H)=pH \quad \text{Eq 74}$$

where pK_a is acid dissociation constant (a quantitative measure of the strength of an acid in solution, no units); $(NR)/(NR^+H)$ is the ratio of reduced NR molecules to oxidized NR molecules and the pH is a unit less measure of the acidity or basicity of an aqueous.

If specific pK_a value for (NR) = 6.8, than, at pH = 6, $(NR)/(NR^+H)$ = 1 (no units) and if pH = =12 than $(NR)/(NR^+H) = 1 \times 10^6$ (no units). This shows that more neutral red (NR) stays in its non polar NR form, if pH is increased. If pH is decreased more NR stays in NR^+H form. NR also seemed not to be efficient in the methods used here for electricity production (Fig 25 – Fig. 28), though NR can also be immobilized and be an effective electron mediator, as discussed in previous studies (Housecroft and Sharpe, 2007).

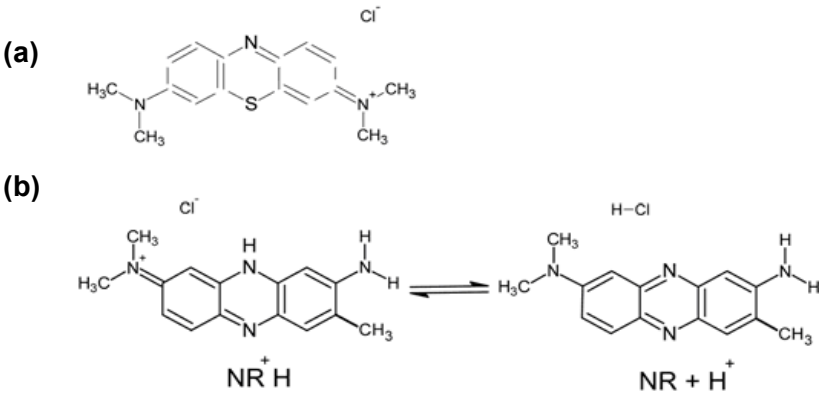

Figure 30 – Molecular structure of MB (30 a) and dissociation equation for neutral red (NR) (pKa = 6.8) (30 b).

The voltages (Fig. 25) indicate that the adsorbed methylene blue (MB) mediator can facilitate rapid initial voltage development in MFCs. When the biofilm developed on the anode electrodes, the average voltage outputs observed (average for all voltage readings recorded from day 71 to day 154) were almost the same for the MFCs with MB treated carbon electrodes and the control (313 and 309 mV, respectively). The neutral red (NR) treated carbon electrode showed significantly lower average voltage output (223 mV) from day 71 to day 154.

The VFA removal rates (Fig. 29) were similar for MB and NR treated electrodes, yet CE values (Table 9), voltage (Fig. 25) and power densities (Fig. 25 – Fig. 28) were lower for MFCs with NR treated anodes.

The comparison of VFA removal rates to electricity production at this time suggested but not fully confirmed that NR had an inhibitory effect on electricity production that has not been reported in literature before. The proposed reason for inferior performance is that NR made anode into poor electron acceptor promoting growth of archaea which act as electron sinks for electricity producing bacteria.

The power density was monitored on a weekly basis and was shown to slowly increase with time (Fig. 27). All microbial fuel cells MFCs were operated at room temperature (23±2 ^{o}C) with highest power densities recorded on weeks 19, 20 and 21, at 40 Ω resistance, when the resistance was increased to open circuit and decreased every hour (see Table 10 and "Analysis" for details). The peak power density P_{max} (MB) was twice as high as P_{max} (control) which was twice as high as P_{max} (NR) (Fig. 28). The percentage of volatile fatty acids (VFAs, in this case acetate) was almost exactly the same on weeks 15-21 (days 105-150) as shown in figure 29. It is likely that this was because of the limited electron current flow between the bacteria and electrode (Logan et al., 2006). The increased power density at higher current obtained in MB treated carbon supports the hypothesis that immobilized MB improves the electron transport from the bacteria to the anode.

The aim of temperature controlled experiment, performed at the end of week 21 (see "Experimental Regime" section 5 for details) was designed to investigate the effect of temperature on microbial culture grown in mesophilic conditions, at room temperature so that data obtained could be compared to results previously obtained by the same team, already published in literature (Michie et al., 2011, Kim et al., 2009b). The enzymatic activity for enzymes in mesophilic bacteria decreases with decrease in temperature and the increase in temperature above 40 ^{o}C - 45 ^{o}C causes enzymes to be denatured. The experiments confirm that the temperature range 30 ^{o}C - 35 ^{o}C is considered to be optimal for most mespohilic bacteria, as in published work by Popov et al (2012) in greater detail. As shown on Table 9 energy recovery (E) values follow the same trend as coulombic efficiency (CE) values.

It could be suggested that most of energy recovered from the substrate is diverted to other metabolic processes than electricity production Strikanth and Venkata Mohan (2012), Logan (2009). Microbial fuel cells MFCs were operated for 21 weeks (21 batch operations) because the biofilm on the anode surface takes a long time to establish. After the initial adhesion of the bacteria driven by weak Van der Waals forces (Busscher et al., 1992) during 1st two weeks, before substrate and sludge in electrolyte are discarded (see "Experimental Regime" section 5 for details) the biofilm continues to colonize the anode surface through microbial division and attachment of cells from the planktonic phase (Davey and O'Toole G, 2000).

This experiment was however was not designed to control these mechanisms but to facilitate the electron transfer from exoelectrogenic bacteria to the anode surface. Since anaerobically digested sludge was used as inoculum, mixed biofilm consisting of archaea, exoelectrogenic and non exoelectrogenic bacteria. It could be argued that microbial fuel cells (MFCs) containing MB treated anodes facilitated electron transfer from bacteria to anodes and there was natural selection towards higher percentage of exoelectrogenic bacteria in the mixed biofilm consortium on the anode surface. Cyclic voltammetry (CV) analysis of effluents (see "Electrochemical Analysis Methods" section 4.7 for details) supports this theory since effluent samples from MFCs with MB treated MFCs show taller cytochrome peaks. Results for three samples obtained per reactor (3 controls, 3MFCs with MB treated anodes and 3 MFCs with NR treated anodes) showed higher oxidation peaks for microbial fuel cells with MB treated anodes (4.36×10^{-2} mA at -0.026 V) compared to the NR (1.97×10^{-2} mA at -0.077 V) and control (1.94×10^{-2} mA at -0.080 V) as shown in figure 24. To test this hypothesis would require molecular biology analysis of samples to confirm CV results.

The gas composition analysis results imply that electrogenesis was activated while methanogenesis decreased, facilitated by an increased electron transfer rate in the MFC, when using the MB treated carbon anode (Table 10). CE values for MB treated anode and control were slightly higher for MB treated anode, at 150 Ω resistance (Table 9). These values show once again that microbial fuel cells (MFCs) with NR treated anodes performed worse than MFCs with MB treated anodes and control (Fig. 25 – Fig. 28). These results show that NR seemed to have inhibitory effect on current generation, which according to our knowledge was not reported in literature before. This result combined with small volumes of methane detected ≈ 2×10^{-3} cm^{-3} in 13 cm^3 head space, on weekly basis (0 cm^3 for MB and control), suggests that NR prevented electron transport from bacteria to anode and therefore promoted growth of methanogenic archaea which act as electron sinks for electricity producing bacteria. Further research however needs to be done in order to identify how MB and NR treatment affects the growth and diversity of mixed culture in the biofilms growing on the anode surface.

Considering there are so many different types of microbial fuel cell (MFC) around it's hard to make a comparison (Tables A-2.1- A-2.4 "Appendix A-2" section 9.2). To make an exact comparison the microbial culture, materials used, the size of the reactors and the composition of the media have to be the same. A small MFC, for example, has the power density that appears to be higher if converted from W mm^{-3} to W m^{-3}, because the distance between anode and cathode is small. If the size of the device is increased its power density would be smaller than expected, because the distance between the electrodes increases and the losses associated with ionic transport through the electrolyte increase for larger MFCs.

Resistance between the cathode and the anode in MFC is another important factor that has to be taken into the account because it can influence the proportion of exoelectrogenic bacteria in the biofilm (Katuri et al., 2011), with lower resistances such as 60-100 Ω producing highest currents and power densities. Mixed microbial cultures acclimated to different resistances from same sludge extracts produce biofilms with different morphology and different percentage of exoelectrogenic if grown in identical microbial fuel cells (MFCs) (Zain et al., 2011). Table 11 shows some results obtained for MFCs previously reported in literature comparable to reactors used in this publication. As shown on Table 11 ferricyanide treated air Pt treated carbon cloth cathode is a more efficient proton acceptor than Pt treated carbon cloth cathode and oxygen in air (Rabaey et al., 2005b). Ferricyanide is however expensive, and it has to be replaced frequently (Logan, 2008, Wei et al., 2012). This is unlikely to be used in continuous flow systems, so it's not fully comparable to the aims of this thesis.

Table 11 – The comparison of single chamber MFCs with air cathodes where acetate, used as substrate, was previously reported in literature.

MFC configuration	Size (L)	Power density (W m^{-3})	Reference
single-chamber MFC with air cathode	0.025	16.98	(Sevda et al., 2013)
tubular single-chamber MFC with air cathode	0.20	6.10	(Kim et al., 2009b)
tubular single-chamber MFC with air cathode	0.20	11.3	this study
tubular single-chamber MFC With ferricyanide soaked air cathode	0.39	90.00	(Rabaey et al., 2005b)
tubular single-chamber MFC with air cathode	1.26	2.00	(Jeon et al., 2013)

Tables in "Appendix A-2" section 9.2 compare different electrode treatments, cathode and anode materials and cathode catalysts. The biggest problem is that there is no standard MFC design and with the multitude of microbial mixed cultures it's hard to make an exact comparison (see "Comparison of Different BES Designs" section 2.14 for more information).

6.2.5 Conclusion

Methylene blue (0.54 mg cm^{-2}) were successfully adsorbed onto carbon from 1.56 mmol L^{-1} solution on the 13 cm^2 carbon cloth electrode surface when pH of the buffer solution containing dye was changed to pH = 12 for 28 h and 0.23 mg cm^{-2} adsorbed at pH 5.5 during a 28 h period. MB treated electrode at pH 12 for 28 h was shown to be improving voltage production in microbial fuel cell (MFC). Adsorption could be used to prepare electron mediator treated anodes for scaled up systems combining dye removal from wastewater with MFC technology to remove other organics, such as lipids, carbohydrates and proteins in food waste liquor that is often used as substrate for MFCs. pH shifting technique used in this work was never attempted to anode material surface treatment that is significantly cheaper than other techniques reported in literature as mentioned "Discussion" section 6.2.4 in greater detail. Since MB remains permanently adsorbed it is possible to use mediator treated anodes in scaled up continuous flow MFC devices.

The anodes from MFCs with MB treated anodes produced high currents ≈ 7.5 mA, power densities P_{max} ≈ 11.78 Wm^{-3} at 35.5 ^oC compared to MFC (control) currents ≈ 5.2 mA and power densities P_{max}= 5.3 Wm^{-3}. Since the anodes performed well in MFCs they are expected to perform well when removed and placed into MECs, as shown in section 6.1 in greater detail, which produced reproducible results comparable to results previously reported in literature. The performance of MB treated anode could be tested against control in continuous flow MEC, which according to our knowledge was not previously assed in detail before.

The anodes from MFCs with NR treated anodes produced currents ≈ 2.29 mA, power densities P_{max} ≈ 2.63 Wm^{-3} at 35.5 ^oC compared to MFC (control) currents ≈ 5.2 mA and power densities P_{max}= 5.3 Wm^{-3}. This result combined with small volumes of methane detected ≈ 2×10^{-3} cm^{-3} in 13 cm^3 head space, on weekly basis (0 cm^3 for MB and control), suggests that NR prevented electron transport from bacteria to anode and therefore promoted growth of methanogenic archaea which act as electron sinks for electricity producing bacteria.

6.3 The Influence of Changes in Acetate and Butyrate Concentrations and Full Substrate Switch on Gas Production from Two Microbial Electrolysis Cells (MECs) Acclimated to either Acetate or Butyrate

The power density of microbial fuel cells (MFCs) and the hydrogen production rate for microbial electrolysis cells (MECs) can be increased not just by the use of mediators but via choice of substrate for the bacteria (Cheng and Logan, 2007a, Logan, 2008). The aim of this work was to investigate the influence of changes in acetate and butyrate concentrations present in the feedstock solution supplied for two BES's with untreated carbon cloth (UCC) anodes operated for either electricity production in MFC mode or for hydrogen production rate in MEC mode. Six 200 cm^3 tubular MFC reactors were prepared as described in "Materials and Methods" in section 4 and "Experimental Regime" in section 5. Acetate and butyrate solutions (20 mmol L^{-1}) were used as feedstock for AC and BU reactors respectively and used for experiment 3.1, which lasted for 9 weeks in order to create biofilms acclimated to these substrates. The pre-acclimated anodes were then transferred into 320 cm^3 anode chambers for MECs experiments 3.2 and 3.3 and were investigated for hydrogen production rate for experiments 3.2 and 3.3.

6.3.1 Results for Microbial Fuel Cell (MFC) Anode Acclimation Experiments

i) Voltage Monitoring

In experiment 3.1 the influence of 20 mmol L^{-1} acetate (AC) or butyrate (BU) on the voltage production from the mixed biofilm consortium was investigated in MFC mode. The cells were operated by feeding 20mmol L^{-1} acetate or 20mmol L^{-1} butyrate at a 1000 Ω resistance and at room temperature (23±2 ^oC) to allow comparison to work previously done by Michie et al (2011). The voltage produced was continuously logged on line (see "Electrochemical Analysis Methods" section 4.7 for details). The sharp voltage decrease to zero was due to the cells being emptied and refilled with fresh substrate once a week (Fig. 31). The comparison between the three replicates is not shown. The replicates 2 and 3 followed a similar pattern and values as replicate 1 and so for clarity and space reasons, the graphs for the reactor replicates 2 and 3 were not included here.

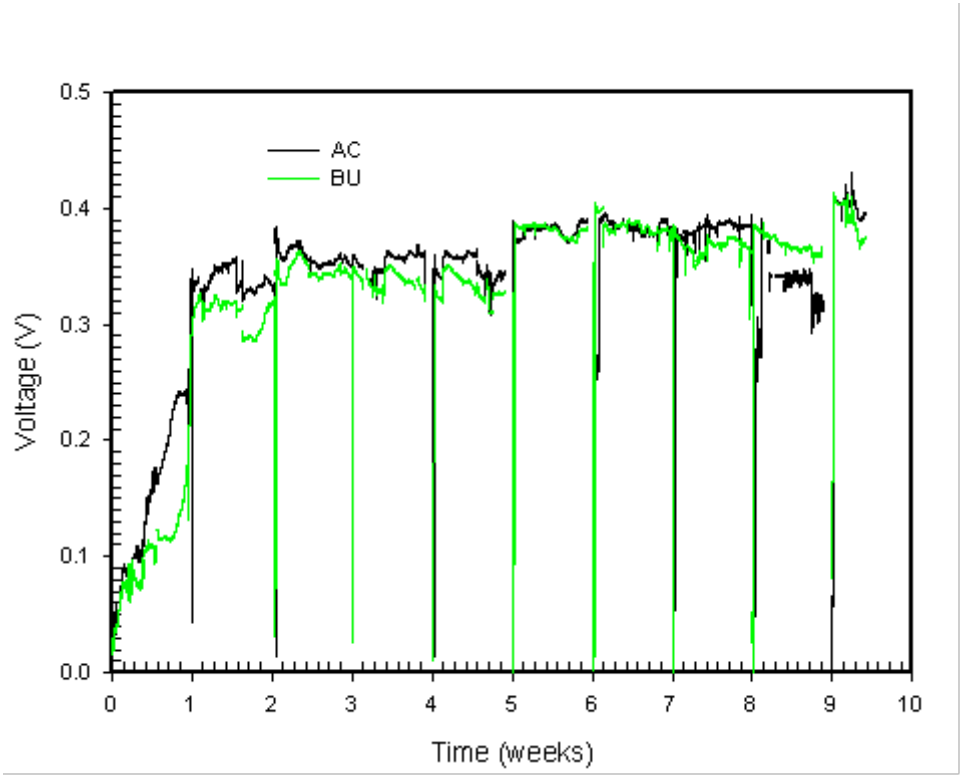

Figure 31 – Voltages vs time plot for microbial fuel cells (MFCs) operated on acetate or butyrate.

Fig. 31 shows that the voltage generation began to increase noticeably from day 1 of the enrichment of the anode electrode (time t=0, when sludge containing bacteria was added to nutrient electrolyte mixture, in the assembled MFCs) reaching 348 mV (0.61 W m^{-3}) for the MFC (AC) on week 1, day 7, during the first batch operation, and continued increasing gradually from 370 mV (0.68 W m^{-3}), to 412 mV (0.85 W m^{-3}), on weeks 2-9, days 14 – 63.

For the MFC (BU) voltage generation began to noticeably increase reaching 321 mV (0.52 W m^{-3}) on week 1, day 7, during the first batch operation, and continued increasing gradually from 343 mV (0.59 W m^{-3}) to 410 mV (0.84 W m^{-3}) for MFC (BU) on weeks 2-9, days 14 – 63.

ii) Coulombic Efficiency (CE) and Energy Efficiency:

One of the aims of microbial fuel cell (MFC) research is to recover as many electrons and as much energy from the biomass substrates as possible. The coulombic efficiency (CE) and energy efficiency for the sequencing batch (SBR) operation were calculated, as previously described in “Electrochemical Analysis Methods” section 4.7.

Table 12 shows that practical coulombic efficiency (CE_p) and energy (E_p) recovered are the same for MFCs AC and BU. For calculating % CE values, it was assumed that 4 electrons were needed for destruction of one butyrate molecule.

As one butyrate molecule produces two acetate molecules when the oxidation reaction occurs. So another 16 electrons are needed to convert these two acetate molecules produced from the butyrate and this has to be taken into consideration when butyrate oxidation is used (Eq 14 – Eq 18) which makes theoretical Coulombic Efficiency value (CE_t) higher for butyrate. This makes % CE lower for butyrate (Table 12). The % energy recovery (E) values for butyrate are lower than for acetate due to the lower ΔH of combustion for acetate (875.200 KJ mol^{-1}) and for butyrate (2183.500 KJ mol^{-1}), which are need to calculate theoretical energy recovery values (E_t).

Table 12 – Comparison of coulombic efficiency (CE) and energy recovery (E) values for MFCs fed with given substrate (20 mmol L^{-1}) enriched at 1000 Ω resistance.

Substrate	MFC	CE_p (c)	CE (%)	E (%)	E_p (J)
butyrate	BU	1851±7	24	7.5	658±2
acetate	AC	1824±5	59	18	637±2

CE_t (AC) = 3088 c, CE_t (BU) = 7719 c, E_t (AC) = 3501 J, E_t (BU) = 876 J
± represents variations from the average for *n* experimental repeats (*n*=3)

iii) Power Density Monitoring:

The power density curves were also used to monitor power density but also enabled to monitor voltage developments at low resistances as well as power density. The power densities were measured once per 7 days (performed as calculations previously described in "Electrochemical Analysis Methods" section 4.7 and "Experimental Regime" section 5). All MFCs were operated at 1000 Ω resistance to compare results to other published research eg: Michie et al (2013). Potential and power in Fig. 32 were calculated from for the average *n* experimental repeats, where *n* = 3. For the production of power density plots currents were monitored at a range of resistances with the lowest possible resistance of 10 Ω. Fig. 32 shows that the power gradually increased over a period of nine weeks. The highest peak power densities were also obtained on day 63 with MFC (AC) P_{max} = 3.15 W m^{-3} (3.24 mA), MFC (BU) P_{max} = 2.00 W m^{-3} (2.00 mA), when the BES's were set up in MFC sequencing batch mode.

From the 2 (or 6, 3 experimental repeats) MFCs data for the power densities currents obtained at a 10 Ω resistance and corresponding to % COD removal (substrate consumption) were used to plot figures 33 a, 33b and 33c. This experiment was conducted to prove the hypothesis that there was a correlation between the currents at the lowest possible resistances, using of two different substrates.

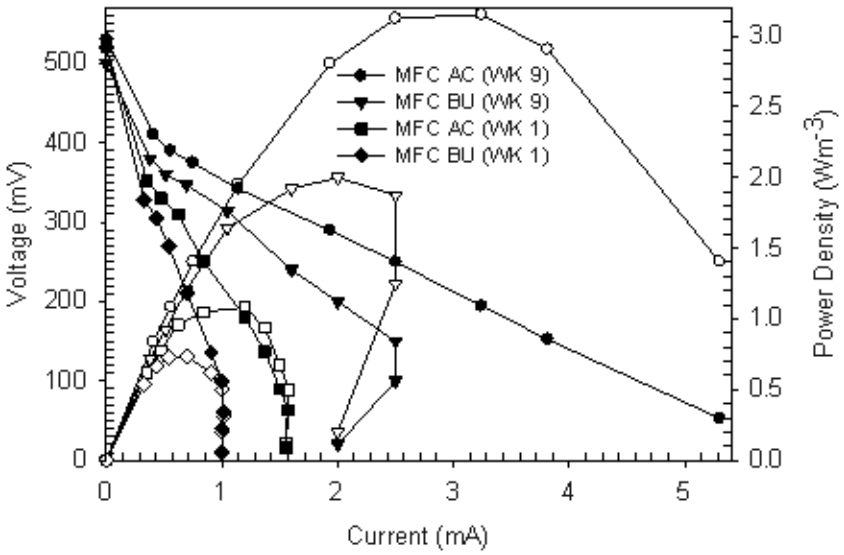

All values were averages calculated for *n* experimental repeats (*n*=3).

Figure 32 – Comparison of current to voltage (closed symbols) and power density (open symbols) for MFCs. For space reasons only closed symbol key shown but symbol shape is same for the reactors for the power densities when the symbol is open.

Fig. 33 a and 33 b show that the power densities at 10 Ω resistance for the MFC (AC) initially decreased from 1 ± 0 mA (0.12 ± 0 W m^{-3}) to 0.6 ± 0mA (0.04 ± 0 W m^{-3}), after the first batch operation. This was due to the removal of some of the inoculum, which contained suspended exoelectrogenic microbes (Logan, 2009). For the MFC (BU), current and power density also decreased from 1 ± 0 mA (0.05 ± 0 W m^{-3}) to 0.6 ± 0mA (0.02 ± 0 W m^{-3}). The current production then increased stabilized at 5.25 ± 0.05 mA for the MFC AC (1.375 ± 0.025 W m^{-3}) and at 2 ± 0.1mA for the MFC (BU) (0.2 ± 0.02 W m^{-3}) on weeks 6-9. These results show that the MFC acclimated to butyrate (BU) produced 2.6 times more electricity than MEC acclimated to acetate (AC). A similar observation was made by by Liu et al (2005 b). Fig. 33 c shows that the average COD removal rates (see "Offline Analysis Methods" section 4.8, for details on COD analysis) which were similar for the MFC systems. The COD removal rates follow the same trend as current output in Fig. 33 a and power output in Fig. 33 b. The percentage COD removal rates for acetate and butyrate were similar. Fig. 33 c shows COD reductions 73 ± 5 % for MFC (AC) and 90 ± 7 % for MFC (BU), week 1, day 7, the end of 1st batch operation, with inoculum (sludge). The COD reductions decreased (due to removal of bacterial biomass suspended in electrolyte solution) to 43 ± 2 % for MFC (AC), 45 ± 5 % for MFC (BU), on week 2, day 14. COD reduction finally stabilized at 46 ± 10 % for MFC (AC), 48 ± 10 % for MFC (BU), on weeks 3 - 9, days 21 - 63. This means that coulombic efficiency (CE) values, which compare current observed to theoretical current produced from substrate consumption by bacteria, were smaller for MFC (BU) than for MFC (AC).

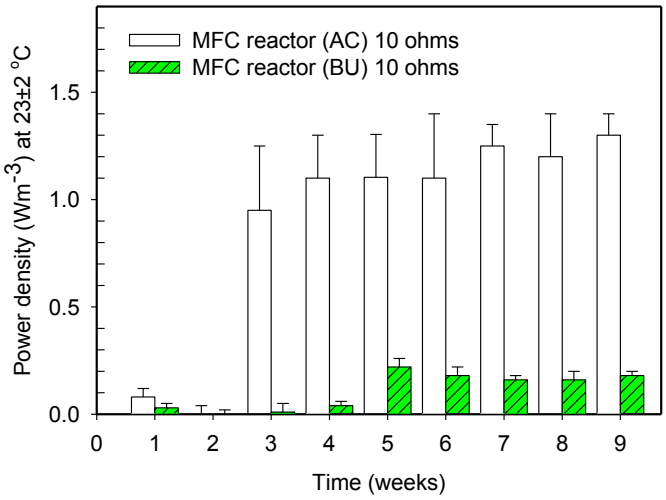

(a)

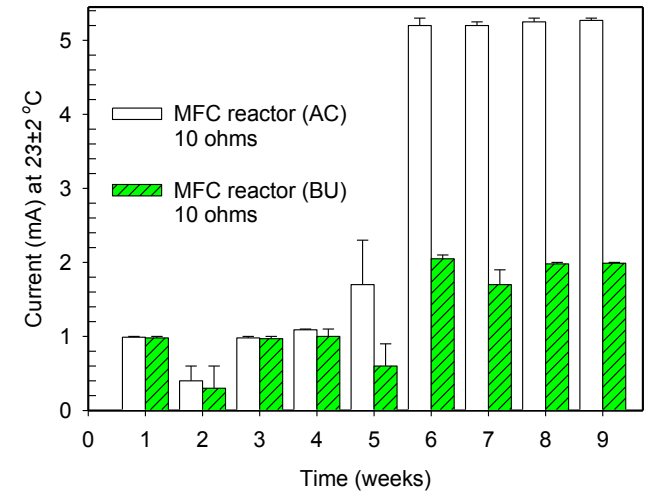

(b)

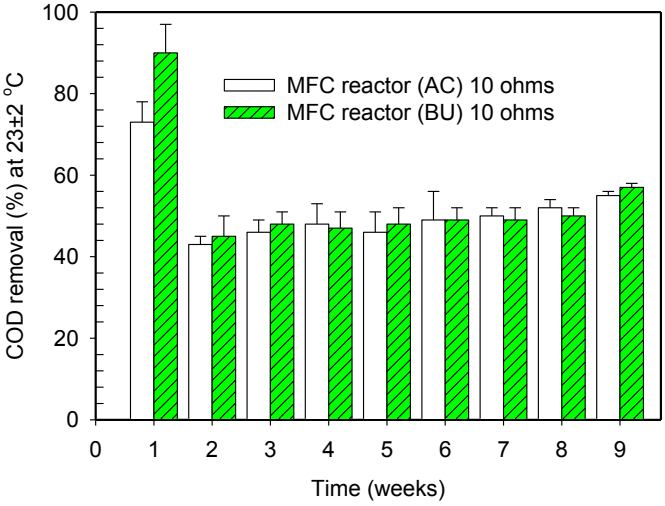

(c)

Error bars represent variations from the average for *n* experimental repeats (*n*=3).

Figure 33 - Comparison of power densities (33 a) currents (33 b) at the resistance 10Ω, as functions of time and percentage COD removal (33 c).

6.3.2 Results for Continuous Flow MEC Experiments

Experiments 3.2 and 3.3 were designed to assess the performance factors associated with changes in acetate and butyrate concentrations for a continuous flow microbial electrolysis (MEC) reactor. The aims of this work are described in "Aims of this Thesis" section 3. A continuous flow MEC was intended to be used as second stage linked to biohydrogen fermentation of biomass e.g. food waste. These biomass feedstocks primarily contain carbohydrates, lipids and proteins, but are converted into volatile fatty acids in approximately a 40 % acetate and 60 % butyrate ratio in the biohydrogen fermentation process. The purpose of this section of work was to assess the effect of changes in concentration in acetate and butyrate on the MEC containing anodes acclimated to either solely acetate or solely butyrate and how the microbial culture on the anode surfaces responded either to acetate and butyrate mixtures or full substrate switch over between acetate to butyrate or vice versa on hydrogen production rate.

Experiment 3.2 investigated the effect of decrease in pure substrate (acetate or butyrate) concentrations on hydrogen production rate in MECs with anodes acclimated to acetate or butyrate. For experiment 3.2 the substrate (acetate for MEC AC and butyrate for MEC (BU)) concentration was decreased from 20 mmol L^{-1} to 10 mmol L^{-1} and than to 5 mmol L^{-1} over 5 day periods (see "Experimental Regime" section 5, for details). Experiment 3.3 investigated the effect of 50 % acetate 50 % butyrate mixtures and full substrate switch on hydrogen production rate in MECs with anodes acclimated to acetate or butyrate. For experiment 3.3 acetate or butyrate was switched for 10 mmol L^{-1} acetate and 10 mmol L^{-1} butyrate mixtures. Finally the substrate was fully switched for (20 mmol L^{-1}) butyrate, for MFC (AC), acclimated to acetate, and substrate for MFC (BU), acclimated to butyrate, was fully switched for (20 mmol L^{-1}) acetate.

Experiment 3.2 i and 3.3 i were repeats of experiment 3.2 and 3.3 designed to confirm the results obtained because only two MECs (one MEC (AC) and one MEC (BU)) could be used at that time.

Calculations for the Performance Factors

All performance factors, described in "Electrochemical Analysis Methods" section 4.7 and "Offline Analysis Methods" section 4.8, such as coulombic efficiency (CE), cathodic hydrogen recovery (r_{cat}), see equation 51 for overall hydrogen recovery (Y_{H2}), see equation 52 hydrogen yield with respect to the substrate consumed ($Y_{H2\ per\ mol\ substrate\ destroyed}$), see equation 53 were calculated, from data obtained, as shown below, based on (Logan, 2008, Logan et al., 2008).

The calculations were exactly the same as in "The Influence of Temperature and Catholyte pH on the Hydrogen Production in Microbial Electrolysis Cells (MECs) " section 6.1 with the only difference being that the hydraulic retention time (HRT), was changed from 8.1 h to 9.6 h instead of 9 h due to peristaltic tube replacement.

i) The Influence of Acetate or Butyrate Concentrations on the Hydrogen Production, Methane Production and Cathodic Current Density in MECs

The data from experiments 3.2 and 3.3 is shown in figures 33 and 34. The results from experiments 3.2 and 3.3 show that with the decrease in the single VFA component substrate concentration from 20 mmol L^{-1} to 5 mmol L^{-1} (acetate for MEC (AC) and butyrate for MEC (BU)), had different outcomes for the acetate fed MEC and the butyrate fed MEC. A decrease in hydrogen production rate and current density was observed for the MEC (AC) which was acclimated on acetate. In contrast an increase in hydrogen production rate and current density was observed when butyrate concentration was decreased from 20 mmol L^{-1} to 10 mmol L^{-1} for MEC (BU) but a decrease in hydrogen production rate and current density when the butyrate concentration was decreased from 10 mmol L^{-1} to 5 mmol L^{-1}.was observed. The reason for the initial increase in hydrogen production rate at 10 mmol L^{-1} butyrate concentration for MEC (BU) could be substrate inhibition which was reported for hydrogen fermentation (Wong et al., 2014) and MFCs (Sharma and Li, 2010b) but according to our knowledge has not been accessed in detail for MECs. The subsequent fall in hydrogen yield when the butyrate was decreased from 10 mmol L^{-1} to 5 mmol L^{-1} would indicate that the bacteria at this point has become substrate limited.

From the results for experiments 3.2, 3.2i and 3.3 and 3.3i it could be suggested that MEC (AC), with anode acclimated to acetate, could only convert the acetate into hydrogen fraction when fed the 10 mmol L^{-1} acetate and 10 mmol L^{-1} butyrate mixtures. The MEC (BU) with anode could utilize both acetate and butyrate for hydrogen production rate. Figure 34 shows data for gas (hydrogen and methane) production and corresponding current densities for experiments 3.2, 3.3 with error bars representing variations from average daily volumetric hydrogen production rate. Experiments 3.2i and 3.3i (data not included) produced very similar results with a decrease in hydrogen concentration for reactor AC for 10 mmol L^{-1} acetate and 10 mmol L^{-1} butyrate mixture due to leak in the gas bag. Figure 35 shows the current density, temperature and pH logged on line for experiments 3.2, 3.3. Figure 35 shows a comparison between the single replicate with repeat 2 not shown. Replicate 2 and 3 followed a similar pattern and values as replicate 1 and so for clarity and space reasons the graphs for replicates for 2 and 3 were not included here.

Results for Experiment 3.2 and 3.2i:-

Experiments 3.2 and 3.2i investigated the effect of decrease of one component substrate concentration on hydrogen production rate for 20 mmol L^{-1}, 10 mmol L^{-1}.and 5 mmol L^{-1} substrate concentrations. This study compared microbial electrolysis cells (MECs) acclimated to acetate (AC) and butyrate (BU).

Hydrogen production rate and current density at 20 mmol L^{-1} substrate concentration on weeks 11-12, days 80- 85 (i-ii), as shown below:-

i) The MEC (AC) produced significant amounts of hydrogen 182 ± 3.0 cm^3 $L_{(anode)}^{-1}$ day^{-1} (*n*=5), where *n* refers to the number of days during which a particular substrate was administered current density (1.68 ± 0.025 A m^{-2}), as shown in figures 34 and 35, and COD reduction of 48 ± 10 %, see Table A-3.1 for details.

ii) The MEC (BU) produced lower 148 ± 2.0 cm^3 $L_{(anode)}^{-1}$ day^{-1} (*n*=5), current density (1.74 ± 0.04 A m^{-2}), as shown in figures 34 and 35, and COD reduction of 59 ± 2 %, see Table A-3.1 for details.

Hydrogen production rate and current density when the substrate concentration was decreased to 10 mmol L^{-1} on week 12, days 85 – 90 (iii-iv), as shown below:-

iii) There was an decrease in hydrogen production rate was observed for the MEC (AC) to 125 ± 3.0 cm^3 $L_{(anode)}^{-1}$ day^{-1} (*n*=5) a small drop in the current density amounting to 1.46 ± 0.045 A m^{-2}, as shown in figures 34 and 35, and COD reduction of 62 ± 4 %, see Table A-3.1 for details.

iv) For the MEC (BU) an increase in hydrogen production rate was observed amounting to 201 ± 2.0 cm^3 $L_{(anode)}^{-1}$ day^{-1} (*n*=5); a decrease in current density to 1.5 ± 0.01 A m^{-2}, as shown in figures 34 and 35, and COD reduction of 70 ± 7 %, see Table A-3.1 for details.

Hydrogen production rate and current density when the substrate concentration was decreased to 5 mmol L^{-1} on weeks 12-13, days 90-95 (v-vi), as shown below:-

v) A decrease in hydrogen production rate was observed for the MEC (AC) 56 ± 2.0 cm^3 $L_{(anode)}^{-1}$ day^{-1} (*n*=5), current density 1.32 ± 0.03 A m^{-2}, as shown in figures 34 and 35, and COD reduction of 38±5 %, see Table A-3.1 for details.

vi) A decrease in hydrogen production rate was also observed for the MEC (BU) 176±3.0 $cm^3 L_{(anode)}^{-1} day^{-1}$ (*n*=5), current density 1.5 ± 0.005 A m^{-2}, as shown in figures 34 and 35, and COD reduction of 97±1 %, see Table A-3.1 for details.

Methane producing archaea convert substrate, otherwise used by hydrogen producing bacteria into methane resulting a decrease the amount of hydrogen produced. It is important to monitor methane as well as rate in order to explain the difference between MEC (AC) and MEC (BU). Levels of methane production were found to decrease in line with decreases in the substrate feed concentrations. Higher methane production was observed for acetate MEC (AC) than for butyrate MEC (BU) on weeks 11 -.13, days 80 – 95 (vii – viii). In experiments 3.2 and 3.2i MEC (BU) produced more hydrogen and less methane than MEC (AC) indicating less archaeal activity, as shown below:-

vii) For the MEC (AC) methane production rate was 89 ± 2.0 $cm^3 L_{(anode)}^{-1} day^{-1}$ (*n* = 5) for 20 mmol L^{-1} acetate concentration on weeks 11 - 12; 69 ± 2.0 $cm^3 L_{(anode)}^{-1} day^{-1}$ (*n*=5) for 10 mmol L^{-1} acetate concentration on week 12; 56 ± 1.0 $cm^3 L_{(anode)}^{-1} day^{-1}$ for 5 mmol L^{-1} acetate concentration on weeks 12 - 13, as shown in figure 34 a.

viii) For the MEC (BU) methane production rate was 47 ± 1.0 $cm^3 L_{(anode)}^{-1} day^{-1}$ (*n* = 5) for 20 mmol L^{-1} butyrate concentration on weeks 11 – 12; 25 ± 1.0 $cm^3 L_{(anode)}^{-1} day^{-1}$ (*n*=5) for 10 mmol L^{-1} butyrate concentration on week 12; 19.5 ± $cm^3 L_{(anode)}^{-1} day^{-1}$ (*n*=5) for 5 mmol L^{-1} butyrate concentration on weeks 12-13, as shown in figure 34 a.

Results for Experiment 3.3 and 3.3i:-

Experiments 3.3 and 3.3i investigated the effect of the decrease of two component substrate concentration on hydrogen production rate for a 10 mmol L^{-1} acetate and 10 mmol L^{-1} butyrate mixture and 20 mmol L^{-1} full substrate switch. This study compared microbial electrolysis cells (MECs) acclimated to acetate (AC) and butyrate (BU). In experiments 3.3 and 3.3i, the MEC (BU) produced more hydrogen and less methane than MEC (AC) indicating less archaeal activity. Hydrogen production rate and current density for 10 mmol L^{-1} acetate and 10 mmol L^{-1} butyrate mixtures on weeks 13 - 14, days 95 - 100 (i-ii), as shown below:-

i) The MEC (AC) produced small volumes of hydrogen 19 ± 1.0 $cm^3 L_{(anode)}^{-1} day^{-1}$ (*n*=5), where *n* refers to the number of days during which a particular concentration was administered; current density (1.63 ± 0.03 A m^{-2}), as shown in figures 34 and 35, and COD reduction of 49 ± 2 %, see Table A-3.1 for details.

ii) The MEC (BU) produced higher volumes of hydrogen 173 ± 3.0 $cm^3 L_{(anode)}^{-1} day^{-1}$ (*n*=5), current density (1.35 ± 0.05 A m^{-2}), as shown in figures 34 and 35, and COD reduction of 8 ± 1.8 %, see Table A-3.1 for details.

Hydrogen production rate and current density when the substrates were fully switched for 20 mmol L^{-1} pure acetate or butyrate solutions on weeks 14 -15, days 100 – 105 (iii - iv), as shown below:-

iii) No hydrogen production rate was observed for the MEC (AC) 0 ± 0.0 $cm^3 L_{(anode)}^{-1} day^{-1}$ (*n*=5), the current density also decreased to 0.15 ± 0.05 A m^{-2}, as shown in figures 34 and 35, and COD reduction also decreased to 2.3 ± 7 %, see Table A-3.1 for details.

iv) For the MEC (BU) increase in hydrogen production rate was observed amounting to 249 ± 3.0 $cm^3 L_{(anode)}^{-1} day^{-1}$ (*n*=5); an increase in current density to 1.71 ± 0.04 A m^{-2}, as shown in figures 34 and 35, and COD reduction of 38 ± 10 %, see Table A-3.1 for details.

Levels of methane production on weeks 13 -.15, days 95 – 105 (v – vi), as shown below:-

v) For the MEC (AC) methane production rate was higher than for MEC (BU) 43 ± 1.0 $cm^3 L_{(anode)}^{-1} day^{-1}$ (*n* = 5) for 10 mmol L^{-1} acetate 10 mmol L^{-1} butyrate mixture concentration on weeks 13 – 14. For 20 mmol L^{-1} butyrate concentration (full substrate switch) on weeks 14 – 15 methane production was lower than for MEC (BU) 1.0 ± 1.0 $cm^3 L_{(anode)}^{-1} day^{-1}$ (*n*=5), as shown in figure 34 a.

vi) For the MEC (BU) methane production rate was 19 ± 2.0 $cm^3 L_{(anode)}^{-1} day^{-1}$ (*n* = 5) for 10 mmol L^{-1} acetate 10 mmol L^{-1} butyrate mixture concentration on weeks 13 – 14; 23 ± 2.0 $cm^3 L_{(anode)}^{-1} day^{-1}$ (*n*=5) for 20 mmol L^{-1} butyrate concentration (full substrate switch) on weeks 14 - 15, as shown in figure 34 a.

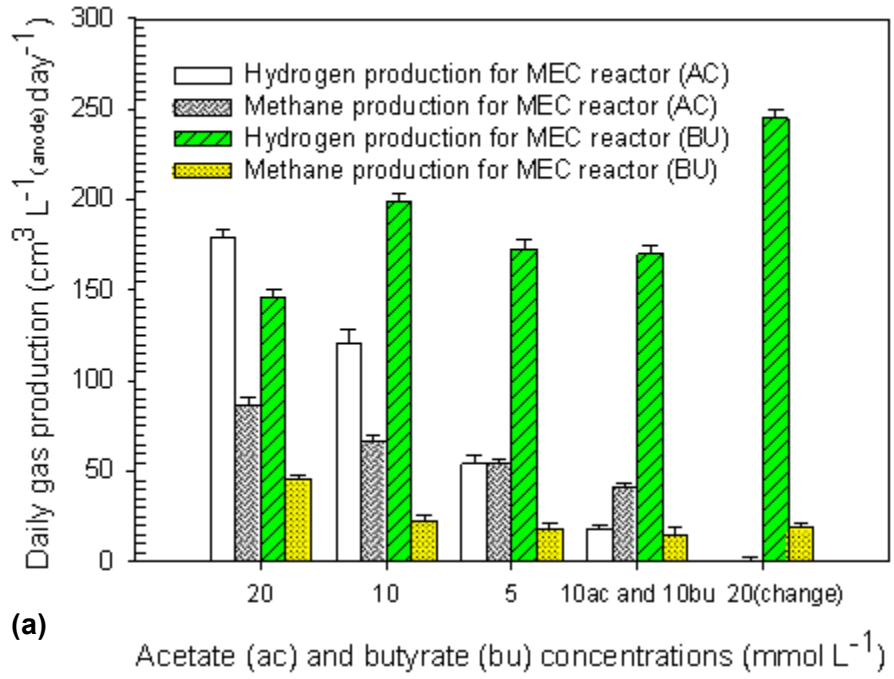

(a)

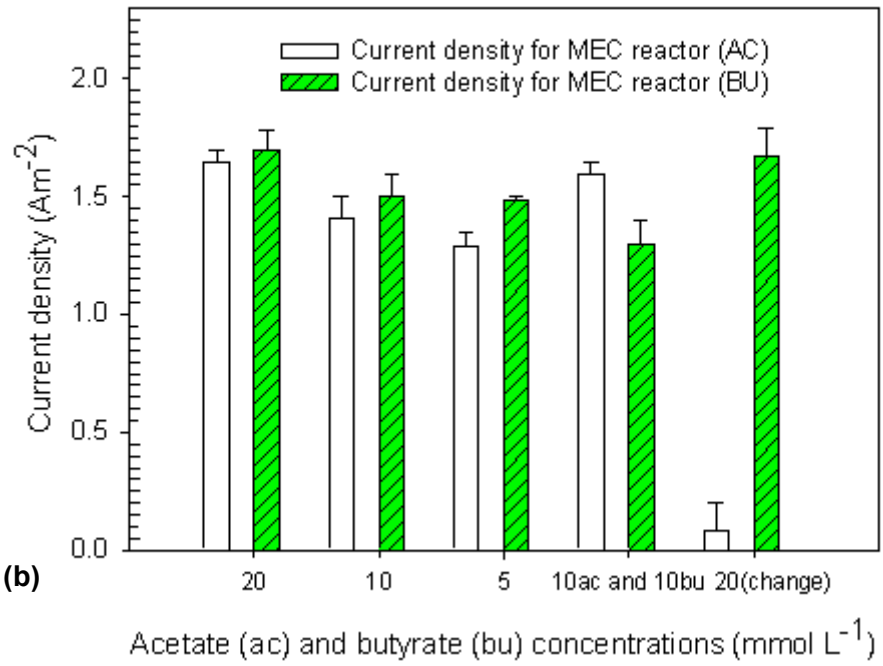

(b)

All errors bars represent variations from the average daily hydrogen production.

Figure 34 – Variations of different hydrogen production rates (34 a), in the cathode chamber, compared to current density (34 b).

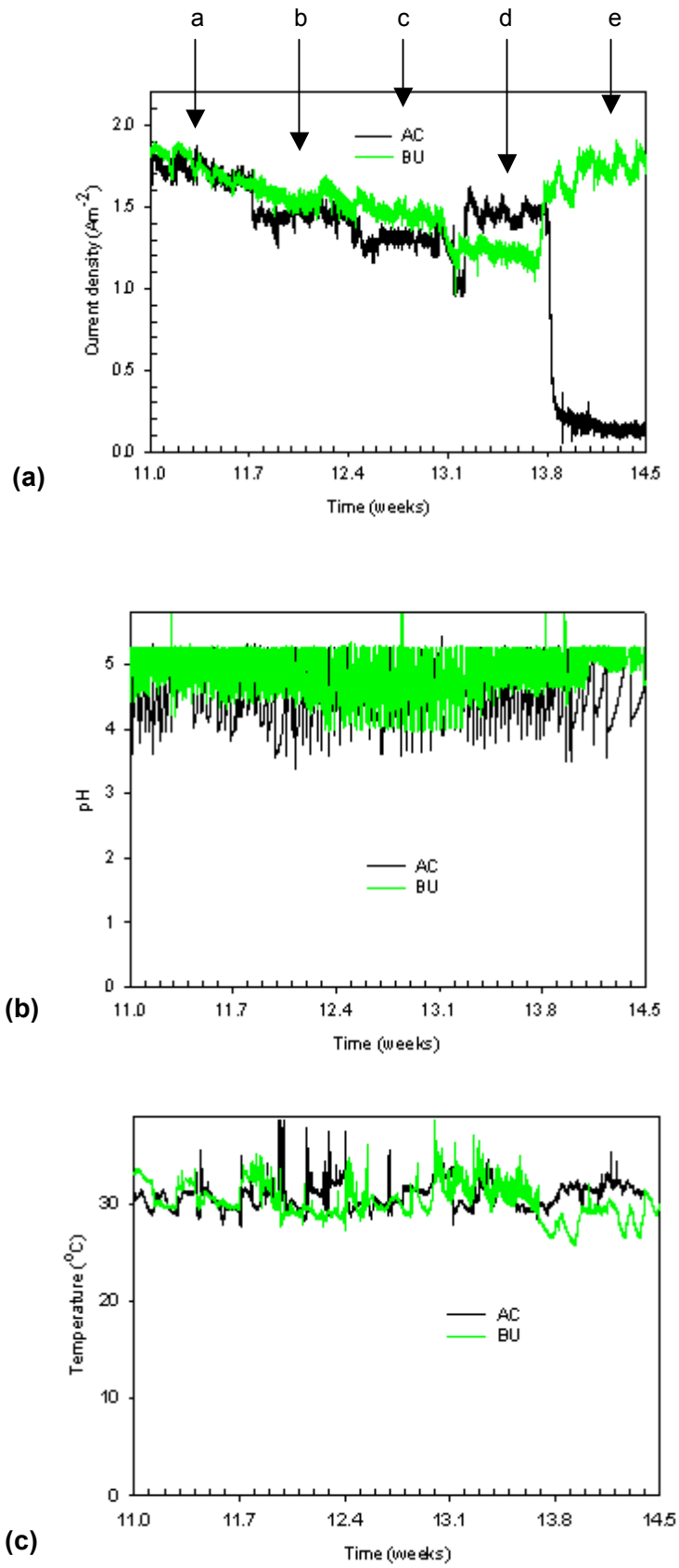

Where a is substrate (acetate for AC or butyrate for BU) fed at 20 mmol L^{-1}, then b at 10 mmol L^{-1} and at c for 5 mmol L^{-1} respectively, in weeks 11 - 13; then d is acetate (10 mmol L-1) / butyrate (10 mmol L^{-1}) mixtures on weeks 13-13.8 and e is a full substrate change over (20 mmol L^{-1}) on weeks 13.8-14.5.

Figure 35 - Variations in the current density (35 a) temperature (35 b) and pH (35 c) with decrease in the substrate concentration.

ii) The Influence of Acetate or Butyrate Concentrations on Coulombic Efficiency (CE) and Hydrogen Yield per mol of Substrate Consumed

Coulombic efficiencies (CEs, see "Electrochemical Analysis Methods" section 4.7 for details) compared the current recorded across 1 Ω resistor between the cathode and the power supply to the theoretical current obtained from the COD reduction. With a decrease in the substrate concentration, the theoretical current obtained from the COD reduction becomes smaller, hence CE values go up. This was observed for pure acetate for MECs (AC), with anode acclimated to acetate, and MEC (BU), with the anode acclimated to butyrate, as shown on Table 13. The hydrogen yields increased slightly from 0.67 $mol_{(hydrogen)}$ $mol_{(acetate)}^{-1}$ to 1.3 $mol_{(hydrogen)}$ $mol_{(acetate)}^{-1}$ for MEC (AC) with a decrease in acetate concentration (as shown on Table 13). The increase in hydrogen yields for MEC (BU) was more abrupt with the decrease in the butyrate concentration from 3.5×10^{-2} $mol_{(hydrogen)}$ $mol_{(acetate)}^{-1}$ to 0.64 $mol_{(hydrogen)}$ $mol_{(acetate)}^{-1}$, as shown on Table 13, which supports the hypothesis that 20 mmol L^{-1} butyrate inhibited the hydrogen production rate (Sharma and Li, 2010b, Wong et al., 2014).

For the acetate and butyrate mixtures the hydrogen production was lower for MEC (AC) than for MEC (BU) but the current density and coulombic efficiency (CE), which was calculated from the current (Fig. 34 and Fig. 35), were higher for MEC (AC), as shown on Table 13. Unlike CE, the hydrogen yield only relates to the amount of substrate consumed that results in hydrogen production rate. If hydrogen producing bacteria in the MEC (AC) were only able to convert acetate in the acetate and butyrate mixtures (10 mmol L^{-1} acetate and 10 mmol L^{-1} butyrate) into hydrogen then the hydrogen yield achieved would be about 50% of the hydrogen yield, that was achieved for the 20 mmol L^{-1} acetate solution. The hydrogen yield for 20 mmol L^{-1} acetate solution was 0.67 $mol_{(hydrogen)}$ $mol_{(acetate)}^{-1}$ and the yield for 10 mmol L^{-1} acetate and 10 mmol L^{-1} butyrate mixtures is 0.2 $mol_{(hydrogen)}$ $mol_{(acetate)}^{-1}$, approximately 30 % of hydrogen yield 20 mmol L^{-1} acetate solution, as shown on Table 13. The current density logged on line for MEC (AC) for 10 mmol L^{-1} acetate and 10 mmol L^{-1} butyrate mixtures same as that for 10 mmol L^{-1} acetate solution, see figure 35 for details. This result supports the theory that only acetate was converted into hydrogen for MEC (AC) and it could also be suggested, but never proven, that butyrate may have also had inhibited the hydrogen production.

The most dramatic change was observed when the substrates were fully switched with current and CE values going up to the same level as for butyrate (10 mmol L^{-1}) for MEC (BU), when butyrate was fully switched to acetate with highest volumetric hydrogen production rate of 251 cm^3 $L_{(anode)}^{-1}$ day^{-1} and smaller then expected hydrogen yield of 0.52 $mol_{(hydrogen)}$ $mol_{(acetate)}^{-1}$ due to changes in the flow rate. MEC (AC) did not produce any current (Fig. 34, and Fig. 35) when substrates were fully switched.

When current decreased to 0, CE values also fell to 0, as shown on Table 13, which again supports hypothesis that hydrogen producing bacteria in MEC (AC) acclimated to acetate were only able to convert acetate into hydrogen. This observation, according to our knowledge, has not been reported in the literature before.

Table 13 – Comparison of coulombic efficiency (CE), cathodic hydrogen recovery and hydrogen yield mol/mol substrate consumed for highest hydrogen productions at given substrate concentrations.

Substrate	Conc. ($mmolL^{-1}$)	H_2 production rate $cm^3 L_{(anode)}^{-1} day^{-1}$		Cathodic H_2 recovery (%)		CE (%)		H_2 yield mol/mol substrate consumed	
		BU	AC	BU	AC	BU	AC	BU	AC
acetate or butyrate	20	148±2	181±3	6±2	31±2	14±2	13±2	3.5×10^{-2}±0	0.67±0
	10	201±2	124±4	56±2	42±4	22±2	15±2	0.5±0	1.2±0
	5	175±2	56±2	51±2	17±2	31±2	56±2	0.64±0	1.3±0
acetate and butyrate mixture	10 and 10	172±3	19±1	70±3	5±1	16±2	82±3	0.51±0	0.2±0
acetate and butyrate fully switched	20	248±3	0	62±3	0	20±1	8±1	0.52±0	0

A STP. Theoretical H_2 yields: 10 mol/per mol butyrate; 4 mol/mol acetate; 12 mol/mol glucose.
Acetate reactor = AC and butyrate reactor = BU. Voltage applied = 850 mV for each MEC.
All errors represent variations from the average daily hydrogen production.
Each concentration was administered for 5 day periods.

6.3.3 Discussion

i) Experiments 3.1, 3.2 and 3.2 i

There was no relationship between, how the anodes acclimated to acetate (AC) and butyrate (BU) performed in MFCs and MECs. The voltage output at 1000 Ω resistance was exactly the same for MFCs (AC and BU). Another good indicator of MFC performance is power density, which slowly increased over the 9 week period. On day 63, the power maximum power density P_{max} was 38 % lower, when the highest power densities were obtained, than that for MFC AC, similar to observations made by Liu et at (2005b). The percentage COD removal was roughly the same for MFCs (AC and BU, Fig. 33 ii).

When the anodes were removed from the MFCs and placed into the MECs, the MEC (BU), containing anode acclimated to butyrate, produced 20% more hydrogen than MEC (AC), with the anode acclimated to acetate, on daily basis (Table 13).

The COD reductions (the amount of substrate consumed) were much lower for MEC (AC), so H_2 yield mol/mol substrate consumed appears to be higher for MEC (AC), see Table A - 3.1 in "Appendix A - 3" section 9.3. It could be suggested that there was more bacteria on the anode surface of the anode acclimated to butyrate that on the anode acclimated to acetate. Another theory is that the anode acclimated to butyrate contained different species of bacteria, which used more substrate.

The 20 mmol L^{-1} butyrate solution produced less hydrogen ≈150 cm^3 $L_{(anode)}^{-1}$ day^{-1} (*n*=5, where *n* refers the number of days during which a particular substrate concentration was used) compared to 26 % increase in hydrogen production rate for 10 mmol L^{-1} butyrate solution,≈203 cm^3 $L_{(anode)}^{-1}$ day^{-1} (*n*=5). This phenomenon is called substrate inhibition of cell multiplication and / or fermentation. Many enzymes (biological catalysts) in bacteria are inhibited by their own substrates, leading to reaction velocity curves (plotted to monitor the rate of product formation) that rise to a maximum and then descend as the substrate concentration increases (Hong, 1986). The reaction velocity curves are typically plotted by varying the concentration of substrate and plotting the rate of product formation as a function of substrate concentration (Kuhl, 1994). From these studies it was determined that substrate inhibition occurs in some 20% of enzymes in MEC reactors (Reed et al., 2010) which is not unusual for fermentation (Wong et al., 2014). The inhibition caused by 20 mmol L^{-1} butyrate solution was not reported in the literature before, to our knowledge.

Other parameters associated with hydrogen production, including the amount of 1.2 mol L^{-1} HCl needed to maintain pH in the cathode chamber at 5.3 was also assessed. When more hydrogen is produced in the MEC, the pH in the cathode chamber increases and HCl consumption, which is proportional to hydrogen production also increases. If the anode, with immobilized microorganisms, is replaced with abiotic anode the hydrogen production and HCl consumption, at the cathode, stops. Daily HCl consumption followed the same trends as daily hydrogen production with highest amounts of HCl consumed by MEC (BU) for 10 mmol L^{-1} butyrate solution and when butyrate was fully switched to 20 mmol L^{-1} acetate, when highest hydrogen production rates were observed, see Table A - 3.1 in "Appendix A - 3" section 9.3.

ii) Experiments 3.3 and 3.3 i

The purpose of the substrate switch experiment was to determine how the anodes, acclimated to acetate or butyrate, respond to 50 % acetate and 50 % butyrate mixture, most likely end product of fermentative hydrogen production (see "Aims of this Thesis" section 3 for more details). The anode acclimated to butyrate had not been tested before and it was important to determine if it responded differently to substrate change.

Acetate and butyrate mixtures did not make much difference to hydrogen production rates compared to pure butyrate solutions for MEC (BU), which contained anode acclimated to butyrate. MEC (AC), with anode acclimated to acetate, produced 88 % less hydrogen than MEC (BU), for 10 mmol L^{-1} acetate and 10 mmol L^{-1} butyrate mixtures, as shown on Table 13. The amount of methane produced by MEC (BU) was 58 ± 5 % smaller than that produced by MEC (AC) for 10 mmol L^{-1} acetate and 10 mmol L^{-1} butyrate mixtures, see Table A-3.1 in "Appendix A-3" section 9.3.

From observations reported in section 6.3.3 it could be suggested that butyrate had an inhibitory effect on methanogenesis, which led to the formation of different biofilms in MECs AC and BU. This may explain lower methane production rate for BU reactor that theoretically contained less archaea. All COD removal rates decreased by 83% for MEC (AC) and by 17 % for MEC (BU) and when 10 mmol L^{-1} acetate and 10 mmol L^{-1} butyrate mixture was introduced, compared to 20 mmol L^{-1} single compound substrate solutions in experiments 2.2 and 2.3. It could be suggested that the reason for this was that bacteria in mixed biofilm consortium on the anodes acclimated to butyrate in MECs (BU) could utilize acetate in the mixtures, however the bacteria on the anodes acclimated to acetate in MECs (AC) could not utilize butyrate in the mixtures.

When the substrates were fully switched, no methane or hydrogen production was observed for the MEC (AC) when acetate was fully switched to butyrate but the MEC (BU) produced ≈ 250 cm^3 $L_{(anode)}^{-1}$ day^{-1} (n=5) of hydrogen corresponding to the hydrogen yield of 0.52 $mol_{(hydrogen)}$ $mol_{(acetate)}^{-1}$, when the butyrate substrates was switched to acetate. The methane production rate for the MEC BU was 74 % lower, when butyrate substrate was fully switched to 20 mmol L^{-1} acetate, if compared to the MEC AC operating on 20 mmol L^{-1} acetate substrate (Fig. 34). The percentage COD reduction remained at 38 ± 10 % for the MEC (BU), when the substrate was fully switched to 20 mmol L^{-1} acetate substrate. For the MEC (AC), the percentage COD reduction decreased to 0, which supports the hypothesis that the bacteria on the anode acclimated to acetate could not utilize butyrate.

A small issue that had to be addressed was the tubing getting stretched during the end of the operation of the system causing higher flow rates and a small decrease in hydrogen yield (which relates the amount of substrate passing through the reactor to the amount of hydrogen produced) for higher volumetric hydrogen production production rates. This issue was addressed by means of recording daily flow rate, which was used in calculating hydrogen yield. The expected hydrogen yield for MEC (BU) with volumetric hydrogen production rate ≈ 250 cm^3 $L_{(anode)}^{-1}$ day^{-1} was 0.6 - 0.7 $mol_{(hydrogen)}$ $mol_{(acetate)}^{-1}$.

The reason why the start up (biofilm acclimation) to acetate or butyrate lasted for 9 instead of 4 weeks (30 days) was to assess the effect of the build up of biomass biofilm in the MEC which can lead up to the production of a conductive barrier. As the result of this, archaeal methanogenesis was not an issue in experiments 1 - 1.4, was an issue in experiments 3.2 – 3.3 using the continuous flow MEC (AC), acclimated to acetate. However not for the MEC BU that was acclimated to butyrate where little methane was detected. The bacteria in the MEC BU were capable of utilizing butyrate probably via converting it into acetate and hydrogen with the remaining acetate converted into hydrogen and CO_2 by different species of bacteria (Liu et al., 2005b). This was confirmed by VFA analysis for MEC (BU), data not shown, which showed that butyrate was fully converted into acetate in two days in a batch reactor (substrate flow through the continuous reactor was stopped for 3 days to prove this theory) and a reduction in acetate concentration was detected on the third day. VFA analysis of effluent samples also showed no changes in butyrate concentration for the MEC (AC) after 3 days of batch operation. In order to provide more evidence to support this hypothesis the effluent samples and the carbon cloth samples were removed from the anode (see "Offline Analysis Methods" section 4.8 for details) were sent for analysis to University of Seoul (Korea) for DNA analysis in order to identify bacteria responsible for butyrate and acetate conversion into hydrogen. This data is not presented here.

iii) Performance of a Two Stage System Consisting of Continuous Flow Fermenter and Microbial Electrolysis Cell (MEC)

Table 14 shows theoretical amounts of hydrogen produced by the integrated system based on practical results for fermentative hydrogen production rates, from hexose, published by Kyazze et al (2006) combined with result for microbial electrolysis cell experiment 3.2 from work mentioned in this thesis.

Table 14 – Theoretical amounts of H_2 from the integrated process compared to highest hydrogen fermentation values for hexose from Kyazze et al.,(2006).

Hexose ($molL^{-1}$)	Butyrate ($molL^{-1}$)	Acetate ($molL^{-1}$)	H_2 fermentation		Integrated process	
			H_2 ($LL^{-1}day^{-1}$)	H_2 ($molmol^{-1}$ hexose)	H_2 ($LL^{-1}day^{-1}$)	H_2 ($molmol^{-1}$ hexose)
56×10^{-3}	50×10^{-3}	28×10^{-3}	4.37	1.65	7.62	2.88
111×10^{-3}	71×10^{-3}	33×10^{-3}	6.79	1.3	10.97	2.10
222×10^{-3}	107×10^{-3}	62×10^{-3}	12.12	1.15	19.22	1.82

For calculating the values in this table the performance for MEC (BU) operated on 5 mmol L^{-1} butyrate and MEC (AC) operated on 5 mmol L^{-1} acetate were used. The reason the fermenter and MEC cells were operated separately was because the concentrations of acetate and / or butyrate had to be exact in order to determine performance factors for different substrate concentrations. Table 14 shows that conversion efficiencies of 0.64 $mol_{(hydrogen)}$ $mol_{(hexose)}^{-1}$ and 1.31 $mol_{(hydrogen)}$ $mol_{(hexose)}^{-1}$ can be achieved for acetate and butyrate respectively. Integrated process showsa potential, ≈ 40 % improvement in hydrogen production rate ($L_{(hydrogen)}$ $L_{(hexose)}^{-1}$ day^{-1}) and efficiency with which hexose is converted into hydrogen ($mol_{(hydrogen)}$ $mol_{(hexose)}^{-1}$), for all concentrations in Table 14.

6.3.4 Conclusion

The effect of different acetate and butyrate concentrations on hydrogen and methane productions was assessed in microbial electrolysis cells (MECs), together with other parameters associated with it, such as COD reduction, pH, conductivity and anodic and cathodic potentials vs reference Ag/AgCl electrodes. The correlation between the current in MEC system, substrate concentration and gas production in MEC with rates of hydrogen production were not assessed in detail in literature before.

The hydrogen yields per mol substrate for MEC acclimated to butyrate, when operated on butyrate, were comparable to what was reported in literature for large scale systems but smaller than what was reported in literature smaller MECs operated on butyrate (see “Discussion” section 6.3.3 for details). The highest hydrogen yield observed was 1.3 $mol_{(hydrogen)}$ $mol_{(acetate)}^{-1}$ for MEC (AC), with its anode acclimated to acetate, for 5 mmol L^{-1} pure acetate solution. The highest hydrogen yield observed for MEC (BU) with its anode acclimated to butyrate was 0.64 $mol_{(hydrogen)}$ $mol_{(butyrate)}^{-1}$ corresponding to volumetric hydrogen production of 177 cm^3 L_{anode}^{-1} day^{-1} for 5 mmol L^{-1} pure butyrate solution. The highest volumetric hydrogen production 251 cm^3 L_{anode}^{-1} day^{-1} corresponding to hydrogen yield 0.52 $mol_{(hydrogen)}$ $mol_{(butyrate)}^{-1}$ was observed for MEC (BU) when butyrate was fully switched to 20 mmol L^{-1} acetate. According to our knowledge the effect of substrate switch on hydrogen production rate was not previously reported in literature before. It was suggested that MEC (BU) contained two microbial cultures. Evidence presented in the “Discussion” section suggests that one metabolic group converted butyrate into acetate and another that converted acetate into carbonate. In MEC (AC) however only one metabolic group converted acetate into carbonate. Pure butyrate, inhibited hydrogen production rate in the MEC (AC) when acetate was fully switched to butyrate. These phenomena have not previously reported in literature. Another observation, according to our knowledge was not reported in literature before, was higher methane concentration in MEC (AC) compared to MEC (BU).

The cause of this could be due to methanogenic archaea, more of which was present MEC (AC), acclimated to acetate.

This work shows that it would be possible to treat the liquid effluent from hydrogen fermenters, which consists of a mixture of acetate and butyrate with MEC reactor improving the overall system hydrogen yield.

6.4 The Comparison of Four Anode Types and their Effect on the Voltage Production in Microbial Fuel Cells (MFCs) and Hydrogen Production in Microbial Electrolysis Cells (MECs)

The power density of microbial fuel cells (MFCs) and the hydrogen production rate of microbial electrolysis cells (MECs) can be increased not only via the use of mediators but also potentially by the choice of anode material configurations (Dumas et al., 2007, Zhu and Logan, 2013). The aim of this work was to investigate the effects of four different anode configurations on the power density in microbial fuel cells (MFCs) and the hydrogen production rates in microbial electrolysis cells (MECs), see "Electrochemical Analysis Methods" section 4.7 for details. Four types of electrodes were prepared, (3 of each, 12 in total):- steel mesh/carbon cloth roll anode (RR), J cloth/carbon cloth roll anode (JC), methylene blue treated carbon cloth (MB, or MBi if referred MB treated anode with microbial culture acclimated to 1000 Ω resistance) and untreated carbon cloth (UCC). Twelve 200 cm^3 tubular MFC reactors were prepared as described in the "Materials and Methods" in section 4 and operated as described in "Experimental Regime" section 5. Acetate solution (20 mmol L^{-1}) was used as feedstock for the MFC reactors used for experiment 4.1, which lasted for 7 weeks in order to create biofilms acclimated to acetate at 1000 Ω resistance. The pre-acclimated anodes were then transferred into 320 cm^3 anode chambers in MECs and investigated for the hydrogen production rates for experiment 4.2 and 4.2 i.

6.4.1 Results for Microbial Fuel Cell (MFC) Anode Acclimation Experiments

i) Voltage Monitoring

In experiment 4.1, the influence of anode material and configuration was investigated. The cells were tested by feeding 20 mmol L^{-1} acetate at 1000 Ω resistance to allow comparison to work previously done by Michie et al (2011) and previous work in this thesis. The voltage was continuously logged on line (see "Electrochemical Analysis Methods" section 4.7 for details). The sharp voltage drops to 0 were due to the cells being emptied and the substrate replaced once a week (Fig. 36). This is comparison between this single replicate with repeats 2 and 3 not shown. Replicates 2 and 3 followed a similar pattern and values as replicate 1 and so for clarity and space reasons the graphs for replicates 2 and 3 were not included here.

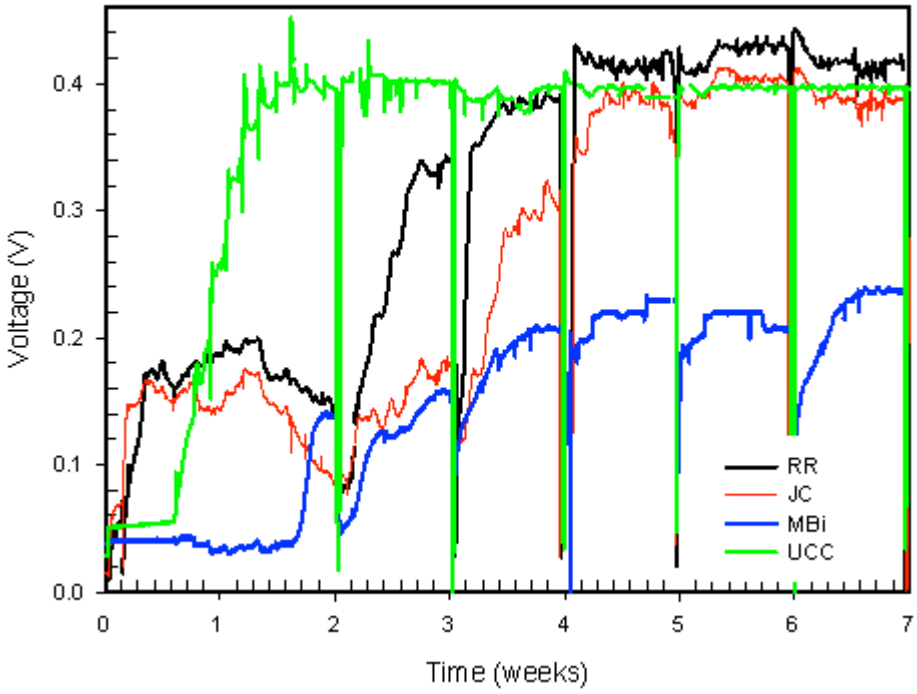

Figure 36 – The development of voltages in microbial fuel cells (MFCs) with 4 different configurations operated on acetate.

Fig. 36 shows that the voltage generation began to noticeably increase from day 1 of the enrichment of the anode electrode (time t=0, when sludge containing bacteria was added to nutrient electrolyte mixture, in the assembled MFCs). This data is described separately for each electrode type as shown below:-

i) For the MFC (RR) the voltage generation reached 197 mV (0.19 W m^{-3}) on week 2, day 9. The voltage slowly increased and stabilized, after three batch operations, on week 4, day 28, at 436.5±4.5 mV (0.95±1.01×10^{-4} W m^{-3}) and remained at that level till the end of week 7, as shown in figure 36.

ii) For the MFC (JC) the voltage generation reached 174 mV (0.15 W m^{-3}) on week 2, day 9. The voltage slowly increased and stabilized, after three batch operations, on week 4, day 30, at 389.5±23.5 mV (0.76±2.8×10^{-3} W m^{-3}) and remained at that level till the end of week 7, as shown in figure 36.

iii) For the MFC (MBi) the voltage generation reached 140 mV (0.1 W m^{-3}) on week 2, day 13. The voltage slowly increased and stabilized, after three batch operations, on week 1, day 28, at 228.5±6.5 mV (0.26±2.1×10^{-4} W m^{-3}) and remained at that level till the end of week 7, as shown in figure 36.

iv) For the MFC (UCC) the voltage generation reached 420mV ($0.80\pm2.31\times10^{-3}$ W m^{-3}) on week 1, day 6. The voltage slowly increased and stabilized, during the first batch operation, on week 1, day 2, at 400±21.5 mV ($0.80\pm2.31\times10^{-3}$ W m^{-3}) and remained at that level till the end of week 7, as shown in figure 36.

i) Coulombic efficiency (CE) and Energy Efficiency:

One of the aims of microbial fuel cell (MFC) research is to extract as many electrons from biomass as possible and to recover as much energy as possible. The coulombic efficiency (CE) and energy efficiency for sequencing batch (SBR) operation were calculated, as previously described in "Electrochemical Analysis Methods" section 4.7 with errors ± representing 3 replicates.

Table 15 – Comparison of coulombic efficiency (CE) and energy recovery values for MFCs fed with acetate (20 mmol L^{-1}) enriched at different resistances.

Resistance		CE_p (c)	CE (%)	E_p (J)	E (%)
1000 Ω	UCC	1143±25	37±1	280±8	8
	RR	1235±83	40±3	450±25	12±1
	JC	1081±60	35±2	335±18	10
	MBi	587±8	19	110±2	3
CE_t (AC) = 3088 c, E_t (AC) = 3501 J					
± represents variations from the average for *n* experimental repeats (*n*=3)					

Table 15 shows the comparison of coulombic efficiency (CE) and energy recovery values (%) for all MFCs used in this study, operated at 1000 Ω resistance, see "Electrochemical Analysis Methods" section 4.7. MFCs (RR) were shown to perform better than all other electrodes. With highest number of coulombs recovered (CE_p), coulombic efficiency (CE), practical energy recovery (J) and % energy recovery (E) compared to standard energy of combustion for acetate, see Table 15.

MFCs (UCC and JC) were shown to have the 2nd best performance factors after MFC's (RR) and MFCs (MBi) performed significantly worse, as shown on Table 15. It could be suggested that MFCs (MBi) with biofilms grown at 1000 Ω resistance (Table 15) performed differently from MFCs (MB) with biofilms grown at 150 Ω previously assessed in "The Effect of Immobilized Methylene Blue and Neutral Red on the Current Production in Microbial Fuel Cells (MFCs)" section 6.2, see (Table 9) due to different microbial cultures developing on the anode surfaces at different resistances (Katuri et al., 2011).

ii) Power Density Monitoring:

The power density curves were used to monitor power density but also enabled to monitor voltage developments at low resistances as well as power density. The power densities were measured once per 7 days (performed as calculations previously described in "Electrochemical Analysis Methods" section 4.7 and "Experimental Regime" section 5). All MFCs were operated at 1000 Ω resistance to compare results to other published research eg: Michie et al (2013). Potential and power in Fig. 37 were calculated from averages for voltages for *n* experimental repeats, where *n* = 3. For the production of power density plots currents were monitored at a range of resistances with the lowest possible resistance of 10 Ω.

The highest peak power densities in MFC mode were also obtained in week 6 on day 48 for all four MFC anode materials (Fig. 37) and MFC UCC P_{max} = 3.13 W m^{-3} (2.85 mA), MFC (RR) P_{max} = 2.85 W m^{-3} (3.08 mA), MFC (JC) P_{max}= 2.32 W m^{-3} (2.78 mA) and MFC (MBi) P_{max}= 1.10 W m^{-3} (0.61 mA).

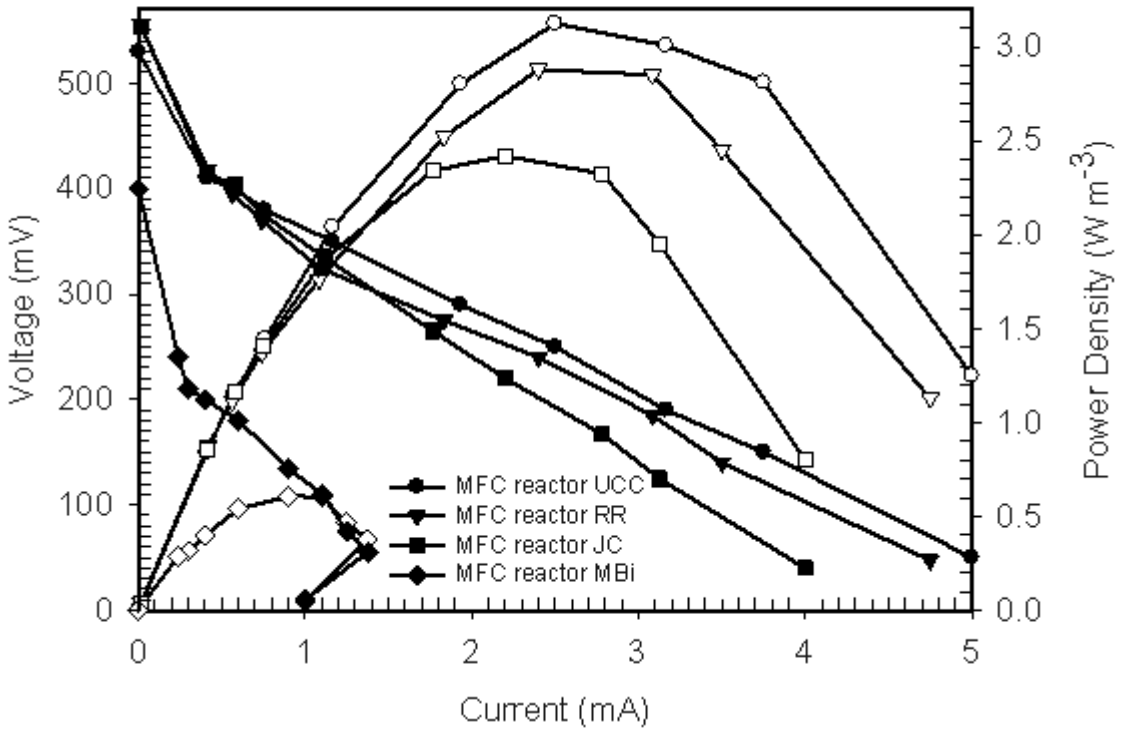

All values are calculated average voltage values for *n* experimental repeats (*n*=3) voltages.

Figure 37 – Comparison of current (closed symbols) to voltage and power density (open symbols) for MFCs, on week 7, day 48, when highest power densities were obtained. For space reasons only closed symbol key shown but symbol shape is same for the reactors for the power densities when the symbol is open.

The data for power densities and currents obtained at a 10 Ω resistance and corresponding % COD removal (substrate consumption) were used to plot figures 38 a, 38 b and 38 c. The currents and power densities for MFC (UCC) were 5 mA (0.125 W m^{-3}), for MFC (RR) were 3.95 mA (0.0078 W m^{-3}), for MFC (JC) were 3.5 mA (0.0061 W m^{-3}) and for MFC (MBi) were 1.5mA (0.001 W m^{-3}). These results were obtained on weeks 6 and 7 at 10 Ω resistance, at the same time as the power density plots were produced, as shown in figures 38 a – 38 b. These results indicate that at 10 Ω resistance MFC (UCC) performed better than the MFC (RR) by producing more current. Similar observations were made by Katuri et al (2011) who compared the biofilm morphology, current and power production for MFCs with bioanodes acclimated to both high and low resistances.

All MFC systems had similar COD (chemical oxygen demand, see "Offline Analysis Methods" section 4.8, for more details) removal rates with from the time when microbial culture was added to MFCs. The decrease of COD removal at the end of 1st batch cycle was when the substrate was replaced and corresponds to the removal of sludge particles with exoelectrogenic bacteria in the suspended phase. The subsequent slow increase in COD removal and voltage indicates that bacterial growth on the bioanode surface (see Fig. 38 c for more details) was occurring. Figure 38 c shows that the COD removal rates were highest for MFCs with untreated and J cloth / carbon cloth anodes (JC) and lowest for metal cloth / carbon cloth anodes (RR). COD removal rates are presented in descending order:- MFC (UCC) 67±2 % (*n*=3), MFC (JC) = 48±3 % (*n*=3), MFC (MBi) = 42±5 % and MFC (RR) = 39±5 % (*n*=3) on week 7, day 49, when highest power densities and voltages were observed. Where *n*=3 where *n* is the number of experimental repeats, see "Experimental Regime" section 5 for details. It could be suggested that stainless carbon cloth / steel cloth anode in MFC (RR) provided poor attachment for bacteria on the anode surface which resulted less substrate consumption, but there was higher percentage of electricity producing bacteria on the anode surface compared to similar voltage and power production to MFCs (UCC) and MFCs (JC) with more substrate consumed. The results of this were lower coulombic efficiencies (CE) in MFCs (JC and MBi) compared to MFCs (UCC) and MFCs (RR). A similar performance to that of MFC (RR) was reported for stainless steel plate anode by Dumas et al (2007).

(a)

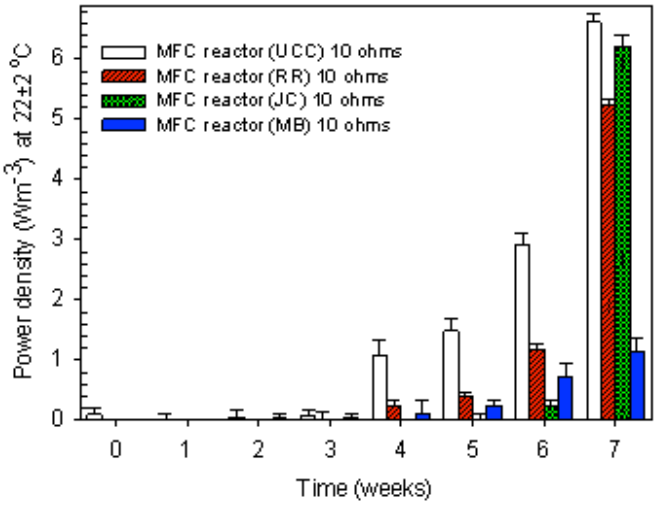

(b)

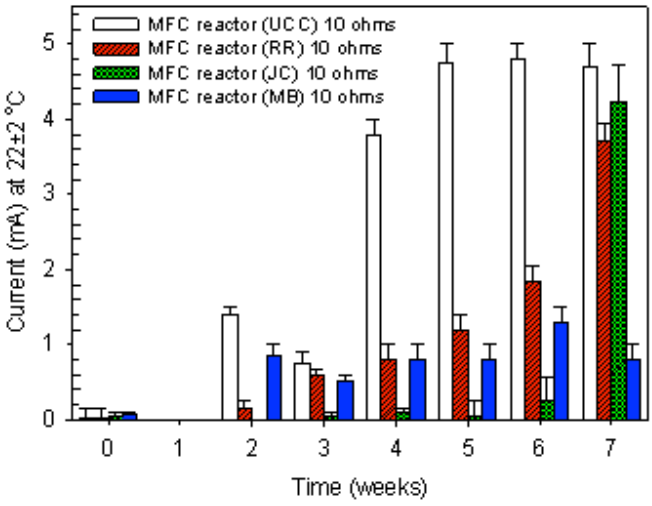

(c)

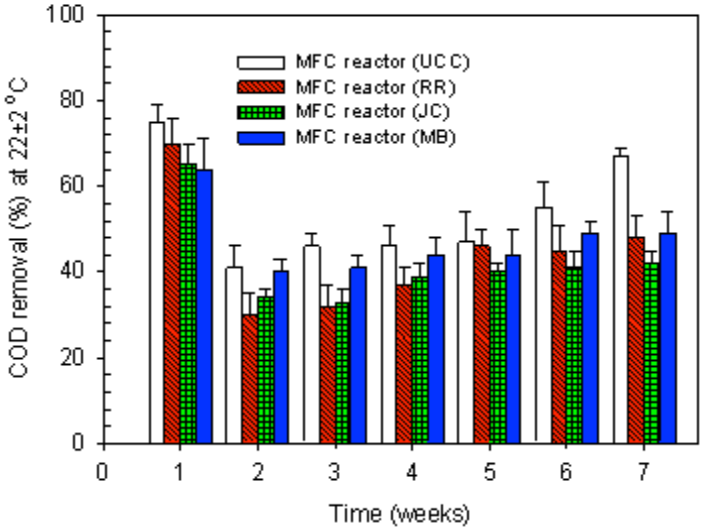

Error bars represent variations from the average for *n* experimental repeats (*n*=3).

Figure 38 - Comparison of power densities (38 a), currents (38 b) and COD removal rates (38 c) for microbial fuel cells (MFCs), as a function of time.

6.4.2 Results for Continuous Flow MEC Experiments with Four Different Anodes

Experiment 4.2 was designed to assess the performance factors associated with changes in acetate concentration for the operation of the continuous flow microbial electrolysis (MEC) reactor. The aims of this work are described in "Aims of this Thesis" section 3. One of the initial aims of the thesis was to assess the use of a continuous flow MEC to be used as second hydrogen production stage linked with fermenative hydrogen production. In this process, which converts biomass, primarily containing carbohydrates, lipids and proteins, into approximately 40 % acetate and 60 % butyrate solution as well as hydrogen. The purpose of this work was to assess the effect of changes in concentration in acetate and butyrate on the MECs containing four different anodes acclimated to either acetate or butyrate on hydrogen production rate. In addition how the microbial culture on the anode responded to acetate and butyrate mixtures and substrate change over. For calculations of the performance factors see "Electrochemical Analysis Methods" section 4.7. For experiment 4.2 the acetate concentration was decreased from 20 mmol L^{-1} to 10 mmol L^{-1} and then to 5 mmol L^{-1} over 5 day periods, (see "Experimental Regime" section 5 for details). For experiment 4.2i acetate was switched to 10 mmol L^{-1} and 10 mmol L^{-1} acetate and butyrate mixtures then fully switched for butyrate (20 mmol L^{-1}) over 5 day periods, see "Experimental Regime" section 5 for details.

Calculations for the Performance Factors

All the performance factors, described in "Electrochemical Analysis Methods" section 4.7 and "Offline Analysis Methods" section 4.8, such as coulombic efficiency (CE), cathodic hydrogen recovery (r_{cat}), see equation 51, overall hydrogen recovery (Y_{H2}), see equation 52 hydrogen yield with respect to the substrate consumed ($Y_{H2\ per\ mol\ substrate\ destroyed}$), see equation 53 were calculated, from data obtained, as shown below, based on (Logan, 2008, Logan et al., 2008). The calculations were exactly the same as in "The Influence of pH and Temperature on Hydrogen Production in Continuous Flow Microbial Electrolysis Cell (MEC) Reactor" with the only difference being the hydraulic retention time (HRT), was changed from 8.1 h to 9.6 h instead of 9 h, because tubing was replaced.

i) Influence of Anode Type on the Hydrogen and Methane Production and Cathodic Current Density in MECs

In experiment 4.2 the influence of 4 anode types and acetate concentration on the hydrogen production rate was investigated for 20 mmol L^{-1} to 10 mmol L^{-1} and then to 5 mmol L^{-1} acetatete solutions. Analysis of other parameters associated with hydrogen production, such as COD reduction, current density, pH of the catalyte at the applied voltage of 850 mV (pH 5.3) was performed.

In experiment 4.3 the influence of 4 electrode configurations and the influence of 10 mmol L^{-1} acetate and 10 mmol L^{-1} butyrate mixtures and a full substrate switch on the hydrogen production rate was also investigated, using same methodology as in experiment 4.2.

Only 4 MECs could be operated at the same time, so *n* refers to number of experimental repeats experiments 4.2, 4.3, 4.2 i (repeat) and 4.3 i (repeat), so *n*=2. Since the MEC (UCC) contained the electrode configuration used in work previously performed all modifications were compared to UCC design and MEC (JC) was control for MEC (RR), see "Materials and Methods" section 4.

Results for Experiments 4.2 and 4.2 i:

The hydrogen production rate decreased with the decrease in acetate concentration from 20 mmol L^{-1} (5 days) to 10 mmol L^{-1} (5 days) to 5 mmol L^{-1} (5 days). A stepwise decrease for in the hydrogen production rate and current density with each step corresponding to five day periods was observed for MFCs UCC, MBi and RR (Fig. 43), when substrate concentration was changed. There were large current and hydrogen production rate fluctuations for MFC JC making it difficult to determine, if how the decrease in acetate concentration affected its performance.

For the MEC (UCC) the hydrogen production rates and current densities are shown below:-

i) At a 20 mmol L^{-1} acetate concentration, the highest hydrogen production rates were obtained, which amounted to 165±5 $cm^3\ L_{(anode)}^{-1}\ day^{-1}$ (*n*=2) were achieved (see figure 39, p.161 for details) with a current density 1.7±0.1 A m^{-2} (see Fig. 42 and Fig. 43) and a COD reduction 58±2 %, for the MEC (UCC) (see Table 3.2 in "Appendix A-3" section 9.3).

ii) At a 10 mmol L^{-1} acetate concentration, the hydrogen production rates of 80.5±0.5 $cm^3\ L_{(anode)}^{-1}\ day^{-1}$ (*n*=2) were achieved (see figure 39, p.161 for details) with a current density 1.5±0.2 A m^{-2} (see Fig. 42 and Fig. 43) and a COD reduction 64±2 %, for the MEC (UCC) (see Table 3.2 in "Appendix A-3" section 9.3).

iii) At a 5 mmol L^{-1} acetate concentration, the hydrogen production rates of 36±1 $cm^3\ L_{(anode)}^{-1}\ day^{-1}$ (*n*=2) were achieved (see figure 39, p.161 for details) with a current density 1.3±0.1 A m^{-2} (see Fig. 42 and Fig. 43) and a COD reduction 53±3 %, for the MEC (UCC) (see Table 3.2 in "Appendix A-3" section 9.3).

For MEC (MBi) the hydrogen production rates and current densities are shown below:-

i) At a 20 mmol L^{-1} acetate concentration, the highest hydrogen production rates for the MEC (MBi) were obtained, which amounted to 20±2 $cm^3\ L_{(anode)}^{-1}\ day^{-1}$ (*n*=2) were achieved (see figure 39, p.161 for details) with a current density 1.25±0.05 A m^{-2} (see Fig. 42 and Fig. 43) and a COD reduction 36±1 %, for MEC (MBi) (see Table 3.2 in "Appendix A-3" section 9.3).

ii) At a 10 mmol L^{-1} acetate concentration, the hydrogen production rates of 5±3 $cm^3\ L_{(anode)}^{-1}\ day^{-1}$ (*n*=2) were achieved (see figure 39, p.161 for details) with a current density 1.1±0.1 A m^{-2} (see Fig. 42 and Fig. 43) and a COD reduction 39±3 %, for MEC (MBi) (see Table 3.2 in "Appendix A-3" section 9.3).

iii) At a 5 mmol L^{-1} acetate concentration, the hydrogen production rates of 2±1 $cm^3\ L_{(anode)}^{-1}\ day^{-1}$ (*n*=2) were achieved (see figure 39, p.161 for details) with a current density 0.7±0.1 A m^{-2} (see Fig. 42 and Fig. 43) and a COD reduction 58±2 %, for MEC (MBi) (see Table 3.2 in "Appendix A-3" section 9.3).

At a 20 mmol L^{-1} acetate concentration, methane production rates of 18.9±0.4 $cm^3\ L_{(anode)}^{-1}\ day^{-1}$ (*n*=2) were achieved; at 10 mmol L^{-1} acetate concentration methane production rates amounted to 11.9±1.9 $cm^3\ L_{(anode)}^{-1}\ day^{-1}$ (*n*=2), and at 5 mmol L^{-1} acetate concentration methane production rates amounted to 5.5±0.7 $cm^3\ L_{(anode)}^{-1}\ day^{-1}$ (*n*=2), for MEC (UCC), see figure 39, p.161 for details.

At a 20 mmol L^{-1} acetate concentration, methane production rates of 32.5±0.5 $cm^3\ L_{(anode)}^{-1}\ day^{-1}$ (*n*=2) were achieved; at 10 mmol L^{-1} acetate concentration methane production rates amounted to 28.1±1.1 $cm^3\ L_{(anode)}^{-1}\ day^{-1}$ (*n*=2), and at 5 mmol L^{-1} acetate concentration methane production rates amounted to 2.2±0.7 $cm^3\ L_{(anode)}^{-1}\ day^{-1}$ (*n*=2), for MEC (MBi); see figure 39, p.161 for details.

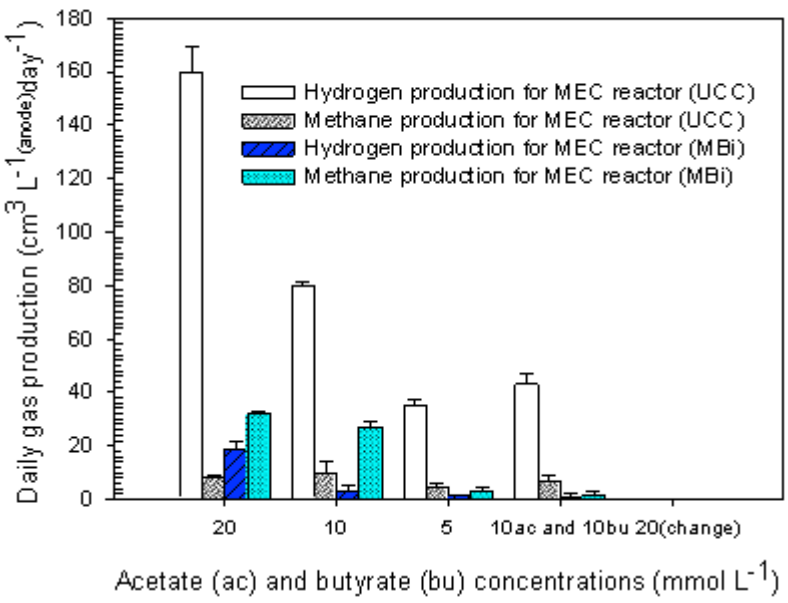

Error bars represent variations from the average for *n* experimental repeats (*n* = 2).

Figure 39 -Variations of different hydrogen production rates, in the cathode chamber, compared to methane production rates for MECs, with MECs with UCC anodes compared to MECs (MBi) under different substrate loadings.

For MEC (RR) hydrogen production rates and current densities were shown below:-

i) At a 20 mmol L^{-1} acetate concentration, the highest hydrogen production rates were obtained which amounted to 175±5 cm^3 $L_{(anode)}^{-1}$ day^{-1} (*n*=2) were achieved (see figure 40, p.162 for details) with a current density 2.2±0.05 A m^{-2} (see Fig. 42 and Fig. 43) and a COD reduction 30±2 %, for the MEC (RR) (see Table 3.2 in "Appendix A-3" section 9.3).

ii) At a 10 mmol L^{-1} acetate concentration, the hydrogen production rates of 51±7 cm^3 $L_{(anode)}^{-1}$ day^{-1} (*n*=2) were achieved (see figure 40, p.162 for details) with a current density 1.44±0.05 A m^{-2} (see Fig. 42 and Fig. 43) and a COD reduction 64±3 %, for the MEC (RR) (see Table 3.2 in "Appendix A-3" section 9.3).

iii) At a 5 mmol L^{-1} acetate concentration, the hydrogen production rates of 4±1 cm^3 $L_{(anode)}^{-1}$ day^{-1} (*n*=2) were achieved (see figure 40, p.162 for details) with a current density 1.03±0.23 A m^{-2} (see Fig. 42 and Fig. 43) and a COD reduction 69±2 %, for the MEC (RR) (see Table 3.2 in "Appendix A-3" section 9.3).

At a 20 mmol L^{-1} acetate concentration, methane production rates of 12.2±1.2 cm^3 $L_{(anode)}^{-1}$ day^{-1} (*n*=2) were achieved; at 10 mmol L^{-1} acetate concentration methane production rates amounted to 16.3±1.3 cm^3 $L_{(anode)}^{-1}$ day^{-1} (*n*=2), and at 5 mmol L^{-1} acetate concentration methane production rates amounted to 12.8±0.8 cm^3 $L_{(anode)}^{-1}$ day^{-1} (*n*=2), for MEC (RR), see figure 40 for details.

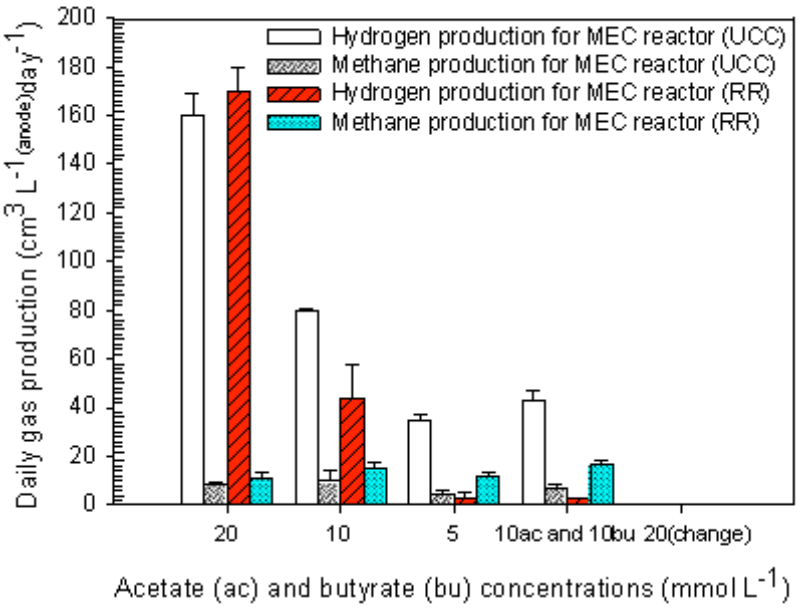

Error bars represent variations from the average for *n* experimental repeats (*n* = 2).

Figure 40 – Variations of different hydrogen production rates, in the cathode chamber, compared to methane production rates for MECs, with RR anodes compared to MECs (UCC) under different substrate loadings.

For the MEC (JC) the following hydrogen production rates and current densities were found:-

i) At a 20 mmol L^{-1} acetate concentration, the highest hydrogen production rates for the MEC (JC) were obtained, which amounted to 7.7±0.2 cm^3 $L_{(anode)}^{-1}$ day^{-1} (*n*=2), (see figure 41, p.163 for details); with a current density of 1.12±0.48 A m^{-2} (Fig. 42 and Fig. 43), a COD reduction of 63±5 %, for MEC (JC) (see Table A-3.2 in "Appendix A-3" section 9.3).

ii) At a 10 mmol L^{-1} acetate concentration, the hydrogen production rates of 8.8±0.2 cm^3 $L_{(anode)}^{-1}$ day^{-1} (*n*=2) were achieved, (see figure 41, p.163 for details) with a current density of 1.2±0.2 A m^{-2} (see Fig. 42 and Fig. 43), and a COD reduction of 55±5 %, for MEC (JC) (see Table A-3.2 in "Appendix A-3" section 9.3).

iii) At a 5 mmol L^{-1} acetate concentration, the hydrogen production rates of 0.3±0.1 cm^3 $L_{(anode)}^{-1}$ day^{-1} (*n*=2) were achieved (see figure 41 for details) with a current density 0.8±0.2 A m^{-2} (see Fig. 42 and Fig. 43) and a COD reduction 74±5 %, for MEC (JC) (see Table 3.2 in "Appendix A-3" section 9.3).

At 20 mmol L^{-1}acetate concentration methane production rates of 46.4±1.4 cm^3 $L_{(anode)}^{-1}$ day^{-1} (*n*=2) were achieved; at 10 mmol L^{-1} acetate concentration methane production rates amounted to 6.7±0.7 cm^3 $L_{(anode)}^{-1}$ day^{-1} (*n*=2), and at 5 mmol L^{-1} acetate concentration methane production rates amounted to 1.8±0.1 cm^3 $L_{(anode)}^{-1}$ day^{-1} (*n*=2), for MEC (JC) (see figure 41 for details).

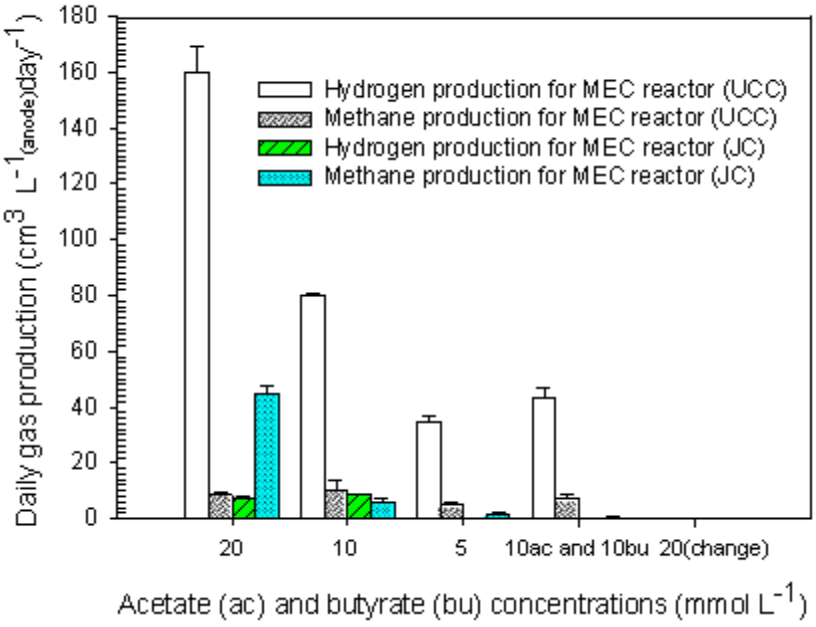

Error bars represent variations from the average for *n* experimental repeats (*n* = 2).

Figure 41 – Variations of different hydrogen production rates, in the cathode chamber, compared to methane production rates for MECs, with JC anodes compared to MECs (UCC) under different substrate loadings.

Results for Experiments 4.3 and 4.3 i:

The hydrogen production rates and current densities, for 10 mmol L^{-1} acetate 10 mmol L^{-1} butyrate solution, for MEC (UCC) increased to the levels similar to that observed for pure 5 mmol L^{-1} acetate solution and decreased to 0, for full substrate switch full substrate switch to from acetate to 20 mmol L^{-1} butyrate.

For MECs MBi, RR and JC the hydrogen production rates and current densities decreased to 0, for 10 mmol L^{-1} acetate 10 mmol L^{-1} butyrate solution and full substrate switch to from acetate to 20 mmol L^{-1} butyrate. These results can be presented as shown below:-

i) For the MEC (UCC), the hydrogen production rates of 45±2 $cm^3 L_{(anode)}^{-1} day^{-1}$ (*n*=2) were achieved, (see figure 39 for details) with a current density 1.5±0.1 A m^{-2} (see Fig. 42 and Fig. 43) and a COD reduction of 2±1 % (see Table A-3.2 in "Appendix A-3" section 9.3).

ii) For the MEC (MBi), the hydrogen production rates of 2±1 $cm^3 L_{(anode)}^{-1} day^{-1}$ (*n*=2) were achieved, (see figure 41 for details) with a current density 0.975±0.03 A m^{-2} (Fig. 42 and Fig. 43) and a COD reduction of 5±1 % (see Table A-3.2 in "Appendix A-3" section 9.3).

iii) For the MEC (RR), the hydrogen production rates of 3±1 $cm^3 L_{(anode)}^{-1} day^{-1}$ (*n*=2) were achieved (see figure 40 for details) with a current density 1.2±0.2 A m^{-2} (Fig. 42 and Fig. 43) and a COD reduction of 43±3 % (see Table A-3.2 in "Appendix A-3" section 9.3).

iv) For the MEC (JC), the hydrogen production rates of 6.5±1.5 × 10^{-2} $cm^3 L_{(anode)}^{-1} day^{-1}$ (*n*=2) were achieved (see figure 41 for details) with a current density 0.55±0.35 A m^{-2} (Fig. 42 and Fig. 43) and a COD reduction of 6±1 % (see Table A-3.2 in "Appendix A-3" section 9.3).

Methane production rates obtained for 10 mmol L^{-1} and 10 mmol L^{-1} acetate and butyrate solutions and for full substrate switch from acetate to 20 mmol L^{-1} butyrate are shown below:-

i) For the MEC (UCC), the methane production rates of 7.8±0.8 $cm^3 L_{(anode)}^{-1} day^{-1}$ (*n*=2) for 10 mmol L^{-1} acetate and 10 mmol L^{-1} butyrate solution and 0.8±0.2 $cm^3 L_{(anode)}^{-1} day^{-1}$ (*n*=2) for 20 mmol L^{-1} butyrate were achieved (see figure 39 for details).

ii) For the MEC (MBi), the methane production rates of 0.1±0.0 $cm^3 L_{(anode)}^{-1} day^{-1}$ (*n*=2) for 10 mmol L^{-1} acetate and 10 mmol L^{-1} butyrate solution and 0.0±0.0 $cm^3 L_{(anode)}^{-1} day^{-1}$ (*n*=2) for 20 mmol L^{-1} butyrate were achieved (see figure 39 for details).

iii) For the MEC (RR), the methane production rates of 0.2±0.1 cm^3 $L_{(anode)}^{-1}$ day^{-1} (*n*=2) for 10 mmol L^{-1} acetate and 10 mmol L^{-1} butyrate solution and 0.0±0.0 cm^3 $L_{(anode)}^{-1}$ day^{-1} (*n*=2) for 20 mmol L^{-1} butyrate were achieved (see figure 40 for details).

iv) For the MEC (JC), the methane production rates of 0.2±0.1 cm^3 $L_{(anode)}^{-1}$ day^{-1} (*n*=2) for 10 mmol L^{-1} acetate and 10 mmol L^{-1} butyrate solution and 0.1±0.0 cm^3 $L_{(anode)}^{-1}$ day^{-1} (*n*=2) for 20 mmol L^{-1} butyrate were achieved (see figure 41 for details).

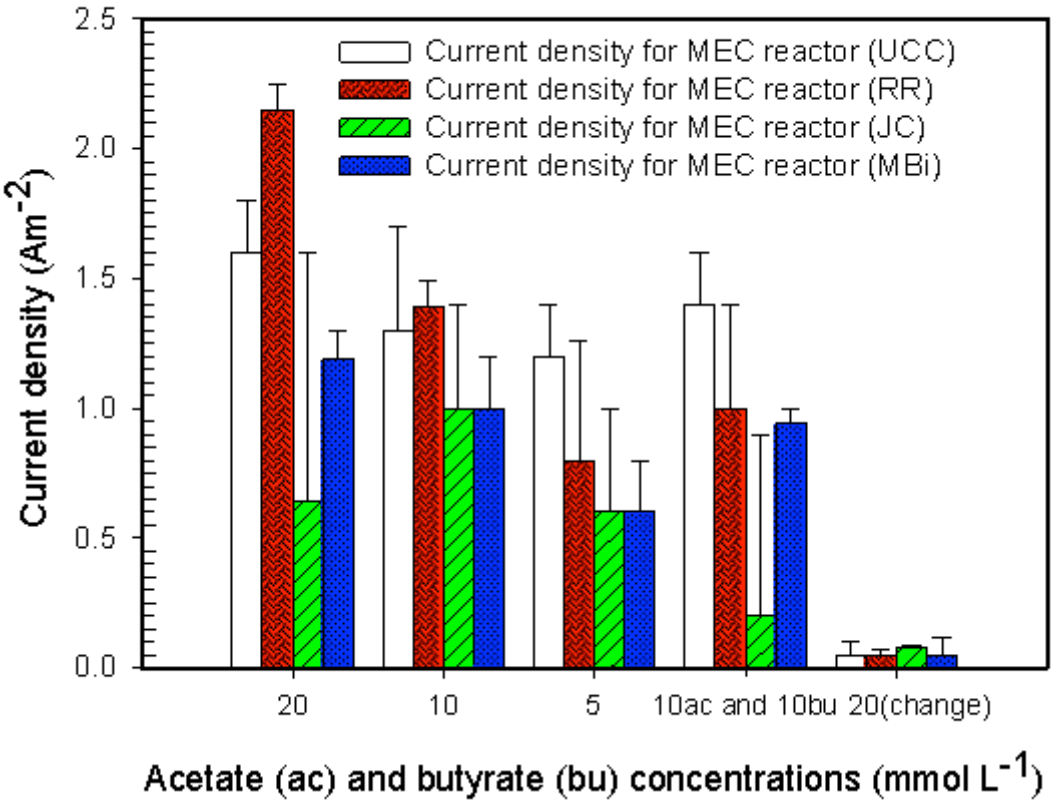

Error bars represent variations from the average for *n* experimental repeats (*n* = 2).

Figure 42 – Variations in current density under different substrate loadings.

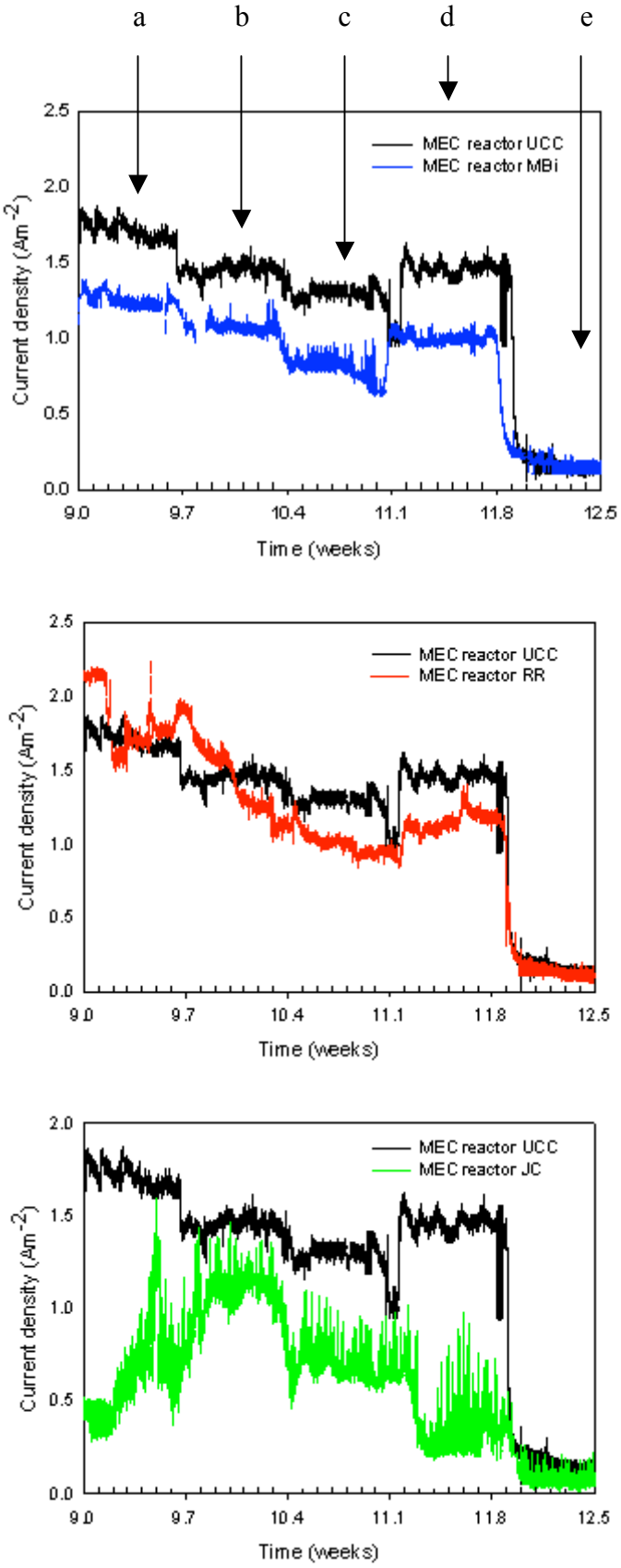

Where a is substrate (acetate or butyrate) 20 mmol L^{-1}, b is 10 mmol L^{-1} and c is 5 mmol L^{-1} respectively, on weeks 11 - 13; d is acetate (10 mmol L-1) / butyrate (10 mmol L^{-1}) mixtures on weeks 13-13.8 and e is full substrate change (20 mmol L^{-1}) on weeks 13.8-14.5.

Figure 43 – The current densities of MEC reactors with four different anode configurations under different substrate loadings.

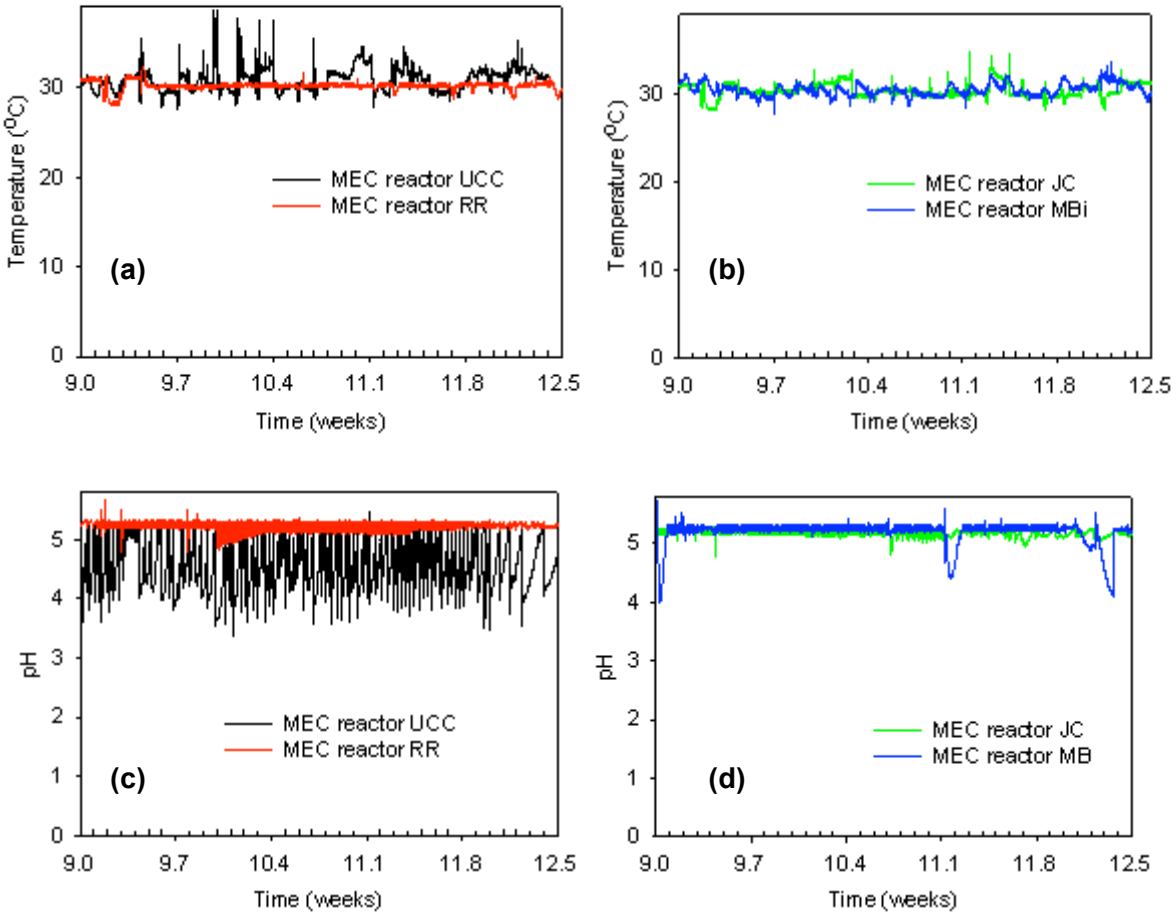

Figure 44 – The pH (44 a and 44 b) and Temperature (44 c and 44 d) of MEC Reactors with Four Different Anode Configurations under Different Substrate Loadings.

The temperature was maintained at 30 ^{o}C (Fig. 44 a and Fig. 44 b) with small fluctuations caused by problems with one temperature controller for MEC (UCC) for less than a day, which was repaired several once, sometimes twice a week during 1st three weeks of operation. It could be suggested that the fluctuations in pH (Fig. 44 c and Fig. 44 d) were caused by microbial activity on the anode surface with biggest drops in pH corresponding to MEC (UCC), which produced most hydrogen.

ii) Effect of Changes in Acetate and / or Butyrate Concentrations on Other Performance Factors such as Coulombic Efficiency (CE) and Hydrogen Recovery per mol of Substrate Consumed

Coulombic efficiencies (CEs), see "Electrochemical Analysis Methods" section 4.7 for details, compared current recorded across 1Ω resistor between the cathode and the power supply to theoretical current obtained from COD reduction. With decrease in the substrate concentration theoretical current obtained from COD reduction becomes smaller, hence CE values go up for MECs (UCC, MBi and JC), as observed for pure acetate for MECs (AC, with anode acclimated to acetate), as shown on Table 16. For MEC (RR, stainless steel cloth carbon cloth roll) however CE values (Table 16) and COD values decreased with decrease in substrate concentration.

The hydrogen yields in table 16 relate COD reduction (the amount of substrate consumed) to hydrogen production rates. Hydrogen yields decreased with decrease in substrate concentration. For MEC (RR) highest hydrogen yield obtained was 0.67 $mol_{(hydrogen)}$ $mol_{(acetate)}^{-1}$ (n=2) at 20 $mmolL^{-1}$ acetate concentration, which quickly decreased to that ≤ 0.03 $mol_{(hydrogen)}$ $mol_{(acetate)}^{-1}$. It could be suggested that stainless carbon cloth / steel cloth anode in MFC (RR) provided poor attachment for bacteria on the anode surface in continuous flow system. COD reduction however remained ≈ 60%, which is 20% higher than that for MECs with other electrode designs to which it was compared. Higher substrate removal indicates that there were more bacteria in the MEC reactor, which could remain in suspended phase substrate solution. According to Logan (2008) electricity producing bacteria exist in symbiotic relationship with archaea that act as electron sinks for electricity producing microorganisms. It could be suggested that in the solution archaea become the electron acceptors for electricity producing bacteria instead of anode. This hypothesis however requires microbiology analysis to be confirmed. MEC (MBi) and MEC (JC) produced small amounts of hydrogen which resulted small hydrogen yields ≤ 0.03 $mol_{(hydrogen)}$ $mol_{(acetate)}^{-1}$, which decreased with decrease in substrate concentration. 10 mmol L^{-1} acetate and 10 mmol L^{-1} butyrate produced even smaller hydrogen yields ≤ 0.02 $mol_{(hydrogen)}$ $mol_{(aceate)}^{-1}$ and full substrate switch gave 0.00 $mol_{(hydrogen)}$ $mol_{(butyrate)}^{-1}$ for all MEC designs.

Table 16 – Comparison of coulombic efficiency (CE), cathodic hydrogen recovery and hydrogen yield mol/mol substrate consumed under varying substrate loads.

Substrate	Conc. (mmol L^{-1})	H_2 production rate $cm^3 L_{(anode)}^{-1} day^{-1}$		Cathodic H_2 recovery (%)		CE (%)		H_2 yield mol/mol substrate consumed	
		RR	JC	RR	JC	RR	JC	RR	JC
acetate	20	175±5.0	7.7±0.2	10±1	19±0	48±2	5±0	0.67±0.1	4×10^{-2}±0
	10	51±7.0	8.8±0.2	4±2	7±0	21±1	11±0	$(3\pm1)\times10^{-2}$	3×10^{2}±0
	5	4±1.0	0.3±0.1	2±0	0.21±0	28±3	23±0	$(2\pm1)\times10^{-2}$	2×10^{-3}±0
acetate and butyrate mixture	10 and 10	3±1.0	6.5±1.5	1.8±1	0.16±0	13±2	42±0	$(2\pm2)\times10^{-2}$	3×10^{-3}±0
butyrate	20	0	0	0	0	0	0	0	0
		MBi	UCC	MBi	UCC	MBi	UCC	MBi	UCC
acetate	20	20±2	165±5	5.6±1	35±2	15±2	29±2	4×10^{-2}±0	0.46±0
	10	5±3	80±1	0.4±2	25±1	16±2	36±2	1×10^{-2} ±0	0.39±0
	5	2±1	36±1	0.8±0	10±0	19±1	40±2	8×10^{-3}±0	0.16±0
acetate and butyrate mixture	10 and 10	2±1	45±2	0.1±0	42±2	18±0	42±2	6×10^{-3}±0	0.1±0
butyrate	20	0	0	0	0	0	0	0	0

A STP. Theoretical H_2 yields: 10 mol/per mol butyrate; 4 mol/mol acetate; 12 $mol/mol_{glucose}$

± represents variations from the average for *n* experimental repeats (*n*=2)

The voltage applied = 850 mV for all MEC reactors.

6.4.3 Discussion

i) Effect of Anode Construction on MFC Performance

Four types of anodes were prepared and tested in MFC and MEC modes. RR and UCC designs performed better than JC and MBi anodes. For the first time the performance of MFC with MB treated carbon anode was assessed and compared at 150 Ω and 1000 Ω resistances. MFC cell with MB treated anode (MB) was shown to perform better with peak power density twice as high as that of control (Fig. 36 – Fig. 38) but similar coulombic efficiency (CE) and energy recovery (E) values (CE=82 % and E=22 %) than MFC with untreated carbon anode (UCC, CE=78 % and E=20 %), if operated at 150 Ω resistance (Table 17 and experiment 2.1 in "The Effect of Immobilized Methylene Blue and Neutral Red on the Current Production in Microbial Fuel Cells (MFCs)" section 6.2 for details). This could be a feasible activation method for carbon electrodes for electrogenic bacteria, which could simultaneously treat contaminated wastewater (e.g. dye), and generate electrical power. If, however, MFC, with MB treated anode, was operated at 1000 Ω resistance MB (MFC MBi) inhibited the current generation and power densities by the factor of 2 (Fig. 37) with coulombic efficiency (CE) significantly lower than for MFC with anode acclimated to 150 Ω resistance (CE=19 %, E=3 %, Table 16), which according to our knowledge was not mentioned in literature before. For MFC with untreated carbon cloth anode (UCC, control) acclimated to 1000 Ω resistance the power densities (Fig. 37) were smaller by the factor of 2 than MFCs with anodes acclimated to 150 Ω (Fig. 26). It could be suggested that different resistances promote the growth of biofilms containing different species bacteria on the anode surfaces in BESs (Gil et al., 2003, Rismani-Yazdi et al., 2011). Other studies suggest that operating MFC at low resistance promotes the growth of exoelectrogenic bacteria, compared to that of MFC operated at high resistance (Rismani-Yazdi et al., 2011, Katuri et al., 2011).

. **Table 17 – Comparison of coulombic efficiency (CE) and energy recovery values for MFCs fed with acetate (20 mmol L^{-1}) enriched at 150 Ω and 1000 Ω.**

Resistance		CE_p (c)	CE (%)	E_p (J)	E (%)
150 Ω	UCC	2419±15	78±1	728±5	21
	MB	2532±8	82	770±2	22
1000 Ω	UCC	1143±25	37±1	280±8	8
	RR	1235±83	40±3	450±25	12±1
	JC	1081±60	35±2	335±18	10
	MBi	587±8	19	110±2	3

CE_t (AC) = 3088 c, E_t (AC) = 3501 J

± represents variations from the average for *n* experimental repeats (*n*=3)

ii) Factors Effecting MEC Performance

When the anode from MFC (UCC) was removed after 7 weeks of sequencing batch operation (SBR) and placed into the anode chamber of MEC (UCC, see "Experimental Regime" section 5 for details) it similar daily hydrogen production rate to that produced by MEC (AC) performance of which was assessed in "The Influence of Changes in Acetate and Butyrate Concentrations and Full Substrate Switch on Gas Production from Two Microbial Electrolysis Cells (MECs) Acclimated to either Acetate or Butyrate" section 6.3, as expected for control reactor.

When the anode from MFC (RR) was removed after 7 weeks of sequencing batch operation (SBR) and placed into the anode chamber of MEC (RR, see "Experimental Regime" section 5 for details) it produced more hydrogen than MEC (UCC, control 1), see Fig. 40 for details. The hydrogen production rate and substrate consumption, however rapidly decreased after 5 days of operation on 20 mmol L^{-1} acetate. Large fluctuations and the drop in hydrogen production rates and anodic current density for MEC with RR anode could be due to poor biofilm attachment (Dumas et al., 2008a, Dumas et al., 2008b), which was coming off when the device was operated in continuous flow mode. Stainless steel provides poor attachment to the bacteria but was better conductivity, so carbon cloth was added to provide attachment to bacteria on the electrode surface. It could be suggested that operation of MEC reactor in continuous flow mode caused bits of biofilm on the electrode surface to come off (Shen et al., 2013), which would explain decrease in hydrogen production rates (Fig. 40), CE (Table 16) and COD removal (Table A-2.1, "Appendix A-2" section 9.2). Stainless steel is also chromium coated, which could be toxic to the bacteria (Jagielski et al., 2000, Nam and Lee, 2007).

When the anode from MFC (MBi) was removed after 7 weeks of sequencing batch operation (SBR) and placed into the anode chamber of MEC (MB, see "Experimental Regime" section 5 for details) it produced less hydrogen than MEC (UCC, control 1), see Fig. 39 for details. It could be suggested that anode from MFC (MB) acclimated to methylene blue at 1000 Ω resistance had exactly the same effect of MEC performance as it did on MFC performance, as described in MFC operation in Discussion section 6.4.3.

When the anode from MFC (JC, control 2) was removed after 7 weeks of sequencing batch operation (SBR) and placed into the anode chamber of MEC (MB, see "Experimental Regime" section 5 for details) it produced least hydrogen and most methane (Fig. 41) because J cloth (see "Materials and Methods" section 4 for details) was not conductive. Non conductive surfaces on bioanode can provide area for the attachment of archaea (Afzal Ghauri et al., 2007, Michie et al., 2011) which produce methane (Thauer et al., 2008).

Methane was detected in both anode and cathode chambers, however the pH in the cathode chamber was kept at 5.3 and the electrolyte solution contained 30 g L^{-1} of salt making it impossible for methanogenesis to occur. It could be suggested that methanogenesis was either occurring on the membrane or in the acetate solution in the anode chamber, where pH was 6.75±2.5. Compared to control 2 MECs (RR and MBi) produced more hydrogen but compared to MEC (UCC, control 1) they performed worse (Fig. 39 – Fig. 41).

6.4.4 Conclusion

This work shows the importance of assessing all possible materials from which the electrodes for a continuous flow MEC system could be built before designing one. Conductivity, surface area available for electrogenic activity and bacterial attachment to electrode surface has on voltage, % of substrate removed and power production have to be assessed in detail prior to building a larger reactor. It shows that anodic structure had an effect on the performances of MFCs and MECs. This study showed that stainless steel carbon cloth roll (RR) material did not increase voltage production and power density in MFCs or hydrogen production rates and cathodic current density in MECs, as expected.

Methylene blue treated anode surface was shown to inhibit electricity production in MFCs and hydrogen production rates in MECs for microbial culture grown at 1000 Ω resistance, which was expected to increase voltage production in the same way it did for microbial culture acclimated to 150 Ω resistance.

The microbial culture acclimated to acetate was shown to be unable to consume butyrate as substrate. Although this was failure this experiment inspired experiments involving microbial cultures acclimated to butyrate described in “The Influence of Changes in Acetate and Butyrate Concentrations and Full Substrate Switch on Gas Production from two Microbial Electrolysis Cells (MECs) Acclimated to Acetate and Butyrate” 6.3.

6.5 Scaled Up Multi Anode Chamber Microbial Electrolysis Cell (Revolver Reactor)

Reports on larger scale microbial (greater than 1 liter) electrolysis cells (MECs) are a relatively rare due to the relatively recent development of this research field, and to date only a few scaled up systems have been built. Studies conducted on a 120 L MEC revealed that even though it is a promising technology for urban and industrial wastewater treatment, several difficulties still need to be overcame such as low hydrogen production rates produced only 15 $cm^3 L^{-1}_{domestic\ wastewater}\ day^{-1}$ (Heidrich et al., 2013), for 10 L MEC which produced 45 $cm^3 L^{-1}_{wastewater}\ day^{-1}$ (Gil-Carrera et al , 2011). Studies conducted by Cusick et al (2011) at 1000 L MEC which produced 190 $cm^3 L^{-1}_{vine\ wastewater}\ day^{-1}$, although most of the product gas was converted to methane (86 ± 6%). The biggest problem with all designs previously reported in literature is that they contained single large anode chambers with plenty of space for archaeal planktonic biofilm to grow, in study by hydrogen. Archaea convert hydrogen and / or substrate into methane hence preventing the growth of methanogens is one of the major issues in scaled up MECs (Thauer, 1998). Another major issue is poor conductivity of wastewater making it a poor electrolyte (Cusick et al., 2011) and the requirement of adding phosphates to convert wastewater into buffer as done in previous experimental work in this thesis is expensive. The aim of this work is describe in “Aims of this Thesis” section 3 in greater detail. The most important aims for this work were:

i) To design a scaled up MEC cell consisting of separate modules that could easily be replaced capable of treating larger volumes of wastewater (>1000 $L_{vine\ wastewater}\ day^{-1}$)

ii) To address the issues associated with a low hydrogen production rate previously reported in literature for scaled up MEC systems.

iii) To design anode chamber modules and novel anodes for a scalable MEC based on conclusions from the experimental work in this thesis.

6.5.1 Results and Discussion

A scaled up microbial electrolysis (MEC) system was designed (Fig. 45) and materials were ordered. It was referred to as Revolver Reactor because of its seven anode rods inside the cathode chamber resembling the barrel of a revolver. It was based around the design for tubular MFCs (see “Appendix A-7” section 9.7 for schematics.

An industrial scale microbial electrolysis (MEC) system has to be run continuously at high volumes (>100 m^3 per day) and should be designed in such a way that it could be possible to move large amounts of liquid through these devices and be scalable. The volume of 1 anode chamber anode rod is 453×7 = 3171 cm^3 = 3.2 L inside 19 L cathode chamber. It has 12.5h HRT (hydraulic retention time, the time needed for 3.2 L day^{-1} of influent to pass through reactor), for details) if the same pump used for upflow MEC in experiment 1 (see "Materials and Methods" section 4) is used to pump the influent into the large scale reactor. If a design in "experiment 3" (also see "Materials and Methods" section 4) is capable of producing 65 cm^3 of hydrogen per 326 cm^3 anode chamber than MEC with 453 cm^3 anode chamber could theoretically produce 65/326×3271=652 cm^3 day^{-1}. This reactor is likely to perform better than designs reported by Heidrich at al (2012) and Gil-Carrera et al (2013). The work on the reactor was sadly never finished due to lack of time.

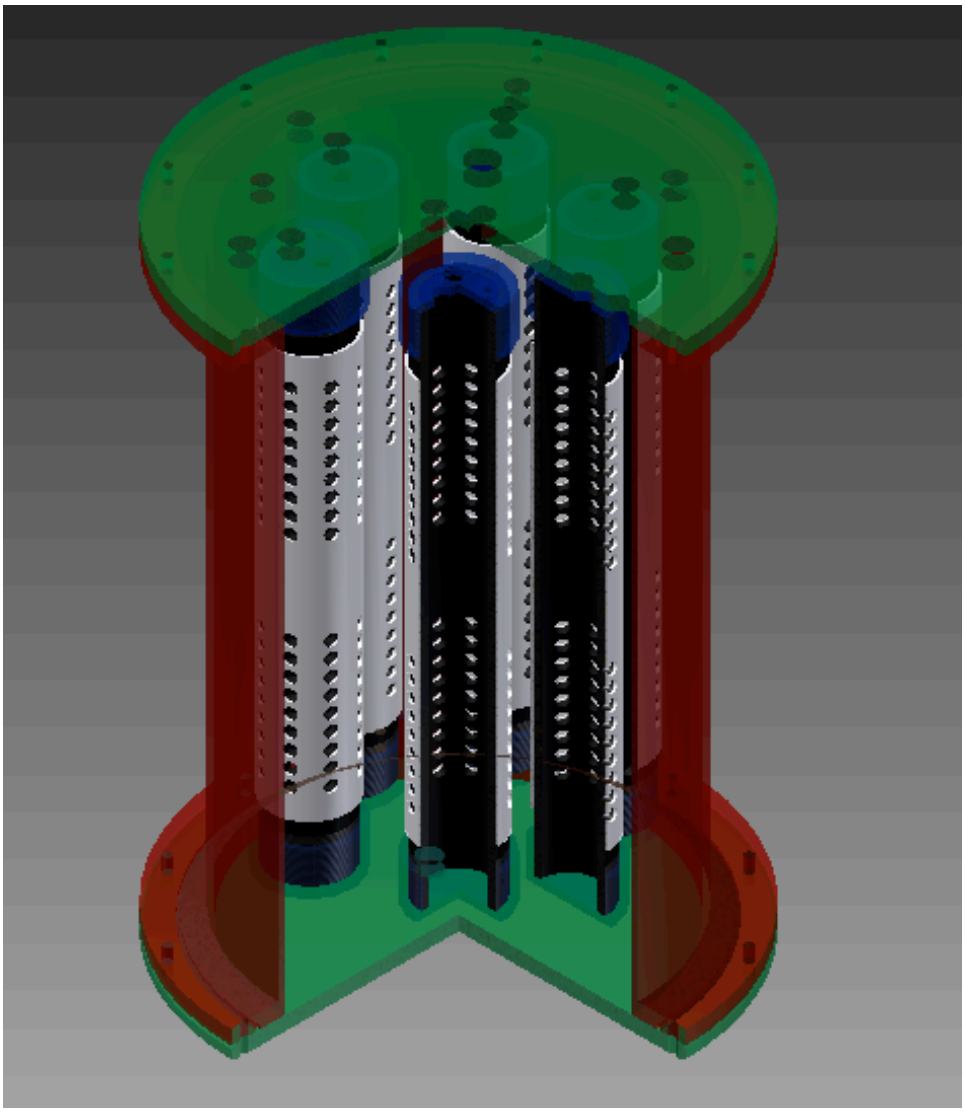

Figure 45 – A 3d drawing of cathode and anode chamber assembly for a scaled up reactor.

6.5.2 Conclusion

A scaled up microbial electrolysis (MEC) reactor was built to address major issues which were reported in literature for the research on scaling up MECs, i.e. the relatively low volumes of substrate treated and the relatively low volumes of gas produced per day. The design was based on the design described in "The Influence of Temperature and Catholyte pH on the Hydrogen Production in Microbial Electrolysis Cells (MECs)" section 6.1, which was shown to perform to required standard (hydrogen production rate at ≈200 $cm^3 L^{-1}_{substrate} day^{-1}$). The proposed seven chamber design was built and assembled for researching scaled up MEC systems, however has not yet been tested.

7. Thesis Conclusions and Further Work

7.1 Conclusions

i) The aims of this work were to assess how an increase in temperature, pH and applied voltage would affect the hydrogen production rates (cm^3 $L_{(anode)}^{-1}$ day^{-1}) for microbial electrolysis cells (MECs). The expected result was that the increase in temperature from 18 ^oC to 35 ^oC would increase the hydrogen production rate followed by decrease in hydrogen production rate at 35 ^oC - 53 ^oC. The hydrogen producing bacterial consortium was expected to be predominantly mesophilic in character, with temperatures above 35^oC and below 19 ^oC inhibiting the hydrogen production rate. The optimal pH for hydrogen production was expected to be pH 7, with a decrease in hydrogen production rate seen for pH 5 and pH 9 because electrogenic hydrogen producing bacteria previously reported in the literature, such as: *Geobacter* species are reported to be most active at neutral pH. The pH in the two chamber MEC cells (biotic anode and abiotic cathode) was kept at the same pH in both chambers to allow efficient ion transport. The effect of temperature and pH on daily hydrogen and daily methane production was assessed together with other associated parameters, such as COD reduction, pH, conductivity and anodic and cathodic potentials vs reference electrodes.

Temperatures within the range of 18 ^oC to 53 ^oC and pH ranging from 5 to 9 were tested. This experiment demonstrated that the 1 L microbial electrolysis cell could be operated at room temperature (≈23 ^oC) with highest hydrogen hydrogen yield 1.1 $mol_{(hydrogen)}$ $mol_{(acetate)}^{-1}$, corresponding to daily volumetric production of 200 cm^3 $L_{(anode)}^{-1}$ day^{-1} at the upper end of the mesophilic temperature range 30 ^oC at an applied voltage of 850 mV, at pH=5. These results were as expected for optimal temperature for hydrogen production as being between 20 ^oC and 25 ^oC but the results did not support that pH 7 was optimal pH in the cathode chamber.

Two applied voltages of 850 mV and 600 mV were tested at the same temperature and pH range. The hydrogen production rate was expected to be higher at an applied voltage of 850 mV and lower at the applied voltage of 600 mV. As expected, a lower hydrogen yield 0.52 $mol_{(hydrogen)}$ $mol_{(acetate)}^{-1}$, corresponding to volumetric production of 92 cm^3 $L_{(anode)}^{-1}$ day^{-1} was produced at the lower applied voltage of 600 mV at pH=5. A lower volumetric hydrogen production rate which makes the process more efficient in terms of the energy consumption but less efficient in terms of substrate conversion into hydrogen was also seen.

It was also shown that the current density, which is proportional to the daily hydrogen production rate, could be logged continuously on line and was successfully used to monitor MEC performance. This would allow industrially deployed units to be monitored and controlled by computer-based systems without the use of expensive hydrogen sensors.

ii) To improve the performance of the biocatalyst (bacteria) in microbial fuel cells (MFCs) electron carriers were immobilized onto the anode surface hence improving the electron transport from bacteria to the anode. The aim of this experiment was to immobilize two artificial electron carriers methylene blue (MB) and neutral red (NR) onto the carbon cloth anode surface and to assess the effect of temperatures 8 ^{o}C, 23 ^{o}C and 35 ^{o}C on performance of MFC cells acclimated to 23 ^{o}C. Both artificial electron carries (MB and NR) were expected to improve the electron transport from electrogenic biofilm grown on the anode surface and highest current was expected to be observed either at 23 ^{o}C or 35 ^{o}C. The electricity producing bacterial consortium was expected to be predominantly mesophilic in character, with temperatures above 35 ^{o}C and below 19 ^{o}C inhibiting electricity production.

A new passive adsorption technique was developed which enabled the immobilization of neutral red (NR) and methylene blue (MB) up to 0.54 mg cm^{-2} onto carbon cloth from 1.56 mmol L^{-1} solutions. Methylene blue was shown to improve maximum power density (P_{max}) and current production (mA) in microbial fuel cells (MFCs) compared to MFCs with untreated carbon anodes (controls), both types of MFCs operated at 150 Ω resistance. The choice of the electron carrier was found to have a significant effect on MFC performance with MB having positive effect and NR having an inhibitory effect on P_{max} and current production. The results were as MFCs (MB) $P_{max} \approx 8.7$ Wm^{-3} (6.6 mA), MFCs (control) $P_{max} \approx$ 4.5 W m^{-3} (4.7 mA) and MFCs (NR) $P_{max} \approx 2.63$ W m^{-3} (2.29 mA) at the room temperature (≈ 23 ^{o}C) on MFCs acclimated to 150 Ω resistance. A new and unexpected finding was the inhibitory effect of NR on electricity production and that the choice of resistance was found to have a large effect on MFC performance with MB having inhibitory effect on P_{max} and current production for microbial culture acclimated to and operated at 1000 Ω resistance, (MFC MBi), as shown in Conclusions part iii).

The effect of temperature on the performance of MFCs with mediator treated anodes acclimated to 150 Ω resistance was also conducted in order to determine the best temperature range for the current production.

The effect of the incubation temperatures of 8 ^{o}C, 35 ^{o}C and 40 ^{o}C was tested on microbial culture acclimated to room temperature ≈ 23 ^{o}C. MFC MB produced maximum power density (P_{max}) twice that of MFCs (control) at temperatures 8 ^{o}C, 23 ^{o}C and 35 ^{o}C. At 35 ^{o}C power densities increased to MFCs (MB) P_{max} ≈ ≈ 11.78 W m^{-3} (7.5 mA), MFCs (control) P_{max} ≈ 5.3 W m^{-3} (5.2 mA) and MFCs (NR) P_{max} ≈ 3.06 W m^{-3} (3.19 mA) and no power or current produced at 40 ^{o}C. This result also shows that mesophilic culture developed at 23 ^{o}C could operate at mesophilic temperatures but not at the meso/thermo crossover area. This method for mediator attachment could be used for anode preparation for scaled up systems hence improving their performance.

iii) The fermentative conversion of organic substrate to biohydrogen produces volatile fatty acid (VFA) rich effluents, typically a 40 % acetate and 60 % butyrate mixture. These VFA products can be used as feedstock for microbial electrolysis (MEC), to recover more hydrogen. The effect of different acetate and butyrate concentrations on hydrogen and methane production and full substrate switch was assessed in microbial electrolysis cells (MECs) acclimated to acetate (AC) and butyrate (BU). Other parameters associated with hydrogen production, such as COD reduction, pH, conductivity and anodic and cathodic potentials vs reference electrodes were also evaluated. It was not known exactly how the changes in substrate concentrations would affect hydrogen production rates (cm^3 $L_{(anode)}^{-1}$ day^{-1}) for microbial electrolysis cells (MECs). The effect of butyrate on methane production in MECs has never been reported in literature before hence it was important to find out if it could inhibit methanogenic Archaea that utilize the hydrogen from the hydrogen producing bacteria. The highest hydrogen yield observed for MEC (BU) with its anode acclimated to butyrate was 0.64 $mol_{(hydrogen)}$ $mol_{(butyrate)}^{-1}$ corresponding to daily volumetric hydrogen production of 177 cm^3 L_{anode}^{-1} day^{-1} was observed for 5 mmol L^{-1} pure butyrate solution. The highest volumetric hydrogen production rate of 251 cm^3 L_{anode}^{-1} day^{-1} corresponding to hydrogen yield of 0.52 $mol_{(hydrogen)}$ $mol_{(acetate)}^{-1}$ was observed for MEC (BU) when butyrate was fully switched to 20 mmol L^{-1} acetate. The bacteria, in mixed biofilm consortium acclimated to butyrate in MEC (BU), were able to utilize acetate when butyrate was fully switched to acetate. The butyrate also had an inhibitory effect on methane production in the MEC (BU) resulting in higher hydrogen yield compared to MEC reactor containing biofilm acclimated to acetate in MEC (AC). Pure butyrate, inhibited hydrogen production rate in the MEC (AC), when acetate was fully switched to butyrate.

These phenomena have not previously reported been in the literature. The reason for this effect was postulated to be the presence of two microbial consortia: one that converted butyrate into butyrate into acetate and hydrogen and another that converted acetate into carbonate and hydrogen. MEC (BU) contained both biofilm consortia and MEC (AC) only contained the biofilm that converted acetate into carbonate and hydrogen. This theory was supported by another experiment where a substrate flow through MEC (BU) was stopped for three days. The VFA analysis of solution samples taken every 7 hours showed a slow drop in butyrate concentration from 20 m mol L^{-1} to 0 m mol L^{-1} and simultaneous increase in acetate concentration, over the period of two days, followed by a decrease in acetate concentration on day 3. Pure butyrate, inhibited hydrogen production rate in the MEC (AC) when acetate was fully switched to butyrate. This work shows that it would be possible to treat the liquid effluent from hydrogen fermenters, which consists of a mixture of acetate and butyrate with MEC reactor improving the overall hydrogen fermenter – MEC system hydrogen yield by 40%.

iv) In order to improve the performance of biocatalyst (bacteria) in microbial fuel cells (MFCs) or microbial electrolysis cells (MECs) carbon stainless steel materials could be used providing attachment to the bacteria hence improving the electron transport from bacteria to the anode. The aim of this experiment was to assess the performance of carbon veil / stainless steel cloth material against two controls: plain carbon veil and non conductive J cloth – carbon cloth. The expected result was that stainless steel would have the same effect on electron transport from the bacteria to anode as electron carriers like methylene blue (MB), in Conclusions part ii), compared to controls. It was also important to determine if a microbial culture acclimated to 1000 Ω resistance would perform differently from microbial culture acclimated to 150 Ω resistance in microbial fuel cells (MFC). When the anodes from MFCs, acclimated to 1000 Ω resistance, were transferred into microbial electrolysis cells (MECs) operated at 1 Ω resistance where voltage was applied a shift in the microbial biofilm population was expected to occur leading to growth hydrogen producing bacterial consortium. It was important to assess any differences in the performance in MECs for anodes acclimated to different resistances, in MFC modes, prior to their transfer because, according to our knowledge, these types of studies were not reported in literature before. Carbon veil / stainless steel cloth russian roll (RR), plain carbon veil (UCC), non conductive J cloth – carbon cloth (JC) and methylene blue treated carbon cloth (MBi) were prepared and tested in MFCs at 1000 Ω resistance and MECs.

For MFCs, factors such as maximum power density (P_{max}) and current production (mA) compared to MFCs with untreated carbon anodes (controls) were assessed. The choice of resistance was found to have a large effect on MFC performance with MB having inhibitory effect on P_{max} and current production for microbial culture acclimated to 1000 Ω resistance. The results could be presented as:- MFC UCC P_{max} = 3.13 W m^{-3} (2.85 mA), MFC (RR) P_{max} = 2.85 W m^{-3} (3.08 mA), MFC (JC) P_{max}= 2.32 W m^{-3} (2.78 mA) and MFC (MBi) P_{max}= 1.10 W m^{-3} (0.61 mA). The difference in the current production found in MFCs for microbial cultures acclimated to 1000 Ω compared to microbial cultures acclimated to 150 Ω resistance was much bigger than expected and previously was not assessed in any detail in the literature previously.

For MECs hydrogen and methane productions were assessed in microbial electrolysis cells (MECs) acclimated to acetate together with other parameters associated with it, such as COD reduction, pH, conductivity and anodic and cathodic potentials vs reference electrodes. The highest volumetric hydrogen productions could be presented as: MEC (UCC) 165±5 cm^3 L_{anode}^{-1} day^{-1} corresponding to hydrogen yield of 0.46±0 $mol_{(hydrogen)}$ $mol_{(acetate)}^{-1}$, MEC (RR) 175±5.0 cm^3 L_{anode}^{-1} day^{-1} corresponding to hydrogen yield of 0.67±0.1 $mol_{(hydrogen)}$ $mol_{(acetate)}^{-1}$, MEC (JC) 7.7±0.2 cm^3 L_{anode}^{-1} day^{-1} corresponding to hydrogen yield of 4×10^{-2}±0 $mol_{(hydrogen)}$ $mol_{(acetate)}^{-1}$, MEC (MBi) 20±2 cm^3 L_{anode}^{-1} day^{-1} corresponding to hydrogen yield of 4×10^{-2}±0 $mol_{(hydrogen)}$ $mol_{(acetate)}^{-1}$. MEC (RR) did not perform as well as expected in the original hypothesis due to poor attachment of biofilm carbon / stainless steel material, but was still able to achieve the highest volumetric hydrogen yield but with less efficient substrate conversion into hydrogen compared to MEC (UCC). This work shows the importance of assessing all possible materials from which the electrodes for a continuous flow MEC system could be built before designing one. Conductivity, surface area available for electrogenic activity and bacterial attachment to electrode surface has on voltage, % of substrate removed and power production have to be assessed in detail prior to building a larger reactor. It shows that anodic structure had an effect on the performances of MFCs and MECs.

This study showed that stainless steel carbon cloth roll (RR) material did not increase voltage production and power density in MFCs, as expected, however it slightly increased hydrogen production rates and cathodic current density in MECs, as expected. MEC (MBi), which contained methylene blue treated carbon anode, was expected to perform better than controls MEC (JC) and MEC (UCC).

Microbial culture acclimated to MB anode at 1000 Ω resistance (MEC MBi) was shown to produce less hydrogen which shows the importance of using low resistance for acclimating the anode, as demonstrated in previous study, see Conclusions part ii).

v) A scaled up microbial electrolysis (MEC) reactor was designed. The design was based on the design described in Conclusions part i) which was shown to perform to required standard (hydrogen production rate at ≈200 cm ^{3} $L^{-1}_{substrate}$ day^{-1} for substrate flow rate 400 $cm^3_{substrate}$ day^{-1}). This can be used to treat 3171 cm^3 = 3.2 L of wastewater; typical laboratory scale hydrogen fermenters and be expected to produce 652 cm^3 day^{-1} of hydrogen, which would be reasonable laboratory scale implementation to show a scalable demonstration of the principle of operation.

7.2 Further Work

The proposed future research areas for BES devices could be split into a number of areas, these include improving various physical design and electrochemical features to develop larger scale devices that would be required for the industrial deployment of MECs and research into identifying and improving the microbial communities used in MECs:-

i) Experimental work shows that it would be possible to treat the liquid effluent from hydrogen fermenters, which consists of a mixture of acetate and butyrate with MEC reactor improving the overall system hydrogen yield. Theoretical amounts of hydrogen produced by the integrated system based on practical results for fermentative hydrogen production rates show that ≈ 40 % improvement in hydrogen production rate ($L_{(hydrogen)}$ $L^{-1}_{(hexose)}$ day^{-1}) and efficiency with which hexose can be converted into hydrogen ($mol_{(hydrogen)}$ $mol^{-1}_{(hexose)}$) can be achieved. MECs operating on effluents from hydrogen fermentation containing acetate and butyrate mixtures to convert organic waste into precious commodity like hydrogen are particularly important for wastewater treatment yet have not been reported in literature before. Natural gas price for hydrogen is $2.70/kg (Thompson et al., 2013), so hydrogen production from waste can produce more profit than wastewater treatment methods currently in use, described in Future Work part iv).

ii) There are many issues involving scaled up systems such as pressure and choice of materials for robust wastewater treatment systems. There is no benchmark for the reactor design of MEC for performance, cost or efficiency. Therefore there is a need to developing benchmarking based on surface areas of electrodes and cathode to anode surface area ratio.

The future of this work may be in introducing designs for tubular systems were plastic tubes are replaced with gutter guards for guttering filters to increase the cathode surface area interacting with contents of the anode chamber through the ion exchange membrane. Cathodes in MFCs and MECs could be made from porous material such as reticulated vitreous carbon treated with catalyst to increase the number of active sites.

iii) Platinum is considered to be the benchmark catalyst for oxygen reduction in MFCs, because it is also the benchmark catalyst in chemical fuel cells (Rozendal et al., 2009b, Rozendal et al., 2009a). Despite its good oxygen reduction properties, many disadvantages are associated with the use of platinum in BESs. The biggest problem is the cost that is associated with the use of platinum as a catalyst (Clauwaert et al., 2007b). Within this scope, replacing expensive cathode catalysts, like platinum, with cheaper materials is an important challenge. More research is put into replacing expensive cathode catalysts, such as platinum with cheaper NiW alloys (Hu et al., 2009) or stainless steel meshs (Cusick et al., 2011), explained in more detail on pages 38 - 47. A good example of such material is stainless steel A286 mesh with hydrogen production rate 1.5±0.04 $m^3\ m^{-3}_{(anode)}\ day^{-1}$ (Selembo et al., 2009a) compared to 3.12 $m^3\ m^{-3}_{(anode)}\ day^{-1}$ for carbon cloth cathode Pt (0.5 mg cm^{-2}). The focus of future research could be in testing various methods of surface treatment of stainless steel particles used as catalyst and using the best catalyst for scaled up systems.

iv) If a MFC or MEC systems are going to be used on an industrial scale they must be able to operate intermittently for long time periods, in continuous flow modes. This work shows that it is possible to build and operate scaled up MEC system. Pilot scale hydrogen fermentation MFC or MEC integrated systems could be used sewerage waste treatment and offer many advantages over techniques currently used. Conventional activated sludge treatment process, which involves pumping air or oxygen into sewage or industrial wastewater in order to promote growth of organisms to develop a biofilm, which reduces the organic content in treated wastewater. Integrated systems require less energy input and MFC integrated with hydrogen fermentation produces gas and electricity and does not require as much energy as activated sludge treatment, which only removes organic waste. The two stage process has been applied in the treatment and conversion of a wide range of wastes including food waste (Han and Shin, 2004) and agro-industrial waste (Rincón et al., 2009).

Hydrogen fermenter and microbial fuel cell (MFC) were used as second stage process to convert byproducts of hydrogen fermentation (first stage), mostly acetate and butyrate mixtures into electricity (Guwy et al., 2011). This thesis proved that the two stage hydrogen fermentation – MFC could be implemented however MEC technology could be a advantage in the more income in the form of hydrogen which is more valuable than electricity could be achieved and therefore should be considered a potential priority for the future work (Heidrich et al., 2013, Thompson et al., 2013).

v) As well as the research aspects of engineering a deployable technology, microbial population analysis can add value to H_2 producing technology. If the microbial species are identified, then it may be possible to have well characterised optimum operating conditions that can be implemented to improve hydrogen production rate for hydrogen fermentation and microbial electrolysis. As molecular biology techniques develop the information on species abundance, metagenomic analysis with 464 pyrosequencing and on proteomics indicating changes in metabolism with operating conditions could prove particularly useful in optimisation studies (Premier et al., 2011, Rabaey et al., 2005a, Rabaey et al., 2004, Rabaey and Verstraete, 2005). According to our knowledge microbial population analysis has not been previously implemented to analyse how immobilized mediators, or substrates, in different concentrations, affect the diversity within microbial communities, on the anode surfaces, in BES. The exact amounts of a particular mediator, needed to facilitate electron transport from the bacteria to the electrode surface, have to be adsorbed on the anode surface. High concentrations of certain mediators may be toxic to the bacteria and low concentrations may not facilitate the electron transport efficiently enough. Different bacterial communities require different amounts of mediator, in order to facilitate the electron transport. Synthetic communities could be created for high hydrogen production rate at particular conditions and, most importantly, mixed microbial communities could be developed, where non exoelectrogenic bacteria produce high quantities of mediators, such as phenazine (Venkataraman et al., 2010), which could then be utilized by exoelectrogenic bacteria on the electrode surface.

8. References

AELTERMAN, P., RABAEY, K., CLAUWAERT, P. & VERSTRAETE, W. 2006a. Microbial fuel cells for wastewater treatment. *Water Science and Technology,* 54**,** 9-15.

AELTERMAN, P., RABAEY, K., PHAM, H. T., BOON, N. & VERSTRAETE, W. 2006b. Continuous electricity generation at high voltages and currents using stacked microbial fuel cells. *Environmental Science & Technology,* 40**,** 3388-3394.

AELTERMAN, P., VERSICHELE, M., MARZORATI, M., BOON, N. & VERSTRAETE, W. 2008. Loading rate and external resistance control the electricity generation of microbial fuel cells with different three-dimensional anodes. *Bioresource Technology,* 99**,** 8895-8902.

AFZAL GHAURI, M., OKIBE, N. & BARRIE JOHNSON, D. 2007. Attachment of acidophilic bacteria to solid surfaces: The significance of species and strain variations. *Hydrometallurgy,* 85**,** 72-80.

AHN, Y. & LOGAN, B. E. 2010. Effectiveness of domestic wastewater treatment using microbial fuel cells at ambient and mesophilic temperatures. *Bioresource Technology,* 101**,** 469-475.

AHN, Y., ZHANG, F. & LOGAN, B. E. 2014. Air humidity and water pressure effects on the performance of air-cathode microbial fuel cell cathodes. *Journal of Power Sources,* 247**,** 655-659.

AJAYI, F. F., KIM, K. Y., CHAE, K. J., CHOI, M. J., KIM, S. Y., CHANG, I. S. & KIM, I. S. 2009. Study of hydrogen production in light assisted microbial electrolysis cell operated with dye sensitized solar cell. *International Journal of Hydrogen Energy,* 34**,** 9297-9304.

AKIMOTO, K., SANO, F., HOMMA, T., TOKUSHIGE, K., NAGASHIMA, M. & TOMODA, T. 2013. Assessment of the emission reduction target of halving CO_2 emissions by 2050: Macro-factors analysis and model analysis under newly developed socio-economic scenarios. *Energy Strategy Reviews*.

AKUTSU, Y., LI, Y.-Y., HARADA, H. & YU, H.-Q. 2009. Effects of temperature and substrate concentration on biological hydrogen production from starch. *International Journal of Hydrogen Energy,* 34**,** 2558-2566.

ALLEN, R. M. & BENETTO, H. P. 1993. Microbial Fuel Cells: Electricity Production from Carbohydrates. *Appl Biochem Biotechnol,* 39/40**,** 27-40.

ANASTASI, A., SPINA, F., ROMAGNOLO, A., TIGINI, V., PRIGIONE, V. & VARESE, G. C. 2012. Integrated fungal biomass and activated sludge treatment for textile wastewaters bioremediation. *Bioresource Technology,* 123**,** 106-111.

ANDERSSON, M., YUAN, J. L. & SUNDEN, B. 2010. Review on modeling development for multiscale chemical reactions coupled transport phenomena in solid oxide fuel cells. *Applied Energy,* 87**,** 1461-1476.

ANGENENT, L. T., HE, Z. & SHAO, H. B. 2007. Increased power production from a sediment microbial fuel cell with a rotating cathode. *Biosensors & Bioelectronics,* 22**,** 3252-3255.

ANGENENT, L. T., KARIM, K., AL-DAHHAN, M. H. & DOMIGUEZ-ESPINOSA, R. 2004. Production of bioenergy and biochemicals from industrial and agricultural wastewater. *Trends in Biotechnology,* 22**,** 477-485.

APHA, A. Wpcf 1989. *Standard Methods for the Examination of Water & Wastewater, 17th Edition, American Public Health Association, Washington*.

ARALP, L. C., ERDINCLER, A. & ONAY, T. T. 2001. Heavy metal removal from wastewater and leachate co-treatment sludge by sulfur oxidizing bacteria. *Water Sci Technol,* 44**,** 53-8.

ARGUN, H. & KARGI, F. 2009. Effects of sludge pre-treatment method on bio-hydrogen production by dark fermentation of waste ground wheat. *International Journal of Hydrogen Energy,* 34**,** 8543-8548.

ARGUN, H., KARGI, F., KAPDAN, I. K. & OZTEKIN, R. 2008. Batch dark fermentation of powdered wheat starch to hydrogen gas: Effects of the initial substrate and biomass concentrations. *International Journal of Hydrogen Energy,* 33**,** 6109-6115.

BARD, A. J. & FAULKNER, L. R. 1976. Elctrochemical Methods. New York: John Wiley & Sons.

BARD, A. J. & FAULKNER, L. R. 2001. *Electrochemical Methods, Fundamentals and Applications,* New York, John Wiley & Sons.

BENZIGER, J. B., SATTERFIELD, M. B., HOGARTH, W. H. J., NEHLSEN, J. P. & KEVREKIDIS, I. G. 2006. The power performance curve for engineering analysis of fuel cells. *Journal of Power Sources,* 155**,** 272-285.

BERGE, M., COURNET, A., DELIA, M. L., BERGEL, A. & ROQUES, C. 2010. Electrochemical reduction of oxygen catalyzed by a wide range of bacteria including Gram-positive. *Electrochemistry Communications,* 12**,** 505-508.

BIFFINGER, J. C., PIETRON, J., BRETSCHGER, O., NADEAU, L. J., JOHNSON, G. R., WILLIAMS, C. C., NEALSON, K. H. & RINGEISEN, B. R. 2008. The influence of acidity on microbial fuel cells containing *Shewanella oneidensis*. *Biosens Bioelectron,* 24**,** 906-11.

BLANKENSHIP, R. E. & PARSON, W. W. 1979. Involvement of Iron and Ubiquinone in Electron-Transfer Reactions Mediated by Reaction Centers from Photosynthetic Bacteria. *Biochimica Et Biophysica Acta,* 545**,** 429-444.

BLUNT, W. & BRUNIUS, G. 2002. *Carl von Linné*, Bonnier.

BON, E. P. S., FERREIRA-LEITAO, V. S. & CARVALHO, M. E. A. 2007. Lignin peroxidase efficiency for methylene blue decolouration: Comparison to reported methods. *Dyes and Pigments,* 74**,** 230-236.

BOND, D. R., HOLMES, D. E., TENDER, L. M. & LOVLEY, D. R. 2002. Electrode-reducing microorganisms that harvest energy from marine sediments. *Science,* 295**,** 483-485.

BOND, D. R. & LOVLEY, D. R. 2003. Electricity production by *Geobacter sulfurreducens* attached to electrodes. *Applied and Environmental Microbiology,* 69**,** 1548-1555.

BOND, D. R. & LOVLEY, D. R. 2005. Evidence for involvement of an electron shuttle in electricity generation by *Geothrix fermentans*. *Applied and Environmental Microbiology,* 71**,** 2186-2189.

BOYLES, W. D. 1995. *Science of chemical oxygen in demand* [Online]. Available: http://www.hach.com/asset-get.download-en.jsa?code=61786.

BROOIJMANS, R., DE VOS, W. M. & HUGENHOLTZ, J. 2009. Electron transport chains of lactic acid bacteria - walking on crutches is part of their lifestyle. *F1000 Biol Rep,* 1**,** 34.

BUSSCHER, H. J., COWAN, M. M. & VAN DER MEI, H. C. 1992. On the relative importance of specific and non-specific approaches to oral microbial adhesion. *FEMS Microbiology Letters,* 88**,** 199-209.

BUTLER, C. S., CLAUWAERT, P., GREEN, S. J., VERSTRAETE, W. & NERENBERG, R. 2010. Bioelectrochemical Perchlorate Reduction in a Microbial Fuel Cell. *Environmental Science & Technology,* 44**,** 4685-4691.

CALL, D. & LOGAN, B. E. 2008. Hydrogen production in a single chamber microbial electrolysis cell lacking a membrane. *Environmental Science & Technology,* 42**,** 3401-3406.

CALL, D. F., MERRILL, M. D. & LOGAN, B. E. 2009a. High Surface Area Stainless Steel Brushes as Cathodes in Microbial Electrolysis Cells. *Environmental Science & Technology,* 43**,** 2179-2183.

CALL, D. F., WAGNER, R. C. & LOGAN, B. E. 2009b. Hydrogen Production by *Geobacter* Species and a Mixed Consortium in a Microbial Electrolysis Cell. *Applied and Environmental Microbiology,* 75**,** 7579-7587.

CARVER, S. M., VUORIRANTA, P. & TUOVINEN, O. H. 2011. A thermophilic microbial fuel cell design. *Journal of Power Sources,* 196**,** 3757-3760.

CATAL, T., CYSNEIROS, D., O'FLAHERTY, V. & LEECH, D. 2011. Electricity generation in single-chamber microbial fuel cells using a carbon source sampled from anaerobic reactors utilizing grass silage. *Bioresource Technology,* 102**,** 404-410.

CATAL, T., LI, K., BERMEK, H. & LIU, H. 2008. Electricity production from twelve monosaccharides using microbial fuel cells. *Journal of Power Sources,* 175**,** 196-200.

CATANHO, M., MALPASS, G. R. P. & MOTHEO, A. D. 2006. Evaluation of electrochemical and photoelectrochemical methods for the degradation of three textile dyes. *Quimica Nova,* 29**,** 983-989.

CHAE, K. J., CHOI, M. J., LEE, J., AJAYI, F. F. & KIM, I. S. 2008. Biohydrogen production via biocatalyzed electrolysis in acetate-fed bioelectrochemical cells and microbial community analysis. *International Journal of Hydrogen Energy,* 33**,** 5184-5192.

CHAE, K. J., CHOI, M. J., LEE, J. W., KIM, K. Y. & KIM, I. S. 2009. Effect of different substrates on the performance, bacterial diversity, and bacterial viability in microbial fuel cells. *Bioresource Technology,* 100**,** 3518-3525.

CHASSARY, P., VINCENT, T., MARCANO, J. S., MACASKIE, L. E. & GUIBAL, E. 2005. Palladium and platinum recovery from bicomponent mixtures using chitosan derivatives. *Hydrometallurgy,* 76**,** 131-147.

CHAUDHURI, S. K. & LOVLEY, D. R. 2003. Electricity generation by direct oxidation of glucose in mediatorless microbial fuel cells. *Nature Biotechnology,* 21**,** 1229-1232.

CHEN, W. T., LIN, Y. K., YANG, T. T., PU, Y. C. & HSU, Y. J. 2013. Au/ZnS core/shell nanocrystals as an efficient anode photocatalyst in direct methanol fuel cells. *Chem Commun (Camb),* 49**,** 8486-8.

CHENG, J., ZHU, X. P., NI, J. R. & BORTHWICK, A. 2010. Palm oil mill effluent treatment using a two-stage microbial fuel cells system integrated with immobilized biological aerated filters. *Bioresource Technology,* 101**,** 2729-2734.

CHENG, K. Y., CORD-RUWISCH, R. & HO, G. 2009. A new approach for in situ cyclic voltammetry of a microbial fuel cell biofilm without using a potentiostat. *Bioelectrochemistry,* 74**,** 227-231.

CHENG, S., LIU, H. & LOGAN, B. E. 2006a. Increased performance of single-chamber microbial fuel cells using an improved cathode structure. *Electrochemistry Communications,* 8**,** 489-494.

CHENG, S., LIU, H. & LOGAN, B. E. 2006b. Power densities using different cathode catalysts (Pt and CoTMPP) and polymer binders (Nafion and PTFE) in single chamber microbial fuel cells. *Environmental Science & Technology,* 40**,** 364-369.

CHENG, S. & LOGAN, B. E. 2007a. Sustainable and efficient biohydrogen production via electrohydrogenesis. *Proceedings of the National Academy of Sciences of the United States of America,* 104**,** 18871-18873.

CHENG, S. A. & LOGAN, B. E. 2007b. Ammonia treatment of carbon cloth anodes to enhance power generation of microbial fuel cells. *Electrochemistry Communications,* 9**,** 492-496.

CHENG, X. Y. & LIU, C. Z. 2011. Hydrogen Production via Thermophilic Fermentation of Cornstalk by *Clostridium thermocellum*. *Energy & Fuels,* 25**,** 1714-1720.

CHERRYMAN, S. J., KING, S., HAWKES, F. R., DINSDALE, R. & HAWKES, D. L. 2008. An exploratory study of public opinions on the use of hydrogen energy in Wales. *Public Understanding of Science,* 17**,** 397-410.

CHILDERS, S. E., CIUFO, S. & LOVLEY, D. R. 2002. *Geobacter metallireducens* accesses insoluble Fe(III) oxide by chemotaxis. *Nature,* 416**,** 767-769.

CHITNIS, M. & HUNT, L. C. 2012. What drives the change in UK household energy expenditure and associated CO_2 emissions? Implication and forecast to 2020. *Applied Energy,* 94**,** 202-214.

CHOI, Y., KIM, N., KIM, S. & JUNG, S. 2003. Dynamic behaviors of redox mediators within the hydrophobic layers as an important factor for effective microbial fuel cell operation. *Bulletin of the Korean Chemical Society,* 24**,** 437-440.

CHRISTY, A. D., RISMANI-YAZDI, H., CARVER, S. M., YU, Z. T., DEHORITY, B. A. & TUOVINEN, O. H. 2011. Effect of external resistance on bacterial diversity and metabolism in cellulose-fed microbial fuel cells. *Bioresource Technology,* 102**,** 278-283.

CLAASSEN, P. A. M. & DE VRIJE, T. 2006. Non-thermal production of pure hydrogen from biomass: HYVOLUTION. *International Journal of Hydrogen Energy,* 31**,** 1416-1423.

CLAASSEN, P. A. M., DE VRIJE, T., KOUKIOS, E., VAN NIEL, E., EROGLU, I., MODIGELL, M., FRIEDL, A., WUKOVITS, W. & AHRER, W. 2010. Non-thermal production of pure hydrogen from biomass: HYVOLUTION. *Journal of Cleaner Production,* 18**,** S4-S8.

CLAASSEN, P. A. M., DE VRIJE, T. & URBANIEC, K. 2009. Non-thermal production of pure hydrogen from biomass: HYVOLUTION. *Pres'09: 12th International Conference on Process Integration, Modelling and Optimisation for Energy Saving and Pollution Reduction, Pts 1 and 2,* 18**,** 333-338.

CLARK, W. W. & RIFKIN, J. 2006. A green hydrogen economy. *Energy Policy,* 34**,** 2630-2639.

CLAUWAERT, P., RABAEY, K., AELTERMAN, P., DE SCHAMPHELAIRE, L., HAM, T. H., BOECKX, P., BOON, N. & VERSTRAETE, W. 2007a. Biological denitrification in microbial fuel cells. *Environmental Science & Technology,* 41**,** 3354-3360.

CLAUWAERT, P., VAN DER HA, D., BOON, N., VERBEKEN, K., VERHAEGE, M., RABAEY, K. & VERSTRAETE, W. 2007b. Open air biocathode enables effective electricity generation with microbial fuel cells. *Environmental Science & Technology,* 41**,** 7564-7569.

COLLET, C., ADLER, N., SCHWITZGUEBEL, J. P. & PERINGER, P. 2004. Hydrogen production by *Clostridium thermolacticum* during continuous fermentation of lactose. *International Journal of Hydrogen Energy,* 29**,** 1479-1485.

COMPÈRE, C., BELLON‐FONTAINE, M. N., BERTRAND, P., COSTA, D., MARCUS, P., POLEUNIS, C., PRADIER, C. M., RONDOT, B. & WALLS, M. G. 2001. Kinetics of conditioning layer formation on stainless steel immersed in seawater. *Biofouling,* 17**,** 129-145.

CORONADO, J., PERRIER, M. & TARTAKOVSKY, B. 2013. Pulse-width modulated external resistance increases the microbial fuel cell power output. *Bioresour Technol,* 147**,** 65-70.

CROESE, E., PEREIRA, M. A., EUVERINK, G. J., STAMS, A. J. & GEELHOED, J. S. 2011. Analysis of the microbial community of the biocathode of a hydrogen-producing microbial electrolysis cell. *Appl Microbiol Biotechnol,* 92**,** 1083-93.

CUSICK, R. D., BRYAN, B., PARKER, D. S., MERRILL, M. D., MEHANNA, M., KIELY, P. D., LIU, G. L. & LOGAN, B. E. 2011. Performance of a pilot-scale continuous flow microbial electrolysis cell fed winery wastewater. *Applied Microbiology and Biotechnology,* 89**,** 2053-2063.

CUSICK, R. D., KIELY, P. D. & LOGAN, B. E. 2010. A monetary comparison of energy recovered from microbial fuel cells and microbial electrolysis cells fed winery or domestic wastewaters. *International Journal of Hydrogen Energy,* 35**,** 8855-8861.

DAMIAN, A. & OMANOVIC, S. 2005. Ni and Ni-Mo Hydrogen Evolution Electrocatalysis Electrodeposited in Phenylaniline Matrix. *Journal of Power Sources***,** 464-476.

DANIEL, D. K., DAS MANKIDY, B., AMBARISH, K. & MANOGARI, R. 2009. Construction and operation of a microbial fuel cell for electricity generation from wastewater. *International Journal of Hydrogen Energy,* 34**,** 7555-7560.

DANTAS, J. M., MORGADO, L., POKKULURI, P. R., TURNER, D. L. & SALGUEIRO, C. A. 2013. Solution structure of a mutant of the triheme cytochrome PpcA from *Geobacter sulfurreducens* sheds light on the role of the conserved aromatic residue F15. *Biochimica et Biophysica Acta (BBA) - Bioenergetics,* 1827**,** 484-492.

DAS, D. & MOHAN, Y. 2009. Effect of ionic strength, cation exchanger and inoculum age on the performance of Microbial Fuel Cells. *International Journal of Hydrogen Energy,* 34**,** 7542-7546.

DAS, D., MOHAN, Y. & KUMAR, S. M. M. 2008. Electricity generation using microbial fuel cells. *International Journal of Hydrogen Energy,* 33**,** 423-426.

DAS, D. & VEZIROGLU, T. N. 2001. Hydrogen production by biological processes: a survey of literature. *International Journal of Hydrogen Energy,* 26**,** 13-28.

DAVEY, M. E. & O'TOOLE G, A. 2000. Microbial biofilms: from ecology to molecular genetics. *Microbiol Mol Biol Rev,* 64**,** 847-67.

DE BAERE, L. A., DEVOCHT, M., VAN ASSCHE, P. & VERSTRAETE, W. 1984. Influence of high NaCl and NH_4Cl salt levels on methanogenic associations. *Water Research,* 18**,** 543-548.

DE BOER, P. C. T., MCLEAN, W. J. & HOMAN, H. S. 1976. Performance and emissions of hydrogen fueled internal combustion engines. *International Journal of Hydrogen Energy,* 1**,** 153-172.

DE CARCER, D. A., HA, P. T., JANG, J. K. & CHANG, I. S. 2011. Microbial community differences between propionate-fed microbial fuel cell systems under open and closed circuit conditions. *Appl Microbiol Biotechnol,* 89**,** 605-12.

DE SCHAMPHELAIRE, L. & VERSTRAETE, W. 2009. Revival of the Biological Sunlight-to-Biogas Energy Conversion System. *Biotechnology and Bioengineering,* 103**,** 296-304.

DELIA, M. L., COURNET, A., BERGE, M., ROQUES, C. & BERGEL, A. 2010. Electrochemical reduction of oxygen catalyzed by *Pseudomonas aeruginosa*. *Electrochimica Acta,* 55**,** 4902-4908.

DENG, Q., LI, X. Y., ZUO, J. E., LING, A. & LOGAN, B. E. 2010. Power generation using an activated carbon fiber felt cathode in an upflow microbial fuel cell. *Journal of Power Sources,* 195**,** 1130-1135.

DEVRIES, W., VANWYCKK.WM & STOUTHAM.AH 1973. Generation of ATP during Cytochrome Linked Anaerobic Electron-Transport in Propionic-Acid Bacteria. *Journal of General Microbiology,* 76**,** 31-41.

DEWAN, A., BEYENAL, H. & LEWANDOWSKI, Z. 2008. Scaling up Microbial Fuel Cells. *Environmental Science & Technology,* 42**,** 7643-7648.

DEY, A. & MAGBANUA, B. S. 2012. Evaluation of Process Uncertainty in Activated Sludge Treatment by Probabilistic Modeling. *Journal of Environmental Engineering-Asce,* 138**,** 1040-1047.

DI SALVO, E. A., VIDELA, H. A. & ARVÍA, A. J. 1979. Kinetic model of a depolarization-type bioelectrochemical fuel cell. *Journal of Electroanalytical Chemistry and Interfacial Electrochemistry,* 104**,** 493-508.

DIETEL, W., FONTAINE, J. J. & DIELS, J. C. 1983. Intracavity Pulse-Compression with Glass - a New Method of Generating Pulses Shorter Than 60 Fsec. *Optics Letters,* 8**,** 4-6.

DITZIG, J., LIU, H. & LOGAN, B. E. 2007. Production of hydrogen from domestic wastewater using a bioelectrochemically assisted microbial reactor (BEAMR). *International Journal of Hydrogen Energy,* 32**,** 2296-2304.

DOLLHOPF, M. E., NEALSON, K. H., SIMON, D. M. & LUTHER, G. W. 2000. Kinetics of Fe(III) and Mn(IV) reduction by the Black Sea strain of *Shewanella putrefaciens* using in situ solid state voltammetric Au/Hg electrodes. *Marine Chemistry,* 70**,** 171-180.

DOMINGUEZ, A., BLANCO, C., SANTAMARIA, R., GRANDA, M., BLANCO, C. G. & MENENDEZ, R. 2004. Monitoring coal-tar pitch composition changes during air-blowing by gas chromatography. *J Chromatogr A,* 1026**,** 231-8.

DOU, X. X. & ANDREWS, J. 2012. Design of a Dynamic Control System for Standalone Solar-Hydrogen Power Generation. *Procedia Engineering,* 49**,** 107-115.

DUMA, R. & MINTEER, S. D. 2006. Development of bilirubin oxidase cathodes for ethanol/oxygen biofuel cells. *Abstracts of Papers of the American Chemical Society,* 231.

DUMAS, C., BASSEGUY, R. & BERGEL, A. 2008a. Electrochemical activity of *Geobacter sulfurreducens* biofilms on stainless steel anodes. *Electrochimica Acta,* 53**,** 5235-5241.

DUMAS, C., MOLLICA, A., FERON, D., BASSEGUY, R., ETCHEVERRY, L. & BERGEL, A. 2007. Marine microbial fuel cell: Use of stainless steel electrodes as anode and cathode materials. *Electrochimica Acta,* 53**,** 468-473.

DUMAS, C., MOLLICA, A., FERON, D., BASSEGUY, R., ETCHEVERRY, L. & BERGEL, A. 2008b. Checking graphite and stainless anodes with an experimental model of marine microbial fuel cell. *Bioresource Technology,* 99**,** 8887-8894.

ERABLE, B. & BERGEL, A. 2009. First air-tolerant effective stainless steel microbial anode obtained from a natural marine biofilm. *Bioresource Technology,* 100**,** 3302-3307.

ESCAPA, A., GIL-CARRERA, L., GARCIA, V. & MORAN, A. 2012. Performance of a continuous flow microbial electrolysis cell (MEC) fed with domestic wastewater. *Bioresource Technology,* 117**,** 55-62.

FAN, Y., HU, H. & LIU, H. 2007. Enhanced Coulombic efficiency and power density of air-cathode microbial fuel cells with an improved cell configuration. *Journal of Power Sources,* 171**,** 348-354.

FAN, Y. Z., XU, S. T., SCHALLER, R., JIAO, J., CHAPLEN, F. & LIU, H. 2011. Nanoparticle decorated anodes for enhanced current generation in microbial electrochemical cells. *Biosensors & Bioelectronics,* 26**,** 1908-1912.

FANG, H. H. P. & LIU, H. 2002. Effect of pH on hydrogen production from glucose by a mixed culture. *Bioresource Technology,* 82**,** 87-93.

FEDOROV, A. S., TSYGANKOV, A. A., RAO, K. K. & HALL, D. O. 1998. Hydrogen photoproduction by *Rhodobacter sphaeroides* immobilized on polyurethane foam. *Biotechnology Letters,* 20**,** 1007-1009.

FENG, X., XU, Y., CHEN, Y. & TANG, Y. J. 2012. Integrating flux balance analysis into kinetic models to decipher the dynamic metabolism of *Shewanella oneidensis* MR-1. *PLoS computational biology,* 8**,** e1002376.

FENG, Y., WANG, X., LOGAN, B. E. & LEE, H. 2008. Brewery wastewater treatment using air-cathode microbial fuel cells. *Applied Microbiology and Biotechnology,* 78**,** 873-880.

FENG, Y. J., WANG, X., LIU, J., LEE, H., LI, C., LI, N. & REN, N. Q. 2010a. Sequestration of CO_2 discharged from anode by algal cathode in microbial carbon capture cells (MCCs). *Biosensors & Bioelectronics,* 25**,** 2639-2643.

FENG, Y. J., YANG, Q., WANG, X. & LOGAN, B. E. 2010b. Treatment of carbon fiber brush anodes for improving power generation in air-cathode microbial fuel cells. *Journal of Power Sources,* 195**,** 1841-1844.

FERNANDO, E., KESHAVARZ, T. & KYAZZE, G. 2014. External resistance as a potential tool for influencing azo dye reductive decolourisation kinetics in microbial fuel cells. *International Biodeterioration & Biodegradation,* 89**,** 7-14.

FLOHN, H. 1980. CO_2-Induced Climatic Changes Potentially More Dangerous Than Nuclear-Energy. *Umschau in Wissenschaft Und Technik,* 80**,** 114-115.

FOLEY, J. M., ROZENDAL, R. A., HERTLE, C. K., LANT, P. A. & RABAEY, K. 2010. Life Cycle Assessment of High-Rate Anaerobic Treatment, Microbial Fuel Cells, and Microbial Electrolysis Cells. *Environmental Science & Technology,* 44**,** 3629-3637.

FOO, K. Y. & HAMEED, B. H. 2012. Dynamic adsorption behavior of methylene blue onto oil palm shell granular activated carbon prepared by microwave heating. *Chemical Engineering Journal,* 203**,** 81-87.

FRANKE, R. & FRANKE, C. 1999. Model reactor for photocatalytic degradation of persistent chemicals in ponds and wastewater. *Chemosphere,* 39**,** 2651-9.

FRANKS, A. E., NEVIN, K. P., JIA, H., IZALLALEN, M., WOODARD, T. L. & LOVLEY, D. R. 2009. Novel strategy for three-dimensional real-time imaging of microbial fuel cell communities: monitoring the inhibitory effects of proton accumulation within the anode biofilm. *Energy & Environmental Science,* 2**,** 113-119.

FREGUIA, S., MASUDA, M., TSUJIMURA, S. & KANO, K. 2009. *Lactococcus lactis* catalyses electricity generation at microbial fuel cell anodes via excretion of a soluble quinone. *Bioelectrochemistry,* 76**,** 14-18.

FREGUIA, S., RABAEY, K., YUAN, Z. & KELLER, J. 2007a. Non-catalyzed cathodic oxygen reduction at graphite granules in microbial fuel cells. *Electrochimica Acta,* 53**,** 598-603.

FREGUIA, S., RABAEY, K., YUAN, Z. & KELLER, J. R. 2008. Syntrophic Processes Drive the Conversion of Glucose in Microbial Fuel Cell Anodes. *Environmental Science & Technology,* 42**,** 7937-7943.

FREGUIA, S., RABAEY, K., YUAN, Z. G. & KELLER, J. 2007b. Electron and carbon balances in microbial fuel cells reveal temporary bacterial storage behavior during electricity generation. *Environmental Science & Technology,* 41**,** 2915-2921.

FRENCH, J. 2014. Available: http://www.shell.com/global/environment-society/environment/climate-change/biofuels-alternative-energies-transport/hydrogen.html.

FU, Y., XU, Q., ZAI, X., LIU, Y. & LU, Z. 2014. Low electrical potential anode modified with Fe/ferric oxide and its application in marine benthic microbial fuel cell with higher voltage and power output. *Applied Surface Science,* 289**,** 472-477.

FULLER, S. J., MCMILLAN, D. G., RENZ, M. B., SCHMIDT, M., BURKE, I. T. & STEWART, D. I. 2014. Extracellular Electron Transport-Mediated Fe(III) Reduction by a Community of Alkaliphilic Bacteria That Use Flavins as Electron Shuttles. *Appl Environ Microbiol,* 80**,** 128-37.

GAVALA, H. N., SKIADAS, I. V. & AHRING, B. K. 2006. Biological hydrogen production in suspended and attached growth anaerobic reactor systems. *International Journal of Hydrogen Energy,* 31**,** 1164-1175.

GEELHOED, J. S., HAMELERS, H. V. M. & STAMS, A. J. M. 2010. Electricity-mediated biological hydrogen production. *Current Opinion in Microbiology,* 13**,** 307-315.

GENORIO, B., SUBBARAMAN, R., STRMCNIK, D., TRIPKOVIC, D., STAMENKOVIC, V. R. & MARKOVIC, N. M. 2011. Tailoring the selectivity and stability of chemically modified platinum nanocatalysts to design highly durable anodes for PEM fuel cells. *Angew Chem Int Ed Engl,* 50**,** 5468-72.

GERHARDT, P. 1994. *Total carbohydrates protocol* [Online]. Available: http://web.itu.edu.tr/~dulekgurgen/Carbs.pdf.

GESCHER, J., RICHTER, K., BUCKING, C. & SCHICKLBERGER, M. 2010. A simple and fast method to analyze the orientation of c-type cytochromes in the outer membrane of Gram-negative bacteria. *Journal of Microbiological Methods,* 82**,** 184-186.

GIACONIA, A. & CAPUTO, G. 2014. 12 - Membrane technologies for solar-hydrogen production. *In:* GUGLIUZZA, A. & BASILE, A. (eds.) *Membranes for Clean and Renewable Power Applications.* Woodhead Publishing.

GIL-CARRERA, L., ESCAPA, A., CARRACEDO, B., MORÁN, A. & GÓMEZ, X. 2013. Performance of a semi-pilot tubular microbial electrolysis cell (MEC) under several hydraulic retention times and applied voltages. *Bioresource Technology,* 146**,** 63-69.

GIL, G. C., CHANG, I. S., KIM, B. H., KIM, M., JANG, J. K., PARK, H. S. & KIM, H. J. 2003. Operational parameters affecting the performance of a mediator-less microbial fuel cell. *Biosensors & Bioelectronics,* 18**,** 327-334.

GINKEL, S. V., SUNG, S. & LAY, J.-J. 2001. Biohydrogen Production as a Function of pH and Substrate Concentration. *Environmental Science & Technology,* 35**,** 4726-4730.

GIRVAN, M. S., CAMPBELL, C. D., KILLHAM, K., PROSSER, J. I. & GLOVER, L. A. 2005. Bacterial diversity promotes community stability and functional resilience after perturbation. *Environ Microbiol,* 7**,** 301-13.

GORBY, Y., MCLEAN, J., KORENEVSKY, A., ROSSO, K. M., EL-NAGGAR, M. Y. & BEVERIDGE, T. J. 2008. Redox-reactive membrane vesicles produced by *Shewanella*. *Geobiology,* 6**,** 232-241.

GORBY, Y. A. 2006. Bacterial nanowires: Electrically conductive filaments and their implications for en ergytrans formation and distribution in natural and engineered systems. *2006 Bio- Micro- and Nanosystems Conference***,** 20-20.

GORBY, Y. A. 2007. Bacterial nanowires: Extracellular electron transfer and mineral transformation. *Geochimica Et Cosmochimica Acta,* 71**,** A345-A345.

GORBY, Y. A., YANINA, S., MCLEAN, J. S., ROSSO, K. M., MOYLES, D., DOHNALKOVA, A., BEVERIDGE, T. J., CHANG, I. S., KIM, B. H., KIM, K. S., CULLEY, D. E., REED, S. B., ROMINE, M. F., SAFFARINI, D. A., HILL, E. A., SHI, L., ELIAS, D. A., KENNEDY, D. W., PINCHUK, G., WATANABE, K., ISHII, S., LOGAN, B., NEALSON, K. H. & FREDRICKSON, J. K. 2006. Electrically conductive bacterial nanowires produced by *Shewanella oneidensis* strain MR-1 and other microorganisms. *Proceedings of the National Academy of Sciences of the United States of America,* 103**,** 11358-11363.

GUILHERME, M. R., SILVA, R., GIROTTO, E. M., RUBIRA, A. F. & MUNIZ, E. C. 2003. Hydrogels based on PAAm network with PNIPAAm included: hydrophilic-hydrophobic transition measured by the partition of Orange II and Methylene Blue in water. *Polymer,* 44**,** 4213-4219.

GUO, K., TANG, X. H., DU, Z. W. & LI, H. R. 2010. Hydrogen production from acetate in a cathode-on-top single-chamber microbial electrolysis cell with a mipor cathode. *Biochemical Engineering Journal,* 51**,** 48-52.

GUWY, A. J., DINSDALE, R. M., KIM, J. R., MASSANET-NICOLAU, J. & PREMIER, G. 2011. Fermentative biohydrogen production systems integration. *Bioresource Technology,* 102**,** 8534-8542.

HALL-STOODLEY, L., COSTERTON, J. W. & STOODLEY, P. 2004. Bacterial biofilms: from the natural environment to infectious diseases. *Nat Rev Microbiol,* 2**,** 95-108.

HALLENBECK, P. C. & BENEMANN, J. R. 2002. Biological hydrogen production; fundamentals and limiting processes. *International Journal of Hydrogen Energy,* 27**,** 1185-1193.

HAMEED, B. H., AHMAD, A. L. & LATIFF, K. N. A. 2007a. Adsorption of basic dye (methylene blue) onto activated carbon prepared from rattan sawdust. *Dyes and Pigments,* 75**,** 143-149.

HAMEED, B. H., DIN, A. T. M. & AHMAD, A. L. 2007b. Adsorption of methylene blue onto bamboo-based activated carbon: Kinetics and equilibrium studies. *Journal of Hazardous Materials,* 141**,** 819-825.

HAMEED, B. H., MAHMOUD, D. K. & AHMAD, A. L. 2008. Equilibrium modeling and kinetic studies on the adsorption of basic dye by a low-cost adsorbent: Coconut (Cocos nucifera) bunch waste. *Journal of Hazardous Materials,* 158**,** 65-72.

HAMELERS, H. V. M., ROZENDAL, R. A. & BUISMAN, C. J. N. 2006. Effects of membrane cation transport on pH and microbial fuel cell performance. *Environmental Science & Technology,* 40**,** 5206-5211.

HAMELERS, H. V. M., ROZENDAL, R. A., MOLENKMP, R. J. & BUISMAN, J. N. 2007. Performance of single chamber biocatalyzed electrolysis with different types of ion exchange membranes. *Water research,* 41**,** 1984-1994.

HAN, S.-K. & SHIN, H.-S. 2004. Performance of an Innovative Two-Stage Process Converting Food Waste to Hydrogen and Methane. *Journal of the Air & Waste Management Association,* 54**,** 242-249.

HANISCH, C. 1999. Researchers will tap potential of deep-ocean sediment life. *Environmental Science & Technology,* 33**,** 350a-351a.

HAWKES, F. R., DINSDALE, R., HAWKES, D. L. & HUSSY, I. 2002. Sustainable fermentative hydrogen production: challenges for process optimisation. *International Journal of Hydrogen Energy,* 27**,** 1339-1347.

HAWKES, F. R., HUSSY, I., KYAZZE, G., DINSDALE, R. & HAWKES, D. L. 2007. Continuous dark fermentative hydrogen production by mesophilic microflora: Principles and progress. *International Journal of Hydrogen Energy,* 32**,** 172-184.

HE, Z. & ANGENENT, L. T. 2006. Application of bacterial biocathodes in microbial fuel cells. *Electroanalysis,* 18**,** 2009-2015.

HE, Z., HUANG, Y., MANOHAR, A. K. & MANSFELD, F. 2008. Effect of electrolyte pH on the rate of the anodic and cathodic reactions in an air-cathode microbial fuel cell. *Bioelectrochemistry,* 74**,** 78-82.

HE, Z., MINTEER, S. D. & ANGENENT, L. T. 2005. Electricity generation from artificial wastewater using an upflow microbial fuel cell. *Environmental Science & Technology,* 39**,** 5262-5267.

HEIDELBERG, J. F., PAULSEN, I. T., NELSON, K. E., GAIDOS, E. J., NELSON, W. C., READ, T. D., EISEN, J. A., SESHADRI, R., WARD, N., METHE, B., CLAYTON, R. A., MEYER, T., TSAPIN, A., SCOTT, J., BEANAN, M., BRINKAC, L., DAUGHERTY, S., DEBOY, R. T., DODSON, R. J., DURKIN, A. S., HAFT, D. H., KOLONAY, J. F., MADUPU, R., PETERSON, J. D., UMAYAM, L. A., WHITE, O., WOLF, A. M., VAMATHEVAN, J., WEIDMAN, J., IMPRAIM, M., LEE, K., BERRY, K., LEE, C., MUELLER, J., KHOURI, H., GILL, J., UTTERBACK, T. R., MCDONALD, L. A., FELDBLYUM, T. V., SMITH, H. O., VENTER, J. C., NEALSON, K. H. & FRASER, C. M. 2002. Genome sequence of the dissimilatory metal ion-reducing bacterium *Shewanella oneidensis*. *Nature Biotechnology,* 20**,** 1118-1123.

HEIDRICH, E. S., DOLFING, J., SCOTT, K., EDWARDS, S. R., JONES, C. & CURTIS, T. P. 2013. Production of hydrogen from domestic wastewater in a pilot-scale microbial electrolysis cell. *Appl Microbiol Biotechnol,* 97**,** 6979-89.

HIROSE, K. 2010. Materials towards carbon-free, emission-free and oil-free mobility: hydrogen fuel cell vehicles now and in the future. *Philos Trans A Math Phys Eng Sci,* 368**,** 3365-77.

HOGUE, C. 2012. CO_2 EMISSIONS Global releases in 2011 set a record high at 31.6 billion metric tons. *Chemical & Engineering News,* 90**,** 8-8.

HOLMES, D. E., NICOLL, J. S., BOND, D. R. & LOVLEY, D. R. 2004. Potential role of a novel psychrotolerant member of the family *Geobacteraceae*, *Geopsychrobacter electrodiphilus* gen. nov., sp nov., in electricity production by a marine sediment fuel cell. *Applied and Environmental Microbiology,* 70**,** 6023-6030.

HONG, J. 1986. Optimal substrate feeding policy for a fed batch fermentation with substrate and product inhibition kinetics. *Biotechnol Bioeng,* 28**,** 1421-31.

HONG, Y. Y., CALL, D. F., WERNER, C. M. & LOGAN, B. E. 2011. Adaptation to high current using low external resistances eliminates power overshoot in microbial fuel cells. *Biosensors & Bioelectronics,* 28**,** 71-76.

HOUSECROFT, C. & SHARPE, A. G. 2007. *Inorganic Chemistry* Prentice Hall.

HU, H. Q., FAN, Y. Z. & LIU, H. 2008. Hydrogen production using single-chamber membrane-free microbial electrolysis cells. *Water Research,* 42**,** 4172-4178.

HU, H. Q., FAN, Y. Z. & LIU, H. 2009. Hydrogen production in single-chamber tubular microbial electrolysis cells using non-precious-metal catalysts. *International Journal of Hydrogen Energy,* 34**,** 8535-8542.

HU, W.-J., NIU, C.-G., WANG, Y., ZENG, G.-M. & WU, Z. 2011. Nitrogenous heterocyclic compounds degradation in the microbial fuel cells. *Process Safety and Environmental Protection,* 89**,** 133-140.

HUANG, L. P. & ANGELIDAKI, I. 2008. Effect of humic acids on electricity generation integrated with xylose degradation in microbial fuel cells. *Biotechnology and Bioengineering,* 100**,** 413-422.

HUANG, X., ZHANG, X. Y., CHENG, S. A., LIANG, P. & LOGAN, B. E. 2011. Scalable air cathode microbial fuel cells using glass fiber separators, plastic mesh supporters, and graphite fiber brush anodes. *Bioresource Technology,* 102**,** 372-375.

HURLE, D. 2004. Crystal growth for beginners. Edited by Ivan V Markov. Pp. 564. World Scientific Press. USD 68, GBP 46. ISBN 981-238-245-3. *Acta Crystallographica Section A: Foundations of Crystallography,* 60**,** 355-355.

HUSSY, I., HAWKES, F. R., DINSDALE, R. & HAWKES, D. L. 2005. Continuous fermentative hydrogen production from sucrose and sugarbeet. *International Journal of Hydrogen Energy,* 30**,** 471-483.

HWANG, M. J., LEE, S. Y. & HAN, C. S. 2006. A study on electric conductivity of phosphoric acid supported on nano-pore rice husk silica in $H_2/Pt/H_3PO_4$ / RHS/Pt/O_2 fuel cells. *J Nanosci Nanotechnol,* 6**,** 3491-3.

HYUN, M. S., KIM, B. H., CHANG, I. S., PARK, H. S., KIM, H. J., KIM, G. T., KIM, M. & PARK, D. H. 1999. Isolation and identification of an anaerobic dissimilatory Fe(III)-reducing bacterium, *Shewanella putrefaciens* IR-1. *Journal of Microbiology,* 37**,** 206-212.

INMAN, M. 2006. *Bacteria made to sprout conducting nanowires* [Online]. Available: http://www.newscientist.com/article/dn9526-bacteria-made-to-sprout-conducting-nanowires.html [Accessed 12:03 11 July 2006].

INTANOO, P., SUTTIKUL, T., LEETHOCHAWALIT, M., GULARI, E. & CHAVADEJ, S. 2014. Hydrogen production from alcohol wastewater with added fermentation residue by an anaerobic sequencing batch reactor (ASBR) under thermophilic operation. *International Journal of Hydrogen Energy*.

IPCC. 2014. *2013 Revised Supplementary Methods and Good Practice Guidance Arising from the Kyoto Protocol* [Online]. Intergovernmental Panel on Climate Change. Available: http://www.ipcc-nggip.iges.or.jp/public/kpsg/pdf/KP_Supplement_Entire_Report.pdf.

ITO, T. 2014. *The Honda Worldwide Fuel Cell Site* [Online]. Available: http://world.honda.com/FuelCell/.

JADHAV, G. S. & GHANGREKAR, M. M. 2009. Performance of microbial fuel cell subjected to variation in pH, temperature, external load and substrate concentration. *Bioresour Technol,* 100**,** 717-23.

JAGIELSKI, J., KHANNA, A. S., KUCINSKI, J., MISHRA, D. S., RACOLTA, P., SIOSHANSI, P., TOBIN, E., THERESKA, J., UGLOV, V., VILAITHONG, T., VIVIENTE, J., YANG, S. Z. & ZALAR, A. 2000. Effect of chromium nitride coating on the corrosion and wear resistance of stainless steel. *Applied Surface Science,* 156**,** 47-64.

JENKINS, P., TUURALA, S., VAARI, A., VALKIAINEN, M., SMOLANDER, M. & LEECH, D. 2012. A comparison of glucose oxidase and aldose dehydrogenase as mediated anodes in printed glucose/oxygen enzymatic fuel cells using ABTS/laccase cathodes. *Bioelectrochemistry,* 87**,** 172-7.

JEON, Y., KOO, K., KIM, H. J. & KIM, S. 2013. Construction and Operation of a Scaled-up Microbial Fuel Cell. *BULLETIN OF THE KOREAN CHEMICAL SOCIETY,* 34**,** 317-320.

JEREMIASSE, A. W., HAMELERS, E. V. M. & BUISMAN, C. J. N. 2010. Microbial electrolysis cell with a microbial biocathode. *Bioelectrochemistry,* 78**,** 39-43.

JIAN-XIAO, L., GUO-HONG, X., QING-LING, Y., LI, Z., JIAN-MIN, L. & YING, C. 2009. H_2O_2-assisted photolysis of reactive dye BES golden yellow simulated wastewater. *Water Sci Technol,* 60**,** 2329-36.

JIANG, D. Q. & LI, B. K. 2009. Novel electrode materials to enhance the bacterial adhesion and increase the power generation in microbial fuel cells (MFCs). *Water Science and Technology,* 59**,** 557-563.

JONG, B. C., KIM, B. H., CHANG, I. S., LIEW, P. W., CHOO, Y. F. & KANG, G. S. 2006. Enrichment, performance, and microbial diversity of a thermophilic mediatorless microbial fuel cell. *Environ Sci Technol,* 40**,** 6449-54.

JUNG, K. W., KIM, D. H., KIM, S. H. & SHIN, H. S. 2011. Bioreactor design for continuous dark fermentative hydrogen production. *Bioresource Technology,* 102**,** 8612-8620.

JUNG, Y. S., YOON, W. L., SEO, Y. S. & RHEE, Y. W. 2012. The effect of precipitants on Ni-Al_2O_3 catalysts prepared by a co-precipitation method for internal reforming in molten carbonate fuel cells. *Catal Commun,* 26**,** 103-111.

KALATHIL, S., LEE, J. & CHO, M. H. 2011. Granular activated carbon based microbial fuel cell for simultaneous decolorization of real dye wastewater and electricity generation. *N Biotechnol,* 29**,** 32-7.

KAMALASKAR, L. B., DHAKEPHALKAR, P. K., MEHER, K. K. & RANADE, D. R. 2010. High biohydrogen yielding *Clostridium* sp. DMHC-10 isolated from sludge of distillery waste treatment plant. *International Journal of Hydrogen Energy,* 35**,** 10639-10644.

KASEM, E. T., SAITO, Y., TSUJIGUCHI, T. & NAKAGAWA, N. Effect of Anode Material on the Performance and Characteristics of Yeast Operated Microbial Fuel Cell.

KATURI, K. P., SCOTT, K., HEAD, I. M., PICIOREANU, C. & CURTIS, T. P. 2011. Microbial fuel cells meet with external resistance. *Bioresource Technology,* 102**,** 2758-2766.

KESICKI, F. 2012. Costs and potentials of reducing CO_2 emissions in the UK domestic stock from a systems perspective. *Energy and Buildings,* 51**,** 203-211.

KESKIN, T. & HALLENBECK, P. C. 2012. Hydrogen production from sugar industry wastes using single-stage photofermentation. *Bioresour Technol,* 112**,** 131-6.

KHALILNEJAD, A. & RIAHY, G. H. 2014. A hybrid wind-PV system performance investigation for the purpose of maximum hydrogen production and storage using advanced alkaline electrolyzer. *Energy Conversion and Management,* 80**,** 398-406.

KIEFT, T. L., FREDRICKSON, J. K., ONSTOTT, T. C., GORBY, Y. A., KOSTANDARITHES, H. M., BAILEY, T. J., KENNEDY, D. W., LI, S. W., PLYMALE, A. E., SPADONI, C. M. & GRAY, M. S. 1999. Dissimilatory reduction of Fe(III) and other electron acceptors by a *Thermus isolate*. *Applied and Environmental Microbiology,* 65**,** 1214-1221.

KIELY, P. D., CUSICK, R., CALL, D. F., SELEMBO, P. A., REGAN, J. M. & LOGAN, B. E. 2011. Anode microbial communities produced by changing from microbial fuel cell to microbial electrolysis cell operation using two different wastewaters. *Bioresource Technology,* 102**,** 388-394.

KIM, B.-H., KIM, H.-J., HYUN, M.-S. & PARK, D.-H. 1999a. Direct electrode reaction of Fe (III)-reducing bacterium, *Shewanella putrefacien*s. *Journal of Microbiology and Biotechnology,* 9**,** 127-131.

KIM, B. H., PARK, H. S., KIM, H. J., KIM, G. T., CHANG, I. S., LEE, J. & PHUNG, N. T. 2004. Enrichment of microbial community generating electricity using a fuel cell type electrochemical cell. *Appl Microbiol Biotechnol,* 63**,** 672-81.

KIM, H., HYUN, M., CHANG, I. & KIM, B. H. 1999b. A microbial fuel cell type lactate biosensor using a metal-reducing bacterium, *Shewanella putrefaciens*. *J. Microbiol. Biotechnol,* 9**,** 365-367.

KIM, J., PARKEY, J., RHODES, C. & GONZALEZ-MARTIN, A. 2009a. Development of a biofuel cell using glucose-oxidase- and bilirubin-oxidase-based electrodes. *Journal of Solid State Electrochemistry,* 13**,** 1043-1050.

KIM, J. R., CHENG, S., OH, S. E. & LOGAN, B. E. 2007a. Power generation using different cation, anion, and ultrafiltration membranes in microbial fuel cells. *Environmental Science & Technology,* 41**,** 1004-1009.

KIM, J. R., JUNG, S. H., REGAN, J. M. & LOGAN, B. E. 2007b. Electricity generation and microbial community analysis of alcohol powered microbial fuel cells. *Bioresource Technology,* 98**,** 2568-2577.

KIM, J. R., MIN, B. & LOGAN, B. E. 2005. Evaluation of procedures to acclimate a microbial fuel cell for electricity production. *Applied Microbiology and Biotechnology,* 68**,** 23-30.

KIM, J. R., PREMIER, G. C., HAWKES, F. R., DINSDALE, R. M. & GUWY, A. J. 2009b. Development of a tubular microbial fuel cell (MFC) employing a membrane electrode assembly cathode. *Journal of Power Sources,* 187**,** 393-399.

KIM, J. R., PREMIER, G. C., HAWKES, F. R., RODRIGUEZ, J., DINSDALE, R. M. & GUWY, A. J. 2010. Modular tubular microbial fuel cells for energy recovery during sucrose wastewater treatment at low organic loading rate. *Bioresource Technology,* 101**,** 1190-1198.

KNIGHTS, S. D., WILKINSON, D. P., CAMPBELL, S. A., TAYLOR, J. L., GASCOYNE, J. M. & RALPH, T. R. 2001. *Fuel cell anode structure for voltage reversal tolerance*. PCT/CA2000/000970. 21.03.2001.

KOIZUMI, Y., TAKII, S., NISHINO, M. & NAKAJIMA, T. 2003. Vertical distributions of sulfate-reducing bacteria and methane-producing archaea quantified by oligonucleotide probe hybridization in the profundal sediment of a mesotrophic lake. *FEMS Microbiology Ecology,* 44**,** 101-108.

KOTAY, S. M. & DAS, D. 2007. Microbial hydrogen production with *Bacillus coagulans* IIT-BT S1 isolated from anaerobic sewage sludge. *Bioresource Technology,* 98**,** 1183-1190.

KRAMM, U. I., HERRANZ, J., LAROUCHE, N., ARRUDA, T. M., LEFEVRE, M., JAOUEN, F., BOGDANOFF, P., FIECHTER, S., ABS-WURMBACH, I., MUKERJEE, S. & DODELET, J. P. 2012. Structure of the catalytic sites in Fe/N/C-catalysts for O_2-reduction in PEM fuel cells. *Phys Chem Chem Phys,* 14**,** 11673-88.

KUHL, P. 1994. Excess-substrate inhibition in enzymology and high-dose inhibition in pharmacology: a reinterpretation. *Biochem. J,* 298**,** 171-180.

KUNDU, P. P. & SHARMA, V. 2010. Biocatalysts in microbial fuel cells. *Enzyme and Microbial Technology,* 47**,** 179-188.

KURAMOCHI, T., RAMIREZ, A., TURKENBURG, W. & FAAIJ, A. 2012. Effect of CO_2 capture on the emissions of air pollutants from industrial processes. *International Journal of Greenhouse Gas Control,* 10**,** 310-328.

KYAZZE, G., DINSDALE, R., GUWY, A. I., HAWKES, F. R., PREMIER, G. C. & HAWKES, D. L. 2007. Performance characteristics of a two-stage dark fermentative system producing hydrogen and methane continuously. *Biotechnology and Bioengineering,* 97**,** 759-770.

KYAZZE, G., MARTINEZ-PEREZ, N., DINSDALE, R., PREMIER, G. C., HAWKES, F. R., GUWY, A. J. & HAWKES, D. L. 2006. Influence of substrate concentration on the stability and yield of continuous biohydrogen production. *Biotechnology and Bioengineering,* 93**,** 971-979.

KYAZZE, G., POPOV, A., DINSDALE, R., ESTEVES, S., HAWKES, F., PREMIER, G. & GUWY, A. 2010. Influence of catholyte pH and temperature on hydrogen production from acetate using a two chamber concentric tubular microbial electrolysis cell. *International Journal of Hydrogen Energy,* 35**,** 7716-7722.

LALAURETTE, E., THAMMANNAGOWDA, S., MOHAGHEGHI, A., MANESS, P. C. & LOGAN, B. E. 2009. Hydrogen production from cellulose in a two-stage process combining fermentation and electrohydrogenesis. *International Journal of Hydrogen Energy,* 34**,** 6201-6210.

LANAS, V. & LOGAN, B. E. 2013. Evaluation of multi-brush anode systems in microbial fuel cells. *Bioresour Technol,* 148**,** 379-85.

LEBEDEVA, N.D. 1964. Heats of combustion of monocarboxylic acids. *Russ. J. Phys. Chem*. (Engl. Transl.), 38**,** 1435-1437

LEE, H. S., PARAMESWARAN, P., KATO-MARCUS, A., TORRES, C. I. & RITTMANN, B. E. 2008. Evaluation of energy-conversion efficiencies in microbial fuel cells (MFCs) utilizing fermentable and non-fermentable substrates. *Water Res,* 42**,** 1501-10.

LEE, H. S., TORRES, C. I., PARAMESWARAN, P. & RITTMANN, B. E. 2009. Fate of H_2 in an Upflow Single-Chamber Microbial Electrolysis Cell Using a Metal-Catalyst-Free Cathode. *Environmental Science & Technology,* 43**,** 7971-7976.

LEE, J., PHUNG, N. T., CHANG, I. S., KIM, B. H. & SUNG, H. C. 2003. Use of acetate for enrichment of electrochemically active microorganisms and their 16S rDNA analyses. *FEMS Microbiology Letters,* 223**,** 185-191.

LEE, K. Y. & KIM, K. W. 2010. Heavy metal removal from shooting range soil by hybrid electrokinetics with bacteria and enhancing agents. *Environ Sci Technol,* 44**,** 9482-7.

LETTINGA, G., REBAC, S. & ZEEMAN, G. 2001. Challenge of psychrophilic anaerobic wastewater treatment. *Trends Biotechnol,* 19**,** 363-70.

LI, B. K., LI, X., HU, B. X., SUIB, S. & LEI, Y. 2011. Electricity generation in continuous flow microbial fuel cells (MFCs) with manganese dioxide (MnO_2) cathodes. *Biochemical Engineering Journal,* 54**,** 10-15.

LI, H. R., TANG, X. H., GUO, K., DU, Z. W. & TIAN, J. L. 2010a. Microfiltration membrane performance in two-chamber microbial fuel cells. *Biochemical Engineering Journal,* 52**,** 194-198.

LI, N., GUIVER, M. D. & BINDER, W. H. 2013a. Towards high conductivity in anion-exchange membranes for alkaline fuel cells. *ChemSusChem,* 6**,** 1290.

LI, X., YU, Y. & MENG, Y. 2013b. Novel quaternized poly(arylene ether sulfone)/Nano-ZrO_2 composite anion exchange membranes for alkaline fuel cells. *ACS Appl Mater Interfaces,* 5**,** 1414-22.

LI, Z. J., ZHANG, X. W., LIN, J., HAN, S. & LEI, L. C. 2010b. Azo dye treatment with simultaneous electricity production in an anaerobic-aerobic sequential reactor and microbial fuel cell coupled system. *Bioresource Technology,* 101**,** 4440-4445.

LIM, T. Development of fuel cell electric vehicle in Hyundai–Kia Motors. 6th International Hydrogen & Fuel Cell Expo Technical Conference, Tokyo, 2010.

LINSTROM, P. J. & MALLARD, W. G. 2010. *NIST Chemistry WebBook, NIST Standard Reference Database Number 69* [Online]. Available: http://webbook.nist.gov.

LITHGOW, A. M., ROMERO, L., SANCHEZ, I. C., SOUTO, F. A. & VEGA, C. A. 1986. Interception of the Electron-Transport Chain in Bacteria with Hydrophilic Redox Mediators.1. Selective Improvement of the Performance of Biofuel Cells with 2,6-Disulfonated Thionine as Mediator. *Journal of Chemical Research-S***,** 178-179.

LIU, C., GORBY, Y. A., ZACHARA, J. M., FREDRICKSON, J. K. & BROWN, C. F. 2002. Reduction kinetics of Fe(III), Co(III), U(VI), Cr(VI), and Tc(VII) in cultures of dissimilatory metal-reducing bacteria. *Biotechnol Bioeng,* 80**,** 637-49.

LIU, C. H., CHANG, C. Y., LIAO, Q., ZHU, X. & CHANG, J. S. 2013a. Photoheterotrophic growth of *Chlorella vulgaris* ESP6 on organic acids from dark hydrogen fermentation effluents. *Bioresour Technol,* 145**,** 331-6.

LIU, G., YATES, M. D., CHENG, S., CALL, D. F., SUN, D. & LOGAN, B. E. 2011a. Examination of microbial fuel cell start-up times with domestic wastewater and additional amendments. *Bioresour Technol,* 102**,** 7301-6.

LIU, H., CHENG, S. A. & LOGAN, B. E. 2005a. Power generation in fed-batch microbial fuel cells as a function of ionic strength, temperature, and reactor configuration. *Environmental Science & Technology,* 39**,** 5488-5493.

LIU, H., CHENG, S. A. & LOGAN, B. E. 2005b. Production of electricity from acetate or butyrate using a single-chamber microbial fuel cell. *Environmental Science & Technology,* 39**,** 658-662.

LIU, H. & FANG, H. H. P. 2003. Hydrogen production from wastewater by acidogenic granular sludge. *Water Science and Technology,* 47**,** 153-158.

LIU, H., GROT, S. & LOGAN, B. E. 2005c. Electrochemically Assisted Microbial Production of Hydrogen from Acetate. *Environmental Science Technology,* 39**,** 4317-4320.

LIU, H. & LOGAN, B. 2004a. Electricity generation using an air-cathode single chamber microbial fuel cell (MFC) in the absence of a proton exchange membrane. *Abstracts of Papers of the American Chemical Society,* 228**,** U622-U622.

LIU, H. & LOGAN, B. E. 2004b. Electricity generation using an air-cathode single chamber microbial fuel cell in the presence and absence of a proton exchange membrane. *Environmental Science & Technology,* 38**,** 4040-4046.

LIU, H. & WANG, G. 2012. Hydrogen production of a salt tolerant strain *Bacillus* sp. B2 from marine intertidal sludge. *World Journal of Microbiology and Biotechnology,* 28**,** 31-37.

LIU, H., ZHANG, T. & FANG, H. H. P. 2003. Thermophilic H_2 production from a cellulose-containing wastewater. *Biotechnology Letters,* 25**,** 365-369.

LIU, L., TSYGANOVA, O., LEE, D.-J., CHANG, J.-S., WANG, A. & REN, N. 2013b. Double-chamber microbial fuel cells started up under room and low temperatures. *International Journal of Hydrogen Energy,* 38**,** 15574-15579.

LIU, L. H., LEE, C. Y., HO, K. C., NIEN, P. C., SU, A., WANG, A. J., REN, N. Q. & LEE, D. J. 2011b. Occurrence of power overshoot for two-chambered MFC at nearly steady-state operation. *International Journal of Hydrogen Energy,* 36**,** 13896-13899.

LIU, X. W., WANG, Y. P., HUANG, Y. X., SUN, X. F., SHENG, G. P., ZENG, R. J., LI, F., DONG, F., WANG, S. G., TONG, Z. H. & YU, H. Q. 2011c. Integration of a Microbial Fuel Cell With Activated Sludge Process for Energy-Saving Wastewater Treatment: Taking a Sequencing Batch Reactor as an Example. *Biotechnology and Bioengineering,* 108**,** 1260-1267.

LIU, Y., HARNISCH, F., FRICKE, K., SIETMANN, R. & SCHRODER, U. 2008. Improvement of the anodic bioelectrocatalytic activity of mixed culture biofilms by a simple consecutive electrochemical selection procedure. *Biosens Bioelectron,* 24**,** 1012-7.

LLOYD, J. R., BLUNT-HARRIS, E. L. & LOVLEY, D. R. 1999. The periplasmic 9.6-kilodalton c-type cytochrome of *Geobacter sulfurreducens* is not an electron shuttle to Fe(III). *Journal of Bacteriology,* 181**,** 7647-7649.

LLOYD, J. R., LEANG, C., MYERSON, A. L. H., COPPI, M. V., CUIFO, S., METHE, B., SANDLER, S. J. & LOVLEY, D. R. 2003. Biochemical and genetic characterization of PpcA, a periplasmic c-type cytochrome in *Geobacter sulfurreducens*. *Biochemical Journal,* 369**,** 153-161.

LOCHER, C., MEYER, C. & STEINMETZ, H. 2012. Operating experiences with a molten carbonate fuel cell at Stuttgart-Mohringen wastewater treatment plant. *Water Sci Technol,* 65**,** 789-94.

LOGAN, B., CHENG, S., WATSON, V. & ESTADT, G. 2007a. Graphite fiber brush anodes for increased power production in air-cathode microbial fuel cells. *Environmental Science & Technology,* 41**,** 3341-3346.

LOGAN, B., CHENG, S. A. & WATSON, V. 2007b. FUEL 129-Progress and challenges in scale up of electrogenic reactors such as microbial fuel cells. *Abstracts of Papers of the American Chemical Society,* 234.

LOGAN, B. E. 2004a. Extracting hydrogen electricity from renewable resources. *Environmental Science & Technology,* 38**,** 160a-167a.

LOGAN, B. E. 2004b. Potential for wastewater treatment systems based on microbial fuel cells and biological hydrogen production. *Abstracts of Papers of the American Chemical Society,* 228**,** U621-U621.

LOGAN, B. E. 2008. *Microbial Fuel Cells,* New Jersey, John Wiley & Sons.

LOGAN, B. E. 2009. Exoelectrogenic bacteria that power microbial fuel cells. *Nature Reviews Microbiology,* 7**,** 375-381.

LOGAN, B. E. 2010. Scaling up microbial fuel cells and other bioelectrochemical systems. *Applied Microbiology and Biotechnology,* 85**,** 1665-1671.

LOGAN, B. E., CALL, D., CHENG, S., HAMELERS, H. V. M., SLEUTELS, T. H. J. A., JERMIASSE, A. W. & ROZENDAL, R. A. 2008. Microbial Electrolysis Cells for High Yield Hydrogen Gas Production from Organic Matter. *Environmental Science Technology*.

LOGAN, B. E. & CHENG, S. 2007. Sustainable and efficient biohydrogen production via electrohydrogenesis. *Proceedings of the National Academy of Sciences of the United States of America,* 104**,** 18871-18873.

LOGAN, B. E., CHENG, S. A. & XING, D. F. 2011. Electricity generation of single-chamber microbial fuel cells at low temperatures. *Biosensors & Bioelectronics,* 26**,** 1913-1917.

LOGAN, B. E., CUSICK, R. D. & KIELY, P. D. 2010. A monetary comparison of energy recovered from microbial fuel cells and microbial electrolysis cells fed winery or domestic wastewaters. *International Journal of Hydrogen Energy,* 35**,** 8855-8861.

LOGAN, B. E., HAMELERS, B., ROZENDAL, R. A., SCHRORDER, U., KELLER, J., FREGUIA, S., AELTERMAN, P., VERSTRAETE, W. & RABAEY, K. 2006. Microbial fuel cells: Methodology and technology. *Environmental Science & Technology,* 40**,** 5181-5192.

LOGAN, B. E., KIM, J. R., CHENG, S. & OH, S. E. 2007c. Power generation using different cation, anion, and ultrafiltration membranes in microbial fuel cells. *Environmental Science & Technology,* 41**,** 1004-1009.

LOGAN, B. E., MURANO, C., SCOTT, K., GRAY, N. D. & HEAD, I. M. 2005. Electricity generation from cysteine in a microbial fuel cell. *Water Research,* 39**,** 942-952.

LOGAN, B. E. & REGAN, J. M. 2006. Electricity-producing bacterial communities in microbial fuel cells. *Trends in Microbiology,* 14**,** 512-518.

LOGAN, B. E., REZAEI, F. & RICHARD, T. L. 2009a. Analysis of chitin particle size on maximum power generation, power longevity, and Coulombic efficiency in solid-substrate microbial fuel cells. *Journal of Power Sources,* 192**,** 304-309.

LOGAN, B. E., REZAEI, F., RICHARD, T. L. & BRENNAN, R. A. 2007d. Substrate-enhanced microbial fuel cells for improved remote power generation from sediment-based systems. *Environmental Science & Technology,* 41**,** 4053-4058.

LOGAN, B. E., REZAEI, F., XING, D. F., WAGNER, R., REGAN, J. M. & RICHARD, T. L. 2009b. Simultaneous Cellulose Degradation and Electricity Production by *Enterobacter cloacae* in a Microbial Fuel Cell. *Applied and Environmental Microbiology,* 75**,** 3673-3678.

LOVELEY, D. R., HOLMES, D. E. & NEVLIN, K. P. 2004. Dessimilatory Fe (III) and Mn (IV) Reduction *Advanced Microbial Physiology,* 49**,** 219 - 286.

LOVLEY, D. R. 1993. Dissimilatory metal reduction. *Annu Rev Microbiol,* 47**,** 263-90.

LOVLEY, D. R. 1997. Microbial Fe(III) reduction in subsurface environments. *Fems Microbiology Reviews,* 20**,** 305-313.

LOVLEY, D. R., NEVIN, K. P., CHILDERS, S. E., MEHTA, T. & CIUFO, S. A. 2002. Different strategies for Fe(III) oxide reduction in *Geobacter* versus *Shewanella* and *Geothrix* species. *Abstracts of Papers of the American Chemical Society,* 223**,** U598-U598.

LOVLEY, D. R., PHILLIPS, E. J. P., GORBY, Y. A. & LANDA, E. R. 1991. Microbial Reduction of Uranium. *Abstracts of Papers of the American Chemical Society,* 202**,** 8-Geoc.

LOWY, D. A. & TENDER, L. M. 2008. Harvesting energy from the marine sediment-water interface III. Kinetic activity of quinone- and antimony-based anode materials. *Journal of Power Sources,* 185**,** 70-75.

LOWY, D. A., TENDER, L. M., ZEIKUS, J. G., PARK, D. H. & LOVLEY, D. R. 2006. Harvesting energy from the marine sediment-water interface II - Kinetic activity of anode materials. *Biosensors & Bioelectronics,* 21**,** 2058-2063.

LU, L., REN, N. Q., XING, D. F. & LOGAN, B. E. 2009. Hydrogen production with effluent from an ethanol-H_2-coproducing fermentation reactor using a single-chamber microbial electrolysis cell. *Biosensors & Bioelectronics,* 24**,** 3055-3060.

LUBKEN, M., WICHERN, M., LETSIOU, I., KEHL, O., BISCHOF, F. & HORN, H. 2007. Thermophilic anaerobic digestion in compact systems: investigations by modern microbiological techniques and mathematical simulation. *Water Sci Technol,* 56**,** 19-28.

LUO, H., XU, P., ROANE, T. M., JENKINS, P. E. & REN, Z. 2012. Microbial desalination cells for improved performance in wastewater treatment, electricity production, and desalination. *Bioresour Technol,* 105**,** 60-6.

LV, Z., XIE, D., YUE, X., FENG, C. & WEI, C. 2012. Ruthenium oxide-coated carbon felt electrode: A highly active anode for microbial fuel cell applications. *Journal of Power Sources,* 210**,** 26-31.

MACAODHA, D., P, O. C., EGAN, B., KAVANAGH, P. & LEECH, D. 2013. Membraneless glucose/oxygen enzymatic fuel cells using redox hydrogel films containing carbon nanotubes. *Chemphyschem,* 14**,** 2302-7.

MALKI, M., DE LACEY, A. L., RODRFGUEZ, N., AMILS, R. & FERNANDEZ, V. M. 2008. Preferential use of an anode as an electron acceptor by an acidophilic bacterium in the presence of oxygen. *Applied and Environmental Microbiology,* 74**,** 4472-4476.

MANNISTO, M. K. & PUHAKKA, J. A. 2002. Psychrotolerant and microaerophilic bacteria in boreal groundwater. *FEMS Microbiol Ecol,* 41**,** 9-16.

MARGESIN, R. & SCHINNER, F. 2001. Potential of halotolerant and halophilic microorganisms for biotechnology. *Extremophiles,* 5**,** 73-83.

MARSHALL, C. W. & MAY, H. D. 2009. Electrochemical evidence of direct electrode reduction by a thermophilic Gram-positive bacterium, *Thermincola ferriacetica*. *Energy & Environmental Science,* 2**,** 699-705.

MASSANET-NICOLAU, J., DINSDALE, R. & GUWY, A. 2008. Hydrogen production from sewage sludge using mixed microflora inoculum: Effect of pH and enzymatic pretreatment. *Bioresource Technology,* 99**,** 6325-6331.

MASSANET-NICOLAU, J., GUWY, A., DINSDALE, R., PREMIER, G. & ESTEVES, S. 2010. Production of hydrogen from sewage biosolids in a continuously fed bioreactor: Effect of hydraulic retention time and sparging. *International Journal of Hydrogen Energy,* 35**,** 469-478.

MATOS, C. T. & LOPES DA SILVA, T. 2013. Using multi-parameter flow cytometry as a novel approach for physiological characterization of bacteria in microbial fuel cells. *Process Biochemistry,* 48**,** 49-57.

MCHUGH, S., COLLINS, G. & O'FLAHERTY, V. 2006. Long-term, high-rate anaerobic biological treatment of whey wastewaters at psychrophilic temperatures. *Bioresour Technol,* 97**,** 1669-78.

MEHTA, T., COPPI, M. V., CHILDERS, S. E. & LOVLEY, D. R. 2005. Outer membrane c-type cytochromes required for Fe(III) and Mn(IV) oxide reduction in *Geobacter sulfurreducens*. *Applied and Environmental Microbiology,* 71**,** 8634-8641.

MENICUCCI, J., BEYENAL, H., MARSILI, E., VELUCHAMY, R. A., DEMIR, G. & LEWANDOWSKI, Z. 2006. Procedure for determining maximum sustainable power generated by microbial fuel cells. *Environ Sci Technol,* 40**,** 1062-8.

METHE, B. A., NELSON, K. E., EISEN, J. A., PAULSEN, I. T., NELSON, W., HEIDELBERG, J. F., WU, D., WU, M., WARD, N., BEANAN, M. J., DODSON, R. J., MADUPU, R., BRINKAC, L. M., DAUGHERTY, S. C., DEBOY, R. T., DURKIN, A. S., GWINN, M., KOLONAY, J. F., SULLIVAN, S. A., HAFT, D. H., SELENGUT, J., DAVIDSEN, T. M., ZAFAR, N., WHITE, O., TRAN, B., ROMERO, C., FORBERGER, H. A., WEIDMAN, J., KHOURI, H., FELDBLYUM, T. V., UTTERBACK, T. R., VAN AKEN, S. E., LOVLEY, D. R. & FRASER, C. M. 2003. Genome of *Geobacter sulfurreducens*: Metal reduction in subsurface environments. *Science,* 302**,** 1967-1969.

MICHIE, I. S., KIM, J. R., DINSDALE, R. M., GUWY, A. J. & PREMIER, G. C. 2011. The influence of psychrophilic and mesophilic start-up temperature on microbial fuel cell system performance. *Energy & Environmental Science,* 4**,** 1011-1019.

MIDILLI, A., AY, M., DINCER, I. & ROSEN, M. A. 2005. On hydrogen and hydrogen energy strategies: I: current status and needs. *Renewable and Sustainable Energy Reviews,* 9**,** 255-271.

MIN, B., CHENG, S. & LOGAN, B. E. 2005. Electricity generation using membrane and salt bridge microbial fuel cells. *Water research,* 39**,** 1675-1686.

MODIN, O. & WILEN, B. M. 2012. A novel bioelectrochemical BOD sensor operating with voltage input. *Water Res,* 46**,** 6113-20.

MOHAN, S. V., MOHANAKRISHNAA, G., RAMANAIAHA, S. & SARMA, P. N. 2008a. Simultaneous biohydrogen production and wastewater treatment in biofilm configured anaerobic periodic discontinuous batch reactor using distillery wastewater. *International Journal of Hydrogen Energy,* 33**,** 550 - 558.

MOHAN, S. V., RAGHAVULU, S. V., GOUD, R. K. & SARMA, P. N. 2009. Effect of anodic pH microenvironment on microbial fuel cell (MFC) performance in concurrence with aerated and ferricyanide catholytes. *Electrochemistry Communications,* 11**,** 371-375.

MOHAN, Y. & DAS, D. 2009. Effect of ionic strength, cation exchanger and inoculum age on the performance of Microbial Fuel Cells. *International Journal of Hydrogen Energy,* 34**,** 7542-7546.

MOHAN, Y., KUMAR, S. M. M. & DAS, D. 2008b. Electricity generation using microbial fuel cells. *International Journal of Hydrogen Energy,* 33**,** 423-426.

MOON, H., CHANG, I. S. & KIM, B. H. 2006. Continious Electricity Production from Artificial Wastewater Using a Mediator-Less Microbial Fuel Cell. *Bioresource Technol,* 97**,** 621-627.

MORITA, R. Y. 1975. Psychrophilic bacteria. *Bacteriol Rev,* 39**,** 144-67.

MU, Y., RABAEY, K., ROZENDAL, R. A., YUAN, Z. G. & KELLER, J. 2009. Decolorization of Azo Dyes in Bioelectrochemical Systems. *Environmental Science & Technology,* 43**,** 5137-5143.

MU, Y., ROZENDAL, R. A., RABAEY, K. & KELLER, J. 2010. Electrochemically active bacteria assisted nitrobenzene removal from wastewater. *Journal of Biotechnology,* 150**,** S147-S147.

MUNOZ, L. D., ERABLE, B., ETCHEVERRY, L., RIESS, J., BASSEGUY, R. & BERGEL, A. 2010. Combining phosphate species and stainless steel cathode to enhance hydrogen evolution in microbial electrolysis cell (MEC). *Electrochemistry Communications,* 12**,** 183-186.

NAM, D. G. & LEE, H. C. 2007. Thermal nitridation of chromium electroplated AIS1316L stainless steel for polymer electrolyte membrane fuel cell bipolar plate. *Journal of Power Sources,* 170**,** 268-274.

NAM, J. Y., TOKASH, J. C. & LOGAN, B. E. 2011. Comparison of microbial electrolysis cells operated with added voltage or by setting the anode potential. *International Journal of Hydrogen Energy,* 36**,** 10550-10556.

NEVIN, K. P., RICHTER, H., COVALLA, S. F., JOHNSON, J. P., WOODARD, T. L., ORLOFF, A. L., JIA, H., ZHANG, M. & LOVLEY, D. R. 2008. Power output and columbic efficiencies from biofilms of *Geobacter sulfurreducens* comparable to mixed community microbial fuel cells. *Environ Microbiol,* 10**,** 2505-14.

NIEN, P. C., LEE, C. Y., HO, K. C., ADAV, S. S., LIU, L. H., WANG, A. J., REN, N. Q. & LEE, D. J. 2011. Power overshoot in two-chambered microbial fuel cell (MFC). *Bioresource Technology,* 102**,** 4742-4746.

NIESSEN, J., SCHRODER, U., ROSENBAUM, M. & SCHOLZ, F. 2004a. Fluorinated polyanilines as superior materials for electrocatalytic anodes in bacterial fuel cells. *Electrochemistry Communications,* 6**,** 571-575.

NIESSEN, J., SCHRODER, U. & SCHOLZ, F. 2004b. Exploiting complex carbohydrates for microbial electricity generation - a bacterial fuel cell operating on starch. *Electrochemistry Communications,* 6**,** 955-958.

NISSILA, M. E., TAHTI, H. P., RINTALA, J. A. & PUHAKKA, J. A. 2011. Thermophilic hydrogen production from cellulose with rumen fluid enrichment cultures: Effects of different heat treatments. *International Journal of Hydrogen Energy,* 36**,** 1482-1490.

O-THONG, S., PRASERTSAN, P. & BIRKELAND, N.-K. 2009. Evaluation of methods for preparing hydrogen-producing seed inocula under thermophilic condition by process performance and microbial community analysis. *Bioresource Technology,* 100**,** 909-918.

OH, E. O., WHANG, C. M., LEE, Y. R., PARK, S. Y., PRASAD, D. H., YOON, K. J., SON, J. W., LEE, J. H. & LEE, H. W. 2012. Extremely thin bilayer electrolyte for solid oxide fuel cells (SOFCs) fabricated by chemical solution deposition (CSD). *Adv Mater,* 24**,** 3373-7.

OH, S. & LOGAN, B. E. 2005. Hydrogen and Elecricity Production From a Food Processing Wasewater Using Fermentation and Microbial Fuel Cell Technologies. *Water research,* 39**,** 4673-4682.

OH, S., MIN, B. & LOGAN, B. E. 2004. Cathode performance as a factor in electricity generation in microbial fuel cells. *Environmental Science & Technology,* 38**,** 4900-4904.

OH, S. E., KIM, J., MIN, B. & LOGAN, B. E. 2005. Electricity generation from food and animal wastewaters using microbial fuel cells. *Abstracts of Papers of the American Chemical Society,* 230**,** U1691-U1692.

OH, S. E. & LOGAN, B. E. 2007. Voltage reversal during microbial fuel cell stack operation. *Journal of Power Sources,* 167**,** 11-17.

OMIDI, H. & SATHASIVAN, A. 2013. Optimal temperature for microbes in an acetate fed microbial electrolysis cell (MEC). *International Biodeterioration & Biodegradation,* 85**,** 688-692.

PANAGIOTOPOULOS, I. A., BAKKER, R. R., DE VRIJE, T., CLAASSEN, P. A. M. & KOUKIOS, E. G. 2012. Dilute-acid pretreatment of barley straw for biological hydrogen production using *Caldicellulosiruptor saccharolyticus*. *International Journal of Hydrogen Energy,* 37**,** 11727-11734.

PANDIT, S., NAYAK, B. K. & DAS, D. 2012. Microbial carbon capture cell using cyanobacteria for simultaneous power generation, carbon dioxide sequestration and wastewater treatment. *Bioresour Technol,* 107**,** 97-102.

PANDIT, S., SENGUPTA, A., KALE, S. & DAS, D. 2011. Performance of electron acceptors in catholyte of a two-chambered microbial fuel cell using anion exchange membrane. *Bioresour Technol,* 102**,** 2736-44.

PANT, D., VAN BOGAERT, G., DIELS, L. & VANBROEKHOVEN, K. 2010. A review of the substrates used in microbial fuel cells (MFCs) for sustainable energy production. *Bioresource Technology,* 101**,** 1533-1543.

PARAMESWARAN, P., TORRES, C. I., LEE, H.-S., RITTMANN, B. E. & KRAJMALNIK-BROWN, R. 2011. Hydrogen consumption in microbial electrochemical systems (MXCs): The role of homo-acetogenic bacteria. *Bioresource Technology,* 102**,** 263-271.

PARK, D. H., KIM, S. K., SHIN, I. H. & JEONG, Y. J. 2000. Electricity production in biofuel cell using modified graphite electrode with Neutral Red. *Biotechnology Letters,* 22**,** 1301-1304.

PARK, D. H., LAIVENIEKS, M., GUETTLER, M. V., JAIN, M. K. & ZEIKUS, J. G. 1999. Microbial utilization of electrically reduced neutral red as the sole electron donor for growth and metabolite production. *Applied and Environmental Microbiology,* 65**,** 2912-2917.

PARK, D. H. & ZEIKUS, J. G. 1999. Utilization of electrically reduced neutral red by *Actinobacillus succinogenes*: Physiological function of neutral red in membrane-driven fumarate reduction and energy conservation. *Journal of Bacteriology,* 181**,** 2403-2410.

PARK, D. H. & ZEIKUS, J. G. 2000. Electricity generation in microbial fuel cells using neutral red as an electronophore. *Applied and Environmental Microbiology,* 66**,** 1292-1297.

PARK, D. H. & ZEIKUS, J. G. 2002. Impact of Electrode Composition on Electricity Generation in a Single Compartment Fuel Cell Using *Shewanella putrefaciens*. *Appl Biochem Biotechnol,* 59**,** 58-61.

PARK, D. H. & ZEIKUS, J. G. 2003. Improved fuel cell and electrode designs for producing electricity from microbial degradation. *Biotechnology and Bioengineering,* 81**,** 348-355.

PARK, H. S., KIM, B. H., KIM, H. S., KIM, H. J., KIM, G. T., KIM, M., CHANG, I. S., PARK, Y. K. & CHANG, H. I. 2001. A novel electrochemically active and Fe(III)-reducing bacterium phylogenetically related to *Clostridium butyricum* isolated from a microbial fuel cell. *Anaerobe,* 7**,** 297-306.

PATTERSON, T., DINSDALE, R. & ESTEVES, S. 2008. Review of energy balances and emissions associated with biomass-based transport fuels relevant to the United Kingdom context. *Energy & Fuels,* 22**,** 3506-3512.

PATTERSON, T., ESTEVES, S., DINSDALE, R. & GUWY, A. 2011. Life cycle assessment of biogas infrastructure options on a regional scale. *Bioresource technology,* 102**,** 7313-7323.

PEDERSEN, K. 2002. Chapter 10 Microbial processes in the disposal of high level radioactive waste 500 m underground in Fennoscandian Shield rocks. *In:* KEITH-ROACH, M. J. & LIVENS, F. R. (eds.) *Radioactivity in the Environment.* Elsevier.

PENG, L., YOU, S. J. & WANG, J. Y. 2010. Carbon nanotubes as electrode modifier promoting direct electron transfer from *Shewanella oneidensis*. *Biosensors & Bioelectronics,* 25**,** 1248-1251.

PHAM, C. A., JUNG, S. J., PHUNG, N. T., LEE, J., CHANG, I. S., KIM, B. H., YI, H. & CHUN, J. 2003. A novel electrochemically active and Fe(III)-reducing bacterium phylogenetically related to *Aeromonas hydrophila*, isolated from a microbial fuel cell. *Fems Microbiology Letters,* 223**,** 129-134.

PHAM, T. H., RABAEY, K., AELTERMAN, P., CLAUWAERT, P., DE SCHAMPHELAIRE, L., BOON, N. & VERSTRAETE, W. 2006. Microbial fuel cells in relation to conventional anaerobic digestion technology. *Engineering in Life Sciences,* 6**,** 285-292.

PICIOREANU, C., HEAD, I. M., KATURI, K. P., VAN LOOSDRECHT, M. C. M. & SCOTT, K. 2007. A computational model for biofilm-based microbial fuel cells. *Water Research,* 41**,** 2921-2940.

PINO, F. J., VALVERDE, L. & ROSA, F. 2011. Influence of wind turbine power curve and electrolyzer operating temperature on hydrogen production in wind–hydrogen systems. *Journal of Power Sources,* 196**,** 4418-4426.

POPOV, A. L., KIM, J. R., DINSDALE, R. M., ESTEVES, S. R., GUWY, A. J. & PREMIER, G. C. 2012. The effect of physico-chemically immobilized methylene blue and neutral red on the anode of microbial fuel cell. *Biotechnology and Bioprocess Engineering,* 17**,** 361-370.

PREMIER, G. C., KIM, J. R., MICHIE, I., DINSDALE, R. M. & GUWY, A. J. 2011. Automatic control of load increases power and efficiency in a microbial fuel cell. *Journal of Power Sources,* 196**,** 2013-2019.

RABAEY, K., BOON, N., HOFTE, M. & VERSTRAETE, W. 2005a. Microbial phenazine production enhances electron transfer in biofuel cells. *Environmental Science & Technology,* 39**,** 3401-3408.

RABAEY, K., BOON, N., SICILIANO, S. D., VERHAEGE, M. & VERSTRAETE, W. 2004. Biofuel cells select for microbial consortia that self-mediate electron transfer. *Applied and Environmental Microbiology,* 70**,** 5373-5382.

RABAEY, K., CLAUWAERT, P., AELTERMAN, P. & VERSTRAETE, W. 2005b. Tubular microbial fuel cells for efficient electricity generation. *Environmental Science & Technology,* 39**,** 8077-8082.

RABAEY, K., VAN DE SOMPEL, K., MAIGNIEN, L., BOON, N., AELTERMAN, P., CLAUWAERT, P., DE SCHAMPHELAIRE, L., PHAM, H. T., VERMEULEN, J., VERHAEGE, M., LENS, P. & VERSTRAETE, W. 2006. Microbial fuel cells for sulfide removal. *Environmental Science & Technology,* 40**,** 5218-5224.

RABAEY, K. & VERSTRAETE, W. 2005. Microbial fuel cells: novel biotechnology for energy generation. *Trends in Biotechnology,* 23**,** 291-298.

RADER, G. K. & LOGAN, B. E. 2010. Multi-electrode continuous flow microbial electrolysis cell for biogas production from acetate. *International Journal of Hydrogen Energy,* 35**,** 8848-8854.

RAHIMPOUR, M. R. & ELEKAEI, H. 2009. Enhancement of methanol production in a novel fluidized-bed hydrogen-permselective membrane reactor in the presence of catalyst deactivation. *International Journal of Hydrogen Energy,* 34**,** 2208-2223.

RAJALAKSHMI, N., SAMROT, A. V., SENTHILKUMAR, P., PAVANKUMAR, K., AKILANDESWARI, G. C. & DHATHATHREYAN, K. S. 2010. Electricity generation by *Enterobacter cloacae* SU-1 in mediator less microbial fuel cell. *International Journal of Hydrogen Energy,* 35**,** 7723-7729.

RAMASAMY, R. P., REN, Z., MENCH, M. M. & REGAN, J. M. 2008. Impact of initial biofilm growth on the anode impedance of microbial fuel cells. *Biotechnol Bioeng,* 101**,** 101-8.

RAMOS, C., BUITRON, G., MORENO-ANDRADE, I. & CHAMY, R. 2012. Effect of the initial total solids concentration and initial pH on the bio-hydrogen production from cafeteria food waste. *International Journal of Hydrogen Energy,* 37**,** 13288-13295.

RAZA, R., ABBAS, G., LIU, Q., PATEL, I. & ZHU, B. 2012. La0.3Sr0.2Mn0.1Zn0.4 oxide-Sm0.2Ce0.8O1.9 (LSMZ-SDC) nanocomposite cathode for low temperature SOFCs. *J Nanosci Nanotechnol,* 12**,** 4994-7.

REED, M. C., LIEB, A. & NIJHOUT, H. F. 2010. The biological significance of substrate inhibition: a mechanism with diverse functions. *Bioessays,* 32**,** 422-429.

REGAN, J. M. & JUNG, S. 2011. Influence of External Resistance on Electrogenesis, Methanogenesis, and Anode Prokaryotic Communities in Microbial Fuel Cells. *Applied and Environmental Microbiology,* 77**,** 564-571.

REGUERA, G., MCCARTHY, K. D., MEHTA, T., NICOLL, J. S., TUOMINEN, M. T. & LOVLEY, D. R. 2005. Extracellular electron transfer via microbial nanowires. *Nature,* 435**,** 1098-1101.

REGUERA, G., NEVIN, K. P., NICOLL, J. S., COVALLA, S. F., WOODARD, T. L. & LOVLEY, D. R. 2006. Biofilm and nanowire production leads to increased current in *Geobacter sulfurreducens* fuel cells. *Appl Environ Microbiol,* 72**,** 7345-8.

REIMERS, C. E., TENDER, L. M., FERTIG, S. & WANG, W. 2001. Harvesting energy from the marine sediment-water interface. *Environmental Science & Technology,* 35**,** 192-195.

REN, L., TOKASH, J. C., REGAN, J. M. & LOGAN, B. E. 2012. Current generation in microbial electrolysis cells with addition of amorphous ferric hydroxide, Tween 80, or DNA. *International Journal of Hydrogen Energy,* 37**,** 16943-16950.

REN, N.-Q., GUO, W.-Q., WANG, X.-J., XIANG, W.-S., LIU, B.-F., WANG, X.-Z., DING, J. & CHEN, Z.-B. 2008. Effects of different pretreatment methods on fermentation types and dominant bacteria for hydrogen production. *International Journal of Hydrogen Energy,* 33**,** 4318-4324.

REN, Z., WARD, T. E. & REGAN, J. M. 2007. Electricity production from cellulose in a microbial fuel cell using a defined binary culture. *Environ Sci Technol,* 41**,** 4781-6.

REZAEI, F., XING, D. F., WAGNER, R., REGAN, J. M., RICHARD, T. L. & LOGAN, B. E. 2009. Simultaneous Cellulose Degradation and Electricity Production by *Enterobacter cloacae* in a Microbial Fuel Cell. *Applied and Environmental Microbiology,* 75**,** 3673-3678.

RIBOT-LLOBET, E., NAM, J.-Y., TOKASH, J. C., GUISASOLA, A. & LOGAN, B. E. 2013. Assessment of four different cathode materials at different initial pHs using unbuffered catholytes in microbial electrolysis cells. *International Journal of Hydrogen Energy,* 38**,** 2951-2956.

RINCÓN, B., BORJA, R., MARTÍN, M. & MARTÍN, A. 2009. Evaluation of the methanogenic step of a two-stage anaerobic digestion process of acidified olive mill solid residue from a previous hydrolytic–acidogenic step. *Waste management,* 29**,** 2566-2573.

RINGEISEN, B. R., HENDERSON, E., WU, P. K., PIETRON, J., RAY, R., LITTLE, B., BIFFINGER, J. C. & JONES-MEEHAN, J. M. 2006. High power density from a miniature microbial fuel cell using *Shewanella oneidensis* DSP10. *Environmental Science & Technology,* 40**,** 2629-2634.

RISMANI-YAZDI, H., CARVER, S. M., CHRISTY, A. D. & TUOVINEN, I. H. 2008. Cathodic limitations in microbial fuel cells: An overview. *Journal of Power Sources,* 180**,** 683-694.

RISMANI-YAZDI, H., CHRISTY, A. D., CARVER, S. M., YU, Z. T., DEHORITY, B. A. & TUOVINEN, O. H. 2011. Effect of external resistance on bacterial diversity and metabolism in cellulose-fed microbial fuel cells. *Bioresource Technology,* 102**,** 278-283.

ROTH, C., BENKER, N., BUHRMESTER, T., MAZUREK, M., LOSTER, M., FUESS, H., KONINGSBERGER, D. C. & RAMAKER, D. E. 2005. Determination of OH and CO coverage and adsorption sites on PtRu electrodes in an operating PEM fuel cell. *J Am Chem Soc,* 127**,** 14607-15.

ROZENDAL, R. A., HAMELERS, H. V. M. & BUISMAN, C. J. N. 2006a. Effects of membrane cation transport on pH and microbial fuel cell performance. *Environmental Science & Technology,* 40**,** 5206-5211.

ROZENDAL, R. A., HAMELERS, H. V. M., EUVERINK, G. J. W., METZ, S. J. & BUISMAN, C. J. N. 2006b. Principle and perspectives of hydrogen production through biocatalyzed electrolysis. *International Journal of Hydrogen Energy,* 31**,** 1632-1640.

ROZENDAL, R. A., HAMELERS, H. V. M., MOLENKMP, R. J. & BUISMAN, J. N. 2007. Performance of single chamber biocatalyzed electrolysis with different types of ion exchange membranes. *Water Research,* 41**,** 1984-1994.

ROZENDAL, R. A., HAMELERS, H. V. M., RABAEY, K., KELLER, J. & BUISMAN, C. J. N. 2008a. Towards practical implementation of bioelectrochemical wastewater treatment. *Trends in Biotechnology,* 26**,** 450-459.

ROZENDAL, R. A., HARNISCH, F., JEREMIASSE, A. W. & SCHRÖDER, U. 2009a. Chemically catalyzed cathodes in bio-electrochemical systems. *IWA Integrated Environmental Technology.*

ROZENDAL, R. A., JEREMIASSE, A. W., HAMELERS, H. V. M. & BUISMAN, C. J. N. 2008b. Hydrogen production with a microbial biocathode. *Environmental Science & Technology,* 42**,** 629-634.

ROZENDAL, R. A., LEONE, E., KELLER, J. & RABAEY, K. 2009b. Efficient hydrogen peroxide generation from organic matter in a bioelectrochemical system. *Electrochemistry Communications,* 11**,** 1752-1755.

SCOTT, K., RIMBU, G. A., KATURI, K. P., PRASAD, K. K. & HEAD, I. M. 2007. Application of modified carbon anodes in microbial fuel cells. *Process Safety and Environmental Protection,* 85**,** 481-488.

SEELIGER, S., CORD-RUWISCH, R. & SCHINK, B. 1998. A periplasmic and extracellular c-type cytochrome of *Geobacter sulfurreducens* acts as a ferric iron reductase and as an electron carrier to other acceptors or to partner bacteria. *Journal of Bacteriology,* 180**,** 3686-3691.

SEKOMO, C. B., KAGISHA, V., ROUSSEAU, D. & LENS, P. 2012. Heavy metal removal by combining anaerobic upflow packed bed reactors with water hyacinth ponds. *Environ Technol,* 33**,** 1455-64.

SELEMBO, P. A., MERRILL, M. D. & LOGAN, B. E. 2009a. The use of stainless steel and nickel alloys as low-cost cathodes in microbial electrolysis cells. *Journal of Power Sources,* 190**,** 271-278.

SELEMBO, P. A., MERRILL, M. D. & LOGAN, B. E. 2010. Hydrogen production with nickel powder cathode catalysts in microbial electrolysis cells. *International Journal of Hydrogen Energy,* 35**,** 428-437.

SELEMBO, P. A., PEREZ, J. M., LLOYD, W. A. & LOGAN, B. E. 2009b. High hydrogen production from glycerol or glucose by electrohydrogenesis using microbial electrolysis cells. *International Journal of Hydrogen Energy,* 34**,** 5373-5381.

SELL, D., KRAMER, P. & KREYSA, G. 1989. Use of an Oxygen Gas-Diffusion Cathode and a 3-Dimensional Packed-Bed Anode in a Bioelectrochemical Fuel Cell. *Applied Microbiology and Biotechnology,* 31**,** 211-213.

SENTHILKUMAAR, S., VARADARAJAN, P. R., PORKODI, K. & SUBBHURAAM, C. 2005. Adsorption of methylene blue onto jute fiber carbon: kinetics and equilibrium studies. *Journal of Colloid and Interface Science,* 284**,** 78-82.

SEO, H. N., LEE, W. J., HWANG, T. S. & PARK, D. H. 2009. Electricity generation coupled with wastewater treatment using a microbial fuel cell composed of a modified cathode with a ceramic membrane and cellulose acetate film. *J Microbiol Biotechnol,* 19**,** 1019-27.

SEVDA, S., DOMINGUEZ-BENETTON, X., VANBROEKHOVEN, K., SREEKRISHNAN, T. R. & PANT, D. 2013. Characterization and comparison of the performance of two different separator types in air–cathode microbial fuel cell treating synthetic wastewater. *Chemical Engineering Journal,* 228**,** 1-11.

SHARMA, C. S., AWASTHI, R., SINGH, R. N. & SINHA, A. S. 2013. Graphene-cobaltite-Pd hybrid materials for use as efficient bifunctional electrocatalysts in alkaline direct methanol fuel cells. *Phys Chem Chem Phys,* 15**,** 20333-44.

SHARMA, T., REDDY, A. L. M., CHANDRA, T. S. & RAMAPRABHU, S. 2008. Development of carbon nanotubes and nanofluids based microbial fuel cell. *International Journal of Hydrogen Energy,* 33**,** 6749-6754.

SHARMA, Y. & LI, B. 2010a. Optimizing energy harvest in wastewater treatment by combining anaerobic hydrogen producing biofermentor (HPB) and microbial fuel cell (MFC). *International Journal of Hydrogen Energy,* 35**,** 3789-3797.

SHARMA, Y. & LI, B. 2010b. The variation of power generation with organic substrates in single-chamber microbial fuel cells (SCMFCs). *Bioresource Technology,* 101**,** 1844-1850.

SHEN, Y., WANG, M., CHANG, I. S. & NG, H. Y. 2013. Effect of shear rate on the response of microbial fuel cell toxicity sensor to Cu(II). *Bioresour Technol,* 136**,** 707-10.

SHI, X.-X., SONG, H.-C., WANG, C.-R., TANG, R.-S., HUANG, Z.-X., GAO, T.-R. & XIE, J. 2010. Enhanced bio-hydrogen production from sweet sorghum stalk with alkalization pretreatment by mixed anaerobic cultures. *International Journal of Energy Research,* 34**,** 662-672.

SHI, X., FENG, Y., WANG, X., LEE, H., LIU, J., QU, Y., HE, W., KUMAR, S. M. & REN, N. 2012. Application of nitrogen-doped carbon powders as low-cost and durable cathodic catalyst to air-cathode microbial fuel cells. *Bioresour Technol,* 108**,** 89-93.

SLEUTELS, T. H. J. A., HAMELERS, H. V. M., ROZENDAL, R. A. & BUISMAN, C. J. N. 2009a. Ion transport resistance in Microbial Electrolysis Cells with anion and cation exchange membranes. *International Journal of Hydrogen Energy,* 34**,** 3612-3620.

SLEUTELS, T. H. J. A., LODDER, R., HAMELERS, H. V. M. & BUISMAN, C. J. N. 2009b. Improved performance of porous bio-anodes in microbial electrolysis cells by enhancing mass and charge transport. *International Journal of Hydrogen Energy,* 34**,** 9655-9661.

STRANDBERG, G. W., SHUMATE, S. E. & PARROTT, J. R. 1981. Microbial Cells as Biosorbents for Heavy Metals: Accumulation of Uranium by *Saccharomyces cerevisiae* and *Pseudomonas aeruginosa*. *Appl Environ Microbiol,* 41**,** 237-45.

SUKKASEM, C., LAEHLAH, S., HNIMAN, A., O'THONG, S., BOONSAWANG, P., RARNGNARONG, A., NISOA, M. & KIRDTONGMEE, P. 2011. Upflow bio-filter circuit (UBFC): Biocatalyst microbial fuel cell (MFC) configuration and application to biodiesel wastewater treatment. *Bioresource Technology,* 102**,** 10363-10370.

SUMMERS, Z. M., FOGARTY, H. E., LEANG, C., FRANKS, A. E., MALVANKAR, N. S. & LOVLEY, D. R. 2010. Direct exchange of electrons within aggregates of an evolved syntrophic coculture of anaerobic bacteria. *Science,* 330**,** 1413-5.

SUN, M., SHENG, G. P., ZHANG, L., XIA, C. R., MU, Z. X., LIU, X. W., WANG, H. L., YU, H. Q., QI, R., YU, T. & YANG, M. 2008. An MEC-MR-Coupled System for Biohydrogen Production from Acetate. *Environmental Science & Technology,* 42**,** 8095-8100.

SUND, C. J., MCMASTERS, S., CRITTENDEN, S. R., HARRELL, L. E. & SUMNER, J. J. 2007. Effect of electron mediators on current generation and fermentation in a microbial fuel cell. *Appl Microbiol Biotechnol,* 76**,** 561-8.

SURYAWANSHI, P. C., CHAUDHARI, A. B. & KOTHARI, R. M. 2010. Thermophilic anaerobic digestion: the best option for waste treatment. *Crit Rev Biotechnol,* 30**,** 31-40.

TANG, X. H., GUO, K., LI, H. R., DU, Z. W. & TIAN, J. L. 2011. Electrochemical treatment of graphite to enhance electron transfer from bacteria to electrodes. *Bioresource Technology,* 102**,** 3558-3560.

TARTAKOVSKY, B., MANUEL, M. F., NEBURCHILOV, V., WANG, H. & GUIOT, S. R. 2008. Biocatalyzed hydrogen production in a continuous flow microbial fuel cell with a gas phase cathode. *Journal of Power Sources,* 182**,** 291-297.

TARTAKOVSKY, B., MANUEL, M. F., WANG, H. & GUIOT, S. R. 2009. High rate membrane-less microbial electrolysis cell for continuous hydrogen production. *International Journal of Hydrogen Energy,* 34**,** 672-677.

TER HEIJNE, A., HAMELERS, H. V. M., SAAKES, M. & BUISMAN, C. J. N. 2008. Performance of non-porous graphite and titanium-based anodes in microbial fuel cells. *Electrochimica Acta,* 53**,** 5697-5703.

THAUER, R. K. 1998. Biochemistry of methanogenesis: a tribute to Marjory Stephenson. *Microbiology-Uk,* 144**,** 2377-2406.

THAUER, R. K., JUNGERMANN, K. & DECKER, K. 1977. Energy-Conservation in Chemotropic Anaerobic Bacteria. *Bacteriological Reviews,* 41**,** 100-180.

THAUER, R. K., KASTER, A. K., SEEDORF, H., BUCKEL, W. & HEDDERICH, R. 2008. Methanogenic archaea: ecologically relevant differences in energy conservation. *Nature Reviews Microbiology,* 6**,** 579-591.

THOMPSON, L., BARBIER, F., FRIEDLAND, R., KICZEK, E., NOZIK, A., RICHMOND, G., SHAW, R. & WILSON, D. Report of the Hydrogen Production Expert Panel: A Subcommittee of the Hydrogen & Fuel Cell Technical Advisory Committee. *In:* STEVEN CHU, S. C., RICHARD GREENE, LEVI THOMPSON,ROBERT SHAW, LARRY BURNS, MARK CARDILLO, SUNITA SATYAPAL, ed. A Subcommittee of the Hydrogen & Fuel Cell Technical Advisory Committee, 2013 Washington, DC 20585. U.S Department of Energy's Hydrogen and Fuel Cell Technologies Program

TIAN, J., MOROZAN, A., SOUGRATI, M. T., LEFEVRE, M., CHENITZ, R., DODELET, J. P., JONES, D. & JAOUEN, F. 2013. Optimized synthesis of Fe/N/C cathode catalysts for PEM fuel cells: a matter of iron-ligand coordination strength. *Angew Chem Int Ed Engl,* 52**,** 6867-70.

TORRES, C. I., MARCUS, A. K., LEE, H. S., PARAMESWARAN, P., KRAJMALNIK-BROWN, R. & RITTMANN, B. E. 2010. A kinetic perspective on extracellular electron transfer by anode-respiring bacteria. *Fems Microbiology Reviews,* 34**,** 3-17.

TORRES, C. I., MARCUS, A. K. & RITTMANN, B. E. 2008. Proton transport inside the biofilm limits electrical current generation by anode-respiring bacteria. *Biotechnology and Bioengineering,* 100**,** 872-881.

TSAI, H. Y., WU, C. C., LEE, C. Y. & SHIH, E. P. 2009. Microbial fuel cell performance of multiwall carbon nanotubes on carbon cloth as electrodes. *Journal of Power Sources,* 194**,** 199-205.

UK LEE, H., YOUNG YOO, H., LKHAGVASUREN, T., SEOK SONG, Y., PARK, C., KIM, J. & WOOK KIM, S. 2013. Enzymatic fuel cells based on electrodeposited graphite oxide/cobalt hydroxide/chitosan composite-enzyme electrode. *Biosens Bioelectron,* 42**,** 342-8.

VAN EERTEN-JANSEN, M. C. A. A., VELDHOEN, A. B., PLUGGE, C. M., STAMS, A. J. M., BUISMAN, C. J. N. & TER HEIJNE, A. 2013. Microbial Community Analysis of a Methane-Producing Biocathode in a Bioelectrochemical System. *Archaea,* 2013**,** 12.

VENKATA MOHAN, S., LALIT BABU, V. & SARMA, P. N. 2008. Effect of various pretreatment methods on anaerobic mixed microflora to enhance biohydrogen production utilizing dairy wastewater as substrate. *Bioresource Technology,* 99**,** 59-67.

VENKATARAMAN, A., ROSENBAUM, M., ARENDS, J. B. A., HALITSCHKE, R. & ANGENENT, L. T. 2010. Quorum sensing regulates electric current generation of *Pseudomonas aeruginosa* PA14 in bioelectrochemical systems. *Electrochemistry Communications,* 12**,** 459-462.

VILLANO, M., AULENTA, F., CIUCCI, C., FERRI, T., GIULIANO, A. & MAJONE, M. 2010. Bioelectrochemical reduction of CO_2 to CH_4 via direct and indirect extracellular electron transfer by a hydrogenophilic methanogenic culture. *Bioresource Technology,* 101**,** 3085-3090.

WAGNER, R. C., REGAN, J. M., OH, S. E., ZUO, Y. & LOGAN, B. E. 2009. Hydrogen and methane production from swine wastewater using microbial electrolysis cells. *Water Research,* 43**,** 1480-1488.

WAN, C. H., WU, C. L., LIN, M. T. & SHIH, C. 2010. New electrocatalysts for unitized regenerative fuel cell: Pt-Ir alloy deposited on the proton exchange membrane surface by impregnation-reduction method. *J Nanosci Nanotechnol,* 10**,** 4612-8.

WANG, A. J., LIU, L. H., SUN, D., REN, N. Q. & LEE, D. J. 2010a. Isolation of Fe(III)-reducing fermentative bacterium *Bacteroides* sp. W7 in the anode suspension of a microbial electrolysis cell (MEC). *International Journal of Hydrogen Energy,* 35**,** 3178-3182.

WANG, A. J., LIU, W. Z., CHENG, S. A., XING, D. F., ZHOU, J. H. & LOGAN, B. E. 2009a. Source of methane and methods to control its formation in single chamber microbial electrolysis cells. *International Journal of Hydrogen Energy,* 34**,** 3653-3658.

WANG, A. J., SUN, D., CAO, G. L., WANG, H. Y., REN, N. Q., WU, W. M. & LOGAN, B. E. 2011. Integrated hydrogen production process from cellulose by combining dark fermentation, microbial fuel cells, and a microbial electrolysis cell. *Bioresource Technology,* 102**,** 4137-4143.

WANG, A. J., SUN, D., REN, N. Q., LIU, C., LIU, W. Z., LOGAN, B. E. & WU, W. M. 2010b. A rapid selection strategy for an anodophilic consortium for microbial fuel cells. *Bioresource Technology,* 101**,** 5733-5735.

WANG, C. T., CHEN, W. J. & HUANG, R. Y. 2010c. Influence of growth curve phase on electricity performance of microbial fuel cell by *Escherichia coli*. *International Journal of Hydrogen Energy,* 35**,** 7217-7223.

WANG, H., SWEIKART, M. A. & TURNER, J. A. 2003. Stainless steel as bipolar plate material for polymer electrolyte membrane fuel cells. *Journal of Power Sources,* 115**,** 243-251.

WANG, H., WANG, G., LING, Y., QIAN, F., SONG, Y., LU, X., CHEN, S., TONG, Y. & LI, Y. 2013. High power density microbial fuel cell with flexible 3D graphene-nickel foam as anode. *Nanoscale,* 5**,** 10283-10290.

WANG, M., WANG, Z., GONG, X. & GUO, Z. 2014. The intensification technologies to water electrolysis for hydrogen production – A review. *Renewable and Sustainable Energy Reviews,* 29**,** 573-588.

WANG, S. B., ZHU, Z. H., COOMES, A., HAGHSERESHT, F. & LU, G. Q. 2005. The physical and surface chemical characteristics of activated carbons and the adsorption of methylene blue from wastewater. *Journal of Colloid and Interface Science,* 284**,** 440-446.

WANG, X., CHENG, S. A., FENG, Y. J., MERRILL, M. D., SAITO, T. & LOGAN, B. E. 2009b. Use of Carbon Mesh Anodes and the Effect of Different Pretreatment Methods on Power Production in Microbial Fuel Cells. *Environmental Science & Technology,* 43**,** 6870-6874.

WANG, Z., MEI, X., MA, J. & WU, Z. 2012. Recent advances in microbial fuel cells integrated with sludge treatment. *Chemical Engineering & Technology,* 35**,** 1733-1743.
WATSON, R. T., ZINYOWERA, M. C. & MOSS, R. H. 1996. Technologies, Policies and Measures for Mitigating Climate Change. *IPCC Technical Paper* 1**,** 84.
WATSON, V. J. & LOGAN, B. E. 2010. Power production in MFCs inoculated with *Shewanella oneidensis* MR-1 or mixed cultures. *Biotechnology and Bioengineering,* 105**,** 489-498.
WEI, L., HAN, H. & SHEN, J. 2012. Effects of cathodic electron acceptors and potassium ferricyanide concentrations on the performance of microbial fuel cell. *International Journal of Hydrogen Energy,* 37**,** 12980-12986.
WEN, Q., KONG, F. Y., ZHENG, H. T., CAO, D. X., REN, Y. M. & YIN, J. L. 2011. Electricity generation from synthetic penicillin wastewater in an air-cathode single chamber microbial fuel cell. *Chemical Engineering Journal,* 168**,** 572-576.
WHITE, C. M., STEEPER, R. R. & LUTZ, A. E. 2006. The hydrogen-fueled internal combustion engine: a technical review. *International Journal of Hydrogen Energy,* 31**,** 1292-1305.
WILKINSON, S. 2000. "Gastrobots" - Benefits and challenges of microbial fuel cells in food powered robot applications. *Autonomous Robots,* 9**,** 99-111.
WILLENBORG, M., GHALY, H., HATLAPATKA, K., URBAN, K., PANTEN, U. & RUSTENBECK, I. 2010. The signalling role of action potential depolarization in insulin secretion: Metabolism-dependent dissociation between action potential increase and secretion increase by TEA. *Biochemical Pharmacology,* 80**,** 104-112.
WILLNER, I., ARAD, G. & KATZ, E. 1998. A biofuel cell based on pyrroloquinoline quinone and microperoxidase-1 monolayer-functionalized electrodes. *Bioelectrochemistry and Bioenergetics,* 44**,** 209-214.
WINFIELD, J., IEROPOULOS, I. & GREENMAN, J. 2010. The overshoot phenomenon as a function of internal resistance in microbial fuel cells. *Journal of Biotechnology,* 150**,** S23-S23.
WINFIELD, J., IEROPOULOS, I., GREENMAN, J. & DENNIS, J. 2011. The overshoot phenomenon as a function of internal resistance in microbial fuel cells. *Bioelectrochemistry,* 81**,** 22-27.
WONG, Y. M., WU, T. Y. & JUAN, J. C. 2014. A review of sustainable hydrogen production using seed sludge via dark fermentation. *Renewable and Sustainable Energy Reviews,* 34**,** 471-482.
WRIGHTON, K. C., AGBO, P., WARNECKE, F., WEBER, K. A., BRODIE, E. L., DESANTIS, T. Z., HUGENHOLTZ, P., ANDERSEN, G. L. & COATES, J. D. 2008. A novel ecological role of the Firmicutes identified in thermophilic microbial fuel cells. *ISME J,* 2**,** 1146-56.
WU, C.-H., LAI, C.-Y., LIN, C.-W. & KAO, M.-H. 2013a. Generation of Power by Microbial Fuel Cell with Ferricyanide in Biodegradation of Benzene. *CLEAN – Soil, Air, Water,* 41**,** 390-395.
WU, K.-J. & CHANG, J.-S. 2007. Batch and continuous fermentative production of hydrogen with anaerobic sludge entrapped in a composite polymeric matrix. *Process Biochemistry,* 42**,** 279-284.
WU, X. Y., SONG, T. S., ZHU, X. J., WEI, P. & ZHOU, C. C. 2013b. Construction and Operation of Microbial Fuel Cell with *Chlorella vulgaris* Biocathode for Electricity Generation. *Appl Biochem Biotechnol,* 171**,** 2082-92.
XIE, X., HU, L., PASTA, M., WELLS, G. F., KONG, D., CRIDDLE, C. S. & CUI, Y. 2010. Three-Dimensional Carbon Nanotube−Textile Anode for High-Performance Microbial Fuel Cells. *Nano Letters,* 11**,** 291-296.

XING, D. F., ZUO, Y., CHENG, S. A., REGAN, J. M. & LOGAN, B. E. 2008. Electricity generation by *Rhodopseudomonas palustris* DX-1. *Environmental Science & Technology,* 42**,** 4146-4151.

XU, M., FANG, Y., LIU, J., CHEN, X., SUN, G., GUO, J., HUA, Z., TU, Q., WU, L., ZHOU, J. & LIU, X. 2013. Draft Genome Sequence of *Shewanella decolorationis* S12, a Dye-Degrading Bacterium Isolated from a Wastewater Treatment Plant. *Genome Announc,* 1.

YAMAMOTO, K., MATSUMOTO, T., SHIMADA, S., TANAKA, T. & KONDO, A. 2013. Starchy biomass-powered enzymatic biofuel cell based on amylases and glucose oxidase multi-immobilized bioanode. *N Biotechnol,* 30**,** 531-5.

YONG, Y. C., YU, Y. Y., YANG, Y., LIU, J., WANG, J. Y. & SONG, H. 2013. Enhancement of extracellular electron transfer and bioelectricity output by synthetic porin. *Biotechnol Bioeng,* 110**,** 408-16.

YOU, S. J., REN, N. Q., ZHAO, Q. L., WANG, J. Y. & YANG, F. L. 2009. Power Generation and Electrochemical Analysis of Biocathode Microbial Fuel Cell Using Graphite Fibre Brush as Cathode Material. *Fuel Cells,* 9**,** 588-596.

YOUNG, T. G., HADJIPETROU, L. & LILLY, M. D. 1966. The Theoretical Aspects of Biochemical Fuel Cells. *Biotechnology and Bioengineering,* 3**,** 581-593.

YUAN, Y., ZHAO, B., ZHOU, S., ZHONG, S. & ZHUANG, L. 2011. Electrocatalytic activity of anodic biofilm responses to pH changes in microbial fuel cells. *Bioresour Technol,* 102**,** 6887-91.

ZAIN, S. M., ROSLANI, N. S., HASHIM, R., ANUAR, N., SUJA, F., DAUD, W. R. W. & BASRI, N. E. A. 2011. Microbial Fuel Cells using Mixed Cultures of Wastewater for Electricity Generation. *Sains Malaysiana,* 40**,** 993-997.

ZENG, J., HE, B., LAMB, K., DE MARCO, R., SHEN, P. K. & JIANG, S. P. 2013. Phosphoric acid functionalized pre-sintered meso-silica for high temperature proton exchange membrane fuel cells. *Chem Commun (Camb),* 49**,** 4655-7.

ZHANG, F., CHENG, S. A., PANT, D., VAN BOGAERT, G. & LOGAN, B. E. 2009a. Power generation using an activated carbon and metal mesh cathode in a microbial fuel cell. *Electrochemistry Communications,* 11**,** 2177-2179.

ZHANG, F., DING, J., SHEN, N., ZHANG, Y., DING, Z., DAI, K. & ZENG, R. J. 2013. In situ hydrogen utilization for high fraction acetate production in mixed culture hollow-fiber membrane biofilm reactor. *Appl Microbiol Biotechnol,* 97**,** 10233-40.

ZHANG, F. & KEASLING, J. 2011. Biosensors and their applications in microbial metabolic engineering. *Trends Microbiol,* 19**,** 323-9.

ZHANG, F., SAITO, T., CHENG, S. A., HICKNER, M. A. & LOGAN, B. E. 2010. Microbial Fuel Cell Cathodes With Poly(dimethylsiloxane) Diffusion Layers Constructed around Stainless Steel Mesh Current Collectors. *Environmental Science & Technology,* 44**,** 1490-1495.

ZHANG, G., ZHAO, Q., JIAO, Y., WANG, K., LEE, D. J. & REN, N. 2012a. Biocathode microbial fuel cell for efficient electricity recovery from dairy manure. *Biosens Bioelectron,* 31**,** 537-43.

ZHANG, J., ZHANG, Y. & QUAN, X. 2012b. Electricity assisted anaerobic treatment of salinity wastewater and its effects on microbial communities. *Water Research,* 46**,** 3535-3543.

ZHANG, L., LI, C., DING, L., XU, K. & REN, H. 2011a. Influences of initial pH on performance and anodic microbes of fed-batch microbial fuel cells. *Journal of Chemical Technology & Biotechnology,* 86**,** 1226-1232.

ZHANG, L., ZHU, X., LI, J., LIAO, Q. & YE, D. 2011b. Biofilm formation and electricity generation of a microbial fuel cell started up under different external resistances. *Journal of Power Sources,* 196**,** 6029-6035.

ZHANG, X. Y., CHENG, S. A., WANG, X., HUANG, X. & LOGAN, B. E. 2009b. Separator Characteristics for Increasing Performance of Microbial Fuel Cells. *Environmental Science & Technology,* 43**,** 8456-8461.

ZHAO, F., HARNISH, F., SCHRÖDER, U., SCHOLTZ, F. & HERRMANN, I. 2006. Challenges and Constraints of Using Oxygen Cathodes in Microbial Fuel Cells *Evironmental Science and Technology,* 40.

ZHAO, F., RAHUNEN, N., VARCOE, J. R., CHANDRA, A., AVIGNONE-ROSSA, C., THUMSER, A. E. & SLADE, R. C. T. 2008. Activated carbon cloth as anode for sulfate removal in a microbial fuel cell. *Environmental Science & Technology,* 42**,** 4971-4976.

ZHAO, F., SCHRÖDER, F. H. U., SCHOLTZ, F., BOGDANOFF, P. & HERRMANN, I. 2005. Application of Pyrolysed Iron (II) Phthallocyanine and CoTMPP Based Oxygen Reduction Catalysis as Cathode Materials in Microbial Fuel Cells. *Electrochemistry Communications* 7**,** 1405 - 1410.

ZHU, X. & LOGAN, B. E. 2013. Copper anode corrosion affects power generation in microbial fuel cells. *Journal of Chemical Technology and Biotechnology*.

ZHU, X., ZHANG, L., LI, J., LIAO, Q. & YE, D.-D. 2013. Performance of liter-scale microbial fuel cells with electrode arrays: Effect of array pattern. *International Journal of Hydrogen Energy,* 38**,** 15716-15722.

ZHUANG, L., ZHOU, S. G., WANG, Y. Q., LIU, C. S. & GENG, S. 2009. Membrane-less cloth cathode assembly (CCA) for scalable microbial fuel cells. *Biosensors & Bioelectronics,* 24**,** 3652-3656.

ZOBELL, C. E. 1943. The Effect of Solid Surfaces upon Bacterial Activity. *J Bacteriol,* 46**,** 39-56.

ZOU, Y. J., XIANG, C. L., YANG, L. N., SUN, L. X., XU, F. & CAO, Z. 2008. A mediatorless microbial fuel cell using polypyrrole coated carbon nanotubes composite as anode material. *International Journal of Hydrogen Energy,* 33**,** 4856-4862.

ZUO, Y., CHENG, S., CALL, D. & LOGAN, B. E. 2007. Tubular membrane cathodes for scalable power generation in microbial fuel cells. *Environmental Science & Technology,* 41**,** 3347-3353.

ZUO, Y., CHENG, S. & LOGAN, B. E. 2008a. Ion exchange membrane cathodes for scalable microbial fuel cells. *Environmental Science & Technology,* 42**,** 6967-6972.

ZUO, Y., XING, D. F., REGAN, J. M. & LOGAN, B. E. 2008b. Isolation of the exoelectrogenic bacterium *Ochrobactrum anthropi* YZ-1 by using a U-tube microbial fuel cell. *Applied and Environmental Microbiology,* 74**,** 3130-3137.

9. Appendices Electricity and Hydrogen Producing Microorganisms

9.1 Appendix A-1

Taxon (left column) is a term that describes either phylum or class of bacteria. In tables A-1 on and A-2 fermicutes, actinobacteria and proteobacteria are different phylums. *Chlorophyta* is a division (term division in botany is same as phylum in microbiology) for of green algae, informally called *Chlorophytes*, which belongs to different domain eukaryotes, kingdom plantae. Phylum proteobacteria are split is split into 4 classes α, β, γ and δ. Substrates reported in literature degraded by particular taxon of bacteria are placed in the right column.

Word taxon describes the rank-based classification, of bacteria or plants. The higherarchy of biological classification established by Carl von Linné (Blunt and Brunius, 2002) has nine major ranks from highest to lowest: life, domain, kingdom, phylum class, order, family, genus and species. In classification of life, there are three domains (eukaryotes, bacteria and archaea) which, in terms of taxonomy, have several different conventions between them and between their subdivisions as are studied by different disciplines (botany, zoology, mycology and microbiology), for example in microbiology there are type strains and in zoology there are type specimens. In the scientific classification each species (lowest rank) has to be assigned to a genus (a rank one step higher), which in turn is a lower level of a hierarchy of ranks.

Table A-1.1 – Electricity producing microorganisms and substrates used in microbial fuel cells (MFCs).

Taxon:	Microbes:	Substrate:	Application:
α-proteobacteria	*Rhodopseudomonas palustris* DX-1	acetate	self produced mediators detected (Xing et al., 2008)
	Ochrobacterium anthropi YZ-1	acetate	mediatorless MFC, ammonia treated carbon cloth anode (Zuo et al., 2008b)
	Acidiphylium sp. 3.2sup5	glucose	mediatorless MFC (Malki et al., 2008)
β-proteobacteria	*Rhodoferax ferrireducens*	glucose	mediatorless MFC (Chaudhuri and Lovley, 2003)
γ-proteobacteria	*Actinobacillus succinogenes*	fumarate,	dissolved NR and MV mediated MFC (Park et al., 1999)
	Actinobacillus succinogenes	glucose	dissolved NR mediated MFC (Park and Zeikus, 1999, Park and Zeikus, 2000)
	Aeromonas hydrophylia	acetate	c type cytochrome (Pham et al., 2003)
	Enterobacter cloacae	cellulose	mediatorless MFC (Rezaei et al., 2009)
	Enterobacter cloacae	MYG medium	dissolved MB mediated MFC (Mohan and Das, 2009, Mohan et al., 2008b)

Table A-1.1 – Electricity producing microorganisms and substrates used in MFCs (continued).

Taxon:	Microbes:	Substrate:	Application:
Γ-proteobacteria	*Escherichia coli*	beef extract and peptone or yeast extract and peptone	dissolved MB mediated MFC (Wang et al., 2010c)
	Pseudomonas species	wastewater	dissolved MB and NR mediated MFC (Daniel et al., 2009)
	Shewanella putrefaciens IR 1	lactate, pyruvate, glucose	substrate contining (FeOOH) to enhance cytochrome activity (Kim et al., 1999b) mediatorless MFC (Kim et al., 1999a)
	Shewanella oneidensis MR 1	glutamate, lactate, pyruvate	mediatorless MFC (Feng et al., 2012)
	Shewanella oneidensis	lactate	mediatorless MFC (Ringeisen et al., 2006)
	Escherichia coli	glucose	immobilized NR, Fe^{3+} and Mn^{4+} mediated MFC (Park and Zeikus, 2003, Park et al., 2000)
Δ-proteobacteria	*Geobacter metallireducens*	acetate	mediator- less MFC (Min et al., 2005)
	Geobacter sulfurreduciens	acetate	mediator- less MFC (Bond and Lovley, 2003)

Table A-1.1 – Electricity producing microorganisms and substrates used in MFCs (continued).

Taxon:	Microbes:	Substrate:	Application:
Δ-proteobacteria	mixed culture containing *Geobacter* species	nitrate and nitrate supplied with perchlorate	mediatorless MFC (Butler et al., 2010)
	Achromobacter and *Azovibrio* species	propionate fed MFC under closed circuit conditions	mediatorless MFC (de Carcer et al., 2011)
Firmicutes	*Lactococcus lactis*	glucose	ACNQ mediated MFC (Freguia et al., 2009)
	Clostridium cellulolyticum	acetate, lactate	dissolved AQDS, safranine O, resazurin, methylene blue, and humic acid mediated MFC (Sund et al., 2007)
	Clostridium butyricum	starch	mediatorless MFC (Niessen et al., 2004b)
Acidobacteria	*Geothrix fermentans*	acetate, propionate, malate, lactate	self produced mediators detected (Bond and Lovley, 2005)
Actinobacteria	*Propionibacterium freudenreichii*	glucose	produced ACNQ for ACNQ mediated MFC (Freguia et al., 2009)
Chlorophyta	*Chlorella vulgaris*	carbon dioxide	mediatorless MFC (Wu et al., 2013b)

Table A-1.1 – Electricity producing microorganisms and substrates used in MFCs (continued).

Taxon:	Microbes:	Substrate:	Application:
Chlorophyta	*Chlamydomonas reinhardtii* and *Pseudokirchneriella sub-capitata*	carbon dioxide	mediatorless MFC (De Schamphelaire and Verstraete, 2009)
–	mixed culture	methanol, ethanol	mediatorless MFC (Kim et al., 2007b)
	mixed culture	congo red (CR)	mediatorless MFC (Li et al., 2010b)
	mixed culture	butyrate	mediatorless MFC (Liu et al., 2005b)
	mixed culture	palm oil waste	mediatorless MFC coupled with USAB reactor (Cheng et al., 2010)
	mixed culture	M9 medium spiked with iron sulfide	mediatorless MFC (Rabaey et al., 2006)
	mixed culture	carbon dioxide	mediatorless MFC (Villano et al., 2010)
	mixed culture	synthetic penicillin	mediatorless MFC (Wen et al., 2011)
	mixed culture	xylose	mediatorless MFC (Catal et al., 2008)
	mixed culture	humic acid	mediatorless MFC (Huang and Angelidaki, 2008)

Table A-1.2 – Hydrogen producing microorganisms and substrates used in microbial electrolysis cells (MECs).

Taxon:	Microbes or inoculum:	Substrate:	Application:
α-proteobacteria	*Rhodobacter*	carbon dioxide, ormerod medium	mediatorless MEC (Fedorov et al., 1998)
β-proteobacteria and δ-proteobacteria		acetate	two chamber mediatorless MEC (Geelhoed et al., 2010, Chae et al., 2008)
δ-proteobacteria	*Geobacter sulfurreduces* and *Pelobacter propionicus*	acetate	single chamber mediator-less MEC (Selembo et al., 2010)
	Geobacter sulfurreducens	acetate	mediator- less MEC (Call et al., 2009b)
	mixed culture containing *Geobacter sulfurreducens*	potato wastewater containing acetate, glucose and propionate	mediator- less MFC and MEC (Chae et al., 2009, Kiely et al., 2011)
	mixed culture	acetate	mediator- scaled up one chamber MEC (Rader and Logan, 2010)
	Mixed culture	acetate butyrate glucose lactic acid propionic acid valeric acid	Two chamber mediatorless H type MEC (Cheng and Logan, 2007a)
Firmicutes	*Thermo-anaerobacterium* species	cellulose	mediatorless MEC (Nissila et al., 2011, Liu et al., 2003)

Table A-1.2 – Hydrogen producing microorganisms and substrates used in MECs (continued).

Taxon:	Microbes or inoculum:	Substrate:	Application:
Firmicutes	*Desulfitobacterium freudenreichii*	swine wastewater	mediatorless MEC (Wagner et al., 2009)
Unknown	anaerobic sludge	acetate	single chamber mediatorless MEC (Guo et al., 2010)
	marine sediments	acetate	two chamber mediatorless MEC (Munoz et al., 2010)
	effluent from another MEC	acetate	mediatorless MEC (Rozendal et al., 2008b, Sleutels et al., 2009b, Sleutels et al., 2009a)

9.2 Appendix A-2 Perfomance Factors for MFCs and MECs

The references, for microbial fuel cells (MFCs) are arranged in four tables. Comparison of different anode materials and different anode treatments to bacteria taxon, inoculation sources (if mixed cultures are used it has not been established what bacteria these mixed cultures contain) performance factors (Table A-2.1 and A-2.2) and comparison of different cathode materials and different cathode treatments to (P_{max}) values (Table A-2.3 and A-2.4).

The Performance Factors Shown in Tables are:-

Power density (P_{max}), for MFCs only, the amount of power (time rate of energy transfer) per unit volume, to show that and continuous voltage output over the batch cycles to show that MFCs are capable of continuous voltage output, over fixed resistance, until the substrate is exhausted, compared to anode, cathode and / or volumes of anode chambers.

Coulombic efficiencies (described in "Electrochemical Analysis Methods" section 4.7 in greater detail), to show how much substrate consumed by bacteria is converted into current, for both MFCs and MECs.

Table A-2.1 – Comparison of different anode materials and anode configurations, in microbial fuel cells (MFCs).

Electrode materials		Configuration and CE	Electrode size	Inoculation source	Reactor configuration	P_{max}	References
Carbon	carbon cloth	plane	3 mm in diameter, 0.3 mm thick	domestic wastewater	1 chamber air-cathode	1010 Wm^{-3} compared to the anode chamber size	(Fan et al., 2007)
Carbon	carbon veil	plane	22.5 cm^2	primary clarifier overflow	2 chamber air-cathode	600 mWm^{-2} (anode area)	(Logan et al., 2007b)
Carbon	carbon cloth	plane	7 cm^2	preacclimated bacteria from an active MFC	1 chamber cube air- cathode MFCs	46 Wm^{-3} (anode chamber volume)	(Zhang et al., 2009b)
Carbon	activated carbon cloth	plane	1.5 cm^2	*D. desulfuricans* strain Essex 6 (for sulfate removal)	1 chamber air-cathode	0.51mW cm^{-2} (anode area)	(Zhao et al., 2008)
Carbon	graphite plate	plane	155 cm^2	*Shewanella oneidensis* (MR – 1)	2 chamber air-cathode	1410 mWm^{-2} (anode area)	(Dewan et al., 2008)
Carbon	carbon mesh	plane	7 cm^2	preacclimated bacteria from an active MFC	1 chamber air-cathode	893 mWm^{-2} (anode area) 45 Wm^{-3} (anode chamber volume)	(Wang et al., 2009b)

Table A-2.1 – Comparison of different anode materials and anode configurations, in MFCs (continued).

Materials and methods		Configuration	Electrode size	Inoculation source	Reactor configuration	P_{max}	References
carbon	reticulus vitreaous carbon	plane	volume 0.6cm^3	*Shewanella oneidensis* (DSP 10)	2 chamber MFC, catholyte: - K_3FeCN_6	500 Wm^{-3} (anode chamber volume)	(Ringeisen et al., 2006)
carbon	reticulus vitreaous carbon	packed	97cm^2, 190 cm^3 anode chamber	effluent from anaerobic bioreactor used for brewery wastewater treatment	2 chamber MFC, catholyte: - K_3FeCN_6	170 mWm^{-2} (anode area)	(He et al., 2005)
carbon	reticulus vitreaous carbon	packed	97 cm^2, 190 cm^3 anode chamber	effluent from anaerobic bioreactor used for brewery wastewater treatment	2 chamber MFC, catholyte: - K_3FeCN_6	170 mWm^{-2} (anode area)	(He et al., 2005)
carbon	graphene foam	plane	volume 60.7 cm^3	*Shewanella oneidensis* (MR – 1)	–	661 Wm^{-3} (based on the volume of anode material)	(Wang et al., 2013)
carbon	granular graphite	packed	granules O.D. 1.5 – 5 mm in 390 cm^3 anode chamber	preacclimated bacteria from an active MFC	2 chamber MFC	90 Wm^{-3} (anode chamber volume)	(Rabaey et al., 2005b)
carbon	granular activated carbon	packed	450 cm^3 anode chamber	domestic wastewater	1 chamber air-cathode	5 Wm^{-3} (anode chamber volume)	(Jiang and Li, 2009)
carbon	carbon brush	brush	4 cm high, 3 cm wide	preacclimated bacteria from an active MFC	1 chamber air cathode	2400mWm^{-2} (anode area), 73 Wm^{-3} (anode chamber)	(Logan et al., 2007a)
carbon	graphite fiber	plane	cylinder weight 196.0 g	marine sediments	marine sediment MFC	16 mWm^{-2} (anode area)	(Bond et al., 2002)
carbon	graphite felt	packed <10%	–	activated sludge	2 chamber (aerated cathode)	1.3mWm^{-2}, 6.9 mAm^{-2}, (anode area)	(!!! INVALID CITATION !!!)
metal	stainless steel plate	plane	0.12 m^2	marine sediments	marine sediment MFC	23 mWm^{-2} (anode area)	(Dumas et al., 2007)

Table A-2.2 – Comparison of different anode treatments and anode configurations, in microbial fuel cells (MFCs).

Materials and methods		Base material	Electrode size	Inoculation source	Reactor configuration	P_{max} and improvement in performance	References
surface coating	Pt coated titanium	plane metal	22 cm^2	preacclimated bacteria from an active MFC	2 chamber air-cathode cassette MFC with flow channels	not reported	(ter Heijne et al., 2008)
surface treatment	NH_3 gas treatment	carbon cloth	≈36cm^2	domestic wastewater	2 chamber cassette MFC	20% increase in power density, 50% reduction in start up time	(Cheng and Logan, 2007b)
surface treatment	heat treatment	carbon mesh	7 cm^2	domestic wastewater	2 chamber cassette MFC	25% increase in power density	(Wang et al., 2009b)
surface treatment	H_2SO_4 treatment	carbon brush	volume 28cm^3	domestic wastewater	1 chamber, cubic MFC	8% increase in power density	(Feng et al., 2010b)
surface treatment	HNO_3 treatment	graphite felt	9cm^2	brewery wastewater	tubular MFC	50% increase in power density	(Scott et al., 2007)
surface treatment	electro - chemical oxidation	graphite felt	volume 28cm^3	preacclimated bacteria from active MFC	1 chamber, cubic MFC	39.5% increase in power density	(Feng et al., 2010b)
surface treatment	electro - chemical oxidation	graphite plate	volume 14cm^3	marine sediments	2 chamber, cubic MFC	56.8 fold increase in kinetic activity	(Tang et al., 2011)
surface coating	CNT	carbon cloth	volume 57.7cm^3	domestic wastewater	tubular MFC	30.5% increase in power density	(Tsai et al., 2009)
surface coating	glassy carbon	glassy carbon	volume 7.5cm^3	*Shewanella oneidensis* MR-1	tubular MFC	82-fold increase in current density	(Peng et al., 2010)
surface coating	Pt treated carbon nanotubes	carbon veil	volume 250 cm^3	*Escherichia coli* (DH5a strain)	2 chamber, H - type	6 fold increase in power density	(Sharma et al., 2008)
surface coating	polyaniline	graphite felt	9 cm^2	brewery wastewater	tubular MFC	1.8 fold increase in power density	(Scott et al., 2007)
surface coating	AQDS	graphite disk	i.d.=48.3cm, h=1.27cm	marine sediments	tubular MFC	0.7 fold increase in kinetic activity	(Lowy et al., 2006)

Table A-2.2 – Comparison of different anode treatments and anode configurations, in MFCs (continued).

Materials and methods		Base material	Electrode size	Inoculation source	Reactor configuration	P_{max} and improvement in performance	References
surface coating	NQ	graphite disk	i.d.=48.3 cm, h=1.27cm	marine sediments	tubular MFC	0.5 fold increase in kinetic activity	(Lowy et al., 2006)
surface coating	NR	graphite felt	1.27m^2	*Shewanella putrefaciens*	single chamber,	1000 fold increase in power density	(Park and Zeikus, 2003)
surface coating	Au nanoparticle	graphite disk	1.05cm^2	*Shewanella oneidensis* MR-1	one chamber, cubic MFC	20 fold increase in current density	(Fan et al., 2011)
surface coating	Pd nanoparticle	graphite disk	1.05cm^2	*Shewanella oneidensis* MR-1	one chamber, cubic MFC	50 – 150% increase in current density	(Fan et al., 2011)
surface coating	graphite paste containing Fe_3O_4	graphite disk	i.d.=48.3cm, h=1.27cm	marine sediments	tubular MFC	1.1 fold increase in kinetic activity	(Lowy et al., 2006)
electrolytic deposition	surface coating withFe_3O_4 particles	graphite felt and plate	4 cm × 4 cm × 2 cm	marine sediments	tubular MFC	17.4 fold increase in power density ($mWcm^{-2}$)	(Fu et al., 2014)
composite electrode	Sb (V) complex in graphite paste	-	anode volume= 24.58 cm^3	marine sediments		0.9 fold increase in kinetic activity	(Lowy and Tender, 2008)
composite electrode	Mn^{2+}graphite	-	82cm^2	*Shewanella putrefaciens*	two chamber, H - type	10 fold increase in power density	(Park and Zeikus, 2002)
composite electrode	graphite – ceramic containing Mn^{2+} and Ni^{2+}	-	-	marine sediments	tubular MFC	1.2 fold increase in kinetic activity	(Lowy et al., 2006)
surface coating	iron oxide	carbon veil	volume 310 cm^3	anaerobic sludge	two chamber, H - type	2.75 fold increase in power density	(Kim et al., 2005)
surface coating	polypyrrole coated carbon nanotubes composite	carbon veil	7cm^2	*Escherichia coli* (DH5a strain)	two chamber, H - type	228 mWm^{-2}	(Zou et al., 2008)
air-cathode	carbon cloth, nafion binder, no diffusion layer	plane	7cm^2	Pt	single chamber	400±10 – 420±20 mWm^{-2} (cathode area)	(Cheng et al., 2006a)

For microbial fuel cells (MFCs), cathodes can be modified in two possible ways. Carbon veils or cloths used as cathodes can be replaced with precious metal meshes or foams (Table 2.3) or various metal particles, organic substances or bacteria could be immobilized on the electrode surface (Table 2.4)

Table A-2.3 – Comparison of different cathode materials and cathode configurations, in microbial fuel cells (MFCs).

Type	Cathode materials	Configuration and CE	Electrode size	Catalyst	Reactor configuration	P_{max}	References
air-cathode	carbon cloth, PTFE binder, no diffusion layer	plane	7cm^2	Pt	single chamber	766 mWm^{-2} (cathode area)	(Cheng et al., 2006b)
air-cathode	stainless steel mesh, nafion binder, polydimethyl siloxane diffusion layer	plane	7cm^2	Pt	single chamber	1610±56 mWm^{-2} (cathode area)	(Zhang et al., 2010)
aqueous air-cathode	carbon paper	plane	11.25cm^2	Pt	two chamber	33mWm^{-2} (cathode area)	(Logan et al., 2005)
MACA	PEM cathode cloth	plane	7cm^2	Pt	single chamber	262±10 mWm^{-2} (cathode area)	(Liu and Logan, 2004a)
aqueous air-cathode (no catalyst)	ferric sulfate, graphite powder, kaolin and nickel chloride	plane	400 cm^2	-	single chamber	788 mWm^{-2} (cathode area)	(Park and Zeikus, 2003)
biocathode	carbon veil	plane	–	pure *Chlorella vulgaris* culture and Pt	tubular, two chamber	24.4 mWm^{-2} 2.8 times increase in power density	(Wu et al., 2013b)
biocathode	granular graphite	packed	O.D. 1.5-5mm; cathode chamber 444 cm^3	mixture of sediment and sludge	tubular, single chamber	8W m^{-3} (cathode chamber volume)	(Clauwaert et al., 2007a)
biocathode	graphite fiber brush	brush	-	anaerobic sludge	two chamber	68.4 Wm^{-3} (cathodic wet volume)	(You et al., 2009)
aqueous air-cathode (no catalyst)	activated graphite	packed	25 cm^2	-	two chamber	8.1Wm^{-3} (cathode chamber volume)	Erable and Bergel, 2009)
aqueous air-cathode (no catalyst)	activated carbon felt	plane	36cm^2, thickness 5 cm	-	two chamber	315mWm^{-2} (cross sectional area of a separator	(Deng et al., 2010)
air-cathode (no catalyst)	activated carbon, pressed with PTFE	plane	7 cm^2	-	single chamber	1220mW m^{-2} (cathode area)	(Zhang et al., 2009b, Zhang et al., 2009a)

Table A-2.4 – Comparison of different cathode treatments and cathode configurations, in microbial fuel cells (MFCs).

Type	Cathode materials	Configuration and CE	Electrode size	Catalyst	Reactor configuration	P_{max}	References
aqueous air-cathode (no catalyst)	granular graphite with nanoscale pores	packed		-	two chamber	50 Wm^{-3} (cathode chamber volume)	(Freguia et al., 2007a)
aqueous air-cathode (no catalyst)	activated graphite	packed	25 cm^2	-	two chamber	8.1 Wm^{-3} (cathode chamber volume)	(Erable and Bergel, 2009)
aqueous air-cathode (no catalyst)	activated carbon felt	plane	36cm^2, thickness 5 cm	-	two chamber	315 mWm^{-2} (cross sectional area of separator)	(Deng et al., 2010)
MACA	UF membrane coated with graphite coating and catalyst	tubular	54 cm^2	CoTMPP	single chamber	18 W m^{-3} (total reactor volume)	(Zuo et al., 2007)
MACA	AEM, CEM coated with graphite and catalyst	plane	7 cm^2	CoTMPP	single chamber	449±35 and 286±30 mWm^{-2} (cathode area)	(Zuo et al., 2008a)
MACA	canvas cloth coated with Ni based or graphite and MnO_2 based conductive paints	tubular	253.75 cm^2	MnO_2	tubular, single chamber	86.03 mWm^{-2} (cathode area); for Ni based coating and 24.67mWm^{-2} (cathode area) for graphite and MnO_2	(Zhuang et al., 2009)

For microbial electrolysis cells (MECs) tables were arranged in the same way as that for MFCs. Table 2.5 is the comparison of different anode configurations and anode treatments, in MECs, Tables - 2.6 and 2.7 are the comparisons of different cathode configurations and cathode treatments for two and one chamber MECs respectively.

For Table A-2.5 performance factors such as coulombic efficiency (CE) which is related to the amount of anaerobically respiring electricity producing bacteria on the bio-anode surface, where anode acts as artificial electron acceptor; hydrogen production rate and hydrogen yield, in mols of hydrogen obtained per mol of substrate destroyed are performance factors used for MEC comparison, described in "Electrochemical Analysis Methods" section 4.7 in greater detail. (η_{W+S} %) is cathodic energy recovery, which is sometimes used in literature instead of cathodic hydrogen production (described in "Online Analysis Methods" section 4.7.

Cathodic energy recovery is calculated as $\eta_{W+S} = W_{H_2} / (W_s + W_{in})$ Eq 75

Where W_{H_2} is heat of combustion for hydrogen 286 KJ mol^{-1}, W_s is heat of combustion for substrate eg:- acetate 870 KJ mol^{-1}, W_{in} is the electric input, where W_{in} =charge (Coulombs) × voltage applied, corrected to power loss across resistor (Cheng and Logan, 2007a).

Table A-2.5 – Comparison of different anode configurations and anode treatments, in microbial electrolysis cells (MECs).

Electrode materials and anode size	Substrate	Inoculation source	Reactor configuration	(η_{W+S}) (%)	Overall H_2 yield / mol acetate	H_2 production rate ($m^3\ m^{-3}_{(anode)}\ d^{-1}$)	CE (%)	References
anode chamber volume= =14cm^3, graphite granules i.d.= =2-6mm	butyrate	soil (cellulose fed reactor), wastewater	two chamber H type mediator – less MEC	91	8.01	1.10	77	(Cheng and Logan, 2007a)
	acetate			80	3.65	0.45	82	
	lactic acid			91	5.45	1.04	82	
	propionic acid			89	6.25	0.72	79	
	valeric acid			67	8.77	0.14	66	
	glucose			71	8.55	1.23	64	
	cellulose			68	8.20	0.11	63	
carbon felt surface area 0.025 m^2, 1mm thick	acetate	effluent from another MEC	two chamber MEC with air cathode	–	–	5.6	90	(Sleutels et al., 2009b)

Table A-2.5 – Comparison of different anode configurations and anode treatments, in MECs (continued).

Electrode materials and anode size	Substrate	Inoculation source	Reactor configuration	(η_{W+S}) (%)	Overall H_2 yied / mol acetate	H_2 production rate ($m^3\ m^{-3}_{(anode)}\ d^{-1}$)	CE (%)	References
graphite felt disc =400 cm^2, anode chamber volume = 3.3L	acetate	effluent from another MEC	two chamber MEC	–	–	0.3	23	(Rozendal et al., 2008a)
carbon veil= =26.5cm^2, anode chamber volume = = 584 cm^2	acetate	domestic wastewater	two chamber cubic MEC	42	–	–	26	(Ditzig et al., 2007)
carbon felt= =25cm^2	acetate	sludge	two chamber cubic MEC	–	–	–	40±2	(Ajayi et al., 2009)
graphite brush, 0.22m^2 surface area	acetate	started in MFC mode, inoculated with wastewater	one chamber, cubic MEC	58±6	–	–	82	(Nam et al., 2011)
graphite brush, 0.22m^2 surface area	acetate	started in MFC mode, inoculated with wastewater	one chamber, cubic MEC	58±6	–	–	82	(Nam et al., 2011)
graphite granules i.d.= = 3 - 5mm, anode chamber volume= =300 cm^3	acetate	anaerobically digested sludge	one chamber cubic MEC	76	–	1.58	95	(Guo et al., 2010)
ammonia treated graphite brush= =0.22m^2, anode chamber volume= =28cm^3	acetate	effluent from MFC	one chamber MEC	75	–	3.12	97	(Call and Logan, 2008)
carbon cloth, 3.5×4cm^2	acetate	domestic wastewater	one chamber MEC	58	–	0.53	75	(Hu et al., 2008)
carbon cloth, 9 cm^2	acetate	*Shewanella* oneidensis MR-1	one chamber MEC	60	–	0.69	73	(Hu et al., 2008)

Table A-2.6 – Comparison of different cathode configurations and cathode treatments for two chamber microbial electrolysis cells (MECs).

cathode / Pt (mg cm^{-2})	Membrane	Substrate	Anode Volume (cm^3)	E_{ap} (V)	CE (%)	Volumetric yield ($m^3\ m^{-3}_{(anode)}\ d^{-1}$)	I_A (Am^{-2})	References
MECs with graphite felt anodes:								
Ti mesh / 0.5	nafion	acetate	6600	0.5	–	0.02	0.5	(Rozendal et al., 2006b)
graphite felt (biocathode)	CEM	acetate	250	1.2	_	0.63	1.2	(Rozendal et al., 2008b)
MECs with graphite granule anodes:								
carbon cloth / 0.5	AEM	acetate	42	0.6	–	0.11	_	(Cheng and Logan, 2007a)
carbon cloth / 0.5	AEM	cellulose	42	0.6	96	1.1	_	Cheng and Logan, 2007a)
MECs with carbon paper anodes:								
carbon paper / 0.5	PEM	domestic wastewater	512	0.5	23	_	0.2	(Ditzig et al., 2007)
carbon paper /2	PEM	acetate	900	0.35	33	0.015	0.4	(Sun et al., 2008)
MEC with carbon felt anode:								
carbon cloth / 0.5	no membrane	acetate	50	1	95	6.32	4.7	(Tartakovsky et al., 2009)
carbon cloth / 0.5 Pt with 0.5 Pd added	PEM	acetate	50	1.16	67	0.98	_	(Tartakovsky et al., 2008).
MEC with carbon cloth anode:								
carbon paper / 0.5	nafion	acetate	200	0.6	78	_	_	(Liu et al., 2005c)

Table A-2.7 – Comparison of different cathode configurations and cathode treatments for the single chamber microbial electrolysis cells (MECs).

Cathode / Pt (mg cm^{-2})	Substrate	Anode volume (cm^3)	E_{ap} (V)	C_E	Volumetric yield ($m^3\ m^{-3}_{(anode)}\ d^{-1}$)	I_A (Am^{-3})	References
MECs with graphite brush anodes:							
stainless steel brush	acetate	28	0.6	–	1.7	88	(Call et al., 2009a)
stainless steel mesh	winery wastewater	1×10^6	0.9	–	0.19±0.04	7.4	(Cusick et al., 2011)
stainless steel NiO_X	acetate	28	0.6	108	0.76	131	(Jeremiasse et al., 2010)
stainless steel A286	acetate	28	0.9	–	1.5±0.04	222±4	(Selembo et al., 2009a)
nickel 625	acetate	28	0.9	–	0.79±0.27	160±22	(Selembo et al., 2009a)
Nickel	vinery wastewater	90	1.0	–	0.25	–	(Escapa et al., 2012)
carbon cloth / 0.5	acetate	28	0.8	98	3.12	11.6	(Call and Logan, 2008)
MECs with graphite brush anodes:							
carbon cloth / 0.5	swine wastewater	28	0.5	29	0.9	4.2	(Wagner et al., 2009)
carbon cloth / 0.5	glycerol	28	0.9	104	2	8.8	(Selembo et al., 2009b)
carbon cloth / 0.5	cellulose	28	0.5	73	1.11		(Lalaurette et al., 2009)
carbon cloth / 0.5	fermentation effluent	26	0.6	87	1.41	5.6	(Lu et al., 2009)
MEC with graphite granule anode:							
carbon felt	acetate	140	1.06	60	0.57	50	(Lee et al., 2009)
MECs with carbon cloth anodes:							
carbon cloth / 0.5	acetate	300	0.6	75	0.53	9.3	(Lu et al., 2009)
carbon cloth + NiMo	acetate	18	0.6	75	2	12	(Hu et al., 2009)
carbon cloth + NiW	acetate	18	0.6	73	1.5	9	(Hu et al., 2009)

9.3 Appendix A-3 Perfomance Factors for MECs Used in Experiments 3 and 4

Table A-3.1 – Variation of COD reduction, electrode potentials and average daily dosage of acid with substrate concentration for microbial electrolysis cells (MECs) acclimated to acetate and butyrate.

Substrate	Conc. (mmol L^{-1})	COD reduction (%)		Anode potential vs Ag/AgCl (V)		Cathode potential vs Ag/AgCl (V)		Av.HCl, 1.2 mmol L^{-1} dosed per day (cm^3)		pH		Conductivity (mS cm^{-1})	
acetate (AC) or butyrate (BU)		BU	AC	BU	AC	BU	AC	BU	AC	BU	AC	BU	AC
	20	59±2	48±10	-299±106	-177±20	-1004±56	-960±18	15	10	6.3±0.3	6.6±0.3	6.4±0.6	7.3±0.1
	10	70±7	42±4	-199±39	-153±18	-1170±25	-980±25	10	7	6.7	6.6±0.2	6.5±1.5	6.2±0.2
	5	97±1	38±5	-264±8	-130±10	-1075±25	-1060±10	7.7	5	6.8±0.1	6.6±0.2	7.46±0.3	6.2±0.1
acetate and butyrate mixture	10 and 10	49±2	8±1.8	-249±50	-101±10	-1055±15	-975±12	7.6	10	6.8±0.1	6.7±0.1	4.62±0.2	6.1±0.3
acetate and butyrate switched	20	38±10	2.3±7	-180±80	-446±10	-1061±110	-826±75	10	1.7	6.78±0.1	6.9±0.4	8.63±1.3	8.75±0.6

A STP. Theoretical H_2 yields: 10 mol/per mol butyrate; 4 mol/mol acetate; 12 mol/mol glucose. Acetate reactor =AC and butyrate reactor = BU

All tests were performed in triplicates at the applied potential of 850 mV

Tolerance bars represent variations from the average for daily hydrogen production for *n* days (*n*=5) per substrate concentration

Table A-3.2 – Variation of COD reduction, electrode potentials and average daily dosage of acid with substrate concentration for microbial electrolysis cells (MECs) with modified anodes.

Substrate	Conc. (mmol L^{-1})	COD reduction (%)		Anode potential vs Ag/AgCl (V)		Cathode potential vs Ag/AgCl (V)		av.HCl, 1.2 mmol L^{-1} dosed per day (cm^3)		pH		Conductivity (mS cm^{-1})	
acetate		RR	JC	RR	JC	RR	JC	RR	JC	RR	JC	RR	JC
	20	30±2	63±5	-246±20	-277±30	-1064±20	-590±45	25	20	6.7±0.2	6.8±0.1	12.7±0.1	11.9±0.1
	10	64±3	55±5	-290±18	-233±37	-1057±25	-533±60	15	10	6.8±0.1	6.8±0.2	7.6±0.2	7.5±0.1
	5	69±2	74±5	-136±20	-315±45	-1022±30	-523±55	10	5	6.6±0.2	6.6±0.3	3.6±0.3	3.5±0.3
acetate and butyrate	10 and 10	43±3	6±1	-256±30	-257±50	-1056±20	-573±70	10	5	6.4±0.3	6.4±0.4	5.2±0.3	5.5±0.3
butyrate	20	3±1	4±1	-554±20	-158±10	-759±44	-578±75	5	5	6.7±0.2	6.7±0.4	4.45±0.3	4.6±0.3
acetate		MB	UCC	MB	UCC	MB	UCC	MB	UCC	MB	UCC	MB	UCC
	20	36±1	58±2	-421±20	-177±20	-1010±20	-960±18	10	10	6.6±0.3	6.6±0.3	8.1±0.1	7.3±0.1
	10	39±3	64±2	-531±30	-153±18	-971±10	-980±25	7	7	6.5±0.2	6.6±0.2	6.2±0.1	6.2±0.2
	5	58±2	53±3	-472±20	-130±10	-861±20	-1060±10	5	5	6.7±0.1	6.6±0.2	6.2±0.2	6.2±0.1
acetate and butyrate	10 and 10	5±1	2±1	-448±10	-101±10	-917±18	-975±12	10	10	6.7±0.2	6.7±0.1	5.9±0.3	6.1±0.3
butyrate	20	2±1	2±1	-537±17	-446±10	662±42	-826±75	1.7	1.7	6.9±0.2	6.9±0.4	6.8±0.3	6.4±0.6

A STP. Theoretical H_2 yields: 10 mol/per mol butyrate; 4 mol/mol acetate; 12 mol/mol glucose. All tests were performed at the applied voltage of 850 mV.

Error bars represent variations from the average for *n* experimental repeats (*n*=2)

9.4 Appendix A-4 Print Screen Copies of VI Diagrams for Data Logging

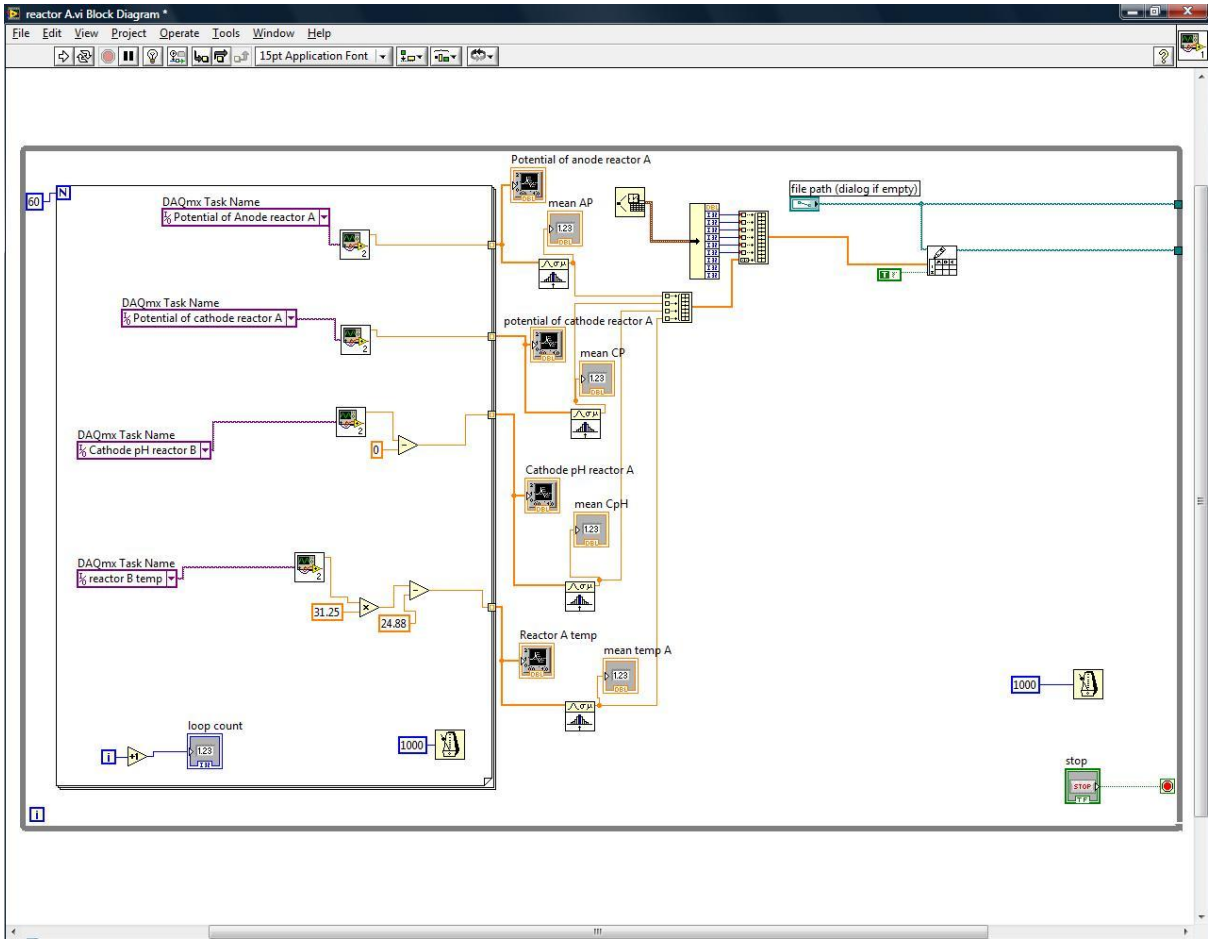

Print screen copy of VI diagram for data – anode potential, pH and temperature – acquisition in Labview used for experiment 1 (see Results, pages 105-112).

Figure 46 – Appendix A – 4.1 – Print screen copy of VI diagram for MEC.

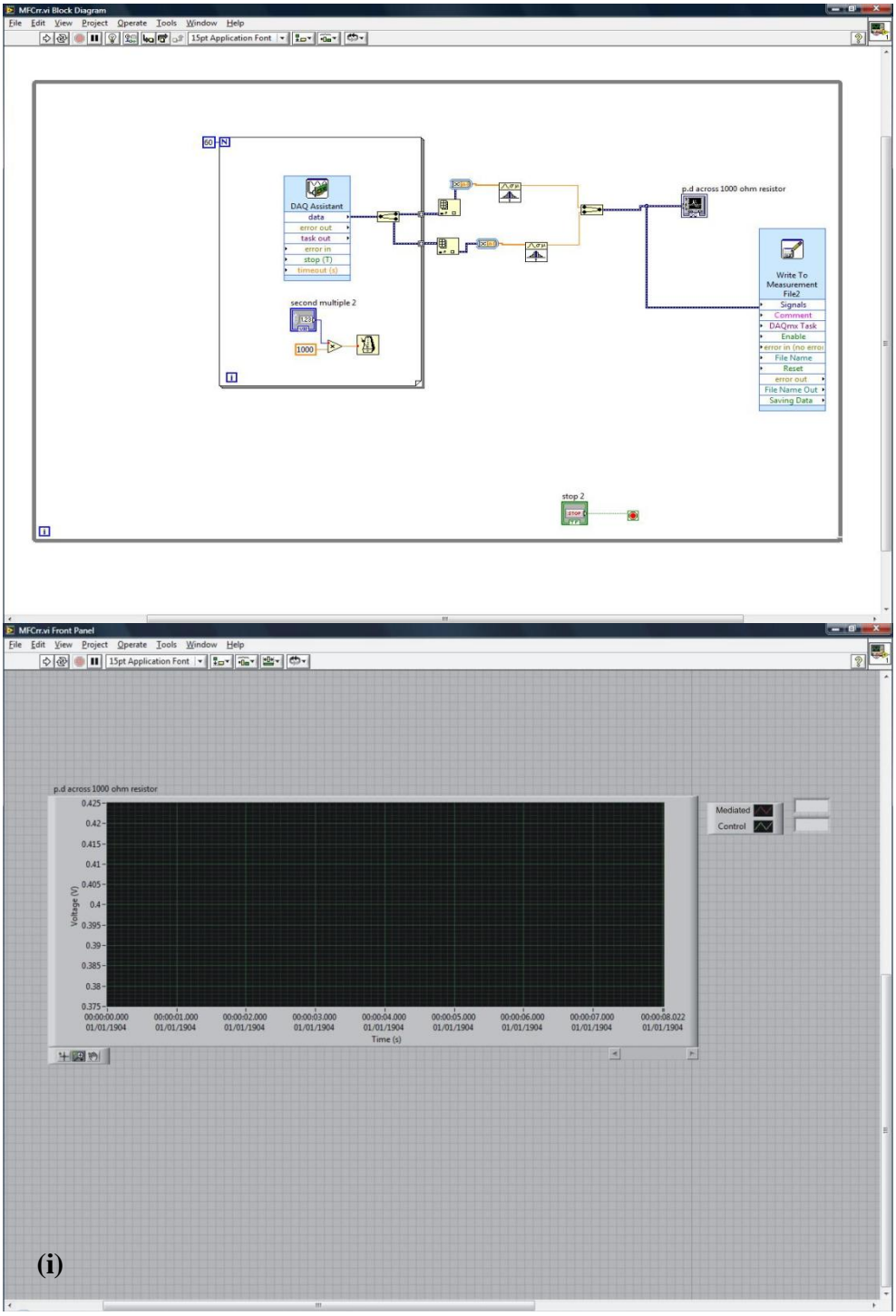

Print screen copy of VI diagram (47) and instrument panel (47i) for data – voltage – acquisition in Labview used for experimental parts 3 and 4 when reactors were operated in MFC mode.

Figure 47 – Appendix A-4.2 – Print screen copies of VI diagrams for MFCs.

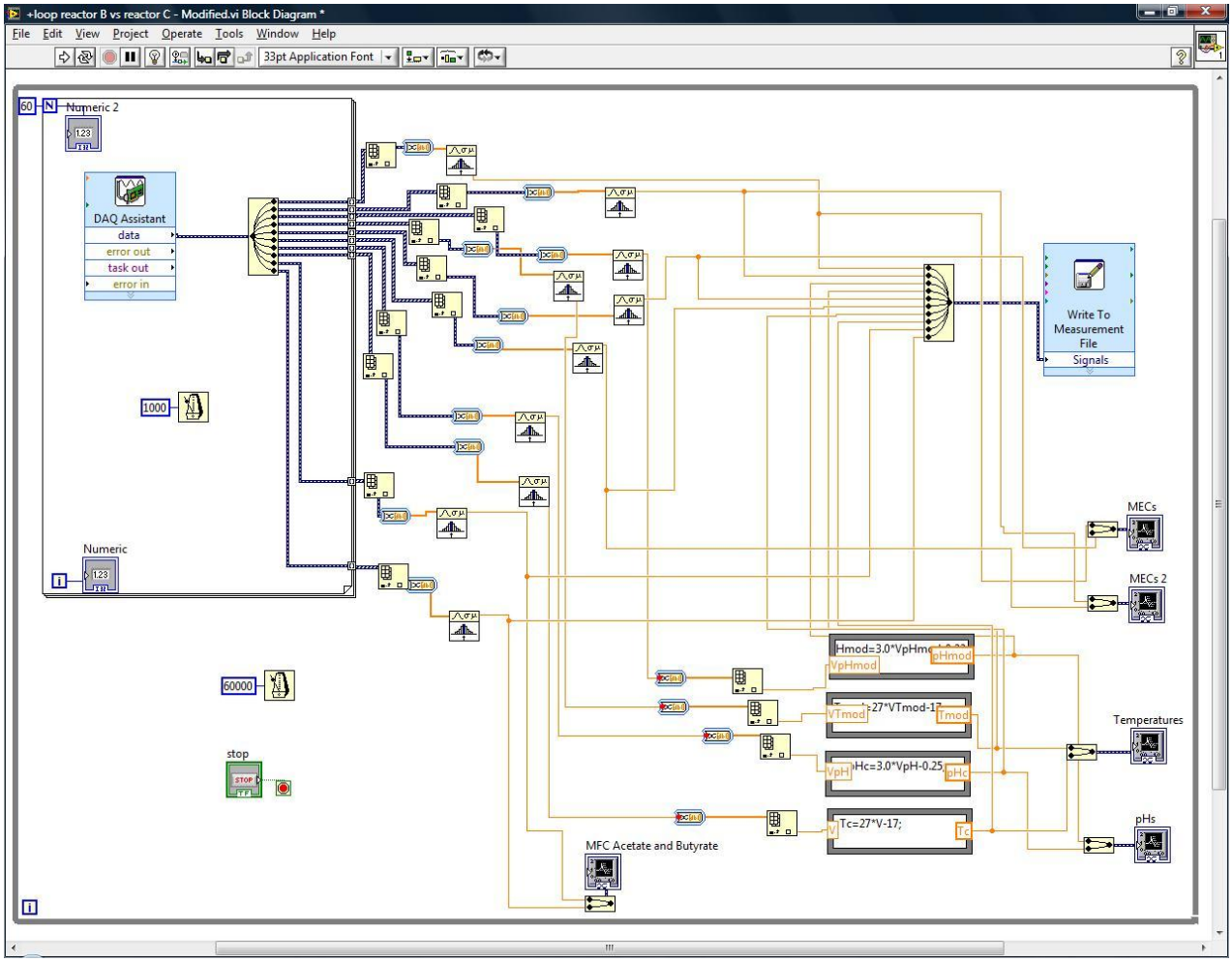

Print screens copies of VI diagrams for data – anode and cathode potentials, pH and temperature – acquisition in Labview used for experiments 3 and 4, see “Results” part 3 and part 4.

Figure 48 – Appendix A-4.3 – Print screen copy of VI diagram for MEC.

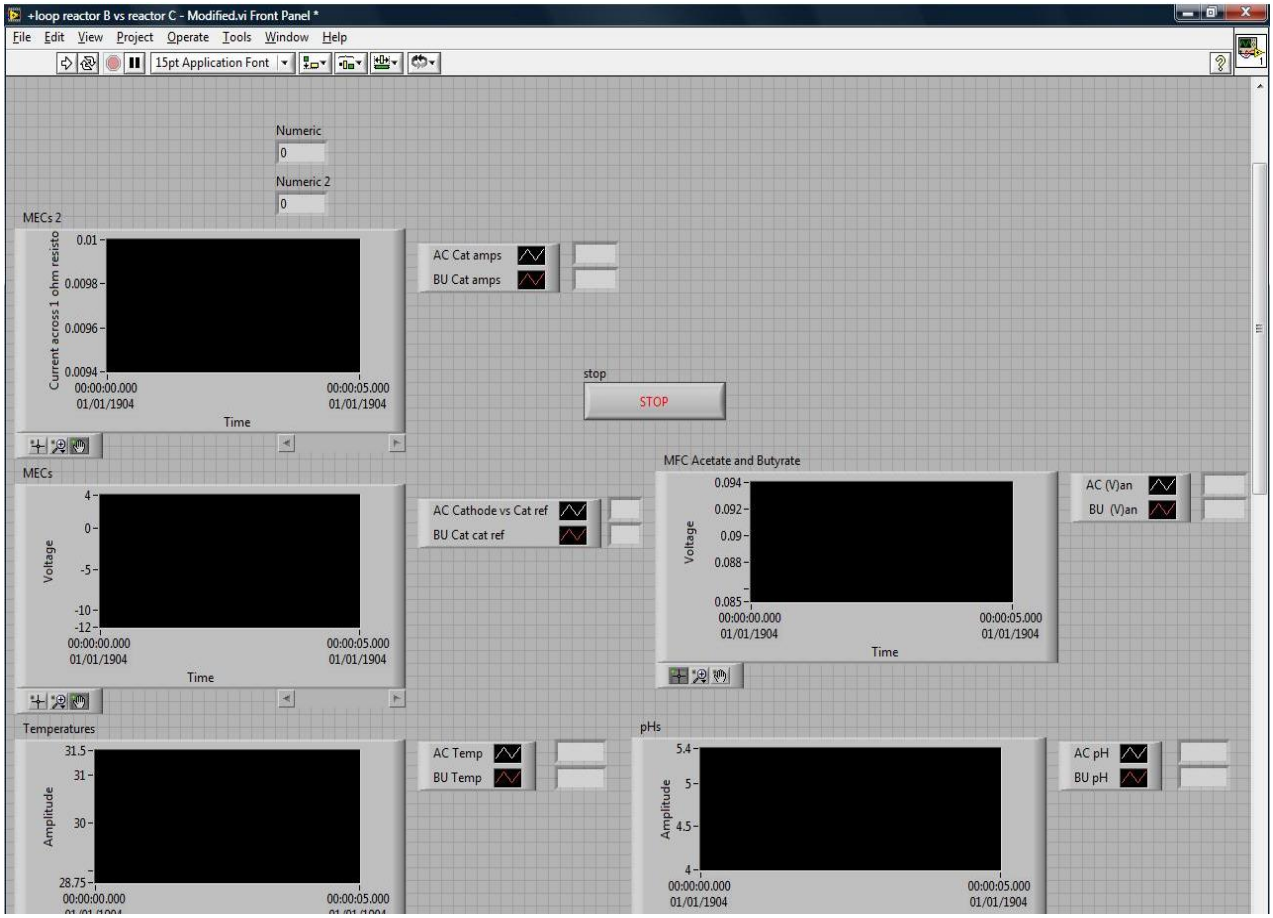

Print screen copy of VI instrument panel for data – potentials, pH and temperature – acquisition in Labview used for all experiments, main window, same for both set diagram.

Figure 49 – Appendix A-4.4 – Print screen copy of VI diagram for MEC.

9.5 Appendix A-5 Published Articles

Available at www.sciencedirect.com

ScienceDirect

journal homepage: www.elsevier.com/locate/he

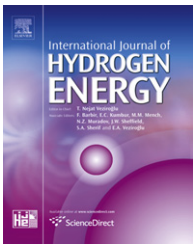

Influence of catholyte pH and temperature on hydrogen production from acetate using a two chamber concentric tubular microbial electrolysis cell

Godfrey Kyazze, Arseniy Popov, Richard Dinsdale, Sandra Esteves, Freda Hawkes, Giuliano Premier, Alan Guwy*

The Sustainable Environment Research Centre, University of Glamorgan, Pontypridd, CF37 1DL, United Kingdom

ARTICLE INFO

Article history:
Received 28 December 2009
Received in revised form
5 May 2010
Accepted 8 May 2010
Available online 11 June 2010

Keywords:
Temperature
Catholyte pH
Microbial electrolysis
BES
Hydrogen
Acetate

ABSTRACT

Microbial electrolysis cells (MECs) could be integrated with dark fermentative hydrogen production to increase the overall system yield of hydrogen. The influence of catholyte pH on hydrogen production from MECs and associated parameters such as electrode potentials (vs Ag/AgCl), COD reduction, current density and quantity of acid needed to control pH in the cathode of an MEC were investigated. Acetate (10 mM, HRT 9 h, 24 °C, pH 7) was used as the substrate in a two chamber MEC operated at 600 mV and 850 mV applied voltage. The effect of catholyte pH on current density was more significant at an applied voltage of 600 mV than at 850 mV. The highest hydrogen production rate was obtained at 850 mV, pH 5 amounting to 200 cm^3_{stp}/l_{anode}/day (coulombic efficiency 60%, cathodic hydrogen recovery 45%, H_2 yield 1.1 mol/mol acetate converted and a COD reduction of 30.5%). Within the range (18.5–49.4 °C) of temperatures tested, 30 °C was found to be optimal for hydrogen production in the system tested, with the performance of the reactor being reduced at higher temperatures. These results show that an optimum temperature (approximately 30 °C) exists for MEC and that lower pH in the cathode chamber improves hydrogen production and may be needed if potentials applied to MECs are to be minimised.

1. Introduction

Research on the use of electrochemically active bacteria for power generation in microbial fuel cells (MFCs) has gained wide interest in the past five years [1,2]. Microbial electrolysis cells (MECs) are a variation on the principles of microbial fuel cells such that, with an electrical energy input, substrates are oxidised at the anode (as in MFCs) but the cathodic reaction involves reduction of protons to hydrogen as the cathode chamber is kept anaerobic [3,4]. Microbial electrolysis can thus be seen as a biological analogue of chemical electrolysis.

Hydrogen is widely reported to be a significant future energy vector (or carrier) and also as the ultimate non polluting fuel if produced sustainably [5]. This proposition, often called the 'hydrogen economy', is driven by the need to reduce the impact of climate change (arising out of increased greenhouse gas levels in the atmosphere), need to secure energy supplies, reduce atmospheric pollution and meet the increasing energy demands of an increasing population [6,7].

* *Corresponding author*. Department of Molecular and Applied Biosciences, University of Westminster, 115 New Cavendish Street, London W1W 6UW, United Kingdom. Tel.: +44 1443 483590; fax: +44 1443 483382
E-mail addresses: gkyazze@yahoo.com, g.kyazze@westminster.ac.uk (G. Kyazze).
0360-3199/$ – see front matter © 2010 Professor T. Nejat Veziroglu. Published by Elsevier Ltd. All rights reserved.
doi:10.1016/j.ijhydene.2010.05.036

One of the challenges that must be overcome before the hydrogen economy becomes a reality is that of producing hydrogen efficiently and affordably using clean technologies. Hydrogen production via microbial electrolysis is advantageous as a variety of substrates can be used; the hydrogen yield is potentially high (1 g COD can liberate 1400 ml at 0 °C and 1 atm); the system can be operated effectively at room temperature and atmospheric pressure and substrates inhibitory or recalcitrant to anaerobic digestion e.g. those with high ammonium can be utilized [8]. Recovery of hydrogen from the cathode should be easier to achieve as the hydrogen simply bubbles out of solution. There should be greater simplicity in cell design and subsequently reduced cost. The simpler design results from the liquid phase operation in MEC cathodes as opposed to the likely gas and liquid (thin film) phase operation of MFC cathodes, with their incumbent oxygen mass transfer limitations. Microbial electrolysis can be used as a second stage process of a fermentative hydrogen reactor to recover more hydrogen from what otherwise would be waste products (volatile fatty acids e.g. acetate and alcohols among others), or used in alternative configurations as presented in Hawkes et al. [9].

Theoretically a hydrogen yield of 12 mol/mol hexose is possible using microbial electrolysis compared to 4 mol/mol hexose using dark fermentation. For thermodynamic reasons a small amount of electrical energy (ca. 120 mV) has to be supplied to drive the reactions that take place in an MEC [10].

To optimise the performance of microbial electrolysis cells the effect of a number of factors needs to be understood, amongst which are catholyte pH and temperature. Previous studies on hydrogen production using microbial electrolysis have mainly been operated as batch processes [11,12] and it has been indicated (at pH 7) that despite the use of Pt as catalyst, the overpotential at the cathode limits the hydrogen evolution reaction [4]. Practical application of microbial electrolysis cells will require continuous operation because of the productivity gains that can be achieved by operation that is not intermittent. In batch culture many parameters are interdependent, e.g. culture growth rate and the physical and chemical environment. It is therefore difficult to extrapolate results obtained from batch studies to steady state continuous operation.

The catholyte pH may be expected to affect the redox potential of the hydrogen evolution reaction. In addition, pH may also be expected to affect any methanogens inadvertently introduced in the cathode. Temperature may also be expected to (a) affect the growth rate of the electrochemically active bacteria (and hence substrate utilisation rate); (b) affect the mass transport of reactants and products to and from the electrodes, (c) influence reaction kinetics and (d) have an effect on the electrode potentials according to the Nernst equation:

$E' = E^{0'}$- $(RT\ln K_{eq})/(nF)$, modified at 25 °C for proton reduction as

$$E' = E^{0'} - 0.0296\log P_{H2} - 0.059\mathrm{pH} \quad (1)$$

To the knowledge of the authors, no information on the effects of catholyte pH and temperature on hydrogen production via microbial electrolysis have been reported. Therefore, in this work we have studied and reported the effects of catholyte pH and temperature on hydrogen production from acetate using microbial electrolysis.

2. Materials and methods

2.1. Microbial electrolysis cell setup

A schematic of the MEC set up is shown in Fig. 1. The MEC consisted of two concentric tubular clear acrylic cells with i.d. 40 mm and 74 mm. The smaller, inner tube (326 ml volume) was radially perforated (39 holes each 8 mm in diameter) on one side of the tube (subtending 150° of the 360° circumference) and inserted in the larger diameter tube (1290 ml inner volume). The inner tube was assembled with an anode electrode (plain carbon cloth, PRF composite materials, Dorset, UK) rolled several times around a plastic rod of diameter 10 mm and length 200 mm and a reference electrode (Ag/AgCl) located 7 mm from the anode. A cation exchange membrane (CMI 7000, Membranes International, NJ, USA) area 240 cm^2 was attached to the outer surface of the inner tube so as to cover the perforations, thus separating the internal volumes of the two tubes. The cathode electrode (carbon cloth, area 75 cm^2 coated with 0.5 mg/cm^2 Pt, BASF fuel cell, NJ, USA) was placed round the cation exchange membrane forming a membrane electrode assembly (see also [13]). The inner tube was equipped with ports for supplying substrate, removing effluent and connecting the anode and a reference electrode. The outer tube was fitted with ports for connecting the cathode, recirculation of catholyte, releasing gas produced in the cathode chamber and for access to the feed and outlet ports of the inner tube. The headspace of the cathode chamber was maintained at 100 cm^3 using an overflow U-tube. Data for anode potential, cathode potential, pH, potential difference across an external resistive load (Section 2.2.2) and temperature were logged online using LabVIEW® virtual instrumentation software (National Instruments, UK). The pH in the cathode chamber was controlled by automatically dosing with 1.2M HCl (Mettler Toledo pH transmitter, Leicester, UK) except during days 30–60 when a gas cathode was used. Except during experimentation on effect of

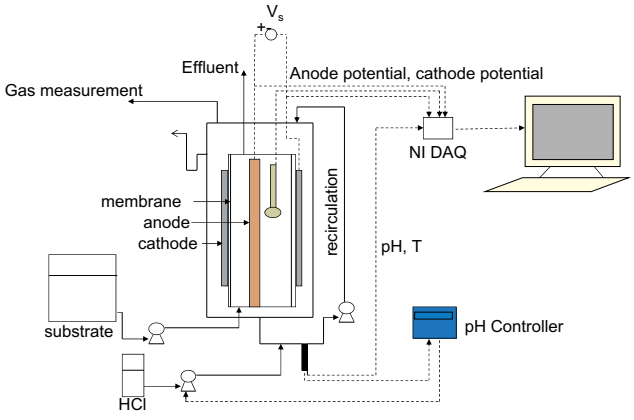

Fig. 1 – Schematic of the MEC used in this study.

catholyte pH, the pH in the cathode was normally controlled to 7.0. The MEC was operated at room temperature except during experimentation on the effect of temperature.

2.2. Operating conditions

2.2.1. Batch start up

The anode was inoculated with anaerobically digested sewage sludge (10% v/v) obtained from a wastewater treatment plant (Cog Moors, Cardiff, UK). The anode medium consisted of 2.4 g/L CH_3COONa, 310 mg/L NH_4Cl, 130 mg/L KCl, 2.690 g/L $NaH_2PO_4.H_2O$, 4.330 g/L Na_2HPO_4, 26.6g/L NaCl, 12.5 cm^3/L of a mineral salt medium and 12.5 cm^3/L of a vitamin medium. The high salt (sodium chloride) concentration in the anode medium was used to mimic salt water from where *Geobacter* sp., identified as integral members of bacteria consortia in MFCs and MECs [14], have been shown to be abundant [15] and also to inhibit methanogens [16]. The recipe of the mineral salts was (mg/L): $MgSO_4$ (3.0), $MnSO_4.H_2O$ (0.5), NTA (1.5), NaCl (1.0), $FeSO_4.7H_2O$ (0.1), $CaCl_2.2H_2O$ (0.1), $CoCl_2.6H_2O$ (0.1), $ZnCl_2$ (0.13), $CuSO_4.5H_2O$ (0.01), $AlK(SO_4)_2.12H_2O$ (0.01), H_3BO_3 (0.01), Na_2MoO_4 (0.025), $NiCl_2.6H_2O$ (0.024), $Na_2WO_4.2H_2O$ (0.025) [17]. The vitamin solution used was formulated according to the recipe (mg/L): biotin (2.0), folic acid (2.0), pyridoxine HCl (10.0), riboflavin (5.0), thiamin (5.0), nicotinic acid (5.0), panthotenic acid (5.0), B12 (0.1), p-aminobenzoic acid (5.0), thioctic acid (5.0) [17]. The catholyte was 50 mM phosphate buffer solution (PBS) with a pH of 7.0 and conductivity of 5.97 mS/cm. Both the anode and cathode chambers were sparged with nitrogen for 10 min to remove air. An anode potential of +300 mV (Vs Ag/AgCl) was applied. This startup procedure lasted 30 days. A control startup was set up without the use of bacterial inocula.

2.2.2. Continuous operation

After batch startup, the sediments in the anode were removed and replaced with 10 mM acetate (600 mg/L). The anode chamber was then fed continuously with 10 mM acetate (600 mg/L) in an aqueous solution which also included 310 mg/L NH_4Cl, 130 mg/L KCl, 2690 mg/L $NaH_2PO_4.H_2O$, 4330 mg/L Na_2HPO_4, 12.5 cm^3/L of the mineral salts medium and 12.5 cm^3/L of the vitamin medium referred to in 2.2.1. This anode media had a pH of 7.4 and a conductivity of 7.24 mS/cm. In days 30–60, 600 mV was applied to the cell and a gas cathode was used with nitrogen sparging (10 ml/min). This was followed in days 60–78 with addition of 50 mM PBS (pH 7.0) to the cathode and collection of gas produced in the cathode using a gas bag with FEP on/off valve (Fisher Scientific, Loughborough UK).

The reactor was used in experiments 1, 2 and 3 as follows: In Experiment 1, which lasted from day 78 to day 110, two applied voltages of 600 mV and 850 mV between anode and cathode were used (Solartron 1470E potentiostat, Solartron Analytical, Farnborough, UK) and in each case the pH in the cathode was controlled for at least 3 days at 5, 7 and 9. The gas produced in the cathode was collected by displacement of water saturated with sodium chloride. The anodic gas was collected in a gas bag.

Experiment 2 was designed to confirm the results of Experiment 1. A power supply unit (model 3644A, Array Electronika Co. Ltd.) was used as the Solartron potentiostat used in experiment 1 had developed a fault, and two applied voltages were used: 670 mV and 920 mV. The MEC used in Experiment 1 was connected to a 3-Ω resistor so that the potential difference (and hence current through the circuit) could be logged online. Higher applied voltages compared to Experiment 1 were used to allow for the potential drop across the external resistor. Again the pH of the cathode was controlled to 5, 7 and 9. There was a time interval of 20 days between end of Experiment 1 and start of Experiment 2 during which the MEC was not fed. Experiment 2 lasted for 69 days.

In Experiment 3, 920 mV was applied to the MEC used in Experiments 1 and 2 using the DC programmable power supply unit with the catholyte pH controlled to 7.0, and the temperature of the cell varied in the range 20 °C–53 °C. The MEC had been operating for 4 months at 23 ± 1.4 °C on 10 mM acetate (600 mg/L). There was a delay of 6 days from the end of Experiment 2 to the start of Experiment 3 during which the MEC was not fed. Fresh PBS (50 mM, pH 7) was used in the cathode. Temperatures of 30.4 ± 1.04 °C (days 0–12), 42.9 ± 0.4 °C (days 12–22), 49.3 ± 3.9 °C (days 22.7–25.8) were set. For purposes of temperature control, silicone tubes were wound round the MEC and connected to a Grant flow heater (Grant Instruments, Cambridge, UK). On day 25.84, temperature control was switched off and the reactor operated at room temperature. After day 46.4, cold water from a refrigerator was re-circulated around the reactor to achieve temperatures below room temperature, up to 18.5 °C on day 49.4 when the experiment was stopped. Gas output from the cathode was metered using a bubble counter (NCBE, Reading, UK) while gas produced in the anode was collected in a gas bag. The counter was calibrated using nitrogen gas from a cylinder with the flow rate regulated using a needle valve in the range 0–2 ml/min.

2.3. Offline analyses

The soluble COD of the influent and effluent was determined using a Hach spectrophotometer (model 2500, Hach Lange, Manchester, UK). The conductivity of the solutions was measured using a conductivity meter (Mettler Toledo, Leicester, UK). Hydrogen and methane composition in the off gases was measured using a CP-4900 MicroGC (Varian Ltd, Oxford, UK). pH was measured using a bench top pH meter from Mettler Toledo. Effluent samples were analysed for volatile fatty acids by headspace GC according to the method of Cruwys et al. [18].

2.4. Evaluation of performance

Hydrogen and methane production rates were evaluated daily by combining the gas volumes recorded with their compositions at standard temperature and pressure (stp). Current density was normalised to the area of the cathode. The cathodic hydrogen recovery was calculated based on the volume of hydrogen recovered *vis a vis* what would be expected by invoking Faraday's second law of electrolysis. The coulombic efficiency was calculated based on the COD reduction and the current recorded for a given time. For example taking a basis of 1 h, the amount of COD degraded could be

determined and the current that would have been expected from this COD degradation determined from the relationship: 16 g COD ≡ 1 mol H_2≡2F (F = faraday). Hydrogen yield was obtained from the relationship: 1 g COD ≡ 1400 ml of hydrogen at stp, neglecting biomass formation. The theory behind these calculations was reviewed in detail by Logan et al. [19].

3. Results and discussion

3.1. *Batch startup and initial operation with a sparged cathode vs liquid cathode*

During batch startup, a small current of 400–600 μA was registered but it was higher than in the control where the current was less than 100 μA. In Experiment 1, continuous sparging of the cathode with nitrogen gave a current of 1.6 mA, far below the current which would be expected from 100% degradation of the substrate (78 mA). Using a liquid cathode improved the current by six times compared to the gas cathode; however as the experiment progressed, methane was found to accumulate in the gas bag at the expense of hydrogen (Fig. 2); the 14% hydrogen measured in the gas bag on day 73, had fallen to 5% by day 77 with an increase in methane from less than 1% on day 73–5% on day 77.

Methane production probably proceeds via the reaction: $2H_2 + CO_2 \rightarrow CH_4 + 2H_2O$ [20] which is accompanied by a reduction of volume. This would explain the negative pressure that was observed when an MGC-1 counter (Litremeter, North Marston, UK) was used to meter the produced gas at 600 mV applied voltage in a separate experiment. This 'sucking back' phenomenon has also been observed by Tartakovsky et al. [21]. The source of the methanogens can be via contamination from outside or from the anode side e.g. due to a defective partitioning (by the membrane) between the anode and cathode.

3.2. *Influence of catholyte pH*

In Experiment 1 the influence of catholyte pH on hydrogen production and associated parameters like COD reduction, current density, electrode potentials and amount of acid needed to maintain the set pH were studied. Fig. 3 shows the variation of hydrogen production rate and current density with pH of the catholyte at the two applied voltages of 600 mV

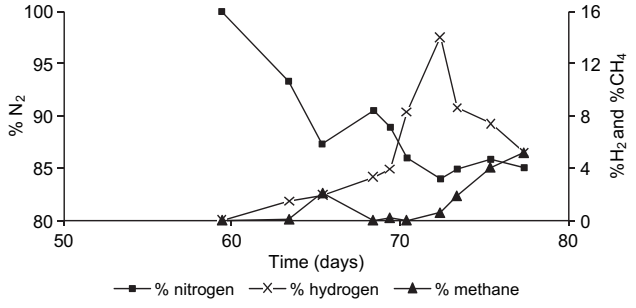

Fig. 2 – Occurrence of methanogenesis in the cathode of an MEC at the expense of hydrogen production. Applied voltage was 600 mV.

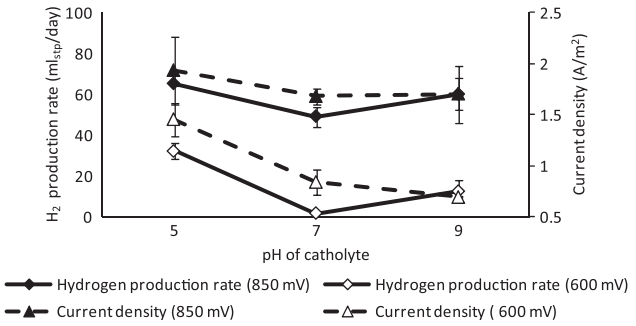

Fig. 3 – Variation of hydrogen production rate and current density with pH of the catholyte.

and 850 mV and Table 1 shows the variation of the remaining parameters with catholyte pH.

Catholyte pH influenced hydrogen production as did the voltage applied. The effect of catholyte pH was more significant at an applied voltage of 600 mV than at 850 mV. At 600 mV applied voltage, current density increased from 0.69 ± 0.01A/m^2 of cathode at pH 9 to 1.45 ± 0.16 A/m^2 cathode at pH 5. At 850 mV, the current densities were: 1.70 ± 0.16 (pH 9), 1.68 ± 0.08 (pH 7) and 1.93 ± 0.33 A/m^2 (pH 5), respectively (Fig. 3).

At 600 mV hydrogen production rates at catholyte pH 5 (32.3 ± 3.7 ml/day) and pH 9 (12.5 ± 5.4 ml/day) were higher than at pH 7 (1.68 ± 1.2 ml/day, Fig. 3). At an applied voltage of 850 mV higher average hydrogen production rates were also obtained at pH 5 (65 ± 1 ml/day ($n = 2$) or 200 ml/l_{anode}/day) and pH 9 (59.8 ± 13.9 ml/day ($n = 3$)) than at pH 7 (49 ± 5 ml/day ($n = 2$)). The difference in hydrogen production rates at pHs 5, 7 and 9 was however not statistically significant at the $P < 0.05$ level. The equivalent coulombic efficiency at 850 mV, catholyte pH 5 was 60%, cathodic hydrogen recovery 45%, H_2 yield 1.1 mol/mol acetate converted and COD reduction of 30.5% (Tables 1 and 2). The low cathodic hydrogen recovery and low hydrogen yield may suggest that some of the hydrogen diffused from the cathode to the anode where it would have been converted to methane.

Methane was detected in the anode chamber in all cases but no methane was detected in the cathode chamber. At 850 mV, catholyte pH 7, methane productivity amounted to 0.8 ml/h. Based on the feeding regime, this is equivalent to a conversion of 10% of the substrate to methane (neglecting biomass formation).

A COD balance for the case of catholyte pH 7 gave the following:

Input: 640 mg/L at 9 h HRT, equivalent to 593.5 mg COD/day based on the size of the anode chamber. Output: methane production rate of 19.2 ml/day equivalent to 59.4 mg COD; H_2 production rate of 49 ml/day equivalent to 17.5 mg COD. Thus 13% of the input COD was recovered as methane and hydrogen [note that the COD reduction in this case was 31%].

The effluent from the anode had a pH of 6.4–6.5 with a conductivity of 6.5 mS/cm. The highest coulombic efficiency was obtained at pH 5 in the cathode (Table 2). Cathodic hydrogen recovery and hydrogen yields were low, with the

Table 1 – Experiment 1. Variation of COD reduction, electrode potentials and daily dosage of acid with the pH of the catholyte.

	600 mV				850 mV			
pH	COD reduction (%)	Anode potential vs Ag/AgCl	Cathode potential vs Ag/AgCl	1.2M HCl dosed per day (ml)	COD reduction (%)	Anode potential vs Ag/AgCl	Cathode potential vs Ag/AgCl	1.2M HCl dosed per day (ml)
5	32 ± 5(2)	−52 ± 20	−652 ± 20	9 ± 1.4(4)	30.5 ± 5.1(2)	100 ± 18	−750 ± 20	6.5 ± 1(2)
7	30 ± 2(4)	−150 ± 86	−750 ± 86	5.4 ± 1.7(8)	31 ± 5.6(2)	−170 ± 2	−1020 ± 15	5.0 ± 0 (2)
9	12 ± 4.7(2)	−256 ± 44	−856 ± 44	7.1 ± 2.5(5)	29.7 ± 6.7(3)	−213 ± 55	−1056 ± 44	7.2 ± 0.7(3)

(*Cf.* theoretical cathodic potentials (vs Ag/AgCl) at pH 5 = −500 mV, pH 7 = −620 mV and pH 9 = −740 mV).

worst hydrogen yield performance obtained at 600 mV, pH 7 (Table 2). In Experiment 2, the trend of hydrogen productivity and current density were similar to those of Experiment 1.

Acetate is one of the main byproducts of fermentative hydrogen reactors and anaerobic digesters. The utilization of acetate for hydrogen production in MECs would be beneficial. The cathodic overpotential for proton reduction has been highlighted as one of the main electrochemical losses in microbial electrolysis cells [4], despite the presence of platinum as a catalyst. However, this has been disputed by some workers [22] indicating that the hydrogen evolution reaction is very reversible.

Electrode potentials are pH dependent and the cathodic potential for hydrogen evolution would be expected to increase (numerically) by +60 mV for every pH unit decrease according to equation (1). Thus, operation at low pH in the cathode would be expected to improve hydrogen production rates and reduce the overall electrical energy added to the system. In the tests performed in this study, at 600 mV applied voltage, the current density and hydrogen production rates increased with a decrease in pH. The cathodic overvoltage was in the order: 152 mV (pH 5) > 132 mV (pH 7) > 116 mV (pH 9). Rozendal et al. [4] reported a higher cathodic overvoltage of 280 mV when 500 mV was applied. The low overvoltage at catholyte pH 9 might explain the low COD conversion of 12% as the physiological conditions of the anode chamber were similar and the anode potentials were more positive than the redox potential for acetate oxidation (i.e. −480 mV vs Ag/AgCl at pH 7 in the anode). At an applied potential of 850 mV, the cathodic overvoltage was in the order of 400 mV (pH 7) > 316 mV (pH 5) > 250 mV (pH 9). The high cathodic overvoltages at these pHs may explain the higher hydrogen production rates compared to 600 mV applied voltage (Fig. 3). The difference in the trend of cathodic overvoltage at 600 mV and 850 mV may be due to differences in dissolved hydrogen concentration (or partial pressure) – see Eq. (1).

Table 2 – Experiment 1. Comparison of performance indicators at different pH of catholyte and applied potential. Calculations based only on average values of current, COD reduction and hydrogen production rates.

	600 mV			850 mV		
pH	CE (%)	Cathodic H_2 recovery (%)	H_2 yield mol/mol acetate consumed	CE (%)	Cathodic H_2 recovery (%)	H_2 yield mol/mol acetate consumed
5	40	32	0.52	60	45	1.1
7	28	2.5	0.13	52	39	0.81
9	54	25	0.50	57	47	1.0

As the H_2 production rate and current density increased with the reduction in catholyte pH at an applied voltage of 600 mV, it suggests that either the concentration of protons in the cathode or the cathodic overvoltage or both was/were limiting the hydrogen evolution reaction at the cathode. Although in Experiment 1, for an applied voltage of 850 mV, the highest H_2 production rate was obtained at pH 5, the differences in hydrogen production rate and current density compared to pH 7 and pH 9 (Fig. 3) was not significant at the $p < 0.05$ level. This suggests that the cathodic reaction for hydrogen evolution was probably not rate limiting. It may be that the transfer of protons across the ion exchange membrane was the limiting factor in this case.

The trend curve of the volume of acid dosed to maintain the pH of the catholyte is similar in shape to that of hydrogen production rates (data in Table 1). However, this volume of acid only reflects the extent of generation of OH^- ions in the cathode and is probably not used for hydrogen generation considering that the dosing of the acid was in the recirculation line; the acid would have been neutralized before reaching the main chamber In Experiment 1, 600 mV applied and catholyte pH 7, if the acid dosed (6.48×10^{-3} mol H^+/day) had been used for hydrogen production, the hydrogen production rate would have been 72.5 ml/day but the recorded rate was only 1.7 ml/day. Hydrogen production rate was lower at pH 7 compared to pH 5 or 9. It is likely that at pH 7 the proton gradient is lower than at pH 9. At pH 5, despite an unfavourable proton gradient (in terms of diffusion), the concentration of protons in the cathode suggests that mass transport is not expected to be the limiting factor.

A comparison of hydrogen yields from continuous flow MECs is shown in Table 3 and indicates that there is a need to further improve the efficiency of MECs. Apart from the problem of methanogenesis in the anode and a low cathodic hydrogen recovery, the COD reduction in MECs (Table 1) needs improvement e.g. by optimizing the growth media. One question that may arise in this respect is whether NH_4Cl is the best source of nitrogen when NH_4^+ ions have been shown to migrate to the cathode [23].

Table 3 – Experiment 1. Comparison of H_2 production with other continuous flow studies.

Substrate conc. (mg/L)	mV applied	H_2 production rate ml/L/d	H_2 yield[a] (mol/mol substrate consumed)	Ref.
Acetate (600 mg/L)	600	100	0.52	This study
Acetate (600 mg/L)	850	200	1.1	This study
Acetate (600 mg/L)	1000	300	0.92	Rozendal et al. [4]
Glucose (600 mg/L)	700	340	1.63	Tartakovsky et al. [21]

a stp. Theoretical H_2 yields : 4 mol/per mol acetate; 12 mol/mol glucose.

3.3. *Influence of temperature*

Current density and hydrogen production were influenced by temperature, increasing in the range 20–30 °C and then decreasing as temperature was increased to 53 °C (Fig. 5). The optimum temperature for operation of the MEC was *circa* 30 °C, where average hydrogen production rate was 56.5 ml/day (173 ml/L_{anode}/day, current density 1.69 A/m^2). At room temperature (23 ± 1.4 °C) the average hydrogen production rate was 42.2 ml/day (current density 1.33 A/m^2).

By the end of operation at 30.4 ± 1.04 °C (day 12.8), the catholyte conductivity had increased from that of 50 mM PBS (5.97 mS/cm) on day 0 to 13.6 mS/cm. Increasing the temperature to 42.9 ± 0.4 °C and then 49.3 ± 3.9 °C led to a decrease in current density and hydrogen production (Fig. 5). However, the MEC could be recovered by reverting to lower temperatures after operation at the higher temperatures. Having switched off the heating on day 25.84, it took 4.7 days for the current to increase to previous levels. Temperatures lower than 30 °C were also shown to decrease current density and hydrogen production rates. The current density at 20 °C (0.89 A/m^2) was almost half that at 30 °C (1.69 A/m^2, Fig. 4). The COD

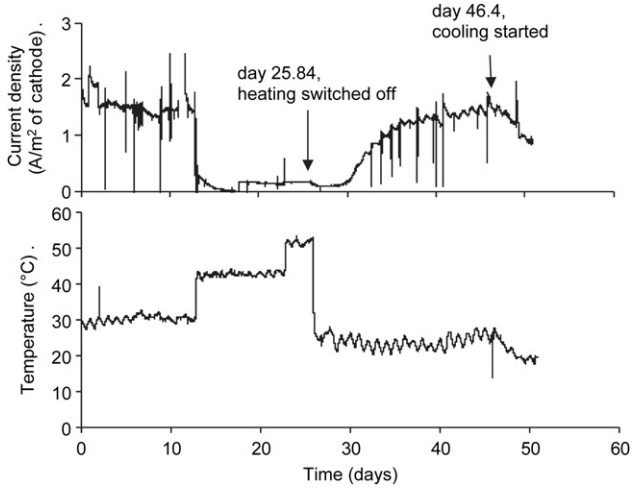

Fig. 4 – Variation of current density and hydrogen production rate with temperature (876 mV effectively applied at a controlled pH of 7 at the cathode).

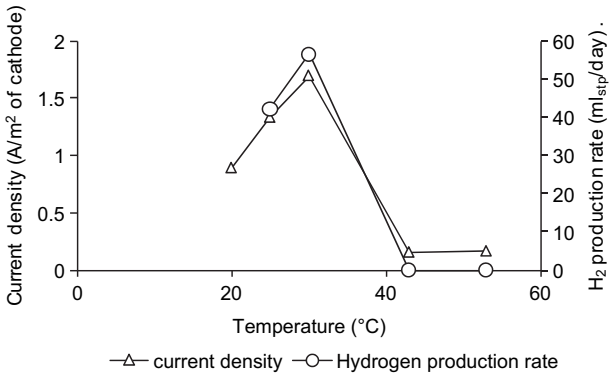

Fig. 5 – Experiment 3. Variation of temperature and current density over the operational period. Day 0 refers to the time 6 days after end o f experiment 2.

reduction at 30 °C (days 13–20) was 42.5% while at 23 °C (days 30–45) was 17.3%. The average potential difference actually applied to the cell was 862 mV and the pH of the effluent averaged 6.50.

Methane production in the anode was also found to vary with temperature. At 30 °C, a methane production rate of 2.96 ml/day was recorded. When the temperature set point was changed to 42.9 °C on day 12.8, temperature increased and the methane production rate in days 13–14 (temp. 41–43 °C) was 12.9 ml/day but it then decreased steadily reaching 1.94 ml/day in days 21–22. No methane was detected in the cathode chamber. It appears methanogenic activity peaks at around 40 °C while electrogenic/anaerobic respiration peaks at around 30 °C. At room temperature, methane production, current density and hydrogen production was lower than at 30 °C.

The optimum temperature for MEC operation appears to be around 30 °C. Interestingly the current density at 30 °C was almost twice that at 20 °C indicating agreement with Arrhenious equation – which relates reaction rates of chemical reactions with temperature – that a doubling of the reaction rate constant accompanies a 10 °C increase in temperature. Studies on the effect of temperature on MFC performance did not give this agreement with the power density decreasing by only 9% when the temperature was lowered from 32 °C to 20 °C [24]. The recovery of the microorganisms' activity by allowing the temperature to decrease to room temperature, following a temperature increase to 52 °C, indicates that the electrochemically active bacteria are resilient to higher temperatures. From an energy standpoint, the optimal temperature of ca. 30 °C suggests that MECs would be suitable for tropical countries.

4. Conclusion

Hydrogen production was improved at catholyte pH 5 compared to pH 7 and 9, the effect being more significant at an applied voltage of 600 mV than at 850 mV. The maximum hydrogen production rate of 200 ml_{stp}/l_{anode}/day was obtained at pH 5 in the cathode and an applied voltage of 850 mV, giving

a H_2 yield of 1.1 mol/mol acetate converted and a COD reduction of 30.5%. The optimum temperature for MEC operation was found to be around 30.4 ± 1.0 °C. Operation at 42.9 °C and 49.3 °C inhibited hydrogen production; however, reverting from 42.9 °C to 23 °C allowed the recovery of current generation in the MEC over 4 days.

Acknowledgements

The authors wish to thank EPSRC for funding the UK SUPERGEN (SHEC) project (grant number EP/E040071/1) of which this work forms a part.

REFERENCES

[1] Du Z, Li H, Gu T. A state of the art review on microbial fuel cells: a promising technology for wastewater treatment and bioenergy. Biotechnol Adv 2007;25:464–82.
[2] Rabaey K, Verstraete W. Microbial fuel cells: novel biotechnology for energy generation. Trends Biotechnol 2005;23:291–8.
[3] Liu H, Grot S, Logan BE. Electrochemically-assisted microbial production of hydrogen from acetate. Environ Sci Technol 2005;39:4317–20.
[4] Rozendal RA, Hamelers HVM, Euverink GJW, Metz SJ, Buisman CJN. Principle and perspectives of hydrogen production through biocatalyzed electrolysis. Int J Hydrogen Energy 2006;31:1632–40.
[5] Sartbaeva A, Kuznetsov VL, Wells SA, Edwards PP. Hydrogen nexus in a sustainable energy future. Energy Environ Sci 2008;1:79–85.
[6] Ipcc, Ipcc. 4th assessment report: climate change 2007. Paris: The Physical Science Basis; 2007.
[7] Rand D, Dell R. Hydrogen energy: challenges and prospects. Cambridge: RSC publishing; 2008.
[8] Clauwaert P, Toledo R, van der Ha D, Crab R, Hu H, Udert KM, et al. Combining biocatalysed electrolysis with anaerobic digestion. Water Sci Technol 2007;57:575–9.
[9] Hawkes FR, Kim J, Kyazze G, Premier GC, Guwy A. Feedstocks for BES conversions. In: Rabaey K, Angenent LT, Shroeder U, Keller J, editors. Biolectrochemical systems: from extracellular electron transfer to biotechnological application. London: IWA Publishing; 2009. p. 369–92.
[10] Rozendal R, Hamelers HVM, Rabaey K, Keller J, Buisman CJN. Towards practical implementation of bioelectrochemical wastewater treatment. Trends Biotechnol 2008;26:450–9.
[11] Call D, Logan BE. Hydrogen production in a single chamber microbial electrolysis cell lacking a membrane. Environ Sci Technol 2008;42:3401–6.
[12] Cheng S, Logan BE. Sustainable and efficient biohydrogen production using electrohydrogenesis. Proc Natl Acad Sci 2007;104:18871–4.
[13] Kim JR, Premier GC, Hawkes FR, Dinsdale RM, Guwy AJ. Development of a tubular microbial fuel cell (MFC) employing a membrane electrode assembly cathode. J Power Sources 2009;187:393–9.
[14] Chae KJ, Choi MJ, Lee J, Ajayi FF, Kim IS. Biohydrogen production via biocatalyzed electrolysis in acetate-fed bioelectrochemical cells and microbial community analysis. Int J Hydrogen Energy 2008;33:5184–92.
[15] Holmes DE, Bond DR, O'Neil RA, Reimers CE, Tender LR, Lovley DR. Microbial communities associated with electrodes harvesting electricity from a variety of aquatic sediments. Microb Ecol 2004;48:178–90.
[16] Kyazze G, Dinsdale R, Guwy AJ, Hawkes FR, Premier GC, Hawkes DL. Performance characteristics of a two stage dark fermentative system producing hydrogen and methane continuously. Biotechnol. Bioeng. 2007;97:759–70.
[17] Loveley D, Phillips E. Novel mode of microbial energy metabolism: organic carbon coupled to dissimilatory reduction of iron or manganese. Appl Environ Microbiol 1988; 54:1472–80.
[18] Cruwys JA, Dinsdale RM, Hawkes FR, Hawkes DL. Development of a static headspace gas chromatographic procedure for the routine analysis of volatile fatty acids in wastewaters. J Chromatogr A 2002;945:195–209.
[19] Logan BE, Call D, Cheng S, Hamelers HVM, Sleutels THJA, Jeremiasse AW, et al. Microbial electrolysis cells for high yield hydrogen gas production from organic matter. Environ Sci Technol 2008;42:8630–40.
[20] Wang A, Liu W, Cheng S, Xing D, Zhou J, Logan BE. Source of methane and methods to control its formation in single chamber microbial electrolysis cells. Int J Hydrogen Energy 2009;34:3653–8.
[21] Tartakovsky B, Manuel MF, Neburchilov V, Wang H, Guiot SR. Biocatalysed hydrogen production in a continuous flow microbial fuel cell with a gas phase cathode. J Power Sources 2008;182:291–7.
[22] Marshall AT, Haverkamp RG. Production of hydrogen by the electrochemical reforming of glycerol-water solutions in a PEM electrolysis cell. Int J Hydrogen Energy 2008;33: 4649–54.
[23] Liu W-Z, Wang A-J, Ren N-Q, Zhao X-Y, Liu L-H, Yu Z-G, et al. Electrochemically assisted biohydrogen production from acetate. Energy and Fuels 2008;22:159–63.
[24] Liu H, Cheng S, Logan BE. Power generation in fed batch microbial fuel cells as a function of ionic strength, temperature and reactor configuration. Environ. Sci. Technol. 2005;39:5488–93.

Biotechnology and Bioprocess Engineering 17: 000-000 (2012)
DOI 10.1007/s12257-011-0493-9

RESEARCH PAPER

The Effect of Physico-chemically Immobilized Methylene Blue and Neutral Red on the Anode of Microbial Fuel Cell

Arseniy L. Popov, Jung Rae Kim, Richard M. Dinsdale, Sandra R. Esteves, Alan J. Guwy, and Giuliano C. Premier

Received: 4 October 2011 / Revised: 11 December 2011 / Accepted: 18 December 2011

Abstract A fast and cost effective immobilization of electron carriers, methylene blue (MB) and neutral red (NR) by pH shift was proposed to improve bioanodic performance. The adsorption of mediators onto the carbon cloth anode was verified using cyclic voltammogram (CV) and the effect of the immobilized mediators on acclimation, power density, and acetate removal of MFCs was investigated. A peak power density of P_{max}(MB) = 11.3 W/m^3 was achieved over days 110 ~ 120, as compared to P_{max}(Control) = 5.4 W/m^3 and P_{max}(NR) = 3.1 W/m^3 for the treated anode after 15 sequential fed-batch operations. The VFA removal rates however were similar for all MFC systems, ranging from 82 to 87%. It could be suggested that the increase in power density for the MB treated electrode resulted from an enhanced electron transport from exo-electrogenic bacteria. MB may also have a selective effect on the bacterial community during the start-up stage, increasing the voltage production and acetate removal from day 1 to 16. However, MFC with NR treated anode produced an initial voltage under 100 mV, with lower coulombic efficiency (CE). NR exhibited less favourable mediator molecule binding to the electrode surface, when subject to pH driven physico-chemical immobilization.

Keywords: microbial fuel cell, air cathode, mediators, enhanced electron transport, methylene blue, neutral red

Arseniy L. Popov, Richard M. Dinsdale*, Sandra R. Esteves, Alan J. Guwy
Faculty of Health, Sport and Science, University of Glamorgan, Pontypridd, Mid-Glamorgan, CF37 1DL, UK
Tel: +44-1443-654-219; Fax: +44-1443-482-285
E-mail: rdinsdal@glam.ac.uk

Jung Rae Kim*, Giuliano C. Premier
Faculty of Advanced Technology, University of Glamorgan, Pontypridd, Mid-Glamorgan, CF37 1DL, UK
Tel: +44-1443-654-387; Fax: +44-1443-483-382
E-mail: jkim@glam.ac.uk

1. Introduction

Microbial fuel cells (MFCs) are bioelectrochemical devices which are able to directly convert chemical energy in resource streams containing biodegradable organic matter into electricity. They are capable of processing a wide range of biomass feedstocks and wastewaters [14]. These devices have been studied as alternatives to conventional wastewater treatment and for sustainable electricity generation with attention to scale up strategy [1,57]. One of the biggest challenges associated with MFCs is the power density, which is several orders of magnitude lower than that of chemical fuel cells [8]. Low power density in MFCs may be improved by the development of novel system designs and the modification of anode structures [4,9,10]. Replacing carbon electrodes with carbon brushes or use of carbon foam does dramatically improve the performance of the devices by increasing surface area [9,10].

Artificial electron mediators allow electricity production by the bacteria such as *E. coli*. [11,12], which are unable to use the electrode directly or only produce low power densities, therefore increasing the viability and performance of bioelectrochemical system [9], from such bacteria depends on facilitated or mediated electron transfer to the electrode. The desirable characteristics for a mediator are (i) capability to penetrate the cell membrane; (ii) capability to receive electron charges from the cell, and discharging on the electrode, (iii) fast electrode reaction, (iv) high solubility and stability, (v) low toxicity to microorganisms and wider environment [13]; finally, (vi) ease of dissociation from the cell membrane and microorganisms [14,15].

Potter *et al.* [16] showed *Saccaromyces cervicae* and *E. coli*, generated an anode potential when a mediator was used (under 100 mV), however they could not produce electricity without the aid of mediators. The mechanisms

were not investigated extensively thereafter and the mediator used in the study was not specified. In the mid 90's, interest in mediator functionalised microbial electricity generation re-appeared due to developments in MFC technology and the desire to increase power density stimulated by the requirement for sustainable bioenergy production. A large variety of chemicals are known to facilitate electron transport from the bacteria to the anode; exogenous mediators such as neutral red (NR) [12], thionin [17,18], potassium ferricyanide [11], ubiquinone [19], methyl viologen (MV) [3,14], methylene blue (MB) [14,20], and natural bacterially produced chemicals (endogeneous mediator) such as phenazine and pyocyanin [21].

MB has been used widely in the dyeing industry, and its redox characteristics have been used in MFC research as a mediator as well. It is readily available at low cost and less toxic than many other known redox mediators, and is soluble in bacterial media in bioelectrochemical systems [22]. MB was reported to have redox potentials of 0.101, 0.047, and 0.011 (*vs* NHE) at pH values of 5, 6, and 7, respectively [23]. Detailed studies were performed on the effect of MB on pure strain of *P. falciparum* with 50% inhibitory concentration (IC_{50}) values in the low concentration (11 nM), in the context of its potential use as an antimalarilal drug [24]. However, no detailed studies on MB toxicity were performed with mixed cultures used in MFCs. It has also been reported that MB can be immobilized on a carbon surface by using a simple pH shifting technique, so preventing interference with the wider ecosystem by being discharged with an effluent, as described in previous studies [13,25].

While various electron carriers or mediators have been used to improve electron transfer from the biofilm to the anode surface [4,9,10], this has been mediated predominantly by free moving electrochemically-active molecules in solution in the anode chamber. As indicated, this could have deleterious polluting effects on the wider environment and therefore is generally not acceptable for continuously operated industrial processes. Physico-chemical immobilization of MB on the electrode might reduce the cost of activation and clean up *e.g.* recalcitrant dye wastewater [26-29], and simultaneously could improve the performance and power production. Carbon generated from saw dust and pre-treated with base, has been used to remove MB, which has been immobilised on the carbon by passive physico-chemical adsorption [27,28]. This process can be used in the activation of 'bioelectrodes' in an MFC; combining dye oxidation with organic removal. Of note to this study, MB has been shown to be efficient electron carrier in MFCs, producing higher power density compared to a control [30,31].

The efficiency of the mediator depends on many factors, including the culture and the substrate used as well as its molecular structure and other characteristics such as ability to dissociate and polarity. It could be suggested that NR interacts differently with bacteria, as shown in the previous studies [11,12,14]. In the first article immobilized NR was shown to improve the performance of an MFC using *E. coli* and *Actinobacillus succinogenes,* however NR results in poor performance in the other study, probably because its performance largely depends on the conditions associated with the culture [11,12]. NR has a redox potential of –325 mV, similar to that of NADH (–320 mV, *vs* NHE, respectively) and it is both highly permeability into the lipid bilayer [32], which is a desirable characteristic in mediation. No detailed studies on NR toxicity studies have been found relating to mixed cultures.

According to the author's knowledge, the physico-chemical adsorption of MB has not been investigated extensively in MFCs. In this report, it has been shown that by using simple pH shift, MB can be adsorbed onto the carbon anode surface more efficiently than NR, even though the solubility of MB (35.5 g/L) was lower than NR (56.4 g/L) in water. This is probably due to the positively charged MB^+ ions, produced when MB-chloride is dissolved at high pH (*e.g.* pH 12), which is likely to easily interact with the carbon surface [33]. We have tested a simple pH shift method for the immobilization of mediator onto the carbon anode surface in order to activate the anode electrode for electrogenic activity of bacteria. The performance of MFCs with MB and NR treated electrodes was compared to controls using cyclic voltametry, power density, and organic removal capability. Such activation was shown to be very effective and might provide a mechanism useful in scale-up, in terms of the cost effective activation of carbon electrodes.

2. Materials and Methods

2.1. MFC configuration with MB- or NR-treated carbon electrode

A carbon veil electrode (plain carbon cloth, PRF composite materials, Dorset, UK) was placed into 1.34 mM MB ([7-(dimethylamino) phenothiazin-3-ylidene]-dimethylazanium chloride C.I. 52015, Fisher Scientific, Loughborough, UK) solution for 28 h and dried for another 28 h (MB-carbon electrode treatment). The same procedure was repeated for NR (8-N,8-N,3-trimethylphenazine-2,8-diamine hydrochloride, C.I.50040, Fisher Scientific, Loughborough, UK) carbon electrode treatment. For physico-chemical adsorption of MB on to the electrode, pH was adjusted from pH 5.5 to 12, using NaOH as described in the previous studies [27,28]. MB is more likely to be adsorbed onto the surface

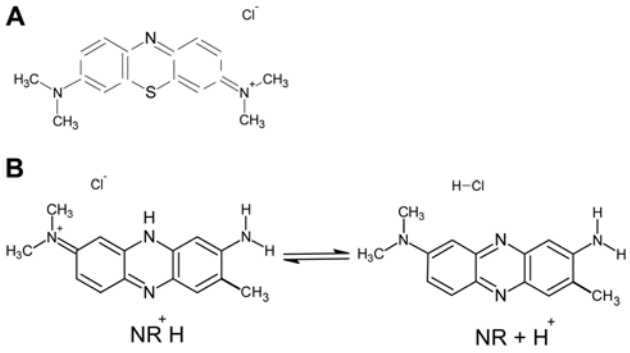

Fig. 1. Molecular structure of MB (A) and dissociation equation for neutral red (NR) (pKa = 6.8) (B).

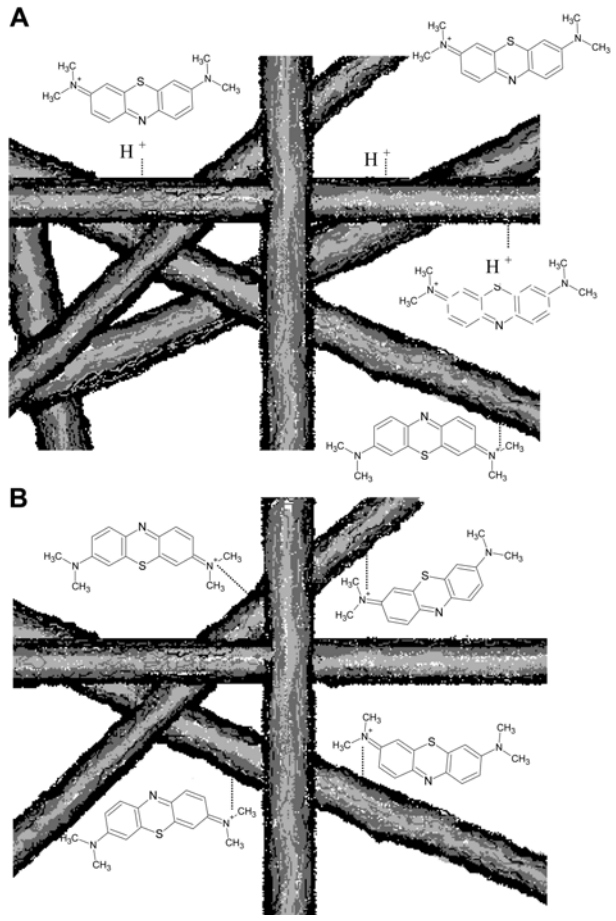

Fig. 2. Interaction between delocolozed electrons on cabon fibers of carbon felt, and positive dipole on suphur atom in methylene blue, (A) pH 5.5 and (B) pH 12.

at high pH (*i.e.* 10 ~ 12) at which most MB molecules exist in oxidized form (Figs. 1A and 2A), as shown in the previous study [34]. The prepared electrodes were assembled into a membrane electrode assembly MFC as previously described [5].

Each MFC consisted of one tubular opaque polypropylene cell with i.d. 40 mm. The tube (200 cm^3 volume) was radially perforated (53 holes each 10 mm in diameter) on one side [5]. Each tubular cell was assembled with the MB or NR adsorbed anode electrode around a carbon rod of diameter 10 mm and length 200 mm. A cation exchange membrane (CMI 7000, Membranes International, NJ, USA), area 240 cm^2, was attached to the outer surface of the tube so as to cover the perforations, thus separating the reactant in the container from the cathode while allowing ion transport to the cathode. The cathode electrode (carbon cloth, area 75 cm^2 coated with 0.5 mg/ cm^2 Pt, BASF fuel cell, NJ, USA) was placed around the cation exchange membrane forming a membrane electrode assembly [1,5,35].

2.2. MFC start up and operation

The anode was inoculated with anaerobic digester sewage sludge (20% v/v) obtained from a wastewater treatment plant (Cog Moors, Cardiff, UK). During the start-up, the media supplied to the anode chamber consisted of 1.64 g/ L CH_3COONa, 310 mg/L NH_4Cl, 130 mg/L KCl, 2.69 g/ L $NaH_2PO_4 \cdot H_2O$, 4.33 g/L Na_2HPO_4, 12.5 mL of minerals, and 12.5 mL of vitamin stock solution [5]. The concentrations and species of the mineral salts in solution were the same as used in the experiments performed by Kim *et al.* [5,36].

After start-up, the sludge in the anode chamber was removed and replaced with fresh anode media once a week. The influent had a pH of 7.0 and a conductivity of 7.24 mS/cm.

2.3. Analyses

2.3.1. Cell potential and power

Each experiment lasted for 210 days, during which the voltage across the load was monitored manually using a multimeter (Fluke 115 true RMS multimeter), while the MFC was maintained at 23 ± 2ºC except where stated otherwise. In order to investigate current-voltage response, the resistance was switched from open to short circuit using a variable resistance box (Tenma, resistance decade box, 72-7270) at 1 hour intervals, at which point pseudo steady state conditions had been established.

2.3.2. Electrochemical measurements

In order to test how much MB was adsorbed onto the carbon veil, CV was performed in the range of 0.7 ~ –0.7 V *vs* Ag/AgCl electrode for the abiotic solution, at a scan rate of 10 mV/sec using a buffer solution prepared as previously described by Kim *et al*. [35,36] (with and without acetate in the media); and from 0.4 to –1.2 V *vs* Ag/AgCl for the effluent samples containing bacteria. This was because CVs of an electrochemically active mixed microbial community may have several oxidation and reduc-

tion peaks, which may not appear if the lower range were used [10,37]. The potentiostat (Model 1287 Electrochemical Interface, Solartron Inc., Farnborough, UK) was operated through a desktop computer running the control software (Corr-Ware 2TM, Scribner Associate Inc., NC) interfaced to the potentiostat *via* a USB to parallel interface (National Instruments GPIB-USB-HS). Three effluent samples were collected from each MFC each week, once the voltage output reached 300 mV. All samples were then scanned, after being flushed with nitrogen for 5 min.

2.3.3. Analysis of volatile fatty acid removal

Liquid samples were collected every week, at the end of each batch operation cycle (1 week) and stored at –80°C before being analysed. Volatile fatty acids content of the samples was determined using a gas chromatograph (Perkin Elmer Ltd, Cambridge, UK) equipped with a headspace sampler (Turbo Matrix 40 trap headspace sampler, Perkin Elmer Ltd, Cambridge, UK), as previously described by Cruwys *et al.* [38]. Hydrogen and methane composition in the off gases were measured using a CP-4900 Micro GC (Varian Ltd, Cambridge, UK), as previously described [39,40]. Conductivity was measured using a portable conductivity meter (Mettler Toledo, SevenGo pro™, SG 7, Leicester, UK).

3. Results

3.1. The effect of MB on enrichment

Fig. 3 shows the development of voltage generation in the MFC with physico-chemically immobilized MB and NR treated carbon electrode, compared to a control with untreated carbon electrode. The voltage generation began to noticeably increase from 6 days of enrichment when using the MB modified anode electrode, reaching and stabilizing at 153 mV (0.78 W/m^3), on day 8 and slowly increased to 286 mV (2.73 W/m^3), on day 20. In the later period of the experiment (days 23 ~ 71), the voltage continuously increased and reached at 366 mV (day 118, 4.47 W/m^3) and then stabilized at 353 mV (day 154, 4.15 W/m^3) with a 150 Ω resistance. The NR treated carbon electrode, however, showed a relatively low voltage, which slowly increased from 0.45 (days 1 ~ 5) to 43.4 mV on day 23 and kept fluctuating between 40 and 50 mV until day 71. The control (without mediator) showed a lag phase of 8 days, then rapidly increased and stabilized to approximately 301.7 mV (3.03 W/m^3) on day 19. In the later period of the experiment (days 23 ~ 71), the voltage slowly increased and subsequently peaked at 338 mV (3.81 W/m^3), on day 147.

These results indicate that the physico-chemically immobilized MB mediator can facilitate rapid initial voltage development in the MFC. However, whenever the media was replaced during fed-batch operation, the voltage fluctuated between 100 and 260 mV, probably due to wash out of the community that had established in suspension/biofilm (days 23 ~ 71), then stabilized at voltages of 280 ± 10 mV for MB, 280 ± 10 mV for control and 40 ± 10 mV for NR. When the biofilm developed on the anode electrodes, the average voltage outputs observed (from 71 to 154 days) were almost the same for the MFCs with MB treated carbon electrodes and the control (313 and 309 mV, respectively). The NR treated carbon electrode showed significantly lower average voltage output (223 mV). The voltage outputs were significantly affected by temperature fluctuations, which ranged between 21 and 25°C. The voltage varied from 310 ± 5 to 350 ± 5 mV, in the MFCs with MB treated carbon electrode (data not shown).

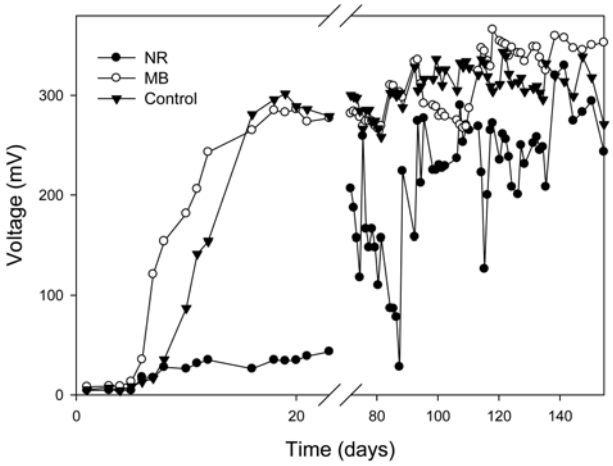

Fig. 3. The development of voltages in MFCs with immobilized MB, NR compared to a control without mediator, during the enrichment process.

3.2. Cyclic voltammetry

In order to investigate physico-chemisorption of MB onto the carbon electrode, cyclic voltametry tests were conducted at pH and pH 12, respectively (Fig. 4). Reduction and oxidation peaks with increased amplitude were obtained from MB treated carbon electrode at pH 12 (0. 69 mA at –0.13 V and –0.85 mA at –0.29 V, respectively), compared to those at pH 5.5 (0.10 mA at –0.20 V and –0.38 mA at –0.27 V, respectively), and MB in solution (1.34 mM) (0.10 mA at 0.20 V and –0. 23 mA at 0.14 V, respectively). Post peaks also appear next to reduction and oxidation peaks for the MB treated carbon electrode at pH 12 (0.33 mA at 0 V and –0.20 mA at –0.07 V, respectively). The post peaks occur when the difference in energies for reduction of adsorbed and dissolved reactant is large, and therefore indicates strong adsorption [41].

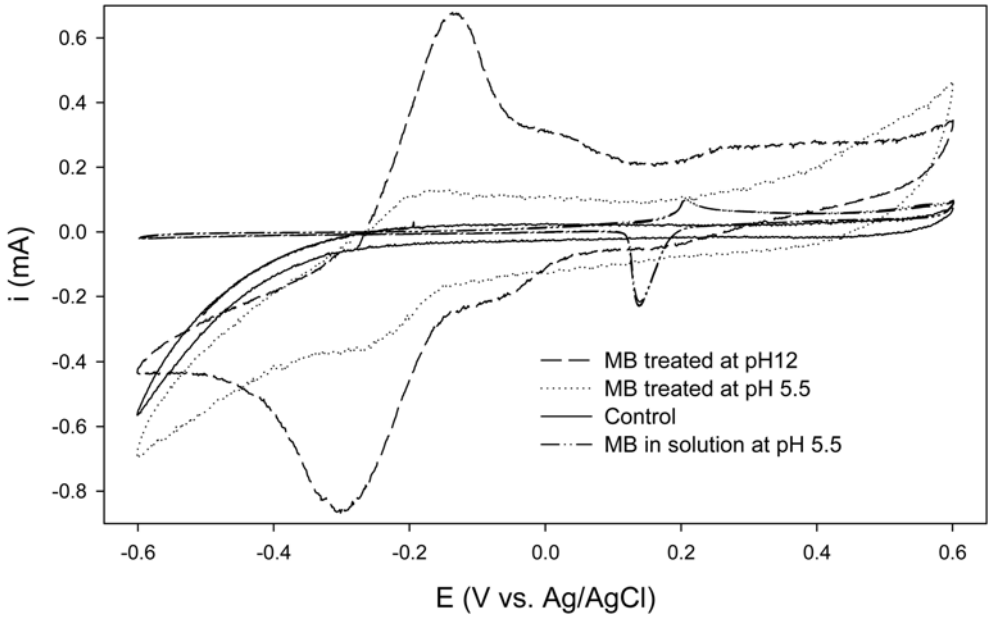

Fig. 4. Cyclic voltammogram showing MB pre-treated carbon electrode at pH 12, and MB pre-treated carbon at pH 5.5 as compared to carbon only control, in sterile electrolyte solution (pH 5.5), and MB in the same solution (not immobilized).

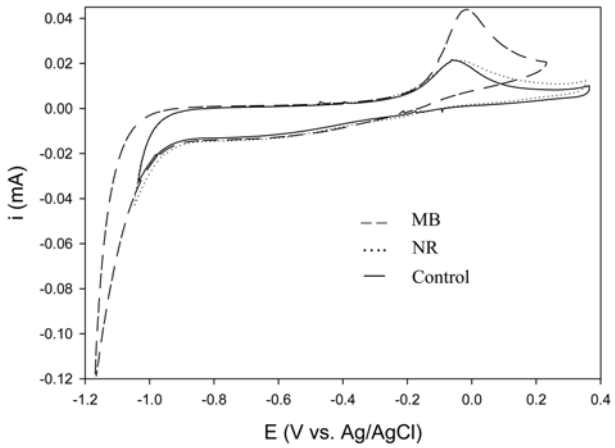

Fig. 5. Cyclic voltammogram of MFC effluent containing bacteria, with MB and NR and carbon only control.

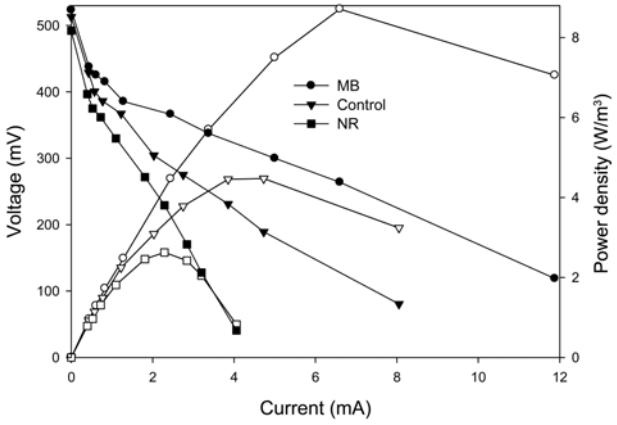

Fig. 6. Comparison of voltages and power densities for MFCs with MB and NR immobilized carbon electrode on day 118. Power densities (open symbols) and cell potentials (closed symbols), are compared for carbon anodes modified with immobilised MB, NR and a carbon only control.

Cyclic voltammograms with different MFC effluent samples containing bacteria were also compared in order to investigate the effect of microbial activity on the current production (Fig. 5). The samples with MB treated carbon showed different CV patterns with a higher oxidation peak (4.36×10^{-2} mA at –0.026 V) compared to the NR (1.97×10^{-2} mA at –0.077 V) and control (1.94×10^{-2} mA at –0.080 V) (Fig. 5). This result suggests that the MB treated carbon anode was populated by different species of bacteria compared to the control and MFCs with NR treated anodes. The absence of reduction peaks supports notion that the exo-electrogenic biofilm transferred electrons to the carbon anode continuously, without selectivity according to potential, therefore only the oxidation reaction was observed [42].

3.3. Cell potentials and power density

The voltage-current response was investigated to compare maximum power density for MB and NR treated carbon anodes as compared to the control. The peak power was higher by a factor of two for the MFC with MB treated anode compared to the control, as well as the power densities at low load resistance and high current regions. The NR treated anode, consistently performed less effectively than the MB or control. The power density obtained at 20ºC at 10 Ω resistance, was 7.06 W/m^3 (11.88 mA) for

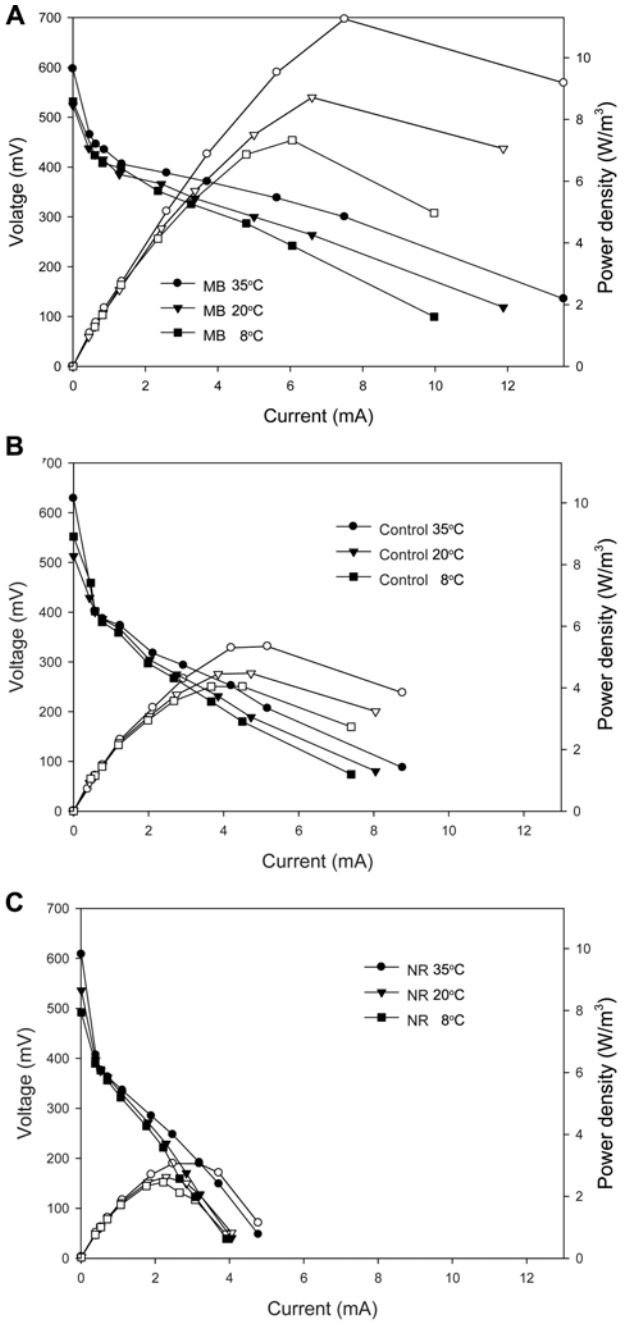

Fig. 7. Comparison of currents to voltages and power densities for MFCs at different temperatures on day 118. Power densities (open symbols) and cell potentials (closed symbols), at 35.5, 20, and 8°C. (A) MB immobilized carbon electrode; (B) carbon electrode (control); (C) NR immobilized carbon electrode.

the MFC with MB treated carbon anode while the power density for the control was 3.24 W/m^3 (8.05 mA) (Fig. 6). It is clearly shown that the *I-V* curve extended to higher currents, probably due to an increase in the rate of electron transport facilitated by MB mediator in the MFC. The maximum power densities were P_{max}(MB) = 8.7 W/m^3 (6.6 mA), P_{max}(Control) = 4.5 W/m^3 (4.7 mA), both obtained at the load of 40 Ω and P_{max}(NR) = 2.63 W/m^3 (2.29 mA), obtained at the load of 60 Ω at 20°C, respectively (Fig. 6).

The highest power density P_{max}(MB) = 11.3 W/m^3 (7.5 mA) was obtained as compared to P_{max}(Control) = 5.3 W/m^3 (5.2 mA) and P_{max}(NR) = 3.06 W/m^3 (3.19 mA) (Fig. 7) at 35°C. The increase in maximum power densities with MB treated carbon electrode was more pronounced compared to those of the control and NR electrode, when the temperature was increased from 8 to 35.5°C, and simultaneously, no methane production indicating lower methanogenic activity with MB electrode (Table 1).

3.4. Effect of immobilized mediators on the VFA removal

VFA (acetate) removal rates using MB and NR treated carbon electrodes and the control are shown in Fig. 8. Initial VFA removal rates in the MFCs were 7.4 mg/L /day (9.7%) for the control, 30.3 mg/L/day (39.7%) for NR, and 23.3 mg/L/day (30.5%) with MB treated carbon anodes, respectively (Fig. 8). The higher VFA removal rate in the MFC with MB treated carbon anode was accompanied by the higher voltage generation during the initial increase in voltage over days 5 ~ 16 during the start-up. The VFA removal rate increased for all reactors, but showed different rates, for example, from 9.7 to 87% (66.5 mg/L/day) for control, 39.7 to 82% (62.6 mg/L/day) for NR; and from 30.5 to 83% (63.4 L/day) for MB. The VFA removal rates for all reactors was almost the same after 118 days, however there was a significant difference in the power densities as previously described, indicating higher exoelectrogenic activity with the MB treated electrode. These results indicate that MB may have affected bacterial selection and/or metabolism on the electrode, thus changing the diversity of the bacterial community on the biofilm and/or in suspension, which are expected to adapt to indirect electron transfer to the electrode with MB treated carbon, as compared to the control.

3.5. Effect of immobilized mediators on gas production in the MFC

An increase in methane production was seen on day 7 and it decreased after the sludge was removed and replaced with fresh media, on day 14 (Table 1) was accompanied by a low carbon dioxide concentration attributable to hydrogenotrophic methanogenesis. Methanogenic activity decreased significantly from days 14 to 147 (data not shown), in the MFC containing an MB treated carbon anodes, while 0.07 ~ 0.14% of methane was detected in the control and NR treated carbon anode MFC. An increase in carbon dioxide production on day 7 was also accompanied by an increase in VFA removal, voltage, power density and a gradual increase in conductivity in all reactors. These results imply that electrogenesis was activated while methano-

Table 1. Gas composition in the tubular MFC reactors (with 12.6 cm^3 head space) for MB, NR and control at days 7, 14 and 154

Time (days)		H_2%	O_2%	N_2%	CH_4%	CO_2 %	Total gas volume (ml/day)
7	NR / carbon anode	0	0	80.51	2.43	0.44	0.5
	MB / carbon anode	0	0	80.13	4.09	0.39	4
	Control (carbon anode)	0	0	77.26	0.27	1.01	0.5
14	NR / carbon anode	0	0	76.48	0	2.05	5
	MB / carbon anode	0	0	76.93	0	1.83	17.5
	Control (carbon anode)	0	0	76.78	0	0.76	2.4
119	NR / carbon anode	0.01	0	74.76	0.14	1.05	1.05
	MB / carbon anode	0	0	77.16	0	4.56	8
	Control (carbon anode)	0	0	74.43	0.07	0.89	0.5

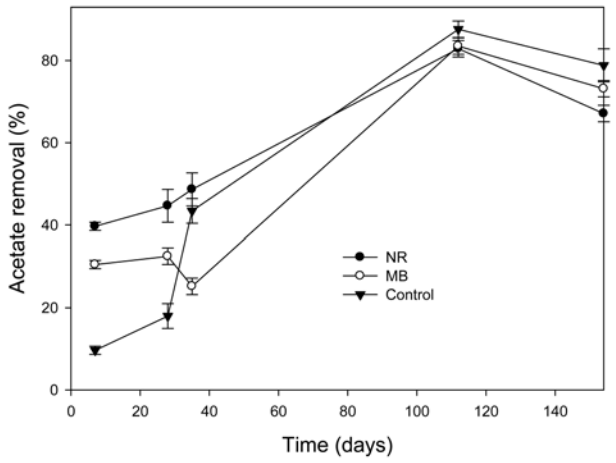

Fig. 8. VFA removal rates in MFCs with MB, NR modified anodes and a control, with carbon electrode.

genesis decreased, facilitated by an increased electron transfer rate in the MFC, when using the MB treated carbon anode.

4. Discussion

MB was successfully immobilized onto the electrode surface by a simple pH shifting method. Although MB has been used as a mediator in many studies [14,30,31], immobilization of MB on the electrode by a physico-chemical adsorption of pH shifting has not been done before in MFCs. This could be a feasible activation method for carbon electrodes for electrogenic bacteria, which could simultaneously treat contaminated wastewater (*e.g.* dye), and generate electrical power. Lower adsorption of MB at acidic pH is probably due to the presence of excess of H^+ ions competing with cation groups [34]. These results are confirmed by the studies on MB adsorption onto the saw dust [43-46], to form an activated MB-carbon anode. It is likely that MB, in its ionic form, interacts with delocolised electrons on carbon. Gravimetric analysis conducted at pH 5.5 showed that 8.0 ± 0.5 mg of MB was adsorbed onto the cabon felt electrode (36.1 ± 1.0 g) at pH 12 as compared to only 3.0 ± 1.0 mg at pH 5.5. Thus the lower adsorption of MB onto the carbon surface could also be the reason for smaller oxidation and reduction peaks on the carbon veil pre-treated at pH 5.5; compared to higher peaks on the carbon veil pre-treated at pH 12 (Fig. 4).

NR was poorly adsorbed onto the carbon suface, as predicted by Henderson-Hasselbalch equation ($6.8 + \log_{10}((NR + H^+)/(NR^+H) = 12)$), which shows that most NR stays in its non polar NR form at pH 12 (Fig. 1). NR also seemed not to be efficient in the methods used here for electricity production, though NR can also be immobilized and be an effective electron mediator, as discussed in previous studies [48]. The proposed reason for inferior performance is that NR molecule interacts differently with different receptors on cell membranes and its performance largely depends on the culture conditions and species selection [14].

The adsorbed MB improved the MFCs power density by a factor of two on day 118 (Fig. 6) and improved the VFA removal rate between days 1 and 23 (Fig. 8). This clearly showed that the MFC with MB treated carbon electrode facilitated the start-up process more rapidly than the control. During the second voltage increase (day 71), MB had a slightly different effect on the performance. The acetate removal rates and average voltage outputs were almost the same for MB and control, between days 71 and 154. The power density was twice as high for MB treated anodes compared to control on day 118 (Fig. 4). The MFC with NR treated carbon electrode, however, showed significantly lower voltage. It is likely that this was because of the limited electron current flow between the bacteria and electrode [3]. The increased power density at higher current obtained in MB treated carbon supports the hypothesis that immobilized MB improves the electron transport from the bacteria to the anode.

Cyclic voltammograms for the samples removed from the reactor with MB treated anode showed higher oxida-

tion peak compared to NR treated anode and the control (Fig. 5). Initial VFA removal rates from the MFC with MB treated carbon anode were three times higher than the control. This suggests that mediators increased the VFA removal rate during start-up, as well as improving power generation. According to Wagner *et al*. [49] the VFA removal would be expected to be higher for the MFCs with higher power densities, as initially observed. It is reasonable to suggest that MB increased the bacterial biofilm metabolism towards exoelectrogenesis more significantly from day 5 to day 16, compared to the control. After several batch cycle replacements of media and innocula, the bacteria capable of using MB for indirect electron transfer [14,50] and capable of attaching themselves to the carbon anode, were more likely to populate the anode with MB immobilized on its carbon surface. This would explain enhanced electron transport on day 118, after 15 fed-batch cycles (Fig. 6). Further research should be done in order to identify how MB and NR treatment affects the growth and diversity of mixed culture in the biofilms growing on the anode surface.

The temperature also significantly affected the cell potential and the power density according to current, probably due to different bacterial communities acting within the biofilm [51,52]. The highest power density with MB treated carbon electrode, P_{max}(MB) = 11.3 W/m^3 (7.5 mA) (Fig. 7A), was approximately two times higher than the control. The maximum power densities increased in MFCs with MB treated carbon electrodes and was significantly higher than the control over the range of 8 ~ 35.5°C. This result indicates that improved bacteria-anode electron transport might enhance the system capability to adapt and increase performance when subject to environmental changes (*e.g.* temperature).

The physico-chemical adsorption of mediator using the simple method presented (*i.e*. pH shift) could readily be applied to large capacity MFC systems for *e.g.* wastewater treatment and/or energy recovery if scale-up barriers were resolved. Some further investigations should however be undertaken; such as ensuring efficient immobilization techniques and scale-up of activation process for carbon materials with mediators (*e.g*. MB) [36]. The immobilised mediator improved the power density of the MFC, and could be used for continuous treatment of organic waste streams, with more efficient energy recovery than carbon electrodes alone. It is believed that chemical treatment can provide an efficient and cost effective activation method for electrodes used in bacterial respiration in MFCs.

This method could also be applied for the removal of other industrial dyes such as resazurin [53]. The results show that a simple physico-chemical method to immobilize the electron carrier onto the carbon electrode surface can activate, bioelectrochemically, a carbon electrode, in order to enhance MFC's performance in continuous flow systems requiring large volumetric capacities in order to treat waste streams. MB may be leached out through a drop in pH caused by bacterial metabolism. Excessive leaching will render the MFC system to be mediated. However, highly localized leaching may contribute to micron-scale electron transportation occurring between attached microorganisms and the anode, driven by local proton accumulation. These methods could be combined with dye removal from industrial wastewater *via* its adsorption onto the activated carbon material, which may then be converted into an anode for bioelectrochemical reactions in the MFC.

Acknowledgement

This research was funded by the RCUK Energy Programme SUPERGEN (SHEC) project (grant number EP/E040071/1) and SUPERGEN Biological Fuel Cell project (EP/D047943/1) supported by grant 68-3A75-3-150. The Energy Programme is an RCUK cross-council initiative led by EPSRC and contributed to by ESRC, NERC, BBSRC and STFC.

References

1. Oh, S. T., J. R. Kim, G. C. Premier, T. H. Lee, C. Kim, and W. T. Sloan (2010) Sustainable wastewater treatment: How might microbial fuel cells contribute. *Biotechnol. Adv.* 28: 871-881.
2. Rabaey, K., K. Van de Sompel, L. Maignien, N. Boon, P. Aelterman, P. Clauwaert, L. De Schamphelaire, H. T. Pham, J. Vermeulen, M. Verhaege, P. Lens, and W. Verstraete (2006) Microbial fuel cells for sulfide removal. *Environ. Sci. Technol*. 40: 5218-5224.
3. Logan, B. E., B. Hamelers, R. Rozendal, U. Schröder, J. Keller, S. Freguia, P. Alterman, W. Verstraetae, and K. Rabaey (2006) Microbial fuel cells: Methodology and technology. *Environ. Sci. Technol*. 40: 5181-5192.
4. Rabaey, K. and W. Verstraete (2005) Microbial fuel cells: Novel biotechnology for energy generation. *Trends Biotechnol*. 23: 291-298.
5. Kim, J. R., G. C. Premiera, F. R. Hawkes, R. M. Dinsdale, and A. J. Guwy (2009) Development of a tubular microbial fuel cell (MFC) employing a membrane electrode assembly cathode. *J. Power Sources* 187: 393-399.
6. Kim, J. R., J. Rodriguez, F. R. Hawkes, R. M. Dinsdale, A. J. Guwy, and G. C. Premier (2011) Increasing power recovery and organic removal efficiency using extended longitudinal tubular microbial fuel cell (MFC) reactors. *Energ. Environ. Sci*. 4: 459-465.
7. Kim, J. R., G. C. Premier, F. R. Hawkes, J. Rodríguez, R. M. Dinsdale, and A. J. Guwy (2010) Modular tubular microbial fuel cells for energy recovery during sucrose wastewater treatment at low organic loading rate. *Bioresour. Technol.* 101: 1190-1198.
8. Zeng, Y. Z., Y. F. Choo, B. H. Kim, and P. Wu (2010) Modelling

and simulation of two-chamber microbial fuel cell. *J. Power Sources*. 195: 79-89.
9. Logan, B. E. (2008) *Microbial Fuel Cells*. pp. 132-133. John Wiley and Sons, NJ.
10. Logan, B. E., B. Hamelers, R. A. Rozendal, U. Schrorder, J. Keller, S. Freguia, P. Aelterman, W. Verstraete, and K. Rabaey (2006) Microbial fuel cells: Methodology and technology. *Environ. Sci. Technol*. 40: 5181-5192.
11. Park, A. H., S. K. Kim, I. H. Shin, and Y. J. Jeong (2000) Electricity Production in biofuel cell using modified graphite felt electrode with neutral red. *Biotechnol. Lett*. 22: 1301-1304.
12. Park, D. H. and J. G. Zeikus (1999) Utilization of electrically reduced neutral red by *Actinobacillus succinogens*: Physiological function of neutral red in membrane driven fumrate reduction and energy concervation. *J. Bacteriol*. 181: 2403-2410.
13. Ferreira-Leitao, V. S., M. E. A. Carvalho, and E. P. S. Bon (2007) Lignin peroxidase efficiency for methylene blue decolouration: Comparison to reported methods. *Dyes Pigments* 74: 230-236.
14. Mohan, Y., S. M. M. Kumar, and D. Das (2008) Electricity generation using microbial fuel cells. *Int. J. Hydrogen Energ*. 33: 423-426.
15. Wang, C. -T., W. -J. Chen, and R. -Y. Huang (2010) Influence of growth curve phase on electricity performance of microbial fuel cell by *Escherichia coli*. *Int. J. Hydrogen Energ*. 36: 1-7.
16. Potter, M. C. (1912) Electrical effects accompanying the decomposition of organic compounds. *Royal Society* 84: 260-276.
17. Choi, Y., N. Kim, S. Kim, and S. Jung (2003) Dynamic behaviors of redox mediators within the hydrophobic layers as an important factor for effective microbial fuel cell operation. *B. Kor. Chem. Soc*. 24: 437-440.
18. Lithgow, A. M., L. Romero, I. C. Sanchez, F. A. Souto, and C. A. Vega (1986) Interception of the electron-transport chain in bacteria with hydrophilic redox mediators .1. Selective improvement of the performance of biofuel cells with 2,6-disulfonated thionine as mediator. *J. Chem. Res.* 5: 178-179.
19. Samrot, A. V., P. Senthilkumar, K. Pavankumar, G. C. Akilandeswari, N. Rajalakshmi, and K. S. Dhathathreyan (2010) Electricity generation by Enterobacter cloacae SU-1 in mediator less microbial fuel cell. *Int. J. Hydrogen Energ*. 35: 7723-7729.
20. Gunawardena, A., S. Fernando, and F. To (2008) Performance of a Yeast-mediated biological fuel cell. *Int. J. Mol. Sci*. 9: 1893-1907.
21. Rabaey, K., N. Boon, M. Hofte, and W. Verstraete (2005) Microbial phenazine production enhances electron transfer in biofuel cells. *Environ. Sci. Technol*. 39: 3401-3408.
22. Das, D. and T. N. Veziroðlu (2001) Hydrogen production by biological process: A survey of literature. *Int. J. Hydrogen Energ*. 26: 13-28.
23. Michaelis, L. and H. Eagle (1930) Some redox mediators. *The J. Biol. Chem*. 88: 713-727.
24. Akoachere, M., K. Buchholz, E. Fischer, J. Burhenne, W. E. Haefeli, R. H. Schirmer, and K. Becker (2005) *In vitro* assessment of methylene blue on chloroquine-sensitive and -resistant Plasmodium falciparum strains reveals synergistic action with artemisinins. *Antimicrob. Agents Ch*. 49: 4592-4597.
25. Auerbach, S. S., D. W. Bristol, J. C. Peckham, G. S. Travlos, C. D. Hebert, and R. S. Chhabra (2010) Toxicity and carcinogenicity studies of methylene blue trihydrate in F344N rats and B6C3F1 mice. *Food and Chemical Toxicol*. 48: 169-177.
26. Hameed, B. H. and A. A. Ahmad (2009) Batch adsorption of methylene blue from aqueous solution by garlic peel, an agricultural waste biomass. *J. Hazard. Mater*. 164: 870-875.
27. Hameed, B. H., A. L. Ahmad, and K. N. A. Latiff (2007) Adsorption of basic dye (methylene blue) onto activated carbon prepared from rattan sawdust. *Dyes Pigments*. 75: 143-149.
28. Hameed, B. H., A. T. M. Din, and A. L. Ahmad (2007) Adsorption of methylene blue onto bamboo-based activated carbon: Kinetics and equilibrium studies. *J. Hazard. Mater*. 141: 819-825.
29. Hameed, B. H. and N. Nasuha (2011) Adsorption of methylene blue from aqueous solution onto NaOH-modified rejected tea. *Chem. Eng. J*. 166: 783-786.
30. Daniel, D. K., B. Das Mankidy, K. Ambarish, and R. Manogari (2009) Construction and operation of a microbial fuel cell for electricity generation from wastewater. *Int. J. Hydrogen Energ*. 34: 7555-7560.
31. Wang, C. T., W. J. Chen, and R. Y. Huang (2010) Influence of growth curve phase on electricity performance of microbial fuel cell by Escherichia coil. *Int. J. Hydrogen Energ*. 35: 7217-7223.
32. McKinlay, J. B. and J. G. Zeikus (2004) Extracellular iron reduction is mediated in part by neutral red and hydrogenase in *Escherichia coli*. *Appl. Environ. Microb*. 70: 3467-3474.
33. Lin, J. X. and L. Wang (2009) Comparison between linear and non-linear forms of pseudo-first-order and pseudo-second-order adsorption kinetic models for the removal of methylene blue by activated carbon. *Frontiers of Env. Sci. Eng. China* 3: 320-324.
34. Senthilkumaar, S., P. R. Varadarajan, K. Porkodi, and C. Subbhuraam (2005) Adsorption of methylene blue onto jute fiber carbon: Kinetics and equilibrium studies. *J. Colloid. Interf. Sci*. 284: 78-82.
35. Kim, J. R., S. Cheng, S. E. Oh, and B. E. Logan (2007) Power generation using different cation, anion, and ultrafiltration membranes in microbial fuel cells. *Environ. Sci. Technol*. 41: 1004-1009.
36. Kim, J. R., G. C. Premier, F. R. Hawkes, J. Rodríguez, R. M. Dinsdale, and A. J. Guwy (2009) Modular tubular microbial fuel cells for energy recovery during sucrose wastewater treatment at low organic loading rate. *Bioresour. Technol*. 101: 1190-1198.
37. Richter, H., K. P. Nevin, H. F. Jia, D. A. Lowy, D. R. Lovley, and L. M. Tender (2009) Cyclic voltammetry of biofilms of wild type and mutant Geobacter sulfurreducens on fuel cell anodes indicates possible roles of OmcB, OmcZ, type IV pili, and protons in extracellular electron transfer. *Energ. Environ. Sci*. 2: 506-516.
38. Cruwys, J. A., R. M. Dinsdalea, F. R. Hawkes, and D. L. Hawkes (2002) Development of a static headspace gas chromatographic procedure for the routine analysis of volatile fatty acids in wastewaters. *J. Chromatography* 945: 195-209.
39. Albrecht, T., Z. P. Chen, E. Knutson, S. Wang, and L. A. Martinez (2007) Stabilization of p53 in human cytomegalovirus-initiated cells is associated with sequestration of HDM2 and decreased p53 ubiquitination. *J. Biol. Chem*. 282: 29284-29295.
40. Rezvani, S., Y. Huang, D. Mcllveen-Wright, N. Hewitt, and Y. Wang (2007) Comparative assessment of sub-critical versus advanced super-critical oxyfuel fired PF boilers with CO(2) sequestration facilities. *Fuel* 86: 2134-2143.
41. Bard, A. J. and L. R. Faulkner (2001) *Electrochemical Methods*. pp. 598-600. John Wiley & sons, Austin.
42. Logan, B. E., J. R. Kim, S. H. Jung, and J. M. Regan (2007) Electricity generation and microbial community analysis of alcohol powered microbial fuel cells. *Bioresour. Technol*. 98: 2568-2577.
43. Cousins, C. S. G. (2003) Elasticity of carbon allotropes. IV. Rhombohedral graphite: Elasticity, zone-center optic modes, and phase transformation using transferred Keating parameters. *Physical Rev. B*. 67: 024110.024111-024110.024111.
44. Cousins, C. S. G. and M. I. Heggie (2003) Elasticity of carbon allotropes. III. Hexagonal graphite: Review of data, previous calculations, and a fit to a modified anharmonic Keating model. *Physical Rev. B*. 67: 024109..024101-024109.024112.
45. Endo, K., S. Koizumi, T. Otsuka, T. Ida, T. Morohashi, J. Onoe, A. Nakao, E. Z. Kurmaev, A. Moewes, and D. P. Chong (2003) Analysis of electron spectra of carbon allotropes (diamond, graphite, fullerene) by density functional theory calculations

using the model molecules. *J. Phys. Chem. A*. 107: 9403-9408.
46. Hirsch, A. (1993) The Chemistry of the Fullerenes - An overview. *Angewandte Chemie-International Edition in English*. 32: 1138-1141.
47. Ye, J. N. and R. P. Baldwin (1988) Catalytic reduction of myoglobin and hemoglobin at chemically modified electrodes containing methylene-blue. *Anal. Chem*. 60: 2263-2268.
48. Housecroft, C. and A. G. Sharpe (2007) *Inorganic Chemistry.* Prentice Hall, NY.
49. Wagner, R. C., D. I. Call, and B. E. Logan (2010) Optimal set anode potentials vary in bioelectrochemical systems. *Environ. Sci. Technol*. 44: 6036-6041.
50. Mccalla, T. M. (1939) Cation adsorption by bacteria. *J. Bacteriol*. 40: 23-32.
51. Michie, I., J. R. Kim, R. Dinsdale, A. Guwy, and G. Premier (2011) Operational temperature regulates anodic biofilm growth and the development of electrogenic activity. *Appl. Microbiol. Biot*. 92: 419-430.
52. Michie, I. S., J. R. Kim, R. M. Dinsdale, A. J. Guwyb, and G. C. Premier (2011) The influence of psychrophilic and mesophilic start-up temperature on microbial fuel cell system performance. *Energ. Environ. Sci*. 4: 1011-1019.
53. Sumner, J. J., C. J. Sund, S. McMasters, S. R. Crittenden, and L. E. Harrell (2007) Effect of electron mediators on current generation and fermentation in a microbial fuel cell. *Appl. Microbiol. Biot*. 76: 561-568.

To the Author:
Kindly check reference number 23.

ISSUES OF SCALE IN MICROBIAL FUEL CELLS AND BIOELECTROCHEMICAL SYSTEMS

Giuliano C. Premier[a*], Jung Rae Kim[a], Iain Michie[b], Arseniy Popov[b],
Hitesh Boghani[a], Katrin Fradler[a], Richard M. Dinsdale[b], Alan J. Guwy[b]
Sustainable Environment Research Centre (SERC)
[a]Faculty of Advanced Technology
[b]Faculty of Health Sport and Science
University of Glamorgan, Treforest, Wales, UK.
[*]Email: gcpremier@glam.ac.uk

ABSTRACT

Bioelectrochemical systems (BES) are expected to have a significant role to play in future energy saving and generation, in the separation of ions and manufacture of bio-derived products; be they energy gasses, liquids or materials. Microbial fuel cells (MFCs) have received the most attention to date, but there are considerable lessons to be derived from this subset of BES, in terms of the minimisation of losses and particularly the performance of the anodic half cell of BES. While interest exists in relation to commercialization of these technologies, there are relatively few examples of increasing scale while maintaining adequate performance. The paper explores some of the issues in relation to scale-up and presents an overview of the work of the authors in this regard.

Keywords: Bioelectrochemical systems (BES), Microbial fuel cell (MFC), Scale-up, Tubular MFC systems.

1. INTRODUCTION

The mitigation of pollution by reducing waste discharges to water courses and the use of fossil fuels has been well rehearsed elsewhere, e.g. (1-6). Several states have passed legislation to drive an agenda of waste reduction, reuse and energy from waste; e.g. the UK Government has passed several acts related to energy and waste treatment/pollution abatement, some of these are driven by EU directives and international commitments, (e.g. UK Energy Act 2010, 2011 (DECC http://www.decc.gov.uk), Climate Change Act 2008, EU Directives on Renewable Energy, Landfill, Water Framework and Urban Wastewater, along with several regulations, plans and targets. The UK is legally committed to an 80% reduction in all GHG emissions by 2050 *c.f.* 1990. Human effects on climate and ecosystems alongside increasing global population and consumption; and a propensity to urbanisation, will exacerbate the problems of waste, energy and resource availability.

The rate at which carbon emissions to the atmosphere would need to reduce for the concentration of CO_2 to stabilise at 550 ppm by the turn of this century, becomes progressively more severe and costly (http://www.direct.gov.uk/en/Nl1/Newsroom/DG_064854). Exactly how green house gas (GHG) emissions may be mitigated is still a prolific and wide ranging field of investigation. However, the International Energy Organisation predict that bioelectrochemical systems (BES) have the potential to contribute by efficient waste treatment and energy from waste; better use of resources and more efficient production of materials.

Microbial Fuel Cells (MFCs) and microbial electrolysis cells (MECs) among other BES have received a significant level of attention to date; particularly since the turn of the millennium (7-9). In essence, BES are electrochemical processes which are catalysed by biological processes. Specifically microbial, whole cell processes are of interest in this treatment, but enzyme focused systems are attracting attention too. The development of such systems started in the early 20th

century(10), but remained a curiosity, with notable exceptions, until the work of (11) which represented at key development, in that the ubiquitous use of electron shuttling (and environmentally damaging) redox were shown not to be essential. This development opened the field to wastewater treatment processes and raised interest from electrochemistry, materials sciences and molecular biology; establishing a multi-disciplinary community well equipped to progress MFC development. Interest in other specialised application such as *in vivo*, benthic/sedimentary MFCs have persisted also.

BES consists of anodic and cathodic chambers in general. The electronic and cationic currents notionally initiated in the anode chamber, can be used in various ways; electricity generation analogous to conventional fuel cells, electrolysis, ion separation and reduction reactions at the cathode references on different BES systems. Although the performance of these systems depends on complex interactions between living and electro-active biofilms and electrochemical systems, with the biocatalysed anode highly coupled to the performance of virtually all other system elements; it is nevertheless useful to empirically and sometimes heuristically consider the common elements in BES. Bacteria, acting alone, or in syntrophic liaisons, have the fortuitous ability to oxidise many different substrates, making use of their versatile metabolic pathways. They may also be considered to be self-regenerating catalysts and may also be useful, in processes, as electron sources or sinks.

The scale-up of the bio-anode has been a focus for the Sustainable Environment Research Centre (SERC), achieving a 2 fold doubling of the system volume with virtually linear correlation to volumetric power density. An elaboration of some key issues of scale-up and of the progress made in anode performance and low temperature operation and the wider context and challenges of the technology will be presented.

2. BES TECHNOLOGIES

BES represents a family of electrochemical processes which use biological catalysts (12). This family includes systems which utilise the natural ability of live microorganisms to use metabolic pathways which can reduce solid electron acceptors, e.g. iron and manganese oxides. As for example in microbial Fuel cells (MFCs), bacteria transfer electrons to reduce an anode electrode which acts as a terminal electron acceptor for their respiration; and so they derive life energy. Conversely the microorganisms may use a cathode as a source of electrons to facilitate reduction reactions in anabolic processes for electrochemical synthesis. Bacterial BES may also generate the potential to drive the movement of ions for e.g. desalination or separation processes (13). A common benefit in BES is the use of low value biodegradable feedstocks (substrates), typically waste streams, as a source of energy. Hence waste treatment is an important collateral feature of BES. The substrates are oxidised by a biofilm (electrogenic microorganisms) delivering electrons to an anode electrode.

2.1 Future development

The deployment of BES technologies is likely to require a simultaneous development of suitable materials, surface and redox chemistry; selection or synthesis of appropriate biofilm, enzymes or planktonic catalysts; identification of suitable and economic BES functions or products; the selection of suitable feed-stocks and the development of optimal operating procedures. Furthermore, these advances must be deployed in viable conceptual arrangements or designs which are able to cost effectively make the transition from laboratory scales to systems which are large enough to find utility as wastewater treatment or production facilities. Integration of BES into existing wastewater treatment system will be of great interest as it can complement and replace the present energy intensive aerobic process.

2.2 Key barriers to development

Arguably, the most significant barrier to BES exploitation lies in the fact that these processes are inherently sensitive to losses which become dominant in scale-up; i.e. it is a typical and important feature of most BES designs, that internal losses typically and rapidly increase with scale. Stacking an enormous number of very small, plate-like BES cells would, in the absence of more elegant concepts, be impractical and costly. It is therefore necessary to find appropriate embodiment concepts to translate the technology from laboratory to the large industrial capacities necessary in e.g. wastewater treatment. Most scale-up concepts proposed to-date generally require modularization and replication of the fundamental BES cell structure to increase volume.

The field of BES awaits a ‘game changing’ strategy, which will allow cost effective scale-up of BES in all their numerous embodiments. These include several highly desirable processes: electricity generating microbial fuel cells (MFCs) (7, 8); hydrogen producing microbial electrolysis (ME) (14), or indeed methane;

microbial electrochemical synthesis (MES), producing renewable materials; desalination (13) and separation processes; waste treatment processes (15-17) and others. Utilizing low value energy sources such as wastewaters, municipal and industrial waste streams, co-products and wet biomass from farming and other sources. The scope for exploitation is therefore manifold.

3. AN OVERVIEW OF MFC/BES SCALE-UP

Specific power and current densities in MFC and BES are considerably lower than conventional fuel cells. They are unlikely to find utility *solely* as power sources, apart from niche applications. Self sustaining waste treatment; energy from waste; low cost production of specialist biosynthesised products or bio-augmented electrochemical processes are more likely to present cost effective exploitation routes. Advanced treatment of recalcitrant organic contaminants include dye wastewater (18, 19) and nitrilotriacetic acid (20). Resource recovery using BES is also of great interest for example: metal from acid mine drainage (21-24). These results indicate that BES could be a versatile field of technology.

3.1 MFC as a model for BES

The basic operating principle of an MFC is similar to Proton Exchange Membrane Fuel Cells (PEM FC) (25). However, as in all BES, they rely on complex interactions between living, electro-active biofilms and the remaining electrochemical system. Metabolic processes oxidise foods through an in-cell electron transport chain, with an extracellular terminal electron acceptor (oxygen in respiration; products such as methane, hydrogen, volatile fatty acids, in fermentation and methanogenesis). BES must present an environment in which it is thermodynamically advantageous for the microorganisms to use metabolic pathways and electron transfer mechanisms, which involved an electrical circuit. In reducing the anode, the microorganisims (generally bacteria) deliver an electrical current to a reduction reaction at the cathode, frequently O_2 in an MFC.

BES typically have a common requirement for an anode catalyzed by microorganisms. MFCs are a subset of BES and may reasonably be employed as an anode half-cell model in considering scale-up. However, the bioelectrochemistry, particularly the ionic species involved and the cathodic reduction reactions will require detailed investigation in each specific case.

The cathode half-cells in BES, which may facilitate product formation through electron transfer to a biologically catalyzed reduction reaction, might be considered to be analogy to the reactions at the anode, but with electron transfer from the electrode to the bio-catalyst; or may draw lessons from optimized anode arrangements.

3.2 Likely sources of energy

Using the chemical energy of municipal and industrial waste streams, co-products and crops, will make significant contributions in mitigating the concerns raised by fossil fuel consumption. It is worth considering the energy lost and consumed from e.g. wastewater; energy which could be utilised in BES, while maintaining some healthy reservations in relation to particulate loading and conductivity for example. We have estimated that $330m^3$/tDM of waste, co-products and crops are available in the UK alone (26), which could be made available as feedstock. Substantial biomass resource is reported to exist in many regions of the. The aim might be for anodic systems in BES processes to have comparable conversion efficiency to anaerobic digestion (12), but with a more direct and efficient utilization of the energy in the various manifestations of BES listed above.

BES are able to use a wide variety of biodegradable materials such as sugars and other carbohydrates, volatile fatty acids and wastewaters, as fuel. Several investigations have been conducted in relation to the use of different materials as substrate and these have been reviewed in (12, 27) have reviewed plausible substrates for MFCs and these are likely to be appropriate for many embodiments of BES. Their most promising application therefore is the utilization of the large volumes of municipal and industrial wastewaters which contain large amounts of chemical and /or biological oxygen demand (COD/BOD) and hence energy. BOD represents pollution potential, and simultaneously incurs large energy costs in its mineralization. In the UK for example approximately 2% of total UK electricity demand is used in aeration, pumping etc in the treatment of waste water (28). BES have the potential to convert this BOD to a resource, but would require large capacity systems to cope with the throughput.

A barrier in ongoing BES research is that the highest current densities are only achievable at very small scales which primarily minimise ohmic losses e.g. power density of ~1 kW/m^3 MFCs (29), despite virtually logarithmic improvements in specific

volumetric power production over the past 10 years or more. The issue of scale is of considerable importance.

3.3 Can MFC/BES technology scale-up?

BES research has focused mainly on laboratory scale devices to-date, e.g. Nevin et al (2008) showed they could achieve greater than 2kW/m^3, specific to reactor volume, which was less than 0.5ml. However there appears to be a swing in emphasis towards applications. Extrapolating laboratory scale performances to an industrial scale has not always considered the difficulties which need to be addressed to achieve scale-up. Dewan et al (30) considered the frequently asserted assumption that increased electrode area would necessarily render greater increased power density. They showed that there was not a direct linear relationship between specific power density and anode area, but a logarithmic relationship instead. They suggested there may be serious questions to address in relation to the plausibility of MFC scale-up.

MFCs are limited in several senses in their current state of development. A critical issue is the spatial arrangement of the anode and cathode, regardless of the presence or absence of an ion-exchange membrane. A tension exists between various over-potentials related to ohmic, activation and mass transfer losses; and volume available for bacteria and the substrate. Fig. 1 indicates the predominant classifications of overpotential losses expected in MFC, where the cell voltage is diminishes as current loading is increased

$$V_{cell} = V_e - \sum \eta_a - \left|\sum \eta_c\right| - IR$$

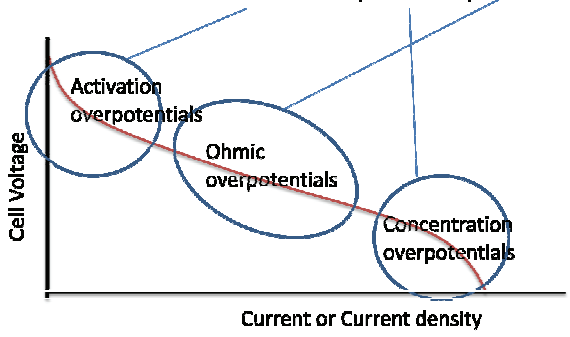

Fig. 1 Indication of overpotential losses and their region of dominance as current loading is increased in an MFC. (after (12))

Concentration overpotentials become a particularly serious issue for large scale BES systems (31, 32). The ion transfer resistivity of wastewater at room temperature is typically between 0.2 Ω m^{-1} (50 mS cm^{-1}, seawater) and 20 Ω m^{-1} (0.5 mS cm^{-1}, drinking water).

One might expect that the larger the volume of the BES cell, the less efficient it will be in transferring charge from the electrochemical reaction site (at the microorganism) to an electrode. The spatial arrangement of the anode and cathode affect the internal impedance, while supply of substrate and removal of biologically derived products (which are frequently inhibitory), are affected by diffusion and hydrodynamic forces; which are also coupled to impedance. The reactor liquid volume is implicated in all these processes and losses (33, 34).

Increased separation between the catalyst and electrode or turbulent fluid flow patterns will induce ohmic losses. Mass transfer and activation losses arise from substrate depletion and/or product inhibition of the biological catalyst or diffusion through concentration gradients limiting access of the microorganisms to the substrate, which represent losses induced by local environments in the vicinity of the catalyst. Ohmic losses in the electrode are also dependent on the scale of the reactor, the distance to the electrode and the surface area of the electrode compared to the fluid volume.

BES are therefore characterised by a series of seemingly conflicting requirements. Electron transfer from bacterial metabolism to serve the purposes of BES requires efficient electron transfer mechanisms. Bacterial proximity to an electrode is implicated in efficient electron transfer, which suggests that that electroactive biofilms with steric access to the electrode/electron donor or acceptor are preferable. Planktonic biomass is not ideal as electron transfer requires synthetic or natural redox mediators to transport electrons through the cell membrane in a cycle of oxidation and reduction; and is susceptable to washout. The use of low value waste streams such as waste waters and municipal solid waste typically requires that large volumes to be processed. Large concentrations of electroactive and/or syntrophic bacteria are necessary to achieve efficient bio-conversion of the biodegradable substrates to energy carriers (electricity, hydrogen, methane etc), or products (H_2O_2, caustic, hydrogen etc and other reduced products). If the biomass is immobilized and localized at the electrode surfaces, this will require a large electrode area. High level of mass transport for substrate supply to electrogens and removal of protons and other localised and inhibitory bio-products and highly conductive electronic and cationic pathways with large electrodes for biomass immobilisation are also required. Such electrodes should exhibit a retained and highly electroactive biofilms, associated with a high surface area to volume ratio electrode. The intent should by some mechanism be to facilitate low ohmic losses, in

a large tank-like reactor (for reasons of cost and throughput). Increased separation between the catalyst and electrode or turbulent fluid flow patterns may induce ohmic losses. Mass transfer and activation losses arise from substrate and/or product inhibition of the biological catalyst or concentration gradients limiting access of the microorganisms to the substrate and those are losses affected by local environments about the catalyst. Ohmic losses in the electrodes are also dependent on the scale of the reactor.

4. SOME PRACTICAL EXAMPLES

Dewan et al (30) amongst others made the observation that power production from MFCs and by implication BES, logarithmically reduced as the area of the anode increases. They showed a rapid drop off in the region of <500 mWm^{-2} and <50 cm^2. They suggested that the cathode should be made as larger than the anode to avoid limitation from this end of the system. This has not stopped attempts to circumvent these limitations. AWMC of the University of Queensland, Australia (http://www.microbialfuelcell.org/www/index.php/Applications/MFC-Pilot.html) have tested a tubular MFC on brewery wastewaters. The system was $1m^3$ and consists of 12 modules. Significant lessons were learned in this ambitious project. High hydrostatic pressures caused concern, as did high overpotential induced by the reactor configuration. Algal biomass also development on the cathode (35). University of Connecticut along with Fuss & Neil and Hydroqual Inc. (http://www.engr.uconn.edu/collaborationcommercialization.php) are conducting scale-up development of graphite granular MFCs and the first pilot MEC is also reported by Pennsylvania State University at the Napa Wine Co, Oakville, CA, USA (35). A small number companies are offering BES solutions e.g. (http://www.engr.uconn.edu/collaborationcommercialization.php).

5. DEVELOPMENTS IN TUBULAR SYSTEMS

A tubular arrangement of MFC/BES has several advantages of many other proposed embodiments of BES processes. Chief amongst these are:
i) A mechanism for increasing volume while simultaneously maintaining critical relative spatial distribution of electrodes and other system components. The cross-sectional geometry remains unaltered while the major axial dimension is extended. There is a crucial requirement that the depletion of substrate and the accumulation of liquid phase products in e.g. the anode chamber, should not deleteriously affect the performance of downstream electrogenesis in an essentially axial flow continuous process.
ii) The manufacturability of the system is enhances by the prismatic geometries employed, in that there is a reasonable prospect of deploying a continuous manufacturing process such as extrusion, pultrusion, lamination etc, which would facilitate a considerable CAPEX reduction with mass production. The OPEX might similarly be expected to be lower than plate-type systems, but this would depend greatly on durability and detailed design.

A step-wise development of a tubular BES concept has been pursued by the authors. A low cost Perspex™ and poly propylene tubular containment and cathode support system has been developed (36) in order to prove the concept. Batch operation allowed a membrane electrode assembly (MEA) system performance to be considered in relation to power generation and chemical oxygen demand (COD) removal. This work established that the membrane/separator selection presents scope for improvement and the cathodic oxygen reduction reaction was limiting and could also be improved. The maximum power generated was using a cation exchange membrane (CEM) with a conductive hydrogel, was 6.1 $W\ m^{-3}$ (reactor - 200 cm^3) (37). It was demonstrated that high coulombic efficiencies ~70% were achievable with this tubular design. The design of a deployable system is in progress, but is not presented here.

Continuous operation was achieved in a modular arrangement which employed replicated tubes of similar capacities and employing relatively low cost carbon veil anode electrodes (38). The applicability of the tubular MFC design has been assessed by twice doubling its scale to 1 l (Fig. 2), while maintaining consistent modules. Power recovery and COD removal efficiency were shown to depend on organic loading rate. The power outputs from modules were considered under different electrical connectivity.

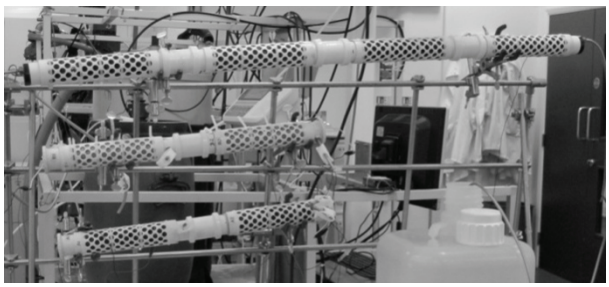

Fig. 2 Twice doubled reactor volume, which achieved virtually proportional increase in power output provided organic loading was adequate.

Above saturation, the cumulative power production lengthwise along the reactor modules, increased to 2.6 mW at higher organic loading rates (OLR) tested (0.8 and 0.38 g/l/d). Power recovery and organic removal could, it was seen, be maximized by extending the number of modules (increased length) in the tubular reactors, which could simultaneously control effluent quality and power, so facilitating scale-up.

Methylene blue was immobilized on the anode electrode to facilitate electron transfer, and was tested in a similar MFC configuration (39). The maximum power and current densities of 8.7Wm^{-3} and 6.6 mA were observed in comparison with 4.5Wm^{-3} and 4.7 mA for untreated carbon cloth of the same dimensions. The aim of this work was to increase hydrogen production from a tubular microbial electrolysis cell. The effect of cathode chamber pH on hydrogen production was also investigated, with the highest hydrogen production rate was obtained at 850 mV, (30^0C, pH5) amounting to 200 cm^3 stp.l_{anode}^{-1}.d^{-1} (coulombic efficiency 60% , H_2 yield 1.1 mol/mol acetate converted and a COD reduction of 30.5%) (40). At pH7 or above, an increase in methane production was observed. At pH 5 and with a salt content of 26g l^{-1}, hydrogenotrophic methanogenisis was completely inhibited as shown by Wang (41).

Successful scaled-up of BES in temperate climates is challenging in terms of energetic (heating) costs and hence carbon footprint. However, low temperature acclimation strategies have been applied to tubular MFC reactors, resulting in MFC biofilms able to operate optimally over a realistic temperature range (42). The effect on the biofilm of such operation was investigated over 1 year and it was observed that 35°C batch operation actually led to a 50% reduction in energy compared to 20°C; this was attributed to the build-up of non-electrogenic biomass at 35°C (43).

Selective membranes can exhibit large internal resistance , but other materials such as cellulose, nylon and polycarbon filters have been used, as have fabrics e,g, (GoreTex®, Canvas) and j-Cloth® or glass wool.

Apart from the serial connection or DC:DC conversion, external capacitors are able to increase potential in MFC systems. An increased voltage to 2.5 V using external capacitors was demonstrated by (44). Similarly Dewan et al (45) increased the maximum power by 111% by harvesting power intermittently and Liang et al (46) increased the average current by 22-32% by capacitive charge/discharge; compared to the intermittent charging. Our own work considered open to closed circuit (1000 ohm) applied to a tubular MFC with carbon veil and stainless steel mesh anode.

Fig. 3 shows the voltage and current development after differing open circuit times (1min to 120min), indicating that the voltage, hence power, increase with increasing open circuit time. This has the potential to increase the power harvested from BES.

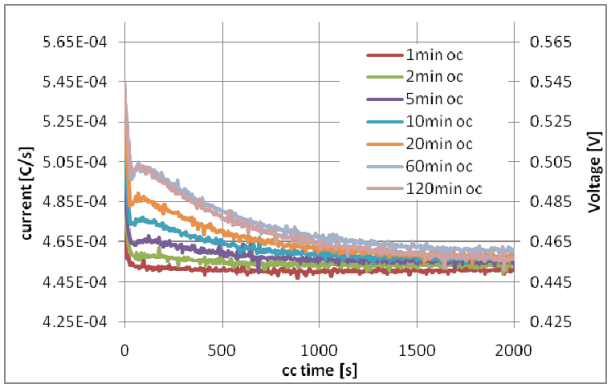

Fig. 3 Voltage and current development (1000 ohm load) after different open circuit times.

The limitations of the anode were considered even though cathode performance was likely to be limiting. To minimise concentration overpotentials, an increase in mass transfer and turnover is necessary. Helical anode designs (Fig. 4) (47), were considered. These induces shear in the fluid flow along the helical path, increasing the mixing. Pillars flow path walls inducing localised eddies increasing the substrate turnover in the MFC.

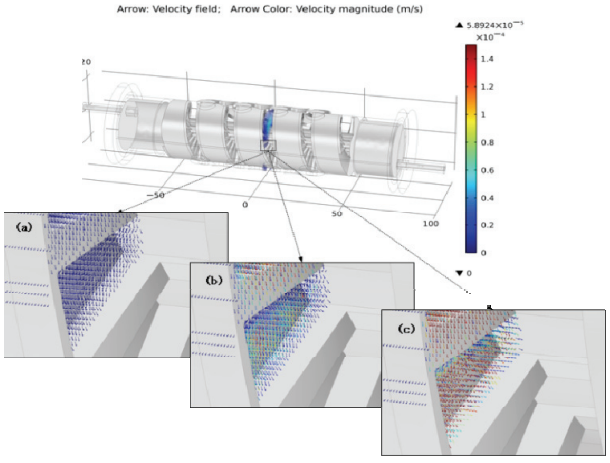

Fig. 4 Fluid dynamic model of the effect of flow rate, indicating increased mixing and reflected in power production.

Fig. 4 shows that increasing flow rate from 0.1ml/min (1.67×10^{-9} m/s) to 7.5ml/min (1.25×10^{-7} m/s) increased the localised eddies as well as fluid particle velocity suggesting that turnover would have increased and/or diffusion layer may have decreased. These effects were seen experimentally, when increased power was seen with increased flow rate.

6. CONCLUSIONS

BES can find utility in waste treatment, ion separation processes, electricity and energy gas and biomaterials production. BES is a promising field of research and development which must combine functions such as waste treatment and energy or product production in order to present a cost effective and deployable industrial process. Scale-up studies aim to minimise overpotential losses are minimised and manufacturability maximised.

7. ACKNOWELDGEMENTS

This research was funded by the RCUK Energy Programme, SUPERGEN Biological Fuel Cell project (EP/D047943/1) supported by grant 68-3A75-3-150 and the SUPERGEN (SHEC) project (grant number EP/E040071/1. The Energy Programme is an RCUK cross-council initiative led by EPSRC and contributed to by ESRC, NERC, BBSRC and STFC.

8. REFERENCES

(1) Fang JY, Zhu JL, Wang SP, Yue C, Shen HH. Global warming, human-induced carbon emissions, and their uncertainties. Science China-Earth Sciences 2011; 54(10): 1458-68. (2) Ramirez-Llodra E, Tyler PA, Baker MC, et al. Man and the Last Great Wilderness: Human Impact on the Deep Sea. Plos One 2011; 6(8). (3) Song Y, Penmatsa V, Wang CL. Recent development of miniaturized enzymatic biofuel cell. In: Dhar NK, Wijewarnasuriya PS, Dutta AK, eds. Energy Harvesting and Storage: Materials, Devices, and Applications Ii, 2011. (4) VijayaVenkataRaman S, Iniyan S, Goic R. A review of climate change, mitigation and adaptation. Renewable & Sustainable Energy Reviews 2012; 16(1): 878-97. (5) Xu DY, Li CL, Zhuang DF, Pan JJ. Assessment of the relative role of climate change and human activities in desertification: A review. Journal of Geographical Sciences 2011; 21(5): 926-36. (6) Smol JP. Climate Change: A planet in flux. Nature 2012; 483(7387): S12-S4. (7) Bullen RA, Arnot TC, Lakeman JB, Walsh FC. Review: Biofuel cells and their development. Biosensors and Bioelectronics 2006; 21: 2015-45. (8) Du Z, Li H, Gu T. A state of the art review on microbial fuel cells: A promising technology for wastewater treatment and bioenergy. Biotechnology advances 2007. (9) Wang H-Y, Bernarda A, Huang C-Y, Lee D-J, Chang J-S. Micro-sized microbial fuel cell: A mini-review. Bioresource Technology 2011; 102(1): 235-43. (10) Potter MC. Electrical effects accompanying the decomposition of organic compounds. Proc R Soc 1911; Ser B(84): 260-76. (11) Kim BH, Ikeda T, Park HS, et al. Electrochemical activity of an Fe(III)-reducing bacterium, Shewanella putrefaciens IR-1, in the presence of alternative electron acceptors. Biotechnology Techniques 1999; 13(7): 475-8. (12) Rabaey K, Angenent LT, Schroder U, Keller J, eds. Bioelectrochemical systems: From extracellular electron transfer to biotechnological application. London, New York: IWA Publishing, 2010 (13) Cao X, Huang X, Liang P, et al. A New Method for Water Desalination Using Microbial Desalination Cells. Environmental Science & Technology 2009; 43(18): 7148-52. (14) Logan BE. Extracting Hydrogen and Electricity from Renewable Resources. Environmental Science and Technology 2004; 38(9): 160-7. (15) Katuri KP, Scott K. Electricity Generation From the Treatment of Wastewater With a Hybrid Up-Flow Microbial Fuel Cell. Biotechnology and Bioengineering 2010; 107(1): 52-8. (16) Oh ST, Kim JR, Premier GC, Lee TH, Kim C, Sloan WT. Sustainable wastewater treatment: How might microbial fuel cells contribute. Biotechnology Advances 2010; 28(6): 871-81. (17) Zhuang L, Zheng Y, Zhou S, Yuan Y, Yuan H, Chen Y. Scalable microbial fuel cell (MFC) stack for continuous real wastewater treatment. Bioresource Technology 2012; 106: 82-8. (18) Kalathil S, Lee J, Cho MH. Granular activated carbon based microbial fuel cell for simultaneous decolorization of real dye wastewater and electricity generation. New Biotechnolog 2011; 29(1): 32-7. (19) Li Z, Zhang X, Lin J, Han S, Lei L. Azo dye treatment with simultaneous electricity production in an anaerobic-aerobic sequential reactor and microbial fuel cell coupled system. Bioresour Technol 2010; 101(12): 4440-5. (20) Jang JK, Chang IS, Moon H, Kang KH, Kim BH. Nitrilotriacetic acid degradation under microbial fuel cell environment. Biotechnol Bioeng 2006; 95(4): 772-4. (21) Cheng S, Dempsey BA, Logan BE. Electricity generation from synthetic acid-mine drainage (AMD) water using fuel cell technologies. Environ Sci Technol 2007; 41(23): 8149-53. (22) Tandukar M, Huber SJ, Onodera T, Pavlostathis SG. Biological Chromium(VI) Reduction in the Cathode of a Microbial Fuel Cell. Environ Sci Technol 2009; 43(21): 8159-65. (23) Ter Heijne A, Hamelers HVM,

Buisman CJN. Microbial Fuel Cell Operation with Continuous Biological Ferrous Iron Oxidation of the Catholyte. Environ Sci Technol 2007; 41(11): 4130-4. (24) Ter Heijne A, Liu F, van der Weijden R, Weijma J, Buisman CJN, Hamelers HVM. Copper Recovery Combined with Electricity Production in a Microbial Fuel Cell. Environ Sci Technol 2010; 44(11): 4376-81. (25) Gamburzev S, Appleby AJ. Recent progress in performance improvement of the proton exchange membrane fuel cell (PEMFC). Journal of Power Sources 2002; 107(1): 5-12. (26) Penumathsa BKV, Modelling biological anaerobic conversion of biomass to energy. Pontypridd: University of Glamorgan; 2010. 190 pp. (27) Pant D, Van Bogaert G, Diels L, Vanbroekhoven K. A review of the substrates used in microbial fuel cells (MFCs) for sustainable energy production. Bioresource Technology 2010; 101(6): 1533-43. (28) Horton B. Climate change: briefing paper. In: Water UK, 2012. (29) Fan YZ, Hu HQ, Liu H. Enhanced Coulombic efficiency and power density of air-cathode microbial fuel cells with an improved cell configuration. Journal of Power Sources 2007; 171(2): 348-54. (30) Dewan A, Beyenal H, Lewandowski Z. Scaling up Microbial Fuel Cells. Environmental Science & Technology 2008; 42(20): 7643-8. (31) Clauwaert P, Aelterman P, Pham TH, et al. Minimizing losses in bio-electrochemical systems: the road to applications. Appl Microbiol Biot 2008; 79(6): 901-13. (32) Clauwaert P, Mulenga S, Aelterman P, Verstraete W. Litre-scale microbial fuel cells operated in a complete loop. Appl Microbiol Biot 2009; 83(2): 241-7. (33) He Z, Wagner N, Minteer SD, Angenent LT. An Upflow Microbial Fuel Cell with an Interior Cathode: Assessment of the Internal Resistance by Impedance Spectroscopy†. Environmental Science & Technology 2006; 40(17): 5212-7. (34) Manohar AK, Bretschger O, Nealson KH, Mansfeld F. The use of electrochemical impedance spectroscopy (EIS) in the evaluation of the electrochemical properties of a microbial fuel cell. Bioelectrochemistry 2008; 72(2): 149-54. (35) Logan BE. Scaling up microbial fuel cells and other bioelectrochemical systems. Applied Microbiology and Biotechnology 2010; 85(6): 1665-71. (36) Kim JR, Premier GC, Hawkes FR, Dinsdale RM, Guwy AJ. Development of a tubular microbial fuel cell (MFC) employing a membrane electrode assembly cathode. Journal of Power Sources 2009; 187(2): 393-9. (37) Kim J, Premier G, Hawkes F, Dinsdale R, Guwy A. Development of a tubular microbial fuel cell (MFC) employing a membrane electrode assembly cathode. Journal of Power Sources 2009; 187(2): 393-9. (38) Kim JR, Premier GC, Hawkes FR, Rodríguez J, Dinsdale RM, Guwy AJ. Modular tubular microbial fuel cells for energy recovery during sucrose wastewater treatment at low organic loading rate. Bioresource Technology 2010; 101(4): 1190-8. (39) Popov AL, Kim JR, Dinsdale RM, Esteves SR, Guwy AJ, Premier GC. The Effect of Physico-chemically Immobilized Methylene Blue and Neutral Red on the Anode of Microbial Fuel Cell. Biotechnology and Bioprocess Engineering In Press. (40) Kyazze G, Popov A, Dinsdale R, et al. Influence of catholyte pH and temperature on hydrogen production from acetate using a two chamber concentric tubular microbial electrolysis cell. International Journal of Hydrogen Energy 2010; 35(15): 7716-22. (41) Wang AJ, Liu WZ, Cheng SA, Xing DF, Zhou JH, Logan BE. Source of methane and methods to control its formation in single chamber microbial electrolysis cells. Int J Hydrogen Energ 2009; 34(9): 3653-8. (42) Michie IS, Kim JR, Dinsdale RM, Guwyb AJ, Premier GC. The influence of psychrophilic and mesophilic start-up temperature on microbial fuel cell system performance. Energy & Environmental Science 2011; 4(3): 1011-9. (43) Michie IS, Kim JR, Dinsdale RM, Guwy AJ, Premier GC. Operational temperature regulates anodic biofilm growth and the development of electrogenic activity. Applied Microbiology and Biotechnology 2011; 92(2): 419-30. (44) Kim Y, Hatzell MC, Hutchinson AJ, Logan BE. Capturing power at higher voltages from arrays of microbial fuel cells without voltage reversal. Energy & Environmental Science 2011; 4(11): 4662-7. (45) Dewan A, Beyenal H, Lewandowski Z. Intermittent Energy Harvesting Improves the Performance of Microbial Fuel Cells. Environmental Science & Technology 2009; 43(12): 4600-5. (46) Liang P, Wu WL, Wei JC, Yuan LL, Xia X, Huang X. Alternate Charging and Discharging of Capacitor to Enhance the Electron Production of Bioelectrochemical Systems. Environmental Science & Technology 2011; 45(15): 6647-53. (47) Kim JR, Boghani H, Amini N, et al. Porous anodes with helical flow pathways in bioelectrochemical systems: The effects of fluid dynamics and operating regimes. Journal of Power Sources In Press.

9.6 Appendix A-6 Continuous Flow MEC Schematics

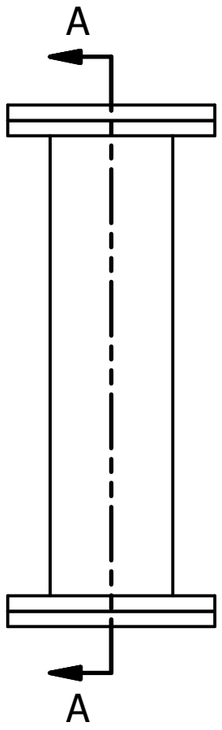

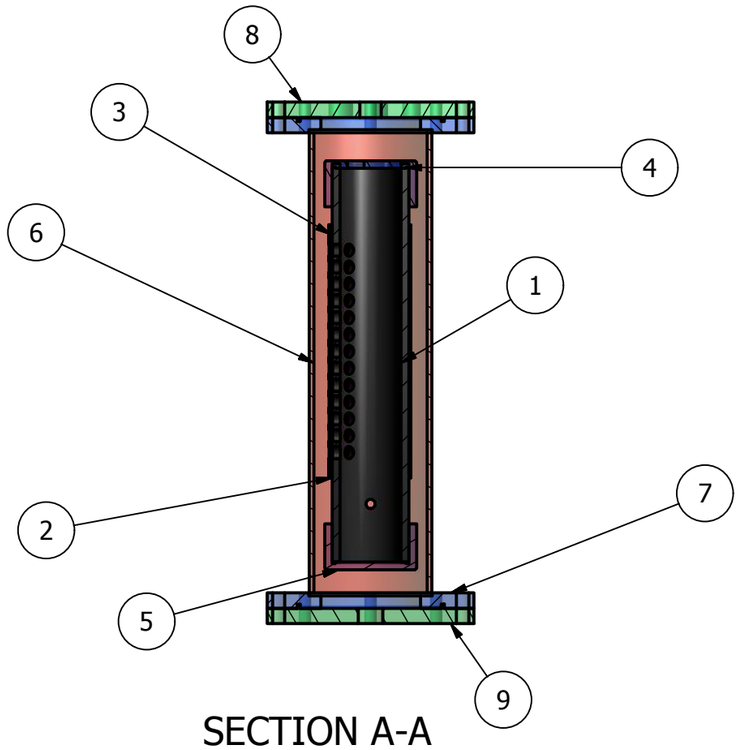

SECTION A-A
SCALE 1 / 4

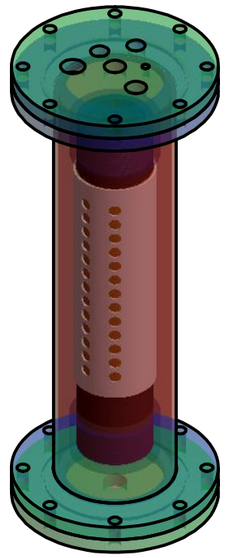

PARTS LIST			
ITEM	QTY	PART NUMBER	DESCRIPTION
1	1	Anode_Chamber_MEC	
2	1	Membrane	
3	1	Cathode_sleeve	
4	1	Anode_top_cap	
5	1	Anode_bottom_cap	
6	1	Cathode_tube	
7	2	Anode_enclosing_caps_cathode	
8	1	Enclosing_top_lid_cathode	
9	1	Anode_enclosing_bottom_lid_cathode	

NOTES:
1. ASSEMBLE PARTS AS SHOWN.

DRAWN hboghani	05/03/2012	SERC, UNIVERSITY OF GLAMORGAN
CHECKED	05/03/2012	TITLE: TUBULAR MEC MODULE
QA		
MFG	05/03/2012	
APPROVED	05/03/2012	
SIZE A3	DWG NO MEC	REV 1
SCALE 1:4		SHEET 1 OF 1

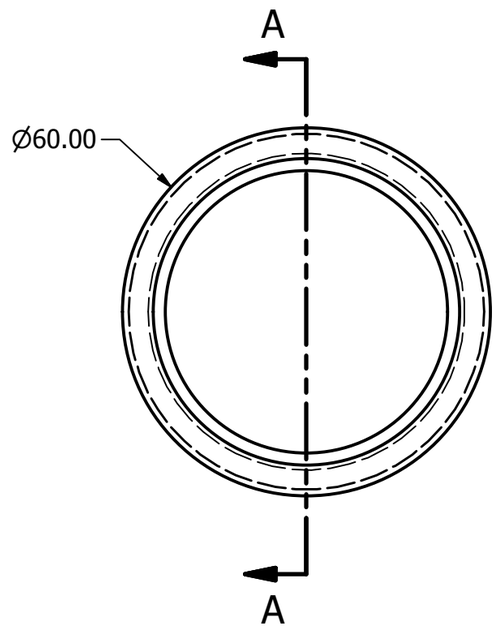

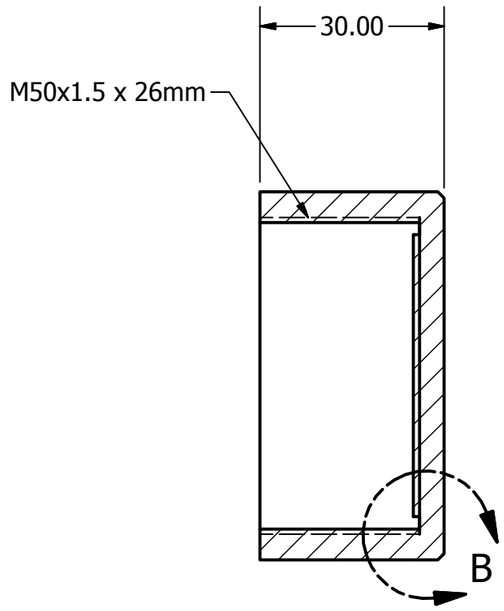

SECTION A-A
SCALE 1 : 1

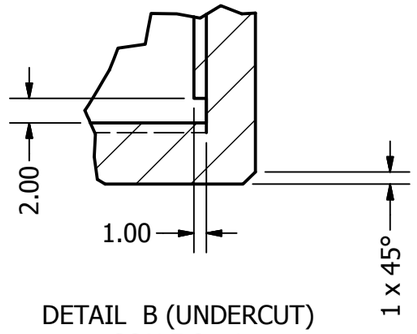

DETAIL B (UNDERCUT)
SCALE 2 : 1

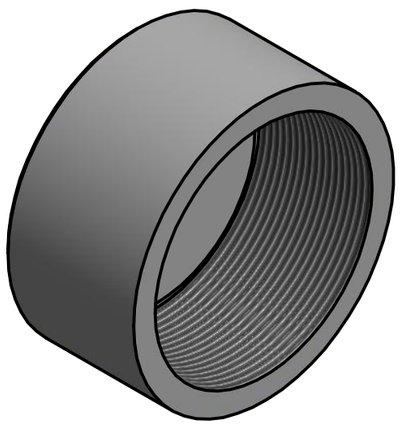

NOTES:
1. DEBURR ALL SHARP EDGES.
2. LINEAR TOLERANCE TO BE ±0.4mm AND
ANGULAR TOLERANCE TO BE ±0.5° UNLESS OTHERWISE SPECIFIED.

DRAWN hboghani	11/02/2012	SERC, UNIVERSITY OF GLAMORGAN
CHECKED		TITLE: ANODE BOTTOM CAP
QA	03/03/2012	
MFG	03/03/2012	
APPROVED	03/03/2012	
SIZE A3	DWG NO Anode_bottom_cap	REV 1
SCALE 1:1		SHEET 1 OF 1

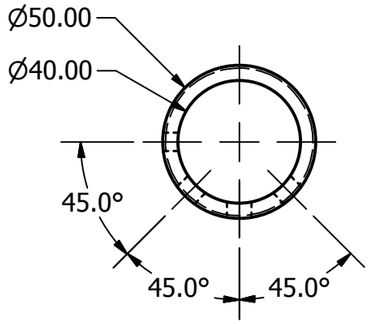

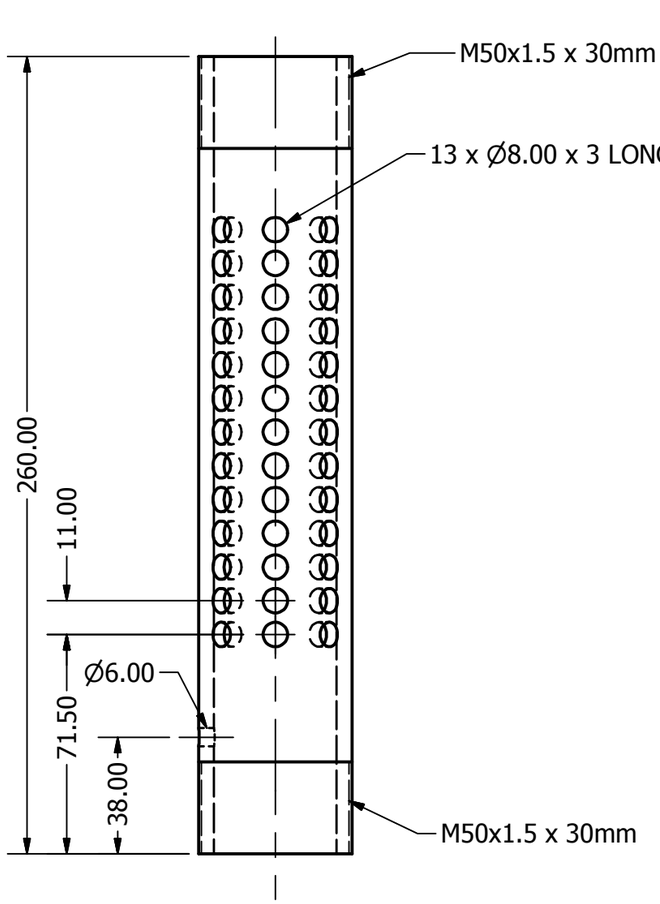

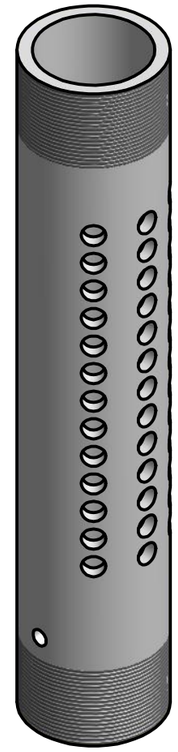

NOTE:
1. DEBURR ALL SHARP EDGES.
2. MATERIAL TO BE PERSPEX.
3. LINEAR TOLERANCE TO BE ±0.4mm AND
ANGULAR TOLERANCE TO BE ±0.5° UNLESS OTHERWISE SPECIFIED.

DRAWN hboghani	03/03/2012	SERC, UNIVERSITY OF GLAMORGAN	
CHECKED	03/03/2012		
QA	03/03/2012	TITLE ANODE CHAMBER MEC	
MFG	03/03/2012		
APPROVED	03/03/2012		
		SIZE A3	DWG NO Anode_Chamber_MEC-1 / REV 1
		SCALE 1:2	SHEET 1 OF 1

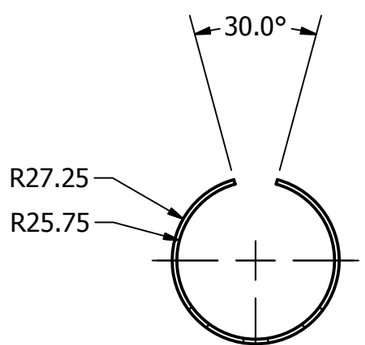

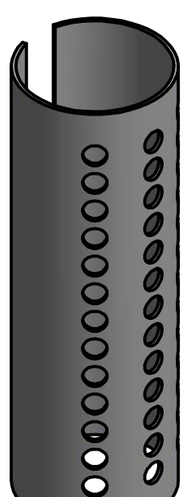

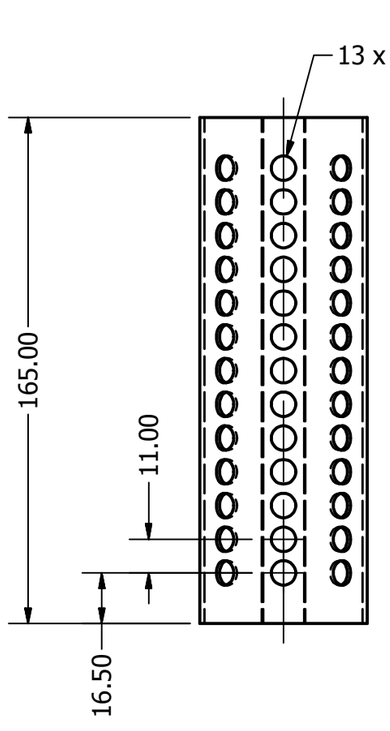

NOTE:
1. DEBURR ALL SHARP EDGES.
2. MATERIAL TO BE POLYPROPYLENE TUBE.
3. LINEAR TOLERANCE TO BE ±0.4mm AND
ANGULAR TOLERANCE TO BE ±0.5° UNLESS OTHERWISE SPECIFIED.

DRAWN hboghani	03/03/2012	SERC, UNIVERSITY OF GLAMORGAN
CHECKED	03/03/2012	TITLE: CATHODE SLEEVE
QA		
MFG	03/03/2012	
APPROVED	03/03/2012	
SIZE A3	DWG NO Cathode_sleeve	REV 1
SCALE 1:2	SHEET 1 OF 1	

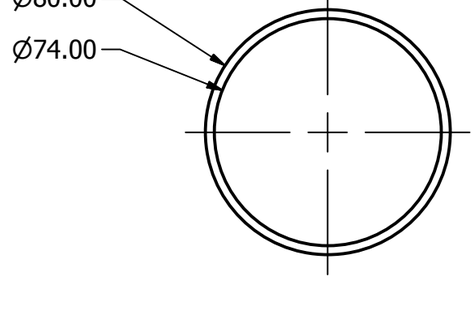

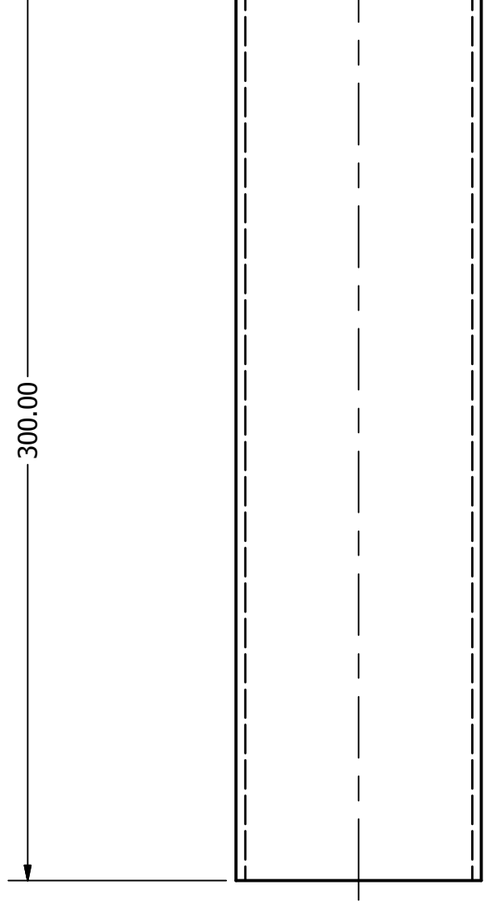

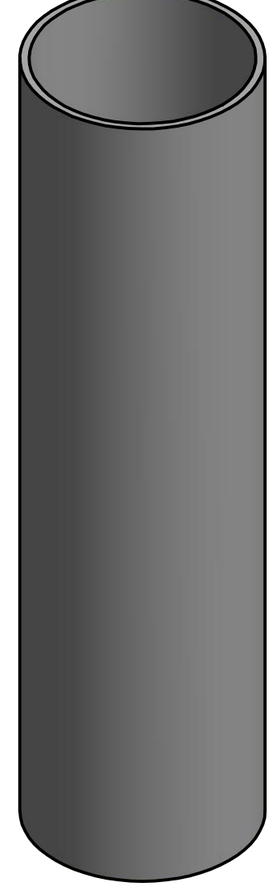

NOTE:
1. DEBURR ALL SHARP EDGES.
2. MATERIAL TO BE PERSPEX.
3. LINEAR TOLERANCE TO BE ±0.4mm AND
ANGULAR TOLERANCE TO BE ±0.5° UNLESS OTHERWISE SPECIFIED.

DRAWN hboghani	03/03/2012	UNIVERSITY OF GLAMORGAN
CHECKED	03/03/2012	
QA		TITLE: CATHODE TUBE
MFG	03/03/2012	
APPROVED	03/03/2012	
		SIZE A3 · DWG NO Cathode_tube · REV 1
		SCALE 1:2 · SHEET 1 OF 1

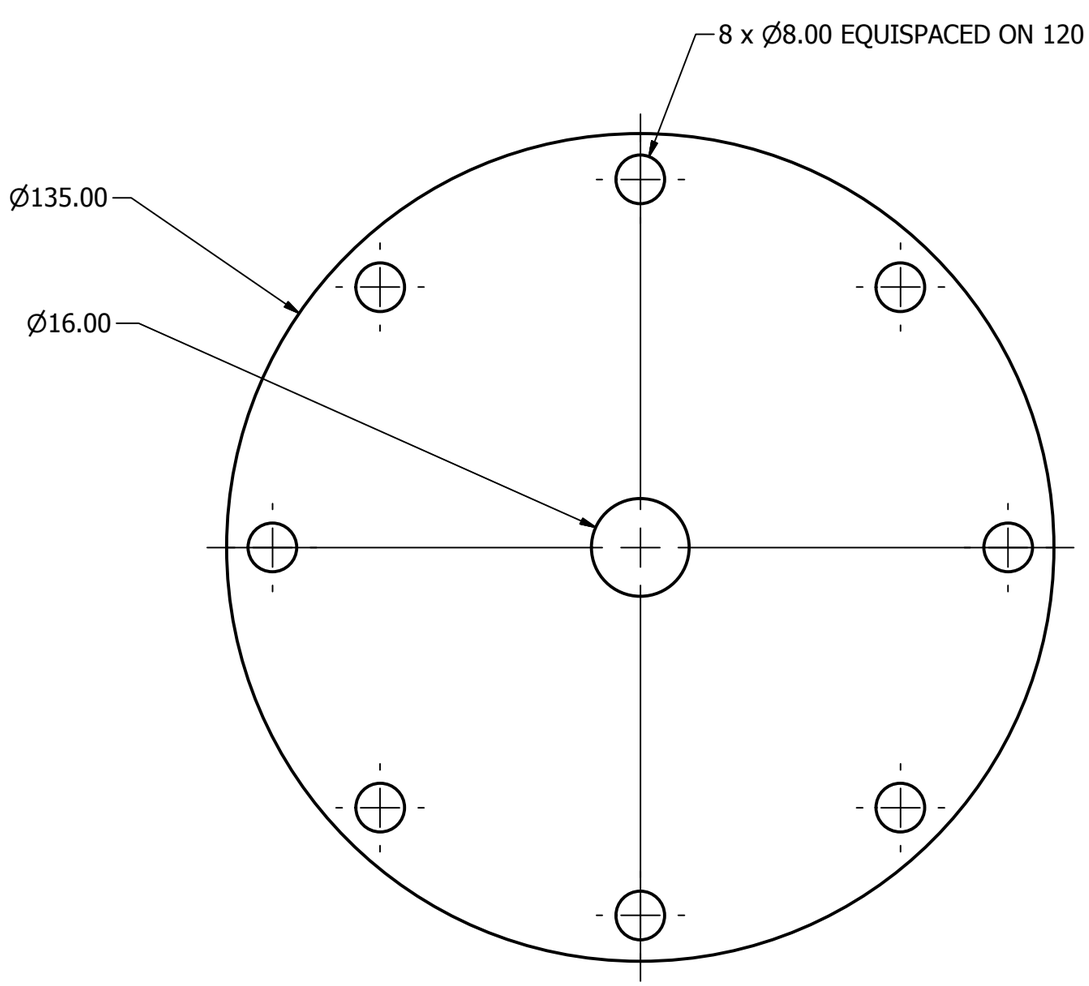

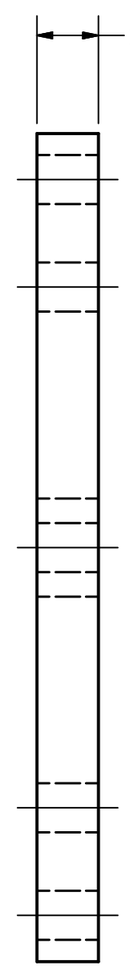

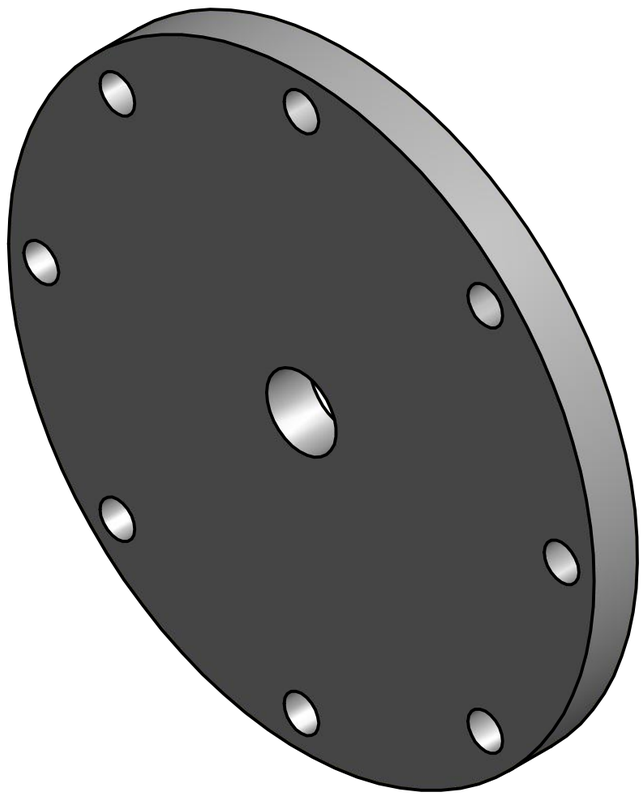

NOTES:
1. DEBURR ALL SHARP EDGES.
2. MATERIAL TO BE PERSPEX.
3. LINEAR TOLERANCE TO BE ±0.4mm AND
ANGULAR TOLERANCE TO BE ±0.5° UNLESS OTHERWISE SPECIFIED.

DRAWN hboghani	03/03/2012	SERC, UNIVERSITY OF GLAMORGAN
CHECKED	03/03/2012	
QA		TITLE: CATHODE BOTTOM LID
MFG	03/03/2012	
APPROVED	03/03/2012	
		SIZE A3 | DWG NO Enclosing_bottom_lid_cathode | REV 1
		SCALE 1:1 | SHEET 1 OF 1

PRODUCED BY AN AUTODESK EDUCATIONAL PRODUCT

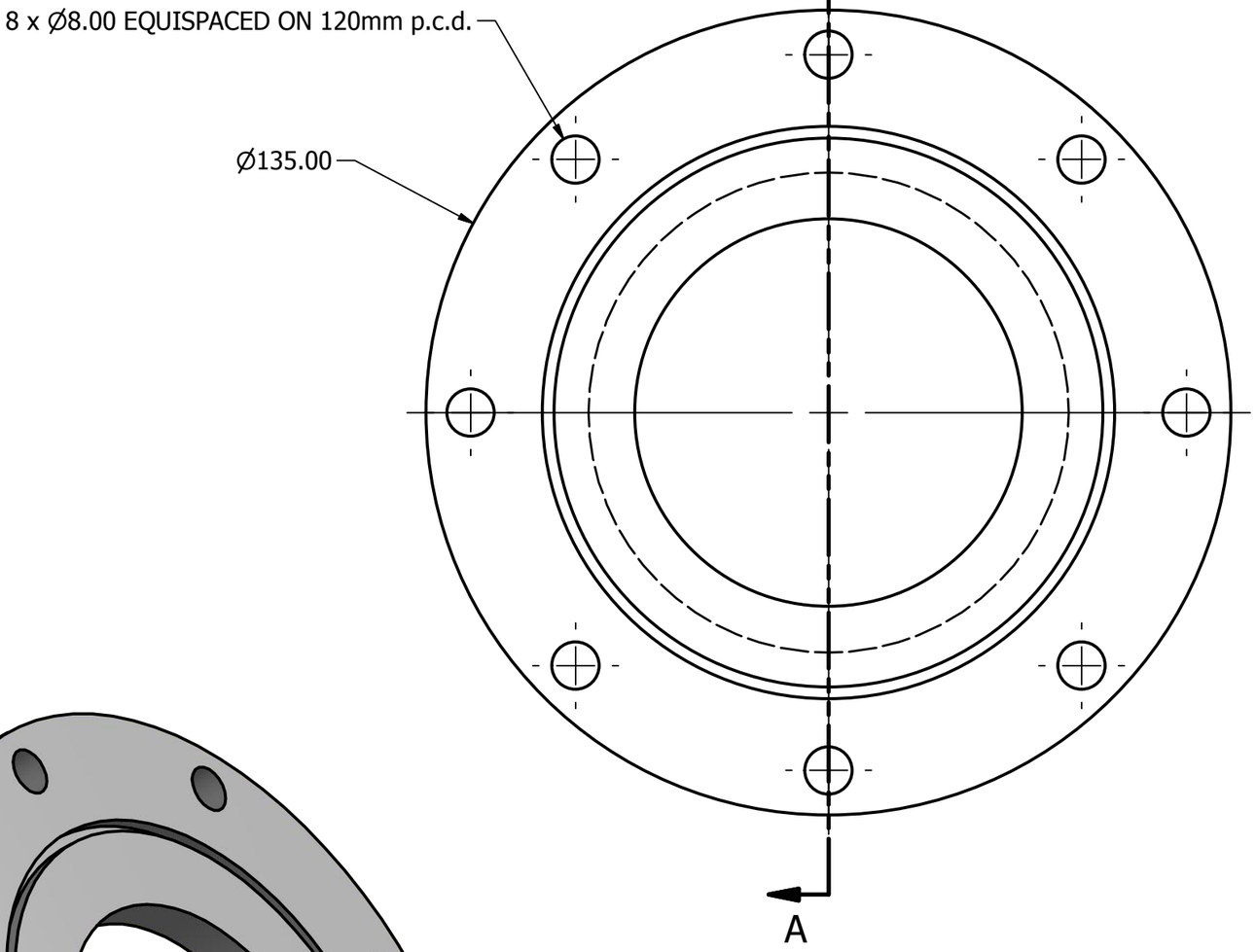

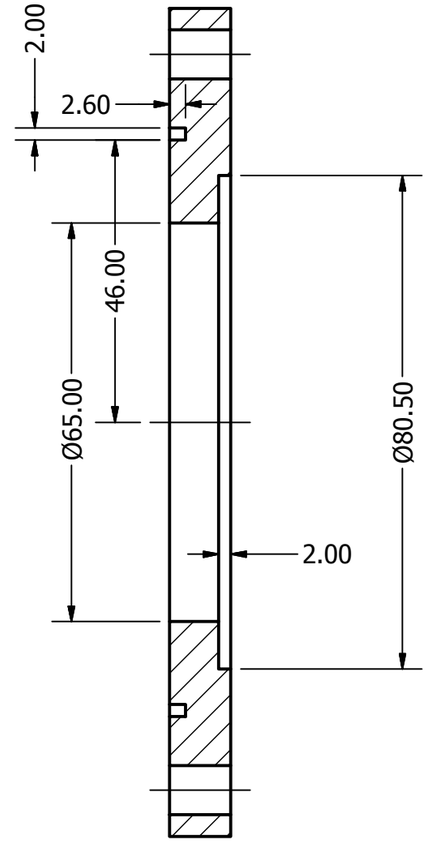

SECTION A-A
SCALE 1 : 1

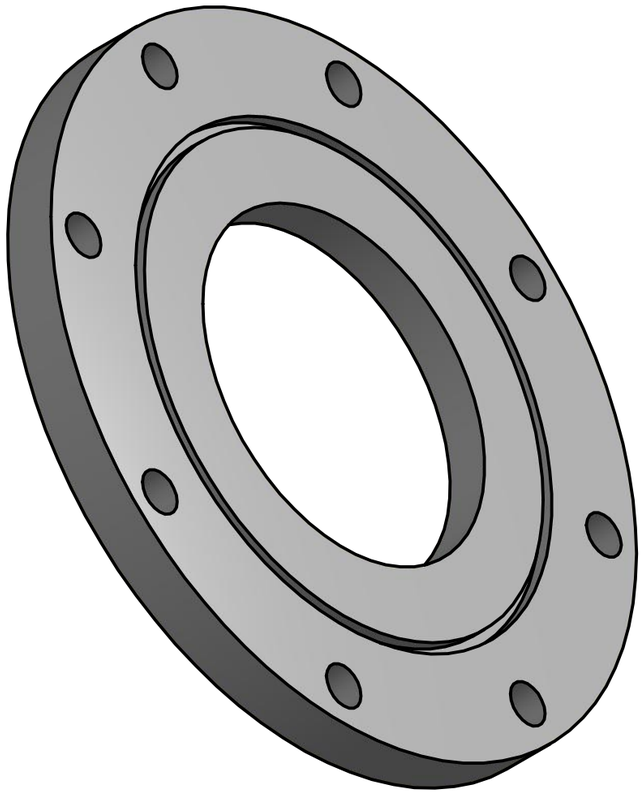

NOTES:
1. DEBURR ALL SHARP EDGES.
2. MATERIAL TO BE PERSPEX.
3. LINEAR TOLERANCE TO BE ±0.4mm AND
ANGULAR TOLERANCE TO BE ±0.5° UNLESS OTHERWISE SPECIFIED.

DRAWN hboghani	03/03/2012	SERC, UNIVERSITY OF GLAMORGAN
CHECKED	03/03/2012	
QA		TITLE: CATHODE ENCLOSING CAPS
MFG	03/03/2012	
APPROVED	03/03/2012	
SIZE A3	DWG NO Enclosing_caps_cathode	REV 1
SCALE 1:1	SHEET 1 OF 1	

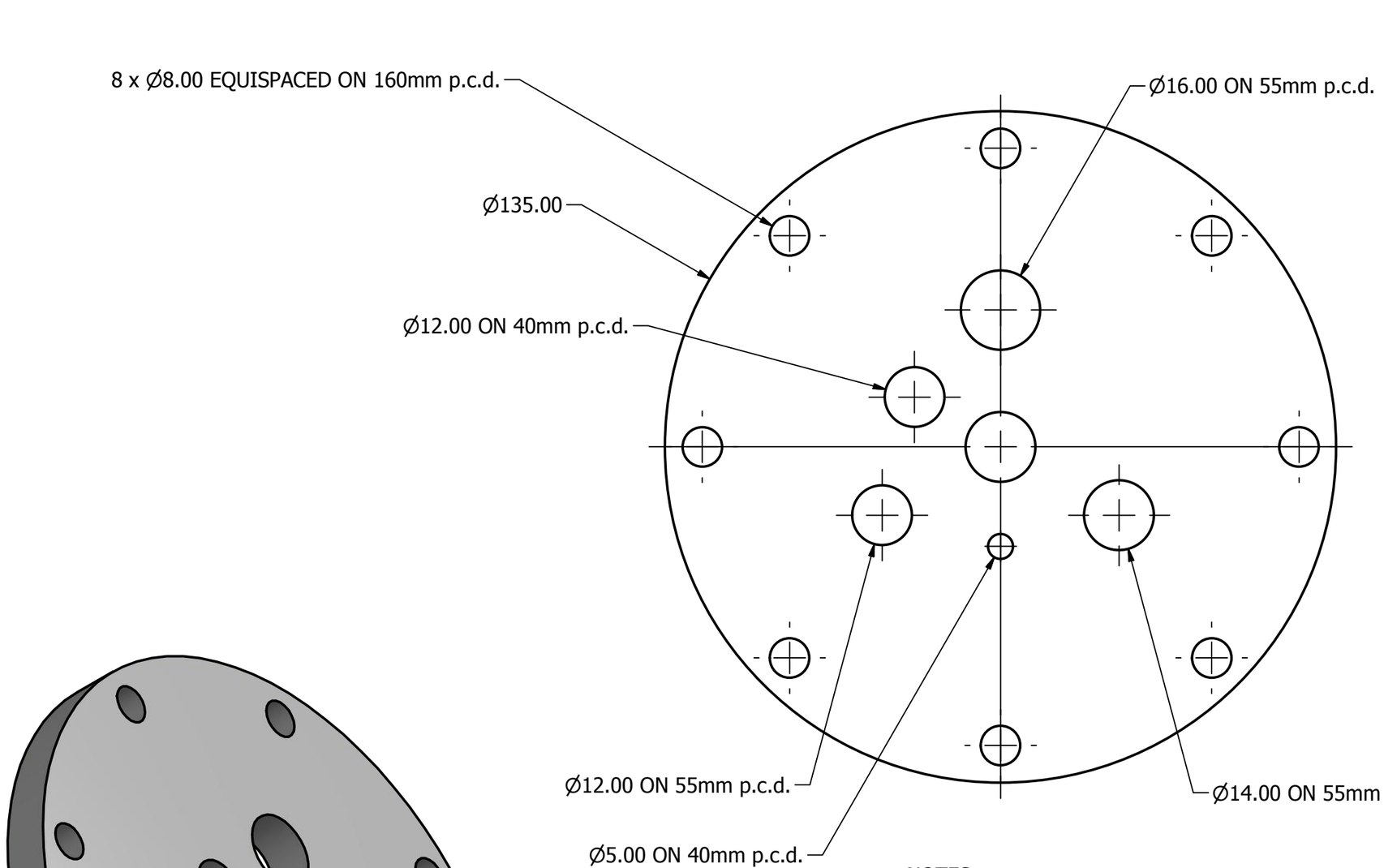

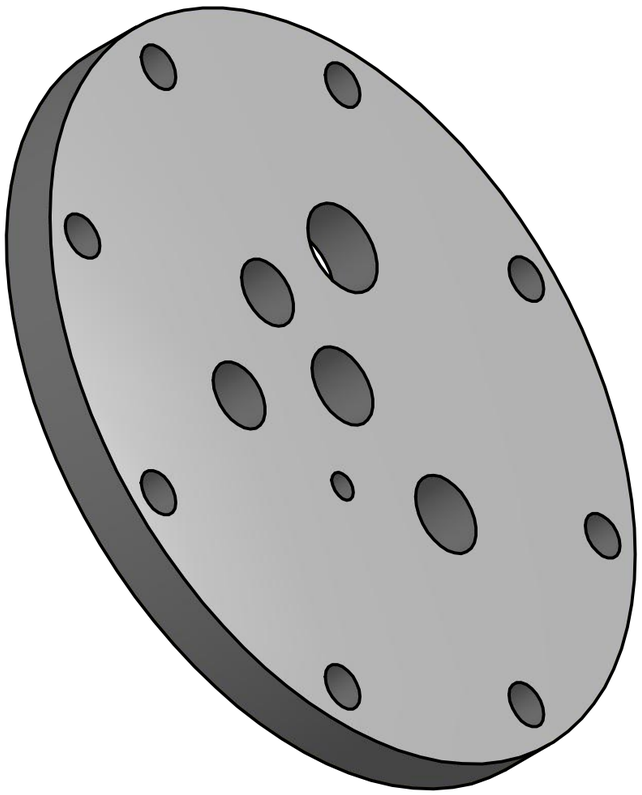

NOTES:
1. DEBURR ALL SHARP EDGES.
2. MATERIAL TO BE PERSPEX.
3. LINEAR TOLERANCE TO BE ±0.4mm AND
ANGULAR TOLERANCE TO BE ±0.5° UNLESS OTHERWISE SPECIFIED.

DRAWN hboghani	03/03/2012	SERC, UNIVERSITY OF GLAMORGAN
CHECKED	03/03/2012	
QA		TITLE: CATHODE TOP LID
MFG	03/03/2012	
APPROVED	03/03/2012	
SIZE A3	DWG NO Enclosing_top_lid_cathode	REV 1
SCALE 1:1		SHEET 1 OF 1

9.7 Appendix A-7 Scaled up Microbial Electrolysis Cell (Revolver Reactor) Schematics

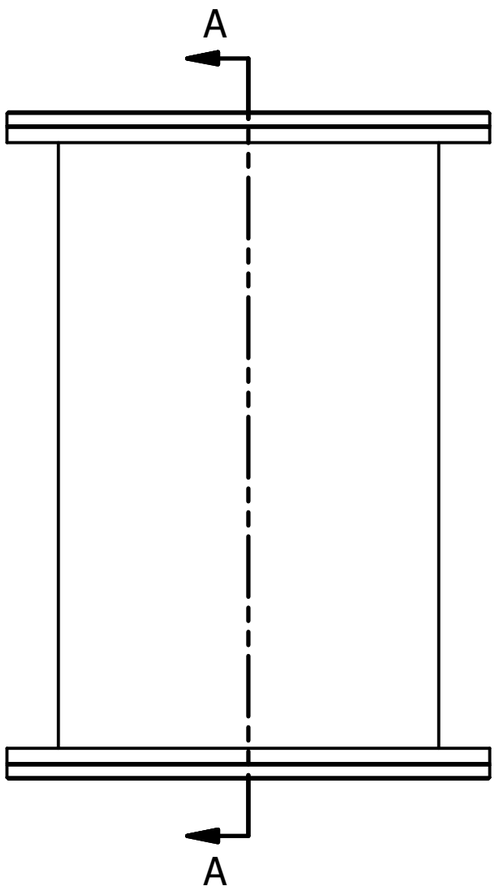

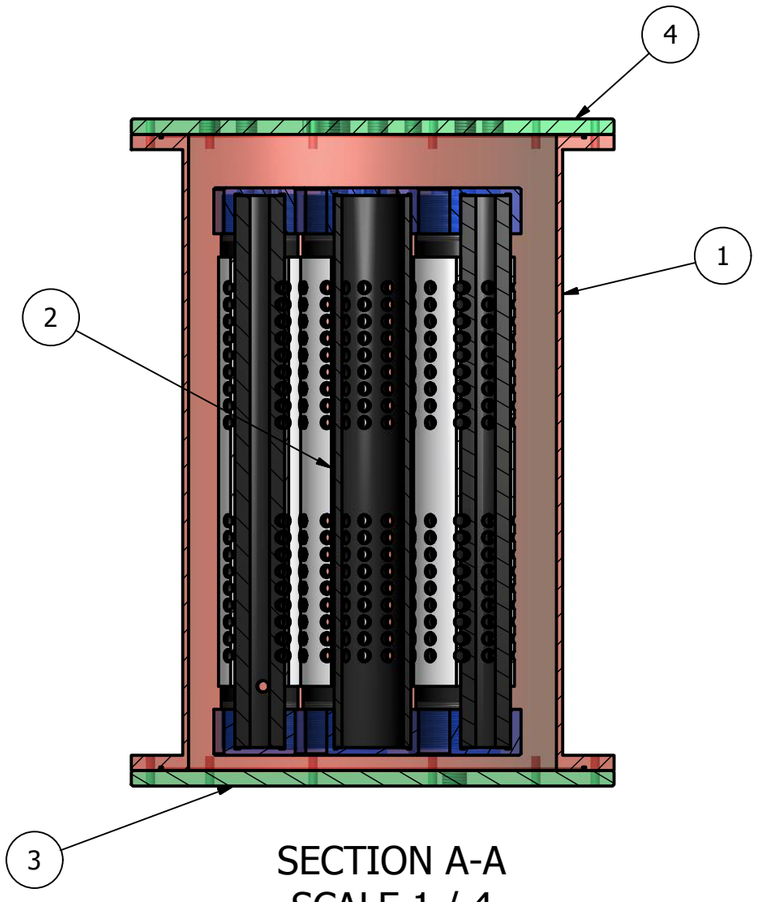

SECTION A-A
SCALE 1 / 4

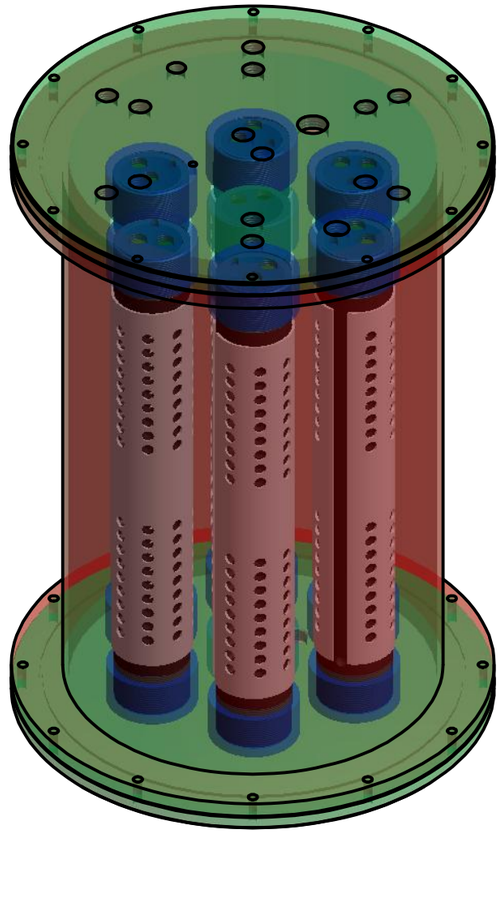

NOTES:
1. ASSEMBLE ALL PARTS AND MODULES AS SHOWN.

PARTS LIST			
ITEM	QTY	PART NUMBER	DESCRIPTION
1	1	Cathode_chamber	
2	7	MFC_module	
3	1	Bottom_lid_cathode	
4	1	Top_lid_cathode	

DRAWN hboghani	05/03/2012	SERC, UNIVERSITY OF GLAMORGAN
CHECKED	05/03/2012	
QA		TITLE: REVOLVER REACTOR
MFG	05/03/2012	
APPROVED	05/03/2012	
		SIZE A3 / DWG NO Revolver_reactor-1 / REV 1
		SCALE 1:4 / SHEET 1 OF 1

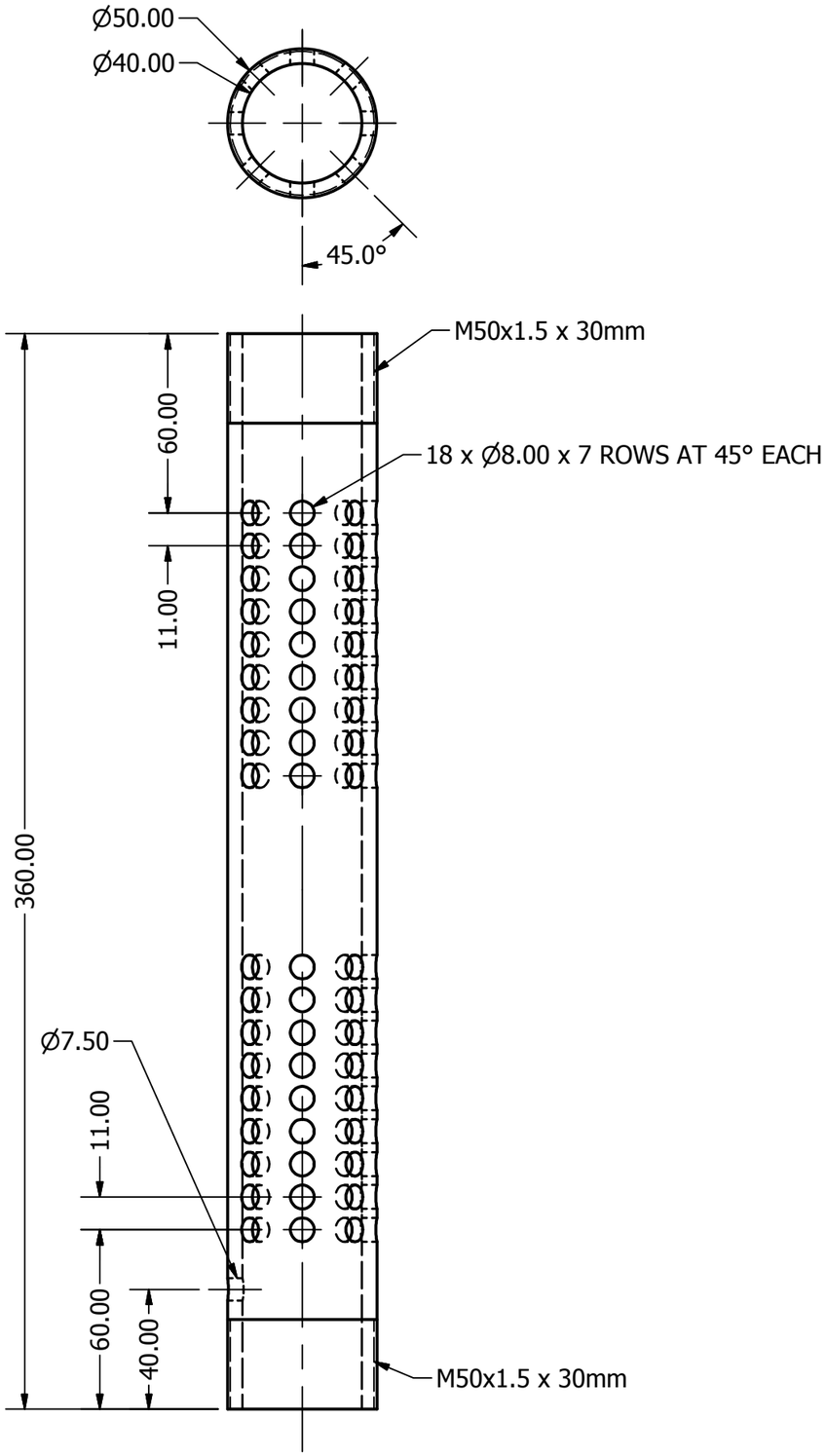

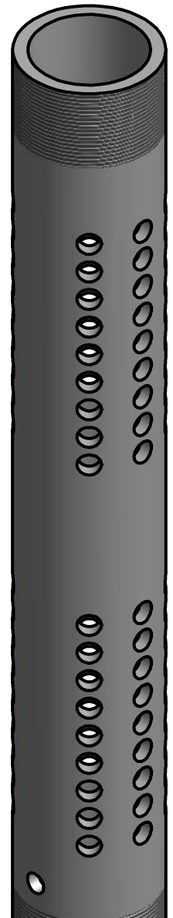

NOTES:
1. DEBURR ALL SHARP EDGES.
2. lINEAR TOLERANCE TO BE ±0.4mm AND
ANGULAR TOLERANCE TO BE ±0.5° UNLESS OTHERWISE SPECIFIED.

DRAWN hboghani	03/03/2012	SERC, UNIVERSITY OF GLAMORGAN
CHECKED	03/03/2012	
QA		TITLE: ANODE CHAMBER
MFG	03/03/2012	
APPROVED	03/03/2012	
		SIZE A3 | DWG NO Anode_Chamber | REV 1
		SCALE 1:2 | SHEET 1 OF 1

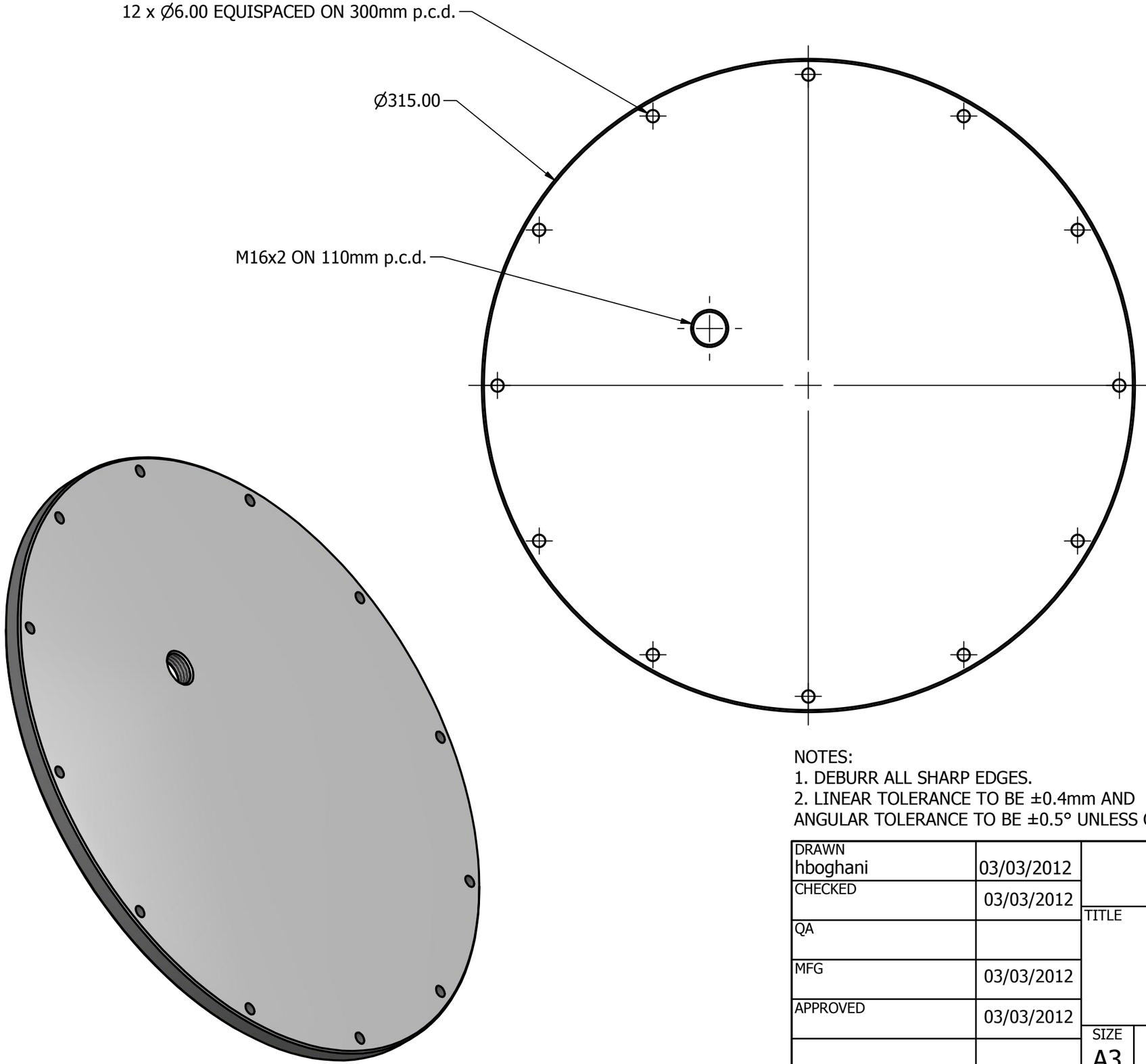

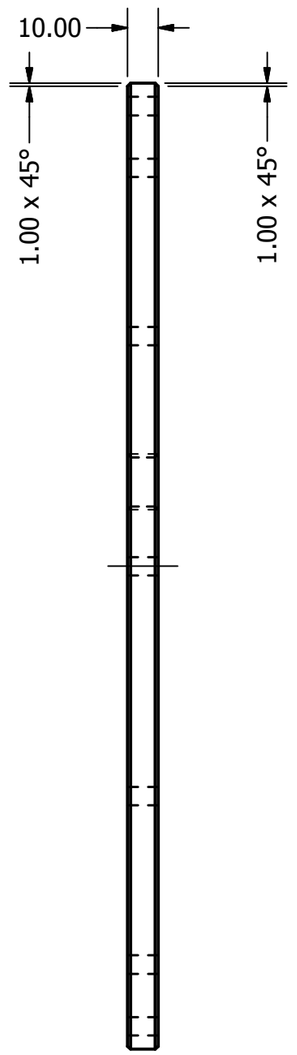

NOTES:
1. DEBURR ALL SHARP EDGES.
2. LINEAR TOLERANCE TO BE ±0.4mm AND
ANGULAR TOLERANCE TO BE ±0.5° UNLESS OTHERWISE SPECIFIED.

DRAWN hboghani	03/03/2012	SERC, UNIVERSITY OF GLAMORGAN
CHECKED	03/03/2012	
QA		TITLE: CATHODE BOTTOM LID
MFG	03/03/2012	
APPROVED	03/03/2012	
SIZE A3	DWG NO Bottom_lid_cathode	REV 1
SCALE 1:2		SHEET 1 OF 1

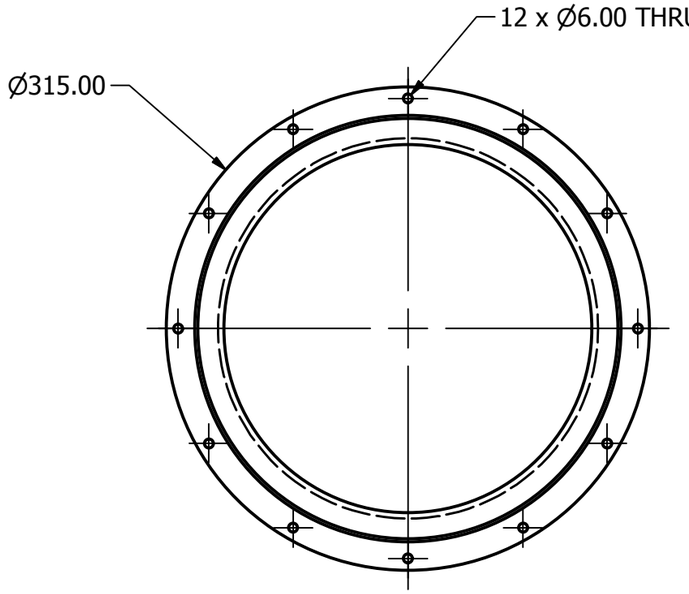

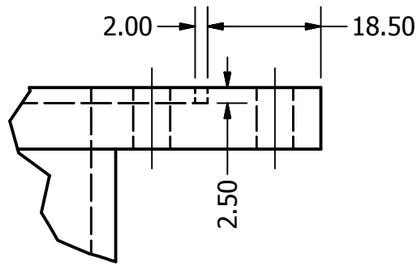

DETAIL B (GROOVE)
SCALE 1 : 1

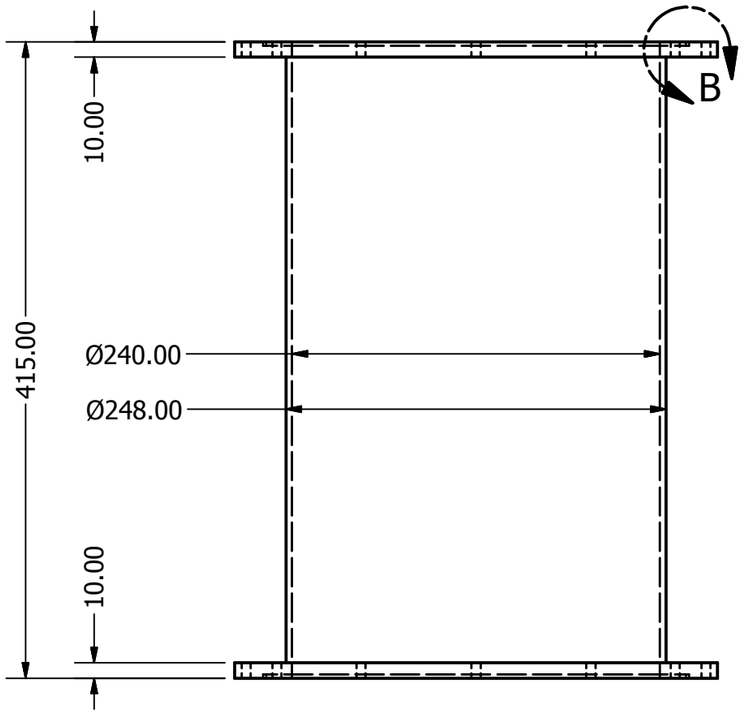

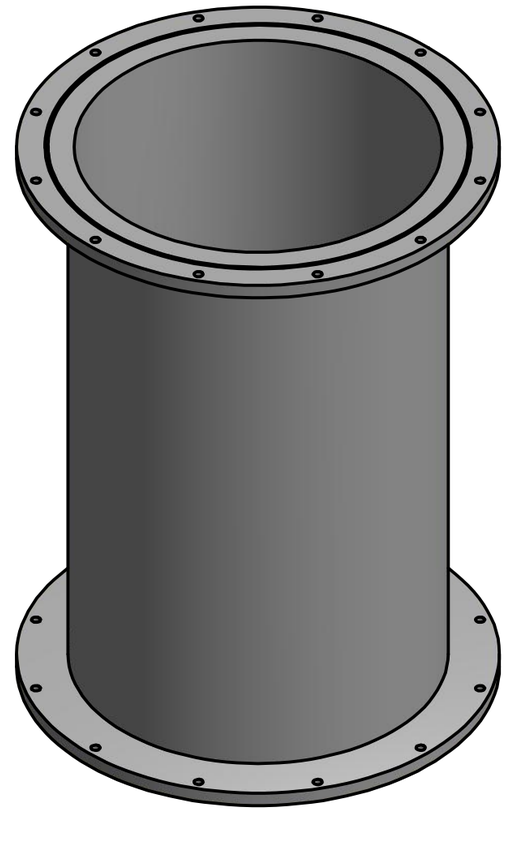

NOTES:
1. DEBURR ALL SHARP EDGES.
2. LINEAR TOLERANCE TO BE ±0.4mm AND
ANGULAR TOLERANCE TO BE ±0.5° UNLESS OTHERWISE SPECIFIED.

DRAWN hboghani	03/03/2012	SERC, UNIVERSITY OF GLAMORGAN
CHECKED	03/03/2012	TITLE: CATHODE CHAMBER
QA		
MFG	03/03/2012	
APPROVED	03/03/2012	
SIZE A3		DWG NO Cathode_chamber / REV 1
SCALE 1:4		SHEET 1 OF 1

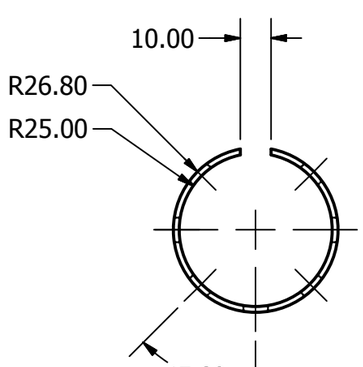

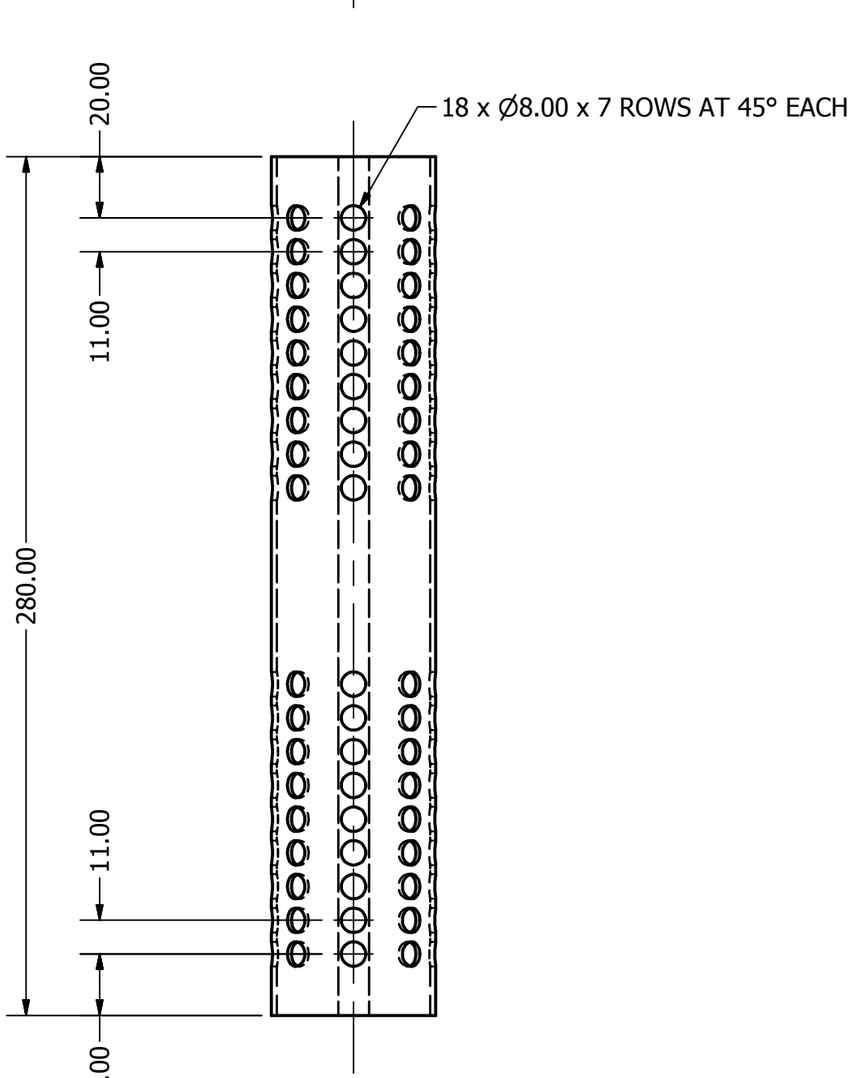

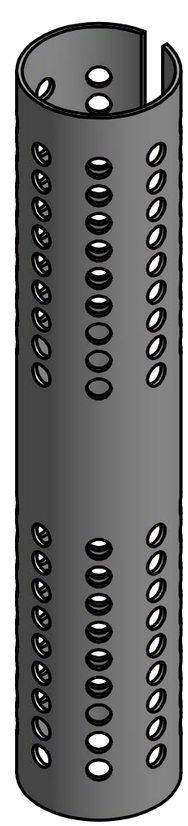

NOTES:
1. DEBURR ALL SHARP EDGES.
2. LINEAR TOLERANCE TO BE ±0.4mm AND
ANGULAR TOLERANCE TO BE ±0.5° UNLESS OTHERWISE SPECIFIED.

DRAWN hboghani	03/03/2012	SERC, UNIVERSITY OF GLAMORGAN
CHECKED	03/03/2012	
QA		TITLE: CATHODE SLEEVE
MFG	03/03/2012	
APPROVED	03/03/2012	
SIZE A3	DWG NO Cathode_sleeve	REV 1
SCALE 1:2	SHEET 1 OF 1	

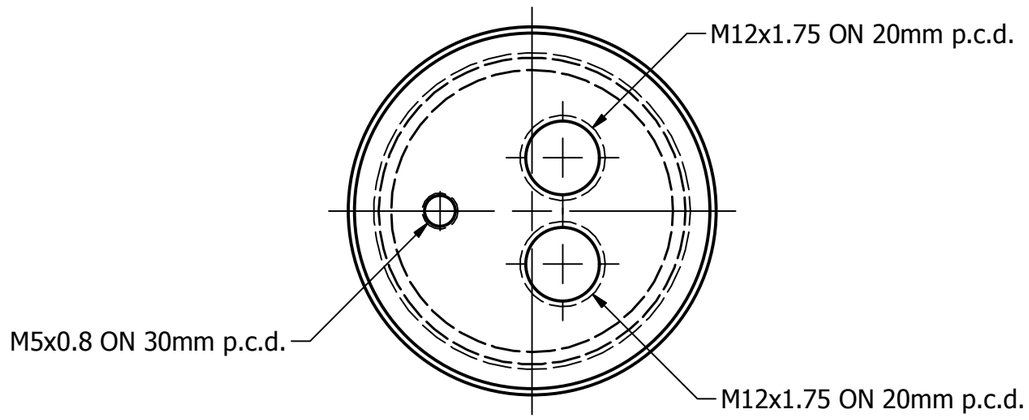

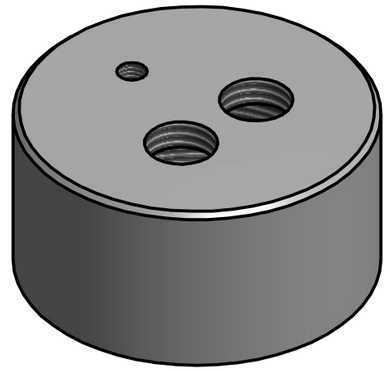

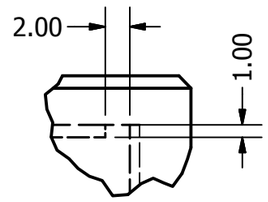

DETAIL A (UNDERCUT)
SCALE 2 : 1

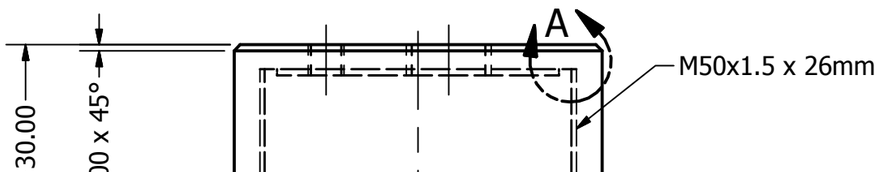

NOTES:
1. DEBURR ALL SHARP EDGES.
2. LINEAR TOLERANCE TO BE ±0.4mm AND
ANGULAR TOLERANCE TO BE ±0.5° UNLESS OTHERWISE SPECIFIED.

DRAWN hboghani	03/03/2012	SERC, UNIVERSITY OF GLAMORGAN
CHECKED	03/03/2012	
QA		TITLE: ANODE END CAP
MFG	03/03/2012	
APPROVED	03/03/2012	
		SIZE A3 / DWG NO End_cap-1 / REV 1
		SCALE 1:1 / SHEET 1 OF 1

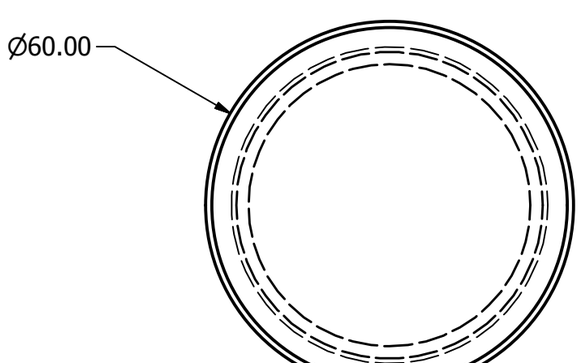

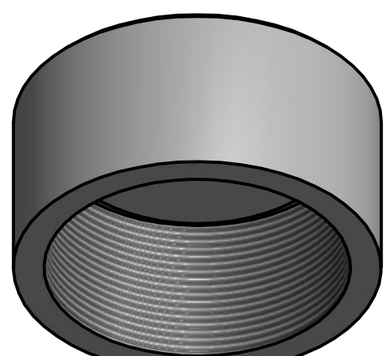

DETAIL A (UNDERCUT)
SCALE 2 : 1

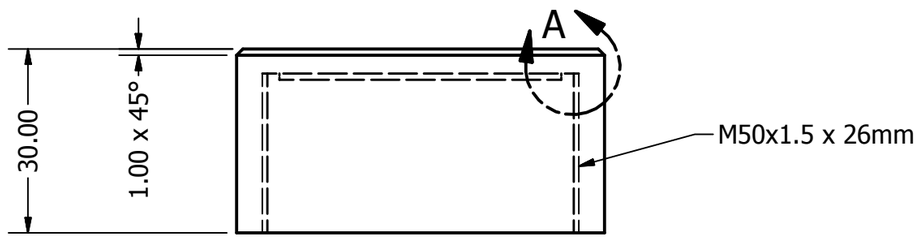

DRAWN hboghani	04/03/2012	SERC, UNIVERSITY OF GLAMORGAN
CHECKED	04/03/2012	TITLE: ANODE BOTTOM CAP
QA		
MFG	04/03/2012	
APPROVED	04/03/2012	
		SIZE A3 · DWG NO End_cap_bottom · REV 1
		SCALE 1:1 · SHEET 1 OF 1

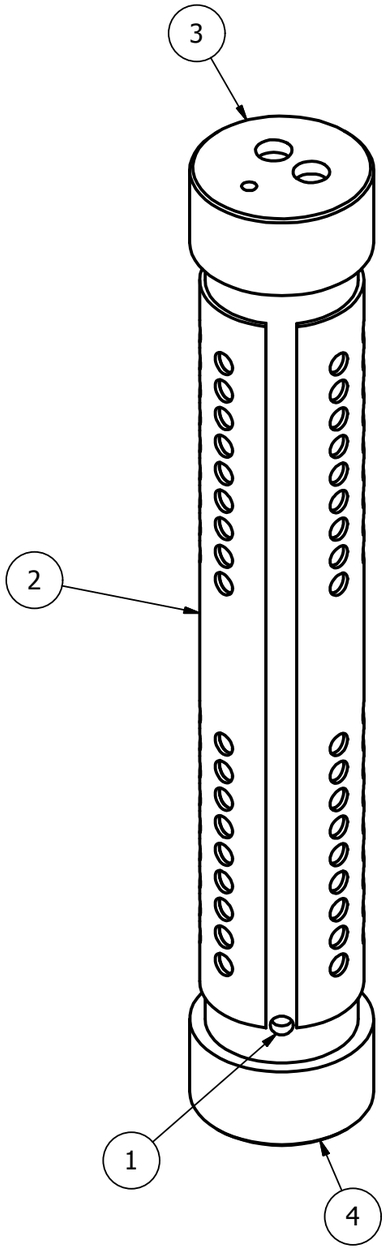

PARTS LIST			
ITEM	QTY	PART NUMBER	DESCRIPTION
1	1	Anode_Chamber	
2	1	Cathode_sleeve	
3	1	End_cap	
4	1	End_cap_bottom	

NOTES:
1. ASSEMBLE THE PARTS AS SHOWN.

DRAWN hboghani	04/03/2012	SERC, UNIVERSITY OF GLAMORGAN
CHECKED	04/03/2012	
QA		TITLE: MFC MODULE
MFG	04/03/2012	
APPROVED	04/03/2012	
SIZE A3	DWG NO MFC_module	REV 1
SCALE 1:2		SHEET 1 OF 1

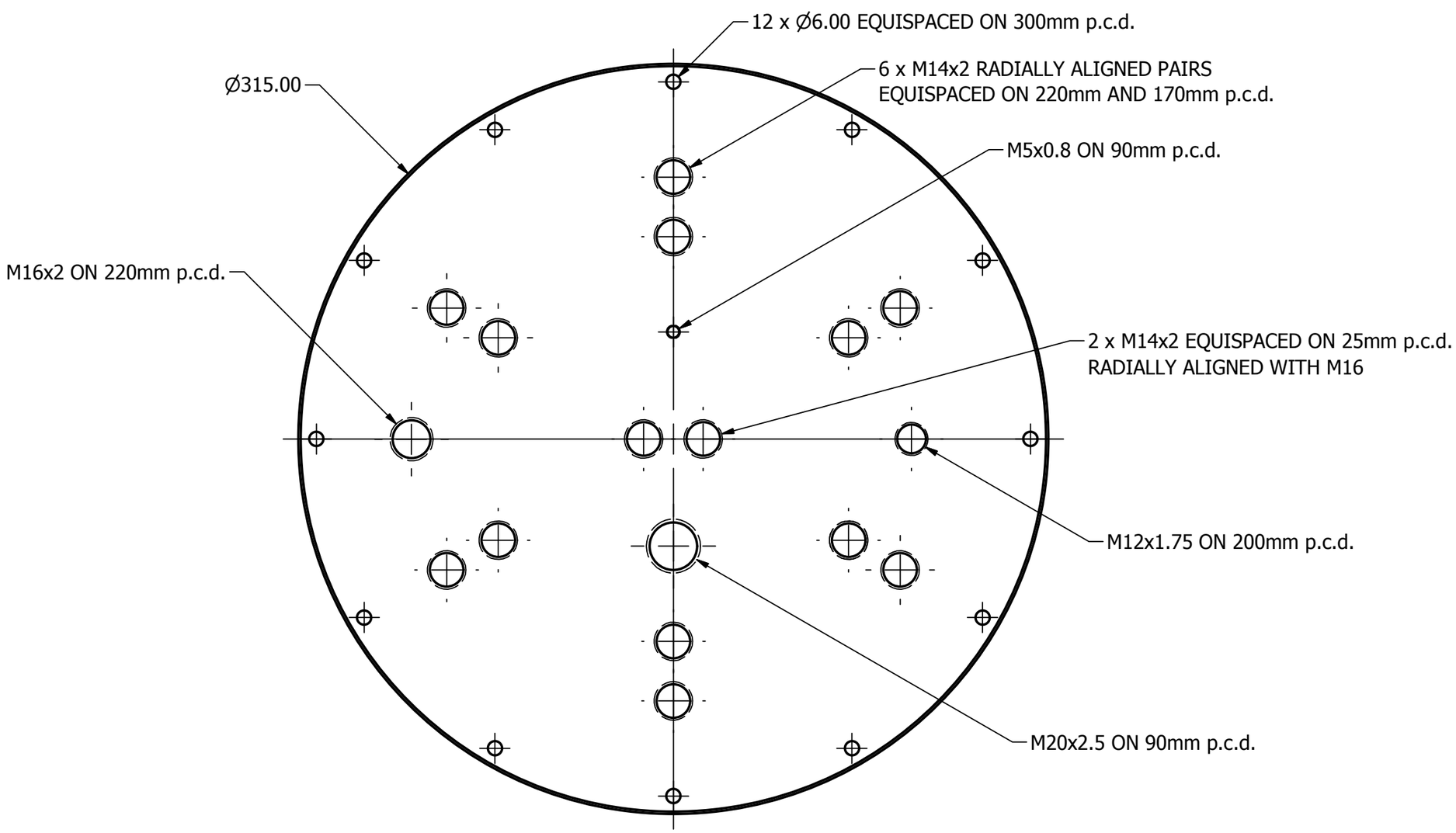

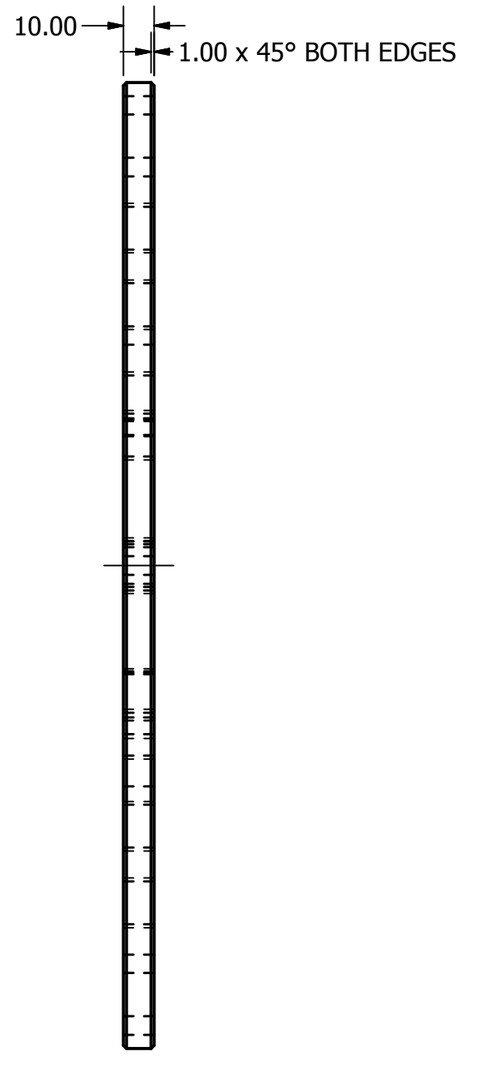

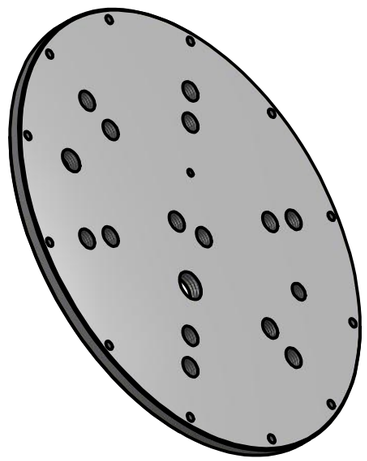

SCALE 1:4

NOTES:
1. DEBURR ALL SHARP EDGES.
2. LINEAR TOLERANCE TO BE ±0.4mm AND
ANGULAR TOLERANCE TO BE ±0.5° UNLESS OTHERWISE SPECIFIED.

DRAWN hboghani	04/03/2012	SERC, UNIVERSITY OF GLAMORGAN
CHECKED	04/03/2012	
QA		TITLE: CATHODE TOP LID
MFG	04/03/2012	
APPROVED	04/03/2012	
SIZE A3	DWG NO Top_lid_cathode	REV 1
SCALE 1:2		SHEET 1 OF 1